

**UNIVERSITA' DEGLI STUDI DI NAPOLI "FEDERICO II"**

**DIPARTIMENTO DI FARMACIA**



**DOTTORATO DI RICERCA IN**

**"SCIENZA DEL FARMACO"**

**XXIX CICLO 2014/2017**

***Semisynthetic bile acid derivatives as human receptor  
modulators***

Dott.ssa Claudia Finamore

**Tutors**

Dott.ssa Valentina Sepe

Prof. Santos Fustero

**Coordinatore**

Prof.ssa Maria Valeria D'Auria

*“To strive, to seek, to find, and not to yield.”*

*“Lottare, cercare, trovare e non cedere mai.”*

***A. Tennyson***

**INDEX**


---



---

<b>ABSTRACT</b> .....	1
 <b>INTRODUCTION: BILE ACIDS AND ENDOGENOUS RECEPTORS</b>	
Bile Acids .....	2
Bile Acid Synthesis .....	3
Farnesoid-X-Receptor (FXR).....	4
FXR: Therapeutic application .....	6
FXR: Ligands from Nature .....	6
FXR: Steroidal and non steroidal agonists.....	7
G-protein coupled receptor 1 (GPBAR1) .....	9
Model of GPBAR1.....	11
 <b>CHAPTER 1</b>	
<b>CHENOCHOLANE AND URSOCHOLANE DERIVATIVES</b>	
1.1 Preparation of Chenocholane derivatives.....	16
1.1.1 Synthesis of 3-deoxychenocholane derivatives .....	16
1.1.2 Synthesis of 3 $\beta$ -chenodeoxycholane derivatives .....	17
1.2 Preparation of Ursocholane derivatives .....	18
1.2.1 Synthesis of 3-deoxyursocholane derivatives.....	18
1.2.2 Synthesis of 5 $\beta$ -cholane derivatives.....	18
1.2.3 Synthesis of 3 $\beta$ -ursodeoxycholane derivatives.....	19
1.3 Pharmacological evaluation .....	19
1.3.1 Pharmacological evaluation on 7 $\alpha$ -hydroxy-5 $\beta$ -cholan-24-sulfate (7) .....	21

## CHAPTER 2

## 6-ETHYLCHENOLANE DERIVATIVES

2.1 Synthesis of 3 $\alpha$ -hydroxy-6-ethylcholane derivatives .....	26
2.2 Pharmacological evaluation of 3 $\alpha$ -hydroxy-6-ethylcholane derivatives .....	31
2.2.1 Pharmacological evaluation on EUDCOH (45).....	31
2.2.1.1 Preclinical <i>in vivo</i> pharmacological evaluation on 45.....	34
2.3 Preparation of 3-deoxy-6-ethylchenodeoxycholane derivatives.....	37
2.4 Preparation of 3 $\beta$ -hydroxy-6-ethylchenodeoxycholane derivatives .....	40
2.5 Pharmacological evaluation of 3-deoxy and 3 $\beta$ -hydroxy derivatives.....	42
2.5.1 <i>In vitro</i> .....	42
2.5.2 <i>In vivo</i> .....	45

## CHAPTER 3

## 6-ETHYLNORCHOLANE AND BIS-HOMO-6-ETHYLCHOLANE DERIVATIVES

3.1 Preparation of 3 $\alpha$ ,7 $\alpha$ -hydroxy-6-ethylnorcholane derivatives .....	50
3.1.1 Pharmacological evaluation of 3 $\alpha$ ,7 $\alpha$ -hydroxy-6-ethylnorcholane derivatives .....	52
3.1.2 Pharmacological evaluation on NorECDCOH (77).....	53
3.1.2.1 Preliminary advanced pharmacological results of 77 .....	58
3.2 Preparation of 3 $\alpha$ -hydroxy-6-ethylnorcholane derivatives.....	62
3.3 Preparation of 3-deoxy- and 3 $\beta$ -hydroxy-6 $\alpha$ -ethylnorcholane derivatives .....	64
3.4 Preparation of bis- <i>homo</i> -6-ethylcholane derivatives .....	65
3.5 Pharmacological evaluation of 3 $\alpha$ -hydroxy-, 3-deoxy-, 3 $\beta$ -hydroxy-6-ethylnorcholane and bis- <i>homo</i> -6-ethylcholane derivatives .....	66

**CHAPTER 4****ASYMMETRIC DIVERSITY-ORIENTED SYNTHESIS OF BENZO-FUSED CYCLIC AMINES**

4.1 Optimization of Intramolecular Heck reaction .....	77
4.2 Ring-closing enyne metathesis (RCEYM) exploration.....	79
4.3 Study of the one-pot condensation/ asymmetric allylation/ intramolecular Pauson–Khand reaction (PKR) sequence.....	82
<b>CONCLUSIONS</b> .....	84
<b>EXPERIMENTAL SECTION</b>	
I. General Experimental procedures.....	86
II. Experimental procedures for chenocholane and ursocholane derivatives.....	90
III. Experimental procedures for 6-ethylchenodeoxycholane derivatives .....	119
IV. Experimental procedures for 6-ethylnorcholane and bis- <i>homo</i> -6-ethylcholane derivatives .....	148
V. Experimental procedures for benzo-fused cyclic amines.....	172
<b>REFERENCES</b> .....	176
<b>ACKNOWLEDGEMENTS</b> .....	190
<b>CURRICULUM VITAE</b> .....	192
<b>PUBLICATIONS</b> .....	193

**ABSTRACT**

---

Next to their primitive role in fat digestion, solubilisation and absorption, nowadays, bile acids (BAs) are considered signaling molecules able to interact with nuclear and membrane endogenous receptors, inducing several cellular networks that regulate lipids, glucose and bile acids homeostasis. Two well-known targets of BAs are the endogenous nuclear receptor FXR (farnesoid-x-receptor) and the membrane receptor GPBAR1 (G-protein coupled receptor 1) and since their activation is linked to the control of different metabolic and enterohepatic functions, they could be considered efficient targets in the treatment of several human diseases. In the last few years, medicinal chemistry modifications on bile acid scaffolds, afforded a large amount of exogenous derivatives with different pharmacological profiles, useful in the treatment of metabolic and enterohepatic disorders, ranging from metabolic syndrome, diabetes, cholestasis and non-alcoholic steatohepatitis. One limit of the therapeutic use of BA derivatives is their promiscuity in binding different receptors and inducing an increase of risk for adverse side effects, due to the activation of several downstream signals controlled by these two receptors. For these reasons, my research work, described in this PhD thesis and developed in this research area, was addressed to the identification of novel selective ligands as potential lead compounds, useful in the treatment of metabolic and enterohepatic disorders, in which the dual modulation is detrimental in terms of side effects. Medicinal chemistry modifications, mainly performed on chenodeoxycholic acid (CDCA) and focused on the length/functionalization of the side chain, as well as on the tetracyclic core, allowed the identification of several lead compounds with promising pharmacological activities in the frame of human FXR-mediated diseases. Another consistent part of my PhD project, in organic synthesis, was spent in the laboratory of the Centro de Investigación Príncipe Felipe of Valencia. During this period, I worked in the asymmetric diversity-oriented synthesis of benzo-fused cyclic amines using homoallylic *o*-halobenzylamines, as starting material, in which the presence of halogen atoms makes them suitable for the asymmetric synthesis of different compounds, such as heterocycles or benzo-fused compounds.

## INTRODUCTION: BILE ACIDS AND ENDOGENOUS RECEPTORS

### BILE ACIDS

Bile acids (BAs) are a class of steroid molecules synthesized in the liver from cholesterol. BAs are the main components of bile and can be divided in primary bile acids, such as chenodeoxycholic acid (CDCA) and cholic acid (CA), in highest concentration, and in secondary bile acids such as lithocholic (LCA), deoxycholic (DCA) and ursodeoxycholic acid (UDCA), contained in a small aliquot (Figure 1). From a structural point of view, they are characterized by a steroid core with a truncated side chain at C17, ending with a carboxyl group. BAs are different from natural steroids for the presence of a *cis* junction between the rings A and B, which confers a “bent form” to the ring A, that is projected out of the plan formed by rings B-C-D.

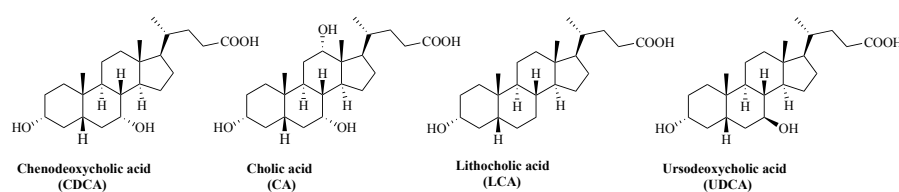


**Figure 1.** Endogenous bile acids

All bile acids possess in their tetracyclic core one or more hydroxyl groups, at C3, C6, C7 or C12, which modulate their physical and chemical properties, as well as their receptor-binding profile. Even though BAs are identified for their ancestral role of lipid digestion and absorption, recently, they are considered key signaling molecules, endowed with both genomic and non genomic effects. These effects are the result of their interaction with several nuclear receptors, such as the farnesoid-X-receptor (FXR), the pregnane-X-receptor (PXR), the constitutive androstane receptor (CAR), the vitamin D receptor (VDR), the liver-X-receptor (LXR), and with G-protein-coupled receptors, such as GPBAR1 (also known as M-BAR, TGR5 or BG37).<sup>1-6</sup> Furthermore, primary and secondary bile acids activate voltage and calcium-gated potassium channels (BKCa or KCa1.1) and interact with tyrosine kinase coupled receptors, inducing the transactivation of the epidermal growth factor receptor or EGFR. The above promiscuity supports the

fact that bile acids exert a variety of patho-physiological and pharmacological activities.

## BILE ACID SYNTHESIS

In bile acid synthesis, cholesterol is first converted by liver in primary bile acids, CA and CDCA that in turn are converted by intestinal microbiota in secondary bile acids, DCA, LCA, UDCA as well as in their glycine (human) and taurine (mouse) conjugated forms. The first pathway (or *classic*) starts from the 7 $\alpha$ -hydroxylase cytochrome P-450 (CYP7A1), differently, the alternative pathway (or *acidic*) is initiated by the sterol 27-hydroxylase (CYP27A1), (Figure 2).

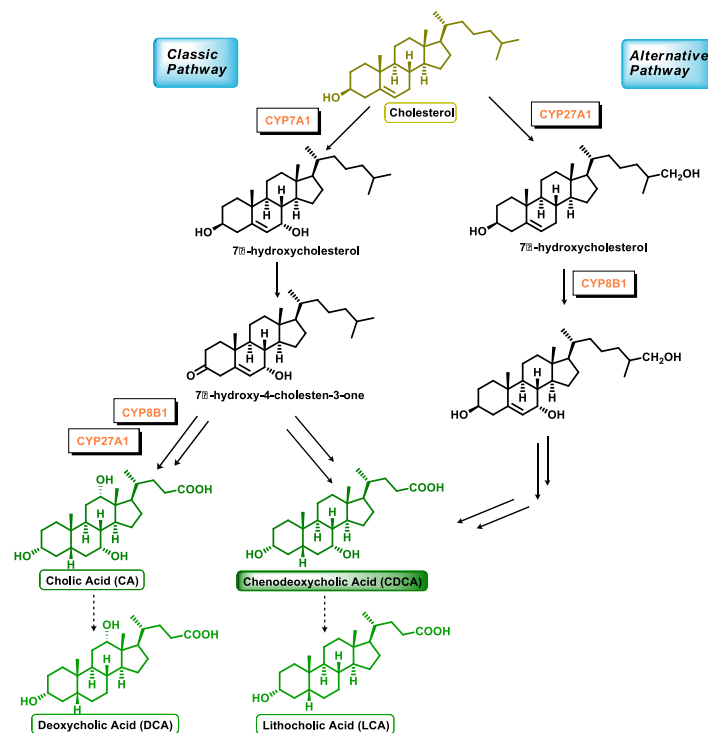


**Figure 2.** Bile acid synthesis

Classic pathway furnishes CA and CDCA in substantial equal amounts, whereas the acidic pathway affords mainly CDCA. After their synthesis, primary bile acids and their conjugates are secreted by liver into the small intestine, where are subjected to deamidation and 7 $\alpha$ -dehydroxylation reactions, by intestinal microbiota, to lead the formation of secondary bile acids, DCA and LCA. These latter are then absorbed by distal ileum, secreted by enterocytes in the portal



circulation and transported back to liver (enterohepatic cycling). The ileal absorption of bile acids is mediated by specific transporters, located at the luminal surface of enterocytes (ASTB), while their secretion in portal circulation is mediated by other specific transporters (OST $\alpha/\beta$ ). The aliquot of un-absorbed bile acids in the terminal ileum reaches the colon and is subjected to deconjugation by microbiota; then the colon can absorb the unconjugated bile acids passively.

### **FARNESOID-X-RECEPTOR (FXR)**

The farnesoid-X-receptor (FXR, NR1H4) belongs to nuclear receptors (NRs) super-family, and is highly expressed in enterohepatic tissues, kidney, adrenal gland, pancreas, reproductive tissues and in lower levels in adipose tissue (Figure 3). FXR presents the typical characteristics common to all hetero-dimeric metabolic NRs and binds to specific DNA responsive

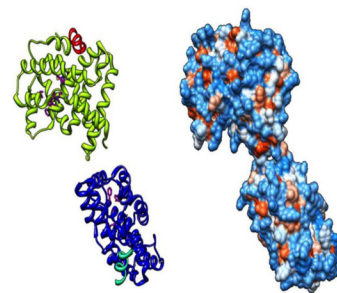


**Figure 3.** FXR 3D structure

elements (FXRE) in complex with the retinoic-X-receptor (RXR). After bile acid binding, a conformational change allows the release of co-repressors such as nuclear co-repressor (NCoR) and the recruitment of co-activators, such as steroid receptor coactivator-1 (Src-1) and others.<sup>7-9,11-13</sup> Thus, the FXR/RXR heterodimer, binds to specific response elements on the promoter of target genes, modulating the expression of enzymes/proteins involved in bile acid homeostasis (synthesis, transport, conjugation, and excretion).<sup>14,15</sup> In the hepatocytes, high intracellular bile acid levels result in the transcriptional activation of FXR. One FXR target gene is the small heterodimer partner (SHP), which is an atypical NR because it lacks a DNA-binding domain. SHP activation and dimerization results in a decrease of CYP7A1 expression/function and in the repression of bile acid synthesis. In addition, FXR ligands negatively regulate basolateral bile acid uptake by repression of the sodium taurocholate cotransporting polypeptide (NTCP) and organic anion transporter polypeptide-1 and 4 (OATP-1 and -4), and also promote BAs excretion by bile ducts, stimulating the expression of canalicular BSEP (bile salt export pump) and basolateral transporters (MRP3, MRP4 and OST $\alpha$  and  $\beta$ ). FXR activation increases the expression of genes encoding for proteins involved in bile acids detoxification (CYP3A4, UGT2Bs

and SULT2A1) and regulates lipoprotein metabolism. In addition, FXR controls lipid metabolism, such as apolipoprotein (apo) C-II, apo C-III, apo A-I, apo E, and phospholipids transfer protein expression. Moreover, FXR induces peroxisome proliferator-activated receptor- $\alpha$  expression, another nuclear receptor controlling triglyceride metabolism. Another important effect is the intestinal activation of FXR that increases the expression and the release of fibroblast growth factor FGF-19.<sup>13,16</sup> This factor binds the type 4 of FGF receptor (FGF-R4) and represses CYP7A1 in hepatocytes, with a subsequent reduction of bile acid synthesis. Additionally, FXR activation in the kidney induces the expression of proteins MRP2 (multidrug resistance-associated protein 2) and OST $\alpha/\beta$ , on the basolateral surface of renal tubular cells, increasing the potential detoxifying effect of this receptor. For its features, FXR is well known as the physiological sensor of bile acids and protects the liver against the toxic effects due to their accumulation. So the enterohepatic bile acids circulation, as well as the selective intestinal and liver FXR activation, are potential therapeutic targets and could be exploited to modulate bile acids homeostasis and lipid metabolism (Figure 4).<sup>10-12</sup>

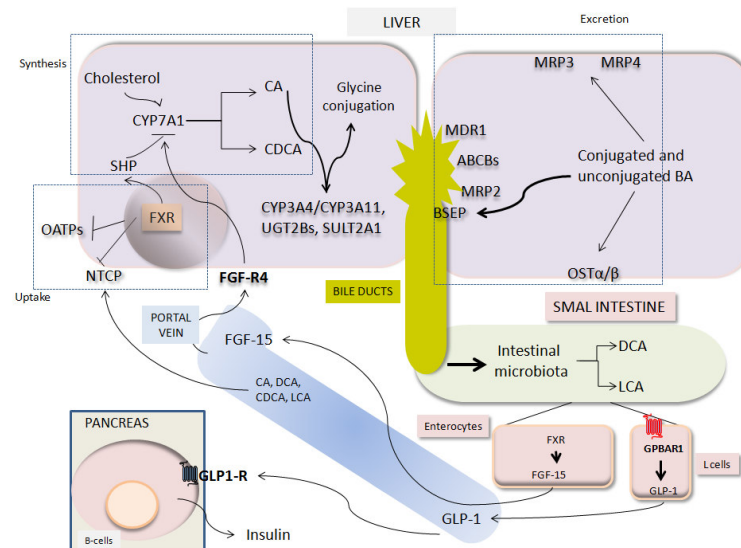


**Figure 4.** Bile acid homeostasis

Of interest, FXR is also involved in the control of glucose homeostasis. The activation of small heterodimer partner (SHP) by FXR decreases the expression of the phosphoenolpyruvate carboxykinase (PEPCK), which plays a key role in

gluconeogenesis, and of glucose 6-phosphatase, which regulates the glycogenolysis.

### **FXR: THERAPEUTIC APPLICATIONS**

FXR ligands have demonstrated beneficial effects in the treatment of several liver disorders, including various types of cholestasis and steatosis.<sup>17</sup> Cholestasis is an abnormal flow of BAs resulting from a functional defect of hepatocytes or from obstruction of intra and extra-hepatic bile ducts, caused by infections, drugs, tumor or genetic disorders. In presence of cholestasis, the elevated levels of bile acids lead to the activation of a complex machinery of coordinated mechanisms, which promote bile acids extrusion from the liver. The most common diseases, which induce cholestasis, are the primary biliary cirrhosis (PBC), the primary biliary cirrhosis-autoimmune hepatitis, the primary sclerosing cholangitis (PSC) and the intrahepatic cholestasis of pregnancy (ICP).<sup>18-21</sup> In addition, there are other rare autosomal recessive disorders, characterized by cholestasis, due to the mutations of genes encoding for hepatocellular transporters. Until now, FXR ligands have shown beneficial effects in the treatment of PBC. As already mentioned, FXR has also an important role in the regulation of glucose homeostasis, through regulation of gluconeogenesis and glycogenolysis in the liver and also of insulin sensitivity in striated muscle and adipose tissue, suggesting potential beneficial effects of FXR agonists in patients affected with type II diabetes, non-alcoholic fatty liver disease (NAFLD) and non-alcoholic steatohepatitis (NASH).<sup>22,23</sup> For all these aspects FXR represents a promising target for drug discovery.

### **FXR: LIGANDS FROM NATURE**

Several natural FXR ligands have been reported, so far. The first example was guggulsterone (GS), which is a vegetable steroid found in the resin of the guggul plant, *Commiphora mukul*,<sup>24-27</sup> a traditional medicinal herb intensively used in Ayurvedic medicine for the treatment of obesity and lipid disorders. A preliminary pharmacological test suggested that guggulsterone could be a FXR antagonist, but successively a deep characterization demonstrated that it is a

partial FXR agonist.<sup>27-30</sup> However, its promiscuity in agonizing different NRs reduced the possibility to be considered a lead to treat metabolic disorders. Starting from the identification of guggulsterone, natural steroid molecules, largely distributed in vegetal and marine worlds, have been affirmed as promising candidates in FXR modulation. A great contribution is derived from high-throughput screening, but also from target-oriented discovery of herbal medicines, affording to the identification of several new FXR ligands. Selected examples are sesquiterpenes and triterpenes from *Alisma orientalis*,<sup>31</sup> widely cultivated in Taiwan, China, and Japan and from *Schisandra glaucescens* Diels (Schisandraceae),<sup>32</sup> whose extracts are used in the treatment of several pathologies, as hyperglycemia and hyperlipidemia.

Stigmasterol acetate (StigAc), a water-soluble semisynthetic derivative of soy, resulted a dose dependent FXR antagonist, suppressing mediated expression of FXR target genes.<sup>33</sup> Also marine ecosystem has been recently demonstrated a promising source of FXR ligands.<sup>34</sup> For example, the family of 4-methylene steroids, isolated from the sponges belonging to *Theonella* species,<sup>35-38</sup> represents a novel class of NRs modulators with peculiar pharmacological profiles, ranging from selective FXR antagonists to dual PXR/FXR modulators. Among these compounds, theonellasterol represents the first example of natural full FXR antagonist identified. In proof of concept study, this compound was tested *in vivo* in a model of obstructive cholestasis,<sup>39</sup> providing the first evidence that FXR antagonism has a potential in the treatment of this type of disease.

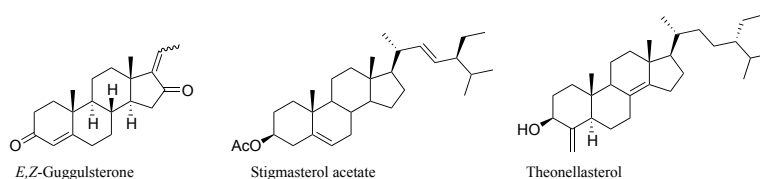


**Figure 5.** Natural FXR ligands

## FXR: STEROIDAL AND NON STEROIDAL AGONISTS

### Steroidal agonists

After FXR de-orphanization by BAs, large medicinal chemistry protocols have been performed on their scaffold. Manipulation on CDCA, which represents the

most potent endogenous FXR agonist, with an  $EC_{50}$  in a range of 4.5-10  $\mu\text{M}$ , with the aim to improve potency, efficacy and metabolic stability, afforded several compounds with promising pharmacological profiles. In detail, the introduction of an ethyl group at C-6 on the CDCA ring B, produced 6-ECDC/OCA (obeticholic acid or INT-747), a potent FXR agonist.<sup>40</sup> OCA has been widely tested *in vitro* and *in vivo*.<sup>41-45</sup> In a phase III clinical trial in patients with non-alcoholic steatohepatitis (NASH), OCA improved several features of NASH,<sup>46</sup> including inflammation and fibrosis. However, in 23% of patients appeared an increase of cholestatic itching with a simultaneous increase of total cholesterol, LDL, and a modest decrease in HDL. Itching was also present in PBC patients and this effect was unsustainable enough to induce drug discontinuation in 40% of patients.<sup>47</sup> Indeed OCA is also a GPBAR1 agonist and this receptor has been recently identified as the physiological mediator of itching in mice.<sup>48-51</sup>

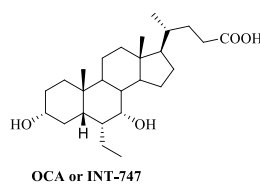


**Figure 6.** Chemical structure of OCA (or INT-747)

### Non steroidal FXR agonists

The most investigated non-steroidal FXR ligand is GW4064 (Figure 7) endowed with a potency of 70 nM and an efficacy of 140% respect the CDCA. Since 2000, an high number of modifications have been performed around this scaffold, with the aim to improve its limited intestinal absorption (<10%) and to reduce its intrinsic photo-instability due to the presence of the widely delocalized  $\pi$ -electron system in the stilbene moiety, that is associated with a potential cell toxicity.

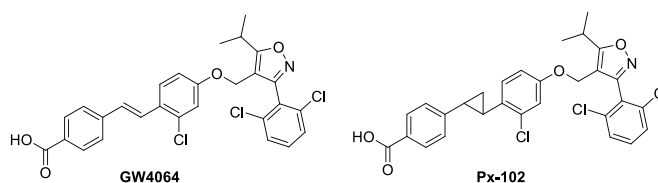


**Figure 7.** GW4064 and Px-102

Thus, several research groups, ranging from academy to industry, have harnessed the chemical space around the stilbene moiety, the position of the carboxyl group on the terminal aryl unit, the nature of classical linker, while the central isoxazole core, the isopropyl group at C-5 and the 2,6-dihalogen substituted phenyl at C-3, have been conserved.<sup>52,53</sup> As depicted in Figure 7, a potent close derivative of GW4064 is the non steroidal FXR agonist PX20606 (Px-102), which was synthesized by Phenex Pharmaceuticals. Currently Px-102 is in a Phase II study in patients with Metabolic Syndrome and Non-Alcoholic Fatty Liver Disease (NAFLD).

### **G-PROTEIN COUPLED RECEPTOR 1 (GPBAR1)**

GPBAR1 (or TGR5, MBAR1) is a member of rhodopsin-like superfamily of G protein coupled receptor (GPCR), mainly expressed in the small intestine,<sup>11,12</sup> in plasma membrane of liver, adipose tissue, colon, skeletal muscle cells, macrophages/monocytes and it is activated by secondary bile acids, lithocholic acid (LCA) and its tauro conjugated form (TLCA). This receptor is coupled to a Gs protein and the binding of a ligand leads to the activation of the adenylate cyclase with a subsequent increase of intracellular concentration of cAMP; then the activation of a protein kinase A (PKA) induces a cascade of events with the activation of different cellular pathways. In fact, after its activation by secondary bile acids, GPBAR1 regulates multiple metabolic functions and increases energy expenditure. In intestinal L-cells, GPBAR1 stimulates the secretion of glucagon-like peptide 1 (GLP-1), a hormone that induces insulin secretion, controls the gastrointestinal transit and suppresses appetite. The GLP-1 release from STC-1 cells, is linked to an increase of intracellular ATP levels, the closure of ATP-dependent potassium channels ( $K_{ATP}$ ) and consequent calcium influx.<sup>54</sup> In the gastrointestinal tract, GPBAR1 plays a key role also in regulating colonic motility and defecation.<sup>55,56</sup> In fact, it is expressed in the inhibitory motor neurons of the myenteric plexus<sup>56</sup> of the large intestine, in which is also present the nitric oxide synthase (NOS). Linked to this co-presence, the activation of GPBAR1 by DCA, a secondary bile acid, induces a phasic contraction of isolated segments of longitudinal muscle induced by a neurogenic and nitrenergic mechanism. Moreover,

the luminal administration of DCA also induces a delay in gastric emptying and small intestinal transit in rodents.<sup>56</sup> GPBAR1 is also co-present with 5-hydroxytryptamine (5-HT) in mouse colon entero-chromaffin cells, and calcitonin gene-related peptide (CGRP) in intrinsic primary afferent neurons.<sup>56,57</sup> In fact, the results of an *in vitro* mucosal application of DCA and LCA (<100  $\mu$ M), to a preparation of mouse colon, showed a response that could be interpreted as the equivalent of *in vivo* peristalsis. Differently, GPBAR1 suppression inhibits this effect and the antagonism of 5-HT<sub>4</sub> and CGRP receptors, blocks GPBAR1-induced peristalsis. These results confirm that GPBAR1 is the mediator of prokinetic actions of bile acids in the colon and that the presence of this receptor is fundamental for the normal defecation process. In fact, genetic defects in GPBAR1, alter intestinal transit in patients with a functional intestine unbalance (for example irritable bowel syndrome).<sup>58</sup> In addition, GPBAR1 presents immunity functions<sup>59</sup> and is highly expressed in macrophages, where its activation reduces macrophage-effector functions activated by pro-inflammatory events, through the negative regulation of NF- $\kappa$ B (nuclear factor kappa-light-chain-enhancer of activated B cells). In animal models of liver inflammation, GPBAR1 activation by 23(S)-methyl-CDCA, a selective semi-synthetic bile acid ligand, attenuates the NF- $\kappa$ B activation through the reduction of I $\kappa$ B $\alpha$  phosphorylation, which inhibits NF- $\kappa$ B translocation into nucleus. In rodent models of colitis, GPBAR1 expression is increased in inflamed tissues, and its absence is correlated with an increased susceptibility to develop colitis and a highest intestinal permeability.<sup>60</sup> Furthermore, GPBAR1 expression in hepatic macrophages (or Kupffer cells), which stimulates the release of pro-inflammatory cytokine, exerts an important role in the development and progression of NAFLD (Non-Alcoholic Fat Liver Disease). For this, GPBAR1 plays an important protective function against steatosis. Therefore, GPBAR1 activation could exert benefic effects in the treatment of atherosclerosis, steatosis, obesity, hyperglycemia, all disorders in partnership to the metabolic syndrome. Moreover, GPBAR1 has been recently demonstrated essential component of the intestinal mucosal barrier and would seem to exert a protective effect against gastrointestinal injury caused by non steroidal anti-inflammatory drugs (FANS).<sup>59</sup> Finally, GPBAR1 activation increases the energy expenditure in the adipose tissue, thereby preventing

obesity.<sup>61</sup> This effect is mediated by the activation of iodothyronine deiodinase enzyme (D2),<sup>62</sup> which stimulates the thermogenesis mediated by thyroid hormones, locally. D<sub>2</sub> hormone, in fact, increases the oxidative mitochondrial phosphorylation in brown adipose tissue, as well as in muscles, through the induction of T4 hormone conversion in the corresponding form activated of T3, which interacts with the receptor inducing an increase of energy expenditure (Figure 8).

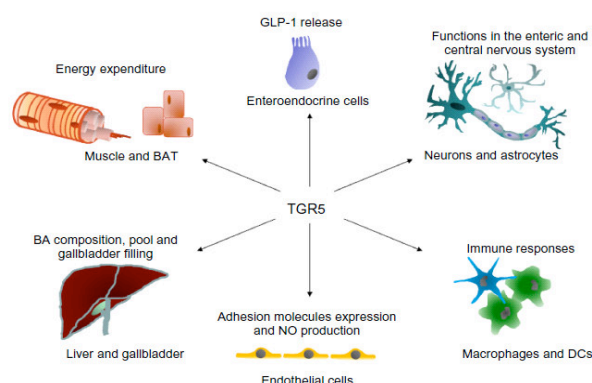


**Figure 8.** GPBAR1 localization and specific tissue functions

In the same way of FXR, GPBAR1 is a negative modulator of bile acids synthesis and re-uptake in biliary tract. In addition, it reduces the accumulation of fats in liver, the blood levels of triglycerides not esterified, and shifts blood cholesterol levels to associations LDL type. Collectively, these findings have prompted the development of dual GPBAR1/FXR agonists as a new frontier in the pharmacological treatment of hypercholesterolemia, hypertriglyceridemia, and diabetes mellitus type 2. However, the concomitant activation of both receptors endorses with potential side effects, and therefore, the discovery of highly selective FXR or GPBAR1 agonists is therapeutically attractive for a large cluster of human diseases. Consequently, my research activity was mainly focused on the design, synthesis and thorough pharmacological investigation of selective agonists generated on bile acid scaffolds.

## MODEL OF GPBAR1

Rational drug design represents an efficient approach in developing novel receptor-agonists. However, as the design of new compounds depends on the availability of structural information of molecular targets, there is a strong



limitation caused from the absence of the tridimensional structure for GPBAR1. Despite this, the large amount of experimental information available on GPCRs and the high number of structures identified in this class of proteins, allowed to transcend this limitation, using known structures as template to project a tridimensional model for this receptor. In particular, multiple sequences of different GPCRs, such as  $\alpha$  and  $\beta$  adrenergic proteins, opioids or adenosine receptor, have been used in order to identify the more conserved regions and the adenosine A<sub>2A</sub>R-GL31 receptor was identified as possible template for the highest sequence identity values (~19%) with GPBAR1. The alignment between the GPBAR1 model and this template was developed considering the sequence homology of extracellular region, where the ligand is bound. In addition, the formation of disulfide bond between the extracellular loop II and the transmembrane helix III (TM3), due to the presence of well-conserved cysteine residues in GPCRs family, induces rigidity in this region, contributing to the design of the ligand-binding site. In fact, as referred in literature<sup>63</sup> this disulfide bond is fundamental to predict the correct GPBAR1 structure. At the end, using Modeler v. 9.11 GPBAR1 tridimensional structure has been built. The receptor was also incorporated in a double phospholipid bilayer (1-palmitoyl-2-oleoyl-*sn*-glycero-3-phosphocholine or POPC), surrounded from water, in order to simulate the extra-membrane environment and finally molecular dynamic (MD) calculations have been performed. The whole system, especially the transmembrane helices, was very stable during the stimulation (90 ms), with a major flexibility observed for the extracellular and the intracellular loops (Figure 9).

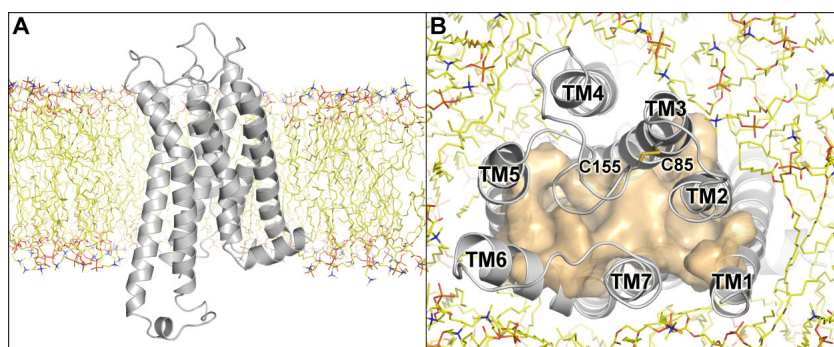


**Figure 9.** Lateral view (A) and superior (B) of GPBAR1 receptor tridimensional model

## CHAPTER 1 CHENOCHOLANE AND URSOCHOLANE DERIVATIVES

The activity of bile acids towards their receptorial counterparts is structure-dependent, with chenodeoxycholic acid (CDCA) and taurolithocholic acid (TLCA), which are the most potent endogenous activators of FXR and GPBAR1 (Figure 10), respectively.<sup>9,49,64</sup> Although FXR activation could be an appealing approach to treat enterohepatic diseases,<sup>65</sup> in this context, the therapeutic use of endogenous bile acids, with the exception of ursodeoxycholic acid (UDCA), is limited by their toxicity and promiscuity in activating different endogenous receptors, such as the G-protein-coupled receptor 1 or GPBAR1. Administration of 6-ECDCA in PBC patients caused itching in approx. 50-60% that was severe enough to cause drug discontinuation in 40% of patients. Indeed, 6-ECDCA is also a ligand for GPBAR1 and therefore the above side effect might be associated to the activation of the membrane bile acid receptor, which is recently demonstrated *bona fide* to be the physiological mediator of itching in mice.<sup>48,49</sup> Thus, the obtainment of selective FXR ligands, without any GPBAR1 effects, represents a new avenue in the treatment of hepatic disorders such as PBC. Differently, GPBAR1 activation could represent a new opportunity in the treatment of metabolic disorders, such as non-alcoholic steatohepatitis (NASH) or type 2 diabetes.

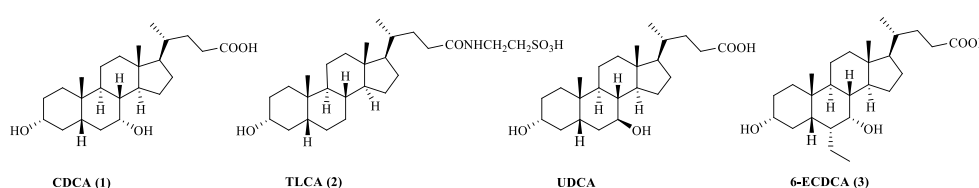


**Figure 10.** Endogenous bile acids and 6-ECDCA

Therefore, selective GPBAR1 ligands could have utility in the treatment of metabolic disorders, in which the increased release of GLP-1 hormone, with a consequent anti-diabetes effect and the regulation of glucose and lipids blood levels, represent an efficacy strategy. In this chapter, the synthesis of a large family of selective FXR and GPBAR1 ligands, starting from the UDCA and CDCA scaffolds, is described. UDCA represents the only endogenous bile acid used in the therapy of cholestasis, with a total safety also when administered in

high doses. However, its mechanism of action is unknown and even though it presents a similar chemical structure to the CDCA, the different configuration of the hydroxyl group at C7 of ring B ( $\beta$  in UDCA,  $\alpha$  in CDCA) with a consequent different spatial disposition, reduces the affinity towards FXR (Figure 11).

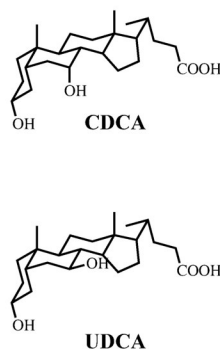


**Figure 11.** Chair conformations of UDCA and CDCA

UDCA and CDCA scaffolds were subjected to intense medicinal chemistry protocols, obtaining a library of derivatives with different pharmacological profiles, ranging from selective modulators to dual modulators towards FXR and GPBAR1.

The main modifications have been focused on:

- ✓ The tetracyclic core, including stereochemistry of ring junctions;
- ✓ The length and functionalization of the side chain.

Modifications on steroid nucleus afforded compounds **4-18**, some of which are deprived of the  $3\alpha$ -OH group on ring A, essential for GPBAR1 activation, and others are completely deoxygenated on the tetracyclic nuclei, whereas compounds **19-24** are inverted at C-3 of ring A (Figure 12). In order to evaluate the influence of a neutral or negative charge in the interaction within two targets, chemical modification has been extended to the side chain, inducing diverse end-groups, such as sulfate, carboxyl or alcoholic functions. All compounds have been structurally characterized by NMR and high-resolution ESI-MS analysis.

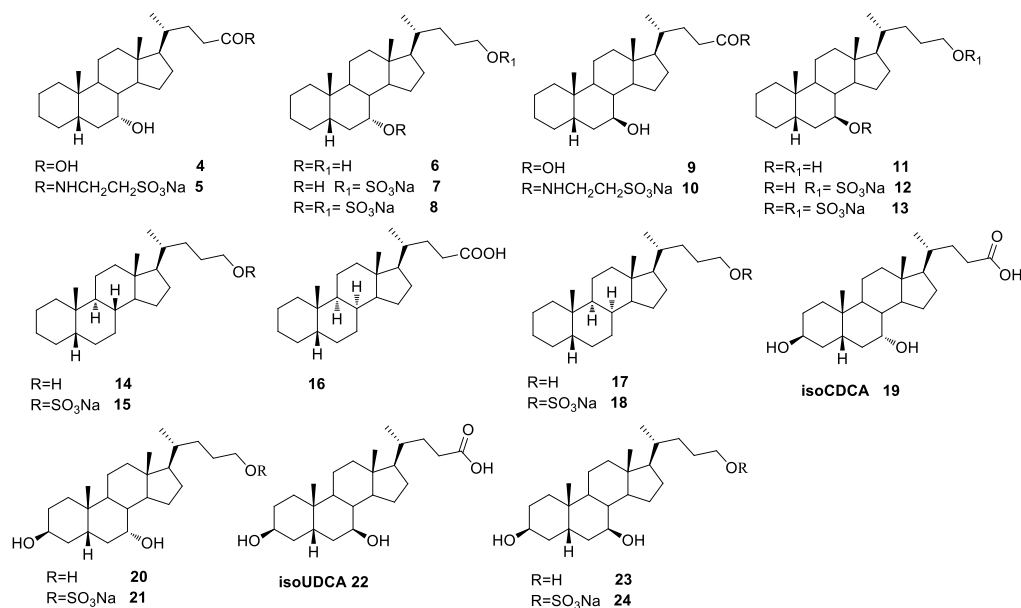


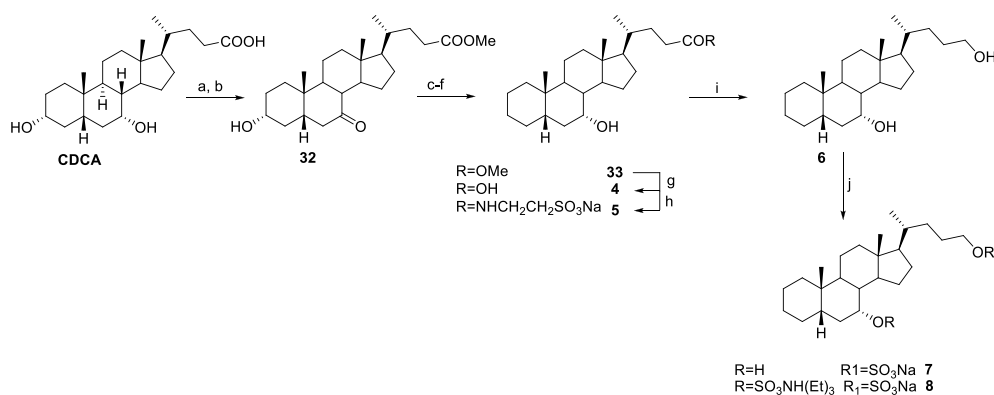
**Figure 12.** Semisynthetic bile acid derivatives generated starting from CDCA and UDCA scaffolds

In particular, we looked for the main chemical modifications, which were the elimination and the inversion of configuration of hydroxyl group in position 3, in the protons spectrum. The occurred elimination was confirmed by the lack of a characteristic signal at  $\delta$  3.35 in the proton spectra of chenodeoxycholic acid scaffold and the only appearance of a singlet at  $\delta$  3.79 corresponding to the proton in  $\beta$ -configuration on C-7 in compounds **4-8** and of another signal at  $\delta$  3.46, as multiplet, corresponding to the proton in  $\alpha$ -configuration on C-7 in compounds **9-13**. The absence of characteristic signals of UDCA scaffold corresponding to protons on C-3 and C-7, in compounds **14-18**, confirmed instead the occurred double elimination. The inverted configuration of hydroxyl group at C-3, was established by the value and the shape of the signal corresponding to the carbinol proton at C-3. In fact, in compounds **19-24**, H-3 resonated around 4 ppm, down-field shifted respect to the value for the above proton in CDCA and in UDCA (3.35 ppm) as singlet, thus demonstrating its equatorial disposition.

Comprehensive pharmacological evaluation allowed the identification of promising lead compounds in several human diseases.

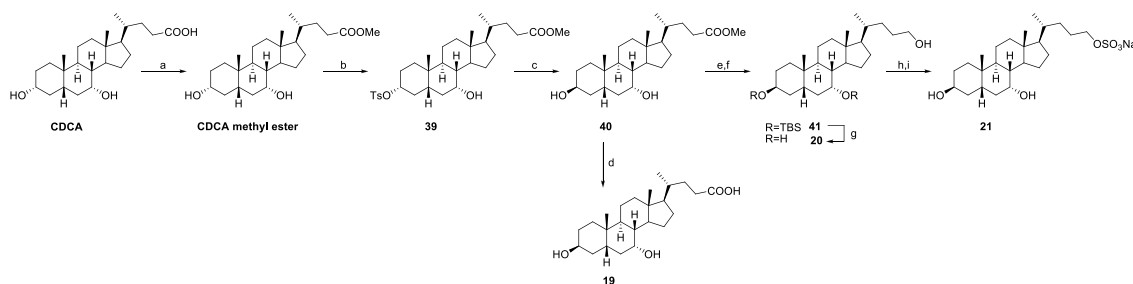
## 1.1 PREPARATION OF CHENOCHOLANE DERIVATIVES

## 1.1.1 Modification on CDCA: Synthesis of 3-deoxychenocholane derivatives



**Scheme 1. 3-Deoxychenocholane derivatives.** a) NaBr, TBABr, NaClO 10%, MeOH:CH<sub>3</sub>COOH: H<sub>2</sub>O:AcOEt 3:1:0.25:6.5; b) *p*-TsOH, MeOH dry, quantitative yield over two steps; c) *p*-TsCl, pyridine; d) LiBr, Li<sub>2</sub>CO<sub>3</sub>, DMF dry, reflux; e) H<sub>2</sub> (1 atm), Pd/C, THF/MeOH 1:1; f) NaBH<sub>4</sub>, THF/H<sub>2</sub>O 4:1 v/v, quantitative yield over four steps; g) NaOH 5% in MeOH/H<sub>2</sub>O 1:1 v/v, quantitative yield; h) DMT-MM, Et<sub>3</sub>N, taurine, DMF dry, 35%; i) LiBH<sub>4</sub>, MeOH dry, THF, 0 °C, 79%; j) Et<sub>3</sub>N·SO<sub>3</sub>, DMF dry, 80 °C.

The synthetic protocol started with CDCA that was subjected to regioselective oxidation with NaClO 10%, NaBr and TBABr, as transfer catalyst of phase, followed by Fischer esterification with *p*-toluenesulfonic acid in MeOH dry, furnishing methyl ester **32**, in quantitative yield.<sup>48</sup> Then tosylation with tosyl chloride and pyridine dry, followed by elimination of tosyl group with Li<sub>2</sub>CO<sub>3</sub> and LiBr and double bond hydrogenation with consequent NaBH<sub>4</sub> reduction at C-7, gave methyl 3-deoxycholanoate **33**, in quantitative chemical yield over four steps (Scheme 1). Alkaline hydrolysis with NaOH 5% in MeOH/H<sub>2</sub>O 1:1 afforded 3-deoxycholanoic acid (**4**) in quantitative chemical yield, which was subjected, in a small aliquot, to amidation with taurine.<sup>66</sup> Purification on RP-18 column, followed by HPLC, gave compound **5** in pure form as sodium salt. Another aliquot of methyl ester **33** was reduced with LiBH<sub>4</sub>, in THF/MeOH dry, at the corresponding C-24 alcohol **6**, which after HPLC purification on a small aliquot, was in turn subjected to sulfation (Et<sub>3</sub>N·SO<sub>3</sub> 1.5 eq. in DMF dry) producing a mixture of compounds **8** and **7**, efficiently separated, as pure sodium salts, by HPLC.

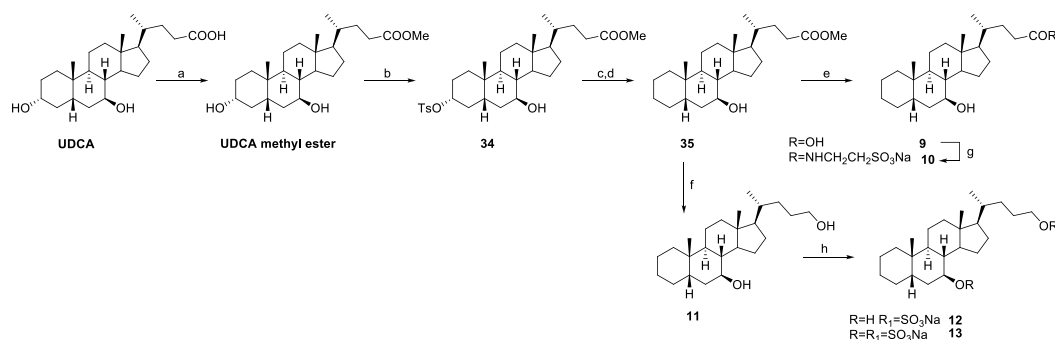
1.1.2 Modification on CDCA: Synthesis of 3 $\beta$ -chenodeoxycholate derivatives

**Scheme 2. 3 $\beta$ -Chenodeoxycholate derivatives.** a) *p*-TsOH, MeOH dry, quantitative yield; b) *p*-TsCl, pyridine, quantitative yield; c) CH<sub>3</sub>COOK, DMF: H<sub>2</sub>O 5:1, reflux, 75%; d) NaOH 5% in MeOH/H<sub>2</sub>O 1:1 v/v, 89%; e) 2,6-lutidine, *t*-butyldimethylsilyl trifluoromethanesulfonate, CH<sub>2</sub>Cl<sub>2</sub>, 0 °C; f) LiBH<sub>4</sub>, MeOH dry, THF dry, 0 °C, 84% over two steps; g) HCl 37%, MeOH, 96%; h) Et<sub>3</sub>N·SO<sub>3</sub>, DMF dry, 80 °C; i) HCl 37%, MeOH, 76% over two steps.

Regioselective tosylation at C-3 (*p*-tosyl chloride in pyridine dry) on CDCA methyl ester furnished intermediate **39**. The preferential tosylation at C-3 results from the major reactivity of equatorial hydroxyl group at C-3 respect to the axial OH at C-7, with the 3 $\alpha$ -OH group pointing in a chemical space free from steric interactions. Treatment of compound **39** with potassium acetate in DMF/H<sub>2</sub>O (Scheme 2), afforded the 3 $\beta$ -hydroxy derivative **40** in 75% yield. Alkaline hydrolysis with NaOH 5% in MeOH/H<sub>2</sub>O 1:1 at C-24 methyl ester and subsequent HPLC purification, gave pure isoCDCA (**19**), in 89% yield. Further, an aliquot of **40** was first protected at C-3 and C-7 hydroxyl groups with *t*-butyldimethylsilyl trifluoromethanesulfonate and 2,6-lutidine in CH<sub>2</sub>Cl<sub>2</sub> dry and then reduced with LiBH<sub>4</sub> in THF/MeOH dry furnishing the protected alcohol **41**. De-protection on compound **41** with HCl 37% (2-3 drops) in MeOH and HPLC purification, afforded isoCDCOH (**20**) in quantitative yield. Finally, a small aliquot of **41** was sulphated and after de-protection and HPLC purification, monosulfate derivative **21** was obtained in 76% yield over two steps.

## 1.2 PREPARATION OF URSOCHOLANE DERIVATIVES

### 1.2.1 Modification on UDCA: Synthesis of 3-deoxyursocholane derivatives

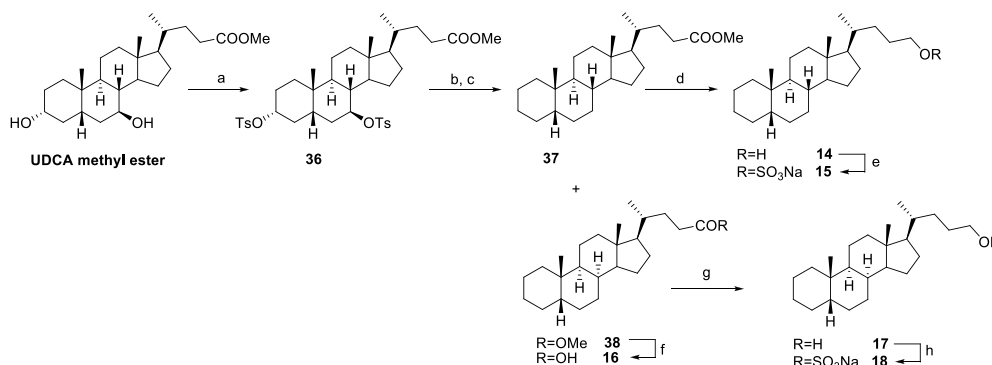


**Scheme 3. 3-Deoxyursocholane derivatives.** a) *p*-TsOH, MeOH dry, quantitative yield; b) *p*-TsCl, pyridine, 58%; c) LiBr, Li<sub>2</sub>CO<sub>3</sub>, DMF dry, reflux, quantitative yield; d) H<sub>2</sub> (1 atm), Pd/C, THF/MeOH dry 1:1, 78%; e) NaOH 5% in MeOH/H<sub>2</sub>O 1:1 v/v, quantitative yield; g) DMT-MM, Et<sub>3</sub>N, taurine, DMF dry, 27%; f) LiBH<sub>4</sub>, MeOH dry, THF dry, 0 °C, 91%; h) Et<sub>3</sub>N·SO<sub>3</sub>, DMF dry, 80 °C.

For the synthesis of 3-deoxyursocholane derivatives (compounds **9-13**, Scheme 3), we performed the same reactions previously described in the Scheme 1 for the preparation of corresponding 3-deoxychenocholane derivatives.

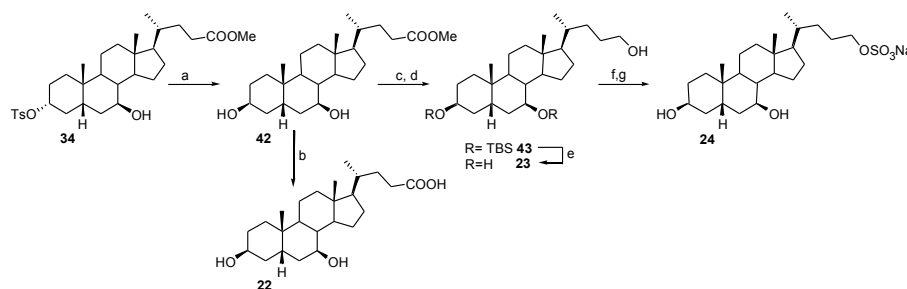
### 1.2.2 Modification on UDCA: Synthesis of 5β-cholane derivatives

UDCA methyl ester was di-tosylated at C-3 and C-6 hydroxyl groups, producing intermediate **36** that was subjected to LiBr/Li<sub>2</sub>CO<sub>3</sub> treatment to obtain the double elimination on ring A and B (Scheme 4). Catalytic hydrogenation (H<sub>2</sub>, Pd/C in THF/MeOH dry) on the crude product, furnished a mixture of the saturated methyl esters **37** and **38**, epimers at C-8. Treatment of methyl ester **37** with LiBH<sub>4</sub> and then with Et<sub>3</sub>N·SO<sub>3</sub>, furnished alcohol **14** and its corresponding sulfated **15**, in 84% and 23% yield, respectively. Alkaline hydrolysis on methyl ester **38** with NaOH 5% in MeOH/H<sub>2</sub>O 1:1, produced carboxylic acid derivative **16** in 78% yield. At last, an aliquot of methyl ester **38** was treated with LiBH<sub>4</sub> and then with Et<sub>3</sub>N·SO<sub>3</sub>, affording alcohol **17** in 78% yield and the corresponding sulfate derivative **18**, in 43% yield.



**Scheme 4. 5β-Cholane derivatives.** a) *p*-TsCl, pyridine, quantitative yield; b) LiBr, Li<sub>2</sub>CO<sub>3</sub>, DMF dry, reflux, quantitative yield; c) H<sub>2</sub> (1 atm), Pd/C, THF/MeOH dry 1:1; d) LiBH<sub>4</sub>, MeOH dry, THF dry, 0 °C, 84%; e) Et<sub>3</sub>N·SO<sub>3</sub>, DMF dry, 80 °C, 23%; f) NaOH 5% in MeOH/H<sub>2</sub>O 1:1 v/v, 78%; g) LiBH<sub>4</sub>, MeOH dry, THF dry, 0 °C, 78%; h) Et<sub>3</sub>N·SO<sub>3</sub>, DMF dry, 80 °C, 43%.

### 1.2.3 Modification on UDCA: Synthesis of 3β-ursodeoxycholane derivatives



**Scheme 5. 3β-Ursodeoxycholane derivatives.** a) CH<sub>3</sub>COOK, DMF: H<sub>2</sub>O 5:1, reflux, 82%; b) NaOH 5% in MeOH/H<sub>2</sub>O 1:1 v/v, 87%; c) 2,6-lutidine, *t*-butyldimethylsilyl trifluoromethanesulfonate, CH<sub>2</sub>Cl<sub>2</sub>, 0 °C; d) LiBH<sub>4</sub>, MeOH dry, THF dry, 0 °C, 94% over two steps; e) HCl 37%, MeOH, 96%; f) Et<sub>3</sub>N·SO<sub>3</sub>, DMF dry, 80 °C; g) HCl 37%, MeOH, 67% over two steps.

The 3β-ursodeoxycholane derivatives **22-24** (Scheme 5) were obtained following the same synthetic protocol illustrated in Scheme 2 for the corresponding chenodeoxycholane derivatives.

## 1.3 PHARMACOLOGICAL EVALUATION

Pharmacological assays were performed by Prof. Fiorucci's group at University of Perugia. In vitro transactivation assays have been executed on HepG2 and HEK-293T cells, transfected with the responsive elements for FXR and GPBAR1, respectively (Figures 13 and 14). As illustrated in Figure 13, the elimination of the hydroxyl group at C-3 on CDCA scaffold furnished potent and selective FXR agonists. In detail, with the exception of the 7, 24-disulfate derivative (**8**), all 3-



deoxychenocholane derivatives were able to transactivate FXR independently from the functional end-group at C-24 (COOH in **4**, CH<sub>2</sub>OH in **6** and CH<sub>2</sub>OSO<sub>3</sub><sup>-</sup> in **7**).

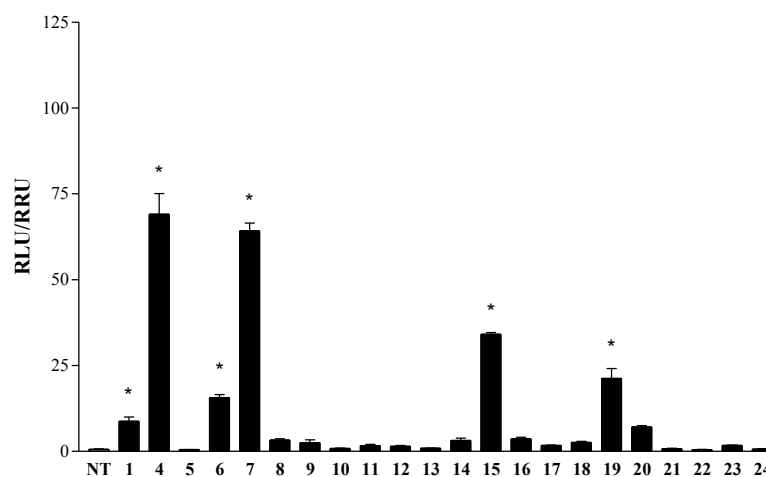


**Figure 13. Transactivation assays on FXR.** HepG2 cells were transfected with pSG5-FXR, pSG5-RXR, pCMV-βgal, and p(hsp27)TKLUC vectors. Cells were stimulated with compounds **4-24** (10 μM). CDCA (**1**, 10 μM) was used as a positive control. Results are expressed as mean ± standard error; \*p < 0.05 versus not treated cells (NT).

Differently, the tauro-conjugation of the carboxyl group on the side chain (compound **5**) completely abolishes the activity on FXR. Of interest, the substitution of carboxyl end-group with a not conjugable functional group, such as a sulfate, produced derivative **7**, with almost the same potency of **4** on FXR and without any GPBAR1 activity (Figure 14). On contrary, the corresponding urso-derivatives **9-13**, all sharing the β-configuration of the hydroxyl group at C-7, were inactive towards FXR, demonstrating that the configuration at C-7 is a key structural feature for FXR interaction. Moreover, even though the sulfate **15** showed a potency of action comparable to the CDCA, the most potent endogenous FXR ligand, the results of transactivation for compounds **14-18**, demonstrated that the deletion of both hydroxyl groups, in particular at C-7, is detrimental for FXR activation (for examples compound **14** respect **6**, and compound **15** respect **7**). Modifications on B/C ring junction produced derivatives **16-18**, deprived of any activity on FXR, thus confirming the importance of bile acids shape in the interaction with FXR-LBD. Of interest are also the results of inverted configuration in position C-3. As shown in Figure 13, isochenodeoxycholic acid (isoCDCA, **19**) was more potent than its precursor CDCA, in activating FXR. Considering the well-known bile acids epimerization

at C-3 that occurs in the intestine by bacterial enzymes, the result of isoCDCA transactivation opens the way to other pharmacological investigations of this compound as FXR modulator.

Transactivation on CREB-responsive elements in HEK-293T cells, transiently transfected with the membrane bile acid receptor GPBAR1 and with a reporter gene containing a cAMP responsive element (Figure 14), showed that the elimination (at C-3 or both positions) or epimerization (at C-3) of hydroxyl groups on the tetracyclic scaffold is detrimental in term of GPBAR1 activity.

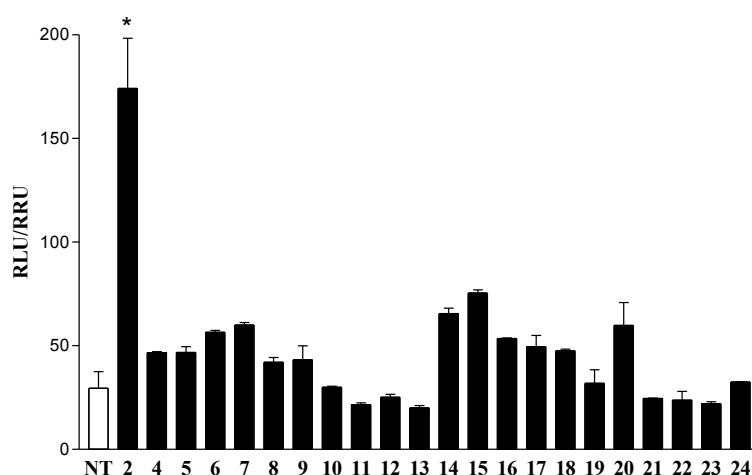


**Figure 14. Transactivation assays on GPBAR1.** HEK-293T cells were co-transfected with GPBAR1 and a reporter gene containing a cAMP responsive element in front of the luciferase gene. Twenty-four hour post transfection cells were stimulated with **4-24** (10  $\mu$ M). Luciferase activity served as a measure of the rise in intracellular cAMP following activation of GPBAR1. TLCA (**2**, 10  $\mu$ M) was used as a positive control. Results are expressed as mean  $\pm$  standard error. \* $p < 0.05$  versus not treated cells (NT).

### 1.3.1 Pharmacological evaluation on 7 $\alpha$ -hydroxy-5 $\beta$ -cholan-24-sulfate (**7**)

In the whole series, compound 7 $\alpha$ -hydroxy-5 $\beta$ -cholan-24-sulfate (**7**), a potent and selective FXR agonist, represents a promising building block to produce selective bile acid receptor modulators. HepG2 and HEK-293T cells were stimulated with increasing concentrations of compound **7** (range from 100 nM to 50  $\mu$ M). As illustrated in Figure 15, panel A, compound **7** was able to transactivate FXR in a dose-dependent manner with an EC<sub>50</sub> of 9  $\mu$ M. Differently, results of GPBAR1 transactivation showed that **7** failed to transactivate GPBAR1 at any concentration tested (Figure 15, panel B). Further, the effect on compound **7** was evaluated on common off-targets, including GR, PPAR $\gamma$ , LXR and PXR.

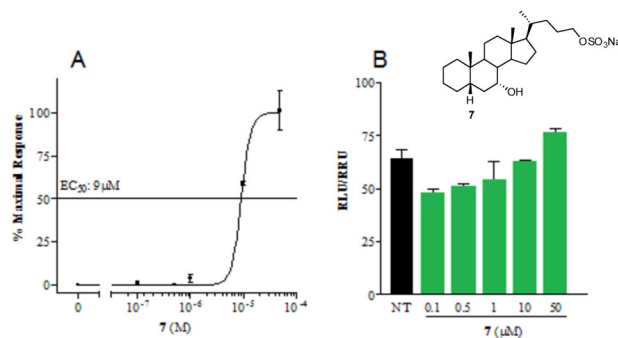


**Figure 15. Concentration-response curve of 7 on FXR (Panel A) and GPBAR1 (Panel B).** FXR transactivation was measured in a luciferase reporter assay using HepG2 cells transfected with FXR. GPBAR1 activity was measured in HEK-293T cells co-transfected with GPBAR1 and a reporter gene containing a cAMP responsive element in front of the luciferase gene (CRE). Twenty-four hour post transfection cells were stimulated with increasing concentrations of the agent: range from 100 nM to 50 μM. Results are expressed as mean ± standard error. \* $p < 0.05$  versus not treated cells (NT).

As shown in Figure 16, panels A-C, this compound failed to transactivate GR, PPAR $\gamma$  and LXR at the concentration of 10 μM. Differently, it was able to transactivate the nuclear receptor PXR at the same concentration (Figure 16 D).

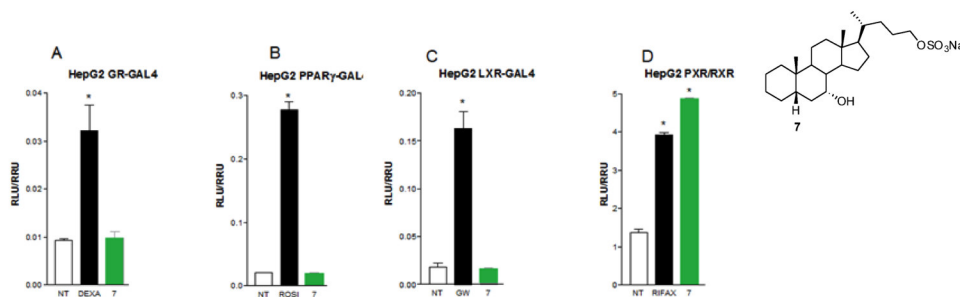


**Figure 16. Specificity of 7 on other nuclear receptors.** (A) (B) and (C) HepG2 cells were co-transfected with the Gal4 luciferase reporter vector and with a series of chimeras in which the Gal4 DNA binding domain is fused to the LBD of the indicated nuclear receptors. Cells were treated 18 h with the specific agonists (10 μM) or with 7 (10 μM). (D) HepG2 cells were co-transfected with pSG5-PXR, pSG5-RXR and with the reporter pCYP3A4 promoter-TKLuc and then stimulated with rifaximin (10 μM), a PXR agonist, or with 7 (10 μM). Data are the mean ± S.E. of three experiments. \* $p < 0.05$  versus not treated cells (NT). DEXA: Dexamethasone; ROSI: Rosiglitazone; GW: GW3965; RIFAX: Rifaximin.

With the purpose to deepen the effects of compound 7, was also evaluated its ability to regulate the canonical functions exerted by FXR and GPBAR1. As shown in Figure 17, panels A and B, compound 7 was evaluated in regulating the expression of FXR and GPBAR1 targeted genes. In detail, RT-PCR analysis revealed that it was not able to induce the expression of pro-glucagon mRNA (GLP-1) in GLUTAg cells,<sup>67</sup> as well as cAMP expression in THP-1 cells, two

well known GPBAR1 targeted genes, thus confirming its inactivity towards this receptor.

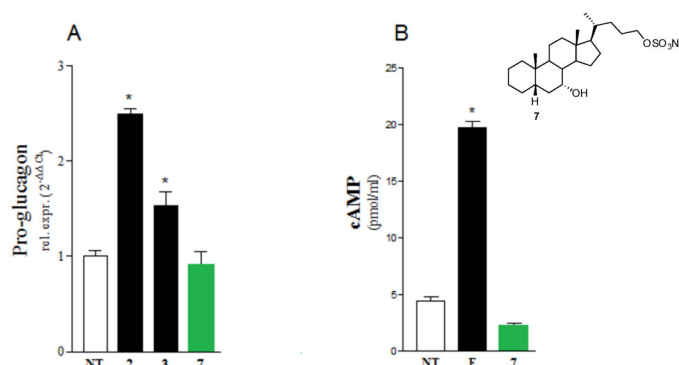


**Figure 17. In vitro pharmacological evaluation of GPBAR1 functions on 7.** (A) Real-time PCR analysis of mRNA expression of GPBAR1 target gene Pro-glucagon in GLUTAg cells primed with 7, (10 μM). TLCA (2) and 6-ECDCA (3) were tested as positive controls (10 μM). Values are normalized relative to GAPDH mRNA and are expressed relative to those of not treated cells (NT), which are arbitrarily set to 1: \*p < 0.05 versus not treated cells (NT). (B) Effect of 7 (10 μM) on intracellular generation of cAMP in THP-1 cells. The data are the mean ± SE of three experiments: \*p < 0.05 versus not treated cells (NT). F: Forskolin 10 μM.

Differently, as illustrated in Figure 18, compound 7 was able in inducing mRNA expression of FXR target genes, OSTα, BSEP and SHP with potency comparable with that of 6-ECDCA (3).

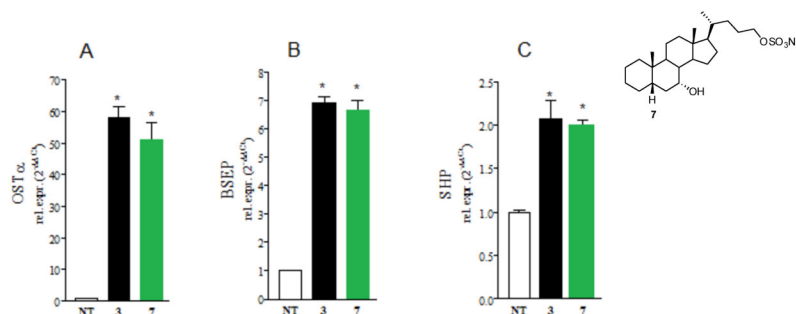


**Figure 18. In vitro pharmacological evaluation of FXR target genes on 7.** Real-time PCR analysis of mRNA expression of FXR target genes OSTα (A), BSEP (B) and SHP (C) in HepG2 cells primed with 7 (10 μM). 6-ECDCA (3) was tested as positive control (10 μM). Values are normalized relative to GAPDH mRNA and are expressed relative to those of not treated cells (NT), which are arbitrarily set to 1: \*p < 0.05 vs NT.

Finally, the ability of compound 7 in the recruitment of SRC-1 (steroid receptor 1 coactivator) was evaluated in cell-free Alphascreen technology. Data shown in Figure 19 clearly confirm the transactivation results. CDCA (1) and 6-ECDCA (3) were used as positive controls and the effect of CDCA was arbitrarily settled as

100%. Compound **7** at the concentration of 4  $\mu$ M showed a moderate recruitment of SRC-1 respect the 6-ECDCA.

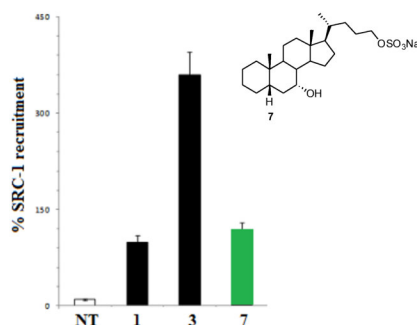


**Figure 19. Coactivator recruitment assay measuring a direct interaction of FXR with Src-1.** Anti-GST-coated acceptor beads captured GST-fusion FXR-LBD and the biotinylated-SRC-1 peptide was captured by the streptavidin donor beads. FXR-LBD recruited SRC-1 in presence of ligand at 4  $\mu$ M and, upon illumination at 680 nm, chemical energy is transferred from Donor to Acceptor beads across the complex streptavidin-Donor/ Src-1-Biotin/ ligand/ GSTFXR-LBD/ Anti-GST-Acceptor and a signal is produced. Results are expressed as percentage of the effect of CDCA (**1**) arbitrarily settled as 100%. NT is referred to the experiment carried out in absence of ligand. Results are expressed as mean  $\pm$  standard error.

In summary, medicinal chemistry on CDCA and UDCA scaffolds led the discovery of compound **7**, a selective FXR ligand which was able to transactivate FXR with an  $EC_{50}$  of  $\sim 9 \mu$ M. Even if compound **7** is approximately 10-15-fold less potent than 6-ECDCA (**3**) in transactivating FXR,<sup>68</sup> its potency in inducing the expression of OST $\alpha$  in the liver is comparable to 6-ECDCA. In addition, respect the 6-ECDCA, compound **7** does not present any effect on GPBAR1, both in transactivation and in RT-PCR analysis. The selectivity of **7** for FXR makes this compound an ideal candidate in the treatment of cholestasis.<sup>17</sup> In fact, it should prevent the risk of itching, a common side effect observed for 6-ECDCA.<sup>41,48,49</sup> Finally, the presence of a stable and not conjugable group (a sulfate) on the side chain increases, from a metabolic point of view, the therapeutical potential of compound **7** in treating human FXR-mediated diseases. Furthermore, compound **7** was chosen as template for further modifications on bile acid scaffolds, in order to improve the selectivity and the potency of action, generating more promising hit compounds.

## CHAPTER 2

### 6-ETHYLCHENOCHOLANE DERIVATIVES

As pointed before, the introduction of an ethyl group at C-6 on the CDCA ring B afforded to the disclosure of the potent FXR agonist 6-ECDCA/OCA, reported in both peer-reviewed literature<sup>40</sup> and in two patent applications of 2002 and 2005.<sup>69</sup> In detail, in the main part of my PhD project I focused my attention on the synthetic modifications of 6-ECDCA scaffold. Starting from this building block, my PhD research activity has been mainly focalized on the synthetic modifications of 6-ECDCA scaffold and large libraries of compounds, modified in the side chain and on the tetracyclic moiety, have been generated. Firstly, we decided to harness the carboxyl group at C-24, generating C-24 alcohols **44-47** and, in the above subset, chemical diversity has been also increased with modification at the configurational assessment between C6/C7 substituents (Figure 20).

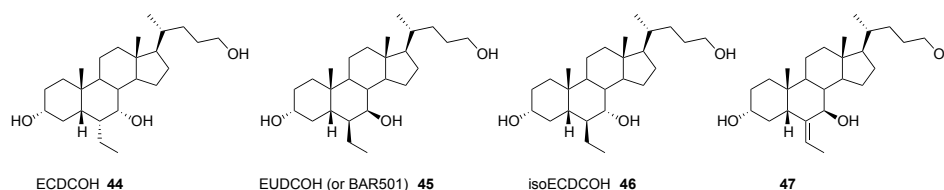


**Figure 20.** 3 $\alpha$ -hydroxy-6-ethylchenocholane derivatives

Second, translating the information that the removal or isomerization of the hydroxyl group at C-3 on CDCA scaffold was detrimental in terms of GPBAR1 activation<sup>70</sup> generating selective FXR agonists to the 6-ECDCA scaffold, compounds **48-62** (Figures 21 and 22) have been obtained. The first subset includes 3-deoxy-6-ethylcholane derivatives (Figure 21) whereas subset B includes the corresponding 3 $\beta$ -hydroxy-6-ethylcholane derivatives. Also in this case, chemical modifications were expanded at the side chain end-group and at the stereochemical arrangement on C-6 and C-7. Structural characterization on compounds **44-62** was performed by NMR and ESI-MS analysis. These huge medicinal chemistry protocols accompanied by an intense pre-clinical pharmacological evaluation afforded the discovery of promising hit compounds as selective and potent bile acid receptors agonists. In particular, compounds **45** (EUDCOH) and **51** have been patented with the name of BAR501 and BAR704

respectively, where the abbreviation BAR is due to the “BAR Pharmaceuticals” company.

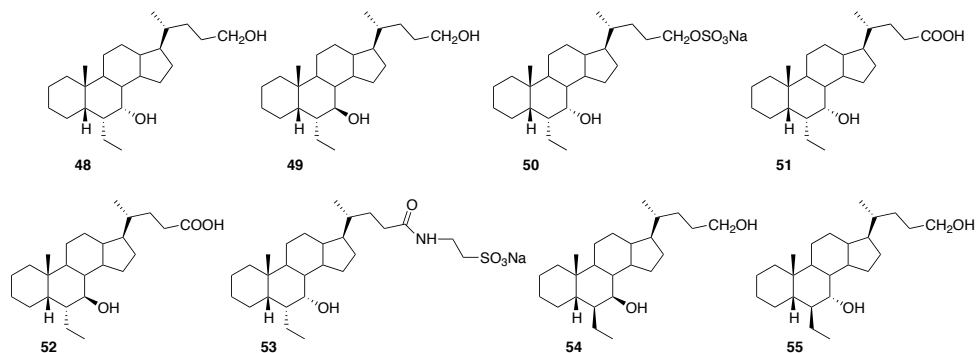


**Figure 21.** Subset A: 3-deoxy-6-ethylchenodeoxycholate derivatives

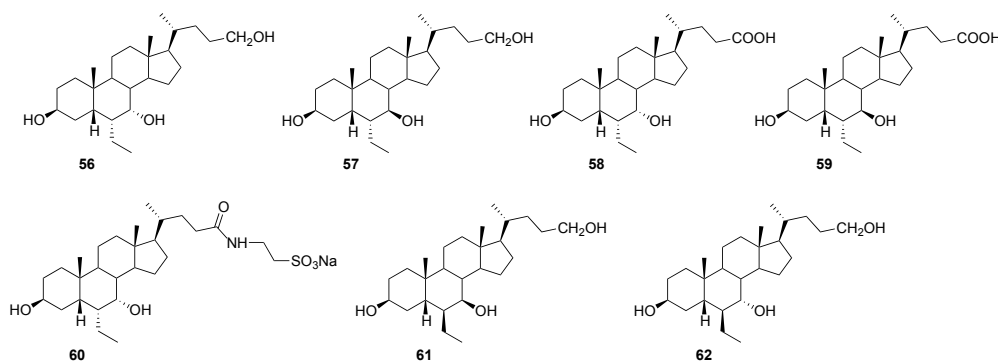
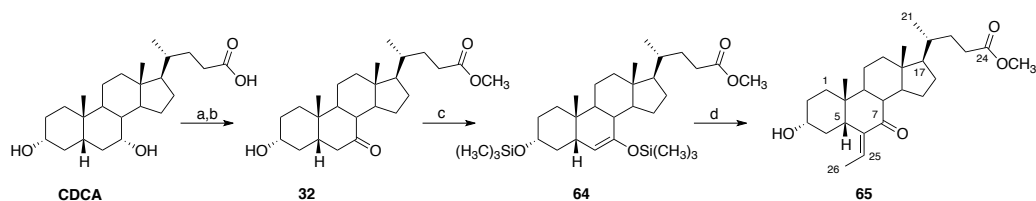


**Figure 22.** Subset B: 3β-hydroxy-6-ethylchenodeoxycholate derivatives

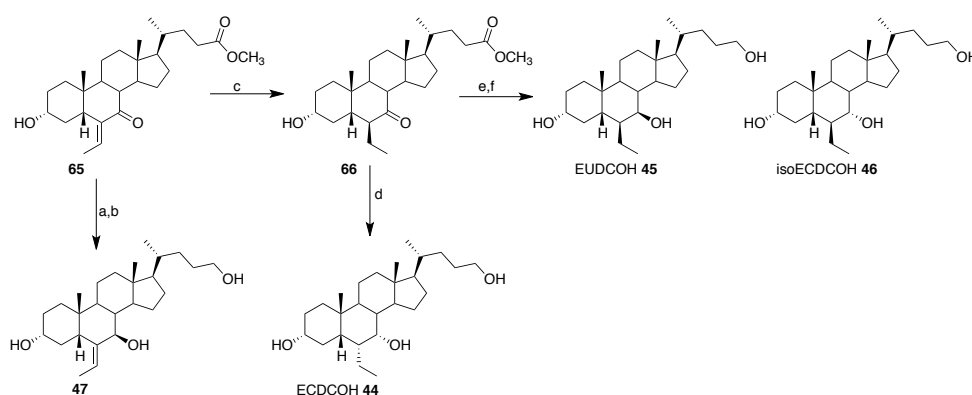
## 2.1 SYNTHESIS OF 3α-HYDROXY-6-ETHYLCHOLANE DERIVATIVES

Alkylation at C-6 on CDCA scaffold represents the key step in the synthetic protocol towards 6-ethylcholate derivatives. As illustrated in the Scheme 6, commercially available chenodeoxycholic acid (CDCA), was regioselectively oxidized at C7 hydroxyl group<sup>37</sup> with NaClO 10%, NaBr and TBABr.



**Scheme 6.** Preparation of 6-ethyl intermediate (65). a) NaBr, TBABr, NaClO 10%, MeOH:CH<sub>3</sub>COOH: H<sub>2</sub>O:AcOEt 3:1:0.25:6.5; b) *p*-TsOH, MeOH dry, 65% over two steps; c) DIPA, *n*-BuLi, TMSCl, TEA dry, THF dry -78 °C; d) acetaldehyde, BF<sub>3</sub>•OEt<sub>2</sub>, CH<sub>2</sub>Cl<sub>2</sub>, -60 °C, 77% over two steps.

Esterification on C7 oxidized intermediate with *p*-TsOH in MeOH dry, gave methyl 7-keto-lithocholanoate (**32**) in 65% yield over two steps.<sup>71</sup> Aldolic addition to a silyl enol-ether intermediate (**64**) with acetaldehyde and BF<sub>3</sub>•OEt<sub>2</sub>,<sup>72</sup> produced methyl 3 $\alpha$ -hydroxy-6-ethylidene-7-keto-5 $\beta$ -cholanoate **65** in 77% chemical yield over two steps. Dipolar couplings H-8/H-25 and Me-26/H-5 in the NOESY spectrum, established the *E* configuration at the exocyclic double bond as represented in **65**. An aliquot of **65** was subjected to NaBH<sub>4</sub> reduction at C-7 ketone<sup>48</sup> followed by a treatment with LiBH<sub>4</sub> in MeOH dry, affording the triol **47** in good chemical yield (Scheme 7).



**Scheme 7. Modification on ring B of 6-ethylcholane scaffold.** a) NaBH<sub>4</sub>, MeOH dry; b) LiBH<sub>4</sub>, MeOH dry, THF dry, 0 °C, 85% over two steps; c) H<sub>2</sub>, Pd/C, THF/MeOH 1:1, quantitative yield; d) LiBH<sub>4</sub>, MeOH dry, THF dry, 0 °C; e) NaBH<sub>4</sub>, MeOH dry; f) LiBH<sub>4</sub>, MeOH dry, THF dry, 0 °C.

The reduction with sodium borohydride on **65** occurred in a stereoselective manner, producing the exclusive formation of 7 $\beta$ -hydroxyl derivative (**47**) as demonstrated by the shape of H-7 (doublet,  $J = 9.8$  Hz) signal in the NMR proton spectrum. The above large value of coupling constant H7/H8 is in full agreement with their trans-diaxial disposition and therefore with the  $\beta$ -orientation of the hydroxyl group at C-7 on ring B. Hydrogenation of the exocyclic double bond (H<sub>2</sub> on Pd/C) on compound **65** afforded exclusively the 6 $\beta$ -ethyl group in **66** as demonstrated by dipolar couplings Me-26 ( $\delta$  0.83)/Me-19 ( $\delta$  1.22) and H-8 ( $\delta$  2.56)/H-25 ( $\delta$  1.83) in Noesy spectrum. The  $\beta$ -configuration in compound **66** after catalytic hydrogenation, depended on the presence of a *cis* junction between the rings A and B, which induced the molecule to assume a bent form; in this spatial disposition the methyl group at C-21 position caused a steric hindrance that forced the attack of hydrogen on the  $\alpha$  face of double bond and gave the  $\beta$ -configuration



of the ethyl group. LiBH<sub>4</sub> treatment furnished alcohol **44** whose stereochemical assessment C6 $\alpha$ /C7 $\alpha$  was substantiated by the almost complete superimposition of proton resonances of all nuclei belonging to the tetracyclic core, with those reported for the 6-ECDCA.<sup>37,48</sup> From a mechanistic point of view, LiBH<sub>4</sub> treatment first induces the epimerization at C-6 through a keto-enol tautomerism where the  $\alpha$  epimer at C-6, thermodynamically more stable, is favored. Then, reduction at C-7 proceeds through the approach of the hydride from the upper-face of the steroid nucleus, in agreement with the steric influence played by the ethyl group at C-6 and by the ring A, both oriented on the  $\alpha$ -face of ring B. For the preparation of the corresponding epimers at C-6 or/and C-7 of compound **44**, NaBH<sub>4</sub> treatment on methyl ester **66** was performed. Interestingly, sodium borohydride treatment does not induce C-6 epimerization, affording directly the reduction at C-7 keto group. Finally, LiBH<sub>4</sub> reduction on the crude reaction furnished a mixture that was then purified in HPLC (88% MeOH:H<sub>2</sub>O) giving pure 6 $\beta$ -ethyl derivatives **45** and **46**, in ratio 7:3. Stereochemical characterization of 6 $\beta$ -ethyl-3 $\alpha$ ,7 $\alpha$ -dihydroxy-5 $\beta$ -cholan-24-ol (isoECDCOH, **46**) was based on careful comparison of NMR data with those of compound **44** (Tables 1 and 2). In compound **46**, H-7 resonated as singlet ( $\delta_{\text{H}}$  3.60), confirming its equatorial disposition and therefore the  $\alpha$ -configuration of C-7 hydroxyl group. The other values in the <sup>1</sup>H NMR spectra were almost similar in the shape and in the chemical shift, with the exception of the down-field shifted signals for H<sub>2</sub>-4 ( $\delta_{\text{H}}$  2.30, 1.55 in **46** vs  $\delta_{\text{H}}$  1.88, 1.73 in **44**) and for Me-26 ( $\delta_{\text{H}}$  0.95 in **46** vs 0.90 in **44**), suggesting the inverted configuration at C-6 in **46**. <sup>13</sup>C NMR spectrum analysis, supported by the two-dimensional HSQC and HMBC experiments, confirmed this hypothesis revealing deep differences in the chemical shift of several carbons adjacent to C-6 (*i.e.* C-4  $\delta_{\text{C}}$  41.4 in **46** respect 34.3 in **44**, C-6  $\delta_{\text{C}}$  51.7 in **46** respect 42.9 in **44**, C-8  $\delta_{\text{C}}$  36.4 in **46** respect 41.3 in **44**). In the <sup>1</sup>H NMR spectrum of 6 $\beta$ -ethyl-3 $\alpha$ ,7 $\beta$ -dihydroxy-5 $\beta$ -cholan-24-ol (EUDCOH, **45**), H-7 appeared as a doublet doublet ( $\delta_{\text{H}}$  3.74, dd,  $J = 10.3, 6.0$  Hz) with a large coupling constant with H-8, due to their *trans* di-axial relationship and consequently in agreement with the  $\beta$ -orientation of the hydroxyl group on C-7. ROESY cross-peaks, H-7/H-9, H-7/H-14 and H-7/H-6 confirm the inverted

configuration at C-7 and suggested the *cis* stereochemical arrangement of the two substituents in positions 6 and 7. Final confirmation of the  $\beta$ -orientation of the 6-ethyl group derived from the perfect overlapping of carbon resonances of all ring A nuclei with those of compound **46** (Table 2).

Position	<b>44</b> $\delta_{\text{H}}^{\text{b}}$	<b>45</b> $\delta_{\text{H}}^{\text{b}}$	<b>46</b> $\delta_{\text{H}}^{\text{b}}$	<b>47</b> $\delta_{\text{H}}^{\text{b}}$
1	1.85 dt (14.2, 3.3) 1.00 m	1.72 dt (14.1, 3.1) 1.07 ovl	1.76 ovl 1.01 m	1.90 dt (14.2, 3.2) 1.07 ovl
2	1.60 m 1.33 ovl	1.62 ovl 1.30 ovl	1.58 ovl 1.29 m	1.65 ovl 1.34 m
3	3.31 <sup>c</sup>	3.51 ovl	3.35 <sup>c</sup>	3.55 m
4	1.88 m 1.73 ovl	1.67 ovl 1.56 ovl	2.30 q (13.5) 1.55 ovl	1.66 ovl 1.54 m
5	1.30 ovl	1.66 ovl	1.40 ovl	2.50 dd (13.1, 4.0)
6	1.55 ovl	1.48 ovl	1.42 ovl	-
7	3.66 s	3.74 dd (10.3, 6.0)	3.60 s	3.90 d (9.8)
8	1.48 ovl	1.59 ovl	1.60 ovl	1.41 ovl
9	1.81 m	1.46 ovl	1.89 ovl	1.71 m
10	-	-	-	-
11	1.50 ovl 1.31 ovl	1.43 ovl 1.33m	1.45 ovl 1.33 ovl	1.48 ovl 1.33 ovl
12	2.00 dt (12.5, 3.2) 1.19 ovl	2.04dt (12.7, 3.2) 1.17 dd (12.7, 3.9)	2.00 dt (12.4, 3.3) 1.19 ovl	2.05 dt (12.6, 3.1) 1.20 m
13	-	-	-	-
14	1.51 ovl	1.23 m	1.53 ovl	1.33 ovl
15	1.75 ovl 1.11 m	2.00 m 1.45 m	1.75 ovl 1.09 ovl	1.96 m 1.49 ovl
16	1.90 m 1.31 ovl	1.85 m 1.29 ovl	1.90 ovl 1.32 ovl	1.87 m 1.28 m
17	1.19 ovl	1.09 ovl	1.20 ovl	1.13 m
18	0.70 s	0.72 s	0.70 s	0.70 s
19	0.92 s	1.00 s	0.94 s	0.81 s
20	1.32 ovl	1.42 ovl	1.42 ovl	1.42 ovl
21	0.97 d (6.6)	0.97 d (6.5)	0.97 d (6.8)	0.97 d (6.8)
22	1.48 ovl 1.08 m	1.48 ovl 1.07 ovl	1.49 m 1.09 ovl	1.49 ovl 1.09 ovl
23	1.42 m 1.20 ovl	1.57 ovl 1.41 ovl	1.62 ovl 1.44 ovl	1.61 ovl 1.41 ovl
24	3.50 m	3.49 ovl	3.51 m	3.50 m
25	1.53 ovl 1.39 m	1.79 m 1.40 ovl	1.42 ovl	5.64 q (6.9)
26	0.90 t (7.2)	0.96 t (7.6)	0.95 t (7.3)	1.62 d (6.9)

**Table 1.** <sup>1</sup>H NMR data (CD<sub>3</sub>OD) of compounds **44**, **45** (700 MHz) and **46**, **47** (400 MHz).  
<sup>b</sup>Coupling constants are in parentheses and in hertz; <sup>c</sup>Ovl: overlapped with solvent signal; Ovl: overlapped with other signals.

Position	<b>44</b> $\delta_C$	<b>45</b> $\delta_C$	<b>46</b> $\delta_C$	<b>47</b> $\delta_C$
1	36.5	37.1	36.6	34.7
2	30.7	30.7	30.1	30.2
3	72.9	71.9	71.8	71.1
4	34.3	40.4	41.4	36.2
5	46.8	45.7	46.7	45.2
6	42.9	51.6	51.7	142.7
7	70.9	75.3	71.9	73.4
8	41.3	40.3	36.4	44.9
9	34.3	42.1	33.2	40.2
10	36.2	35.8	36.0	35.9
11	21.9	22.1	20.7	21.5
12	40.7	41.5	40.1	40.7
13	43.5	44.9	42.5	44.2
14	51.5	57.5	50.5	57.1
15	24.4	28.3	23.9	27.4
16	29.4	29.6	28.5	28.8
17	57.3	56.5	56.8	56.1
18	11.9	12.7	11.4	11.7
19	23.4	26.2	25.3	22.6
20	36.7	35.8	36.2	36.3
21	18.9	19.4	18.4	18.5
22	33.0	32.4	32.4	32.4
23	29.7	29.7	29.5	29.5
24	63.4	63.6	62.7	63.6
25	23.5	23.4	28.8	114.5
26	11.6	14.8	13.7	11.8

**Table 2.**  $^{13}\text{C}$  NMR data ( $\text{CD}_3\text{OD}$ ) at 175 MHz (**44** and **45**) and 100 MHz (**46** and **47**).

## 2.2 PHARMACOLOGICAL EVALUATION OF 3 $\alpha$ -HYDROXY-6-ETHYLCHOLANE DERIVATIVES

Compounds **44-47** were tested *in vitro* in a luciferase reporter assay on HepG2 and HEK-293T cells, transfected with the responsive elements for FXR and GPBAR1, respectively (Figure 23, panels A and B).

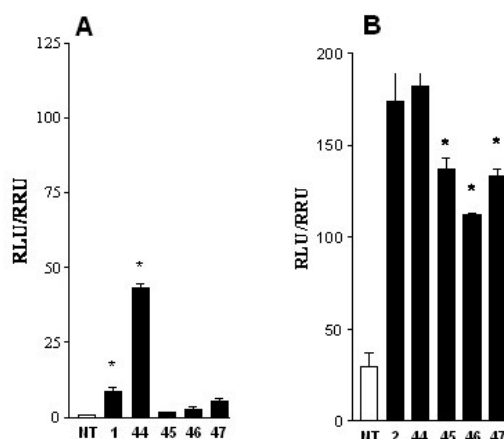


**Figure 23. Transactivation assays on FXR (Panel A) and GPBAR1 (Panel B):** (A) HepG2 cells were transfected with pSG5-FXR, pSG5-RXR, pCMV- $\beta$ gal, and p(hsp27)TKLUC vectors. Cells were stimulated with compounds **44-47** (10  $\mu$ M). CDCA (**1**, 10  $\mu$ M) was used as positive control. Results are expressed as mean  $\pm$  standard error; \* $p < 0.05$  versus not treated cells (NT). (B) HEK-293T cells were co-transfected with GPBAR1 and a reporter gene containing a cAMP responsive element in front of the luciferase gene. Twenty-four hour post transfection cells were stimulated with **44-47** (10  $\mu$ M). Luciferase activity served as a measure of the rise in intracellular cAMP following activation of GPBAR1. TLCA (**2**, 10  $\mu$ M) was used as a positive control. Results are expressed as mean  $\pm$  standard error. \* $p < 0.05$  versus not treated cells (NT).

Results illustrated in Figure 23 confirm the fact that the stereochemical arrangement at C-6 and C-7 positions is a key aspect for FXR activation, whereas doesn't influence GPBAR1 interaction. In fact, alcohols **45-47** resulted potent and selective GPBAR1 agonists whereas derivative **44**, with both ethyl and the hydroxyl groups on ring B  $\alpha$ -oriented, resulted a dual agonist.

### 2.2.1 Pharmacological evaluation on EUDCOH (45)

Compound **45** (EUDCOH), a potent and selective GPBAR1 agonist, was further evaluated. Concentration-response curves, revealed its inactivity on FXR at any concentration tested, whereas demonstrated its agonistic behavior toward GPBAR1 with an  $EC_{50}$  of 1.03  $\mu$ M (panels A and B in Figure 24).

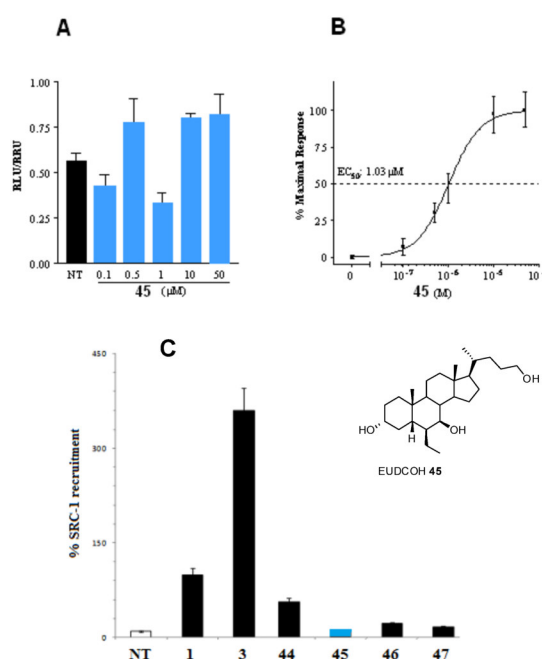


**Figure 24. Concentration-response curve of 45 on FXR (A) and GPBAR1 (B).** FXR transactivation was measured in a luciferase reporter assay using HepG2 cells transfected with FXR. GPBAR1 activity was measured in HEK-293T cells co-transfected with GPBAR1 and a reporter gene containing a cAMP responsive element in front of the luciferase gene (CRE). Twenty-four hour post transfection cells were stimulated with increasing concentrations of each agent: range from 100 nM to 50 μM. Results are expressed as mean ± standard error. \* $p < 0.05$  versus not treated cells (NT). (C) Coactivator recruitment assay measuring a direct interaction of FXR with Src-1. Anti-GST-coated acceptor beads captured GST-fusion FXR-LBD and the biotinylated-SRC-1 peptide was captured by the streptavidin donor beads. FXR-LBD recruited SRC-1 in presence of ligand at 4 μM and, upon illumination at 680 nm, chemical energy is transferred from Donor to Acceptor beads across the complex streptavidin-Donor/Src-1-Biotin/ligand/GSTFXR-LBD/Anti-GST-Acceptor and a signal is produced. Results are expressed as percentage of the effect of CDCA (**1**) arbitrarily settled as 100%. NT is referred to the experiment carried out in absence of ligand. Results are expressed as mean ± standard error.

Moreover, Alphascreen assay confirms the complete absence of activity on FXR for compounds **44-47**. In fact, this assay measures the ability of molecules to induce the recruitment of a coactivator (such as SRC-1) in a receptor ligand-binding domain. This event is fundamental for FXR activation and the consequent activation of transcriptional machinery. As shown in Figure 24 panel C, CDCA (**1**) and 6-ECDCA (**3**) were used as positive control and the results were compared to the assay carried out in absence of ligand (response at 10%). Data collected confirmed that compounds **44-47** are completely unable to recruit the coactivator (**45-47**) when tested at the fixed concentration of 4 μM. Moreover, in order to evaluate the ability of derivative **45** to act selectively on G-protein coupled receptor 1, its effect was evaluated in transactivation assay on common off-targets

such as GR, PPAR $\gamma$ , LXR and PXR (Figure 25). As shown in Figure 25 (panels A-D), except a residual activity on PXR (Figure 25 D), compound **45** failed to transactivate the receptors GR, PPAR $\gamma$  and LXR at the concentration of 10  $\mu$ M. Furthermore, to confirm transactivation assays, compound **45** was evaluated in the regulation of FXR and GPBAR1 canonical functions. As depicted in Figure 26, compound **45** was able in inducing the expression of pro-glucagon mRNA (GLP-1) in GLUTAg cells and cAMP intracellular concentrations in THP-1 cells, while fails in inducing the expression of OST $\alpha$ , BSEP and SHP, three FXR-targeted genes.

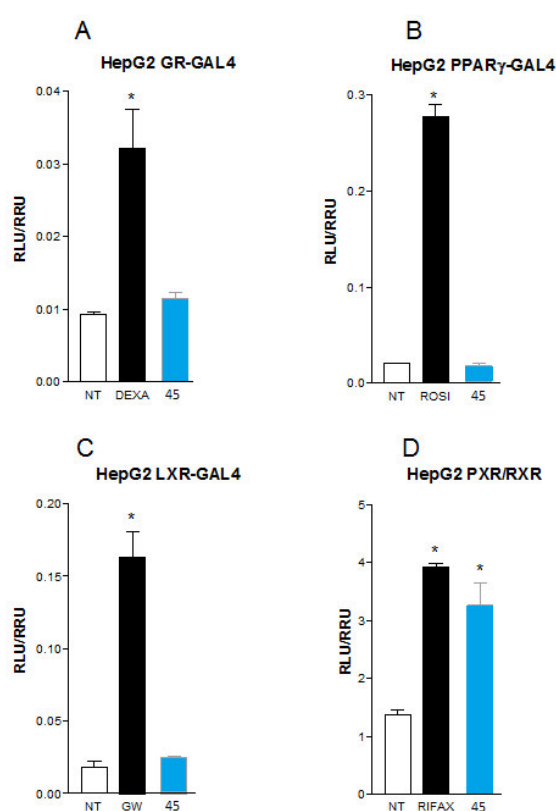


**Figure 25. Specificity of **45** on other nuclear receptors.** (A) (B) and (C) HepG2 cells were co-transfected with the Gal4 luciferase reporter vector and with a series of chimeras in which the Gal4 DNA binding domain is fused to the LBD of the indicated nuclear receptors. Cells were treated 18 h with the specific agonists (10  $\mu$ M) or with **45** (10  $\mu$ M). (D) HepG2 cells were co-transfected with pSG5-PXR, pSG5-RXR and with the reporter pCYP3A4 promoter-TKLuc and then stimulated with rifaximin (10  $\mu$ M), a PXR agonist, or with **45** (10  $\mu$ M). Data are the mean  $\pm$  S.E. of three experiments. \* $p < 0.05$  versus not treated cells (NT). DEXA: Dexamethasone; ROSI: Rosiglitazone; GW: GW3965; RIFAX: Rifaximin.

Collectively, these data affirm compound **45** as a potent and selective GPBAR1 agonist.

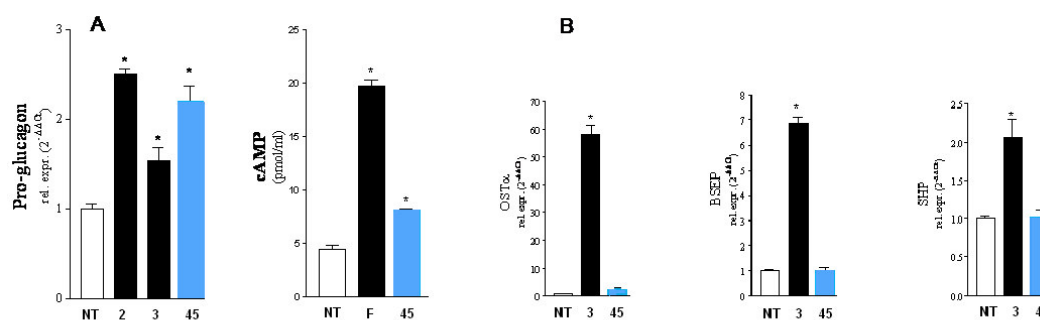


**Figure 26. In vitro pharmacological evaluation of FXR/GPBAR1 functions on 45.** (A) Real-time PCR analysis of mRNA expression of GPBAR1 target genes: Pro-glucagon in GLUTAg cells primed with 45 (10  $\mu$ M); effect of 45 (10  $\mu$ M) on intracellular generation of cAMP in THP-1 cells. The data are the mean  $\pm$  SE of three experiments: \* $p < 0.05$  versus not treated cells (NT). F: Forskolin 10  $\mu$ M. TLCA (2) and 6-ECDCA (3) were tested as positive controls (10  $\mu$ M). Values are normalized relative to GAPDH mRNA and are expressed relative to those of not treated cells (NT), which are arbitrarily set to 1: \* $p < 0.05$  versus not treated cells (NT). (B) Real-time PCR analysis of mRNA expression of FXR target genes: OST $\alpha$ , BSEP and SHP in HepG2 cells primed with 45 (10  $\mu$ M). 6-ECDCA (3) was tested as positive control (10  $\mu$ M). Values are normalized relative to GAPDH mRNA and are expressed relative to those of not treated cells (NT), which are arbitrarily set to 1: \* $p < 0.05$  vs NT.

### 2.2.1.1 Preclinical *in vivo* pharmacological evaluation on 45

The interesting *in vitro* pharmacological results on compound 45 led the attention of our pharmacological partner to a comprehensive investigation on its *in vivo* effects. Compound 45 (or BAR501) demonstrated beneficial effects on portal hypertension in a rodent model of liver cirrhosis, by exerting genomic and non-genomic effects on cystathione- $\gamma$ -lyase (CSE), nitric oxide synthase (eNOS) and endothelin (ET)-1, in liver sinusoidal cells.<sup>73</sup> Portal hypertension is a common symptom of liver cirrhosis, in which the fibrosis combined with a vasculogenic component contributes to an endothelial dysfunction. This last, in turn, induces contraction of the perisinusoidal hepatic stellate cells (HSC) and increases intrahepatic vascular resistance to portal flow.<sup>74-76</sup> Because GPBAR1 expression is limited only to Kupffer and sinusoidal (LSEC) hepatic cells, whose activation regulates the endothelial nitric oxide (NO) synthase (eNOS) activity,<sup>77</sup> this suggests the effective role of GPBAR1 in the treatment of endothelial dysfunction in presence of liver cirrhosis. Hepatic cirrhosis was induced in mice by carbon tetrachloride (CCl<sub>4</sub>) administration for 9 weeks and the dose of BAR501 administered was of 15 mg/kg/day. After 9 weeks treatment, BAR501 effectively protected against occurrence of endothelial dysfunction, by increasing liver CSE

expression and activity and by reducing expression of endothelin (ET)-1 gene. Moreover, this last mechanism was due to the FOXO1 phosphorylation by BAR501, which inhibits ET-1 transcription in liver sinusoidal cells. As illustrated in Figure 27, BAR501 effectively reduced hepatic perfusion pressure in naïve rats and contrasted the vasoconstriction activity of norepinephrine (NE) and of methoxamine, two  $\alpha_1$ -adrenergic receptor agonists.

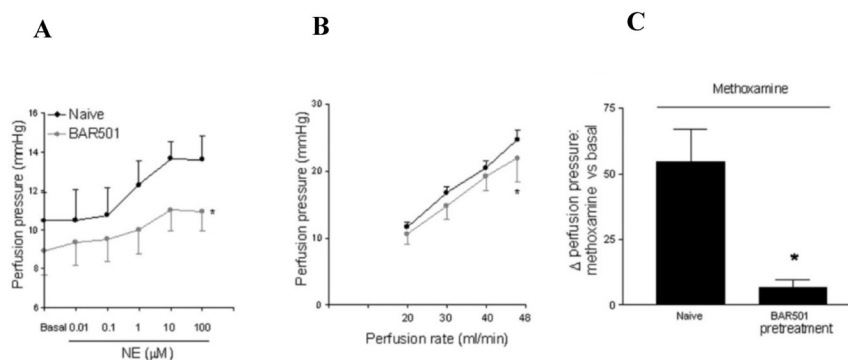


**Figure 27. Pharmacological evaluation on BAR501.** (A) Effect of BAR501 on vasomotor activity of norepinephrine (NE), after administration of 15 mg/kg/day for 6 days. (B) Effect of BAR501 on liver perfusion pressure caused by shear stress in rats. Data are mean  $\pm$  SE of 4–6 animals per group. \* $p < 0.05$  versus shear stress alone (C) BAR501 attenuates vasomotor effect of methoxamine in rats.

Successively, the vasodilatory activity of BAR501 was evaluated in a  $\text{CCl}_4$  model of cirrhosis/fibrosis. As illustrated in Figure 28, after  $\text{CCl}_4$  administration for 9 weeks, mouse developed a severe liver injury (increase of AST levels), liver fibrosis and alteration of albumin levels. After BAR501 administration, the portal pressure and AST plasma levels were reduced without effect on biochemical values of alkaline phosphatase, albumin and bilirubin (Figures 28 A-E). However, BAR501 was unable to improve fibrosis developed in mice model of  $\text{CCl}_4$  (Figure 28, panels F-H and I-N). These results were also confirmed by quantitative Real-Time PCR results. As illustrated in Figure 29, BAR501 failed to contrast, in mice administered with  $\text{CCl}_4$ , the expression of pro-fibrogenic (*i.e.*  $\text{TGF}\beta 1$ ,  $\text{Col}1\alpha 1$  and  $\alpha\text{-SMA}$ ) and pro-inflammatory agents (*i.e.*  $\text{TNF}\alpha$ ).



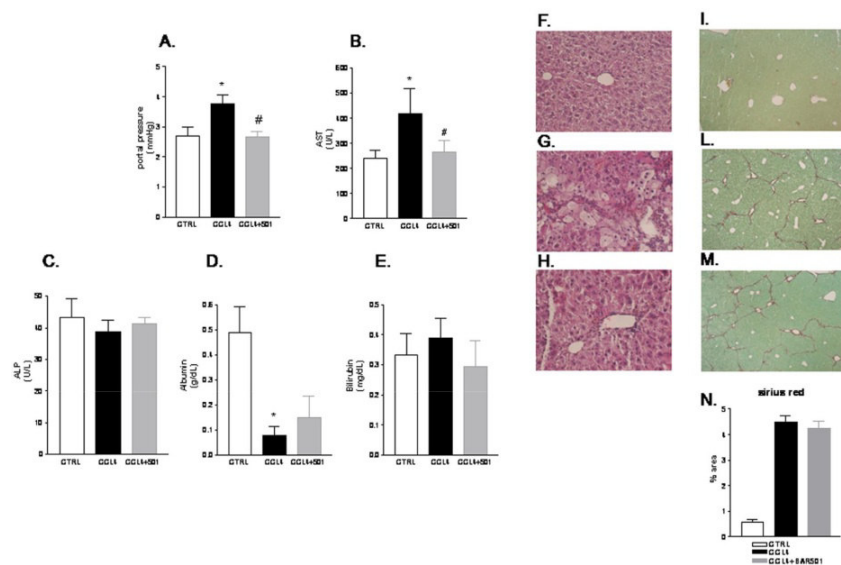


**Figure 28. Vasodilatory activity of BAR501 in the CCl<sub>4</sub> model.** (A) Effect on portal pressure, (B) Effect on AST, (C) Effect on alkaline phosphatase (ALP), (D) Effect on albumin, (E) Effect on bilirubin in mice rendered cirrhotic by administration with CCl<sub>4</sub>. (F-H) Hematoxylin and eosin staining. (I-M) Sirius red staining (Fibrosis). (N) Quantification of Sirius red staining. Data are mean  $\pm$  SE of 8–10 animals per group. \* $p$ <0.05 versus naïve mice. # $p$ <0.05 versus CCl<sub>4</sub>.

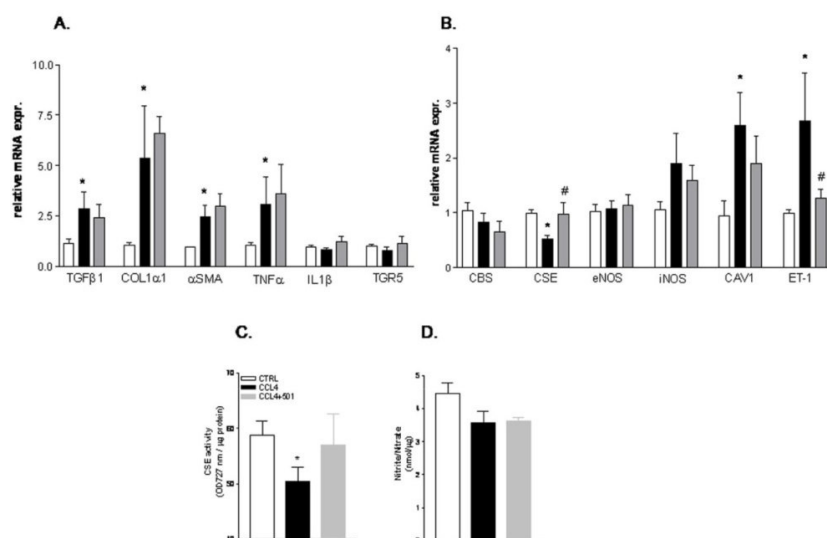


**Figure 29. Expression of CSE and ET-1 in the CCl<sub>4</sub> model of liver cirrhosis.** C57BL6 mice were treated for 9 weeks with CCl<sub>4</sub> or with the combination of CCl<sub>4</sub> plus BAR501 15 mg/kg. The relative hepatic mRNA expression of TGF $\beta$ 1, COL1 $\alpha$ 1,  $\alpha$ SMA, TNF $\alpha$ , IL1 $\beta$ , GPBAR1 (panel A) and CBS, CSE, eNOS, iNOS, CAV-1 ET-1 (panel B) was assayed by Real-Time PCR. (C) Effect of BAR501 on CSE activity in the CCl<sub>4</sub> model. (D) Effect of BAR501 on nitrite/nitrate in CCl<sub>4</sub> treated mice. Results are the mean  $\pm$  SE of 4–8 mice per group. \* $p$ <0.05 versus naïve mice. # $p$ <0.05 versus CCl<sub>4</sub> alone.

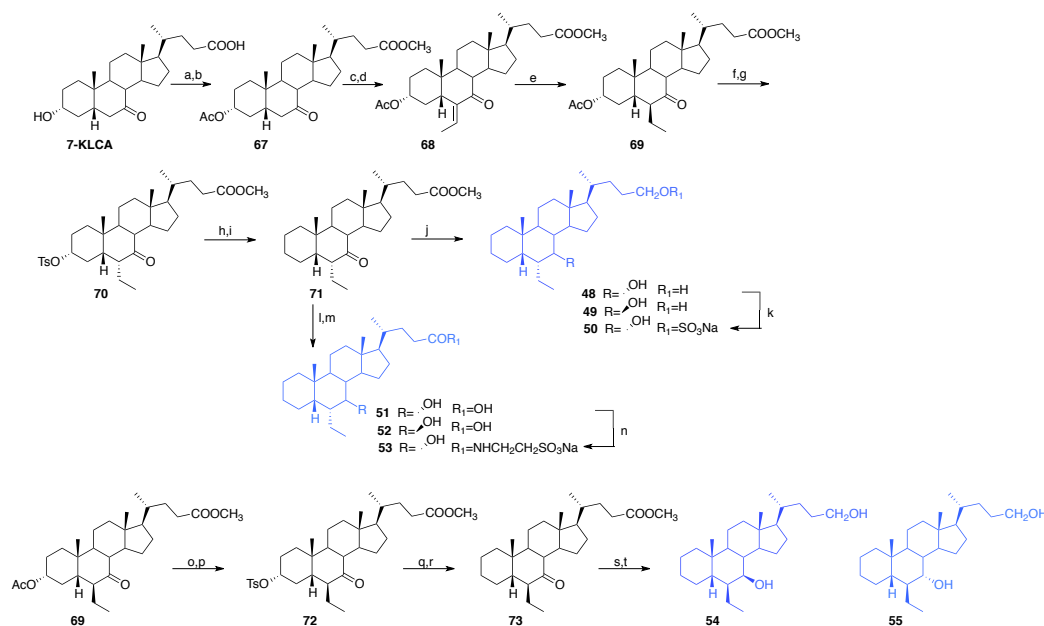
Interestingly are the results on CSE expression/activity where BAR501 administration in combination with CCl<sub>4</sub>, increased the expression of CSE gene, an enzyme involved in the vasodilatation for the release of H<sub>2</sub>S, whereas had no

effect on nitrite/nitrate concentrations (Fig. 29 C and 29 D). Therefore, this result suggests a potential role of this compound in the regulation of endothelial mechanisms in the liver microcirculation. In addition, the ET-1 gene, that is a potent vasoconstrictor factor, was strongly down-regulated by BAR501. Thus, BAR501 effectively reduces vasoconstriction caused by NE and methoxamine in naïve rats and protects against development of portal hypertension in rodent models of cirrhosis and consequent endothelial dysfunction, which was mainly due to insufficient NO production and increased ET-1 generation.<sup>74-76,78-95</sup> However, it failed to attenuate liver fibrosis and it is probably due to the absence of GPBAR1-expression in hepatic stellate cells.<sup>96</sup>

In addition, BAR501 increased the expression of CSE but had no effect on nitrites/nitrates levels. In conclusion, BAR501, a UDCA derivative endowed with robust and selective GPBAR1 agonistic activity, was demonstrated able in attenuating the deleterious consequences of liver cirrhosis.

### **2.3 PREPARATION OF 3-DEOXY-6-ETHYLCHENOCHOLANE DERIVATIVES**

For the preparation of 3-deoxy-6-ethylchenocholane derivatives (compounds **48-55**, Scheme 8), the key step was the elimination of the hydroxyl group at C-3. This modification, as already discussed, was chosen in order to increase the selectivity of these molecules towards FXR, because the hydroxyl group at C-3 is fundamental for GPBAR1 activation.<sup>71</sup> Intermediate **69** (obtained in quantitative yield from 7-KLCA) was prepared as described for **66**, with the exception of acetylation at C-3 before the alkylation at C-6, in order to improve the chemical yield. Compound **69** was then treated over night with MeONa in methanol dry, in order to de-acetylate at C-3 and to invert the configuration at C-6 followed by tosylation at C-3, affording **70** in quantitative yield over two steps.

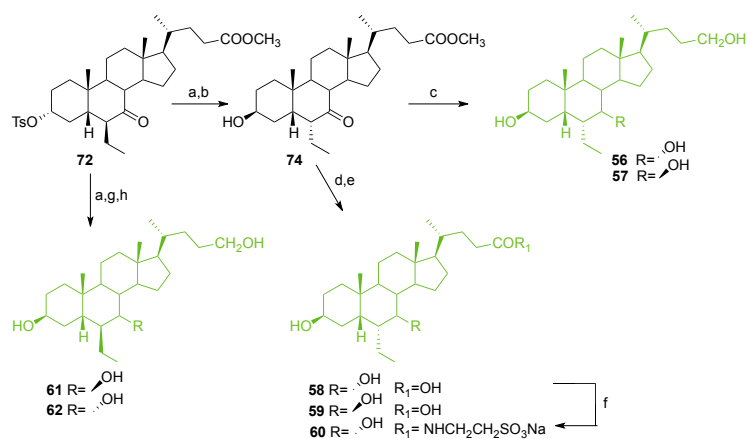


**Scheme 8. Preparation of 3-deoxy-6-ethylchenocholane derivatives (subset A).** a) *p*-TsOH, MeOH dry; b) acetic anhydride, pyridine, 84% yield over two steps; c) DIPA, *n*-BuLi, TMSCl, TEA dry, THF dry -78 °C; d) acetaldehyde, BF<sub>3</sub>(OEt)<sub>2</sub>, CH<sub>2</sub>Cl<sub>2</sub>, -60 °C, 80% over two steps; e) H<sub>2</sub>, Pd(OH)<sub>2</sub>, THF/MeOH 1:1, quantitative yield; f) MeONa, MeOH over night; g) *p*-TsCl, pyridine, quantitative yield over two steps; h) LiBr, Li<sub>2</sub>CO<sub>3</sub>, DMF dry, reflux, i) H<sub>2</sub>, Pd(OH)<sub>2</sub>, THF/MeOH 1:1, room temperature, 88% over two steps; j) LiBH<sub>4</sub>, MeOH dry, THF dry, 0 °C, 77%; k) Et<sub>3</sub>N·SO<sub>3</sub>, DMF, 95 °C; l) NaOH, MeOH:H<sub>2</sub>O 1:1 v/v, 98%; m) LiBH<sub>4</sub>, MeOH dry, THF dry, 0 °C, 83%; n) DMT-MM, Et<sub>3</sub>N, taurine, DMF dry; o) MeONa, MeOH, 2 h; p) *p*-TsCl, pyridine, quantitative yield over two steps; q) LiBr, Li<sub>2</sub>CO<sub>3</sub>, DMF dry, reflux; r) H<sub>2</sub>, Pd(OH)<sub>2</sub>, THF/MeOH 1:1, room temperature, 94% over two steps; s) NaBH<sub>4</sub>, MeOH dry; t) LiBH<sub>4</sub>, MeOH dry, THF, 0 °C, 78% over two steps.

Elimination by LiBr/Li<sub>2</sub>CO<sub>3</sub> treatment and hydrogenation of the unsaturated ring A transient intermediate, furnished the key derivative **71**. LiBH<sub>4</sub> reduction produced the concomitant reduction on side chain methyl ester and at C-7 carbonyl group, generating compound **48** in high chemical yield and a small aliquot of the corresponding epimer at C-7 (**49**), which were efficiently separated in HPLC. In the NMR proton spectra of compounds **48** and **49**, the main differences were in the shape and in the chemical shift value for H-7 signal. In **48**, H-7 resonated as singlet (δ<sub>H</sub> 3.65), thus determining the equatorial disposition for this proton and the consequent α-configuration of the hydroxyl group on C-7. Differently, in **49**, the corresponding proton signal appeared as a triplet (δ<sub>H</sub> 3.07, *t*, *J* = 10.0 Hz) with a large coupling constant with H-8 and H-6, respectively, confirming their reciprocal *trans* di-axial relationship and therefore the β-orientation of the hydroxyl group at C-7. Chemoselective sulfation on a small aliquot of **48** gave the corresponding side chain mono-sulphate **50**. Intermediate

**71** was also used as starting material for the preparation of compounds **51** and **52**. Basic hydrolysis with NaOH in MeOH:H<sub>2</sub>O 1:1 at methyl ester on side chain and then reduction at C-7 by LiBH<sub>4</sub> treatment, furnished **51** in high chemical yield, with about 10% of its epimer at C-7 (**52**), which were separated by HPLC. Amidation with taurine on **51** using the coupling agent DMT-MM in ET<sub>3</sub>N and RP18/HPLC purification, furnished the corresponding tauro-conjugated **53**. As previously demonstrated,<sup>71</sup> the stereochemical arrangement at C-6 and C-7 on ring B profoundly influences bile acid receptor selectivity.<sup>71</sup> The presence of a 6 $\alpha$ -ethyl and a 7 $\alpha$ -hydroxyl group produced potent dual agonists, whereas the 6-epimers (6 $\beta$ -ethyl derivatives) were characterized by selective GPBAR1 activity. To produce the 3-deoxy-6 $\beta$ -ethyl-chenodeoxycholate derivatives, the intermediate **69** was subjected to a controlled treatment with MeONa in MeOH (for 2 h) affording de-acetylation at C-3 position without any epimerization at C-6. Tosylation on the crude reaction product gave **72**, that was subjected to the same protocol described for compound **70**, producing **73** in 94% yield over two steps. NaBH<sub>4</sub> treatment on **73** followed by LiBH<sub>4</sub> reduction on the crude product, gave a mixture that was purified in HPLC, giving pure **54** in a 54% yield respect its C-7 epimer, compound **55**. The good match between <sup>1</sup>H and <sup>13</sup>C NMR resonances of all nuclei belong to rings B-D of the tetracyclic core in **55** with those referred for 6 $\beta$ -ethyl-3 $\alpha$ ,7 $\alpha$ -dihydroxy-5 $\beta$ -cholan-24-ol (**46**),<sup>71</sup> allowed the definition of 6 $\beta$ /7 $\alpha$  orientation in **55**. The inverted configuration at C-7 in **54** was first suggested from H-7 signal shape, a dd ( $\delta_{\text{H}}$  3.67,  $J = 8.7, 4.7$  Hz) in <sup>1</sup>H NMR with a large coupling constant with H-8, confirming their *trans* diaxial relationship and the  $\beta$ -orientation of the hydroxyl group at C-7. Definitive confirmation derived from C-14 chemical shift at  $\delta_{\text{C}}$  57.6, invariably down-fielded shifted respect to the corresponding 7 $\alpha$ -hydroxycholane derivatives.<sup>71</sup> Of interest, the above protocol was unsuccessful in preparing 6 $\beta$ -ethyl C-24 carboxylic acid derivatives. In fact, the basic conditions for the hydrolysis at C-24 methyl ester invariably produced complete epimerization at C-6 forming the more stable thermodynamically 6 $\alpha$ -ethyl isomer of **73**, thus producing the formation of 6 $\alpha$ -ethyl-cholanoic acid derivatives.

## 2.4 PREPARATION OF 3 $\beta$ -HYDROXY-6-ETHYLCHENOCHOLANE DERIVATIVES

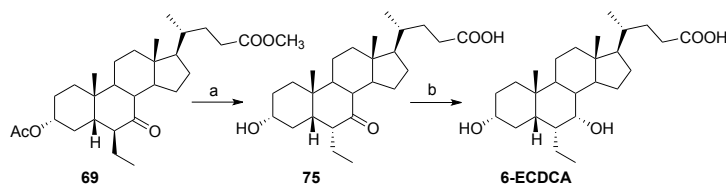


**Scheme 9. Preparation of 3 $\beta$ -hydroxy-6-ethylchenocholane derivatives (subset B).** a) CH<sub>3</sub>COOK, DMF:H<sub>2</sub>O 5:1 v/v; b) NaOMe, MeOH, 74% over two steps; c) LiBH<sub>4</sub>, MeOH dry, THF dry, 0 °C, 58%; d) NaOH, MeOH:H<sub>2</sub>O 1:1 v/v; e) LiBH<sub>4</sub>, MeOH dry, THF dry, 0 °C, 74% over two steps; f) DMT-MM, Et<sub>3</sub>N, taurine, DMF dry; g) NaBH<sub>4</sub>, MeOH dry; h) LiBH<sub>4</sub>, MeOH dry, THF dry, 0 °C, 74% over three steps.

As previously demonstrated, modification at C-3 exerts a great impact on BAs selectivity towards FXR and GPBAR1. In particular, as proved for the removal of 3 $\alpha$ -hydroxyl group, also the isomerization of the same function on LCA scaffold robustly attenuated the agonistic activity on GPBAR1. In fact, isoLCA resulted less potent compound than LCA in transactivating GPBAR1,<sup>71</sup> whereas isochenodeoxycholic acid (iso-CDCA) resulted more potent than CDCA in transactivating FXR and was devoid of any activity towards GPBAR1.<sup>71</sup> With this background in mind, we expanded our library producing the corresponding 3 $\beta$ -hydroxyl derivatives **56-60** (Scheme 9). Treatment with potassium acetate in DMF/H<sub>2</sub>O on intermediate **72** produced inversion at C-3 position on ring A. At this point two divergent protocols have been performed.

First, treatment over night with MeONa/MeOH gave intermediate **74** (74% over two steps), with the  $\alpha$ -configuration of the ethyl group at C-6 that was used as starting material in the synthesis of derivatives **56-60**. In detail, alkaline hydrolysis followed by LiBH<sub>4</sub> treatment gave a mixture of **58** and the corresponding 7 $\beta$ -hydroxyl derivative **59**, in a small amount, efficiently separated by HPLC. A small amount of **58** was tauro-conjugated with the formation of derivative **60** in good chemical yield. In parallel, LiBH<sub>4</sub> reduction on **74** furnished

alcohol **56** and a small amount of the corresponding epimer 6 $\alpha$ -ethyl-3 $\beta$ ,7 $\beta$ -dihydroxy-5 $\beta$ -cholan-24-ol (**57**). In the second protocol, NaBH<sub>4</sub> and then LiBH<sub>4</sub> treatment on **72**, as starting material, were used for the preparation of **61** and **62** as a mixture, efficiently purified in HPLC. Finally methyl ester **69** was also used for the preparation of 6-ECDCA (**3**), the reference compound used in the pharmacological evaluation of our library of 6-ethylcholine derivatives (Scheme 10). Prolonged basic treatment (NaOH, MeOH:H<sub>2</sub>O 1:1) on **69** furnishing the concomitant side chain methyl ester hydrolysis, de-acetylation at C-3 and inversion at C-6 ethyl group. Finally, LiBH<sub>4</sub> treatment on intermediate **75** furnished 6-ECDCA (**3**), in 69% yields over two steps.



**Scheme 10.** a) NaOH, MeOH:H<sub>2</sub>O 1:1 v/v; b) LiBH<sub>4</sub>, MeOH dry, THF dry, 0 °C, 69% over two steps.

## 2.5 PHARMACOLOGICAL EVALUATION OF 3-DEOXY AND 3 $\beta$ -HYDROXY DERIVATIVES

### 2.5.1 *In vitro* pharmacological evaluation

Derivatives **48-62** were tested on FXR and GPBAR1, in a luciferase reporter assay using HepG2 and HEK-293T cells, which were previously transfected with responsive elements for FXR and GPBAR1, respectively (Figures 30 and 31). As reported in Figure 30 A, all compounds with 6 $\alpha$ /7 $\alpha$ -configuration (**48**, **50**, **51** in subset A and **56**, **58** in subset B) were potent FXR agonists. In particular, in this group of compounds with a 6 $\alpha$ /7 $\alpha$  stereochemical arrangement, the presence of a negative charge on side chain (for example carboxyl or sulfate groups) improved their activity on FXR. In fact, compound **51** and the sulfate derivative **50** resulted potent FXR activators, whereas the alcoholic function at C-24 improved the effect of the corresponding 3 $\beta$ -hydroxyl derivatives on FXR (comparison between **51-58** and **56-48**). Of interest, substitutions on ring B in  $\beta$ -configuration (C-6 $\alpha$ /C-7 $\beta$  or C-6 $\beta$ /C-7 $\alpha$ ) produced a strong decrease in FXR activity.

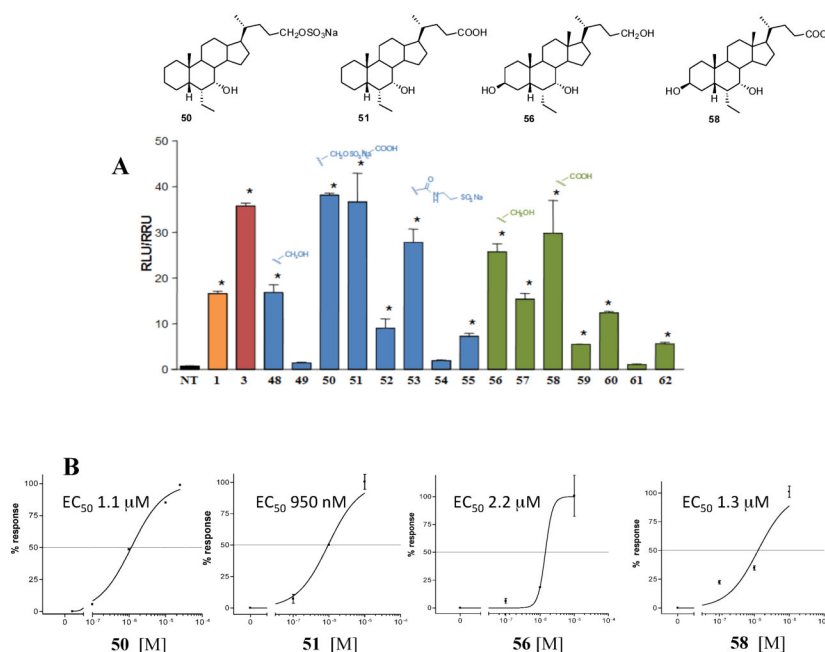


**Figure 30. Transactivation assays on FXR.** A) HepG2 cells were transfected with pSG5-FXR, pSG5-RXR, pCMV- $\beta$ gal, and p(hsp27)TKLUC vectors. Cells were stimulated with compounds **48-62** (10  $\mu$ M). CDCA (**1**, 10  $\mu$ M) and 6-ECDCA (**3**, 1  $\mu$ M) were used as a positive control. Results are expressed as mean  $\pm$  standard error; \*p < 0.05 *versus* not treated cells (NT); B) Concentration-response curve of **50**, **51**, **56** and **58** on FXR in a luciferase reporter assay using HepG2 cells transfected with FXR. Twenty-four hour post transfection cells were stimulated with increasing concentrations of each agent: range from 100 nM to 10  $\mu$ M.

In detail, once again, the activity is related to the nature of the functional end-group on the side chain and to the presence/absence of the hydroxyl group at C-3. In fact, the C3-deoxy/C24-alcohol derivative **49**, with the C-6 $\alpha$ /C-7 $\beta$ -configuration, was completely inactive towards FXR, whereas the corresponding carboxylic acid **52**, even though less potent than CDCA (**1**), maintained a considerable activity. Different is the behavior of the corresponding 3 $\beta$ -hydroxyl derivatives, in which the presence of the alcoholic end-group on the side chain improved their FXR activity (compare **57** vs **59**). At the end, the complete loss of activity for compounds **54** and **61** evidenced that the presence of a 6 $\beta$ /7 $\beta$  stereochemical arrangement, is detrimental in terms of FXR activation (Figure 30 A). The relative potency of the most interesting members (**50**, **51**, **56** and **58**) of this library was then investigated by a careful measurement of their concentration-response curves. As illustrated in Figure 30 B, compounds **50**, **51**, **56** and **58** transactivated FXR with an EC<sub>50</sub> of 1.1  $\mu$ M, 950 nM, 2.2  $\mu$ M and 1.3  $\mu$ M respectively, with compound **51** showing a comparable potency with the reference compound, 6-ECDCA (EC<sub>50</sub>=500 nM, Figure 31).

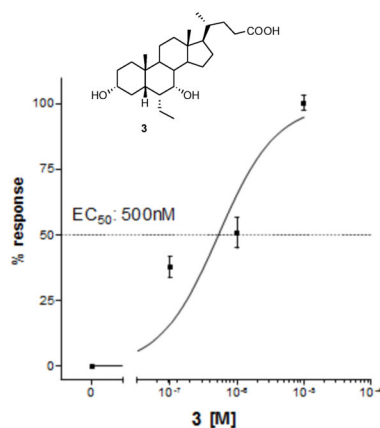


**Figure 31.** Concentration-response curve of 6-ECDCA (**3**) on FXR in a luciferase reporter assay using HepG2 cells transfected with FXR. Twenty-four hour post transfection cells were stimulated with increasing concentrations of **3**: range from 100 nM to 10  $\mu$ M. Results are expressed as mean  $\pm$  standard error.

Notable, the ability to transactivate FXR was also maintained by the corresponding tauro-conjugated **53** (Figure 30 A, compare **51** vs **53**), thus confirming the potential clinical application of 6 $\alpha$ -ethyl-7 $\alpha$ -hydroxy-5 $\beta$ -cholan-24-oic acid (**51**) in FXR-mediated disorders. On the contrary, the tauro-conjugate derivative of the carboxylic acid **58**, showed a considerable decrease in FXR



activity (tauro-conjugates **60** vs carboxyl acid **58** in Figure 30 A). This demonstrated that a longer negative charged side chain was detrimental in terms of FXR activation in presence of a 3 $\beta$ -hydroxyl group and this aspect strongly reduces the possible therapeutic impact of compound **58**. The efficacy of the more active compounds in FXR transactivation was also measured in Alphascreen assay, in order to evaluate the recruitment of the coactivator SRC-1 for FXR. In this assay, 6-ECDCA (**3**) was used as positive control and its effect was set at 100% (Figure 32). Among all derivatives tested, 6 $\alpha$ -ethyl-7 $\alpha$ -hydroxy-5 $\beta$ -cholan-24-oic acid (**51**), 6 $\alpha$ -ethyl-3 $\beta$ ,7 $\alpha$ -dihydroxy-5 $\beta$ -cholan-24-ol (**56**) and the corresponding carboxylic acid, 6 $\alpha$ -ethyl-3 $\beta$ ,7 $\alpha$ -dihydroxy-5 $\beta$ -cholan-24-oic acid (**58**) resulted very potent in the recruitment of SRC-1 co-activator and presented an high affinity to FXR, almost comparable with the reference molecule **3**.

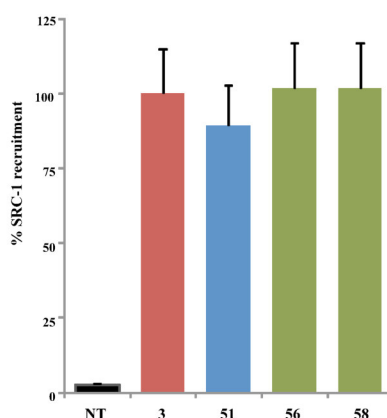


**Figure 32. Coactivator recruitment assay measuring a direct interaction of FXR with SRC-1.** Anti-GST-coated acceptor beads captured GST-fusion FXR-LBD and the biotinylated-SRC-1 peptide was captured by the streptavidin donor beads. FXR-LBD recruited SRC-1 in the presence of ligand at 2  $\mu$ M and, upon illumination at 680 nm, chemical energy is transferred from donor to acceptor beads across the complex streptavidin-donor/Src-1-biotin/ligand/GSTFXR-LBD/anti-GST-acceptor and a signal is produced. Results are expressed as percentage of the effect of **3** arbitrarily settled as 100%. NT is referred to the experiment carried out in absence of ligand. Results are expressed as mean  $\pm$  standard error.

Results of transactivation on CREB-responsive elements in HEK-293T transiently transfected with the membrane bile acid receptor GPBAR1 (Figure 33 A), revealed that the modifications at C-3 hydroxyl group shift the selectivity towards FXR. In fact, independently of the stereochemical arrangement on C6/C7 and of the presence/absence of the hydroxyl group at C-3, all compounds produced in this study are less potent than TLCA (**2**) in transactivating GPBAR1. Of interest are the results on compound **51**, devoid of any activity on GPBAR1 in agonistic

mode. When administered in presence of 10  $\mu\text{M}$  TLCA (**2**), compound **51** showed inhibitory activity against GPBAR1 transactivation induced by TLCA (Figure 33 B). The above result was also confirmed by a concentration-response curve on HEK-293T transiently transfected with GPBAR1, revealing for **51** an  $\text{IC}_{50}$  value of 11  $\mu\text{M}$ . This result affirms **51** as the first example of 6-ethylcholanoic acid derivative with potent FXR agonistic activity and antagonistic effect on GPBAR1. This discovery opens the way to further speculations. At first, starting from this result, we thought to test the *in vivo* effects of this compound in the identification of a new lead compound in the treatment of FXR-mediated liver disorders, in which the concomitant activation of GPBAR1 is associated with several unwanted effects. Second, compound **51** could represent a useful constituent of research on BAs scaffolds, in the effort to shed light on the complex physiological pathways under GPBAR1 control.

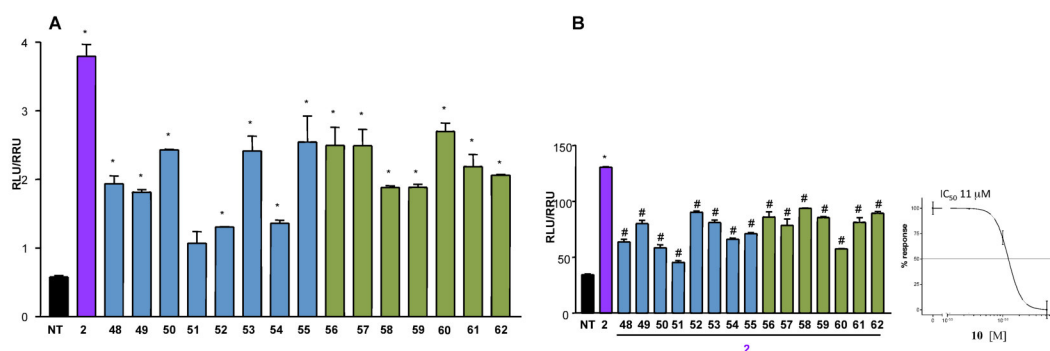


**Figure 33. A) Agonism on GPBAR1 by transactivation assays.** HEK-293T cells were co-transfected with GPBAR1 and a reporter gene containing a cAMP responsive element in front of the luciferase gene. Twenty-four hour post transfection cells were stimulated with **48-62** (10  $\mu\text{M}$ ). Luciferase activity served as a measure of the rise in intracellular cAMP following activation of GPBAR1. TLCA (**2**, 10  $\mu\text{M}$ ) was used as a positive control. Results are expressed as mean  $\pm$  standard error. \* $p < 0.05$  versus not treated cells (NT). **B) Antagonism on GPBAR1 by transactivation assays.** HEK-293T cells were transfected as described in Figure 33. 24 hours post transfection cells were stimulated with 10  $\mu\text{M}$  TLCA (**2**) alone or in combination with 25  $\mu\text{M}$  compounds **48-62**. # $p < 0.05$  versus TLCA stimulated cells; concentration-response curve of **51** on GPBAR1 in combination with TLCA (**2**, 10  $\mu\text{M}$ ) and with increasing concentrations of **51** range from 5 to 25  $\mu\text{M}$ . Results are expressed as mean  $\pm$  standard error.

### 2.5.2 *In vivo* pharmacological evaluation

To further investigate the potency of interaction of compound **51** on FXR, we tested its ability to regulate FXR canonical functions in an ex-vivo Real-time PCR assay. Initially, C57BL6 mice were administered with compound **51** (15 mg/kg, ip). At 6 h post-treatment, livers and blood were collected. As shown in Figure 34,

compound **51** significantly up-regulated the mRNA expression of FXR target genes such as OST $\alpha$ , SHP and BSEP in the liver exposed for 6 h to **51** (\* $p$ <0.05 versus control mice). Because these three genes are endowed with canonical FXR-responsive elements in their promoter, their expression is in full agreement with the profile of compound **51** as a potent FXR ligand. Furthermore, this view was confirmed by the analysis of bile acid levels in the blood of mice after the administration of compound **51**. As depicted in Figure 35, the exposure to this agent induced the reduction of both total and single un-conjugated bile acids, while the quote of tauro-conjugated tMu, tCA, tHCA, tCDCA, tDCA and tLCA was identical (Figure 35, \* $p$ <0.05 versus control mice). Moreover, compound **51** was only found in the conjugated form with taurine (data not shown).

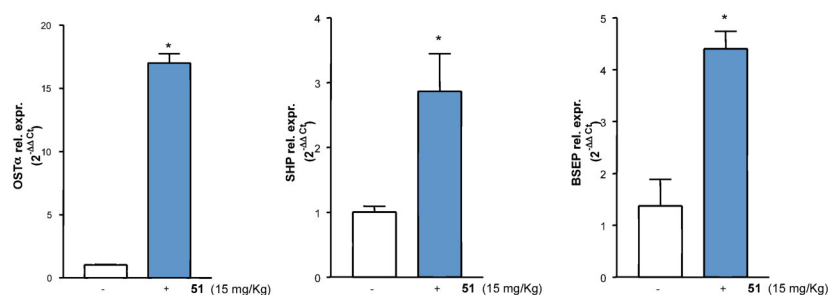


**Figure 34. In vivo effect of 51 on FXR target genes.** C57BL6 mice were administered with **51** (15 mg/kg) for 6 h. After treatment liver were removed and the relative mRNA expression of OST $\alpha$ , SHP and BSEP was assayed by quantitative Real-Time PCR. \* $p$ <0.05 versus control mice.

Finally, to further confirm its FXR agonistic profile, **51** resulted able to reduce the blood concentrations levels of 7 $\alpha$ -hydroxy-4-cholesten-3-one (Figure 35 D), a key intermediate in the synthesis of primary bile acids. This reduction in mice stimulated with compound **51** further supports the fact that this compound represented a potent FXR agonist.

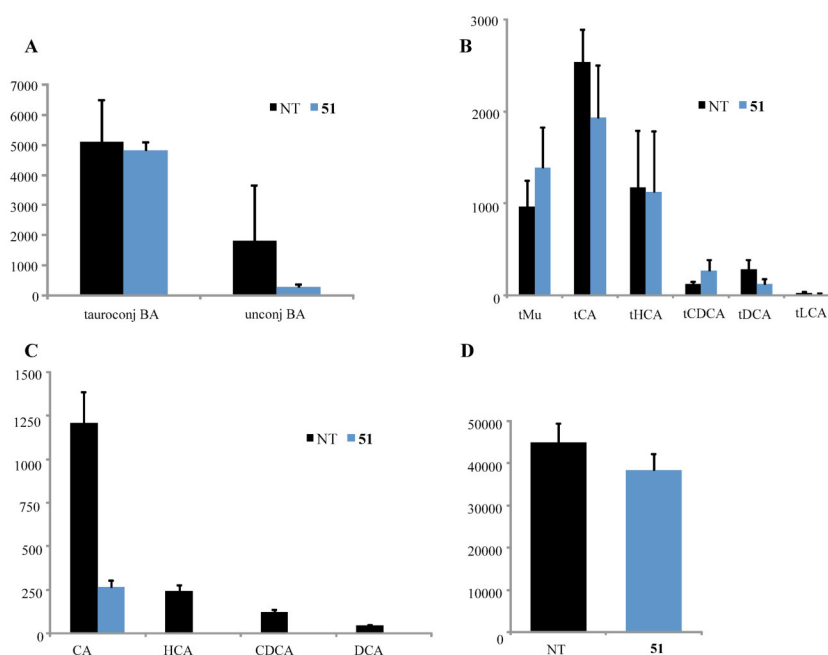


**Figure 35.** Blood concentrations of A) total tauro-conjugated and total unconjugated bile acids, B) individual conjugated and C) unconjugated bile acids, D)  $7\alpha$ -hydroxy-4-cholesten-3-one before and after *in vivo* administration of **51** at 15 mg/kg.

In summary, as medicinal chemistry on 6-ECDCA scaffold afforded in these years several derivatives,<sup>97,98</sup> which in most cases covered the same chemical space and were promiscuous towards FXR and GPBAR1, behaving as dual modulators,<sup>98</sup> in this report we have modified BAs scaffolds in order to produce a library of 6-ethylcholane derivatives with peculiar activity towards FXR and GPBAR1. In way of exception, we obtained selective FXR and GPBAR1 ligands such as compound **45**,<sup>71</sup> a selective GPBAR1 ligand and compound **51**, a potent FXR agonist with also a GPBAR1 antagonistic activity.<sup>99</sup>

From a SAR perspective, our modifications have been focused on three specific areas:

1. Modifications at C-3 hydroxyl group (removal/inversion) on the 6-ethylcholane scaffold
2. Modifications of the end-group on side chain
3. Modifications of configurations at C6/C7 substituents on ring B.

The first observation to be draw is that all 6-ethylcholane derivatives prepared in this study were weak GPBAR1 agonists, with the exception of C-24 alcohol **45**, with maintained the  $3\alpha$ -OH group; thus affirming the key pharmacophoric role of this function in GPBAR1 activation. The second observation was that the

presence of both substituents on ring B in  $\alpha$ -configuration produced potent FXR agonists (such as compounds **50**, **51**, **56** and **58**).<sup>100</sup> Compound **45** (EUDCOH or BAR501) represented the first example of UDCA derivative with a  $\beta$ -ethyl group at C-6. Results of its transactivation demonstrated that it was devoid of any FXR agonistic activity as its precursor UDCA. However, when compared with UDCA, EUDCOH (**45**) resulted more potent on GPBAR1 and able to stimulate the expression of pro-glucagon mRNA in GLUTAg cells and consequently to produce GLP-1. The increased production of this hormone (GLP-1) by **45** could be an important effect in the regulation of glucose levels in the diabetes.<sup>101</sup> Moreover EUDCOH (**45**) has been subjected to a thorough pharmacological investigation showing a protective effect against liver cirrhosis. Differently, compound **44**, which belonged to the same series, with both ethyl and the hydroxyl groups on ring B in  $\alpha$ -configuration, resulted a dual agonist. Among the second library, 3-deoxycholanoic compounds **50** and **51** (subset A), differing in the nature of side chain end-group (sulfate in **50** and carboxylic acid in **51**), presented potency on FXR comparable with the 6-ECDCA (**3**), with  $EC_{50}$  values of 1.1  $\mu$ M and 950 nM, respectively. The same potency was shared by the corresponding 3 $\beta$ -hydroxyl carboxylic acid **58** ( $EC_{50}$  value of 1.3  $\mu$ M, subset B).

Their *in vitro* and *in vivo* pharmacological characterization has led to the discovery of compound **51** as first example of selective FXR agonist. Its therapeutic use could have a potential utility in the treatment of cholestasis and other FXR-mediated disorders, avoiding side effects due to the unwanted activation of GPBAR1.

### CHAPTER 3 6-ETHYLNORCHOLANE AND BIS-HOMO-6-ETHYLCHOLANE DERIVATIVES

In this section, the preparation and the pharmacological characterization of a large family of 6-ethylcholane derivatives modified in the length of the side chain will be discussed. Firstly, we started with the synthesis of derivatives **76-78**, sharing the typical 6-ECDCA scaffold, with the two hydroxyl groups in  $\alpha$ -configuration at C-3 and C-7, but characterized to one carbon less on side chain (Figure 36).

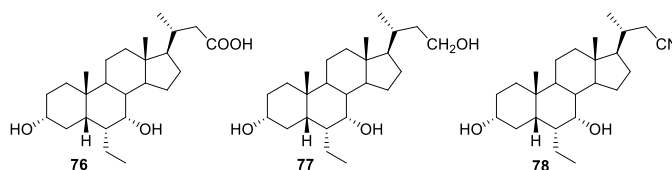


**Figure 36.**  $3\alpha,7\alpha$ -dihydroxy-6-ethylnorcholane derivatives

In addition, we also decided to manipulate the stereochemical arrangement at C-6/C-7 positions as well as the substituent/configuration at C-3 and the nature of the side chain (OH, COOH or  $\text{CH}_2\text{OSO}_3^-$ ), producing another small library of C23 6-ethylcholane derivatives (**79-87**), which have been explored in term of potency/selectivity towards FXR and GPBAR1 (Figure 37).

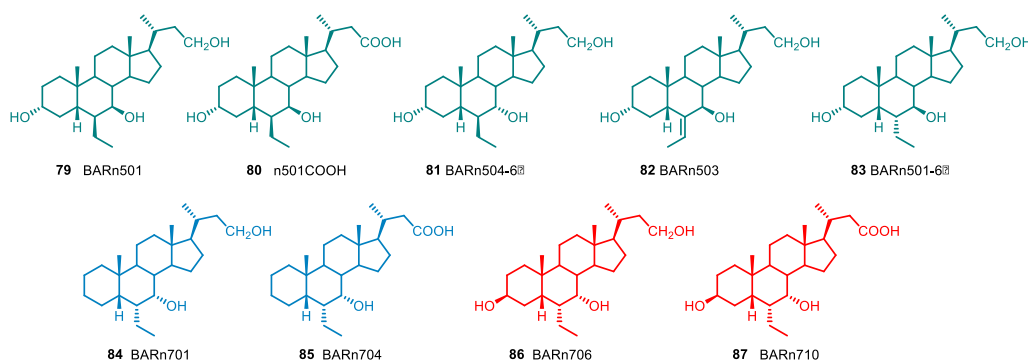


**Figure 37.** 6-Ethylnorcholane derivatives generated in this study.

Finally, the chemodiversity of available bile acid receptor modulators was further expanded, preparing bis-homo-6-ethylcholane derivatives **88-91** (Figure 38).

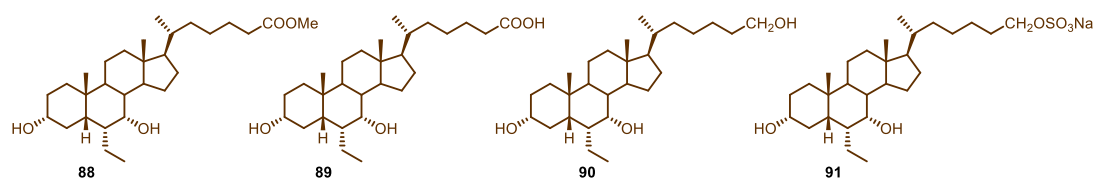
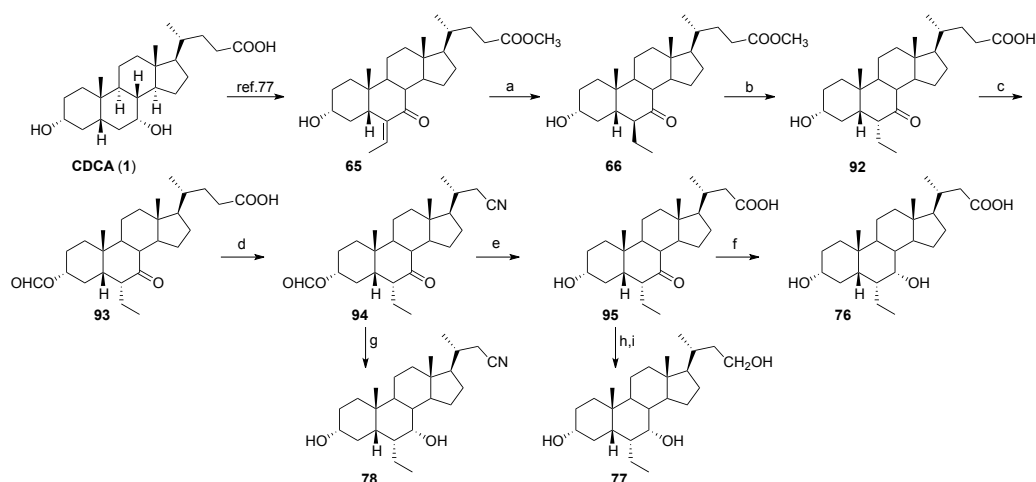


**Figure 38.** Bis-homo-6-ethylcholan-24-yl derivatives generated in this study.

Thorough pharmacological investigation resulted in the identification of several interesting molecules with differentiated activity profiles ranging from dual modulation to selective agonism towards FXR and /or GPBAR1. Among all compounds prepared in this study, the best hit, compound **77**, a dual modulator, has been patented with the name of BAR502.

### 3.1 PREPARATION OF 3 $\alpha$ ,7 $\alpha$ -DIHYDROXY-6-ETHYLNORCHOLANE DERIVATIVES

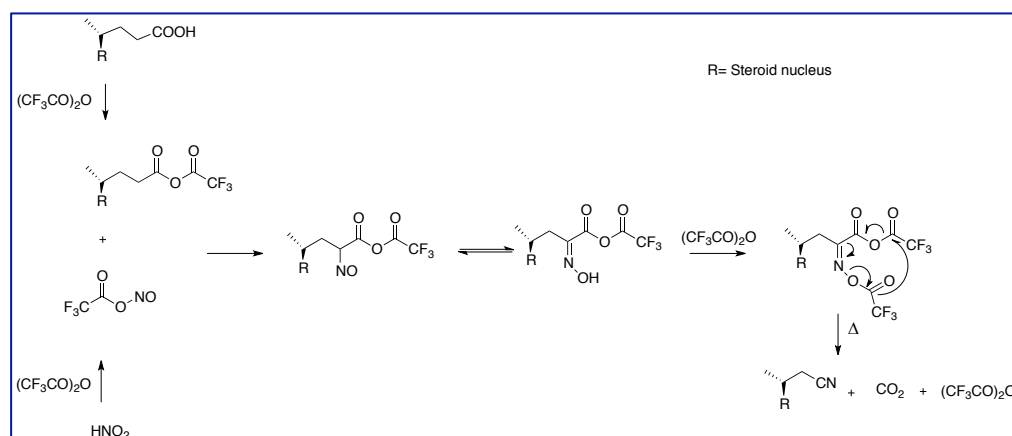


**Scheme 11. Modification on the side chain of 6 $\alpha$ -ethylcholan-24-yl scaffold.** a) H<sub>2</sub>, Pd/C, THF/MeOH 1:1, quantitative yield; b) NaOH 5% in MeOH/H<sub>2</sub>O 1:1 v/v, quantitative yield; c) HCOOH, HClO<sub>4</sub>, 81%; d) TFA, trifluoroacetic anhydride, NaNO<sub>2</sub>; e) KOH 30% in MeOH/H<sub>2</sub>O 1:1 v/v, 86% over two steps; f) LiBH<sub>4</sub>, MeOH dry, THF dry, 0 °C, 89%; g) LiBH<sub>4</sub>, MeOH dry, THF dry, 0 °C, 79%; h) *p*-TsOH, MeOH dry; i) LiBH<sub>4</sub>, MeOH dry, THF, 0 °C, 98% over two steps.

CDCA was alkylated as previously described to obtain the key intermediate **65**.<sup>71</sup> Exocyclic double bond hydrogenation (H<sub>2</sub> on Pd/C) followed by alkaline hydrolysis of methyl ester group on side chain, afforded the 3 $\alpha$ -hydroxy-6 $\alpha$ -ethyl-7-keto-5 $\beta$ -cholan-24-oic acid **92** in quantitative yield. The prolonged alkaline hydrolysis with NaOH 5% in H<sub>2</sub>O:MeOH induced the epimerization at C-6 with

the exclusive formation of the  $\alpha$ -isomer at C-6. In compound **92**, H-6 proton signal at  $\delta_{\text{H}}$  2.83 presented a large coupling constant (dd,  $J = 13.0, 5.5$  Hz) and this demonstrated its axial disposition and as consequence the  $\alpha$ -orientation of the ethyl group on C-6. Then, Fischer's esterification on derivative **92** with formic acid and acetic anhydride<sup>102,103</sup> formed the derivative protected at C-3 (**93**) in 81% yield, which was subjected to "Beckmann rearrangement" using sodium nitrite in trifluoroacetic anhydride and trifluoroacetic acid (Scheme 11).<sup>104</sup>

This mechanism of reaction is concerted, and provided an initial reaction between the carboxyl function at C-24 and the trifluoroacetic acid (TFA) to form a mixed anhydride, essential for the activation of the carbon in  $\alpha$  position at the carboxyl group, and the subsequent nitrosation, realized by a carrier of NO. This last compound is the trifluoro acetyl nitrite, generated started from TFA and  $\text{NaNO}_2$ , which in strong acidic condition ( $\text{HClO}_4$ ) produced nitrous acid ( $\text{HNO}_2$ ). The product of nitrosation reaction is  $\alpha$ -nitroso anhydride, which gives tautomerism forming an oxime, that after the interaction with trifluoroacetic anhydride (TFAA), results acetylated. Finally, heating results in the formation of nitrile through a concerted mechanism as shown in Scheme 12. To prevent the hydrolysis of the formyl group, the temperature of reaction was set at 38-40°C (Scheme 12).



**Scheme 12.** Mechanism of Beckmann rearrangement

The resulting nor-nitrile **94** was subjected to  $\text{LiBH}_4$  reduction at C-7 carbonyl group, affording 6 $\alpha$ -ethyl-3 $\alpha$ ,7 $\alpha$ -dihydroxy-24-nor-5 $\beta$ -cholan-23-nitrile or NorECDCN (**78**) in 79% yield as single diastereoisomer (HPLC purity >95%). Nor-nitrile **94** was also used in the preparation of compound **76** and the



corresponding alcohol **77**. Prolonged alkaline hydrolysis with KOH 30% in MeOH:H<sub>2</sub>O 1:1 furnished the 6 $\alpha$ -ethyl-24-nor-7-keto-lithocholic acid (**95**) in 86% yield over two steps, that was subjected as crude reaction product, to LiBH<sub>4</sub> reduction at C-7. Purification by silica gel (CH<sub>2</sub>Cl<sub>2</sub>:MeOH 9:1) gave NorECDCA (**76**) as a white solid in 89% chemical yield. Analysis of <sup>1</sup>H NMR spectrum revealed that the lithium borohydride reduction evolved in a stereoselective manner, affording the exclusive production of 3 $\alpha$ ,7 $\alpha$ -dihydroxy-6 $\alpha$ -ethyl-24-nor-5 $\beta$ -cholan-23-oic acid as confirmed by the shape of H-7 (3.62, br s), in agreement with the equatorial disposition of this proton, and therefore with the  $\alpha$ -orientation of the hydroxyl group. Fischer's esterification on intermediate **95** followed by concomitant reduction on C-23 methyl ester group and on C-7 position, afforded compound NorECDCOH (**77**) in 98% yield. In this case, no epimerization was observed, precluding the obtainment of alternative configurations at C-6 and C-7 on 6-ethylnorcholane scaffold.

### 3.1.1 PHARMACOLOGICAL EVALUATION OF 3 $\alpha$ ,7 $\alpha$ -DIHYDROXY-6-ETHYLNORCHOLANE DERIVATIVES

Compounds **76-78** were tested for their activities on FXR and GPBAR1 in a luciferase reporter assay using HepG2 and HEK-293T cells transfected with responsive elements for FXR and GPBAR1, respectively (Figure 39).

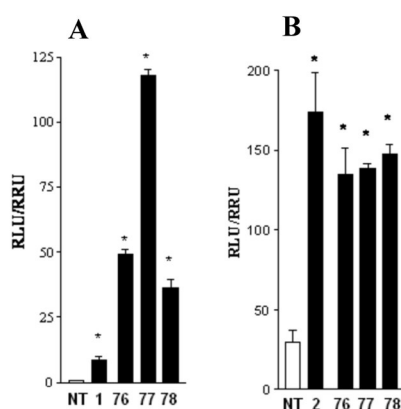


**Figure 39. Transactivation assays on FXR and GPBAR1.** (A) HepG2 cells were transfected with pSG5-FXR, pSG5-RXR, pCMV- $\beta$ gal, and p(hsp27)TKLUC vectors. Cells were stimulated with compounds **76-78** (10  $\mu$ M). CDCA (**1**, 10  $\mu$ M) was used as a positive control. Results are expressed as mean  $\pm$  standard error; \* $p$  < 0.05 versus not treated cells (NT). (B) HEK-293T cells were co-transfected with GPBAR1 and a reporter gene containing a cAMP responsive element in front of the luciferase gene. Twenty-four hour post transfection cells were stimulated with **76-78**

(10  $\mu\text{M}$ ). Luciferase activity served as a measure of the rise in intracellular cAMP following activation of GPBAR1. TLCA (**2**, 10  $\mu\text{M}$ ) was used as a positive control. Results are expressed as mean  $\pm$  standard error. \* $p < 0.05$  versus not treated cells (NT).

As shown in the Figure 39 (panels A and B), the analysis of the biological results of these compounds confirmed, as observed in the previous work for the C24 6-ethyl derivatives,<sup>99</sup> that the  $\alpha$ -configuration at C-6 and C-7 positions represented a key structural feature for FXR activity. In particular, of interest, were the pharmacological results on compound (**77**), the corresponding nor-derivative of **44**,<sup>71</sup> that resulted the most potent FXR agonist generated in this study, even if it showed a residual GPBAR1 activity. The activity of compound **77** was completely modified replacing the C-23 alcoholic function with a carboxyl or a nitrile group in **76** and **78**, respectively, demonstrating a clear shift of their selectivity towards GPBAR1.

### 3.1.2 Pharmacological evaluation on NorECDCOH (**77**)

#### *In vitro*

Among the C23 6-ethyl compounds tested, NorECDCOH (**77**) represents a promising template to consider for further pharmacological experimentations. In Alphascreen assay, compound **77** was demonstrated very potent in the recruitment of SRC-1 co-activator with an efficacy comparable to that of 6-ECDCO (**3**). Differently, compounds **76** and **78** showed a moderate recruitment of SRC-1. Successively, the specific potency of derivative **77** was investigated by a careful measurement of its concentration-response curve on FXR and GPBAR1 transactivation. As illustrated in Figure 40 panel B, **77** was able in transactivating FXR with an  $\text{EC}_{50}$  of 2  $\mu\text{M}$ , while transactivates GPBAR1 with an  $\text{EC}_{50}$  of 0.4  $\mu\text{M}$  (panel C), demonstrating its dual activity. Also, the selectivity was evaluated, testing its activity on other nuclear receptors, such as GR, PPAR $\gamma$ , LXR and PXR (Figure 41). As illustrated in Figure 41, panels A-C, compound **77** at the concentration of 10  $\mu\text{M}$  failed to transactivate GR, PPAR $\gamma$  and LXR. Differently, the results of panel D confirmed its activity on nuclear receptor PXR. In order to elucidate the effective activity of this compound, we have analyzed its ability to regulate FXR and GPBAR1 canonical functions.

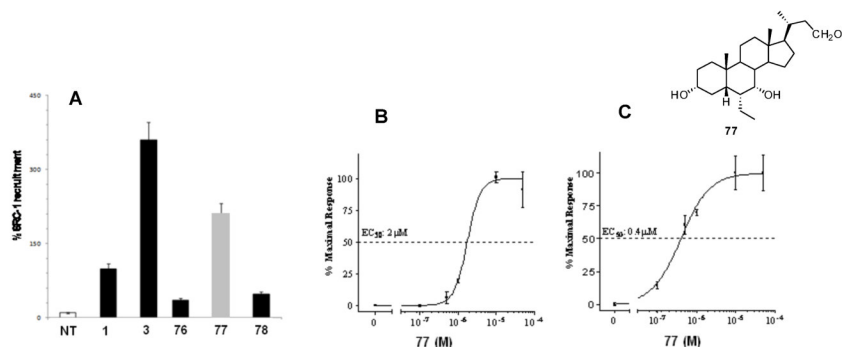


**Figure 40.** Concentration-response curve of **77** on FXR (A) and GPBAR1 (B). FXR transactivation was measured in a luciferase reporter assay using HepG2 cells transfected with FXR. GPBAR1 activity was measured in HEK-293T cells co-transfected with GPBAR1 and a reporter gene containing a cAMP responsive element in front of the luciferase gene (CRE). Twenty-four hour post transfection cells were stimulated with increasing concentrations of each agent: range from 100 nM to 50  $\mu$ M. Results are expressed as mean  $\pm$  standard error. \* $p < 0.05$  versus not treated cells (NT). (C) Coactivator recruitment assay measuring a direct interaction of FXR with Src-1. Anti-GST-coated acceptor beads captured GST-fusion FXR-LBD and the biotinylated-SRC-1 peptide was captured by the streptavidin donor beads. FXR-LBD recruited SRC-1 in presence of ligand at 4  $\mu$ M and, upon illumination at 680 nm, chemical energy is transferred from Donor to Acceptor beads across the complex streptavidin-Donor/Src-1-Biotin/ligand/GSTFXR-LBD/Anti-GST-Acceptor and a signal is produced. Results are expressed as percentage of the effect of CDCA (**1**) arbitrarily settled as 100%. NT is referred to the experiment carried out in absence of ligand. Results are expressed as mean  $\pm$  standard error.

As shown in Figure 42 (panels A-E), **77** was able to induce both the expression of pro-glucagon mRNA in GLUTAg cells and to increase cAMP intracellular concentration in THP-1 cells, but also to induce the expression of FXR target genes (OST $\alpha$ , BSEP and SHP). Therefore, these results confirmed that compound **77** is endowed with an agonistic profile on FXR and GPBAR1 receptors, behaving as dual modulator.

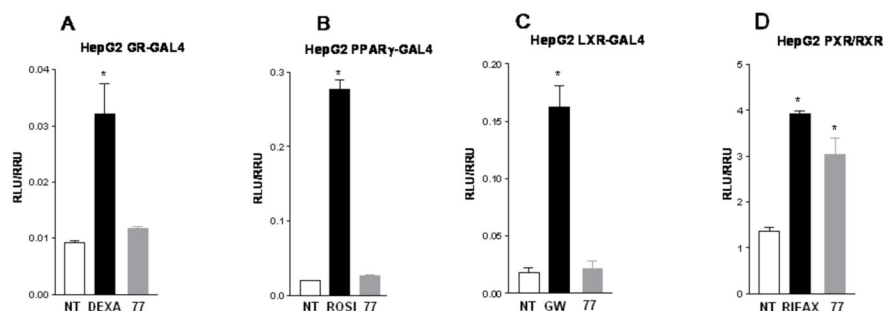


**Figure 41. Specificity of 77 on other nuclear receptors.** (A) (B) and (C) HepG2 cells were co-transfected with the Gal4 luciferase reporter vector and with a series of chimeras in which the Gal4 DNA binding domain is fused to the LBD of the indicated nuclear receptors. Cells were treated 18 h with the specific agonists (10  $\mu$ M) or with **77** (10  $\mu$ M). (D) HepG2 cells were co-transfected with pSG5-PXR, pSG5-RXR and with the reporter pCYP3A4promoter-TKLuc and then stimulated with rifaximin (10  $\mu$ M), a PXR agonist, or with **77** (10  $\mu$ M). Data are the mean  $\pm$  S.E. of three experiments. \* $p < 0.05$  versus not treated cells (NT). DEXA: Dexamethasone; ROSI: Rosiglitazone; GW: GW3965; RIFAX: Rifaximin.

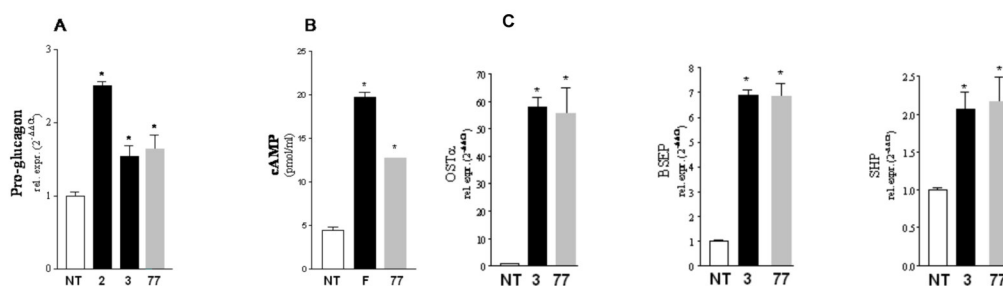


**Figure 42. In vitro pharmacological evaluation of GPBAR1 and FXR functions on 77.** (A) Real-time PCR analysis of mRNA expression of GPBAR1 target gene Pro-glucagon in GLUTAg cells primed with 77 (10 μM). TLCA (2) and 6-ECDCA (3) were tested as positive controls (10 μM). Values are normalized relative to GAPDH mRNA and are expressed relative to those of not treated cells (NT), which are arbitrarily set to 1: \* $p < 0.05$  versus not treated cells (NT). (B) Effect of 77 (10 μM) on intracellular generation of cAMP in THP-1 cells. The data are the mean  $\pm$  SE of three experiments: \* $p < 0.05$  versus not treated cells (NT). F: Forskolin 10 μM. OST $\alpha$  (C), BSEP (D) and SHP (E) mRNA expression in HepG2 cells primed with 77 (10 μM). 6-ECDCA (3) was tested as positive control (10 μM). Values are normalized relative to GAPDH mRNA and are expressed relative to those of not treated cells (NT), which are arbitrarily set to 1: \* $p < 0.05$  vs NT.

### *In vivo*

Compound 77 (or BAR502) was investigated in itching.<sup>49,105</sup> For this purpose, GPBAR1<sup>+/+</sup> and GPBAR1<sup>-/-</sup> mice were subjected to intradermal injection of BAR502, secondary bile acids (DCA and TLCA), oleanolic and betulinic acid.<sup>49</sup> In addition, mice were administered with a PAR2-agonist to evaluate if itching is a GPBAR1-dependent activity. As indicated in Figure 43 A, BAR502 caused a GPBAR1-mediated itching. Then, was also investigated if the pruritogenic response to GPBAR1 agonism was attenuated in a second treatment with the same agents. The results in Figure 43 B-D, shown that the pruritogenic effect of DCA, TLCA and betulinic acid was reduced approximate of 50% after the administration of their second dose. Because under cholestatic conditions bile acid accumulation cause the manifestation of a sever itching, was then investigated if BAR502, a dual bile acid ligand, trigger itching in a rodent model of cholestasis, induced by prolonged treatment with alpha-naphthyl isothiocyanate (ANIT). For this aim, GPBAR1<sup>-/-</sup> mice were treated with ANIT alone (25 mg/kg/day) or in combination with BAR502 (15 mg/kg/day) for 10 days.

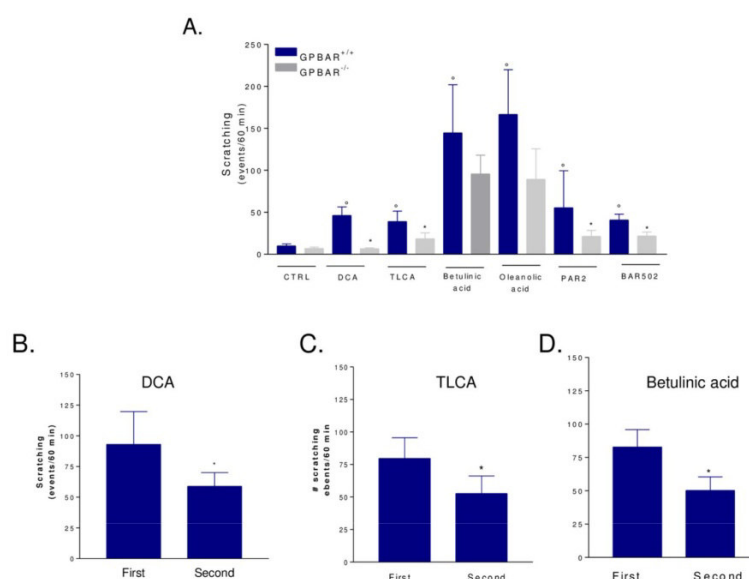


**Figure 43. Effects of BAR502 on scratching behavior in GPBAR1<sup>+/+</sup> and GPBAR1<sup>-/-</sup> mice.** (A) GPBAR1<sup>+/+</sup> and GPBAR1<sup>-/-</sup> mice were subjected to intradermal injection of DCA, TLCA, betulinic acid, oleanolic acid, PAR-2 agonist and BAR502. Each agent was tested at the dose of 25  $\mu$ g. Results are expressed as the number of scratching events during 60 minutes of observation. Results are the mean  $\pm$  SE of 4–8 mice per group.  $^{\circ}$ p<0.05 versus control group (CTRL); \*p<0.05 versus GPBAR1<sup>+/+</sup> mice. (B–D) Desensitization of the itching pathway by a second administration of a GPBAR1 ligand. Animals were administered DCA, TLCA or betulinic acid at the dose of 50  $\mu$ g. After counting scratching for 60 minutes animals were rechallenged with a second dose of the given agonist and the scratching response was recorded for a further 60 minutes of observation. Data are mean  $\pm$  SE of 6–7 animals per group. p>0.01 versus first dose.

Exposure to ANIT caused 100% of lethality at day 10 in GPBAR1<sup>-/-</sup> mice, while BAR502 administration saved mice from death. The scratching test was performed at day 5 and as shown in Figure 44, BAR502 failed to trigger itching. Moreover, ANIT treatment significantly increased total bilirubin and alkaline phosphatase levels in GPBAR1<sup>-/-</sup> respect GPBAR1<sup>+/+</sup> mice, but not plasma levels of AST. BAR502 attenuated the modifications of alkaline phosphatase and AST level, but had no effect on bilirubin level (Figure 45, panels A-B). At last, a histopathology examination shown that while ANIT caused a severe liver necrosis in GPBAR1<sup>-/-</sup> mice, this effect was reduced treating GPBAR1<sup>-/-</sup> and GPBAR1<sup>+/+</sup> mice with BAR502 (Figure 45, panel D).

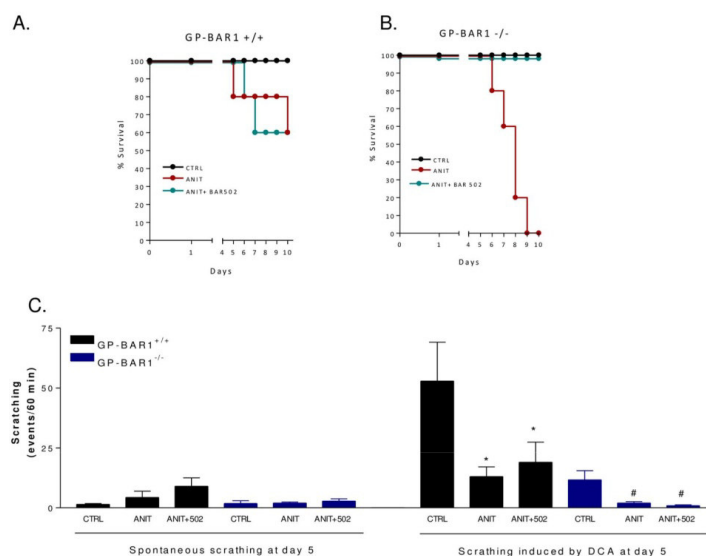


**Figure 44. Effects of BAR502 on scratching behavior in GPBAR1<sup>+/+</sup> and <sup>-/-</sup> mice administered with ANIT.** GPBAR1<sup>+/+</sup> and GPBAR1<sup>-/-</sup> mice were treated for 10 days with ANIT or with the combination of ANIT plus BAR502. At the end of the treatments mice were subjected to intradermal injection of DCA. (A-B) Survival of GPBAR1<sup>+/+</sup> and GPBAR1<sup>-/-</sup> mice in response to ANIT administration. (C) Effect of ANIT on spontaneous scratching and scratching induced by DCA. Scratching tests were performed at day 5. Results are expressed as the number of scratching events during 60 minutes of observation. Results are the mean  $\pm$  SE of 4–8 mice per group. \* $p < 0.05$  versus GPBAR1<sup>+/+</sup> mice subjected to intradermal injection of DCA. # $p < 0.05$  versus GPBAR1<sup>-/-</sup> mice subjected to intradermal injection of DCA.

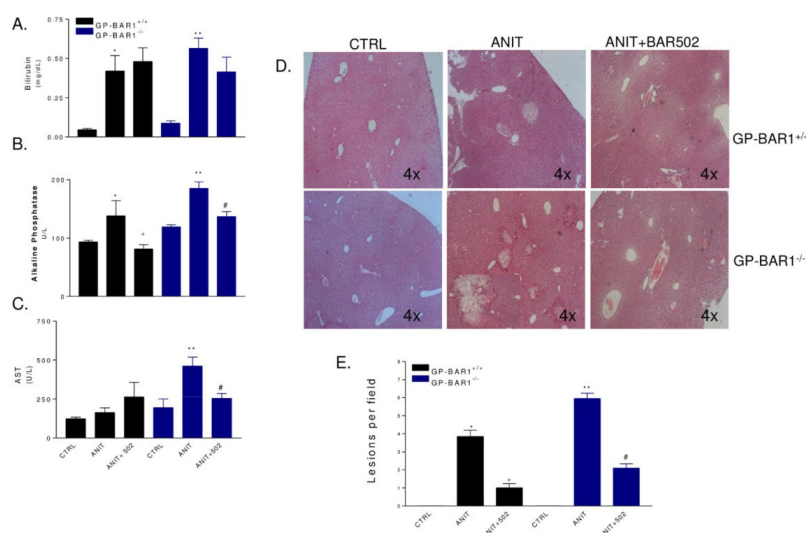


**Figure 45. Dual FXR/TGR5 agonist BAR502 improves liver injury in both GPBAR1<sup>+/+</sup> and GPBAR1<sup>-/-</sup> mice.** GPBAR1<sup>+/+</sup> and GPBAR1<sup>-/-</sup> mice were treated for 10 days with ANIT or with the combination of ANIT plus BAR502. Serum levels of (A) bilirubin, (B) alkaline phosphatase and (C) AST. Results are the mean  $\pm$  SE of 4–8 mice per group. \* $p < 0.05$  versus GPBAR<sup>+/+</sup> mice. ° $p < 0.05$  versus GPBAR1<sup>+/+</sup> mice treated with ANIT. \*\* $p < 0.05$  versus GPBAR1<sup>-/-</sup> mice. # $p < 0.05$  versus GP-BAR<sup>-/-</sup> mice administered with ANIT. (D) Representative histological pictures of H&E-stained livers. (E) Analysis of the number of lesions per field. Results are the mean  $\pm$  SE of 4–8 mice per group. \* $p < 0.05$  versus GPBAR1<sup>+/+</sup> mice. ° $p < 0.05$  versus GPBAR1<sup>+/+</sup> mice treated with

ANIT. \*\* $p < 0.05$  versus GPBAR1<sup>-/-</sup> mice. # $p < 0.05$  versus GPBAR1<sup>-/-</sup> mice administered with ANIT.

### 3.1.2.1 Preliminary advanced pharmacological results of 77

In a recent study BAR502 was evaluated in NASH. Non-alcoholic fatty liver disease (NAFLD) and steatohepatitis (NASH) are two prevalent human disorders, which don't present a specific treatment.<sup>106</sup> In fact, NASH is correlated with other complications such as obesity, insulin resistance, dyslipidemia, cardiovascular disorders, cirrhosis and hepatic carcinoma.<sup>107-109</sup> In the rodent model of NASH, HFD and fructose were administered to C57BL6 mice for 18 weeks. After four weeks of treatment, the food was reduced and the trend was maintained for all the period of study (Figures 46 A and B). After nine weeks, the mice administered with HFD were more heavy (Figure 46 A) than naïve mice ( $\approx 30\%$  increase of body weight compared to 10%), presented high glucose levels and were insulin resistant. HFD insulin-resistant mice were then divided into two groups: HFD administered alone or in combination with BAR502 (15 mg/kg/day). At the end of the study, HFD mice developed the typical features of NASH, which includes elevated AST, cholesterol and HDL plasma levels, while plasma triacylglycerol levels were comparable to naïve mice. As illustrated in Figure 46 E, the liver weight and its percent respect to the body weight were unmodified in this model, in comparison with naïve mice of the same age, whereas the histopathology analysis showed HFD with a severe steatohepatitis and extensive fat deposition (Figure 46 D). Moreover, HFD mice had a significant increased in liver content of triacylglycerol and cholesterol than the control (Figures 46 F and 46 G). In addition, HFD mice developed a moderate liver fibrosis (Figures 46 H and 46 I) and caused the recruitment of inflammatory factor such as IL-1 $\beta$ , IL-6, MCP-1, RANTES and TNF $\alpha$  mRNA (Figure 46 L). These NASH-features were reverted with the administration of BAR502. This treatment was initiated after nine weeks of HFD; from week 9 to week 18 mice were administered only with HFD showing an increase of 3% in body weight, while the treatment with BAR502 resulted in  $\approx 10\%$  decrease of body weight. BAR502 treatment increased HDL levels (Figure 46 C), reversed the lipid accumulation in liver, inducing a robust reduction of liver steatosis and content of lipids (Figures 46 D–G). In addition, it was able to reduce liver fibrosis by 70% and expression of pro-fibrogenetic genes ( $\alpha$ SMA and

$\alpha$ 1-collagen) as well as the expression of pro-inflammatory agents (Figures 46 H–L).

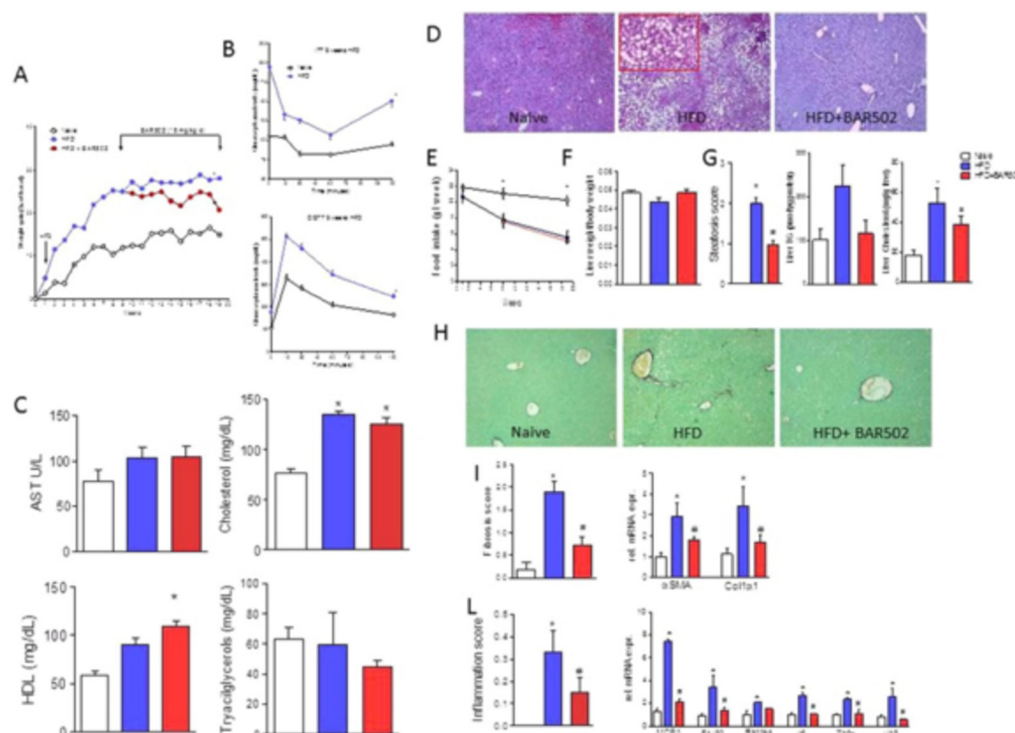


**Figure 46. BAR502 reduced body weight gain and reduced hepatic lipid partition in mice fed HFD.** Mice were fed a HFD and fructose for 18 weeks. BAR502 was administered at the dose of 15 mg/kg/day starting on day 63 (week 9). The data shown are (A) body weight (% delta weight); (B) glycemic response to oral glucose tolerance test (OGTT) and to insulin-tolerance test (ITT) (both after 9 weeks of HFD). (C) plasma levels of AST, cholesterol, HDL and triacylglycerols measured at the end of the study. The data shown in Panels (A–C), are mean  $\pm$ SE of 9 mice. (D) Hematoxylin and eosin (H&E) staining on mice liver tissues showing severe steatosis and ballooning of hepatocytes in mice feed a HFD for 19 weeks. These changes were significantly attenuated by treating the HFD mice with BAR502. The data are mean  $\pm$ SE of 9 mice. (E) Food intake through the study expressed as mg/week/mouse. The data shown in Panels A–C, are mean  $\pm$ SE of 9 mice. Panels F–L. Impact of BAR502 on (F) liver weight, (G) steatosis (Steatosis score) and liver TG and Cholesterol content. (H) Sirius red staining of liver sections; (I) fibrosis score and hepatic expression of  $\alpha$ SMA and COL1 $\alpha$ 1 mRNA; (L) inflammation score and hepatic expression of pro-inflammatory genes. F4/80 is a markers for macrophages. Results are the mean  $\pm$  SE of 5–9 mice per group. \* $p$ < 0.05 versus naïve mice, # $p$ <0.05 versus HFD mice. Values are normalized to B2M and ACT $\beta$ , the relative mRNA expression is expressed as  $2^{-(Ct)}$ .

As shown in Figure 47, HFD treatment increased the expression of proteins involved in the regulation of cholesterol and triacylglycerol metabolism (Fig. 47 A–C), while the expression of nuclear receptors such as LXR, FXR and SHP was unmodified. In Figure 47 A-C is also demonstrated that BAR502 represented an *in vivo* effective FXR agonist because it reduced Cyp7 $\alpha$ 1 while induced BSEP and SHP expression (Figure 47). Moreover, the reason of its beneficial effects on hepatic steatosis was linked to the modulation of cholesterol metabolism in the



liver.<sup>14</sup> In fact, BAR502 significantly reduced the expression of CD36,<sup>110</sup> while up-regulated the expression of ABCG5, a transporter involved in cholesterol extrusion from hepatocytes (Figure 47 B).<sup>111</sup>

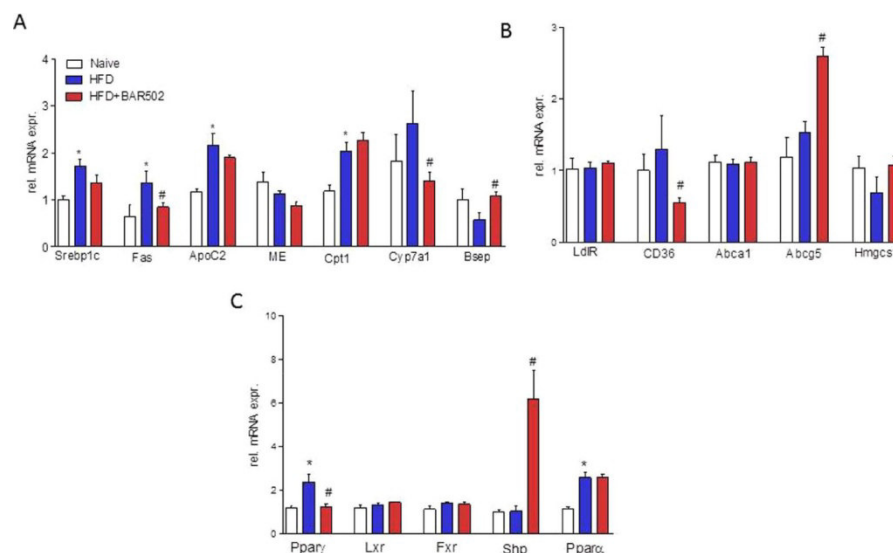


**Figure 47. BAR502 represses fatty acid synthesis, activates export of lipids from hepatocytes and activates FXR target genes in the liver.** Relative hepatic mRNA expression of genes involved in (A) Triacylglycerols and fatty acid metabolism, (B) Cholesterol metabolism, and (C) Nuclear receptors. Results are the mean  $\pm$ SE of 5 mice per group. \* $p < 0.05$  versus naïve mice, # $p < 0.05$  versus HFD mice. Values are normalized to B2M and ACT $\beta$ , the relative mRNA expression is expressed as  $2^{-(Ct)}$ .

In conclusion, 9 weeks of treatment with BAR502 were able to reverse the steatohepatitis and fibrosis in mice subjected to HFD. BAR502 was able to reduce liver cholesterol and to slightly increase HDL levels, indicating a beneficial effect in the control of hepatic cholesterol homeostasis. Because BAR502 was able to attenuate fibrosis in HFD model, this compound was evaluated in reverting liver fibrosis in a rodent model of CCl<sub>4</sub> administration. As illustrated in Figure 48, CCl<sub>4</sub> administration caused a severe liver disorder measured from AST and bilirubin levels, reduction of albumin plasma levels and increased portal pressure (Figures 48 A and B). These biochemical modifications were associated to a severe fibrosis, as demonstrated by a morphological analysis. BAR502 administration reversed these features and exerted a protective effect against liver fibrosis development. In addition, it reduced AST and bilirubin plasma levels, increased level of albumin and reduced extracellular matrix deposition (Figure 48).

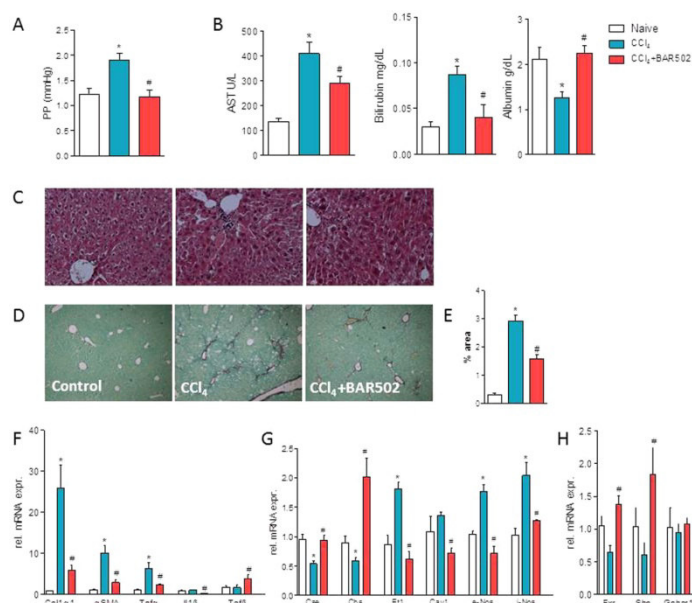
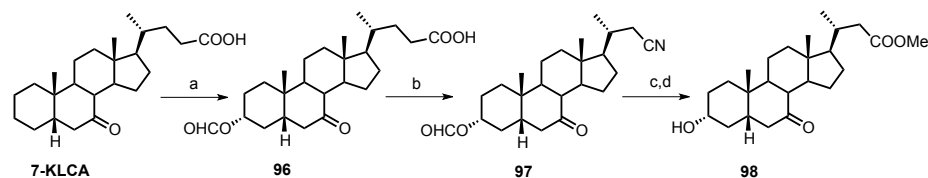


**Figure 48. BAR502 protects against liver fibrosis induced by CCl<sub>4</sub>.** Liver fibrosis was induced by carbon tetrachloride (CCl<sub>4</sub>) administration (i.p. 500 μL/Kg body weight, twice a week for 8 weeks). CCl<sub>4</sub> mice were randomized to receive BAR502 (15 mg/kg daily by gavage) or vehicle (distilled water). Data shown are (A) Portal pressure, (B) plasmatic levels of AST, bilirubin and albumin. (C) Hematoxylin and eosin (H&E) staining and (D) Sirius red staining on mice liver tissues; (E) Image J quantification of Sirius red staining. Total RNA extracted from liver was used to evaluate by RT-PCR the relative mRNA expression of (F) marker genes of fibrosis, (G) genes involved in endothelial function and (H) Nuclear receptor genes. Results are the mean ±SE of 6–12 mice per group. \*p<0.05 versus naïve mice. #p<0.05 versus CCl<sub>4</sub> alone.

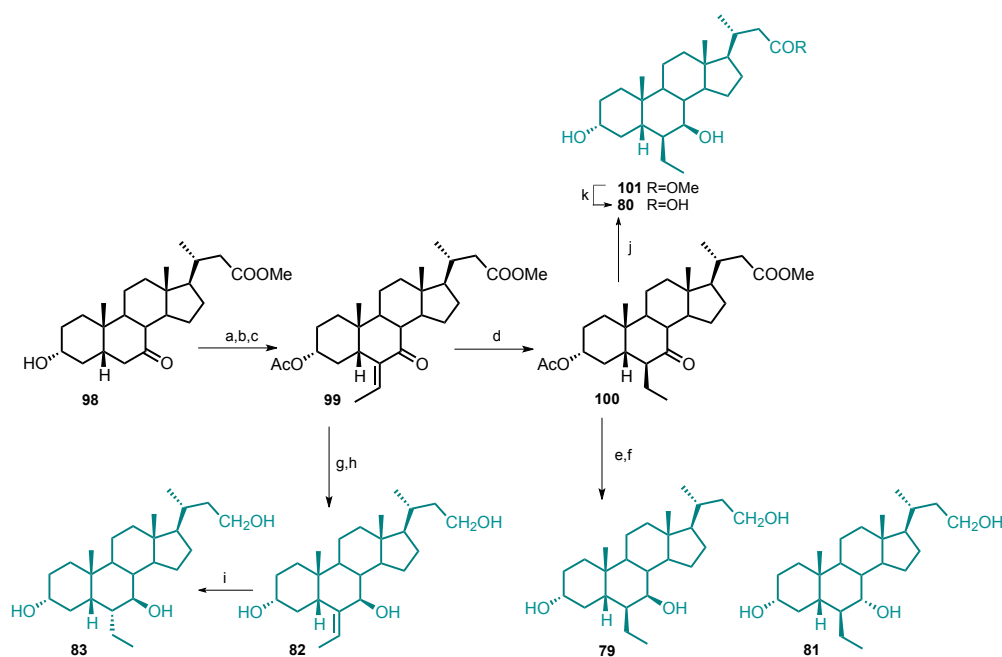
In addition, mice treatment with BAR502 protected against portal hypertension caused by CCl<sub>4</sub> administration. This was the result of induction of both eNOS and CSE genes, which induced vasodilatation by producing nitric oxide (NO) and hydrogen sulfide (H<sub>2</sub>S), respectively. Because these two genes are expressed in liver sinusoidal cells, which in turn express GPBAR1, this effect could be considered a signal of hepatic GPBAR1 activation.<sup>73,112</sup> In summary, in this recent discovery, BAR502 resulted able to exert protective effects against NASH-features, induced in a mice model of HFD. Collectively these data suggest that the dual FXR/GPBAR1 modulation could be a useful tool in treating NASH.

### 3.2 PREPARATION OF 3 $\alpha$ -HYDROXY-6-ETHYLNORCHOLANE DERIVATIVES



**Scheme 13. Preparation of intermediate 98.** a) HCOOH, HClO<sub>4</sub>; b) TFA, trifluoroacetic anhydride, NaNO<sub>2</sub>; c) KOH 30% in MeOH/H<sub>2</sub>O 1:1 v/v, 66% over three steps; d) *p*-TsOH, MeOH dry, quantitative yield.

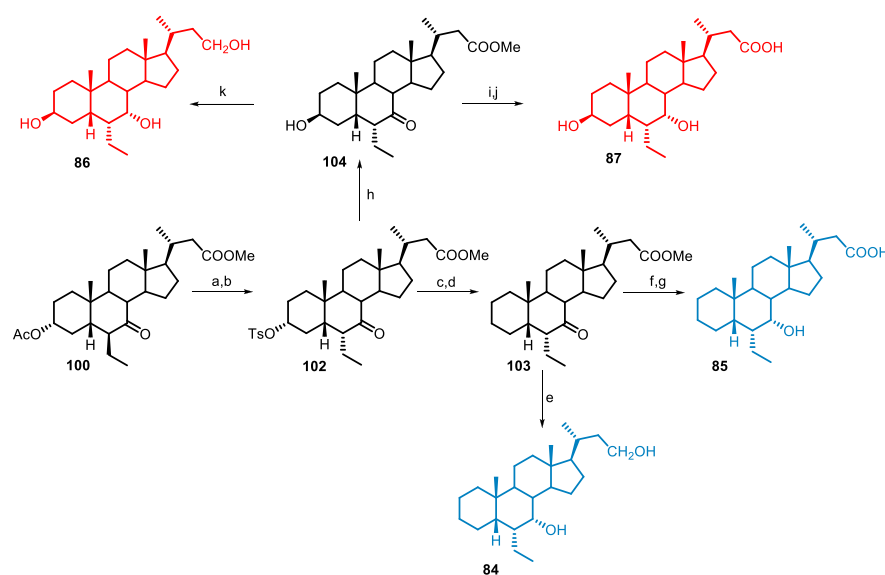
For the preparation of 3 $\alpha$ -hydroxy-6-ethylnorcholane derivatives **79–83**, the first step was the preparation of the key intermediate methyl ester of 7-keto-norLCA (**98**) starting from the 7-KLCA as previously reported (Scheme 13).<sup>48</sup> Fischer's esterification with formic acid and perchloric acid on 7-KLCA intermediate, generated the formiate derivative **96**, that was successively subjected to a Beckmann rearrangement by treatment with sodium nitrite in a mixture of trifluoroacetic anhydride/trifluoroacetic acid, obtaining the nor-nitrile derivative **97**.<sup>104</sup> Prolonged alkaline hydrolysis using KOH 30%, furnished the corresponding carboxylic acid that was in turn transformed with methanol and *p*-toluenesulfonic acid, in the corresponding derivative methylated **98** (66% yield starting from 7-KLCA). Acetylation at C-3 and a consequent Knoevenagel condensation to a silyl enol ether intermediate produced the intermediate **99** (60% over three steps, Scheme 14) that was hydrogenated on the exocyclic double bond with H<sub>2</sub> and Pd(OH)<sub>2</sub> giving the exclusive formation of the 6 $\beta$ -epimer **100** (quantitative yield). Compound **100** was then treated with an excess of NaBH<sub>4</sub> in methanol dry and subjected to LiBH<sub>4</sub> reduction directly on the crude product, to give the contemporary deacetylation at C-3 and reduction on C-7 and C-23 positions. HPLC purification afforded the derivative **79** as main product and a small aliquot of its epimer at C-7, compound **81**.



**Scheme 14. Synthesis of 3α-hydroxy-6-ethylnorcholane derivatives.** a) acetic anhydride, pyridine; b) DIPA, *n*-BuLi, TMSCl, TEA dry, THF dry -78 °C; c) acetaldehyde, BF<sub>3</sub>•OEt<sub>2</sub>, CH<sub>2</sub>Cl<sub>2</sub>, -60 °C, 60% over three steps; d) H<sub>2</sub>, Pd(OH)<sub>2</sub>, THF/MeOH dry 1:1, quantitative yield; e) NaBH<sub>4</sub>, MeOH dry, 0 °C; f) LiBH<sub>4</sub>, MeOH dry, THF dry, 0 °C, 77% over two steps; g) NaBH<sub>4</sub>, MeOH dry; h) LiBH<sub>4</sub>, MeOH dry, THF dry, 0 °C, 85% over two steps; i) H<sub>2</sub>, Pd(OH)<sub>2</sub>, THF:MeOH dry 1:1 v/v, quantitative yield; j) NaBH<sub>4</sub>, MeOH dry, 0 °C; k) NaOH, MeOH:H<sub>2</sub>O 1:1 v/v, 82% over two steps.

In parallel, intermediate **100** was subjected to a controlled NaBH<sub>4</sub> reaction, in order to reduce the C-7 ketone group, and maintaining the methyl ester function on compound **101**, which was subjected to basic hydrolysis affording the carboxylic acid **80** in 82% over two steps. Intermediate **99** was also used as starting material to prepare derivatives **82** and **83**. NaBH<sub>4</sub> reaction followed by LiBH<sub>4</sub> treatment on **99** produced the 7β-hydroxyl derivatives, as confirmed by the shape of H-7 as a doublet ( $J = 9.8$  Hz), which justified the axial disposition of this proton, and as consequence the β-orientation of the hydroxyl group in the same position. The analysis of NOESY spectrum revealed dipolar couplings H-7/H-24 and Me-25/H-5 defining the *E* configuration of the exocyclic double bond as illustrated in **82**. At the end, catalytic hydrogenation with Pd(OH)<sub>2</sub> gave derivative **83**, with the presence of a 6α-ethyl group.

### 3.3 PREPARATION OF 3-DEOXY- AND 3 $\beta$ -HYDROXY-6 $\alpha$ -ETHYLNORCHOLANE DERIVATIVES



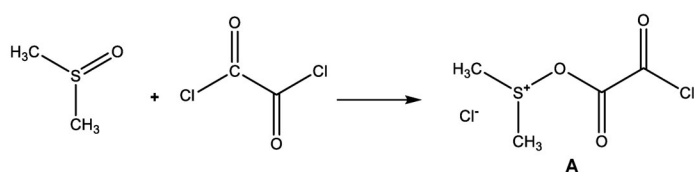
**Scheme 15. Synthesis of 3-deoxy- and 3 $\beta$ -hydroxy-6 $\alpha$ -ethylnorcholeane derivatives.** a) MeONa, MeOH dry; b) *p*-TsCl, pyridine, 73% over two steps; c) LiBr, Li<sub>2</sub>CO<sub>3</sub>, DMF dry, reflux; d) H<sub>2</sub>, Pd(OH)<sub>2</sub>, THF/MeOH dry 1:1, room temperature, quantitative yield over two steps; e) LiBH<sub>4</sub>, MeOH dry, THF dry, 0 °C, 70%; f) NaOH, MeOH:H<sub>2</sub>O 1:1 v/v; g) LiBH<sub>4</sub>, MeOH dry, THF dry, 0 °C, 92% over two steps; h) CH<sub>3</sub>COOK, DMF:H<sub>2</sub>O 5:1 v/v; i) NaOH, MeOH:H<sub>2</sub>O 1:1 v/v; j) LiBH<sub>4</sub>, MeOH dry, THF dry, 0 °C, 58% over two steps; k) LiBH<sub>4</sub>, MeOH dry, THF dry, 0 °C, 57%.

To prepare 3-deoxy- and 3 $\beta$ -hydroxy-6-ethylnorcholeane derivatives **84–87**, the key intermediate **100** was subjected to a treatment with MeONa in methanol, in order to de-acetylate the C-3 position and to invert the C-6 position and then to tosylation reaction, using *p*-tosyl chloride, in order to produce compound **102**, in 73% yield over two steps (Scheme 15). Basic treatment with LiBr/Li<sub>2</sub>CO<sub>3</sub> and then hydrogenation on the unsaturated ring A gave **103**, which was used as starting material for the preparation of compounds **84** and **85**. LiBH<sub>4</sub> reduction at C-7 keto and C-23 methyl ester groups gave **84** in 70% chemical yield after purification, whereas alkaline hydrolysis of the methyl ester group followed by LiBH<sub>4</sub> treatment and HPLC, gave the carboxyl acid **85** in 92% yield. Finally, the tosyl derivative **102** was also used for the preparation of compounds **86** and **87**. Potassium acetate in DMF/H<sub>2</sub>O treatment furnished the key intermediate **104**, with the 3 $\beta$ -hydroxyl group. Reduction at C-7 and C-23 positions using LiBH<sub>4</sub> gave, after HPLC purification, compound **86** in 57% yield, while basic hydrolysis

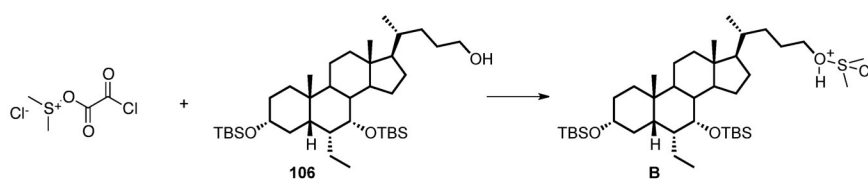
followed by  $\text{LiBH}_4$  treatment and successive HPLC purification, produced the carboxyl derivative **87**, in 58% yield over two steps.

### 3.4 PREPARATION OF BIS-*HOMO*-6-ETHYLCHOLANE DERIVATIVES

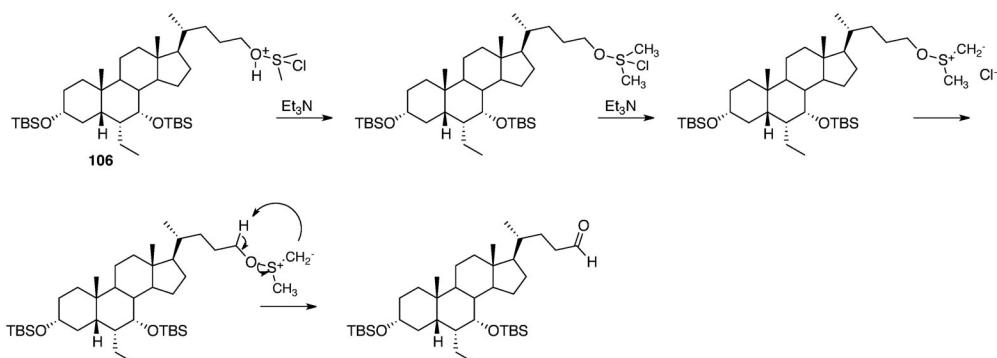
For the synthesis of bis-*homo*-6-ethylcholine derivatives, key step was the C2 homology on the side chain. Thus, 6-ECDCA methyl ester (**105**) was protected at C-3 and C-6 positions using *t*-butyldimethylsilyl trifluoromethane sulfonate, 2,6-lutidine in  $\text{CH}_2\text{Cl}_2$  dry. Reduction of the methyl ester group on side chain furnished the alcohol protected **106**, as the starting material for the one pot Swern oxidation-Horner homologation (Scheme 16). Swern oxidation involves the initial activation of dimethyl sulfoxide (DMSO) using oxalyl chloride ( $\text{COCl}_2$ ), through the nucleophilic attack of the oxygen of DMSO to one of the acyl groups of ( $\text{COCl}_2$ ), obtaining a positive charge on the sulphur group in the intermediate A.



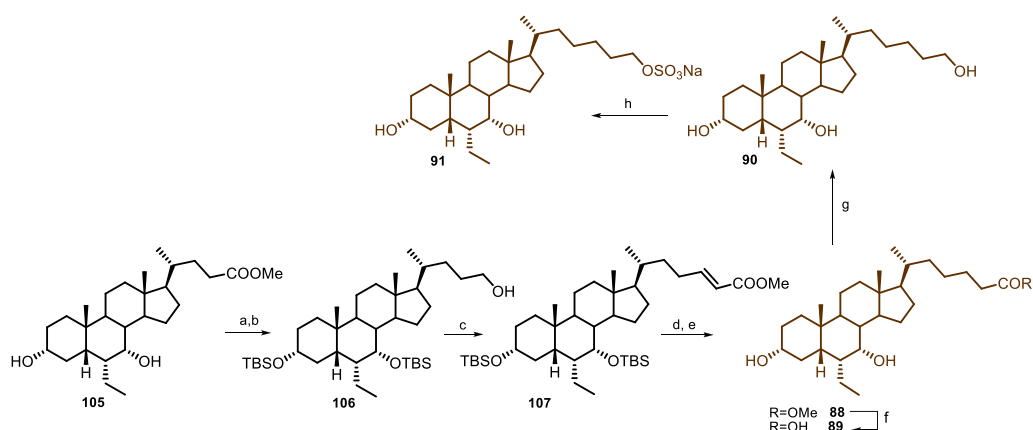
Addition of the alcohol **106** produces the nucleophilic attack on the sulfonium ion with the formation of intermediate B.



Addition of triethylamine (TEA) produces the de-protonation and the consequent intermolecular re-arrangement furnishing the desired aldehyde.



The aldehyde was then used as substrate for the following Horner-homologation reaction with methyl (triphenylphosphoranylidene)acetate, giving the protected  $\Delta^{24,25}$  bis-*homo*-ECDCA methyl ester **107**, in 79% chemical yield (Scheme 16). Hydrogenation on side chain double bond, followed by de-protection with HCl 37% on **107**, gave the methyl ester **88** that was used as starting material for the preparation of the carboxylic acid (**89**) through treatment with NaOH and of the corresponding alcohol **90**, using LiBH<sub>4</sub> reduction. Further, a small amount of alcohol **90** was subjected to a chemoselective sulfation on C-26 hydroxyl group, giving after RP18 column and HPLC purification, the corresponding sulfate derivative **91** in 25% yield.<sup>113</sup>

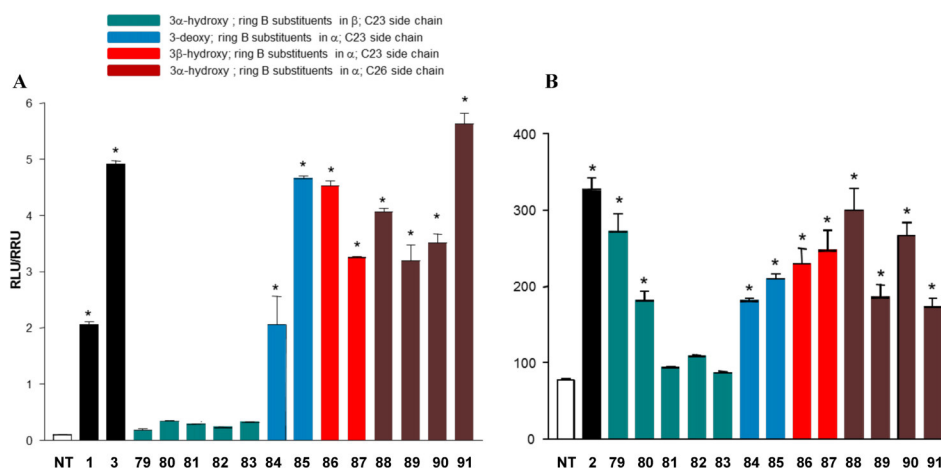


**Scheme 16. Preparation of bis-*homo*-6-ethylcholine derivatives.** a) 2,6-lutidine, *t*-butyldimethylsilyl trifluoromethanesulfonate, CH<sub>2</sub>Cl<sub>2</sub>, 0 °C; b) LiBH<sub>4</sub>, MeOH dry, THF dry, 0 °C, 68% over two steps; c) DMSO, oxalyl chloride, TEA dry, CH<sub>2</sub>Cl<sub>2</sub>, -78 °C then methyl (triphenylphosphoranylidene)acetate, 79%; d) H<sub>2</sub>, Pd(OH)<sub>2</sub>/C Degussa type, THF/MeOH 1:1, quantitative yield; e) HCl 37%, MeOH, 88%; f) NaOH 5% in MeOH/H<sub>2</sub>O 1:1 v/v, 89%; g) LiBH<sub>4</sub>, MeOH dry, THF dry, 0 °C, 78%; h) Et<sub>3</sub>N SO<sub>3</sub>, DMF dry, 95 °C, 25%.

### 3.5 PHARMACOLOGICAL EVALUATION OF 3 $\alpha$ -HYDROXY-, 3-DEOXY-, 3- $\beta$ -HYDROXY-6-ETHYLNORCHOLANE AND BIS-*HOMO*-6-ETHYLCHOLANE DERIVATIVES

Compounds **79-91** were tested on FXR and GPBAR1 in a luciferase reporter assay on HepG2 and HEK-293T cells, previously transfected with responsive elements for the two receptors. Data shown in Figure 49, panel A, reported the results of FXR transactivations. Once again, the 6 $\alpha$ /7 $\alpha$ -configuration on ring B represents a peculiar feature for FXR activation. In fact derivatives **79-83**, with one or two substituents in  $\beta$ -configuration on ring B, were devoid of any activity on FXR when administered at fixed concentration of 10  $\mu$ M. Of interest are the

results of derivatives **84-87**, with both substituents on ring B in  $\alpha$ -configuration and a truncate (C23) side chain. In the above subset, the presence of a negative charge on the side chain (compounds **85** respect **84**) favors the activity of 3-deoxy derivatives, while the presence of a hydroxyl group at C-24 position improves the activity of the corresponding 3 $\beta$ -hydroxyl derivative (compound **86** respect **87**). Finally, results of FXR transactivation on derivatives **88-91** demonstrate that the presence of an elongated side chain on the 6-ECDCA scaffold generates potent FXR agonists. Noteworthy the nature of the side chain end-group considerably influences the effect of FXR transactivation with derivative **91**, a C26-sulfate derivative, the most potent FXR ligand produced in this study.



Results of GPBAR1 transactivation are illustrated in Figure 49, panel B. Compounds **79** and **80**, with the two groups at C-6 and C-7  $\beta$ -orientated, are potent and selective GPBAR1 activators, with compound **79** showing a potency comparable with TLCA (**2**). In addition, all derivatives with both substituents on ring B  $\alpha$ -orientated (**84-91**) are dual FXR/GPBAR1. The potency of the most interesting members of this family was successively investigated by a careful measurement of their concentration-response curves.  $EC_{50}$  on FXR and GPBAR1 for the 3-deoxy C-23 carboxylic acid derivative **85**, the 3 $\beta$ -hydroxyl C-23 alcohol



**86** and the C-26 sulfate derivative **91**, all sharing the 6  $\alpha$ /7 $\alpha$  stereochemical arrangement, were calculated. As depicted in Figure 50, the above compounds transactivated FXR with an EC<sub>50</sub> of 2.3  $\mu$ M (**85**), 5.3  $\mu$ M (**86**) and 1.7  $\mu$ M (**91**). In addition, they transactivated GPBAR1 with an EC<sub>50</sub> of 4.3  $\mu$ M, 1.0  $\mu$ M and 0.95  $\mu$ M, respectively (Figure 51). Comparing these results, sulfate derivative **91** resulted the most potent FXR/GPBAR1 dual agonist generated in this study. Finally, the concentration-response curve of compound **79**, a selective GPBAR1 agonist, was also determined on GPBAR1 with an EC<sub>50</sub> value of 0.91  $\mu$ M (Figure 51).

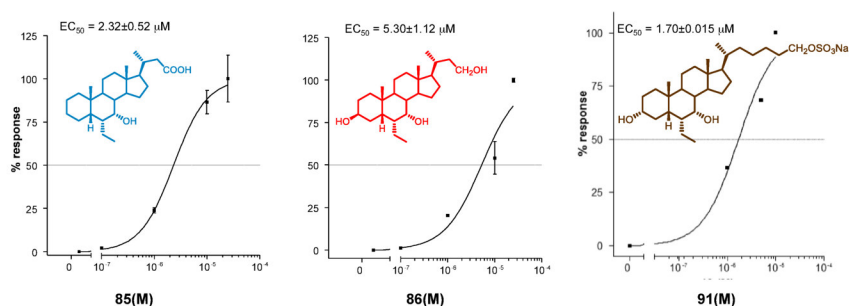


**Figure 50.** Concentration-response curve of **85**, **86** and **91** on FXR. HepG2 cells were transfected with FXR as described above and used in a luciferase reporter assay. Twenty-four hour post transfection cells were stimulated with increasing concentrations of each agent: range from 100 nM to 25  $\mu$ M. Results are expressed as mean  $\pm$  standard error.

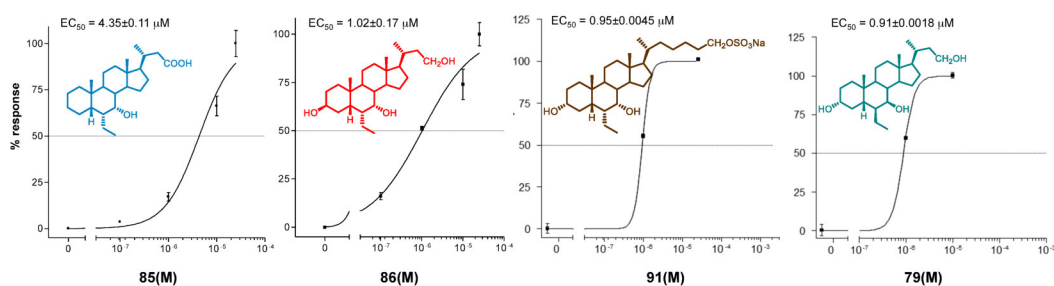


**Figure 51.** Concentration-response curve of compounds **79**, **85**, **86** and **91** on GPBAR1. HEK-293T cells were co-transfected with GPBAR1 and a reporter gene containing a cAMP responsive element in front of the luciferase gene (CRE). Twenty-four hour post transfection cells were stimulated with increasing concentrations of each agent: range from 100 nM to 25  $\mu$ M. Results are expressed as mean  $\pm$  standard error.

The most potent FXR agonist generated in these series (**91**) was also tested in Alphascreen technology assay with CDCA (**1**) and 6-ECDCA (**3**) used as positive controls at the concentration of 2  $\mu$ M and the effect of 6-ECDCA (**3**) arbitrarily settled as 100%. As shown in Figure 52, panel A, compound **91** recruits the SRC-1 co-activator in a comparable way with compound **3**, thus confirming the

transactivation result. Interestingly, the presence of the not conjugable functional group such as the sulfate group on the side chain, points the attention on the positive pharmacokinetic properties of compound **91** and therefore on its therapeutical potential in FXR-mediated diseases. Results on Figure 52, panel A, confirm the inactivity of compounds **79**, **81**, and **82** towards FXR and indirectly affirm compound **79** as a selective GPBAR1 agonist. RT-PCR in Figure 52, panels B-D, confirmed **91** as dual FXR/GPBAR1 agonist, able to induce the expression of BSEP and OST $\alpha$ , two canonical FXR targeted genes,<sup>114</sup> and of GLP-1, a GPBAR1-regulated effect.

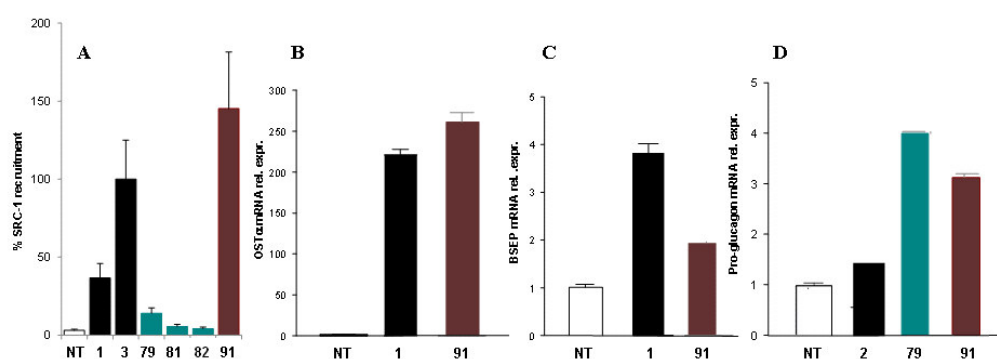


**Figure 52.** (A) Coactivator recruitment assay measuring a direct interaction of FXR with SRC-1; ligands at 2  $\mu$ M. Results are expressed as percentage of the effect of **3** arbitrarily settled as 100%. NT is referred to the experiment in absence of ligand. Results are expressed as mean  $\pm$  standard error. (B, C) Real-time PCR analysis of mRNA expression on FXR target genes BSEP (C), and OST $\alpha$  (B) in HepG2 cells primed with 10  $\mu$ M of compound **91**. CDCA (**1**) was used as a positive control at 10  $\mu$ M. (D) Real-time PCR analysis of mRNA expression of GPBAR1 target gene Pro-glucagon (GLP-1) in GLUTAg cells stimulated with 10  $\mu$ M of compounds **79** and **91**, and TLCA (**2**) used as a positive control at 10  $\mu$ M. Values are normalized to GAPDH and are expressed relative to those of not treated cells (NT), which are arbitrarily settled to 1. The relative mRNA expression is expressed as  $2^{-\Delta\Delta Ct}$ .

In summary, in this chapter I have presented additional chemical modifications on 6-ECDCA scaffold that include the length/nature of the side chain end-group and the stereochemical arrangement of the tetracyclic core. Looking to the pharmacological results on nor-derivatives **76-78**, with all substituents on rings A and B in  $\alpha$ -configuration, it is possible to establish that the side chain exerts an important influence on the receptor selectivity. Shortened side chain with a hydroxyl terminal group produces a potent FXR agonist (NorECDCOH or **77**, EC<sub>50</sub> of 2  $\mu$ M) while the introduction of a negative charge, NorECDCa (**76**), or a neutral end-group, NorECDCN (**78**), improves GPBAR1 activity. Indeed, **77** was also endowed with GPBAR1 activity and was able to increase pro-glucagon gene

expression in GLUTAg cells. However, because it was most potent to induce FXR canonical functions, it could be considered a preferential FXR ligand. Supporting this view, **77** does not induce itching when administered in *in vivo* rodent model of cholestasis and presents benefic effects in rodent model of NASH. Furthermore, derivatives **79-91** add important information in term of SAR. As expected, also in this series, the  $\alpha$ -orientation of both substituents at C-6 and C-7 positions plays a significant role in FXR and GPBAR1 activities, with all derivatives showing this feature invariably dual agonists (**84-91**), independently from the length or functional group on side chain as well as the substitution at C-3. On the contrary, modifications on the configuration of one or both substituents on ring B is clearly detrimental in terms of FXR activation, but result an appealing strategy in the identification of selective GPBAR1 agonists, such as compound **79**, which was the most potent GPBAR1 activator identified in this study, devoid of any FXR activity.<sup>115</sup>

**CHAPTER 4  
ASYMMETRIC DIVERSITY-ORIENTED SYNTHESIS OF  
BENZO-FUSED CYCLIC AMINES**

---

Another consistent part of my Ph.D. project was spent in the Centro de Investigación Príncipe Felipe of Valencia, under the supervision of Prof. Santos Fustero. In this period I have participated in the asymmetric diversity-oriented synthesis of benzo-fused cyclic amines. Diversity-oriented synthesis (DOS) is an emerging field consisting in the synthesis of different libraries of molecules for biological screening, which can be used to identify novel ligands for a variety of targets. Modern drug discovery often is based on the screening of small molecules able to bind specific protein target and this target-oriented synthesis, towards individual molecules or focused libraries, can be obtained by retrosynthetic analysis. Also, drug discovery involves screening of small molecules able to modulate biological pathways in the organisms, without any particular activities for specific target. So in the context of this need to reach an efficient and versatile synthetic approach capable to generate complex and different molecular libraries, the diversity-oriented synthesis (DOS) of small molecules is the access key towards new chemotypes with high chemical diversity. One desired goal of DOS is to synthesize a collection of small molecules able to perturb a particular biological pathway, giving eventually the identification of therapeutic proteins that are target of small molecules.

DOS provides to obtain different chemical libraries using the minimum number of synthetic steps, starting from a common precursor.<sup>116-121</sup> The key for a successful result of this strategy is the use of a suitable substrate with appropriate functional groups in strategic positions. These substituents also must be able to participate in as many different transformations as possible, increasing the complexity of molecules achieved. In the last years, Fustero's group worked hard in the asymmetric synthesis of benzo-fused carbo-<sup>122-128</sup> and heterocycles,<sup>127-130</sup> using the 2-halobenzaldehyde as building block (Figure 53).<sup>131</sup>

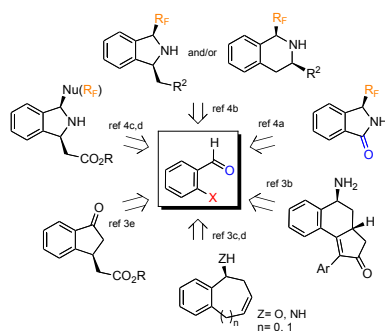


**Figure 53.** 2-halobenzaldehyde in Diversity-oriented synthesis

Starting from this strategy, they have synthesized interesting building blocks, such as fluorinated<sup>128,129</sup> and non-fluorinated isoindolines,<sup>129</sup> indanones,<sup>126</sup> fluorinated isoindolinones<sup>127</sup> and aminosteroid derivatives.<sup>123</sup>

In literature there are many examples of using of 2-halobenzaldehyde in different synthetic processes for its versatility and ability to produce diverse chemical scaffolds. One example of the involvement of 2-halobenzaldehyde is the synthesis of the antidepressant sertraline by Fustero's group. In fact, through DOS the 2-halobenzaldehyde was recognized as the starting material of different benzo-fused carbo- and heterocycles such as isoquinolines, indanones and in particular the tetrahydronaphthalene nucleus, which respect the others is more commonly found in natural products or drugs. The more important examples of drugs, which present the tetrahydronaphthalene core are the analgesic morphine and the antidepressant sertraline.<sup>124</sup>

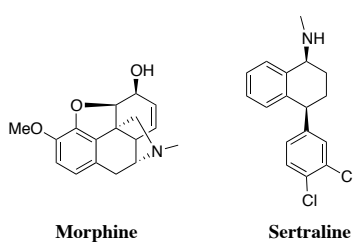


**Figure 54.** The analgesic morphine and the antidepressant sertraline

So with this aim the synthesis of sertraline was performed and consisted in the three-step one-pot protocol starting from the corresponding aldehyde (Figure 55).<sup>124</sup>

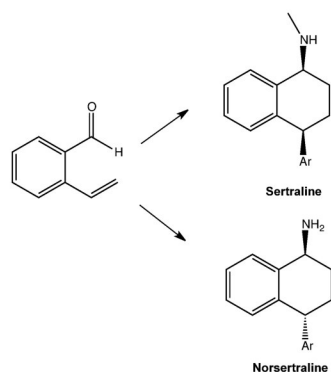


**Figure 55.** Synthesis of Sertraline and Norsertaline

Other applications of 2-halobenzaldehyde are reported in the asymmetric allylation/Pauson–Khand reaction sequence, for the synthesis of tricyclic amines.

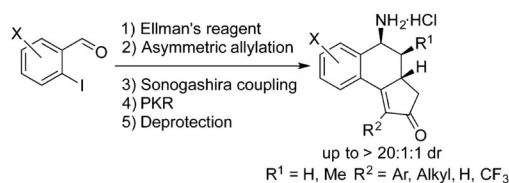


**Figure 56.** Synthesis of tricyclic amines

Firstly, the *o*-iodobenzylidene *tert*-butanesulfinamide intermediates (**2a–e**) were prepared and then they were used as starting material for the next step of Sonogashira cross-coupling, in order to obtain derivatives **4a–I**.

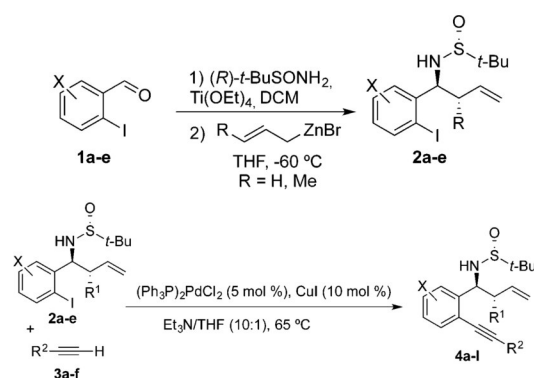


**Figure 57.** Sonogashira cross-coupling reaction of substrates **2a–e**

In this case, the Sonogashira reaction conditions were investigated and this gave the possibility to rise the end-concentration of desired product **4a**, while the formation of the intramolecular Heck reaction byproduct **5a** was almost completely suppressed.

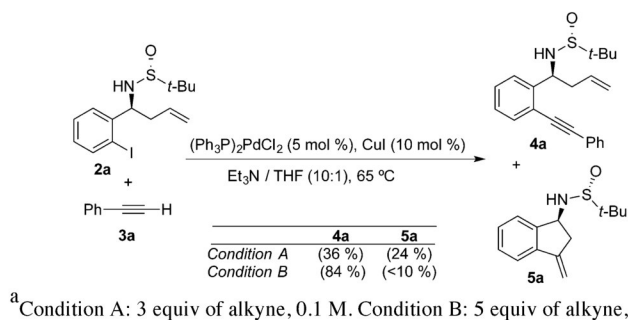


**Figure 58.** Optimization of the reaction conditions for Sonogashira cross-coupling

At the end, in order to obtain tricyclic amines **6a-m** the Pauson-Khand reaction was applied, producing the desired products in high chemical yields.

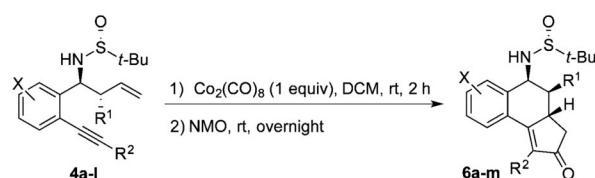


**Figure 59.** Pauson-Khand reaction on substrates **4a-I**

Finally, the same modifications described for polycyclic amines were applied in the synthesis of aminosteroid derivatives, which are an important subclass of steroids, some of which present interesting biological properties, mostly used in the field of anesthesia.

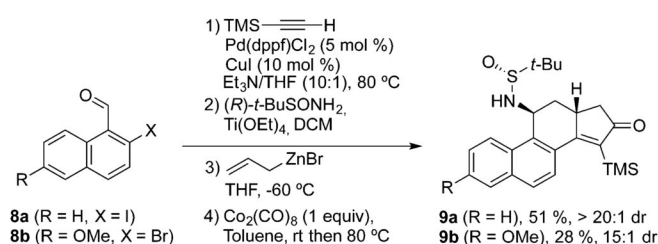


**Figure 60.** Application of the protocol on the synthesis of aminosteroid derivatives

At last, in the effort to expand the use of 2-halobenzaldehyde derivatives in the context of diversity-oriented synthesis (DOS), was envisioned the asymmetric synthesis of fluorine derivatives containing 1-amino-1,2-dihydronaphthelene core. Specifically, 2-halobenzaldehyde was used as a common precursor for the one-pot allylation/RCM procedure.

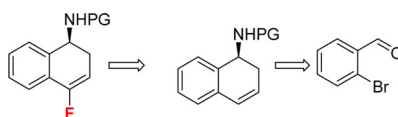


**Figure 61.** Hypothesized retrosynthesis for 1-amino-1,2-dihydronaphthalene-derived vinyl fluorides

The interest to produce fluorine derivatives depends on the great impact that organofluorine compounds have exerted in key industrial fields such as pharmaceutical, agrochemical, or materials industries. For examples many fluorolefins were found in antidiabetes and anti-HIV drugs. The most interesting characteristic is their bioisosterism with an amide group, which confers to fluorolefins the possibility to be incorporated in peptidomimetics, conferring a resistance from proteolytic degradation.

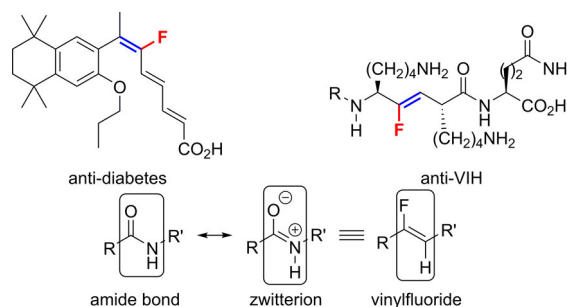


**Figure 62.** Fluorolefin-containing drugs and bioisosterism with amides

For their synthesis the reaction conditions were explored, producing a small library of fluorine derivatives (**12a-g**) where the bromine atom adjacent to the fluorine was removed through an optimized treatment with 4 equivalents of NaH in DMF dry.

Finally, to reduce the number of steps necessary to afford benzo-fused fluorolefin derivatives, was discovered that the *o*-(1-fluorovinyl)-benzaldehyde derivative (OFVBA) was a suitable starting material for the condensation/asymmetric allylation/RCM reaction sequence (Figure 64).



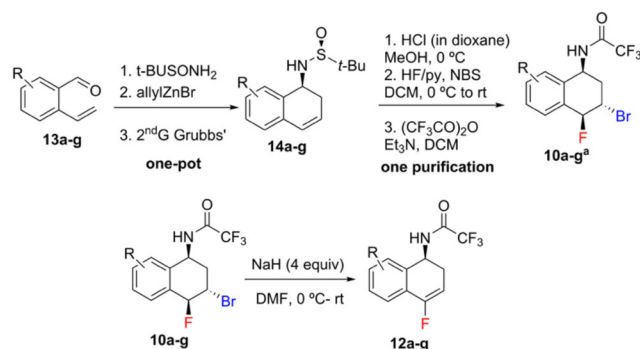


**Figure 63.** Optimized conditions for the synthesis of fluorolefins

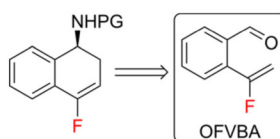
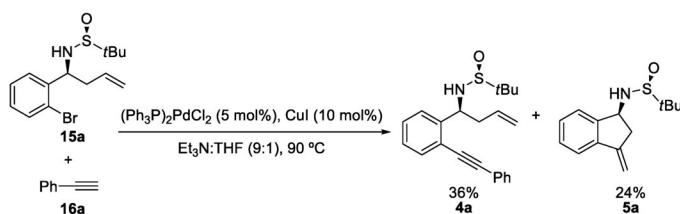


**Figure 64.** Alternative retrosynthetic approach

In the course of the latter studies on DOS, using 2-halobenzaldehyde as starting material, as already mentioned, was discovered that during Sonogashira cross-coupling reaction a significant amount of an undesired by-product (**5a**) respect the main product of intramolecular Heck reaction (**4a**), was found (Scheme 17).

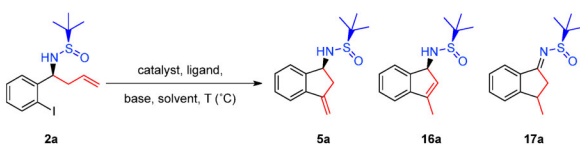


**Scheme 17.** Production of byproduct **5a**

The synthesis of compound **5a** was determined by the observation of two characteristic methylene protons at  $\delta_{\text{H}}$  5.1 and 5.5 in the  $^1\text{H}$  NMR, as well as the appearance of a characteristic corresponding signal at  $\delta_{\text{C}}$  104.4 in the carbon spectra. In the previous report,<sup>123</sup> was observed that the formation of this undesired by-product (**5a**) could be suppressed by increasing of alkyne equivalents (from 3 to 5) and amount of solvent (from 0.1 to 0.5 M). These modifications favored the intermolecular Sonogashira cross-coupling respect the intramolecular Heck reaction.

## 4.1 OPTIMIZATION OF INTRAMOLECULAR HECK REACTION

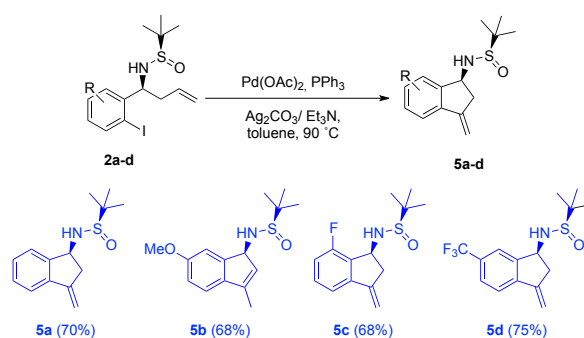
Starting from data collected, my research work in Valencia has been focalized to the optimization of the intramolecular Heck reaction conditions, implementing a one-pot condensation/asymmetric allylation or Pauson-Khand reaction (PKR) protocol, in order to synthesize tricyclic amines. Also we explored the Ring-closing metathesis (RCEYM) on the intermediate **21a**, synthesized as previously illustrated for compound **4a**, from Fustero's group. With this aim we started from the halogenated intermediate **15a** (Scheme 17), which was a versatile building block due to the presence of a halogen atom in *ortho* position to a homoallylic amine. This type of substitution made compound **15a** a suitable molecule to be subjected to different Pd catalyzed processes, such as the intramolecular Heck reaction or the Sonogashira cross-coupling. The intramolecular Heck reaction conditions were intensely explored: initially, CuI and no-longer necessary alkyne (**16a**) were removed increasing the chemical yield but giving a considerable amount of an undesired isomer (**17**). Then Et<sub>3</sub>N was replaced with an inorganic base (Ag<sub>2</sub>CO<sub>3</sub>), suppressing the formation of this isomer **17** and producing exclusively the desired product **5a** in 66% (Table 3, Entry 2).



Entry	Catalyst	Ligand	Base	Solvent	T(LC)	15a (%)	5a (%)	16a (%)	17a (%)
1	Pd(OAc) <sub>2</sub>	PPh <sub>3</sub>	Et <sub>3</sub> N	Tol.	120	–	25	–	31
2	Pd(OAc) <sub>2</sub>	PPh <sub>3</sub>	Ag <sub>2</sub> CO <sub>3</sub>	Tol.	120	–	66	–	–
3	Pd(dba) <sub>2</sub>	PPh <sub>3</sub>	Ag <sub>2</sub> CO <sub>3</sub>	Tol.	120 MW	–	50	–	–
4	Pd(dba) <sub>2</sub>	PPh <sub>3</sub>	Ag <sub>2</sub> CO <sub>3</sub>	THF	100 MW	–	25	25	–
5	Pd(dba) <sub>2</sub>	XANP	Ag <sub>2</sub> CO <sub>3</sub>	THF	100 MW	–	37.5	12.5	–
6	Pd(dba) <sub>2</sub>	JOHNP	Ag <sub>2</sub> CO <sub>3</sub>	THF	100 MW	80	–	–	–
7	Pd(OAc) <sub>2</sub>	PPh <sub>3</sub>	Et <sub>3</sub> N/Ag <sub>2</sub> CO <sub>3</sub>	Tol.	90	–	70	–	–

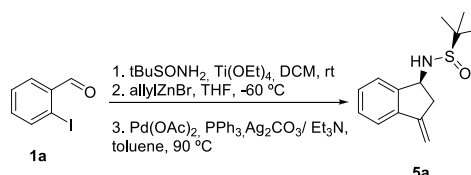
**Table 3.** Optimization of Heck reaction conditions

Microwave irradiations in toluene or THF didn't effort any beneficial effects on the reaction and finally the optimal condition was identified when was used an equimolar ratio of Ag<sub>2</sub>CO<sub>3</sub> and Et<sub>3</sub>N, furnishing 70% of **5a** (Table 3, Entry 7). After this optimization, starting from the intermediates **2a-d** with different substitutions on the aromatic nucleus, a series of 3-methylene-1-aminoindane derivatives **5** was produced, from moderate to good chemical yields (Scheme 18).



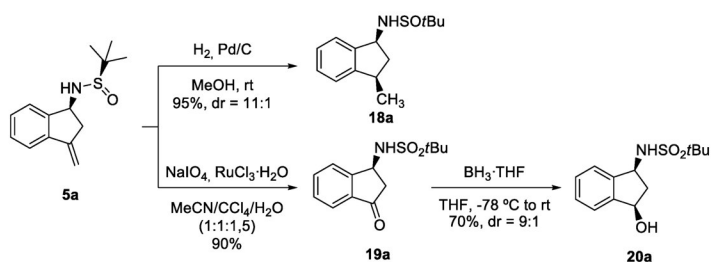
**Scheme 18.** Preparation of 3-methylene-1-aminoindane derivatives

In order to reach a sustainable methodology, we decided to apply on the 2-iodobenzaldehyde **1a** the same optimal reaction conditions showed for compound **2a**, to produce the Heck product **5a** in one-pot reaction. As illustrated in the Scheme 19, the Ellman amine was firstly added to 2-iodobenzaldehyde **1a** in order to produce the imine intermediate. Then it was subjected to an asymmetric allylation with allylzinc bromide and finally to intramolecular Heck reaction. In this way we obtained the derivative **5a** in 70% yield over three steps as single diastereoisomer.



**Scheme 19.** Preparation of derivative **5a** in one-pot condensation/asymmetric allylation/Heck reaction sequence

Moreover, to expand the series of achievable molecules, **5a** was submitted to two different processes: first, this compound was subjected to a catalytic hydrogenation with Pd/C in MeOH at room temperature giving *cis* compound **18a** in high chemical yield, whereas an oxidative cleavage of the methylene group, afforded the 3-aminoindanone derivative **19a** in 90% yield. At the end, this last intermediate **19a** was subjected to a stereoselective reduction on ketone group affording the *cis*-1,3-aminoalcohol derivative **20a**, in 70% yield (Scheme 20).



**Scheme 20.** Chemical modifications applied on derivative **5a**

The stereochemistry of compounds **18a** and **20a** was established according to the analysis of their bidimensional NOESY spectrums: in particular, we observed two cross peaks between the NH and CH<sub>3</sub> and between the two benzylic protons (H<sub>a</sub> and H<sub>b</sub>, Figure 65). In both molecules the assignment was agreed with a *cis* configuration. In particular, for compound **18a** the *cis* arrangement probably was due the attack of hydrogen on the  $\alpha$  face of the olefin, which is less hindered by the NHSOtBu group.

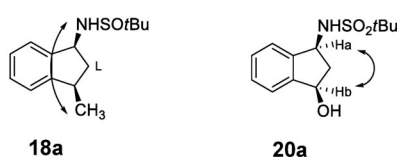


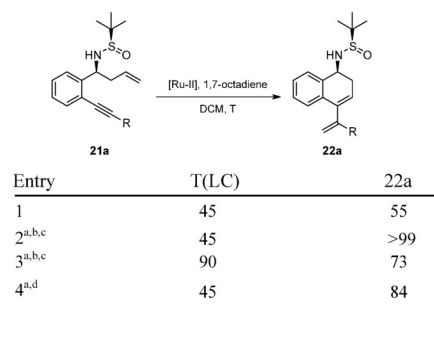
**Figure 65.** Stereochemistry assignments of **18a** and **20a**

## 4.2 RING-CLOSING ENYNE METATHESIS (RCEYM) EXPLORATION

Also we have investigated the reactivity of intermediates from **21a** to **21f**, previously synthesized in another report from Fustero's laboratory.<sup>123</sup> In particular the ring closing enyne metathesis (RCEYM) on these derivatives was explored, because it represents a useable tool for the synthesis of carbo- and heterocycles in which the presence of an exocyclic vinyl group is suitable for successive chemical transformations.<sup>132</sup> For this reason, the intermediate previously obtained **21a** has been subjected to the same conditions of a reference compound<sup>133,134</sup> which was treated with the second generation Grubb's catalyst (Ru-II), DCM and 1,7-octadiene. In order to increase the moderate yield obtained for the reference compound (55%, Table 4, Entry 1) we explored different reaction conditions. When we added two portions of catalyst and 1,7-octadiene, in a sealed tube, **22a**

was obtained with a high chemical yield (>99%) (Table 4, Entry 2). On the other hand, an increase of temperature provided shorter reactions times, but unfortunately the yield was reduced (Table 4, Entry 3).

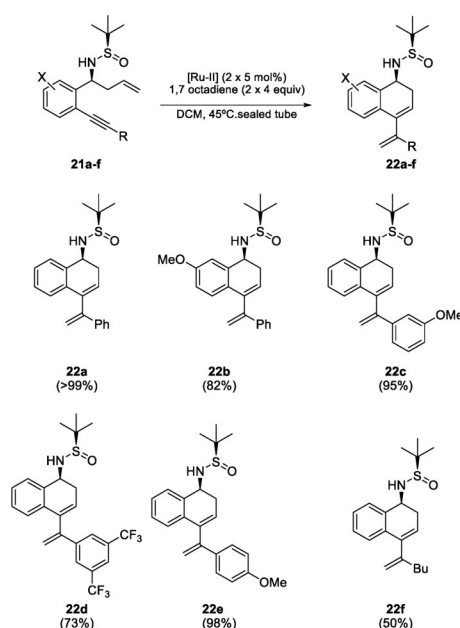
At the end, when we added a Lewis acid (Table 4, Entry 4), even if it improved the catalytic activity, the results in terms of yield were not satisfactory respect the conditions illustrated in the Entry 2.



<sup>a</sup>Sealed tube, <sup>b</sup>2 x 5 mol % catalyst loading, <sup>c</sup>2 x 4 equiv 1,7-octadiene, <sup>d</sup>1 equiv Ti(OEt)<sub>4</sub>

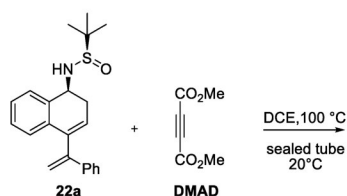
**Table 4.** Optimization of the RCEYM conditions

The optimized reaction conditions found for this RCEYM (Table 4, Entry 2) gave us the possibility to prepare the synthesis of a small library of enyne derivatives (Scheme 21).



**Scheme 21.** Optimization of enyne derivatives synthesis

With these results, we noted that substitutions on aromatic rings were well tolerated without significant modifications in the chemical yield (Scheme 21, **22a-e**). However, the replacement of the aryl substituent on triple bond by an alkyl led to a significant drop of yield (50% yield, Scheme 21, **22f**). The better performance of aryl- substituents over alkyl- triple bonds group, can be rationalized by the higher stabilization of the resulting diene for the conjugation with the aromatic ring. With the aim to expand our library of compounds, a Diels–Alder reaction was applied on diene **22a** through the treatment with dimethyl acetylene dicarboxylate (DMAD). However, **22a** did not react even after prolonged heating in DCE (Scheme 22).



**Scheme 22.** Failed Diels-Alder reaction on derivative **22a**

The low reactivity of diene **22a** in Diels–Alder reaction was probably explained by its preference to assume an *s-trans* conformation respect the required *s-cis* conformation for the reaction, due to the steric hindrance between the protons in ortho positions on the aromatic rings of the dienic moiety, which reduces in *s-trans* conformation the clashing of the protons in these positions (Figure 66).

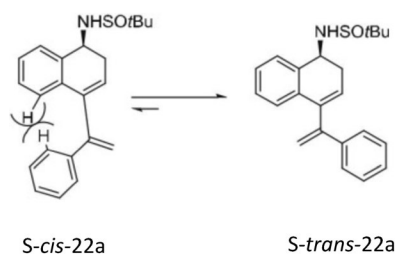
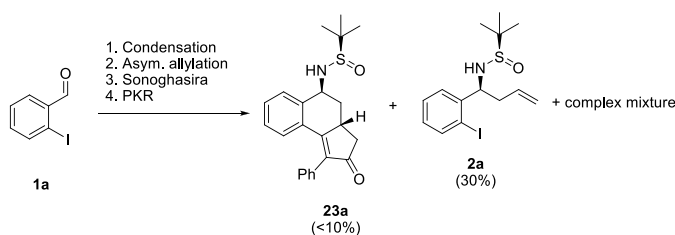


**Figure 66.** *S-cis/S-trans* conformational equilibrium of **22a**

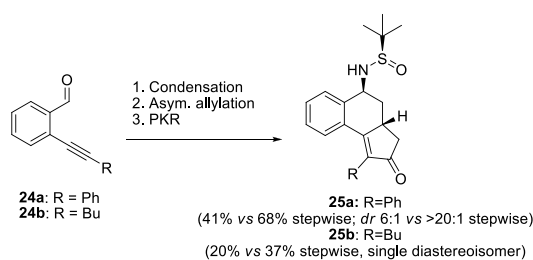
### 4.3 STUDY OF THE ONE-POT CONDENSATION/ASYMMETRIC ALLYLATION/INTRAMOLECULAR PAUSON-KHAND REACTION (PKR) SEQUENCE

Starting from the notable experience in terms of one-pot Ellman's sulfinimides transformations,<sup>124</sup> we decided to apply another one-pot protocol for the asymmetric synthesis of tricyclic enones, using the intramolecular PKR.<sup>123</sup> We started our study applying the four-step one-pot transformation: condensation/allylation/Sonogashira/ PKR. However, after the reaction, the desired product **23a** was obtained in low concentration (<10%), while compound **2a** was obtained in 30% chemical yield, suggesting that the Sonogashira reaction conditions were not fully compatible with the previous protocol of condensation/allylation reactions (Scheme 23).



**Scheme 23.** One-pot condensation/asymmetric allylation/Sonogashira coupling/PKR

As Sonogashira coupling seemed to be the obstacle for this one-pot procedure, we decided to perform this step independently and then to apply the one-pot procedure for the corresponding *o*-alkynylbenzaldehyde derivatives **24a** and **24b** (Scheme 24). As we can observe, the chemical yield of the one-pot procedure is significantly lower than the corresponding stepwise protocol (Scheme 24), even though the one-pot methodology presents a considerable operational simplicity. Moreover, the diastereoselectivity of compound **24a** was affected, as expected, in the one-pot procedure (Scheme 24). This is linked to the dependence of the diastereoselectivity with the substitution at the triple bond, as described in a previous report.<sup>123</sup> Differently, the isolation of a single diastereoisomer for compound **24b** might be due to a loss of small quantities of minor diastereoisomers during the purification, in accord to the low comprehensive chemical yield obtained (20%, Scheme 24).



**Scheme 24.** One-pot condensation/asymmetric allylation/PKR sequence

Concluding, in this report we have described the diversity-oriented synthesis of different substrates starting from available starting material. In particular the 2-iodobenzaldehyde has demonstrated its superior performance as a substrate for diversity-oriented synthesis. Specifically, we have explored the optimization of intramolecular Heck reaction conditions after the obtainment of an undesired product during the Sonogashira cross-coupling reaction. After this, an asymmetric allylation on Ellman's imines followed by intramolecular Heck reaction afforded 3-methylene-1-aminoindane derivatives, which were subjected to other chemical modifications. On the other hand, also the RCEYM reaction was explored and was observed that the introduction of an alkynyl group in *ortho*-position to the *tert*-butylsulfonyl amines, formed substrates suitable to achieve conjugated dienes. Also, we applied the one-pot procedures of asymmetric allylation/intramolecular Heck reaction and of condensation/asymmetric allylation/Pauson–Khand reaction sequence, observing that even though it was a good strategy in an operative point of view, however, it is at expense of chemical yields, which were notable more high in stepwise reaction than in the one-pot procedures.



## CONCLUSIONS

---

In my PhD research activity, different libraries of promising molecules have been prepared and pharmacologically evaluated in their interaction with bile acid receptors, FXR and GPBAR1. Medicinal chemistry modifications have been performed on endogenous bile acids CDCA and UDCA and on the most potent dual and semisynthetic derivative 6-ECDCA, in order to obtain selective bile acid receptor modulators. In a first phase, compound **7** has been identified as a FXR ligand with an EC<sub>50</sub> of ~9 μM. Even though compound **7** resulted less potent than the 6-ECDCA, it induced the expression of FXR targeted genes, mainly OSTα, with a comparable potency with that of the reference molecule. Moreover, compound **7** has been demonstrated a selective FXR agonist without activity towards GPBAR1 in transactivation assay and without inducing the expression of GPBAR1-regulated genes, such as pro-glucagon (or GLP-1), in RT-PCR. The above profile affirms this compound an ideal candidate in the treatment of hepatic FXR-mediated disorders<sup>17</sup> where the concomitant GPBAR1 activation induces exacerbation of cholestatic itching. Further, starting from compound **7**, we decided to harness the 6-ECDCA scaffold applying these peculiar chemical modifications:

- 1 Modifications at C-3 hydroxyl group (deletion/inversion)
- 2 Modifications of the nature of the side chain end-group
- 3 Modifications on stereochemical arrangement at C6/C7.

Except compound **45**, which preserves the 3α-OH group, all 6-ethylcholane derivatives prepared in this study were weak GPBAR1 agonists, thus confirming the key role of this functional group in GPBAR1 activation. In addition, the presence of both substituents on ring B in α-configuration produced potent FXR agonists (such as compounds **50**, **51**, **56** and **58**).<sup>100</sup> In this part of my project, further pharmacological investigations have been focalized on compounds **45** and **51**. Compound **45** is a selective GPBAR1 ligand, which maintains the tetracyclic core of UDCA. In transactivation assay, compound **45** resulted a potent GPBAR1 ligand with an EC<sub>50</sub> of 1 μM and devoid of any FXR agonistic activity. Of interest, *in vivo* pharmacological evaluation affirmed this molecule as a promising candidate in liver cirrhosis. Compound **51** has been demonstrated a selective FXR

agonist with a potency ( $EC_{50}$  value of 950 nM) comparable with that of 6-ECDC (3). Further, compound 51 induces the expression of FXR regulated genes in an *ex-vivo* RT-PCR assay, also reducing *in vivo* blood concentration of 7 $\alpha$ -hydroxy-4-cholesten-3-one, a key intermediate in the primary bile acid synthesis. Finally, in the third year of Ph.D. activity, I have turned my attention on 6-ECDC side chain, modifying the length and the nature of the end-group. In this way, the chemical diversity was expanded producing a large library of molecules with truncate or elongated side chains and differentiated in the stereochemical arrangements at C-6/C-7 positions and in the substitution at C-3. In the context of nor-derivatives, the side chain end-group exerts an important influence on receptor selectivity, with the alcohol 77, a potent FXR agonist, while a negative charged end-group, such as in compound 76, or a neutral end-group (78), improved GPBAR1 activity. The most interesting was compound 77, which resulted a potent FXR ligand with an  $EC_{50}$  of 2  $\mu$ M. Also, it presents a residual activity on GPBAR1 resulting a dual modulator.

In addition, further *in vivo* pharmacological investigations on this compound have been performed. When administered in rodent model of cholestasis, compound 77 did not induce exacerbation of cholestatic itching and in contemporary, it was able to exert protective effects against NASH-features in a mice model of HFD.

Moreover, all derivatives with both C-6 and C-7 groups  $\alpha$ -orientated, showed a dual activity (84–91), independently by the length of the side chain and by the nature of the end-group, with the bis-*homo* derivative 91, a potent and selective FXR agonist.

Finally, in Valencia, I worked in the diversity-oriented synthesis of different substrates starting from available starting material. Specifically, the optimization of intramolecular Heck reaction conditions have been performed, and after this, an asymmetric allylation on Ellman's imines followed by intramolecular Heck reaction was applied, affording a class of 3-methylene-1-aminoindane derivatives, which were subjected to further chemical modifications. In contemporary, the RCEYM reaction has been explored demonstrating that the presence of an alkynyl group in *ortho* to the *tert*-butyl sulfonyl amines, is instrumental in the preparation of conjugated dienes.

**EXPERIMENTAL SECTION**

---

**I. General experimental procedures**

**Chemistry.** Specific rotations were measured on a Jasco P-2000 polarimeter. High-resolution ESI-MS spectra were performed with a Micromass Q-TOF mass spectrometer. NMR spectra were obtained on Varian Inova 400, 500 and 700 NMR spectrometers ( $^1\text{H}$  at 400, 500 and 700 MHz,  $^{13}\text{C}$  at 100, 125 and 175 MHz, respectively) equipped with a SUN microsystem ultra5 hardware and recorded in  $\text{CD}_3\text{OD}$  ( $\delta_{\text{H}} = 3.31$  and,  $\delta_{\text{C}} = 49.0$  ppm) and  $\text{CDCl}_3$  ( $\delta_{\text{H}} = 7.26$  and,  $\delta_{\text{C}} = 77.0$  ppm). All of the detected signals were in accordance with the proposed structures. Coupling constants ( $J$  values) are given in Hertz (Hz), and chemical shifts ( $\delta$ ) are reported in ppm and referred to  $\text{CHD}_2\text{OD}$  and  $\text{CHCl}_3$  as internal standards. Spin multiplicities are given as s (singlet), br s (broad singlet), d (doublet), or m (multiplet). Through-space  $^1\text{H}$  connectivities were evidenced using a ROESY experiment with mixing times of 200 and 250 ms, respectively. HPLC was performed with a Waters Model 510 pump equipped with Waters Rheodine injector and a differential refractometer, model 401. Reaction progress was monitored via thin-layer chromatography (TLC) on Alugram silica gel G/UV254 plates. Silica gel MN Kieselgel60 (70-230 mesh) from Macherey-Nagel Company was used for column chromatography. All chemicals were obtained from Sigma-Aldrich, Inc. Silica gel (200-400 mesh) from Macherey-Nagel Company was used for flash chromatography. All chemicals were obtained from Sigma-Aldrich, Inc. Solvents and reagents were used as supplied from commercial sources with the following exceptions. Hexane, ethyl acetate, chloroform, dichloromethane, tetrahydrofuran and triethylamine were distilled from calcium hydride immediately prior to use. Methanol was dried from magnesium methoxide as follow. Magnesium turnings (5 g) and iodine (0.5 g) were refluxed in a small (50-100 mL) quantity of methanol until all of the magnesium has reacted. The mixture was diluted (up to 1 L) with reagent grade methanol, refluxed for 2-3 h then distilled under nitrogen. All reactions were carried out under argon atmosphere using flame-dried glassware. The purities of compounds were determined to be greater than 95% by HPLC.

**Cell cultures.** HepG2 cells were cultured in E-MEM supplemented with 10% FBS, 1% glutamine, 1% penicillin/streptomycin. GLUTAg cells were originally donated by Dr. Drucker D.J., Banting and Best Diabetes Centre, University of Toronto, Toronto General Hospital, 200 Elizabeth Street MBRW-4R402, Toronto, Canada M5G 2C4. GLUTAg cells were cultured in D-MEM, supplemented with 10% FBS, 1% glutamine, 1% penicillin/streptomycin. THP-1 cells were cultured in RPM-I supplemented with 10% FBS, 1% glutamine, 1% penicillin/streptomycin.

**Transactivation assay.** For FXR mediated transactivation, HepG2 cells were plated at  $5 \times 10^4$  cells/well in a 24-well plate. Cells were transfected with 200 ng of the reporter vector p(hsp27)-TK-LUC containing the FXR response element IR1 cloned from the promoter of heat shock protein 27 (hsp27), 100 ng of pSG5-FXR, 100 ng of pSG5-RXR, and 100 of pGL4.70 (Promega), a vector encoding the human Renillagene. The reporter plasmid p(hsp27)-TKLUC has been developed and validated for FXR reporter activity as previously reported.<sup>136</sup> At 24 h post-transfection, cells were stimulated 18 h with 10  $\mu$ M CDCA (**1**), and compounds tested. For GP-BAR1 mediated transactivation, HEK-293T cells were plated at  $1 \times 10^4$  cells/well in a 24 well-plate and transfected with 200 ng of pGL4.29 (Promega), a reporter vector containing a cAMP response element (CRE) that drives the transcription of the luciferase reporter gene luc2P, with 100 ng of pCMVSPORT6-human GP-BAR1, and with 100 ng of pGL4.70. At 24 h post-transfection, cells were stimulated 18 h with 10  $\mu$ M TLCA (**2**) and compounds tested. After treatments, 10  $\mu$ L of cellular lysates were read using Dual Luciferase Reporter Assay System (Promega Italia s.r.l., Milan, Italy) according manufacturer specifications using the Glomax 20/20 luminometer (Promega Italia s.r.l., Milan, Italy). For dose-response curves, cells were transfected as described above and then treated with increasing concentrations of compounds tested (0.1, 0.5, 1 and 10 and 50  $\mu$ M); luciferase activities were assayed and normalized with Renilla activities. To investigate the specificity of some compounds HepG2 cells were transiently transfected with 200 ng reporter vector p(UAS)<sub>5x</sub>TKLuc, 100 ngpGL4.70 and with a series of vectors containing the ligand binding domain of various nuclear receptors (PPAR $\gamma$ , LXR and GR) cloned upstream of the GAL4-DNA binding domain (*i.e.* pSG5-PPAR $\gamma$ LBD-GAL4DBD, pSG5-LXRLBD-

GAL4DBD and pSG5-GRLBD-GAL4DBD). At 48 h post-transfection, cells were stimulated 18 h with the appropriate nuclear receptor agonist or with compounds of interest. To investigate the PXR mediated transactivation, HepG2 cells were transfected with 100 ng pSG5-PXR, 100 ng pSG5-RXR, 100 ng pGL4.70 and with 200 ng of the reporter vector containing the PXR target gene promoter (CYP3A4 gene promoter) cloned upstream of the luciferase gene (pCYP3A4promoter-TKLuc). At 48 h post-transfection, cells were stimulated 18 h with 10  $\mu$ M rifaximin or with compounds tested.

**Real-Time PCR.** Total RNA was isolated using the TRIzol reagent according to the manufacturer's specifications (Invitrogen). One microgram of purified RNA was treated with DNaseI for 15 min at room temperature, followed by incubation at 95 °C for 3 min in the presence of 2.5 mmol/L EDTA. The RNA was reverse transcribed with Superscript III (Invitrogen) in 20  $\mu$ L reaction volume using random primers. For Real Time PCR, 10 ng template was dissolved in a 25  $\mu$ L containing 200 nmol/L of each primer and 12.5  $\mu$ L of 2X SYBR FAST Universal ready mix (Invitrogen). All reactions were performed in triplicate, and the thermal cycling conditions were as follows: 2 min at 95 °C, followed by 40 cycles of 95 °C for 20 s, 60 °C for 30 s in iCycleriQ instrument (Biorad). The relative mRNA expression was calculated and expressed as  $2^{-(\Delta\Delta C_t)}$ . Forward and reverse primer sequences were the following:

human GAPDH: gaaggtgaaggtcggagt and catgggtggaatcatattggaa;

human OST $\alpha$ : tgttgggccctttccaatac and ggctcccatgttctgctcac;

human BSEP: gggccattgtacgagatcctaaandtcaccgtcttttcactttctg;

human SHP: gctgtctggagtccttctgg and ccaatgatagggcgaaagaagag;

mouse GAPDH: ctgagtatgtcgtggagtctac and gttggtggtgcaggatgcattg;

mouse Pro-glucagon: tgaagacaaacgccactcac and caatgttgttccggttctc.

**cAMP measurement.** cAMP generation in THP-1 cells was assayed using the Direct Cyclic AMP enzyme Immunoassay Kit (Arbor Assay cat. Number K019-H1). THP-1 cells were serum starved over night and then stimulated for 30 min with 10  $\mu$ M Forskolin or compounds of interest.

**Direct interaction on FXR by Alphascreen technology in a coactivator recruitment assay.** Anti-GST-coated acceptor beads were used to capture the GST-fusion FXR-LBD whereas the biotinylated-SRC-1 peptide was captured by

the streptavidin donor beads. Upon illumination at 680 nm, chemical energy is transferred from donor to acceptor beads across the complex streptavidin-Donor/Src-1-Biotin/GSTFXR-LBD/Anti-GST-Acceptor and a signal is produced. The assay was performed in white, low-volume, 384-well Opti plates (PerkinElmer) using a final volume of 25  $\mu$ L containing final concentrations of 10 nM of purified GST-tagged FXR-LBD protein, 30 nM biotinylated Src-1 peptide, 20  $\mu$ g/mL anti-GST acceptor beads acceptor beads and 10  $\mu$ g/mL of streptavidin donor bead (PerkinElmer). The assay buffer contained 50 mM Tris (pH 7.4), 50 mM KCl, 0.1% BSA, and 1 mM DTT. The stimulation times with 1  $\mu$ L of tested compound (dissolved in 50% DMSO/H<sub>2</sub>O) were fixed to 30 min at room temperature. The concentration of DMSO in each well was maintained at a final concentration of 4%. After the addition of the detection mix (acceptor and donor beads) the plates were incubated in the dark for 4 h at room temperature and then were read in Envision microplate analyzer (PerkinElmer).

## II. Experimental procedures for chenocholane and ursocholane derivatives

### Synthesis of 3-deoxychenocholane derivatives

*Methyl 3 $\alpha$ -hydroxy-7-keto-5 $\beta$ -cholan-24-oate (32)*. An oven-dried 250 mL flask was charged with chenodeoxycholic acid (2.0 g, 5.1 mmol), sodium bromide (30.0 mg, 0.250 mmol), tetrabutylammonium bromide (5.40 g, 16.8 mmol), and 43 mL of a solution of MeOH/CH<sub>3</sub>COOH/H<sub>2</sub>O/AcOEt, 3:1:0.25:6.5 v/v. The mixture was stirred at room temperature until a homogeneous solution formed and then cooled at 0 °C. Sodium hypochlorite solution (10%, 5.0 mL, 5.6 mmol) was added, until the test for hypochlorite (peroxide test paper) was positive, and the yellow suspension was stirred. The mixture was stirred at room temperature for 6 h. Aqueous sodium bisulfite (3.3%) was added to afford a white suspension (negative test for peroxide). Water (50 mL) was added and the mixture stirred at 15 °C for 5 min. Aqueous solution was extracted with AcOEt (3 × 50 mL). The combined organic layer was washed with aqueous sodium bisulfite (50 mL) and water (50 mL) and then dried over anhydrous MgSO<sub>4</sub> and evaporated *in vacuo* to give 2.0 g of 3 $\alpha$ -hydroxy-7-keto-5 $\beta$ -cholan-24-oic acid, which was subjected to the next step without any purification. To a solution of this latter intermediate (2.0 g, 5.1 mmol) in MeOH dry (30 mL), *p*-toluenesulfonic acid (4.40 g, 25.5 mmol) was added. The solution was left to stand at room temperature for 2 h. The mixture was quenched by addition of NaHCO<sub>3</sub> saturated solution. After the evaporation of the methanol, the residue was extracted with EtOAc (3 x 150 mL). The combined extract was washed with brine, dried with Na<sub>2</sub>SO<sub>4</sub>, and evaporated to give the methyl esters as amorphous solid **32** (1.5 g, 72.7% over two steps).  $[\alpha]_D^{25} = -7.0$ ,  $c = 0.4$ . Selected <sup>1</sup>H NMR (400 MHz, CDCl<sub>3</sub>):  $\delta$  3.65 (3H, s), 3.55 (1H, m), 2.81 (1H, dd,  $J = 5.9$  e 12.3 Hz), 2.33 (1H, m), 2.17 (1H, m), 1.19 (3H, s), 0.88 (3H, d,  $J = 6.4$  Hz), 0.60 (3H, s). <sup>13</sup>C NMR (100 MHz, CDCl<sub>3</sub>):  $\delta$  212, 178.3, 71.3, 55.1, 49.9, 49.3, 46.3, 45.6, 43.0, 39.2, 39.0, 37.7, 35.5, 34.5, 31.1, 30.9, 30.2, 29.3, 28.6, 23.3, 22.0, 18.7, 14.4, 12.7.

*Methyl 7 $\alpha$ -hydroxy-5 $\beta$ -cholan-24-oate (33)*. To a solution of methyl ester of 7-keto-lithocholic acid (**32**) (130 mg, 0.32 mmol) in dry pyridine (10 mL), tosyl chloride (613 mg, 3.22 mmol) was added, and the mixture was stirred at room temperature for 4 h. It was poured into cold water (10 mL) and extracted with CH<sub>2</sub>Cl<sub>2</sub> (3 × 10 mL). The combined organic layer was washed with saturated

NaHCO<sub>3</sub> solution (10 mL), and water (10 mL), and then dried over anhydrous MgSO<sub>4</sub> and evaporated *in vacuo* to give 180 mg of methyl 3 $\alpha$ -tosyloxy-7-keto-5 $\beta$ -cholan-24-oate (quantitative yield) in the form of colorless needles, that was subjected to next step without any purification. Lithium bromide (55 mg, 0.64 mmol) and lithium carbonate (47 mg, 0.64 mmol) were added to a solution of methyl 3 $\alpha$ -tosyloxy-7-keto-5 $\beta$ -cholan-24-oate (180 mg, 0.32 mmol) in dry DMF (10 mL), and the mixture was refluxed for 3 h. After cooling to room temperature, the mixture was slowly poured into 10% HCl solution (50 mL) and extracted with CH<sub>2</sub>Cl<sub>2</sub> (3  $\times$  30 mL). The combined organic layer was washed successively with water, saturated NaHCO<sub>3</sub> solution and water, and then dried over anhydrous MgSO<sub>4</sub> and evaporated to dryness to give 124 mg of oily residue (quantitative yield), that was subjected to next step without any purification. An oven-dried 10 mL flask was charged with 10% palladium on carbon (30 mg) and the previously obtained crude intermediate (124 mg, 0.320 mmol) and the flask was evacuated and flushed with argon. Absolute methanol (5 mL) and dry THF (5 mL) were added, and the flask was flushed with hydrogen. The reaction was stirred at room temperature under H<sub>2</sub> (1 atm) over night. The mixture was filtered through Celite, and the recovered filtrate was concentrated to give 125 mg of methyl 7-keto-5 $\beta$ -cholan-24-oate (quantitative yield), that was subjected to next step without any purification. Methyl 7-keto-5 $\beta$ -cholan-24-oate (125 mg, 0.320 mmol) was dissolved in a solution of tetrahydrofuran/water (10 mL, 4/1 v/v) and treated at 0 °C with NaBH<sub>4</sub> (720 mg, 1.9 mmol). After 2 h, water and MeOH were added dropwise during a period of 15 min at 0 °C with effervescence being observed. Then after evaporation of the solvents, the residue was diluted with water, acidified with HCl 1 M and extracted with AcOEt (3  $\times$  10 mL). The combined organic phases were washed with brine, dried over Na<sub>2</sub>SO<sub>4</sub> anhydrous and evaporated under reduced pressure to obtain 125 mg of **33** (quantitative yield).  $[\alpha]_D^{25} = +3.5$  ( $c = 2.82$ , CH<sub>3</sub>OH); selected <sup>1</sup>H NMR (500 MHz, CDCl<sub>3</sub>):  $\delta$  3.84 (1H, s), 3.66 (3H, s), 2.34 (1H, m), 2.22 (1H, m), 0.92 (3H, d,  $J = 6.5$  Hz), 0.90 (3H, s), 0.66 (3H, s); HRMS-ESI  $m/z$  391.3216 [ $M + H$ ]<sup>+</sup>, C<sub>25</sub>H<sub>43</sub>O<sub>3</sub> requires 391.3212.

*7 $\alpha$ -hydroxy-5 $\beta$ -cholan-24-oic acid (4)*. Compound **33** (56 mg, 0.15 mmol) was hydrolyzed with a methanol solution of sodium hydroxide (5%, 10 mL) in H<sub>2</sub>O



(2 mL) overnight under reflux. The resulting solution was then concentrated under vacuum, diluted with water, acidified with HCl 6 M and extracted with ethyl acetate (3 x 50 mL). The collected organic phases were washed with brine, dried over Na<sub>2</sub>SO<sub>4</sub> anhydrous and evaporated under reduced pressure to give compound **4** in quantitative yield (58 mg). An analytical sample was obtained by HPLC on a Nucleodur 100-5 C18 (5 μm; 4.6 mm i.d. x 250 mm) with MeOH/H<sub>2</sub>O (95:5) as eluent (flow rate 1 mL/min, *t<sub>R</sub>*=8.2 min); [α]<sub>D</sub><sup>25</sup> = -5.3 (*c* = 0.03, CH<sub>3</sub>OH); selected <sup>1</sup>H NMR (400 MHz, CD<sub>3</sub>OD): δ 3.79 (1H, s), 2.33 (1H, m), 2.23 (1H, m), 0.96 (3H, d, *J* = 6.4 Hz), 0.93 (3H, s), 0.70 (3H, s); <sup>13</sup>C NMR (100 MHz, CD<sub>3</sub>OD): δ 178.3, 69.4, 57.3, 51.5, 44.9, 43.7, 41.1, 40.8, 38.8, 37.0, 36.2, 34.1, 32.4, 31.6, 30.8, 29.2, 29.0, 24.6, 24.2, 23.4, 22.6, 21.8, 18.8, 12.2; HRMS-ESI *m/z* 375.2903 [M-H]<sup>-</sup>, C<sub>24</sub>H<sub>39</sub>O<sub>3</sub> requires 375.2899.

*7α-hydroxy-5β-cholan-24-oyl taurine sodium salt (5)*. Compound **4** (15.0 mg, 39.9 x 10<sup>-3</sup> mmol) in DMF dry (3 mL) was treated with DMT-MM (33 mg, 0.12 mmol) and triethylamine (140 μL, 1.00 mmol) and the mixture was stirred at room temperature for 10 min. Then to the mixture was added taurine (30.0 mg, 0.240 mmol). After 24 h, the reaction mixture was concentrated *in vacuo* and dissolved in water (5 mL). The solution was poured over a C18 silica gel column. Fraction eluted with H<sub>2</sub>O/MeOH 99:1 gave a mixture that was further purified by HPLC on a Nucleodur 100-5 C18 (5 μm; 4.6 mm i.d. x 250 mm) with MeOH/H<sub>2</sub>O (83:17) as eluent (flow rate 1 mL/min), to give 7 mg (35%) of compound **5** (*t<sub>R</sub>*=7.6 min); [α]<sub>D</sub><sup>25</sup> = -58.2 (*c* = 0.02, CH<sub>3</sub>OH); selected <sup>1</sup>H NMR (500 MHz CD<sub>3</sub>OD): δ 3.79 (1H, s), 3.59 (2H, t, *J* = 7.3 Hz), 2.96 (2H, t, *J* = 7.3 Hz), 0.97 (3H, d, *J* = 7.1 Hz), 0.93 (3H, s), 0.69 (3H, s); HRESIMS *m/z* 482.2951 [M-Na]<sup>+</sup>, C<sub>26</sub>H<sub>44</sub>NO<sub>5</sub>S requires 482.2940.

*7α-hydroxy-5β-cholan-24-ol (6)*. Dry methanol (50.0 μL, 1.26 mmol) and LiBH<sub>4</sub> (630 μL, 2 M in THF, 1.26 mmol) were added to a solution of the compound **33** (70 mg, 0.3 mmol) in dry THF (10 mL) at 0 °C under argon and the resulting mixture was stirred for 3 h at 0 °C. The mixture was quenched by addition of NaOH (1 M, 4 mL) and then allowed to warm to room temperature. Ethyl acetate was added and the separated aqueous phase was extracted with ethyl acetate (3 × 15 mL). The combined organic phases were washed with water, dried (Na<sub>2</sub>SO<sub>4</sub>) and concentrated. Purification by silica gel eluting with

ethyl acetate- hexane (85:15) gave the alcohol **6** as a white solid (52 mg, 79%). An analytical sample was obtained by HPLC on a Nucleodur 100-5 C18 (5  $\mu$ m; 4.6 mm i.d. x 250 mm) with MeOH/H<sub>2</sub>O (95:5) as eluent (flow rate 1 mL/min,  $t_R$ =8 min);  $[\alpha]_D^{25} = +5.2$  ( $c = 0.53$ , CH<sub>3</sub>OH); selected <sup>1</sup>H NMR (400 MHz CD<sub>3</sub>OD):  $\delta$  3.79 (1H, br s), 3.51 (2H, t,  $J = 6.6$  Hz), 0.97 (3H, d,  $J = 6.6$  Hz), 0.93 (3H, s), 0.70 (3H, s); <sup>13</sup>C NMR (100 MHz, CD<sub>3</sub>OD):  $\delta$  69.4, 63.6, 57.6, 51.6, 45.6, 43.6, 42.8, 41.1, 40.9, 38.9, 37.0, 36.2, 34.1, 33.3, 31.6, 30.3, 29.3, 29.0, 24.7, 24.5, 22.6, 21.8, 19.2, 12.2; HRMS-ESI  $m/z$  363.3271 [M+H]<sup>+</sup>, C<sub>24</sub>H<sub>42</sub>O<sub>2</sub> requires 363.3263.

*7 $\alpha$ -hydroxy-5 $\beta$ -cholan-24-yl-24-sodium sulfate (7)* and *5 $\beta$ -cholan-7 $\alpha$ ,24-diol-7,24-disodium disulfate (8)*. At a solution of diol **6** (40 mg, 0.1 mmol) in DMF dry (3 mL) was added triethylamine-sulfur trioxide complex (88 mg, 0.55 mmol) under an argon atmosphere, and the mixture was stirred at 80 °C for 24 h. Most of the solvent was evaporated and the residue was poured over a RP18 column to remove excess SO<sub>3</sub>·NEt<sub>3</sub>. Fraction eluted with MeOH:H<sub>2</sub>O 45:55 gave a mixture that was further purified by HPLC on a Nucleodur 100-5 C18 (5  $\mu$ m; 4.6 mm i.d. x 250 mm) with MeOH/H<sub>2</sub>O (50:50) as eluent (flow rate 1 mL/min), to give 24 mg (39%) of compound **8** ( $t_R$ =20.4 min).  $[\alpha]_D^{25} = -9.3$  ( $c = 0.14$ , CH<sub>3</sub>OH); selected <sup>1</sup>H NMR (400 MHz, CDCl<sub>3</sub>):  $\delta$  4.42 (1H, s), 3.95 (2H, br t,  $J = 6.5$  Hz), 0.96 (3H, d,  $J = 6.5$  Hz), 0.94 (3H, s), 0.69 (3H, s); HR ESIMS  $m/z$  543.2070 [M-Na]<sup>-</sup>, C<sub>24</sub>H<sub>40</sub>O<sub>8</sub>S<sub>2</sub>Na requires 543.2062. Fraction eluted with MeOH gave a mixture that was further purified by on a Nucleodur 100-5 C18 (5  $\mu$ m; 4.6 mm i.d. x 250 mm) with MeOH/H<sub>2</sub>O (90:10) as eluent (flow rate 1 mL/min), to give 28 mg (55%) of compound **7** ( $t_R$ =6.6 min).  $[\alpha]_D^{25} = -7.0$  ( $c = 0.28$ , CH<sub>3</sub>OH); selected <sup>1</sup>H NMR (400 MHz CD<sub>3</sub>OD):  $\delta$  3.96 (2H, t,  $J = 6.6$  Hz), 3.78 (1H, br s), 3.30 (1H, ovl), 0.96 (3H, d,  $J = 6.5$ ), 0.92 (3H, s), 0.69 (3H, s); <sup>13</sup>C NMR (100 MHz, CD<sub>3</sub>OD):  $\delta$  69.7, 69.4, 57.7, 51.6, 45.0, 43.8, 41.2, 41.0, 39.0, 37.1, 36.3, 34.2, 33.3, 34.2, 33.3, 31.7, 29.5, 29.0, 27.3, 24.3, 22.7, 21.9, 19.2, 12.3; HR ESIMS  $m/z$  441.2679 [M-Na]<sup>-</sup>, C<sub>24</sub>H<sub>41</sub>O<sub>5</sub>S requires 441.2675.

### **Synthesis of 3 $\beta$ -chenodeoxycholane derivatives**

*3 $\alpha$ -tosyloxy-7 $\alpha$ -hydroxy-5 $\beta$ -cholan-24-oate (39)*. To a solution of CDCA methyl ester (400 mg, 1 mmol) in dry pyridine (10 mL), tosyl chloride (382 mg, 2 x 10<sup>-3</sup>

mol) was added, and the mixture was stirred at room temperature for 4 h. It was poured into cold water (20 mL) and extracted with CH<sub>2</sub>Cl<sub>2</sub> (3 × 50 mL). The combined organic layer was washed with saturated NaHCO<sub>3</sub> solution (30 mL), and water (30 mL), and then dried over anhydrous MgSO<sub>4</sub> and evaporated *in vacuo* to give 555 mg of **39** (quantitative yield) in the form of colourless oil.  $[\alpha]_D^{25} = +22.6$  ( $c = 0.93$ , CH<sub>3</sub>OH); selected <sup>1</sup>H NMR (500 MHz, CDCl<sub>3</sub>): δ 7.80 (2H, d,  $J = 8.7$  Hz), 7.34 (2H, d,  $J = 8.5$ ), 4.38 (1H, m), 3.83 (1H, s), 3.62 (3H, s), 2.40 (3H, s), 2.35 (1H, m), 2.23 (1H, m), 0.93 (3H, d,  $J = 6.4$  Hz), 0.89 (3H, s), 0.65 (3H, s); HR ESIMS  $m/z$  561.3288 [M+H]<sup>+</sup>, C<sub>32</sub>H<sub>49</sub>O<sub>6</sub>S requires 561.3283.

*Methyl 3β,7α-dihydroxy-5β-cholan-24-oate (40)*. A solution of **39** (555 mg, 0.990 mmol) and CH<sub>3</sub>COOK (97 mg, 0.99 mmol) dissolved in water (2 mL) and *N,N*-dimethylformamide (DMF, 10 mL) was refluxed for 2 h. The solution was cooled at room temperature and then ethyl acetate and water were added. The separated aqueous phase was extracted with ethyl acetate (3 × 30 mL). The combined organic phases were washed with water, dried (Na<sub>2</sub>SO<sub>4</sub>) and evaporated to dryness to give 600 mg of mixture. Purification by silica gel (hexane-ethyl acetate 7:3 and 0.5% TEA) gave **40** as oily oil (300 mg, 75%).  $[\alpha]_D^{25} = +2.6$  ( $c = 1.5$ , CH<sub>3</sub>OH); selected <sup>1</sup>H NMR (400 MHz, CD<sub>3</sub>OD): δ 3.96 (1H, s), 3.79 (1H, s), 3.63 (3H, s), 2.47 (dt,  $J = 2.3, 13.7$  Hz), 2.36 (1H, m), 2.26 (1H, m), 0.95 (3H, s), 0.94 (3H, ovl), 0.68 (3H, s); <sup>13</sup>C NMR (100 MHz, CD<sub>3</sub>OD): δ 171.7, 69.3, 67.7, 57.3, 52.0, 51.6, 43.7, 41.1, 40.7, 37.5 (2C), 36.7 (2C), 35.5, 33.4, 32.3, 31.9, 31.0, 29.3, 28.6, 24.6, 23.8, 22.1, 18.8, 12.2; HR ESIMS  $m/z$  407.3173 [M+H]<sup>+</sup>, C<sub>25</sub>H<sub>43</sub>O<sub>4</sub> requires 407.3161.

*3β,7α-dihydroxy-5β-cholan-24-oic acid (19)*. Compound **40** (70.0 mg, 0.172 mmol) was hydrolyzed with a methanol solution of sodium hydroxide (5%, 5 mL) in H<sub>2</sub>O (1 mL) overnight under reflux. The resulting solution was then concentrated under vacuum, diluted with water, acidified with HCl 6 M and extracted with ethyl acetate (3 × 50 mL). The collected organic phases were washed with brine, dried over Na<sub>2</sub>SO<sub>4</sub> anhydrous and evaporated under reduced pressure. HPLC purification on a Nucleodur 100-5 C18 (5 μm; 5 mm i.d. × 250 mm) with MeOH/H<sub>2</sub>O (75:25) as eluent (flow rate 1 mL/min), gave 60 mg of **19** as a white solid (89%,  $t_R = 22$  min).  $[\alpha]_D^{25} = +11$  ( $c = 0.07$ , CH<sub>3</sub>OH); selected <sup>1</sup>H

NMR (400 MHz, CD<sub>3</sub>OD):  $\delta$  3.97 (1H, s), 3.79 (1H, s), 2.47 (1H, dt,  $J = 2.34$ , 13.8 Hz), 2.28 (1H, m), 2.13 (1H, m), 0.96 (3H, d, ovl), 0.95 (3H, s), 0.69 (3H, s); HR ESIMS  $m/z$  391.2856 [M-H]<sup>-</sup>, C<sub>24</sub>H<sub>39</sub>O<sub>4</sub> requires 391.2848.

*3 $\beta$ ,7 $\alpha$ -dihydroxy-5 $\beta$ -cholan-24-ol (20)*. 2,6-lutidine (570  $\mu$ L, 4.90 mmol) and *tert*-butyldimethylsilyl trifluoromethanesulfonate (336  $\mu$ L, 1.50 mmol) were added at 0 °C to a solution of **40** (200 mg, 0.5 mmol) in 10 mL of CH<sub>2</sub>Cl<sub>2</sub>. After 2 h stirring at 0 °C, the reaction was quenched by addition of aqueous NaHSO<sub>4</sub> (1 M, 30 mL). The layers were separated and the aqueous phase was extracted with CH<sub>2</sub>Cl<sub>2</sub> (3  $\times$  100 mL). The combined organic layers were washed with NaHSO<sub>4</sub>, water, saturated aqueous NaHCO<sub>3</sub>, and brine and evaporated *in vacuo* to give 310 mg of methyl 3 $\beta$ , 7 $\alpha$ -di(*tert*-butyldimethylsilyloxy)-5 $\beta$ -cholan-24-oate (quantitative yield) in the form of colorless needles, that was subjected to next step without any purification. To a solution of methyl ester (310 mg, 0.49 mmol) in dry THF (10 mL) at 0 °C, dry methanol (140  $\mu$ L, 3.4 mmol) and LiBH<sub>4</sub> (1.7 mL, 2M in THF, 3.4 mmol) were added. The resulting mixture was stirred for 1 h at 0 °C. The mixture was quenched by addition of 1 M NaOH (1 mL) and then ethyl acetate. The organic phase was washed with water, dried (Na<sub>2</sub>SO<sub>4</sub>) and concentrated to give 250 mg of **41** as a white solid (84%). Methyl ester **41** (200 mg, 0.3 mmol) was dissolved in methanol (5 mL) and 500  $\mu$ L of HCl 37% v/v were added. After 2 h, silver carbonate was added at the solution to precipitate chloride. Then the reaction mixture was centrifuged and the supernatant was concentrated *in vacuo*. HPLC purification on a Nucleodur 100-5 C18 (5  $\mu$ m; 5 mm i.d.  $\times$  250 mm) with MeOH/H<sub>2</sub>O (9:1) as eluent (flow rate 1 mL/min), gave 120 mg of compound **20** as a white solid (96%,  $t_R$ =7 min).  $[\alpha]_D^{25} = +22.8$  ( $c = 0.06$ , CH<sub>3</sub>OH); selected <sup>1</sup>H NMR (500 MHz, CD<sub>3</sub>OD):  $\delta$  3.98 (1H, s), 3.80 (1H, s), 3.50 (2H, m), 0.97 (3H, d,  $J = 6.7$  Hz), 0.96 (3H, s), 0.70 (3H, s). <sup>13</sup>C NMR (125 MHz, CD<sub>3</sub>OD):  $\delta$  69.3, 67.7, 63.6, 57.6, 51.6, 43.7, 41.1, 40.7, 37.5, 37.4, 37.1, 36.7, 35.5, 33.4, 33.2, 31.0, 30.3, 29.3, 28.5, 24.6, 23.8, 22.1, 19.2, 12.2; HR ESIMS  $m/z$  379.3219 [M+H]<sup>+</sup>, C<sub>24</sub>H<sub>43</sub>O<sub>3</sub> requires 379.3212.

*3 $\beta$ ,7 $\alpha$ -dihydroxy-5 $\beta$ -cholan-24-yl-24-sodium sulphate (21)*. The triethylamine-sulfur trioxide complex (65.6 mg, 0.410 mmol) was added to a solution of **41**

(50.0 mg,  $82.5 \times 10^{-3}$  mmol) in DMF dry (5 mL) under an argon atmosphere, and the mixture was stirred at 80°C over night. The solution was then concentrated under vacuum to give 100 mg of crude mixture. The solid was dissolved in methanol (5 mL) and the solution was added 300  $\mu$ L of HCl 37% v/v. After 1h, silver carbonate was added at the solution to precipitate chloride. Then the reaction mixture was centrifuged and the supernatant was concentrated *in vacuo*. HPLC purification on a Nucleodur 100-5 C18 (5  $\mu$ m; 5 mm i.d. x 250 mm) with MeOH/H<sub>2</sub>O (55:45) as eluent (flow rate 1 mL/min), gave 30 mg of **21** as colorless amorphous solid (76% over two steps,  $t_R$ =11.4 min).  $[\alpha]_D^{25} = +18.4$  ( $c = 0.04$ , CH<sub>3</sub>OH); selected <sup>1</sup>H NMR (500 MHz, CD<sub>3</sub>OD):  $\delta$  3.97 (3H, m), 3.80 (1H, s), 2.49 (1H, t,  $J = 14.3$  Hz), 0.97 (3H, d, ovl), 0.96 (3H, s), 0.70 (3H, s); HR ESIMS  $m/z$  457.2632 [M-Na]<sup>-</sup>, C<sub>24</sub>H<sub>41</sub>O<sub>6</sub>S requires 457.2624.

### Synthesis of 3-deoxyursocholane derivatives

*Methyl 3 $\alpha$ -tosyloxy-7 $\beta$ -hydroxy-5 $\beta$ -cholan-24-oate (34)*. To a solution of UDCA methyl ester (400 mg, 1 mmol) in dry pyridine (10 mL), tosyl chloride (280 mg, 1.5 mmol) was added, and the mixture was stirred at room temperature for 2 h. It was poured into cold water (10 mL) and extracted with CH<sub>2</sub>Cl<sub>2</sub> (3  $\times$  10 mL). Purification by silica gel eluting with ethyl acetate-hexane (8:2) gave compound **34** (320 mg, 58%) as a white solid.  $[\alpha]_D^{25} = +37.6$  ( $c = 0.70$ , CH<sub>3</sub>OH); selected <sup>1</sup>H NMR (400 MHz, CDCl<sub>3</sub>):  $\delta$  7.79 (2H, d,  $J = 8.5$  Hz), 7.33 (2H, d,  $J = 8.5$ ), 4.40 (1H, m), 3.52 (1H, m), 2.46 (3H, s), 2.35 (1H, m), 2.23 (1H, m), 0.92 (3H, ovl), 0.91 (3H, s), 0.66 (3H, s); HR ESIMS  $m/z$  561.3259 [M+H]<sup>+</sup>, C<sub>32</sub>H<sub>49</sub>O<sub>6</sub>S requires 561.3250.

*7 $\beta$ -hydroxy-5 $\beta$ -cholan-24-oic acid (9)*. Lithium bromide (73 mg, 0.84 mmol) and lithium carbonate (62 mg, 0.84 mmol) were added to a solution of methyl ester **34** (220 mg, 0.42 mmol) in dry DMF (10 mL), and the mixture was refluxed for 2 h. After cooling to room temperature, the mixture was slowly poured into 10% HCl solution (10 mL) and extracted with CH<sub>2</sub>Cl<sub>2</sub> (3  $\times$  30 mL). The combined organic layer was washed successively with water, saturated NaHCO<sub>3</sub> solution and water, and then dried over anhydrous MgSO<sub>4</sub> and evaporated to dryness to give 162 mg of oily residue (quantitative yield), that was subjected to next step without any purification.

An oven-dried 10 mL flask was charged with 10% palladium on carbon (5 mg) and the product obtained (162 mg, 0.420 mmol) and the flask was evacuated and flushed with argon. Absolute methanol (5 mL) and dry THF (5 mL) were added, and the flask was flushed with hydrogen. The reaction was stirred at room temperature under H<sub>2</sub> (1 atm) over night. The mixture was filtered through celite, and the recovered filtrate was concentrated to give 128 mg of compound **35** (78%). An amount of compound **35** (40 mg, 1.02 x 10<sup>-1</sup> mmol) was hydrolyzed with a methanol solution of sodium hydroxide (5%, 5 mL) in H<sub>2</sub>O (1 mL) overnight under reflux. The resulting solution was then concentrated under vacuum, diluted with water, acidified with HCl 6 M and extracted with ethyl acetate (3 x 20 mL). The collected organic phases were washed with brine, dried over Na<sub>2</sub>SO<sub>4</sub> anhydrous and evaporated under reduced pressure to give **9** in a quantitative yield (39.5 mg). An analytical sample was obtained by HPLC on a Nucleodur 100-5 C18 (5 μm; 4.6 mm i.d. x 250 mm) with MeOH/H<sub>2</sub>O (78:22) as eluent (flow rate 1 mL/min, *t<sub>R</sub>*=13.2 min). [α]<sub>D</sub><sup>25</sup> = -95.0 (*c* = 0.08, CH<sub>3</sub>OH); selected <sup>1</sup>H NMR (400 MHz, CD<sub>3</sub>OD): δ 3.45 (1H, m), 2.32 (1H, m), 2.21 (1H, m), 0.96 (3H, s), 0.95 (3H, ovl), 0.71 (3H, s); HR ESIMS *m/z* 375.2901 [M-H]<sup>-</sup>, C<sub>24</sub>H<sub>39</sub>O<sub>3</sub> requires 375.2899.

*7β-hydroxy-5β-cholan-24-oyl taurine sodium salt (10)*. Compound **9** (9.0 mg, 2.4 x 10<sup>-2</sup> mmol) in DMF dry (3 mL) was treated with DMT-MM (20.0 mg, 71.7 x 10<sup>-3</sup> mmol) and triethylamine (85 μL, 0.60 mmol) and the mixture was stirred at room temperature for 10 min. Then to the mixture was added taurine (18 mg, 0.14 mmol). After 24 h, the reaction mixture was concentrated *in vacuo* and dissolved in water (5 mL). The solution was poured over a C18 silica gel column. Fraction eluted with H<sub>2</sub>O/MeOH 99:1 gave a mixture that was further purified by HPLC on a Nucleodur 100-5 C18 (5 μm; 4.6 mm i.d. x 250 mm) with MeOH/H<sub>2</sub>O (73:27) as eluent (flow rate 1 mL/min), to give 3.3 mg of **10** (27%, *t<sub>R</sub>*=18 min). [α]<sub>D</sub><sup>25</sup> = +4.8 (*c* = 0.08, CH<sub>3</sub>OH); selected <sup>1</sup>H NMR (400 MHz, CD<sub>3</sub>OD): δ 3.57 (2H, t, *J* = 7.2), 3.46 (1H, m), 2.95 (2H, t, *J* = 7.2), 0.96 (6H, ovl), 0.70 (3H, s); HR ESIMS *m/z* 482.2945 [M-Na]<sup>+</sup>, C<sub>24</sub>H<sub>39</sub>O<sub>3</sub> requires 482.2940.

*7β-hydroxy-5β-cholan-24-ol (11)*. Dry methanol (22 μL, 0.55 mmol) and LiBH<sub>4</sub> (276 μL, 2 M in THF, 0.550 mmol) were added to a solution of the compound

**35** (72 mg,  $18.4 \times 10^{-2}$  mmol) in dry THF (10 mL) at 0 °C under argon and the resulting mixture was stirred for 3 h at 0 °C. The mixture was quenched by addition of NaOH (1.0 M, 0.36 mL) and then allowed to warm to room temperature. Ethyl acetate was added and the separated aqueous phase was extracted with ethyl acetate ( $3 \times 15$  mL). The combined organic phases were washed with water, dried ( $\text{Na}_2\text{SO}_4$ ) and concentrated to give 61 mg of **11** as a white solid (91% yield). An analytical sample was obtained by HPLC on a Nucleodur 100-5 C18 (5  $\mu\text{m}$ ; 4.6 mm i.d. x 250 mm) with MeOH/ $\text{H}_2\text{O}$  (95:5) as eluent (flow rate 1 mL/min,  $t_{\text{R}}$ =16 min).  $[\alpha]_{\text{D}}^{25} = +114.6$  ( $c = 0.04$ ,  $\text{CH}_3\text{OH}$ ); selected  $^1\text{H}$  NMR (400 MHz,  $\text{CD}_3\text{OD}$ ):  $\delta$  3.51 (2H, t,  $J = 6.5$  Hz), 3.46 (H, m), 0.96 (3H, s), 0.95 (3H, d, ovl), 0.71 (3H, s); HRMS-ESI  $m/z$  363.3268  $[\text{M}+\text{H}]^+$ ,  $\text{C}_{24}\text{H}_{42}\text{O}_2$  requires 363.3263.

*5 $\beta$ -cholan-7 $\beta$ ,24-diyl-7,24-disodium disulfate (13)* and *7 $\beta$ -hydroxy-5 $\beta$ -cholan-24-yl-24-sodium sulfate (12)*. At a solution of diol **11** (50.0 mg, 0.138 mmol) in DMF dry (5 mL) was added triethylamine-sulfur trioxide complex (125 mg, 0.690 mmol) under an argon atmosphere, and the mixture was stirred at 80°C for 24 h. Most of the solvent was evaporated and the residue was poured over a RP18 column to remove excess  $\text{SO}_3 \cdot \text{NEt}_3$ . Fraction eluted over a RP18 column with  $\text{H}_2\text{O}:\text{MeOH}$  1:1 gave a mixture that was further purified by HPLC on a Nucleodur 100-5 C18 (5  $\mu\text{m}$ ; 4.6 mm i.d. x 250 mm) with MeOH/ $\text{H}_2\text{O}$  (65:35) as eluent (flow rate 1 mL/min), to give 32 mg of **13** (41%,  $t_{\text{R}}$ =12.4 min);  $[\alpha]_{\text{D}}^{25} = -15.4$  ( $c = 0.03$ ,  $\text{CH}_3\text{OH}$ ); selected  $^1\text{H}$  NMR (400 MHz  $\text{CD}_3\text{OD}$ ):  $\delta$  3.96 (2H, m), 3.49 (1H, m), 0.97 (6H, ovl), 0.71 (3H, s); HR ESIMS  $m/z$  543.2069  $[\text{M}-\text{Na}]^-$ ,  $\text{C}_{24}\text{H}_{40}\text{O}_8\text{S}_2\text{Na}$  requires 543.2062.

Fraction eluted over a RP18 column with MeOH gave a mixture that was further purified by HPLC on a Nucleodur 100-5 C18 (5  $\mu\text{m}$ ; 4.6 mm i.d. x 250 mm) with MeOH/ $\text{H}_2\text{O}$  (83:17) as eluent (flow rate 1 mL/min), to give 26 mg of compound **12** (41%,  $t_{\text{R}}$ =5.4 min);  $[\alpha]_{\text{D}}^{25} = +21.4$  ( $c = 1.46$ ,  $\text{CH}_3\text{OH}$ ); selected  $^1\text{H}$  NMR (400 MHz  $\text{CD}_3\text{OD}$ ):  $\delta$  4.28 (1H, m), 3.96 (2H, m), 0.99 (3H, s), 0.98 (3H, ovl), 0.72 (3H, s);  $^{13}\text{C}$  NMR (100 MHz,  $\text{CD}_3\text{OD}$ ):  $\delta$  81.0, 70.9, 56.6 (2C), 45.4, 44.8, 42.6, 41.3, 40.5, 38.3, 36.8, 35.6, 35.2, 33.1, 29.5, 28.8, 28.2, 27.0, 26.9,

24.6, 22.1, 21.8, 19.1, 12.5; HR ESIMS  $m/z$  441.2681  $[M-Na]^-$ ,  $C_{24}H_{41}O_5S$  requires 441.2675.

### Synthesis of 5 $\beta$ -cholane derivatives

*Methyl 3 $\alpha$ ,7 $\beta$ -ditosyloxy-5 $\beta$ -cholan-24-oate (36)*. To a solution of UDCA methyl ester (300 mg, 0.7 mmol) in dry pyridine (20 mL), tosyl chloride (1.39 g, 7.30 mmol) was added, and the mixture was stirred at room temperature for 6 h. It was poured into cold water (30 mL) and extracted with  $CH_2Cl_2$  (3  $\times$  30 mL). Purification by silica gel eluting with ethyl acetate-hexane (8:2) gave **36** (521 mg, quantitative yield) as a white solid.  $[\alpha]_D^{25} = -11$  ( $c = 0.48$ ,  $CH_3OH$ ); selected  $^1H$  NMR (400 MHz,  $CDCl_3$ ):  $\delta$  7.79 (2H, d,  $J = 8.3$  Hz), 7.75 (2H, d,  $J = 8.3$  Hz), 7.36 (2H, d,  $J = 8.3$  Hz), 7.32 (2H, d,  $J = 8.3$  Hz), 4.58 (1H, m), 4.38 (1H, m), 3.67 (3H, s), 2.47 (3H, s), 2.45 (3H, s), 2.33 (1H, m), 2.22 (1H, m), 0.91 (3H, d,  $J = 6.5$  Hz), 0.88 (3H, s), 0.61 (3H, s); HR ESIMS  $m/z$  715.3333  $[M+H]^+$ ,  $C_{39}H_{55}O_8S_2$  requires 715.3338.

*Methyl 5 $\beta$ -cholan-24-oate (37)* and *8 $\alpha$  epimer 38*. Lithium bromide (45 mg, 0.52 mmol) and lithium carbonate (38 mg, 0.52 mmol) were added to a solution of **36** (190 mg, 0.26 mmol) in dry DMF (20 mL), and the mixture was refluxed for 3 h. After cooling to room temperature, the mixture was slowly poured into 10% HCl solution (50 mL) and extracted with  $CH_2Cl_2$  (3  $\times$  30 mL). The combined organic layer was washed successively with water, saturated  $NaHCO_3$  solution and water, and then dried over anhydrous  $MgSO_4$  and evaporated to dryness to give 124 mg of oily residue (quantitative yield), that was subjected to next step without any purification.

An oven-dried 10 mL flask was charged with 10% palladium on carbon (10 mg) and the crude product (124 mg, 0.230 mmol) and the flask was evacuated and flushed with argon. Absolute methanol (5 mL) and dry THF (5 mL) were added, and the flask was flushed with hydrogen. The reaction was stirred at room temperature under  $H_2$  (1 atm) over night. The mixture was filtered through celite, and the recovered filtrate was concentrated to give 95 mg of crude product, that was further purified by HPLC on a Nucleodur 100-5 C18 (5  $\mu$ m; 10 mm i.d.  $\times$  250 mm) with  $MeOH:H_2O$  (995:5) as eluent (flow rate 3 mL/min), to give 25 mg of compound **38** (26%,  $t_R = 25.5$  min) and 32 mg of compound **37** (33%;  $t_R = 33$  min).



*Methyl 5 $\beta$ -cholan-24-oate (37)*.  $[\alpha]_D^{25} = -3.0$  ( $c = 0.03$ , CH<sub>3</sub>OH); selected <sup>1</sup>H NMR (400 MHz, CDCl<sub>3</sub>):  $\delta$  3.66 (3H, s), 2.33 (1H, m), 2.20 (1H, m), 0.91 (6H, ovl), 0.65 (3H, s); <sup>13</sup>C NMR (100 MHz, CDCl<sub>3</sub>):  $\delta$  171.9, 56.6, 56.0, 51.5, 43.8, 40.5 (2C), 40.3, 37.7, 35.9, 35.4 (2C), 31.0 (2C), 28.2, 27.5, 27.3, 27.1, 26.5, 24.2 (2C), 21.3, 20.8, 18.2, 12.0; HR ESIMS  $m/z$  375.3267 [M+H]<sup>+</sup>, C<sub>25</sub>H<sub>43</sub>O<sub>2</sub> requires 375.3263.

*Compound 38*.  $[\alpha]_D^{25} = +19.7$  ( $c = 0.02$ , CH<sub>3</sub>OH); selected <sup>1</sup>H NMR (400 MHz, CDCl<sub>3</sub>):  $\delta$  3.68 (3H, s), 2.46 (1H, m), 2.35 (1H, dd,  $J = 10.1, 5.3$ ), 0.95 (3H, d,  $J = 6.5$  Hz), 0.84 (3H, s), 0.81 (3H, s); <sup>13</sup>C NMR (100 MHz, CDCl<sub>3</sub>):  $\delta$  172.2, 56.6, 51.5, 43.9 (2C), 37.3, 37.1, 36.7, 35.9, 35.3 (2C), 34.1, 31.0, 30.8, 27.7, 27.1 (2C), 26.6, 25.7, 24.9, 24.6, 21.7, 19.4, 18.7, 18.3; HR ESIMS  $m/z$  375.3265 [M+H]<sup>+</sup>, C<sub>25</sub>H<sub>43</sub>O<sub>2</sub> requires 375.3263.

*5 $\beta$ -cholan-24-ol (14)*. Dry methanol (8.0  $\mu$ L, 0.19 mmol) and LiBH<sub>4</sub> (95  $\mu$ L, 2 M in THF, 0.19 mmol) were added to a solution of **37** (10.0 mg,  $26.7 \times 10^{-3}$  mmol) in dry THF (5 mL) at 0 °C under argon and the resulting mixture was stirred for 3 h at 0 °C. The mixture was quenched by addition of NaOH (1.0 M, 55  $\mu$ L) and then allowed to warm to room temperature. Ethyl acetate was added and the separated aqueous phase was extracted with ethyl acetate (3  $\times$  15 mL). The combined organic phases were washed with water, dried (Na<sub>2</sub>SO<sub>4</sub>) and concentrated to give 7.8 mg of **14** (84%). An analytical sample was obtained by HPLC on a Nucleodur 100-5 C18 (5  $\mu$ m; 4.6 mm i.d.  $\times$  250 mm) with MeOH/H<sub>2</sub>O (999.5:0.5) as eluent (flow rate 1 mL/min,  $t_R = 18$  min);  $[\alpha]_D^{25} = +20.5$  ( $c = 0.20$ , CH<sub>3</sub>OH); selected <sup>1</sup>H NMR (400 MHz, CDCl<sub>3</sub>):  $\delta$  3.62 (2H, m), 0.94 (3H, d, ovl), 0.92 (3H, s), 0.65 (3H, s); <sup>13</sup>C NMR (100 MHz, CDCl<sub>3</sub>):  $\delta$  63.7, 56.7, 56.3, 43.9, 42.8, 40.6 (2C), 40.3, 37.8, 36.0, 35.6, 31.9, 29.5, 28.3, 27.6, 27.3 (2C), 27.0, 26.8, 24.4, 21.4, 20.9, 18.7, 12.2; HR ESIMS  $m/z$  347.3321 [M+H]<sup>+</sup>, C<sub>24</sub>H<sub>43</sub>O requires 347.3314.

*5 $\beta$ -cholan-24-yl-24-sodium sulfate (15)*. At a solution of **14** (5.0 mg,  $1.45 \times 10^{-2}$  mmol) in DMF dry (3 mL) was added triethylamine-sulfur trioxide complex (12 mg,  $7.25 \times 10^{-2}$  mmol) under an argon atmosphere, and the mixture was stirred at 80 °C for 24 h. Most of the solvent was evaporated and the residue was poured over a RP18 column to remove excess SO<sub>3</sub>·NET<sub>3</sub>. Fraction eluted with MeOH

give 1.5 mg of compound **15** (23%). An analytical sample was obtained by HPLC on a Nucleodur 100-5 C18 (5  $\mu\text{m}$ ; 4.6 mm i.d. x 250 mm) with MeOH/H<sub>2</sub>O (98:2) as eluent (flow rate 1 mL/min,  $t_{\text{R}}$ =9.9 min);  $[\alpha]_{\text{D}}^{25} = +9.0$  ( $c = 0.88$ , CH<sub>3</sub>OH); selected <sup>1</sup>H NMR (400 MHz, CD<sub>3</sub>OD):  $\delta$  3.64 (2H, m), 0.96 (3H, d, ovl), 0.95 (3H, s), 0.69 (3H, s); <sup>13</sup>C NMR (100 MHz, CD<sub>3</sub>OD):  $\delta$  69.7, 57.6, 47.9, 45.2, 43.8, 41.9, 41.6, 38.7, 37.3, 36.8, 36.5, 33.2, 29.3, 28.6, 28.4, 28.2, 27.7, 27.1, 25.3, 24.8, 22.4, 22.0, 19.2, 12.5; HR ESIMS  $m/z$  425.2732 [M-H]<sup>-</sup>, C<sub>24</sub>H<sub>41</sub>O<sub>4</sub>S requires 425.2726.

*Compound 16.* Compound **38** (12.0 mg, 32.0 x 10<sup>-3</sup> mmol) was hydrolyzed with a methanol solution of sodium hydroxide (5%, 5 mL) in H<sub>2</sub>O (1 mL) overnight under reflux. The resulting solution was then concentrated under vacuum, diluted with water, acidified with HCl 6 M and extracted with ethyl acetate (3 x 50 mL). The collected organic phases were washed with brine, dried over Na<sub>2</sub>SO<sub>4</sub> anhydrous and evaporated under reduced pressure to give 9 mg of carboxylic acid **16** (78%). An analytical sample was obtained by HPLC on a Nucleodur 100-5 C18 (5  $\mu\text{m}$ ; 4.6 mm i.d. x 250 mm) with MeOH/H<sub>2</sub>O (99:1) as eluent (flow rate 1 mL/min,  $t_{\text{R}}$ =21 min);  $[\alpha]_{\text{D}}^{25} = +12.7$  ( $c = 0.28$ , CHCl<sub>3</sub>); selected <sup>1</sup>H NMR (400 MHz, CD<sub>3</sub>OD):  $\delta$  2.42 (1H, m), 2.28 (1H, m), 0.97 (3H, d,  $J = 6.8$  Hz), 0.85 (3H, s), 0.81 (3H, s); HR ESIMS  $m/z$  359.2958 [M-H]<sup>-</sup>, C<sub>24</sub>H<sub>39</sub>O<sub>2</sub> requires 359.2950.

*Compound 17.* Compound **17** (18 mg, 97%) was synthesized, starting from compound **38** (20.0 mg, 53.5 x 10<sup>-3</sup> mmol), by analogous procedures to those detailed above for compound **14**. An analytical sample was obtained by HPLC on a Nucleodur 100-5 C18 (5  $\mu\text{m}$ ; 4.6 mm i.d. x 250 mm) with MeOH/H<sub>2</sub>O (999.5:0.5) as eluent (flow rate 1 mL/min,  $t_{\text{R}}$ =15.8 min);  $[\alpha]_{\text{D}}^{25} = +2.9$  ( $c = 0.18$ , CHCl<sub>3</sub>); selected <sup>1</sup>H NMR (400 MHz, CDCl<sub>3</sub>):  $\delta$  3.64 (2H, m), 0.97 (3H, d,  $J = 6.3$ ), 0.85 (3H, s), 0.81 (3H, s); <sup>13</sup>C NMR (100 MHz, CDCl<sub>3</sub>):  $\delta$  63.6, 56.9, 44.1 (2C), 42.6, 37.4 (2C), 36.7, 36.1, 35.3, 34.2, 31.7, 29.3, 27.7, 27.2, 27.1, 26.6, 25.8, 24.9, 24.6, 21.7, 19.5, 19.1, 18.1; HR ESIMS  $m/z$  347.3318 [M+H]<sup>+</sup>, C<sub>24</sub>H<sub>43</sub>O requires 347.3314.

*Compound 18.* Compound **18** (8.8 mg, 43%) was synthesized, starting from compound **17** (16.0 mg, 46.2 x 10<sup>-3</sup> mmol), by an analogous procedure to that detailed above for compound **15**. An analytical sample was obtained by HPLC

on a Nucleodur 100-5 C18 (5  $\mu$ m; 4.6 mm i.d. x 250 mm) with MeOH/H<sub>2</sub>O (98:2) as eluent (flow rate 1 mL/min,  $t_R$ =9 min);  $[\alpha]_D^{25} = +9.7$  ( $c = 0.15$ , CH<sub>3</sub>OH); selected <sup>1</sup>H NMR (400 MHz, CD<sub>3</sub>OD):  $\delta$  3.96 (2H, m), 0.98 (3H, d,  $J = 6.3$  Hz), 0.87 (3H, s), 0.81 (3H, s); HR ESIMS  $m/z$  425.2733[M-Na]<sup>-</sup>, C<sub>24</sub>H<sub>41</sub>O<sub>4</sub>S requires 425.2726.

### Synthesis of 3 $\beta$ -ursodeoxycholate derivatives

*Methyl 3 $\beta$ ,7 $\beta$ -dihydroxy-5 $\beta$ -cholan-24-oate (42)*. A solution of compound **34** (0.10 g, 0.18 mmol) and CH<sub>3</sub>COOK (18 mg, 0.18 mmol) dissolved in water (1 mL) and *N,N*-dimethylformamide (DMF, 4 mL) was refluxed for 3 h. The solution was cooled at room temperature and then ethyl acetate and water were added. The separated aqueous phase was extracted with ethyl acetate (3  $\times$  30 mL). The combined organic phases were washed with water, dried (Na<sub>2</sub>SO<sub>4</sub>) and evaporated to dryness. Purification by silica gel (hexane-ethyl acetate 7:3 and 0.5% TEA) gave **42** as an oil (60 mg, 82%).  $[\alpha]_D^{25} = +27.4$  ( $c = 0.10$ , CH<sub>3</sub>OH); selected <sup>1</sup>H NMR (500 MHz, CDCl<sub>3</sub>):  $\delta$  4.06 (1H, s), 3.65 (3H, s), 3.54 (1H, m), 2.34 (1H, m), 2.21 (1H, m), 0.98 (3H, s), 0.92 (3H, d,  $J = 6.8$  Hz), 0.67 (3H, s); HR ESIMS  $m/z$  407.3169 [M+H]<sup>+</sup>, C<sub>25</sub>H<sub>43</sub>O<sub>4</sub> requires 407.3161.

*3 $\beta$ ,7 $\beta$ -dihydroxy-5 $\beta$ -cholan-24-oic acid (22)*. Compound **42** (30.0 mg, 73.9  $\times 10^{-3}$  mmol) was hydrolyzed with a methanol solution of sodium hydroxide (5%, 5 mL) in H<sub>2</sub>O (1 mL) overnight under reflux. The resulting solution was then concentrated under vacuum, diluted with water, acidified with HCl 6 M and extracted with ethyl acetate (3  $\times$  50 mL). The collected organic phases were washed with brine, dried over Na<sub>2</sub>SO<sub>4</sub> anhydrous and evaporated under reduced pressure. HPLC purification on a Nucleodur 100-5 C18 (5  $\mu$ m; 5 mm i.d. x 250 mm) with MeOH/H<sub>2</sub>O (75:25) as eluent (flow rate 1 mL/min), gave 25 mg of **22** as white solid (87%,  $t_R = 10.5$  min).  $[\alpha]_D^{25} = +38.1$  ( $c = 0.14$ , CH<sub>3</sub>OH); selected <sup>1</sup>H NMR (400 MHz, CD<sub>3</sub>OD):  $\delta$  4.00 (1H, s), 3.44 (1H, m), 0.99 (3H, s), 0.96 (3H, d,  $J = 6.3$  Hz), 0.69 (3H, s); HR ESIMS  $m/z$  391.2853 [M-H]<sup>-</sup>, C<sub>25</sub>H<sub>39</sub>O<sub>4</sub> requires 391.2848.

*3 $\beta$ ,7 $\beta$ -dihydroxy-5 $\beta$ -cholan-24-ol (23)*. 2,6-lutidine (86  $\mu$ L, 0.74 mmol) and *tert*-butyldimethylsilyl trifluoromethanesulfonate (51  $\mu$ L, 9.0 mmol) were added at 0  $^{\circ}$ C to a solution of **42** (30.0 mg, 73.9  $\times 10^{-3}$  mmol) in 5 mL of CH<sub>2</sub>Cl<sub>2</sub>. After

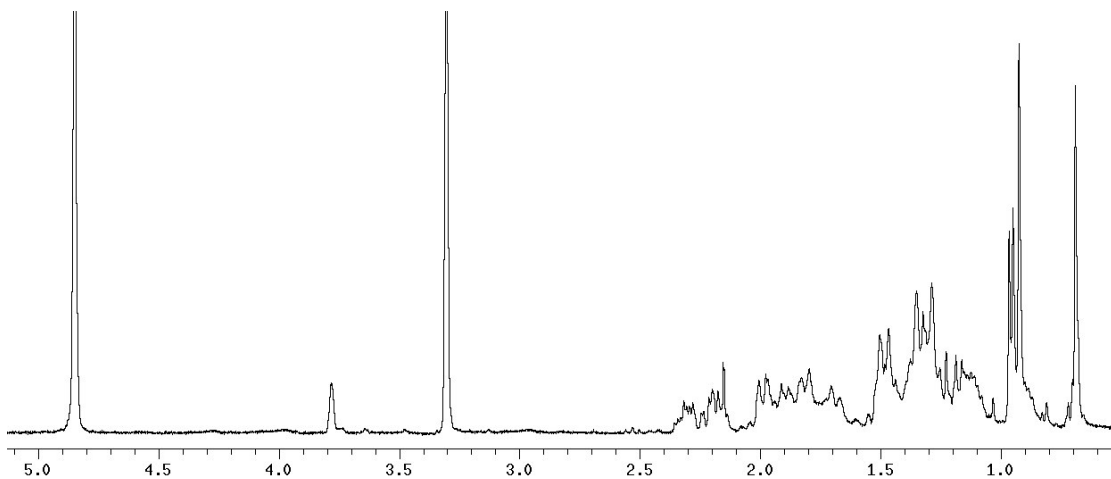
2 h stirring at 0 °C, the reaction was quenched by addition of aqueous NaHSO<sub>4</sub> (1.0 M, 10 mL). The layers were separated and the aqueous phase was extracted with CH<sub>2</sub>Cl<sub>2</sub> (3 × 20 mL). The combined organic layers were washed with NaHSO<sub>4</sub>, water, saturated aqueous NaHCO<sub>3</sub>, and brine and evaporated *in vacuo* to give 45 mg of methyl 3β,7β-di(*tert*-butyldimethylsilyloxy)-5β-cholan-24-oate (96%) in the form of colorless needles, that was subjected to next step without any purification. To a solution of methyl ester (45.0 mg, 71 × 10<sup>-3</sup> mmol) in dry THF (5 mL), at 0 °C dry methanol (20 μL, 0.50 mmol) and LiBH<sub>4</sub> (250 μL, 2M in THF, 0.50 mmol) was added. The resulting mixture was stirred for 1 h at 0 °C. The mixture was quenched by addition of 1.0 M NaOH (35 μL) and then ethyl acetate. The organic phase was washed with water, dried (Na<sub>2</sub>SO<sub>4</sub>) and concentrated to give 40 mg of **43** as a white solid (94%), that was dissolved in methanol (3 mL) and treated with 100 μL of HCl 37% v/v. After 2 h, silver carbonate was added at the solution to precipitate chloride. Then the reaction mixture was centrifuged and the supernatant was concentrated *in vacuo*. HPLC purification on a Nucleodur 100-5 C18 (5 μm; 10 mm i.d. x 250 mm) with MeOH/H<sub>2</sub>O (9:1) as eluent (flow rate 1 mL/min), gave 18 mg of compound **23** as a white solid (96%, *t*<sub>R</sub> = 6.5 min). [α]<sub>D</sub><sup>25</sup> = +32.5 (*c* = 0.31, CH<sub>3</sub>OH); selected <sup>1</sup>H NMR (400 MHz, CD<sub>3</sub>OD): δ 4.00 (1H, s), 3.52 (2H, m), 3.43 (1H, m), 1.00 (3H, s), 0.96 (3H, d, *J* = 6.5 Hz), 0.72 (3H, s); <sup>13</sup>C NMR (100 MHz, CD<sub>3</sub>OD): δ 72.0, 67.4, 63.6, 57.6, 56.7, 44.8, 44.4, 41.6, 40.1, 38.6, 38.3, 37.0, 35.6, 35.2, 33.3, 30.8, 30.3, 29.7, 28.4, 27.9, 24.5, 22.7, 19.4, 12.7; HR ESIMS *m/z* 379.3219 [M+H]<sup>+</sup>, C<sub>24</sub>H<sub>43</sub>O<sub>3</sub> requires 379.3212.

*3β,7β-dihydroxy-5β-cholan-24-yl-24-sodium sulfate (24)*. The triethylamine-sulfur trioxide complex (20.0 mg, 0.120 mmol) was added to a solution of **43** (15.0 mg, 24.7 × 10<sup>-3</sup> mmol) in DMF dry (5 mL) under an argon atmosphere, and the mixture was stirred at 80 °C for 24h. The solution was then concentrated under vacuum. The solid was dissolved in methanol (3 mL) and at the solution was added 50 μL of HCl 37% v/v. After 1h, silver carbonate was added at the solution to precipitate chloride. Then the reaction mixture was centrifuged and the supernatant was concentrated *in vacuo*. HPLC purification on a Nucleodur 100-5 C18 (5 μm; 5 mm i.d. x 250 mm) with MeOH/H<sub>2</sub>O (55:45) as eluent (flow

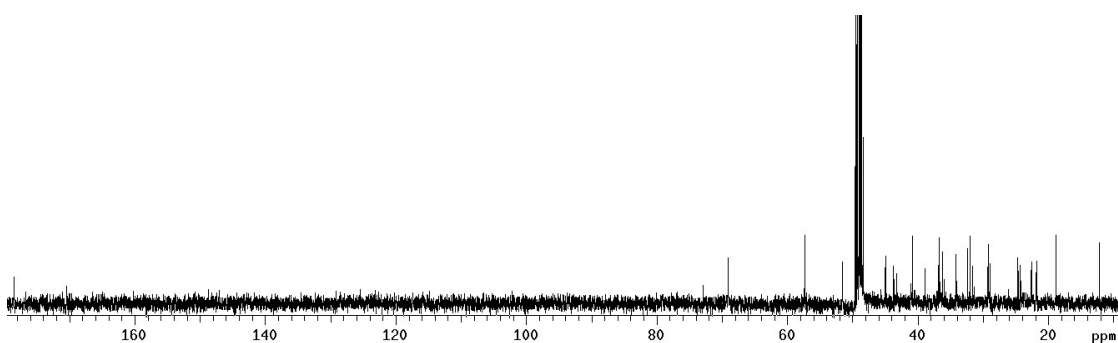
rate 1 mL/min), gave 8 mg of **24** as colourless amorphous solid (67% over two steps,  $t_R = 13.5$  min).  $[\alpha]_D^{25} = +30$  ( $c = 0.26$ , CH<sub>3</sub>OH); selected <sup>1</sup>H NMR (500 MHz, CD<sub>3</sub>OD):  $\delta$  4.00 (1H, s), 3.96 (2H, m), 3.44 (1H, m), 0.99 (3H, s), 0.97 (3H, d,  $J = 6.6$  Hz), 0.72 (3H, s); HR ESIMS  $m/z$  457.2631 [M-Na]<sup>-</sup>, C<sub>24</sub>H<sub>41</sub>O<sub>6</sub>S requires 457.2624.

**Spectroscopic Data**

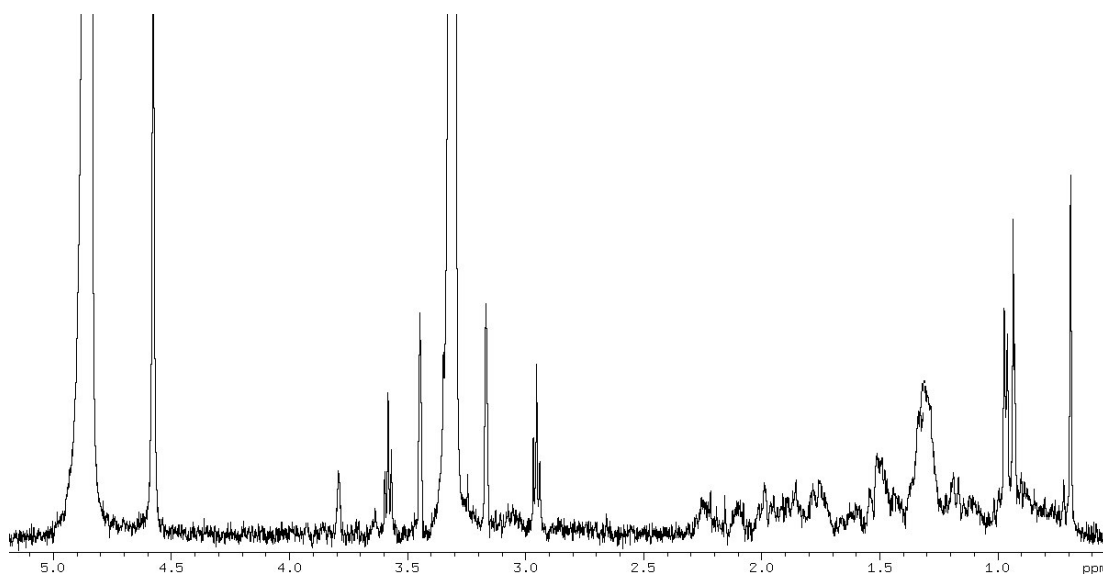
$^1\text{H}$  NMR (400 MHz,  $\text{CD}_3\text{OD}$ ) of compound **4**



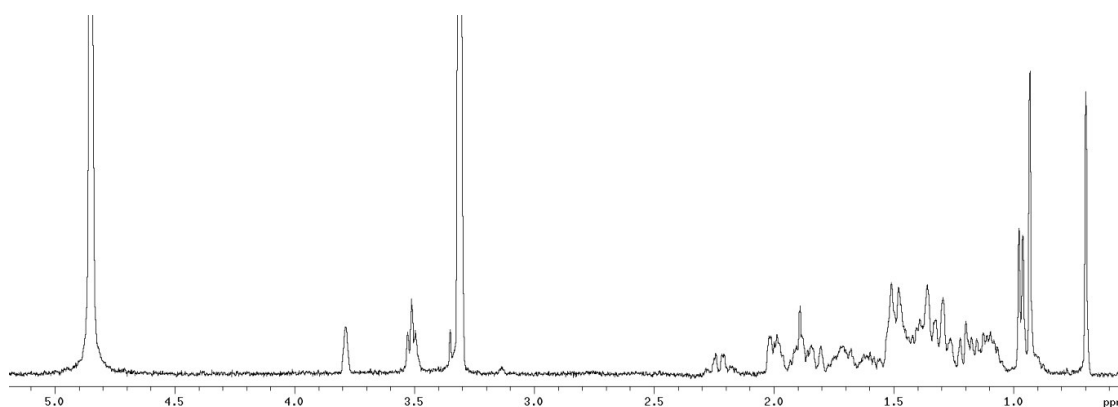
$^{13}\text{C}$  NMR (100 MHz,  $\text{CD}_3\text{OD}$ ) of compound **4**



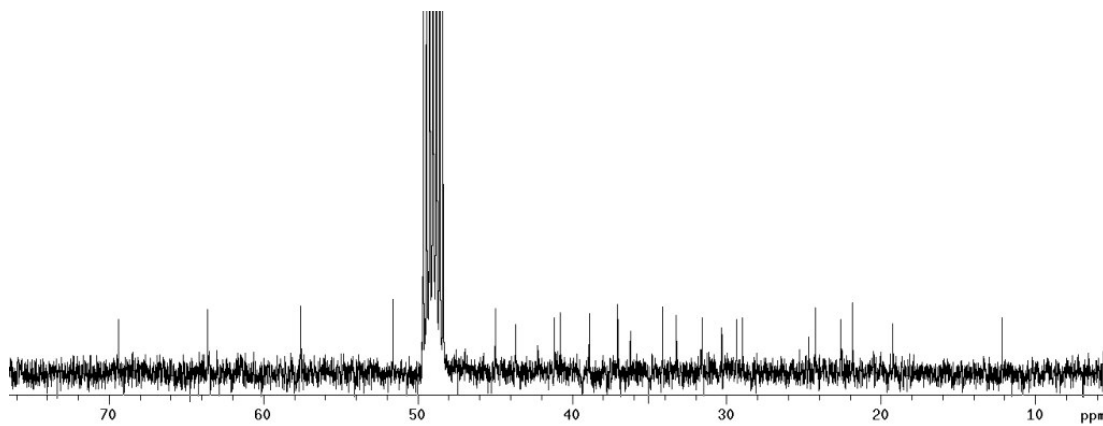
$^1\text{H}$  NMR (500 MHz,  $\text{CD}_3\text{OD}$ ) of compound **5**



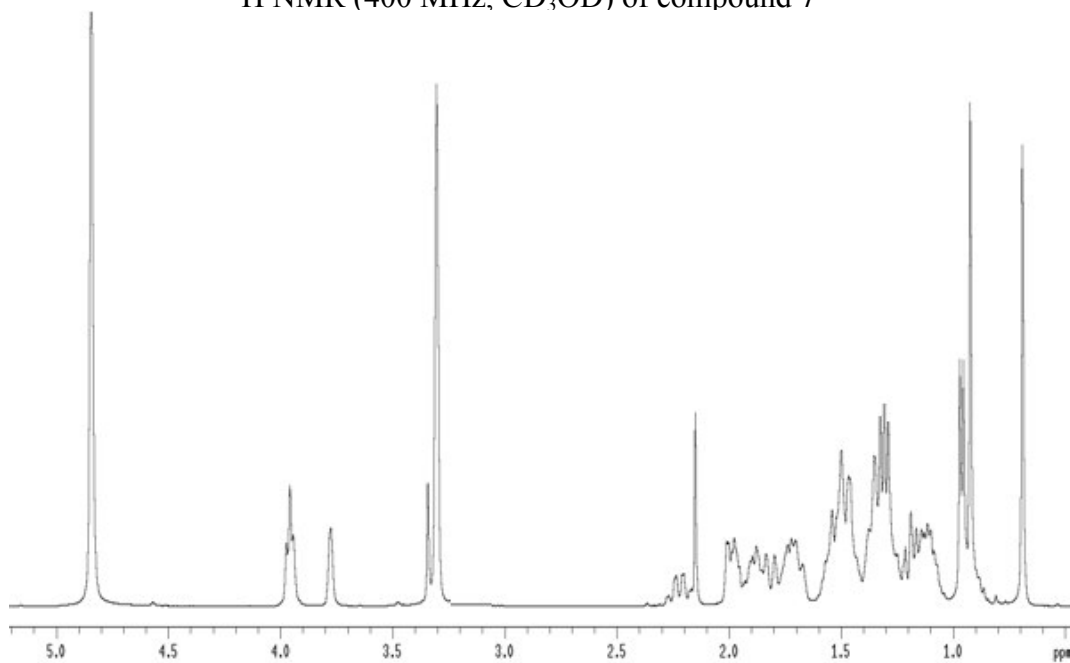
$^1\text{H}$  NMR (400 MHz,  $\text{CD}_3\text{OD}$ ) of compound **6**



$^{13}\text{C}$  NMR (100 MHz,  $\text{CD}_3\text{OD}$ ) of compound 6

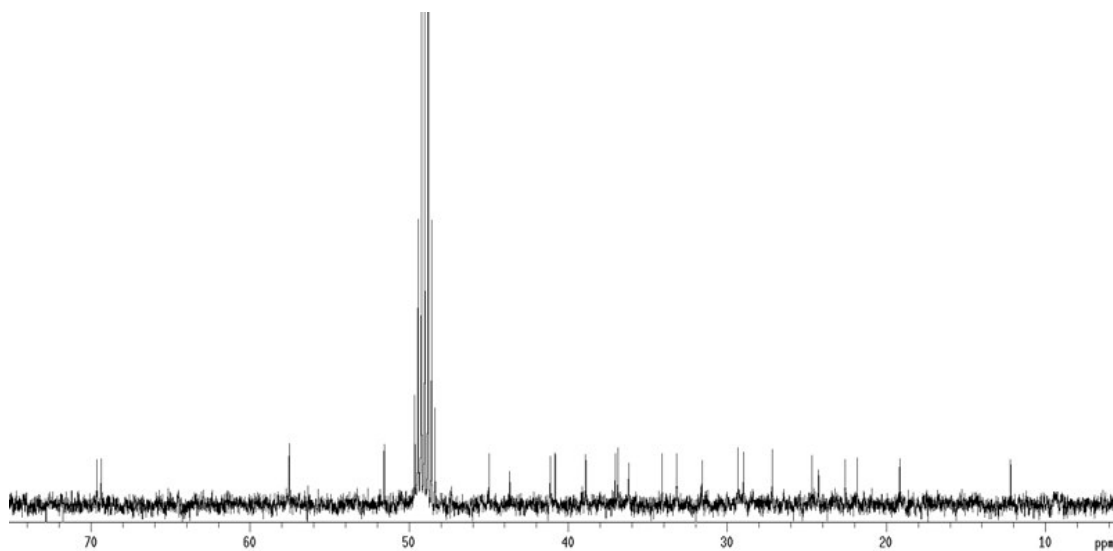


$^1\text{H}$  NMR (400 MHz,  $\text{CD}_3\text{OD}$ ) of compound 7

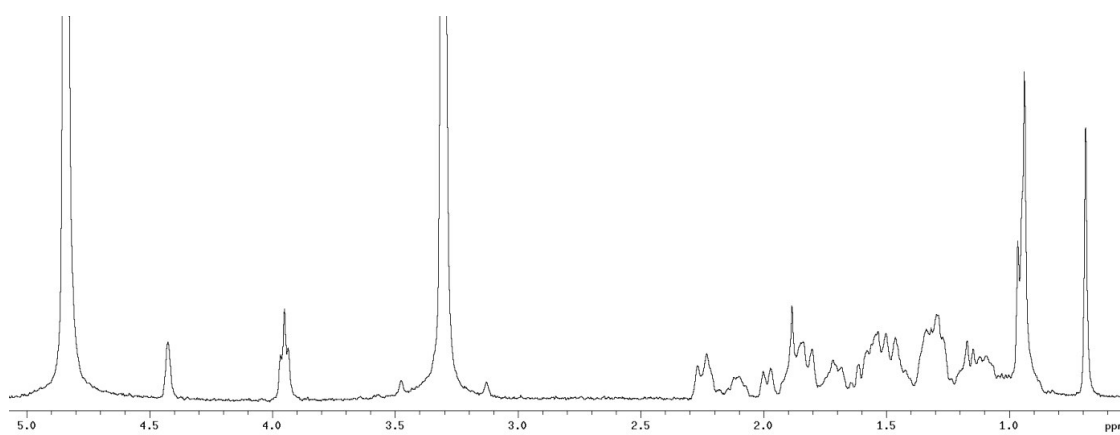




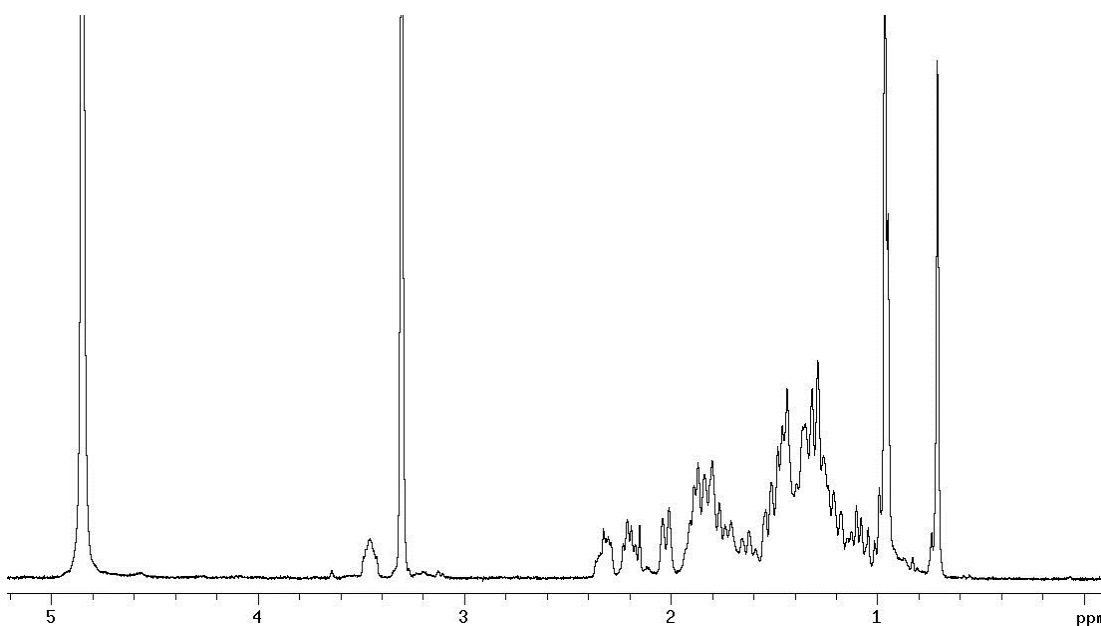
$^{13}\text{C}$  NMR (100 MHz,  $\text{CD}_3\text{OD}$ ) of compound **7**



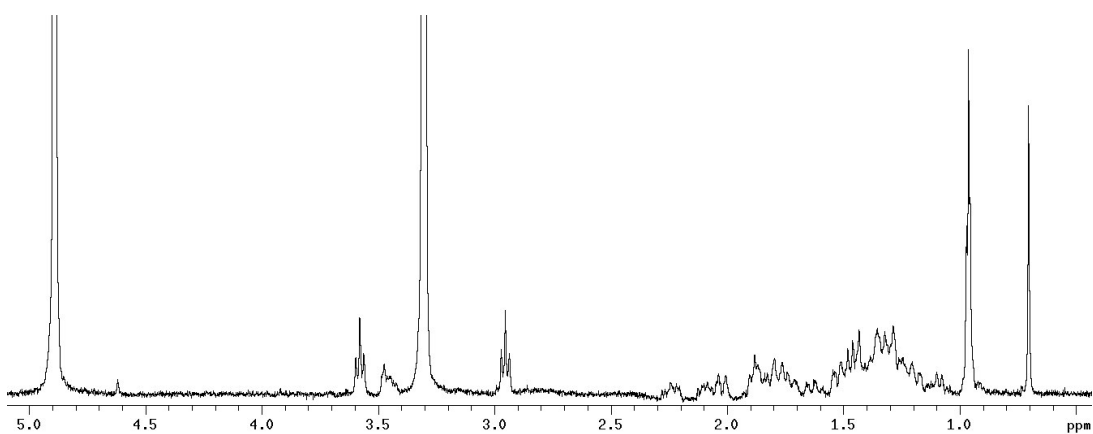
$^1\text{H}$  NMR (400 MHz,  $\text{CD}_3\text{OD}$ ) of compound **8**



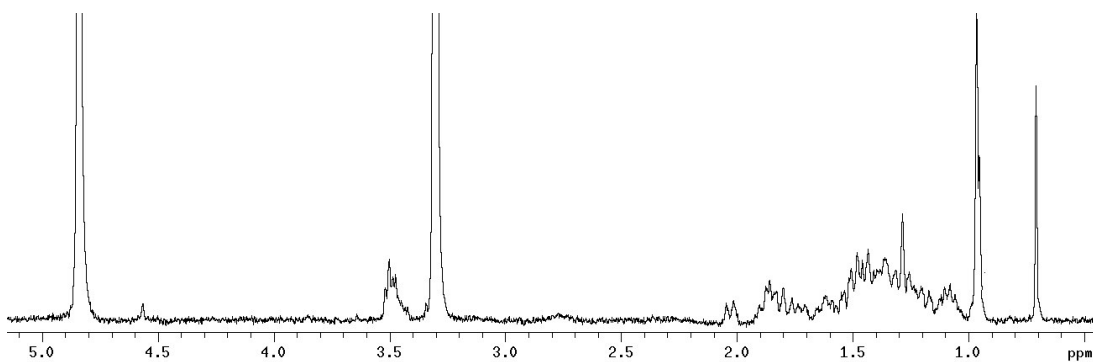
$^1\text{H}$  NMR (400 MHz,  $\text{CD}_3\text{OD}$ ) of compound **9**



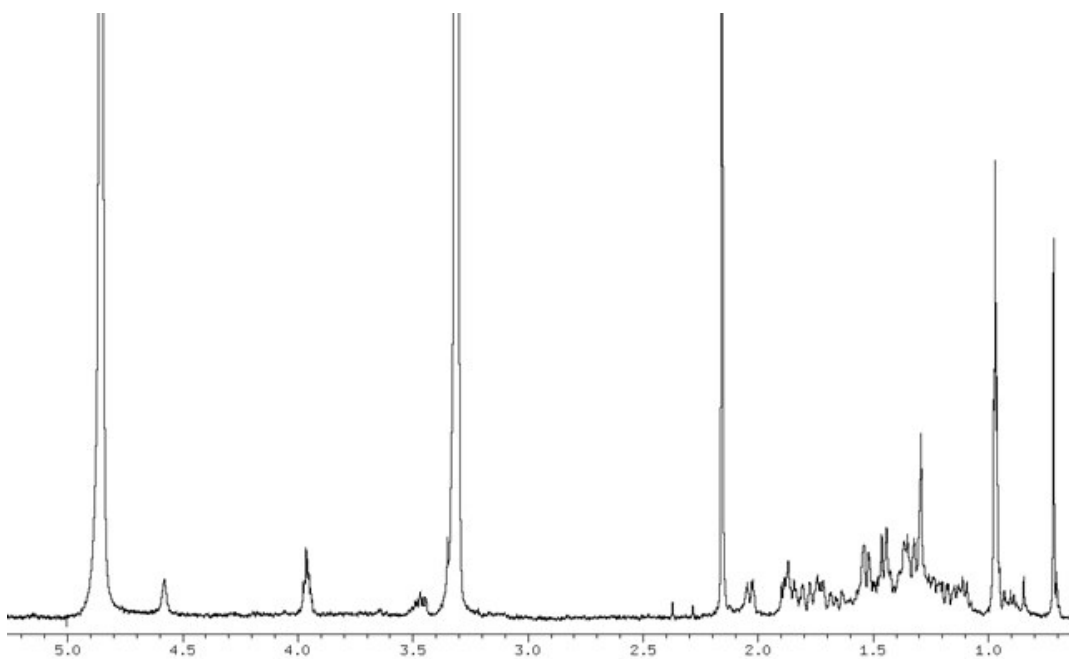
$^1\text{H}$  NMR (400 MHz,  $\text{CD}_3\text{OD}$ ) of compound **10**



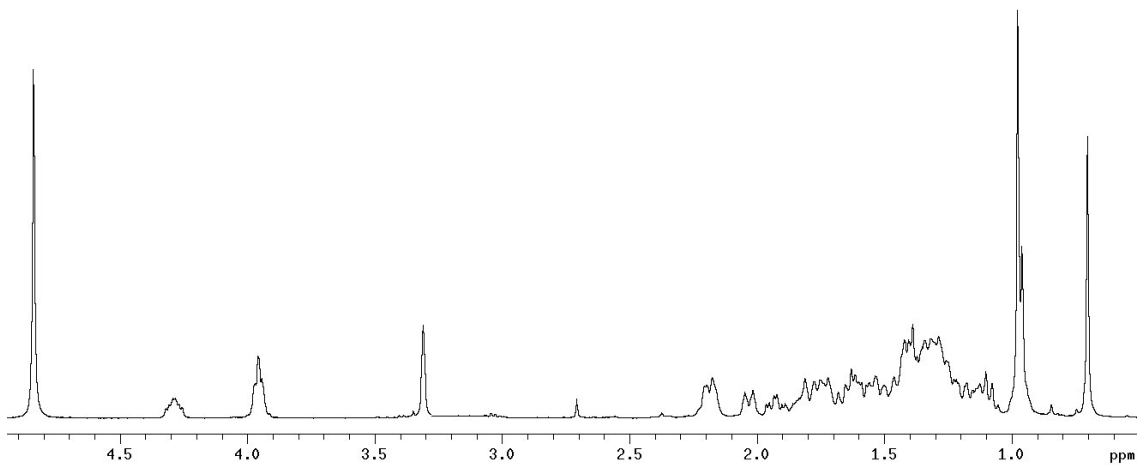
$^1\text{H}$  NMR (400 MHz,  $\text{CD}_3\text{OD}$ ) of compound **11**



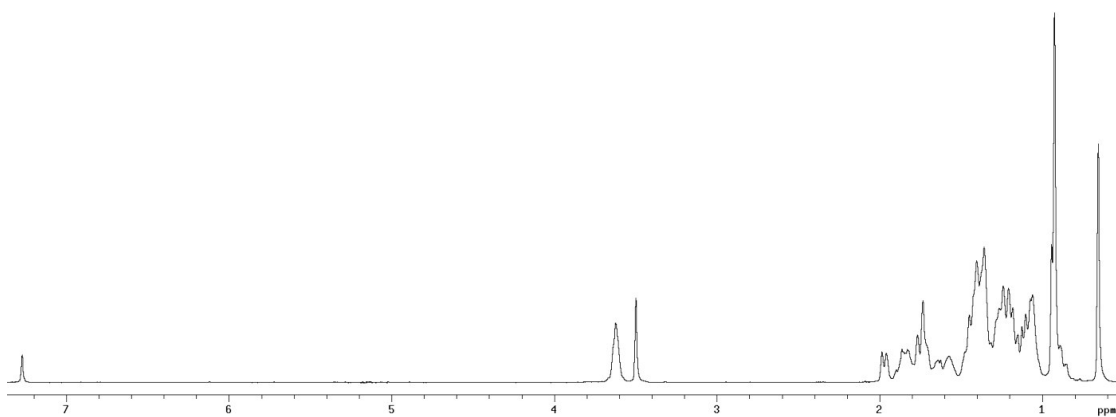
$^1\text{H}$  NMR (400 MHz,  $\text{CD}_3\text{OD}$ ) of compound **12**



$^1\text{H}$  NMR (400 MHz,  $\text{CD}_3\text{OD}$ ) of compound **13**

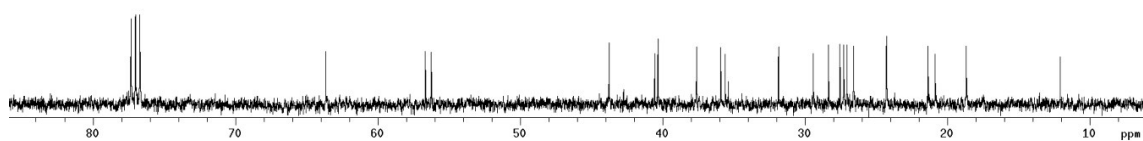


$^1\text{H}$  NMR (400 MHz,  $\text{CDCl}_3$ ) of compound **14**

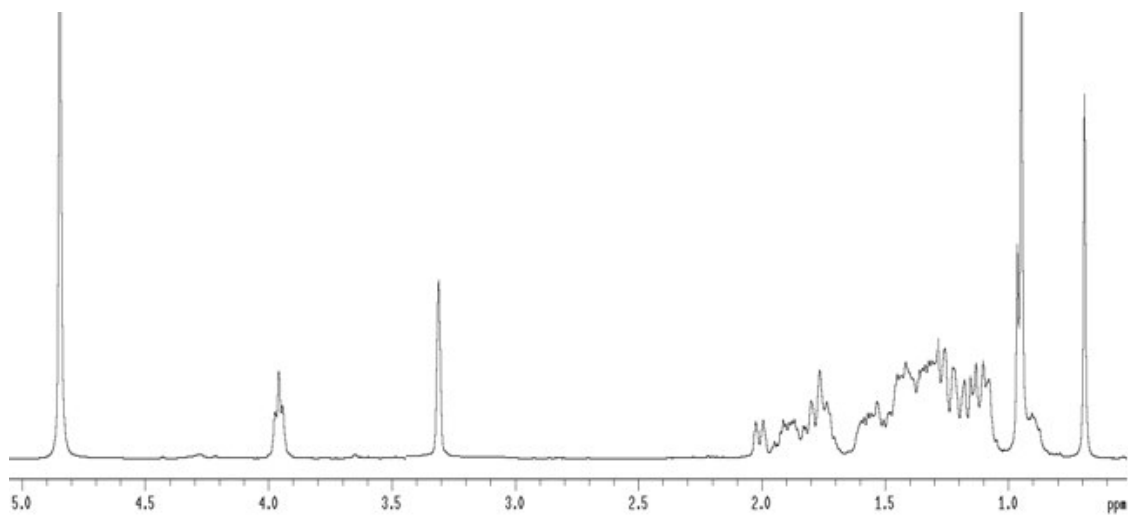


*Experimental Section II*

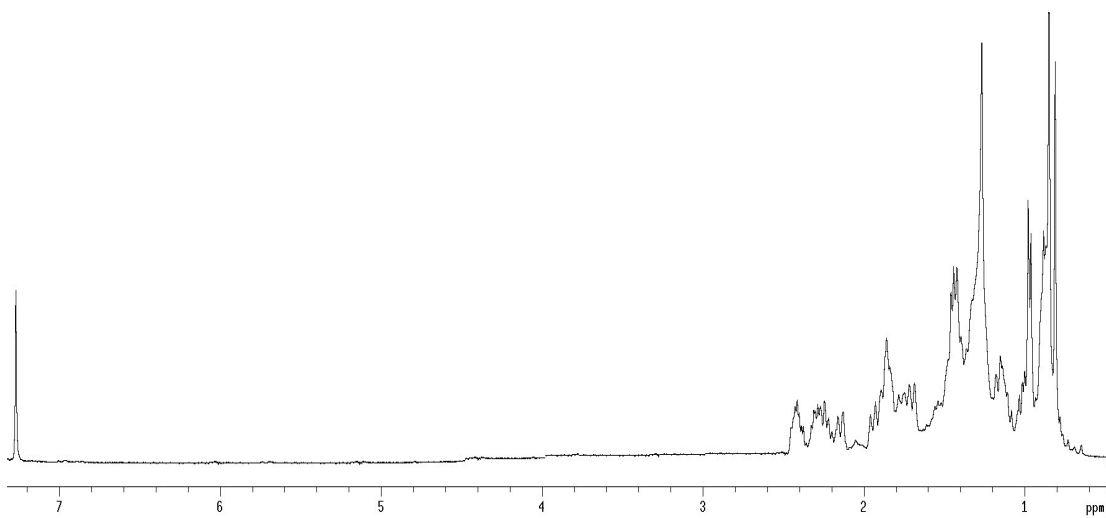
$^{13}\text{C}$  NMR (100 MHz,  $\text{CDCl}_3$ ) of compound **14**



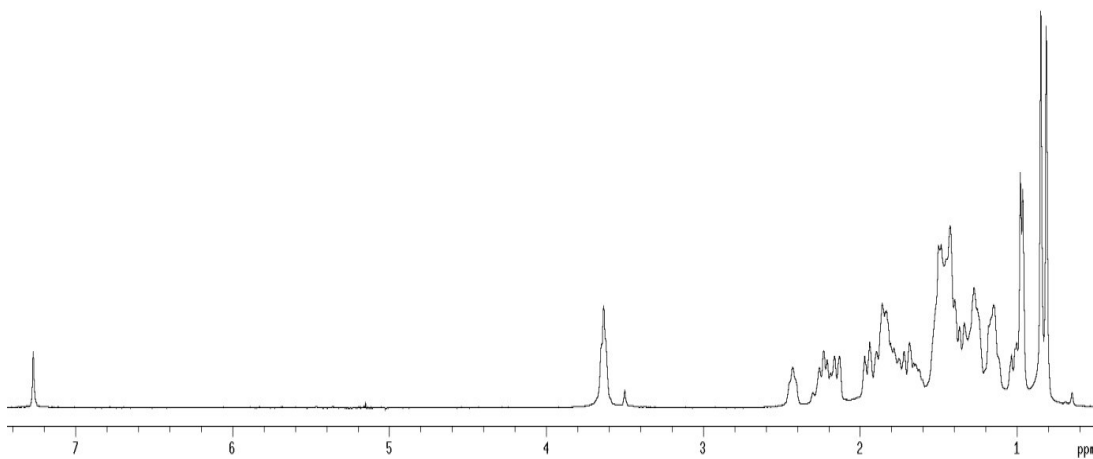
$^1\text{H}$  NMR (400 MHz,  $\text{CD}_3\text{OD}$ ) of compound **15**



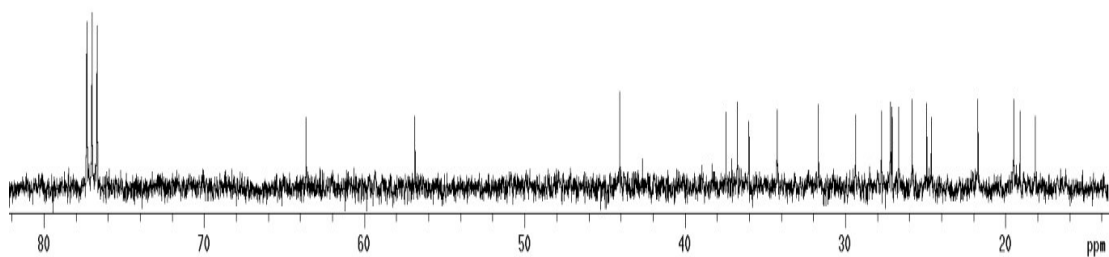
$^1\text{H}$  NMR (400 MHz,  $\text{CDCl}_3$ ) of compound **16**



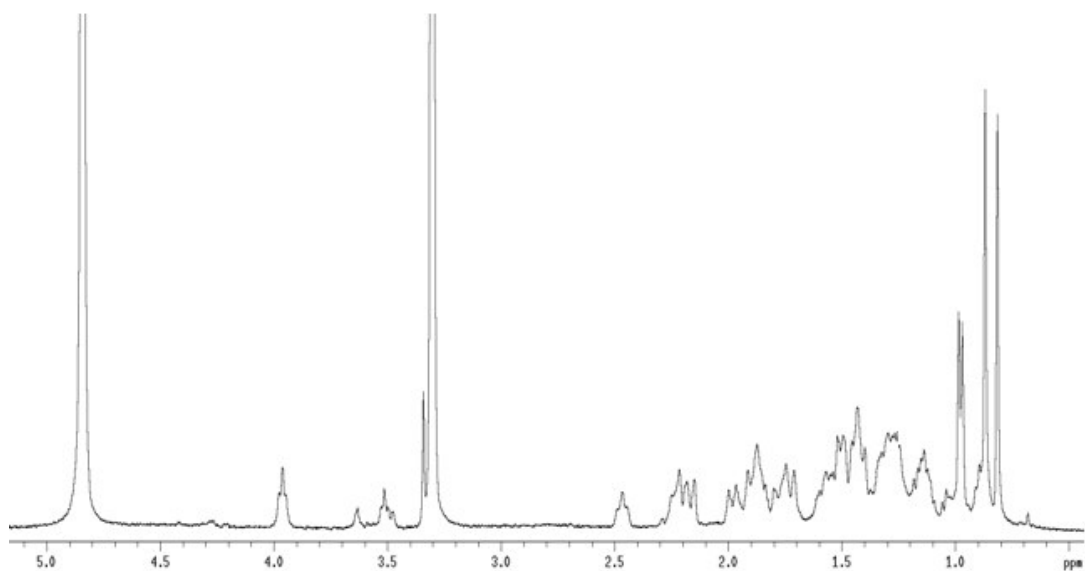
$^1\text{H}$  NMR (400 MHz,  $\text{CDCl}_3$ ) of compound **17**



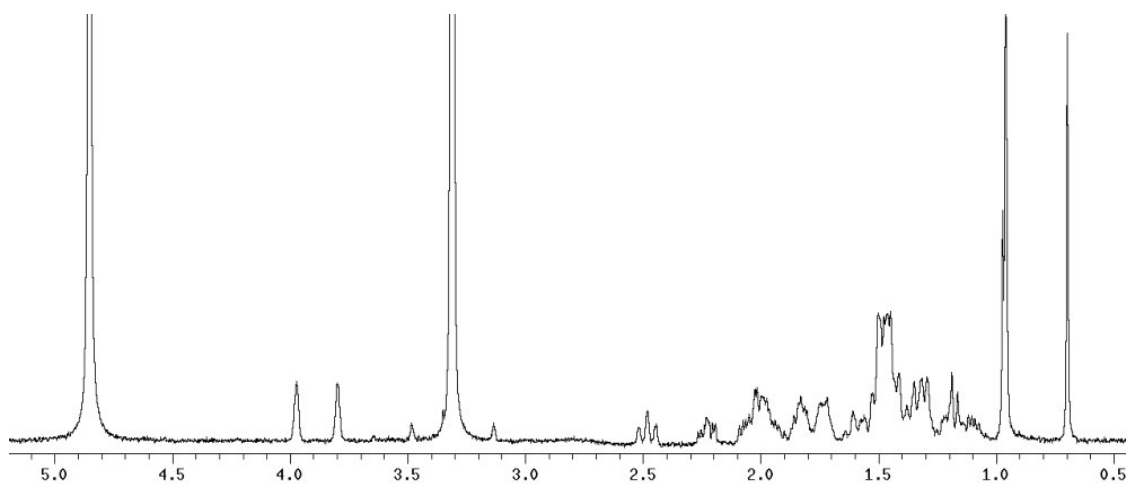
$^{13}\text{C}$  NMR (100 MHz,  $\text{CDCl}_3$ ) of compound **17**



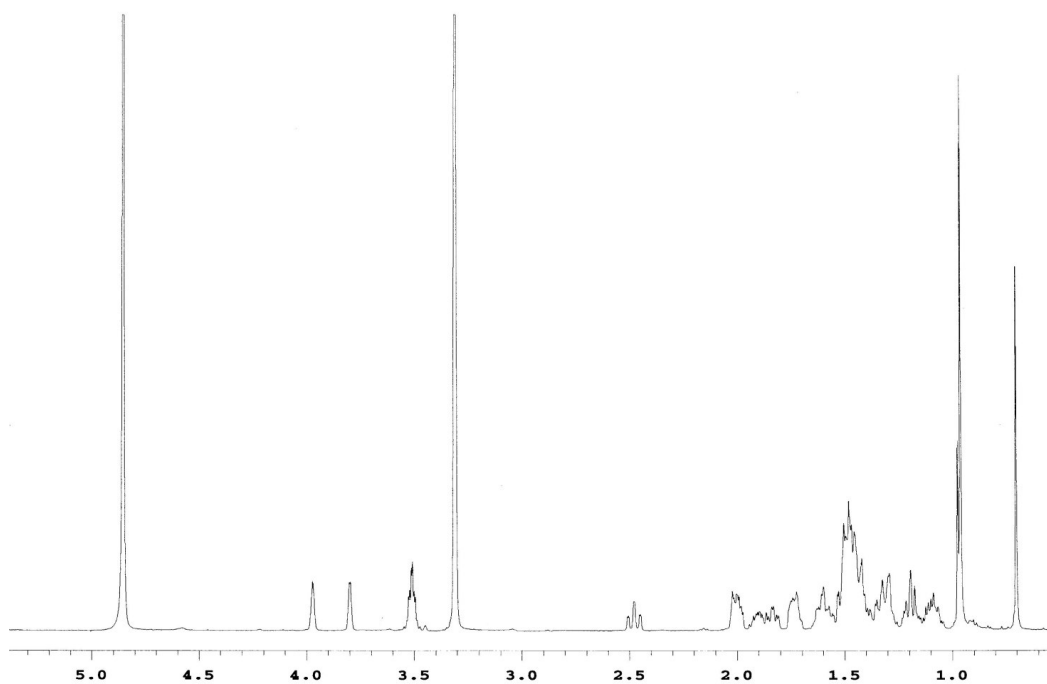
$^1\text{H}$  NMR (400 MHz,  $\text{CD}_3\text{OD}$ ) of compound **18**



$^1\text{H}$  NMR (400 MHz,  $\text{CD}_3\text{OD}$ ) of compound **19**

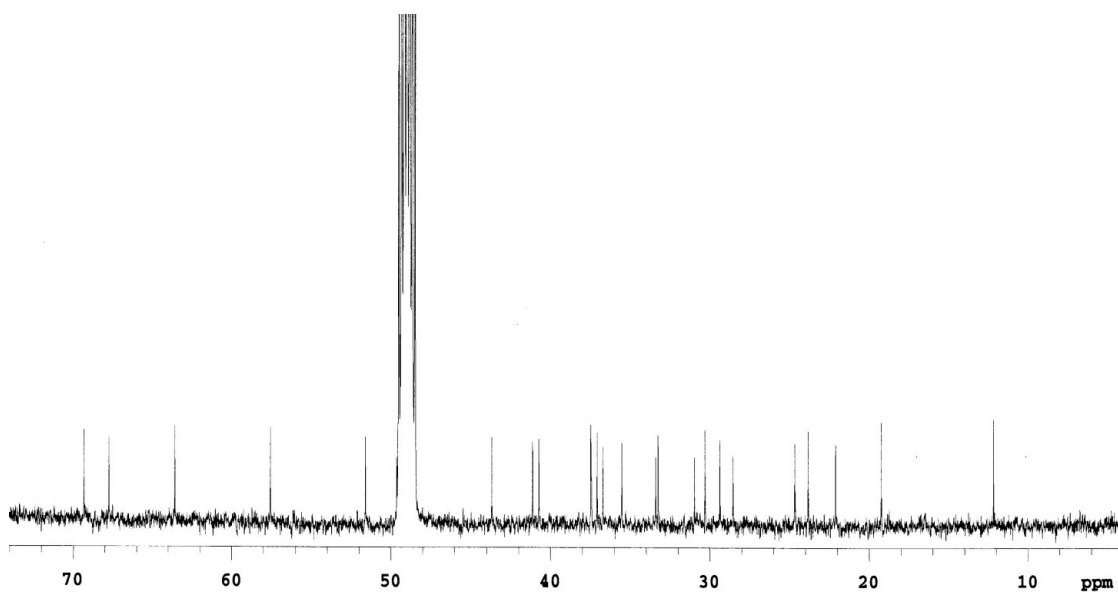


$^1\text{H}$  NMR (500 MHz,  $\text{CD}_3\text{OD}$ ) of compound **20**

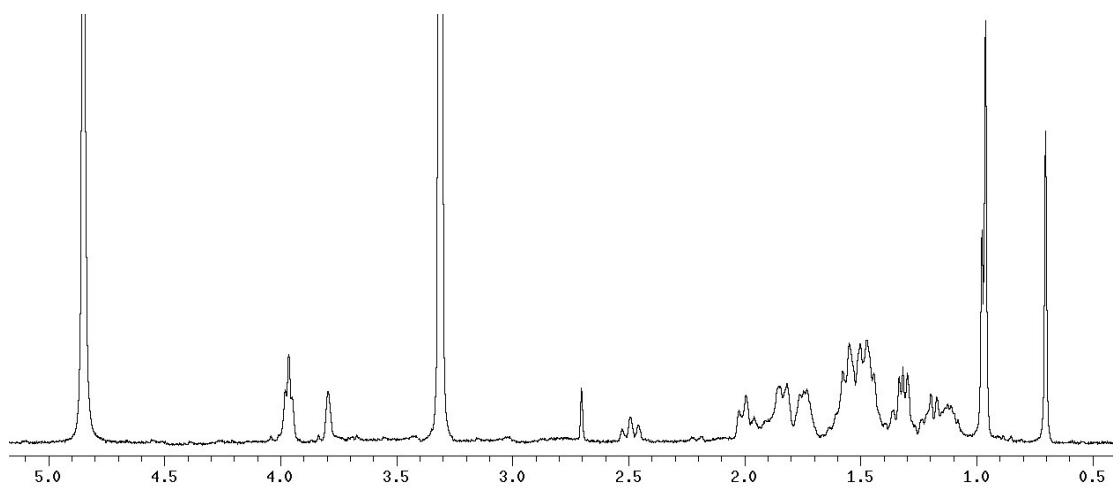




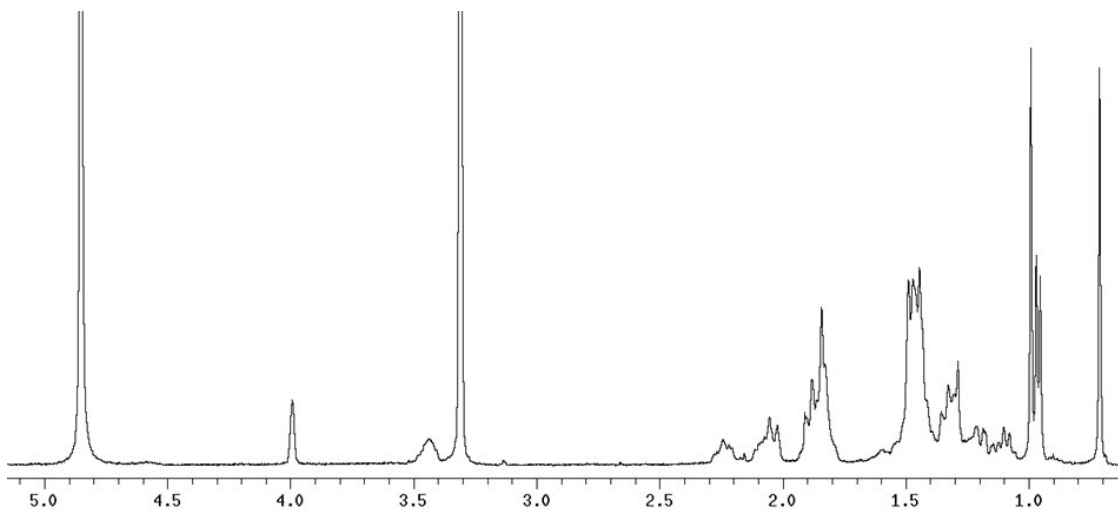
$^{13}\text{C}$  NMR (150 MHz,  $\text{CD}_3\text{OD}$ ) of compound **20**



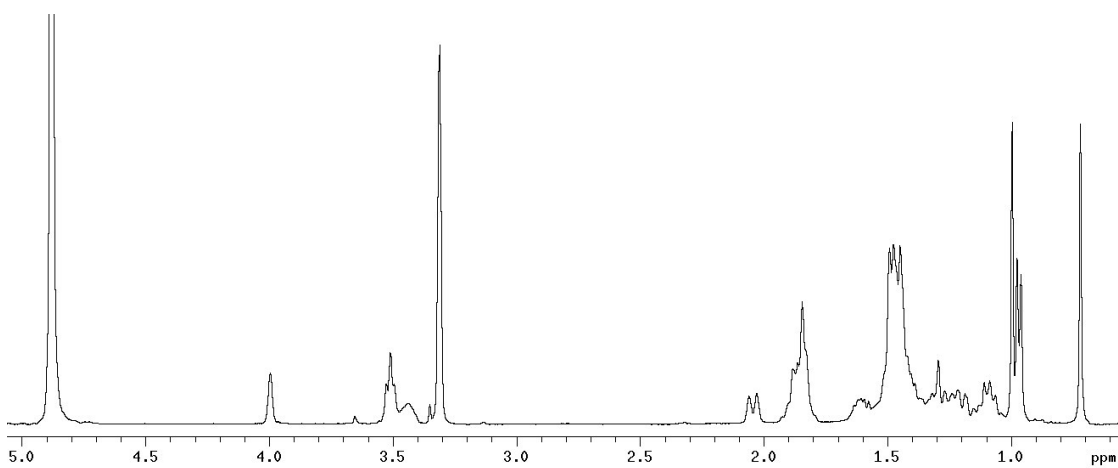
$^1\text{H}$  NMR (400 MHz,  $\text{CD}_3\text{OD}$ ) of compound **21**



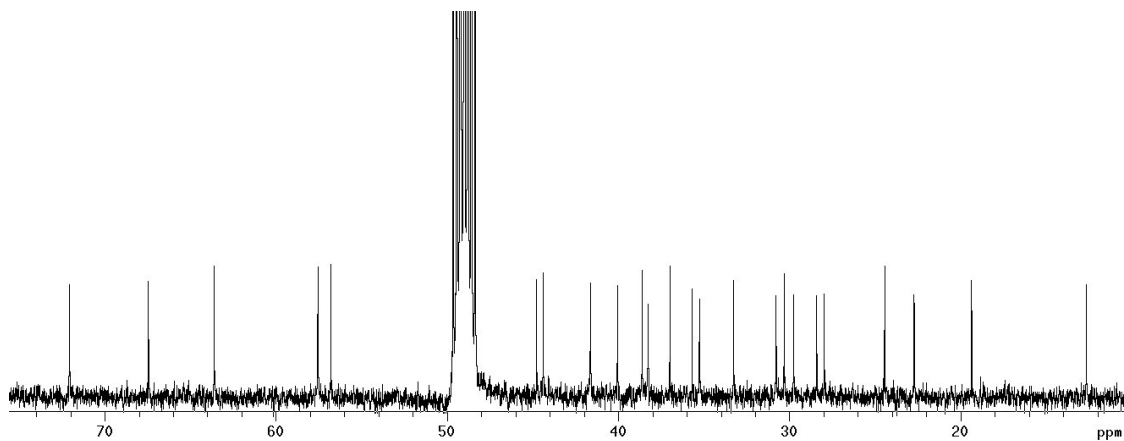
$^1\text{H}$  NMR (400 MHz,  $\text{CD}_3\text{OD}$ ) of compound **22**



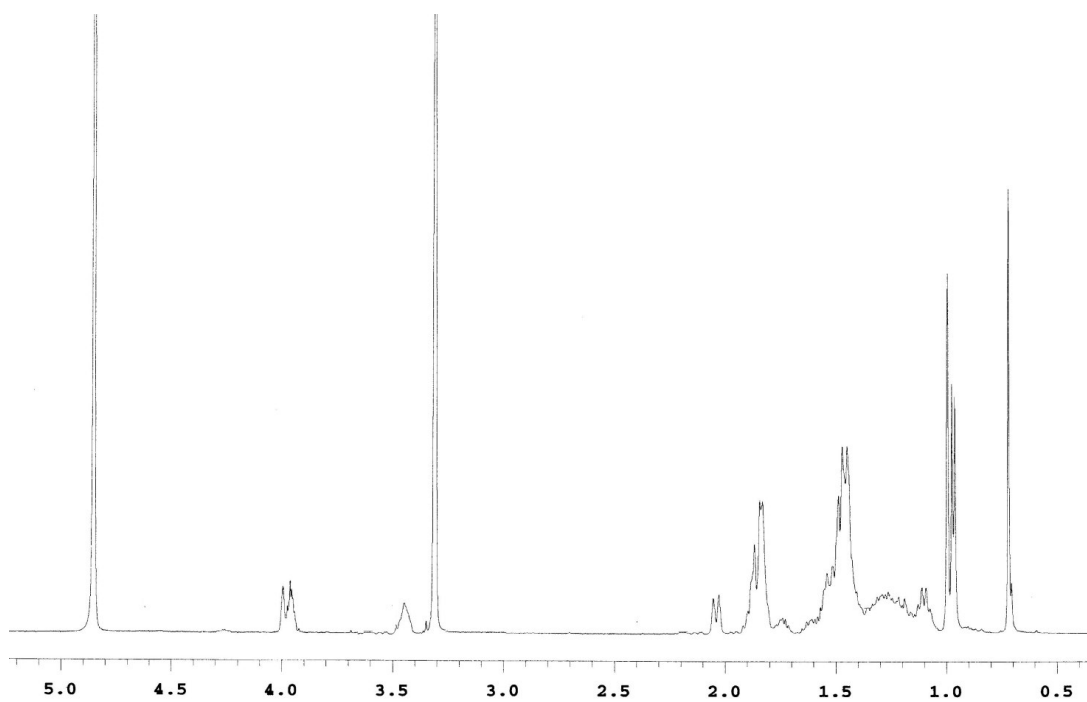
$^1\text{H}$  NMR (400 MHz,  $\text{CD}_3\text{OD}$ ) of compound **23**



$^{13}\text{C}$  NMR (100 MHz,  $\text{CD}_3\text{OD}$ ) of compound **23**



$^1\text{H}$  NMR (500 MHz,  $\text{CD}_3\text{OD}$ ) of compound **24**



### III. Experimental procedures for 6-ethylchenodeoxycholate derivatives

*Methyl 3 $\alpha$ ,7 $\alpha$ -trimethylsilyloxy-5 $\beta$ -cholan-6-en-24-oate (64)*. To a solution of diisopropylamine (6.80 mL, 48.1 mmol) in dry THF (10 mL) was added dropwise a solution of *n*-butyllithium (18 mL, 2.5 M in hexane, 45 mmol) at  $-78$  °C under nitrogen atmosphere. After 30 min, trimethylchlorosilane (8.10 mL, 64.2 mmol) was added, and the resulting mixture was reacted for an additional 20 min. A solution of methyl 3 $\alpha$ -hydroxy-7-keto-5 $\beta$ -cholan-24-oate (**32**) (1.30 g, 3.21 mmol), previously prepared, in dry THF (10 mL) was added dropwise in 10 min. The mixture was stirred at  $-78$  °C for an additional 45 min, and then triethylamine (16.3 mL,  $115.6 \times 10^{-3}$  mol) was added. After 1 h, the reaction mixture was allowed to warm to  $-20$  °C, treated with aqueous saturated solution of NaHCO<sub>3</sub> (10 mL), and brought up to room temperature in 2 h. The organic phase was separated, and the aqueous phase was extracted with ethyl acetate (3  $\times$  50 mL). The combined organic phases were washed several times with a saturated solution of NaHCO<sub>3</sub>, water, and brine. After the mixture was dried over anhydrous Na<sub>2</sub>SO<sub>4</sub>, the residue was evaporated under vacuum to give 3 g of **64** as a yellow residue, which was subjected to next step without any purification.  $[\alpha]_D^{25} = +2.6$ ,  $c = 0.16$ ; selected <sup>1</sup>H NMR (400 MHz, CDCl<sub>3</sub>):  $\delta$  3.67 (3H, s), 3.61 (1H, m), 2.86 (1H, dd,  $J = 6.8$  e 13.4 Hz), 2.36 (1H, m), 2.22 (1H, m), 1.20 (3H, s), 0.92 (3H, d,  $J = 6.3$  Hz), 0.65 (3H, s), 0.0- 0.20 (s' s, 18H); <sup>13</sup>C NMR (100 MHz, CDCl<sub>3</sub>):  $\delta$  174.7, 142.8, 109.0, 71.6, 54.8, 51.5, 44.3, 42.6, 40.9, 40.8, 40.3, 40.0, 35.3, 34.6, 32.9, 30.6, 28.6, 27.0, 22.5, 20.9, 18.6, 12.3, 1.3 (2C), 0.3 (2C), 0.2 (2C).

*Methyl 3 $\alpha$ -hydroxy-6-ethyliden-7-keto-5 $\beta$ -cholan-24-oate (65)*. To a cooled ( $-60$  °C) and stirred solution of acetaldehyde (1.50 mL, 27.5 mmol) and methyl 3 $\alpha$ ,7 $\alpha$ -trimethylsilyloxy-5 $\beta$ -cholan-6-en-24-oate (**64**) (3.0 g, 5.5 mmol) in dry CH<sub>2</sub>Cl<sub>2</sub> (30 mL) was added dropwise BF<sub>3</sub>•OEt<sub>2</sub> (7.0 ml, 55 mmol). The reaction mixture was stirred for 2 h at  $-60$  °C and allowed to warm to room temperature. The mixture was quenched with saturated aqueous solution of NaHCO<sub>3</sub> and extracted with CH<sub>2</sub>Cl<sub>2</sub>. The combined organic phases were washed with brine, dried over anhydrous MgSO<sub>4</sub>, and concentrated under vacuum. Purification on silica gel column, eluting with hexane/AcOEt (9:1) and 0.5% Et<sub>3</sub>N, afforded pure **65** (1.3 g,

85% over two steps).  $[\alpha]_D^{25} = +88.0$   $c = 0.17$ ; selected  $^1\text{H}$  NMR (400 MHz,  $\text{CDCl}_3$ ):  $\delta$  6.15 (1H, q,  $J = 7.12$  Hz), 3.65 (3H, s), 3.55 (1H, m), 1.62 (3H, d), 0.95 (3H, s), 0.85 (3H, d), 0.60 (3H, s);  $^{13}\text{C}$  NMR (100 MHz,  $\text{CDCl}_3$ ):  $\delta$  205.0, 174.6, 143.3, 129.8, 70.4, 54.4, 50.6, 48.6, 45.4, 43.4, 39.0, 38.8, 37.4, 35.1, 34.4, 31.0, 30.9, 29.6 (2C), 28.3, 22.8, 21.2, 18.3, 14.1, 11.3.

*Compound 47.* To a methanol solution of compound **65** (0.40 g, 0.93 mmol), a large excess of  $\text{NaBH}_4$  was added at 0 °C. The mixture was left at room temperature for 10 h and then water and MeOH was added dropwise during a period of 15 min at 0 °C with effervescence being observed. Then after evaporation of the solvents, the residue was diluted with water and extracted with AcOEt (3 x 50 mL). The combined extract was washed with brine, dried with  $\text{Na}_2\text{SO}_4$ , and evaporated to give 400 mg of a crude residue that was subjected to the next step without further purification. To a solution of crude residue (0.40 g, 0.93 mmol) in dry THF (30 mL), at 0 °C dry methanol (260  $\mu\text{L}$ , 6.5 mmol) and  $\text{LiBH}_4$  (3.20 mL, 2M in THF, 6.51 mmol) were added. The resulting mixture was stirred for 2 h at 0 °C. The mixture was quenched by addition of 1 M NaOH (2 mL) and then ethyl acetate. The organic phase was washed with water, dried ( $\text{Na}_2\text{SO}_4$ ) and concentrated. HPLC purification on a Nucleodur 100-5 C18 (5  $\mu\text{m}$ ; 10 mm i.d. x 250 mm) with MeOH/ $\text{H}_2\text{O}$  (88:12) as eluent (flow rate 3 mL/min), gave 320 mg of **47** (85% over two steps,  $t_R = 9.2$  min).  $[\alpha]_D^{25} = +18.1$  ( $c = 0.36$ ,  $\text{CH}_3\text{OH}$ );  $^1\text{H}$  and  $^{13}\text{C}$  NMR spectroscopic data in  $\text{CD}_3\text{OD}$  given in Tables 1 and 2; HR ESIMS  $m/z$  405.3373  $[\text{M}+\text{H}]^+$ ,  $\text{C}_{26}\text{H}_{45}\text{O}_3$  requires 405.3369.

*Methyl 3 $\alpha$ -hydroxy-6 $\beta$ -ethyl-7-keto-5 $\beta$ -cholan-24-oate (66).* A solution of **65** ( $800 \times 10^{-3}$  g, 1.92 mmol) in THF dry/MeOH dry (20 mL, 1:1 v/v) was hydrogenated in presence of  $\text{Pd}(\text{OH})_2$  20% wt on activated carbon (25 mg) Degussa type. The mixture was transferred to a standard Parr apparatus and flushed with nitrogen and then with hydrogen several times. The apparatus was shacked under 50 psi of  $\text{H}_2$ . The reaction was stirred at room temperature for 8 h. The catalyst was filtered through Celite, and the recovered filtrate was concentrated under vacuum to give **66** (800 mg, quantitative yield). The  $\beta$ -configuration of ethyl group at C-6 was determined by dipolar couplings  $\text{H}_3$ -26 ( $\delta$  0.83)/  $\text{H}_3$ -19 ( $\delta$  1.22) and H-8 ( $\delta$  2.56)/H-25 ( $\delta$  1.83) in Noesy spectrum (400

MHz, mixing time 400 ms).  $[\alpha]_D^{25} = -3.7$ ,  $c = 0.5$ ; selected  $^1\text{H}$  NMR (400 MHz,  $\text{CDCl}_3$ ):  $\delta$  3.67 (3H, s), 3.57 (1H, m), 2.57 (1H, t,  $J = 11.5$  Hz), 2.37 (1H, m), 2.24 (1H, dd,  $J = 6.6, 9.6$  Hz), 2.20 (1H, m), 1.22 (3H, s), 0.93 (3H, d,  $J = 6.2$  Hz), 0.85 (3H, t,  $J = 7.3$  Hz), 0.67 (3H, s);  $^{13}\text{C}$  NMR (100 MHz,  $\text{CDCl}_3$ ):  $\delta$  215.1, 178.4, 71.6, 56.3, 50.6, 50.4, 47.5, 46.4, 44.4, 43.8, 40.4, 38.2, 36.6, 36.3, 35.2, 32.4, 32.0, 30.6, 29.3, 25.8, 23.5 (2C), 22.8, 18.8, 12.5; HRMS-ESI  $m/z$  433.3323  $[\text{M}+\text{H}]^+$ ,  $\text{C}_{27}\text{H}_{45}\text{O}_4$  requires 433.3318.

*6 $\beta$ -ethyl-3 $\alpha$ ,7 $\beta$ -dihydroxy-5 $\beta$ -cholan-24-ol* (**45**) and *6 $\beta$ -ethyl-3 $\alpha$ ,7 $\alpha$ -dihydroxy-5 $\beta$ -cholan-24-ol* (**46**). To a methanol solution of **66** (0.50 g, 1.2 mmol) a large excess of  $\text{NaBH}_4$  was added at 0 °C. The mixture was left at room temperature for 10 h and then water and MeOH was added dropwise during a period of 15 min at 0 °C with effervescence being observed. Then after evaporation of the solvents, the residue was diluted with water and extracted with AcOEt (3 x 50 mL). The combined extract was washed with brine, dried with  $\text{Na}_2\text{SO}_4$ , and evaporated to give 900 mg of a crude residue that was subjected to the next step without further purification. To a solution of crude residue (900 x  $10^{-3}$  g, 2.20 mmol) in dry THF (25 mL), at 0 °C dry methanol (623  $\mu\text{L}$ , 15.4 mmol) and  $\text{LiBH}_4$  (7.70 mL, 2M in THF, 15.4 mmol) were added. The resulting mixture was stirred for 2 h at 0 °C. The mixture was quenched by addition of 1.0 M NaOH (4.4 mL) and then ethyl acetate. The organic phase was washed with water, dried ( $\text{Na}_2\text{SO}_4$ ) and concentrated. HPLC purification on a Nucleodur 100-5 C18 (5  $\mu\text{m}$ ; 10 mm i.d. x 250 mm) with MeOH/ $\text{H}_2\text{O}$  (88:12) as eluent (flow rate 3 mL/min), gave 338 mg of **45** (69% over two steps,  $t_R = 11$  min) and 154 mg of **46** (31.4% over two steps,  $t_R = 20.4$  min).

*6 $\beta$ -ethyl-3 $\alpha$ ,7 $\beta$ -dihydroxy-5 $\beta$ -cholan-24-ol* (EUDCOH, **45**).  $[\alpha]_D^{25} = +15.2$  ( $c = 1.21$ ,  $\text{CH}_3\text{OH}$ );  $^1\text{H}$  and  $^{13}\text{C}$  NMR spectroscopic data in  $\text{CD}_3\text{OD}$  given in Tables 1 and 2. HR ESIMS  $m/z$  407.3529  $[\text{M}+\text{H}]^+$ ,  $\text{C}_{26}\text{H}_{47}\text{O}_3$  requires 407.3525.

*6 $\beta$ -ethyl-3 $\alpha$ ,7 $\alpha$ -dihydroxy-5 $\beta$ -cholan-24-ol* (IsoECDCOH, **46**).  $[\alpha]_D^{25} = +5.1$  ( $c = 5.74$ ,  $\text{CH}_3\text{OH}$ );  $^1\text{H}$  and  $^{13}\text{C}$  NMR spectroscopic data in  $\text{CD}_3\text{OD}$  given in Tables 1 and 2. HR ESIMS  $m/z$  407.3532  $[\text{M}+\text{H}]^+$ ,  $\text{C}_{26}\text{H}_{47}\text{O}_3$  requires 407.3525.

*6 $\alpha$ -ethyl-3 $\alpha$ ,7 $\alpha$ , 24-5 $\beta$ -cholantriol* (**44**). Methyl ester **66** (300 mg, 0.7 mmol) was dissolved in dry THF (5 mL) at 0 °C in presence of dry methanol (195  $\mu\text{L}$ , 4.83 mmol) and  $\text{LiBH}_4$  (2.40 mL, 2M in THF, 4.83 mmol). After 8 h, a solution 1.0 M

NaOH (1.4 mL) was added and then allowed to warm to room temperature. Ethyl acetate was added and the separated aqueous phase was extracted with ethyl acetate (3 × 30 mL). The combined organic phases were washed with water, dried (Na<sub>2</sub>SO<sub>4</sub>) and concentrated. Purification by silica gel (CH<sub>2</sub>Cl<sub>2</sub>/MeOH 95:5) gave triol derivative **44** as a colorless oil (250 mg, 89%); <sup>1</sup>H and <sup>13</sup>C NMR spectroscopic data in CD<sub>3</sub>OD given in Tables 1 and 2; HR ESIMS *m/z* 407.3531 [M+H]<sup>+</sup>, C<sub>26</sub>H<sub>47</sub>O<sub>3</sub> requires 407.3525.

*Methyl 3α-acetoxy-7-keto-5β-cholan-24-oate (67)*. To a solution of 7-ketolithocholic acid (5.0 g, 13 mmol), dissolved in 100 mL of dry methanol was added *p*-toluenesulfonic acid (11.0 g, 64.1 mmol). The solution was left to stand at room temperature for 2 h. The mixture was quenched by addition of NaHCO<sub>3</sub> saturated solution. After the evaporation of the methanol, the residue was extracted with EtOAc (3 x 150 mL). The combined extract was washed with brine, dried with Na<sub>2</sub>SO<sub>4</sub>, and evaporated to give the methyl esters as amorphous solid (5.13 g, quantitative yield). At the solution of the methyl ester (5.13 g, 12.7 mmol) in dry pyridine (100 mL), an excess of acetic anhydride was added. When the reaction was complete, the pyridine was concentrated under vacuum. The residue was poured into cold water (100 mL) and extracted with ethyl acetate (3 × 150 mL). The combined organic phases were dried (Na<sub>2</sub>SO<sub>4</sub>) and concentrated to give a residue that was further purified by flash chromatography on silica gel using hexane/ethyl acetate 8:2 and 0.5% of triethylamine as eluent (4.8 g of **67** as a white solid, 84% yield over two steps).

*Methyl 3α-acetoxy-6-ethylidene-7-keto-5β-cholan-24-oate (68)*. To a solution of diisopropylamine (23 mL, 0.16 mol) in dry THF (50 mL) was added dropwise a solution of *n*-butyllithium (60.0 mL, 2.5 M in hexane, 0.150 mol) at -78 °C. After 30 min, trimethylchlorosilane (27.1 mL, 0.210 mol) was added. After additional 30 min, a solution of compound **67** (4.80 g, 10.7 mmol) in dry THF (70 mL) was added. The reaction was stirred at -78 °C for an additional 45 min and then triethylamine (54 mL, 0.38 mol) was added. After 1 h, the reaction mixture was allowed to warm to -20 °C, treated with aqueous saturated solution of NaHCO<sub>3</sub> (100 mL) and brought up to room temperature in 2 h. The aqueous phase was extracted with ethyl acetate (3 x 50 mL). The combined organic phases were washed then with saturated solution of NaHCO<sub>3</sub>, water and brine. After drying

over anhydrous Na<sub>2</sub>SO<sub>4</sub>, the residue was evaporated under vacuum to give 6 g of yellow residue, that was diluted in dry CH<sub>2</sub>Cl<sub>2</sub> (50 mL) and cooled at -78 °C. At this stirred solution acetaldehyde (3.0 mL, 53 mmol) and BF<sub>3</sub>•OEt<sub>2</sub> (13.5 mL, 0.107 mol) were added dropwise. The reaction mixture was stirred for 2 h at -60 °C and allowed to warm to room temperature. The mixture was quenched with saturated aqueous solution of NaHCO<sub>3</sub> and extracted with CH<sub>2</sub>Cl<sub>2</sub>. The combined organic phases were washed with brine, dried over anhydrous Na<sub>2</sub>SO<sub>4</sub> and concentrated under *vacuum*. Purification by silica gel (hexane-ethyl acetate 9:1 and 0.5% TEA) gave compound **68** (4.1 g, 80% over two steps). NMR analysis demonstrated a diastereomeric ratio *E/Z* >95%. The *E* configuration at the exocyclic double bond was established by dipolar coupling H<sub>3</sub>-26 (δ 1.67)/H-5 (δ 2.62) in Noesy spectrum (400 MHz, mixing time 400 ms); selected <sup>1</sup>H NMR (400 MHz, CDCl<sub>3</sub>): δ 6.16 (1H, q, *J* = 7.0 Hz, H-25), 4.74 (1H, m, H-3), 3.64 (3H, s, COOCH<sub>3</sub>), 2.62 (1H, dd, *J* = 13.0, 3.6 Hz, H-5), 1.98 (3H, s, COCH<sub>3</sub>), 1.67 (3H, d, *J* = 7.0 Hz, H<sub>3</sub>-26), 1.00 (3H, s, H<sub>3</sub>-19), 0.92 (3H, d, *J* = 6.0 Hz, H<sub>3</sub>-21), 0.67 (3H, s, H<sub>3</sub>-18); <sup>13</sup>C NMR (100 MHz, CDCl<sub>3</sub>): δ 204.5, 174.6, 170.7, 143.1, 130.2, 72.5, 54.5, 51.4, 50.7, 48.6, 45.2, 43.5, 39.1, 38.9, 35.1, 34.9, 34.1, 33.4, 31.0, 30.9, 28.4, 25.9 (2C), 22.8, 21.4, 21.2, 18.4, 12.7, 12.2; HR ESIMS *m/z* 473.3271 [M+H]<sup>+</sup>, C<sub>29</sub>H<sub>45</sub>O<sub>5</sub> requires 473.3267.

*Methyl 3α-acetoxy-6β-ethyl-7-keto-5β-cholan-24-oate (69)*. A solution of **68** (4.0 g, 8.5 mmol) in THF dry/MeOH dry (100 mL, 1:1 v/v) was hydrogenated in presence of Pd(OH)<sub>2</sub> 20% wt on activated carbon (100 mg) Degussa type. The mixture was transferred to a standard Parr apparatus and flushed with nitrogen and then with hydrogen several times. The apparatus was shacked under 50 psi of H<sub>2</sub>. The reaction was stirred at room temperature for 8 h. The catalyst was filtered through Celite, and the recovered filtrate was concentrated under vacuum to give **69** (4.0 g, quantitative yield). The β-configuration of ethyl group at C-6 was determined by dipolar couplings H<sub>3</sub>-26 (δ 0.83)/ H<sub>3</sub>-19 (δ 1.22) and H-8 (δ 2.56)/H-25 (δ 1.83) in Noesy spectrum (400 MHz, mixing time 400 ms); selected <sup>1</sup>H NMR (400 MHz, CD<sub>3</sub>OD): δ 4.65 (1H, m, H-3), 3.66 (3H, s, COOCH<sub>3</sub>), 2.56 (1H, t, *J* = 11.5 Hz, H-8), 2.35 (1H, m, H-23a), 2.22 (1H, m, H-23b), 1.99 (3H, s, COCH<sub>3</sub>), 1.22 (3H, s, H<sub>3</sub>-19), 0.92 (3H, d, *J* = 6.3 Hz, H<sub>3</sub>-21), 0.83 (3H, t, *J* = 7.2



Hz, H<sub>3</sub>-26), 0.67 (3H, s, H<sub>3</sub>-18); <sup>13</sup>C NMR (100 MHz, CD<sub>3</sub>OD): δ 214.7, 174.3, 170.2, 72.6, 61.7, 54.8, 51.3, 49.0, 48.5, 45.3, 42.7, 42.3 (2C), 38.6, 35.4, 35.1, 35.0, 31.0, 30.8, 28.0 (2C), 26.4, 25.7, 24.7, 21.3, 21.1, 18.2, 12.9, 11.9; HR ESIMS *m/z* 475.3430 [M+H]<sup>+</sup>, C<sub>29</sub>H<sub>47</sub>O<sub>5</sub> requires 475.3423.

*Methyl 6α-ethyl-7-keto-5β-cholan-24-oate (71)*. Compound **69** (500 x 10<sup>-3</sup> g, 1.05 mmol) was treated with MeONa in methanol to obtain deacetylation at C-3 and inversion at C-6. Tosylation, in the same operative condition previously described,<sup>71</sup> furnished 620 mg of **70** (quantitative yield over two steps) that was subjected to the next step without further purification. Lithium bromide (148 mg, 1.70 mmol) and lithium carbonate (125 mg, 1.70 mmol) were added to a solution of 6α-ethyl-3α-tosyloxy-7-keto-5β-cholan-24-oate (500 x 10<sup>-3</sup> g, 0.850 mmol) in dry DMF (30 mL), and the mixture was refluxed for 2 h. After cooling to room temperature, the mixture was slowly poured into 10% HCl solution (20 mL) and extracted with CH<sub>2</sub>Cl<sub>2</sub> (3 × 50 mL). The combined organic layer was washed successively with water, saturated NaHCO<sub>3</sub> solution and water, and then dried over anhydrous MgSO<sub>4</sub> and evaporated to dryness to give 400 mg of oleous residue (quantitative yield), that was subjected to next step without any purification. Hydrogenation on Pd(OH)<sub>2</sub> in the same operative condition previously described furnished 312 mg of **71** (88% over two steps).

*6α-ethyl-7α-hydroxy-5β-cholan-24-ol (48)* and *6α-ethyl-7β-hydroxy-5β-cholan-24-ol (49)*. Dry methanol (70.0 μL, 1.70 mmol) and LiBH<sub>4</sub> (850 μL, 2 M in THF, 1.7 mmol) were added to a solution of the compound **71** (100 mg, 0.2 mmol) in dry THF (5 mL) at 0 °C under argon and the resulting mixture was stirred for 5 h at 0 °C. The mixture was quenched by addition of NaOH (1.0 M, 480 μL) and then allowed to warm to room temperature. Ethyl acetate was added and the separated aqueous phase was extracted with ethyl acetate (3 × 15 mL). The combined organic phases were washed with water, dried (Na<sub>2</sub>SO<sub>4</sub>) and concentrated to give a mixture of alcohols **48** and **49**. HPLC purification on a Nucleodur 100-5 C18 (5 μm; 10 mm i.d. x 250 mm) with MeOH/H<sub>2</sub>O (92:8) as eluent (flow rate 3 mL/min), gave 64 mg of 6α-ethyl-7α-hydroxy-5β-cholan-24-ol **48** (69%, *t<sub>R</sub>* = 31 min) and a small amount of 6α-ethyl-7β-hydroxy-5β-cholan-24-ol **49** (8 mg, *t<sub>R</sub>* = 24.8 min).

*6α-ethyl-7α-hydroxy-5β-cholan-24-ol* (**48**). Selected <sup>1</sup>H NMR (400 MHz, CD<sub>3</sub>OD): δ 3.65 (1H, br s, H-7), 3.51 (2H, m, H<sub>2</sub>-24), 0.97 (3H, d, *J* = 6.3 Hz, H<sub>3</sub>-21), 0.92 (3H, s, H<sub>3</sub>-19), 0.89 (3H, t, *J* = 7.3 Hz, H<sub>3</sub>-26), 0.71 (3H, s, H<sub>3</sub>-18); <sup>13</sup>C NMR (100 MHz, CD<sub>3</sub>OD): δ 71.6, 63.6, 57.6, 51.8, 48.7, 43.7, 43.3, 41.5, 41.1, 39.3, 37.5, 37.0, 34.6, 33.2, 30.3, 29.4, 28.8, 25.1, 24.6 (2C), 23.5, 22.5, 22.0, 19.2, 12.3, 12.1; HR ESIMS *m/z* 391.3579 [M+H]<sup>+</sup>, C<sub>26</sub>H<sub>47</sub>O<sub>2</sub> requires 391.3576.

*6α-ethyl-7β-hydroxy-5β-cholan-24-ol* (**49**). Selected <sup>1</sup>H NMR (500 MHz, CD<sub>3</sub>OD): δ 3.51 (2H, m, H<sub>2</sub>-24), 3.07 (1H, t, *J* = 10.0 Hz, H-7), 0.96 (3H, d, *J* = 6.6 Hz, H<sub>3</sub>-21), 0.96 (3H, t, *J* = 7.3 Hz, H<sub>3</sub>-26), 0.95 (3H, s, H<sub>3</sub>-19), 0.71 (3H, s, H<sub>3</sub>-18); <sup>13</sup>C NMR (100 MHz, CD<sub>3</sub>OD): δ 76.3, 63.6, 57.9, 56.8, 46.3, 45.3, 45.0, 44.7, 41.7, 41.1, 38.8, 37.0, 36.3, 33.3, 30.3, 28.1, 27.9 (2C), 25.0 (2C), 22.0, 21.9 (2C), 19.4, 12.7, 11.6; HR ESIMS *m/z* 391.3581 [M+H]<sup>+</sup>, C<sub>26</sub>H<sub>47</sub>O<sub>2</sub> requires 391.3576.

*6α-ethyl-7α-hydroxy-5β-cholan-24-yl 24-sodium sulfate* (**50**). Sulfation on C-24 on a small aliquot of diol **48** (20 mg, 0.05 mmol) was performed in the same operative conditions previously described.<sup>71,138</sup> RP18/HPLC on a Nucleodur 100-5 C18 (5 μm; 10 mm i.d. x 250 mm) with MeOH/H<sub>2</sub>O (82:18) as eluent (flow rate 3 mL/min) afforded compound **50** (*t<sub>R</sub>* = 14.2 min) as sodium salt. Selected <sup>1</sup>H NMR (400 MHz, CD<sub>3</sub>OD): δ 3.96 (2H, t, *J* = 6.3 Hz, H<sub>2</sub>-24), 3.64 (1H, br s, H-7), 0.96 (3H, d, *J* = 6.6 Hz, H<sub>3</sub>-21), 0.91 (3H, s, H<sub>3</sub>-19), 0.88 (3H, t, *J* = 7.4 Hz, H<sub>3</sub>-26), 0.69 (3H, s, H<sub>3</sub>-18); HR ESIMS *m/z* 469.2991 [M-H]<sup>-</sup>, C<sub>26</sub>H<sub>45</sub>O<sub>5</sub>S requires 469.2988.

*6α-ethyl-7α-hydroxy-5β-cholan-24-oic acid* (**51**) and *6α-ethyl-7β-hydroxy-5β-cholan-24-oic acid* (**52**). Compound **71** (200 mg, 0.5 mmol) was hydrolyzed with NaOH (96 mg, 2.4 mmol) in a solution of MeOH:H<sub>2</sub>O 1:1 v/v (10 mL). The mixture was stirred for 4 h at reflux. The resulting solution was then acidified with HCl 6 M and extracted with ethyl acetate (3 × 50 mL). The collected organic phases were washed with brine, dried over Na<sub>2</sub>SO<sub>4</sub> anhydrous and evaporated under reduced pressure to give the carboxylic acid intermediate. Crude carboxylic acid intermediate (190 mg, 0.47 mmol) was treated with LiBH<sub>4</sub> (1.65 mL, 2M in THF, 3.30 mmol) and MeOH (133 μL, 3.30 mmol) in THF dry (5 mL). Purification by silica gel (CH<sub>2</sub>Cl<sub>2</sub>-MeOH 99:1) furnished 157 mg of *6α-ethyl-7α-*

hydroxy-5 $\beta$ -cholan-24-oic acid (**51**, 83%). In same embodiments LiBH<sub>4</sub> treatment after alkaline hydrolysis produced small amounts (about 10%) of 6 $\alpha$ -ethyl-7 $\beta$ -hydroxy-5 $\beta$ -cholan-24-oic acid (**52**) that was isolated by HPLC purification on a Nucleodur 100-5 C18 (5  $\mu$ m; 10 mm i.d. x 250 mm) with MeOH/H<sub>2</sub>O (88:12) as eluent (flow rate 3 mL/min,  $t_R$ = 16 min).

*6 $\alpha$ -ethyl-7 $\alpha$ -hydroxy-5 $\beta$ -cholan-24-oic acid (51)*. Selected <sup>1</sup>H NMR (400 MHz, CD<sub>3</sub>OD):  $\delta$  3.65 (1H, brs, H-7), 2.34 (1H, m, H-23a), 2.20 (1H, m, H-23b), 0.96 (3H, d,  $J$  = 6.3 Hz, H<sub>3</sub>-21), 0.92 (3H, s, H<sub>3</sub>-19), 0.89 (3H, t,  $J$  = 7.4 Hz, H<sub>3</sub>-26), 0.70 (3H, s, H<sub>3</sub>-18); <sup>13</sup>C NMR (100 MHz, CD<sub>3</sub>OD):  $\delta$  178.0, 71.6, 57.4, 51.7, 48.7, 43.8, 43.3, 41.5, 41.1, 39.3, 37.4, 36.8, 34.6, 32.5 (2C), 29.3, 28.8, 25.1, 24.6 (2C), 23.5, 22.5, 22.0, 18.8, 12.2, 12.1; HR ESIMS  $m/z$  403.3214 [M-H]<sup>-</sup>, C<sub>26</sub>H<sub>43</sub>O<sub>3</sub> requires 403.3212.

*6 $\alpha$ -ethyl-7 $\beta$ -hydroxy-5 $\beta$ -cholan-24-oic acid (52)*. Selected <sup>1</sup>H NMR (500 MHz, CD<sub>3</sub>OD):  $\delta$  3.08 (1H, t,  $J$  = 9.6 Hz, H-7), 2.32 (1H, m, H-23a), 2.20 (1H, m, H-23b), 0.96 (3H, d,  $J$  = 6.2 Hz, H<sub>3</sub>-21), 0.95 (3H, s, H<sub>3</sub>-19), 0.85 (3H, t,  $J$  = 7.0 Hz, H<sub>3</sub>-26), 0.70 (3H, s, H<sub>3</sub>-18); HR ESIMS  $m/z$  403.3217 [M-H]<sup>-</sup>, C<sub>26</sub>H<sub>43</sub>O<sub>3</sub> requires 403.3212.

*6 $\alpha$ -ethyl-7 $\alpha$ -hydroxy-5 $\beta$ -cholan-24-oyl taurine sodium sulfate (53)*. An aliquot of **51** (10.0 mg, 0.0240 mmol) in DMF dry (5 mL) was treated with DMT-MM (20.5 mg, 70 x 10<sup>-3</sup> mmol) and triethylamine (83  $\mu$ L, 0.60 mmol) and the mixture was stirred at room temperature for 10 min. Then to the mixture was added taurine (18 mg, 0.14 mmol). After 3 h, the reaction mixture was concentrated *in vacuo* and dissolved in water (5 mL). Purification on C18 silica gel column and then HPLC on a Nucleodur 100-5 C18 (5  $\mu$ m; 10 mm i.d. x 250 mm) with MeOH/H<sub>2</sub>O (83:17) as eluent (flow rate 3 mL/min), gave 4.5 mg of 6 $\alpha$ -ethyl-7 $\alpha$ -hydroxy-5 $\beta$ -cholan-24-oyl taurine sodium sulfate (**53**) ( $t_R$ =10 min); selected <sup>1</sup>H NMR (400 MHz, CD<sub>3</sub>OD):  $\delta$  3.65 (1H, br s, H-7), 3.58 (2H, t,  $J$  = 7.0 Hz, CH<sub>2</sub>-N), 2.96 (2H, t,  $J$  = 9.6 Hz, CH<sub>2</sub>-S), 2.25 (1H, m, H-23a), 2.10 (1H, m, H-23b), 0.97 (3H, d,  $J$  = 6.4 Hz, H<sub>3</sub>-21), 0.92 (3H, s, H<sub>3</sub>-19), 0.89 (3H, t,  $J$  = 7.1 Hz, H<sub>3</sub>-26), 0.70 (3H, s, H<sub>3</sub>-18); HR ESIMS  $m/z$  510.3257 [M-H]<sup>-</sup>, C<sub>28</sub>H<sub>48</sub>NO<sub>5</sub>S requires 510.3253.

*Methyl 6 $\beta$ -ethyl-7-keto-5 $\beta$ -cholan-24-oate (73)*. Compound **73** (400 mg, 94% over two steps) was synthesized, starting from compound **72** (600 x 10<sup>-3</sup> g, 1.02

mmol), by an analogous procedure to that detailed above for compound **71**. Compound **72** (620 mg, quantitative yield over two steps) was obtained from **69** ( $500 \times 10^{-3}$  g, 1.05 mmol) by an analogous procedure to that detailed above for compound **70**, except for reaction time (2 h) of the deacetylation step; selected  $^1\text{H}$  NMR (400 MHz,  $\text{CD}_3\text{OD}$ ):  $\delta$  3.63 (3H, s,  $\text{COOCH}_3$ ), 2.53 (1H, t,  $J = 11.4$  Hz, H-8), 2.33 (1H, m, H-23a), 2.19 (1H, m, H-23b), 1.18 (3H, s, H<sub>3</sub>-19), 0.89 (3H, d,  $J = 6.2$  Hz, H<sub>3</sub>-21), 0.81 (3H, t,  $J = 7.4$  Hz, H<sub>3</sub>-26), 0.64 (3H, s, H<sub>3</sub>-18);  $^{13}\text{C}$  NMR (100 MHz,  $\text{CD}_3\text{OD}$ ),  $\delta$  217.0, 174.9, 62.4, 54.7, 51.5, 50.7, 48.7, 45.7, 43.2, 42.5, 38.8, 37.5, 36.3, 35.2, 31.0, 30.9, 30.3, 28.2, 26.7 (2C), 26.3, 24.9, 21.4, 20.4, 18.3, 13.0, 12.0; HR ESIMS  $m/z$  417.3373  $[\text{M}+\text{H}]^+$ ,  $\text{C}_{27}\text{H}_{43}\text{O}_3$  requires 417.3369.

*6 $\beta$ -ethyl-7 $\beta$ -hydroxy-5 $\beta$ -cholan-24-ol (54)* and *6 $\beta$ -ethyl-7 $\alpha$ -hydroxy-5 $\beta$ -cholan-24-ol (55)*. To a methanol solution of **73** (350 mg, 0.84 mmol), a large excess of  $\text{NaBH}_4$  was added at 0 °C. The mixture was left at room temperature for 2 h and then water and MeOH were added dropwise during a period of 15 min at 0 °C with effervescence being observed. After evaporation of the solvents, the residue was diluted with water and extracted with ethyl acetate (3 x 50 mL). The combined extract was washed with brine, dried with  $\text{Na}_2\text{SO}_4$ , and evaporated to give 1.3 g of a crude residue that was subjected to the next step without further purification. The crude residue was treated with  $\text{LiBH}_4$  (2 M in THF) in the same operative condition described for the synthesis of compounds **48** and **49**. HPLC purification on a Nucleodur 100-5 C18 (5  $\mu\text{m}$ ; 10 mm i.d. x 250 mm) with MeOH/ $\text{H}_2\text{O}$  (92:8) as eluent (flow rate 3 mL/min), furnished 180 mg of *6 $\beta$ -ethyl-7 $\beta$ -hydroxy-5 $\beta$ -cholan-24-ol (54)*, 54%,  $t_{\text{R}} = 25$  min) and 75.4 mg of *6 $\beta$ -ethyl-7 $\alpha$ -hydroxy-5 $\beta$ -cholan-24-ol (55)*, 23%,  $t_{\text{R}} = 13$  min).

*6 $\beta$ -ethyl-7 $\beta$ -hydroxy-5 $\beta$ -cholan-24-ol (54)*. Selected  $^1\text{H}$  NMR (700 MHz,  $\text{CD}_3\text{OD}$ ):  $\delta$  3.67 (1H, dd,  $J = 8.7, 4.7$  Hz, H-7), 3.51 (2H, m, H<sub>2</sub>-24), 0.98 (3H, s, H<sub>3</sub>-19), 0.97 (3H, d,  $J = 6.6$  Hz, H<sub>3</sub>-21), 0.96 (3H, t,  $J = 7.4$  Hz, H<sub>3</sub>-26), 0.71 (3H, s, H<sub>3</sub>-18);  $^{13}\text{C}$  NMR (175 MHz,  $\text{CD}_3\text{OD}$ ):  $\delta$  75.5, 63.8, 57.6, 56.5, 44.2, 43.7, 42.8, 41.0, 40.9, 40.8, 38.2 (2C), 36.9, 34.4, 32.8, 29.7, 28.9, 27.0, 26.1, 24.7, 22.2, 22.0 (2C), 19.2, 13.9, 12.3; HR ESIMS  $m/z$  391.3580  $[\text{M}+\text{H}]^+$ ,  $\text{C}_{26}\text{H}_{47}\text{O}_2$  requires 391.3576.

*6β-ethyl-7α-hydroxy-5β-cholan-24-ol* (**55**). Selected <sup>1</sup>H NMR (700 MHz, CD<sub>3</sub>OD): δ 3.59 (1H, s, H-7), 3.51 (2H, m, H<sub>2</sub>-24), 2.23 (1H, dq, *J* = 13.9, 4.0 Hz, H-4a), 0.97 (3H, d, *J* = 6.6, H<sub>3</sub>-21), 0.95 (3H, t, *J* = 7.1 Hz, H<sub>3</sub>-26), 0.94 (3H, s, H<sub>3</sub>-19), 0.70 (3H, s, H<sub>3</sub>-18); <sup>13</sup>C NMR (175 MHz, CD<sub>3</sub>OD): δ 73.1, 63.2, 57.3, 52.8, 51.4, 49.4, 43.8, 41.3, 39.7, 37.4 (2C), 37.2, 34.2, 32.6 (2C), 29.9, 29.5, 28.9, 28.3, 27.3, 24.5, 21.7, 21.2, 18.8, 14.3, 12.3; HR ESIMS *m/z* 391.3578 [M+H]<sup>+</sup>, C<sub>26</sub>H<sub>47</sub>O<sub>2</sub> requires 391.3576.

*Methyl 6α-ethyl-3β-hydroxy-7-keto-5β-cholan-24-oate* (**74**). A solution of **72** (900 × 10<sup>-3</sup> g, 1.50 mmol) and CH<sub>3</sub>COOK (147 mg, 1.53 mmol) dissolved in water (2 mL) and *N,N*-dimethylformamide (DMF, 10 mL) was refluxed for 2 h. The solution was cooled at room temperature and then ethyl acetate and water were added. The separated aqueous phase was extracted with ethyl acetate (3 × 30 mL). The combined organic phases were washed with water, dried (Na<sub>2</sub>SO<sub>4</sub>) and evaporated to dryness to give 1.0 g of mixture. Purification by silica gel (hexane-ethyl acetate 7:3 and 0.5% TEA) gave 500 mg of intermediates oily oil. C-6 inversion in the same operative condition as described for the synthesis of compound **70**, furnished compound **74** (500 mg, 74% over two steps); selected <sup>1</sup>H NMR (400 MHz, CD<sub>3</sub>OD): δ 3.96 (1H, m, H-3), 3.64 (3H, s, COOCH<sub>3</sub>), 2.85 (1H, dd, *J* = 5.6, 12.3 Hz, H-6), 2.50 (1H, t, *J* = 11.2 Hz, H-8), 2.33 (1H, m, H-23a), 2.20 (1H, m, H-23b), 1.27 (3H, s, H<sub>3</sub>-19), 0.95 (3H, d, *J* = 6.4 Hz, H<sub>3</sub>-21), 0.81 (3H, t, *J* = 7.2 Hz, H<sub>3</sub>-26), 0.71 (3H, s, H<sub>3</sub>-18); <sup>13</sup>C NMR (100 MHz, CD<sub>3</sub>OD): δ 213.4, 174.8, 65.9, 54.8, 51.8, 51.2, 50.0, 49.0, 45.7, 43.2, 42.7, 39.0, 36.2, 35.2, 31.0 (2C), 29.2, 29.0, 28.3, 27.2, 24.6, 24.0, 22.1, 18.7, 18.4, 12.0 (2C); HR ESIMS *m/z* 433.3322 [M + H]<sup>+</sup>, C<sub>27</sub>H<sub>45</sub>O<sub>4</sub> requires 433.3318.

*6α-ethyl-3β,7α-dihydroxy-5β-cholan-24-ol* (**56**) and *6α-ethyl-3β,7β-dihydroxy-5β-cholan-24-ol* (**57**). Intermediate **74** (500 × 10<sup>-3</sup> g, 1.16 mmol) was treated with LiBH<sub>4</sub> as previously described. HPLC purification on a Nucleodur 100-5 C18 (5 μm; 10 mm i.d. × 250 mm) with MeOH/H<sub>2</sub>O (88:12) as eluent (flow rate 3 mL/min), gave 250 mg of compound **56** as a white solid (53%, *t<sub>R</sub>* = 12.6 min) and a small amount of compound **57** (23 mg, 5%, *t<sub>R</sub>* = 8.2 min).

*6α-ethyl-3β,7α-dihydroxy-5β-cholan-24-ol* (**56**). Selected <sup>1</sup>H NMR (500 MHz CD<sub>3</sub>OD): δ 3.97 (1H, brs, H-3), 3.66 (1H, brs, H-7), 3.51 (2H, m, H<sub>2</sub>-24), 0.96

(3H, d,  $J = 6.6$  Hz, H3-21), 0.94 (3H, s, H3-19), 0.91 (3H, t,  $J = 7.5$  Hz, H3-26), 0.70 (3H, s, H3-18);  $^{13}\text{C}$  NMR (125 MHz,  $\text{CD}_3\text{OD}$ ):  $\delta$  71.4, 67.4, 63.6, 57.6, 51.7, 43.7, 42.8, 41.5, 41.2, 41.1, 37.1 (2C), 33.8, 33.2, 31.3 (2C), 30.3, 29.4, 28.3, 24.6, 24.2, 23.3, 22.3, 19.2, 12.7, 12.1; HR ESIMS  $m/z$  407.3531  $[\text{M}+\text{H}]^+$ ,  $\text{C}_{26}\text{H}_{47}\text{O}_3$  requires 407.3525.

*6 $\alpha$ -ethyl-3 $\beta$ ,7 $\beta$ -dihydroxy-5 $\beta$ -cholan-24-ol (57)*. Selected  $^1\text{H}$  NMR (500 MHz  $\text{CD}_3\text{OD}$ ):  $\delta$  4.01 (1H, brs, H-3), 3.51 (2H, m, H2-24), 3.05 (1H, t,  $J = 9.7$  Hz, H-7), 0.97 (3H, s, H3-19), 0.96 (3H, d,  $J = 6.4$  Hz, H3-21), 0.88 (3H, t,  $J = 7.6$  Hz, H3-26), 0.72 (3H, s, H3-18);  $^{13}\text{C}$  NMR (100 MHz  $\text{CD}_3\text{OD}$ ):  $\delta$  76.3, 67.1, 63.6, 57.8, 56.8, 45.0, 44.8, 44.5, 41.7, 40.3, 39.1, 37.0, 35.9, 33.0, 31.2, 30.2, 29.8, 28.4, 28.0, 27.9, 24.8, 22.9, 21.8, 19.3, 12.8, 11.6; HR ESIMS  $m/z$  407.3529  $[\text{M}+\text{H}]^+$ ,  $\text{C}_{26}\text{H}_{47}\text{O}_3$  requires 407.3525.

*6 $\alpha$ -ethyl-3 $\beta$ ,7 $\alpha$ -dihydroxy-5 $\beta$ -cholan-24-oic acid (58)* and *6 $\alpha$ -ethyl-3 $\beta$ ,7 $\beta$ -dihydroxy-5 $\beta$ -cholan-24-oic acid (59)*. Compounds **58** and **59** (215 mg, 74% over two steps) were synthesized, starting from compound **74** (320 mg, 0.74 mmol), by an analogous procedure to that detailed above for compounds **51** and **52**. HPLC purification on a Nucleodur 100-5 C18 (5  $\mu\text{m}$ ; 10 mm i.d. x 250 mm) with  $\text{MeOH}/\text{H}_2\text{O}$  (88:12) as eluent (flow rate 3 mL/min), gave 208 mg of **58** as a white solid (65%,  $t_{\text{R}} = 11$  min). In same embodiments  $\text{LiBH}_4$  treatment after alkaline hydrolysis produced small amounts (about 10%) of **59** that was isolated by HPLC purification on a Nucleodur 100-5 C18 (5  $\mu\text{m}$ ; 10 mm i.d. x 250 mm) with  $\text{MeOH}/\text{H}_2\text{O}$  (88:12) as eluent (flow rate 3 mL/min, 28 mg of **59**, 9%,  $t_{\text{R}} = 8$  min).

*6 $\alpha$ -ethyl-3 $\beta$ ,7 $\alpha$ -dihydroxy-5 $\beta$ -cholan-24-oic acid (58)*. Selected  $^1\text{H}$  NMR (400 MHz,  $\text{CD}_3\text{OD}$ ):  $\delta$  3.97 (1H, brs, H-3), 3.67 (1H, br s, H-7), 2.33 (1H, m, H-23a), 2.21 (1H, m, H-23b), 0.96 (3H, d,  $J = 6.5$  Hz, H3-21), 0.94 (3H, s, H3-19), 0.91 (3H, t,  $J = 7.6$  Hz, H3-26), 0.70 (3H, s, H3-18);  $^{13}\text{C}$  NMR (100 MHz,  $\text{CD}_3\text{OD}$ ):  $\delta$  178.3, 71.3, 67.5, 57.4, 51.7, 43.8, 42.8, 41.5, 41.2, 41.0, 37.0, 36.7, 33.8, 32.4, 32.0, 31.1 (2C), 29.3, 28.3, 24.6, 24.2, 23.3, 22.2, 18.8, 12.3, 12.2; HR ESIMS  $m/z$  419.3169  $[\text{M}-\text{H}]^-$   $\text{C}_{26}\text{H}_{43}\text{O}_4$  requires 419.3167.

*6 $\alpha$ -ethyl-3 $\beta$ ,7 $\beta$ -dihydroxy-5 $\beta$ -cholan-24-oic acid (59)*. Selected  $^1\text{H}$  NMR (500 MHz,  $\text{CD}_3\text{OD}$ ):  $\delta$  4.01 (1H, brs, H-3), 3.06 (1H, t,  $J = 9.7$  Hz, H-7), 2.32 (1H, m, H-23a), 2.19 (1H, m, H-23b), 0.97 (3H, s, H3-19), 0.96 (3H, d, ovl, H3-21), 0.87

(3H, t,  $J = 7.7$  Hz, H3-26), 0.71 (3H, s, H3-18); HR ESIMS  $m/z$  419.3169 [M-H]<sup>-</sup> C<sub>26</sub>H<sub>43</sub>O<sub>4</sub> requires 419.3167.

*6 $\alpha$ -ethyl-3 $\beta$ ,7 $\alpha$ -dihydroxy-5 $\beta$ -cholan-24-oyl taurine sodium sulfate (60)*. Compound **60** was synthesized, starting from compound **58** (10.0 mg, 0.0230 mmol), by an analogous procedure to that detailed above for compound **53**; selected <sup>1</sup>H NMR (500 MHz, CD<sub>3</sub>OD):  $\delta$  3.97 (1H, brs, H-3), 3.67 (1H, br s, H-7), 3.59 (2H, t,  $J = 6.8$  Hz, CH<sub>2</sub>-N), 2.96 (2H, t,  $J = 6.8$  Hz, CH<sub>2</sub>-S), 0.97 (3H, d,  $J = 6.4$  Hz, H<sub>3</sub>-21), 0.95 (3H, s, H<sub>3</sub>-19), 0.91 (3H, t,  $J = 7.1$  Hz, H3-26), 0.70 (3H, s, H<sub>3</sub>-18); HR ESIMS  $m/z$  526.3206 [M-H]<sup>-</sup>, C<sub>28</sub>H<sub>48</sub>NO<sub>6</sub>S requires 526.3202.

*6 $\beta$ -ethyl-3 $\beta$ ,7 $\beta$ -dihydroxy-5 $\beta$ -cholan-24-ol (61)* and *6 $\beta$ -ethyl-3 $\beta$ ,7 $\alpha$ -dihydroxy-5 $\beta$ -cholan-24-ol (62)*. Compound **72** was treated with CH<sub>3</sub>COOK as previously described for compound **74**. NaBH<sub>4</sub>/LiBH<sub>4</sub> reduction on the corresponding 7-keto intermediate (100 x 10<sup>-3</sup> g, 0.230 mmol) in the same operative conditions described for the synthesis of compounds **54** and **55** afforded a mixture whose HPLC purification on a Nucleodur 100-5 C18 (5  $\mu$ m; 10 mm i.d. x 250 mm) with MeOH/H<sub>2</sub>O (88:12) as eluent (flow rate 3 mL/min), gave 48.3 mg of **61** (52 % over two steps,  $t_R = 11$  min) and 20.7 mg of **62** (22 % over two steps,  $t_R = 13$  min).

*6 $\beta$ -ethyl-3 $\beta$ ,7 $\beta$ -dihydroxy-5 $\beta$ -cholan-24-ol (61)*. Selected <sup>1</sup>H NMR (700 MHz, CD<sub>3</sub>OD):  $\delta$  3.59 (1H, brs, H-3), 3.57 (1H, dd,  $J = 12.6, 2.3$  Hz, H-7), 3.51 (2H, m, H<sub>2</sub>-24), 0.98 (3H, s, H3-19), 0.96 (3H, ovl, H3-21), 0.96 (3H, t, ovl, H3-26), 0.70 (3H, s, H3-18); <sup>13</sup>C NMR (175 MHz, CD<sub>3</sub>OD):  $\delta$  75.2, 68.3, 63.6, 58.3, 57.1, 45.7 (2C), 44.2, 41.8 (2C), 41.2, 40.0, 37.0, 35.9, 33.3, 31.1, 30.3, 29.4 (2C), 26.6 (2C), 23.2 (2C), 19.3, 13.0, 12.3; HR ESIMS  $m/z$  407.3530 [M+H]<sup>+</sup>, C<sub>26</sub>H<sub>47</sub>O<sub>3</sub> requires 407.3525.

*6 $\beta$ -ethyl-3 $\beta$ ,7 $\alpha$ -dihydroxy-5 $\beta$ -cholan-24-ol (62)*. Selected <sup>1</sup>H NMR (700 MHz, CD<sub>3</sub>OD):  $\delta$  3.91 (1H, brs, H-3), 3.60 (1H, br s, H-7), 3.51 (2H, m, H<sub>2</sub>-24), 2.45 (1H, t,  $J = 13.3$  Hz, H-4a), 0.97 (3H, s, H<sub>3</sub>-19), 0.97 (3H, ovl, H<sub>3</sub>-21), 0.95 (3H, t,  $J = 7.4$  Hz, H<sub>3</sub>-26), 0.71 (3H, s, H<sub>3</sub>-18); <sup>13</sup>C NMR (175 MHz, CD<sub>3</sub>OD):  $\delta$  72.8, 67.4, 63.4, 57.2, 51.3, 51.2, 43.2, 41.6, 40.5, 37.3, 37.1 (2C), 36.9, 34.0, 33.3, 32.1, 30.3, 29.3, 28.9, 28.6, 26.3, 24.9, 22.0, 19.3, 13.8, 12.1; HR ESIMS  $m/z$  407.3528 [M+H]<sup>+</sup>, C<sub>26</sub>H<sub>47</sub>O<sub>3</sub> requires 407.3525.

*6 $\alpha$ -ethyl-chenodeoxycholic acid* (**3**). Compound **69** ( $500 \times 10^{-3}$  g, 1.05 mmol) was hydrolyzed with NaOH (208 mg, 5.20 mmol) in a solution of MeOH:H<sub>2</sub>O 1:1 v/v (10 mL), as previously described. The mixture was stirred for 5 h at reflux. The resulting solution was then acidified with HCl 6 M and extracted with ethyl acetate (3 x 50 mL). The collected organic phases were washed with brine, dried over Na<sub>2</sub>SO<sub>4</sub> anhydrous and evaporated under reduced pressure to give the carboxylic acid intermediate **75**. This compound was subjected to the LiBH<sub>4</sub> reduction of the C7-carbonyl group. Purification gave 305 mg of 6-ECDCA (**3**) as a white solid (69% over two steps).

### **Specific biological assays**

#### **Bile acids determination**

**Sample preparation.** The stock solutions of the individual tauro-conjugated and un-conjugated bile acids were prepared separately in methanol at a concentration of 1 mg/mL. All stock solutions were stored at  $-20^{\circ}\text{C}$ . Calibration standards were prepared by combining appropriate volumes of each bile acid stock solution and methanol. The calibration range was from 10 nM to 100  $\mu\text{M}$  of each bile acid in the final solution. Mice serum sample aliquots of 100  $\mu\text{L}$  were deproteinized with 1 mL of cold acetonitrile with 5% of NH<sub>4</sub>OH vortexing for 1 min. After centrifugation at 16000 g for 10 min, the clear supernatant was transferred to a new vial, snap frozen and lyophilized. The sample was then re-dissolved in methanol-water (2:1, v/v) for tauro-conjugated bile acids determination and in methanol-ammonium acetate 10 mM with 0.005% formic acid (3:2, v/v) for un-conjugated bile acids determination. A bile acids extraction yield of 95% has been estimated.

**Liquid chromatography and mass spectrometry.** For LC–MS/MS analysis, chromatographic separation was carried out on the HPLC–MS system LTQ XL ThermoScientific equipped with Accelera 600 Pump and Accelera AutoSampler system. The mixture was separated on a Jupiter 5  $\mu\text{C}18$  column from Phenomenex (150 x 2.00 mm). Tauro-conjugated bile acids were separated at a flow rate of 200  $\mu\text{L}/\text{min}$  using a methanol-aqueous ammonium acetate (NH<sub>4</sub>OAc) gradient. Mobile phase A was 5% methanol in water containing 2 mM ammonium



acetate at pH 7, mobile phase B was methanol, containing ammonium acetate at 2 mM. The gradient started at 30 % B and increased to 100% B in 20 min, kept at 100% B for 5 min then decreased to 30% B in 1 min and kept at 30% B for 10 min. ESI was performed in negative ion mode, the ion source temperature was set at 280 °C. The tune page parameters were automatically optimized injecting taurocholic acid at 1 µM as standard. The MS/MS detection was operated in MRM mode using a collision energy of 20 (arbitrary units), the observed transitions were:

tauromuricholic acid (t-MCA) at 13.5 min MRM of 514.28 Th→514.28 Th, taurohyocholic acid (t-HCA) at 15.6 min MRM of 498.29 Th→498.29 Th, taurocholic acid (t-CA) at 16.6 min MRM of 514.28 Th→514.28 Th, taurochenodeoxycholic acid (t-CDCA) at 18.5 min MRM of 498.29 Th→498.29 Th, taurodeoxycholic acid (t-DCA) at 18.9 min MRM of 498.29 Th→498.29 Th, tauroolithocholic acid (t-LCA) at 22.3 min MRM of 482.29 Th→482.29 Th and tauro-10 (t-10) at 25.3 min MRM of 510.29 Th→510.63 Th. Un-conjugated bile acids were separated at a flow rate of 200 µL/min using 10 mM ammonium acetate in water at 0.005% formic acid as the mobile phase A 10 mM ammonium acetate in methanol at 0.005% formic acid as mobile phase B. The gradient program started at 60% B and increased to 95% B in 25 min, kept at 95% B for 9 min then decreased to 60% B in 1 min and kept at 60% B for 10 min. ESI was performed in negative ion mode, the ion source temperature was set at 280 °C. The tune page parameters were automatically optimized injecting CA at 1 µM as standard. The MS/MS detection was operated in MRM mode using a collision energy of 15 (arbitrary units). The observed transitions were: hyocholic acid (HCA) at 8.9 min MRM of 391.29 Th→391.29 Th, cholic acid (CA) at 10.2 min MRM of 407.28 Th→407.28 Th, chenodeoxycholic acid (CDCA) at 13.8 min MRM of 391.29 Th→391.29 Th, deoxycholic acid (DCA) at 14.4 min MRM of 391.29 Th→391.29 Th, lithocholic acid (LCA) at 17.5 min MRM of 375.28 Th→375.28 Th and 10 at 20.5 min MRM of 403.63 Th→403.63Th.

### **Determination of 7 $\alpha$ -hydroxy-4-cholesten-3-one**

**Sample preparation.** Stock solutions of 7  $\alpha$ -hydroxy-4-cholesten-3-one were separately prepared at 5 mg/mL using MeOH as solvent. Five dilutions were obtained mixing 1 ng, 10 ng, 100 ng, 1  $\mu$ g and 10  $\mu$ g of 7 $\alpha$ -hydroxy-4-cholesten-3-one in 50  $\mu$ L of MeOH. Later on, 10  $\mu$ L of glacial acetic acid and 10 mg of Girard T reagent (diluted in 40  $\mu$ L of water) were added and kept in the dark at r.t. overnight (final volume of 100  $\mu$ L).<sup>137</sup>

Mice serum sample aliquots of 50  $\mu$ L were deproteinized with 500  $\mu$ L of cold acetonitrile with 5% of NH<sub>4</sub>OH vortexing for 60 min. After centrifugation at 16000 g for 10 min, the clear supernatant was transferred to a new vial, snap frozen and lyophilized. The sample was then re-dissolved in 50  $\mu$ L of MeOH. Later on, 10  $\mu$ L of glacial acetic acid and 10 mg of Girard T reagent (diluted in 40  $\mu$ L of water) were added and kept in the dark at r.t. overnight (final volume of 100  $\mu$ L).

**Liquid chromatography and mass spectrometry analysis.** For LC-MS/MS analysis, chromatographic separation was carried out on the HPLC–MS system LTQ XL ThermoScientific equipped with Accelera 600 Pump and Accelera AutoSampler system. The mixture was separated on a Jupiter C18 column from Phenomenex (150 x 2.00 mm) and the column flow rate was set at 150  $\mu$ L/min. Samples were separated using a acetonitrile-metanol-aqueous gradient. Mobile phase A was water/MeOH/ACN at 50/33.3/16.7% in 0.1% TFA, mobile phase B was MeOH/ACN at 66.6/33.4% in 0.1% TFA. The gradient started at 35% B and increased to 95% B in 15 min, kept at 95% B for 10 min then decreased to 35% B in 1 min and kept at 35% B for 10 min. ESI was performed in positive ion mode, the ion source temperature was set at 280 °C. The MS/MS detection was operated using a collision energy of 40 (arbitrary units). 7 $\alpha$ -hydroxy-4-cholesten-3-one modified by GT reagent gave a positive ion at  $m/z$  of 514.5 at 12.0 min and MS/MS analysis gave fragments at  $m/z$  of 455.4, 437.4, 427.4, 163.1, 151.1, 135.1, 123.1.

### **Specific biological assay used for compound 45**

**Chemicals.** Compound 45 or BAR501 was synthesized as described. Norepinephrine (NE), L-methionine, methoxamine, TLCA, oleanolic acid, betulinic acid, UDCA and LY294002 were from Sigma Aldrich (Milan, Italy).

**Animals.** C57BL6 and male Wistar rats were from Harlan Nossan (Udine, Italy). GPBAR1 null mice (generated directly into C57BL/6NCrI background), and congenic littermates on C57BL/6NCrI mice were originally donated by Dr. Galya Vassileva (Schering-Plough Research Institute, Kenilworth).<sup>73</sup> The colonies were maintained in the animal facility of University of Perugia. Mice were housed under controlled temperatures (22 °C) and photoperiods (12:12-hour light/ dark cycle), allowed unrestricted access to standard mouse chow and tap water and allowed to acclimate to these conditions for at least 5 days before inclusion in an experiment. A total number of 96 mice and 21 rats were used in this study. The study was conducted in agreement with the Italian law and the protocol was approved by a ethical committee of University of Perugia and by a National committee of Ministry of Health (permission n. 245/2013-B). The health and body conditions of the animals were monitored daily by the veterinarian in the animal facility. The study protocol caused minor suffering, however, animals that lost more than 25% of the initial body weight were euthanized. At the day of sacrifice (prior to measure the portal pressure the animals (mice) were deeply anesthetized with a mixture of tiletamine hydrochloride and zolazepam hydrochloride/xylazine at a dose of 50/5 mg/kg. Similarly rats, at the day of sacrifice rats were deeply anesthetized with a lethal dose tiletamine hydrochloride and zolazepam hydrochloride/xylazine and liver were isolated and perfused.

**Animal models.** Liver cirrhosis was induced by carbon tetrachloride (CCl<sub>4</sub>) administration. For this purpose, C57BL6 mice (40 animals) were administered i.p. 500 µL/Kg body weight of CCl<sub>4</sub> in an equal volume of paraffin oil twice a week for 9 weeks. CCl<sub>4</sub> mice were randomized to receive BAR501 (15 mg/kg daily by gavage) or vehicle (distilled water). In another experimental setting, wild type C57BL6 mice were administered 500 µL/Kg body weight of CCl<sub>4</sub> in an equal volume of paraffin oil twice a week for 3 weeks. CCl<sub>4</sub> mice were then randomized to receive BAR501 (30 and 45 mg/kg daily by gavage) or vehicle (distilled water). Serum bilirubin, albumin, aspartate aminotransferase (AST), alanine aminotransferase (ALT) and alkaline phosphatase (ALP) were measured by routine biochemical clinical chemistry. For histological examination, portions of the right and left liver lobes were fixed in 10% formalin, embedded in paraffin, sectioned and stained with Sirius red and hematoxylin/ eosin (H&E). In a further

model, moderate hyperhomocysteinemia<sup>77</sup> was induced in Gpbar1<sup>+/+</sup> and Gpbar1<sup>-/-</sup> mice (56 animals) by administration of L-methionine (1 g/kg daily by gavage) for a period of 4 weeks (n = 20). Mice administered L-methionine were randomized to receive BAR501 (20 mg/kg daily by gavage) or vehicle (distilled water).

**Isolated and perfused rat liver preparation.** To investigate the effect of BAR501 on intrahepatic microcirculation, naïve rats were administered BAR501 (15 mg/kg daily by gavage) or water for 6 days. At the end of this period, analysis of hepatic vascular responses to NE (from 0.01 to 100 µmol/L) or methoxamine (100 µM) was performed using the isolated and perfused rat liver preparation, as described previously.<sup>77,84,140-141</sup> The vasomotor responses to changes of liver flow (shear stress) was measured as described previously<sup>77,84-87,140-141</sup> During these studies, the global viability of livers was assessed by standard criteria: *i.e.* inspection of gross appearance, stable pH of the perfusate, stable perfusion pressure for 20 min and bile flow >1 µL/min per g liver. The flow rate during each individual perfusion was maintained at a constant rate of 20 mL/min (S1 Table).

**Cell cultures.** Human liver sinusoidal cells (LSEC) were from Innoprot (cat. N° P10652, Barcelona, Spain). LSEC were cultured in endothelial cell medium (Innoprot) additioned with 5% fetal bovine serum, endothelial cell growth supplement (ECGS) (Innoprot) and antibiotics. HepG2 (HB-8065), THP1 (TIB-202) and HEK293T (CRL-1573) cell lines were from ATCC (Manassas, VA; USA). HepG2 cells were cultured in E-MEM supplemented with 10% FBS, 1% glutamine, 1% penicillin/streptomycin. HEK293T cells were cultured in DMEM supplemented with 10% FBS, 1% glutamine, and 1% penicillin/streptomycin. GLUTAg cells, a murine intestinal endocrine cell line, were kindly donated by Dr. D. J. Drucker, Banting and Best Diabetes Centre, University of Toronto, Toronto, Canada, and cultured in D-MEM, supplemented with 10% FBS, 1% glutamine, and 1% penicillin/streptomycin.

**RNA extraction and Real-Time PCR.** Total RNA was isolated from LSEC or tissues using the TRIzol reagent according to the manufacturer's specifications (Life Technologies). One microgram of RNA was purified from genomic DNA by DNase-I treatment (Life Technologies) and reverse-transcribed using random hexamer primers with Superscript-II (Life Technologies) in a 20-µL reaction

volume. Ten ng cDNA were amplified in a 20 µl solution containing 200 nM of each primer and 10 µl of KAPA SYBR FAST Universal qPCR Kit (KAPA BIOSYSTEMS). All reactions were performed in triplicate, and the thermal cycling conditions were as follows: 3 min at 95 °C, followed by 40 cycles of 95 °C for 15 s, 56 °C for 20 s and 72 °C for 30 s. The relative mRNA expression was calculated accordingly to the Ct method. PCR primers were designed using the software PRIMER3 (<http://frodo.wi.mit.edu/primer3/>) using published data obtained from the NCBI database. Forward and reverse primer sequences were as follows:

hGAPDH: gaaggtgaaggtcggagt and catgggtggaatca tattggaa;

hCSE: cactgtccaccacgttcaag and gtggctgctaaacctgaagc;

hCBS: tcgtgatccagagaagatg and ttggggatttcgttcttcag;

hTGR5: cactgttgc cctcctctcc and acactgctttggctgcttg;

heNOS: agtgaaggcgacaatcctgtat and agggacaccacgtcatactcat;

hET1: agggctgaagacattatggaga and cctggtttgccttaggtgttcc;

mGAPDH: ctgagtatgtcgtggagtctac and gttgggtggtgcaggatgcattg;

mpro-glucagon: tgaagacaaacgccactcac and caatgttgttccggttctctc;

mTGFb1: ttgcttcagctccacagaga and tggttgta gagggcaaggac;

mCOL1A1: acgtcctgggtgaagttggtc and cagggaagcctcttt ctct;

maSMA: tgtgctggactctggagatg and gaaggaatagccacgctcag;

mTNFa: acggcatggatctcaaagac and gtgggtgaggagcacgtagt;

mTGR5: ggcttgaactctgttatcg and gtccctcttggctcttctc;

mIL1b: tcacagcagca catcaaaa and tgcctcatcctcgaaggtc;

mCBS: agaagtgccctggctgtaaa and caggactgtcgggatgaagt;

mCSE: tgctgccaccattacgatta and gatgccaccctcc tgaagta;

meNOS: agaagagtccagcgaacagc and tgggtgctgaactgacagag;

miNOS: acgagacggatagccagaga and cacatgcaaggaagggaact;

mET1: tgccaagcagg aaaagaact and acgaaaagatgccttgatgc;

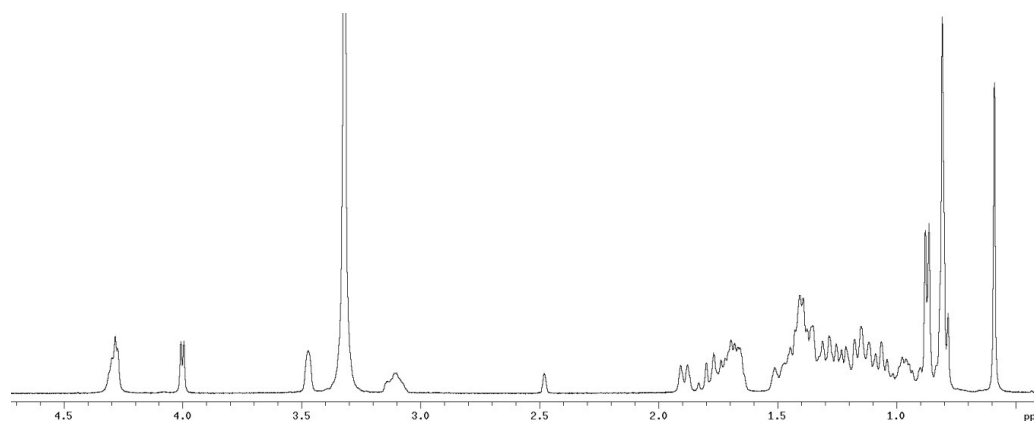
mCAV1: ttgaagatgtgattgcagaacc and tcgtagacaacaagcggtaaaa.

**CSE activity.** CSE activity was measured in liver tissues or in serum starved LSEC administered with 10 µM TLCA or BAR501 for 24 and 48 hr according to a previously published method.<sup>84</sup>

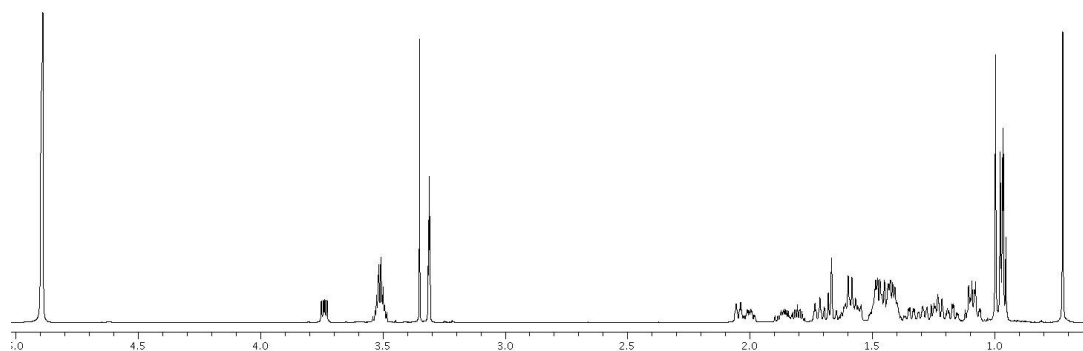
**Nitrite/Nitrate.** Hepatic nitrate/nitrite concentrations were measured by a colorimetric assay (Cayman Chemical, Ann Arbor, Michigan; USA).

**Spectroscopic Data**

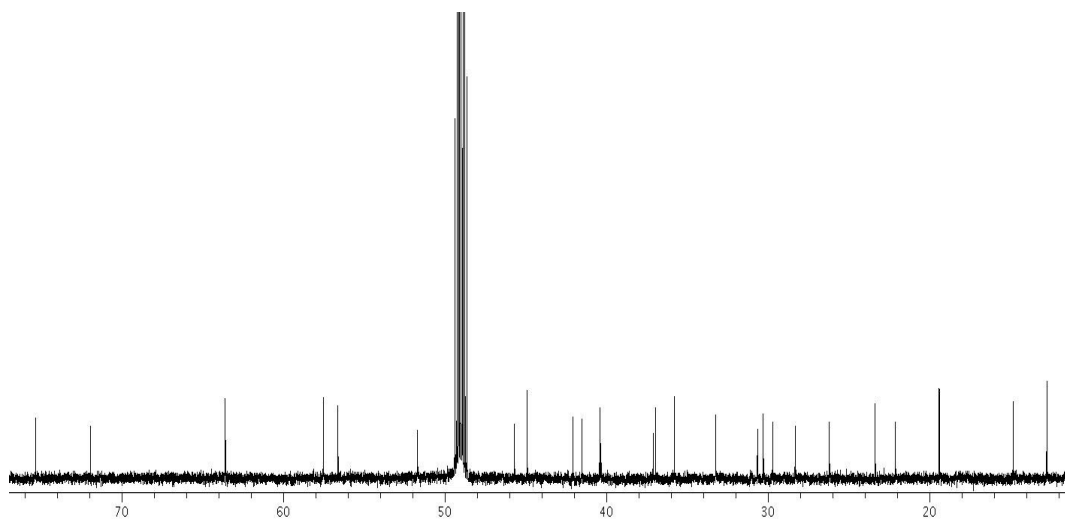
$^1\text{H}$  NMR (400 MHz, DMSO) of compound **44**



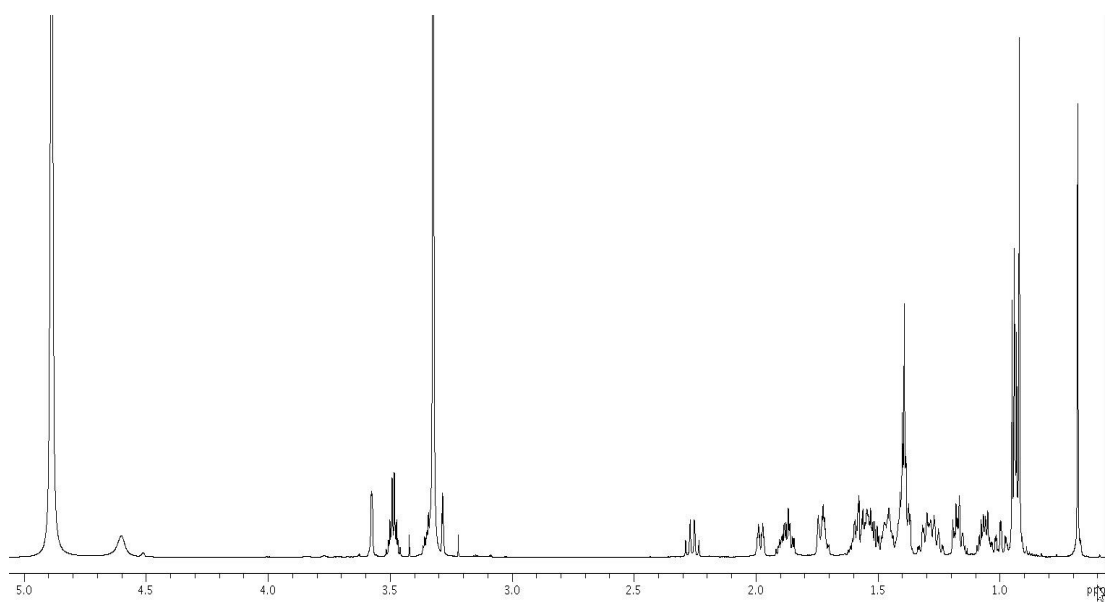
$^1\text{H}$  NMR (700 MHz,  $\text{CD}_3\text{OD}$ ) of compound **45**



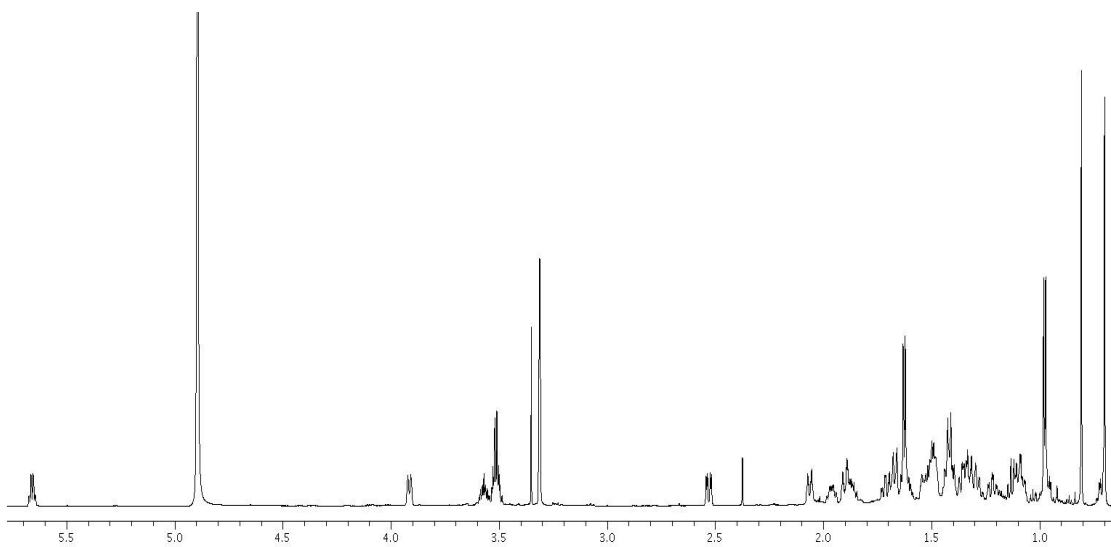
$^{13}\text{C}$  NMR (175 MHz,  $\text{CD}_3\text{OD}$ ) of compound **45**



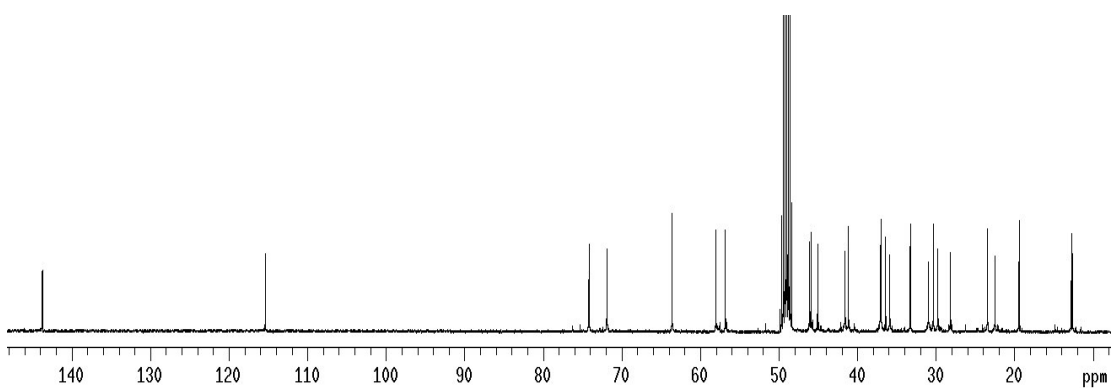
$^1\text{H}$  NMR (700 MHz,  $\text{CD}_3\text{OD}$ ) of compound **46**



$^1\text{H}$  NMR (500 MHz,  $\text{CD}_3\text{OD}$ ) of compound **47**

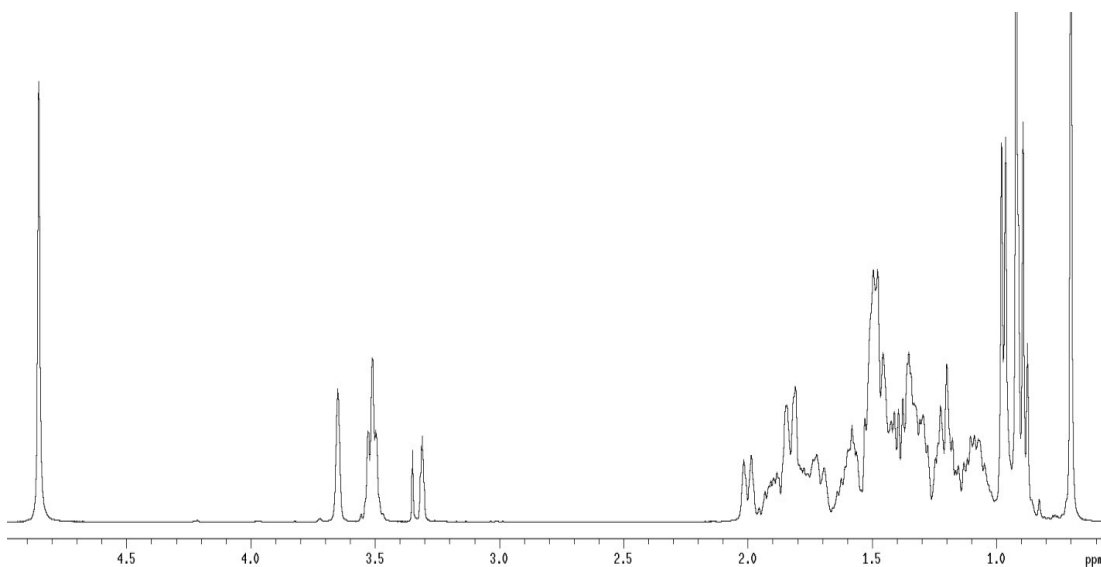


$^{13}\text{C}$  NMR (100 MHz,  $\text{CD}_3\text{OD}$ ) of compound **47**

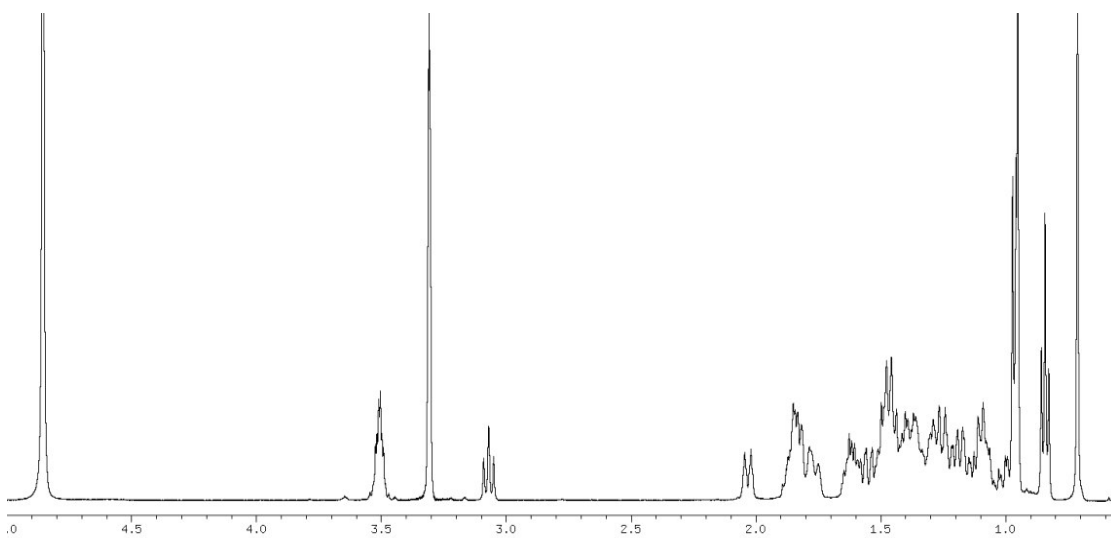




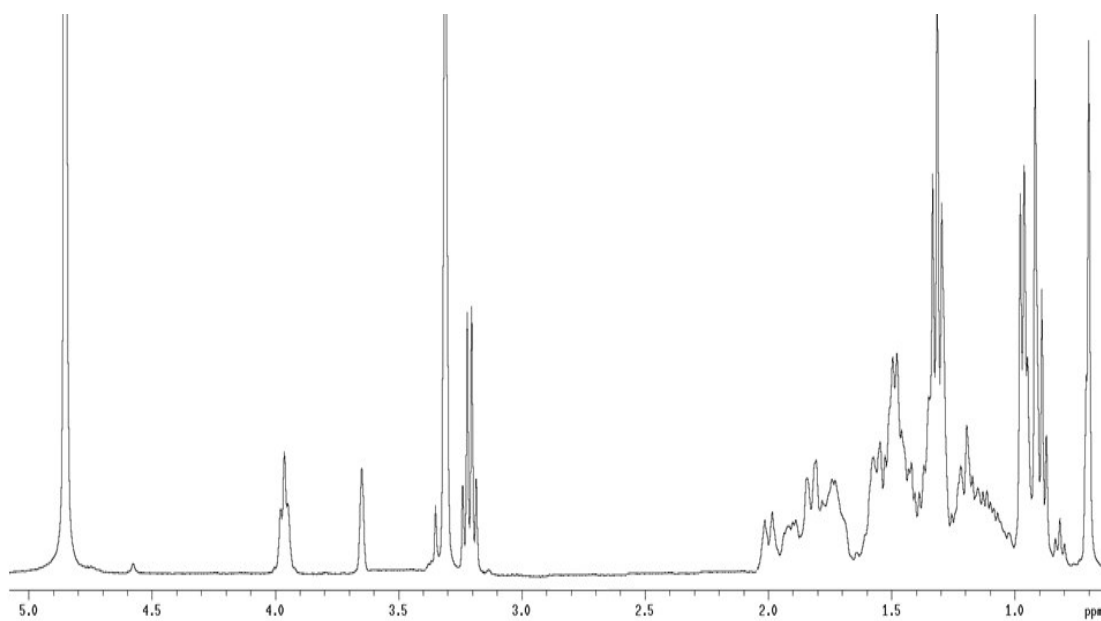
$^1\text{H}$  NMR (400 MHz,  $\text{CD}_3\text{OD}$ ) of compound **48**



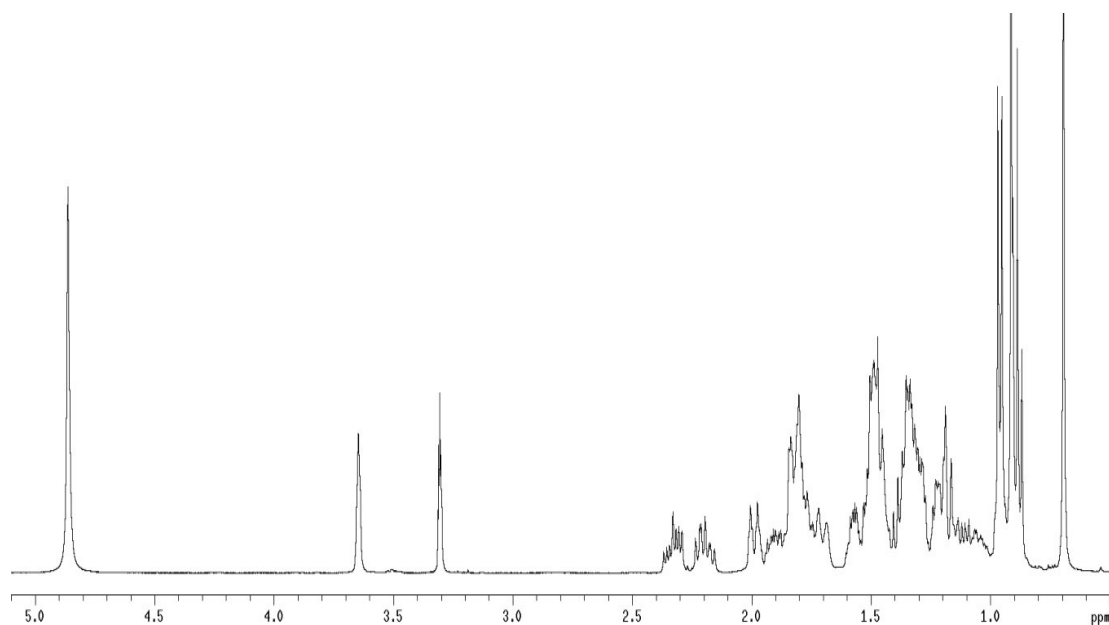
$^1\text{H}$  NMR (500 MHz,  $\text{CD}_3\text{OD}$ ) of compound **49**



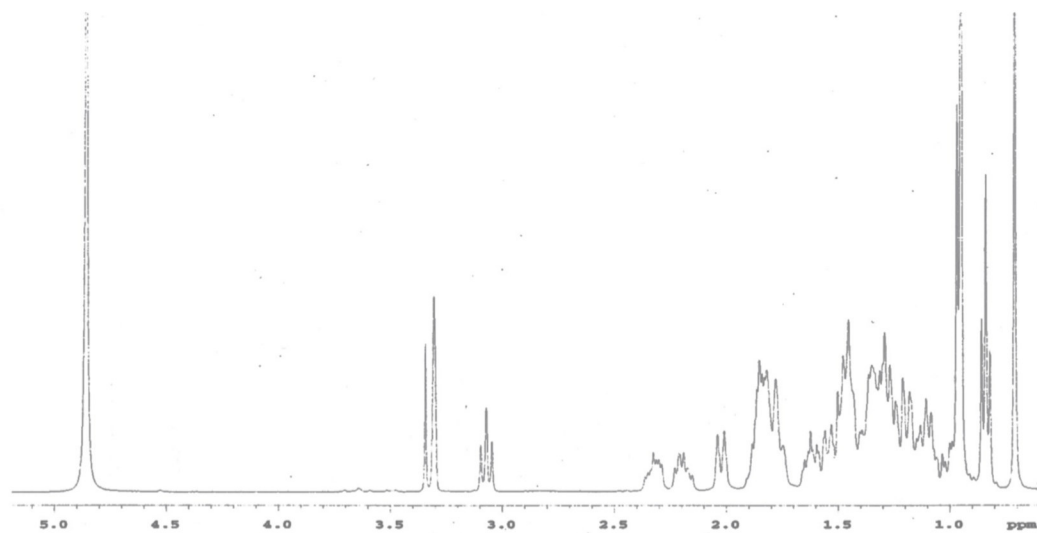
$^1\text{H}$  NMR (400 MHz,  $\text{CD}_3\text{OD}$ ) of compound **50**



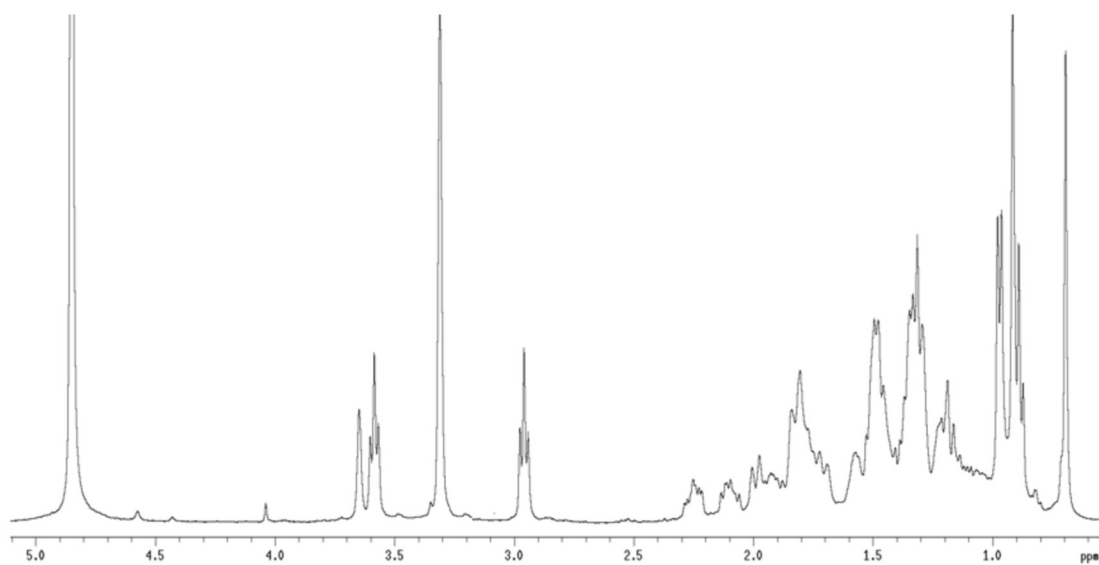
$^1\text{H}$  NMR (400 MHz,  $\text{CD}_3\text{OD}$ ) of compound **51**



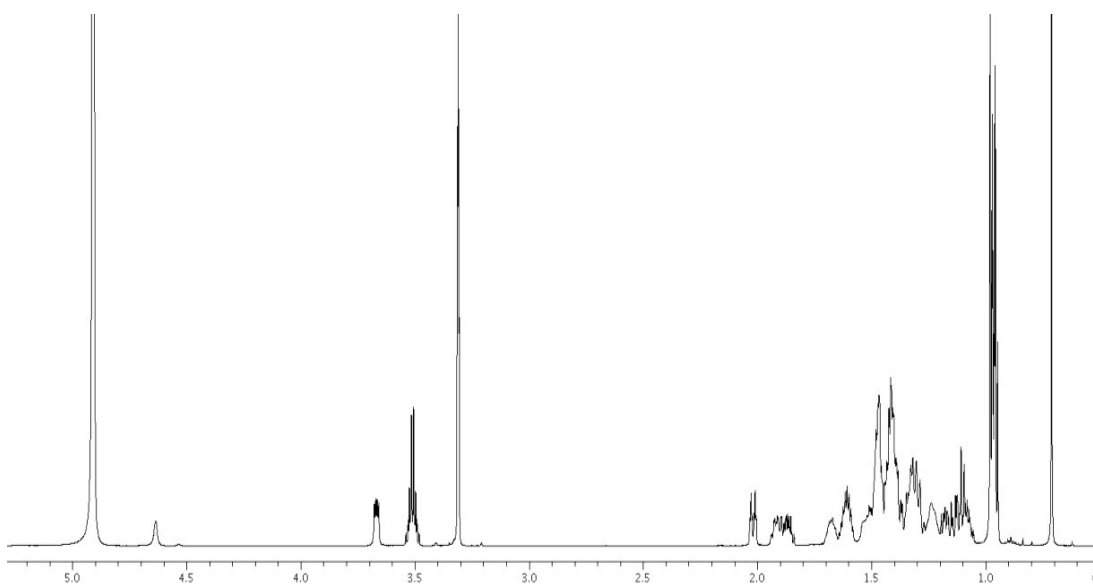
$^1\text{H}$  NMR (500 MHz,  $\text{CD}_3\text{OD}$ ) of compound **52**



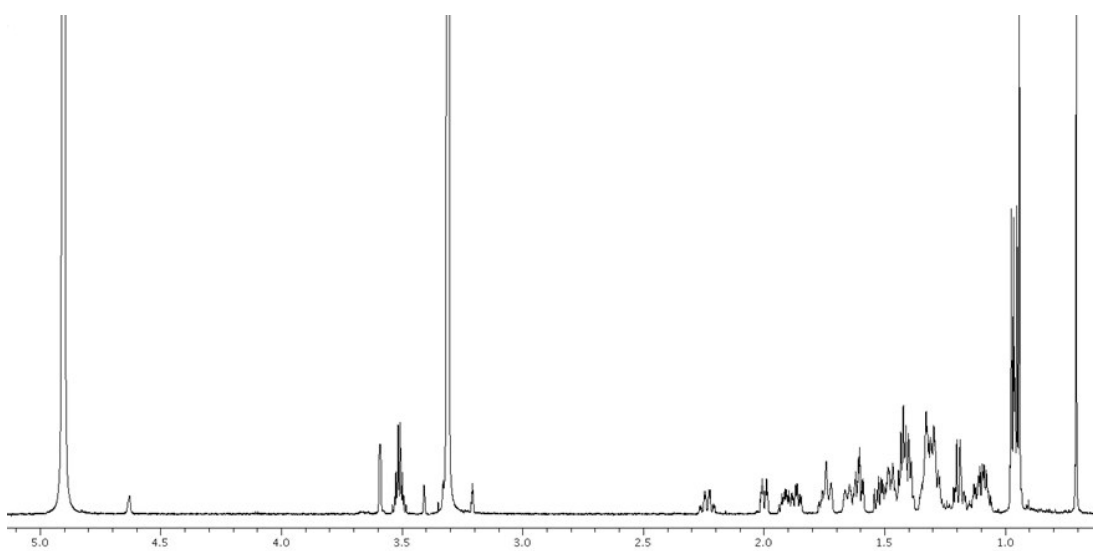
$^1\text{H}$  NMR (500 MHz,  $\text{CD}_3\text{OD}$ ) of compound **53**



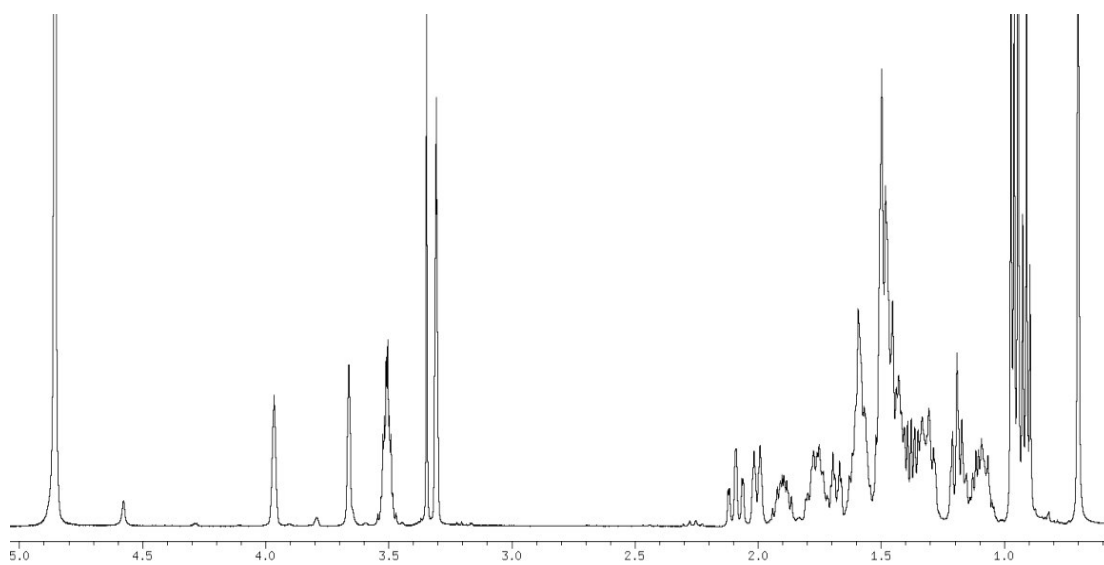
$^1\text{H}$  NMR (700 MHz,  $\text{CD}_3\text{OD}$ ) of compound **54**



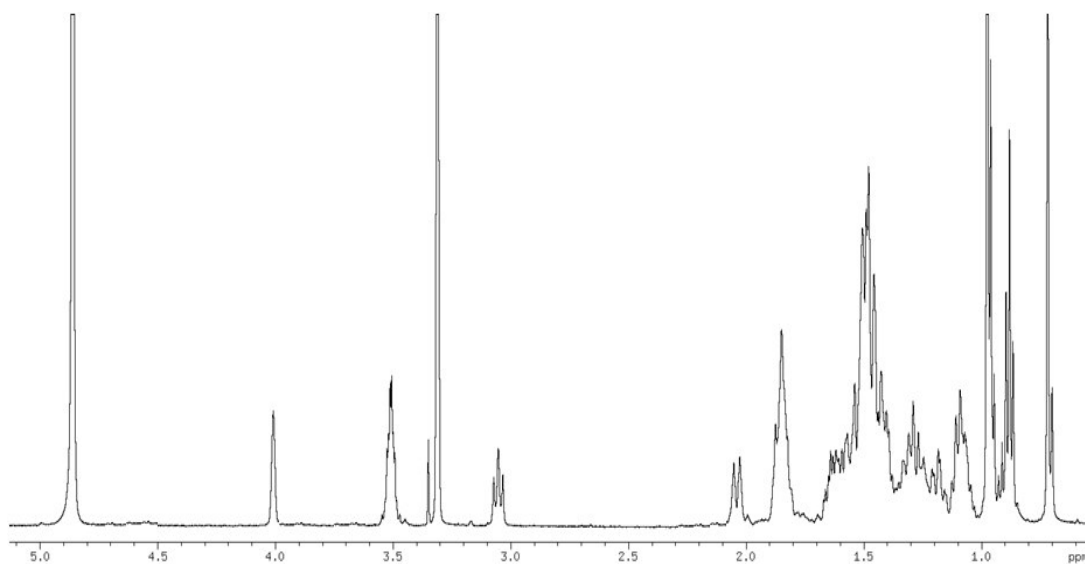
$^1\text{H}$  NMR (700 MHz,  $\text{CD}_3\text{OD}$ ) of compound **55**



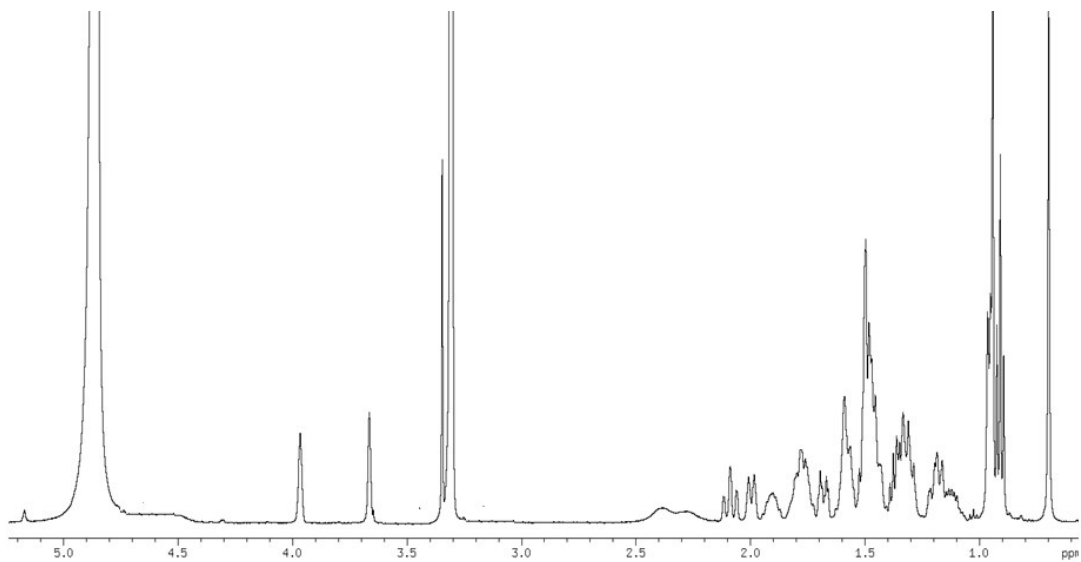
$^1\text{H}$  NMR (500 MHz,  $\text{CD}_3\text{OD}$ ) of compound **56**



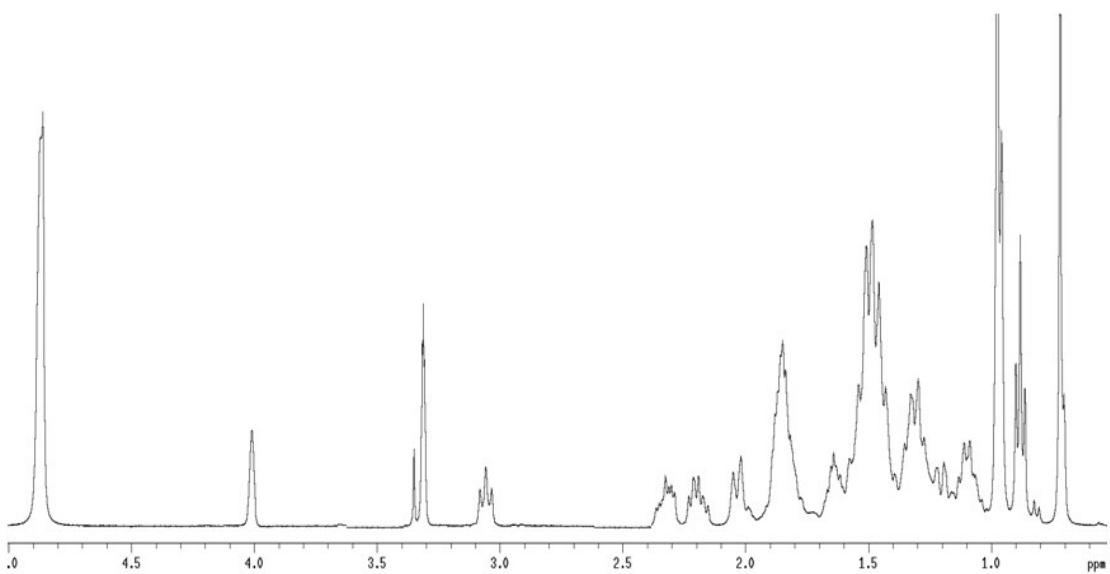
$^1\text{H}$  NMR (500 MHz,  $\text{CD}_3\text{OD}$ ) of compound **57**



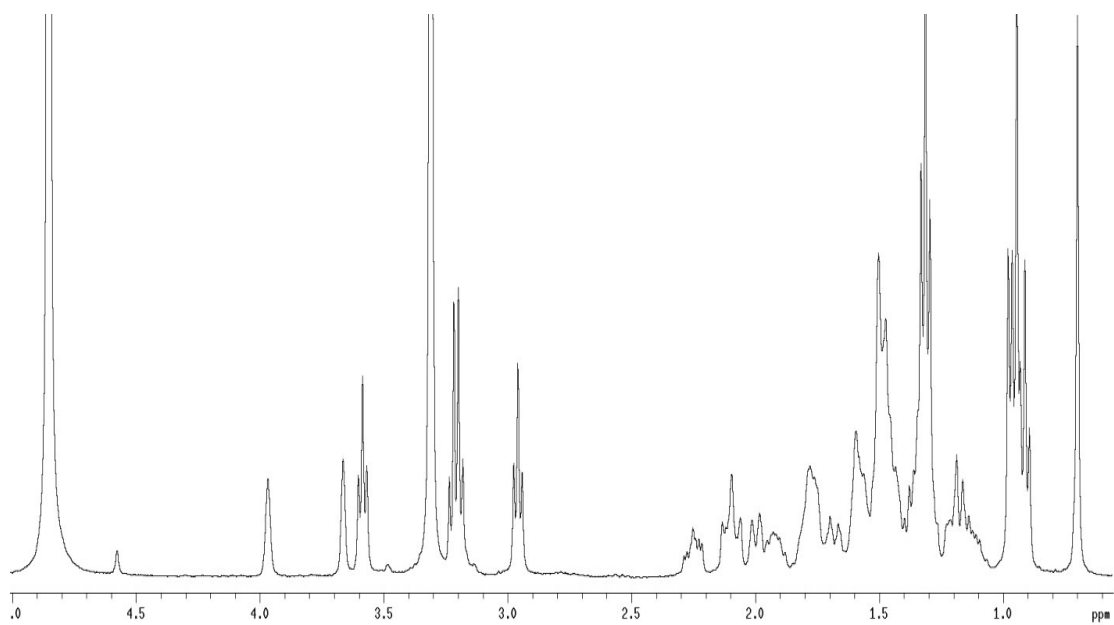
$^1\text{H}$  NMR (500 MHz,  $\text{CD}_3\text{OD}$ ) of compound **58**



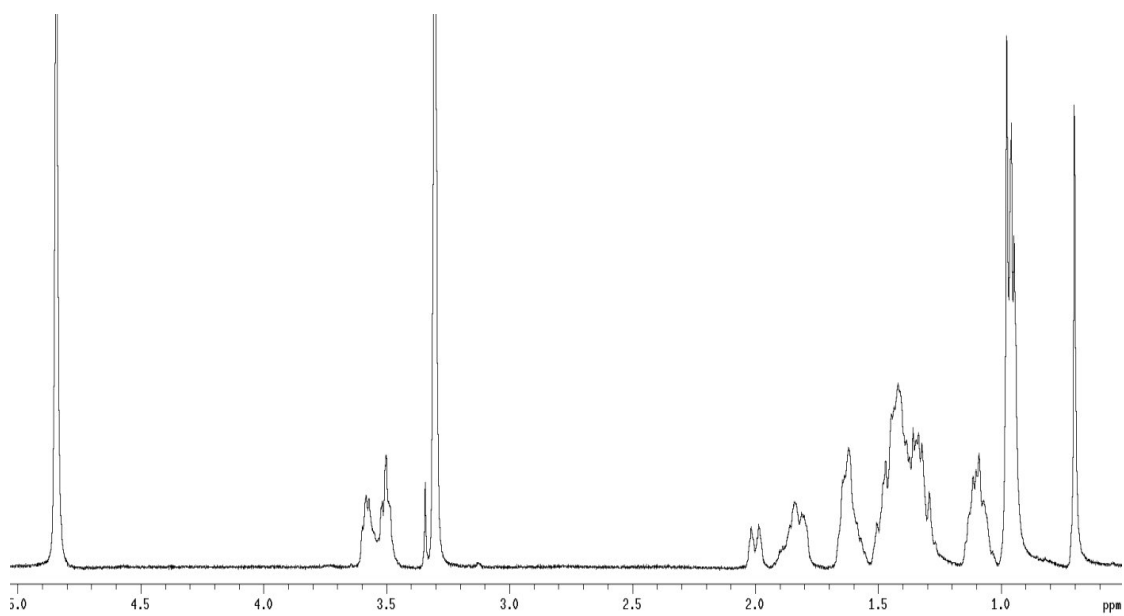
$^1\text{H}$  NMR (500 MHz,  $\text{CD}_3\text{OD}$ ) of compound **59**



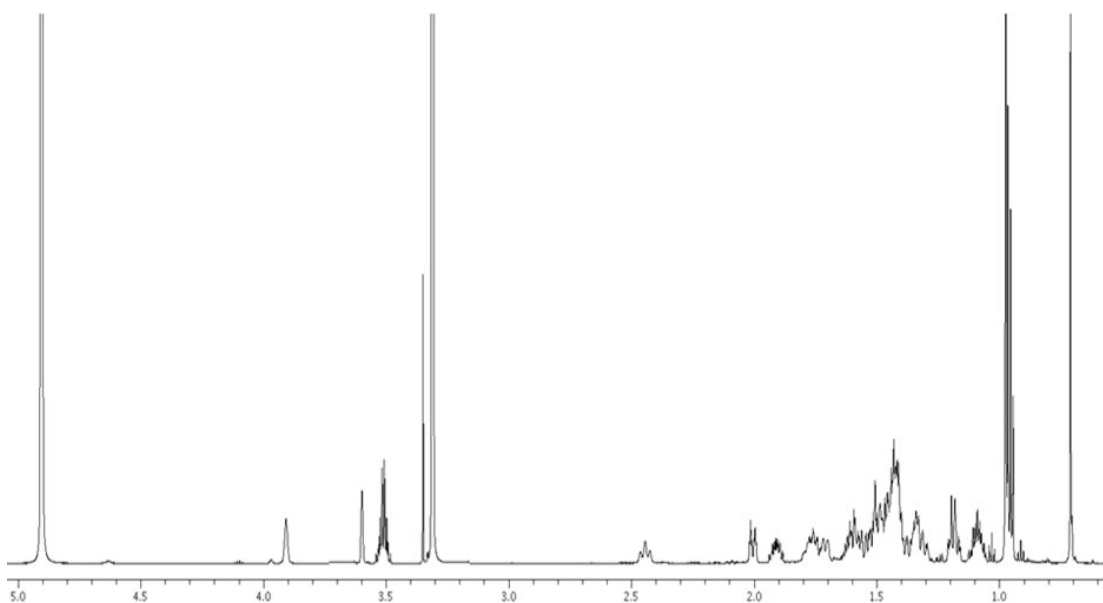
$^1\text{H}$  NMR (500 MHz,  $\text{CD}_3\text{OD}$ ) of compound **60**



$^1\text{H}$  NMR (500 MHz,  $\text{CD}_3\text{OD}$ ) of compound **61**



$^1\text{H}$  NMR (700 MHz,  $\text{CD}_3\text{OD}$ ) of compound **62**





#### IV. Experimental procedures for 6-ethylnorcholane and bis-homo-6-ethylcholane derivatives

##### Synthesis of 3 $\alpha$ ,7 $\alpha$ -dihydroxy-6-ethylnorcholane derivatives

*6 $\alpha$ -ethyl-3 $\alpha$ -hydroxy-7-keto-5 $\beta$ -cholan-24-oic acid (92)*. Compound **66** prepared as previously illustrated in Experimental section II (1.1 g, 2.5 mmol) was hydrolyzed with a methanol solution of sodium hydroxide (5%, 30 mL) in H<sub>2</sub>O (6 mL) overnight under reflux. The resulting solution was then concentrated under vacuum, diluted with water, acidified with HCl 6 M and extracted with ethyl acetate (3 x 50 mL). The collected organic phases were washed with brine, dried over Na<sub>2</sub>SO<sub>4</sub> anhydrous and evaporated under reduced pressure to give **92** in a quantitative yield (1.1 g). An analytical sample was obtained by silica gel chromatography eluting with CH<sub>2</sub>Cl<sub>2</sub>/MeOH 95:5.  $[\alpha]_D^{25} = -21.5$  ( $c = 0.35$ , CH<sub>3</sub>OH); selected <sup>1</sup>H NMR (400 MHz, CD<sub>3</sub>OD):  $\delta$  3.46 (1H, m), 2.83 (1H, dd,  $J = 13.0, 5.5$  Hz), 2.50 (1H, t,  $J = 11.2$  Hz), 2.34 (1H, m), 2.20 (1H, m), 1.22 (3H, s), 0.96 (3H, d,  $J = 6.6$  Hz), 0.81 (3H, t,  $J = 7.3$  Hz), 0.71 (3H, s); <sup>13</sup>C NMR (100 MHz, CD<sub>3</sub>OD):  $\delta$  215.5, 187.0, 71.7, 56.4, 53.3, 52.2, 51.2, 50.5, 45.4, 43.8, 40.4, 36.8, 36.6, 35.3, 32.6, 32.3, 32.0, 30.6, 29.3, 25.6, 23.9, 23.0, 20.8, 18.8, 12.5, 12.3; HRMS-ESI  $m/z$  419.3164 [M+H]<sup>+</sup>, C<sub>26</sub>H<sub>43</sub>O<sub>4</sub> requires 419.3161.

*6 $\alpha$ -ethyl-3 $\alpha$ -formyloxy-7-keto-5 $\beta$ -cholan-24-oic acid (93)*. A solution of **92** (1.0 g, 2.6 mmol) in 30 mL of 90% formic acid containing 90  $\mu$ L of 70% perchloric acid was stirred at 47-50 °C for 6 h. The temperature of the heating bath was lowered to 40 °C, then 24 mL of acetic anhydride was added over 10 min and the mixture was stirred for 10 min more. The solution was cooled to room temperature, poured into 50 mL of water and extracted with diethyl ether. The organic layers were washed with water to neutrality, dried over Na<sub>2</sub>SO<sub>4</sub>, and evaporated to give 940 mg of **93** (81%). An analytical sample was obtained by silica gel chromatography eluting with CH<sub>2</sub>Cl<sub>2</sub>/MeOH 95:5.  $[\alpha]_D^{25} = -25.9$  ( $c = 0.56$ , CH<sub>3</sub>OH); selected <sup>1</sup>H NMR (400 MHz CDCl<sub>3</sub>):  $\delta$  7.99 (1H, s), 4.79 (1H, m), 2.71 (1H, dd,  $J = 5.9, 12.8$  Hz), 1.29 (3H, s), 0.93 (3H, d,  $J = 6.3$  Hz), 0.80 (3H, t,  $J = 7.2$  Hz), 0.66 (3H, s); <sup>13</sup>C NMR (100 MHz CDCl<sub>3</sub>):  $\delta$  212.5, 180.0, 160.6, 73.2, 54.8, 51.9, 50.6, 49.9, 48.9, 43.6, 42.6, 38.9, 35.7, 35.1, 33.8, 30.9, 30.7, 30.3, 28.2, 27.6, 25.9, 24.5, 23.4, 21.8, 18.8, 12.0, 11.9; HRMS-ESI  $m/z$  447.3116 [M+H]<sup>+</sup>, C<sub>27</sub>H<sub>43</sub>O<sub>5</sub> requires 447.3110.

*6 $\alpha$ -ethyl-3 $\alpha$ -formyloxy-7-keto-24-nor-5 $\beta$ -cholan-23-nitrile (94)*. Crude **93** (930 mg, 2.1 mmol), 6.7 mL of cold trifluoroacetic acid, and 1.80 mL (15.6 mmol) of trifluoroacetic anhydride were stirred at 0-5 °C until dissolution. Sodium nitrite (435 mg, 6.30 mmol) was added in small portions. After the addition was complete, the reaction mixture was stirred first at 0-5 °C for 1 h, then at 38-40 °C for 2 h. On completion, the reaction was neutralized with NaOH 2 M, then the product was extracted with 50 mL of diethyl ether (3 x 50 mL), followed by washing with brine and dried over anhydrous Na<sub>2</sub>SO<sub>4</sub>. The ether was removed under reduced pressure to afford 860 mg of **94** in quantitative yield, that was subjected to next step without any purification.

*6 $\alpha$ -ethyl-3 $\alpha$ -hydroxy-7-keto-24-nor-5 $\beta$ -cholan-23-oic acid (95)*. Crude compound **94** (860 mg, 2.1 mmol) was refluxed with 30% KOH in *ca.* 50 mL of methanol/water 1:1. After 48 h stirring, the basic aqueous solution was neutralized with HCl 6 M. Then methanol was evaporated and the residue was extracted with AcOEt (3 x 50 mL). The combined organic layers were washed with brine, dried and evaporated to dryness to give white solid residue **95** (723 mg, 86%). An analytical sample was obtained by silica gel chromatography eluting with CH<sub>2</sub>Cl<sub>2</sub>/MeOH 95:5.  $[\alpha]_D^{25} = -25.2$  ( $c = 0.22$ , CH<sub>3</sub>OH); selected <sup>1</sup>H NMR (400 MHz CD<sub>3</sub>OD):  $\delta$  3.46 (1H, m), 2.82 (1H, dd,  $J = 6.4, 12.6$  Hz), 1.25 (3H, s), 1.25 (3H, d ovl), 0.81 (3H, t,  $J = 7.3$  Hz), 0.74 (3H, s); <sup>13</sup>C NMR (100 MHz CD<sub>3</sub>OD):  $\delta$  215.7, 177.6, 71.7, 56.3, 53.3, 51.2, 50.6, 50.5, 45.3, 43.8, 42.5, 40.4, 36.8, 35.3, 35.0, 32.6, 30.5, 29.4, 25.6, 23.9, 22.9, 20.9, 19.6, 12.5, 12.3; HRMS-ESI  $m/z$  405.3008 [M+H]<sup>+</sup>, C<sub>25</sub>H<sub>41</sub>O<sub>4</sub> requires 405.3005.

*6 $\alpha$ -ethyl-3 $\alpha$ ,7 $\alpha$ -dihydroxy-24-nor-5 $\beta$ -cholan-23-oic acid (NorECDCA, 76)*. To a solution of **95** (500 x 10<sup>-3</sup> g, 1.20 mmol) in dry THF (30 mL), at 0 °C dry methanol (360  $\mu$ L, 8.4 mmol) and LiBH<sub>4</sub> (4.2 mL, 2M in THF, 8.4 mmol) was added. The resulting mixture was stirred for 1 h at 0 °C. The mixture was quenched by addition of 1.0 M NaOH (2.4 mL) and then ethyl acetate. The organic phase was washed with water, dried (Na<sub>2</sub>SO<sub>4</sub>) and concentrated. Purification by silica gel (CH<sub>2</sub>Cl<sub>2</sub>:MeOH 9:1) gave **76** as a white solid (400 mg, 82%). An analytical sample was obtained by HPLC on a Nucleodur 100-5 C18 (5  $\mu$ m; 4.6 mm i.d. x 250 mm) with MeOH/H<sub>2</sub>O (88:12) as eluent (flow rate 1 mL/min,  $t_R = 9.6$  min);  $[\alpha]_D^{25} = +3.3$  ( $c = 1.04$ , CH<sub>3</sub>OH); selected <sup>1</sup>H NMR (500

MHz, CD<sub>3</sub>OD):  $\delta$  3.66 (1H, s), 3.32 (1H, ovl), 2.35 (1H, dd,  $J = 13.4, 3.3$  Hz), 1.00 (3H, d,  $J = 6.4$  Hz), 0.92 (3H, s), 0.90 (3H, t,  $J = 7.1$  Hz), 0.74 (3H, s); <sup>13</sup>C NMR (125 MHz, CD<sub>3</sub>OD):  $\delta$  178.0, 72.9, 70.9, 57.6, 51.4, 46.7, 43.7, 43.6, 42.8, 41.2, 40.8, 36.8, 36.0, 34.8, 34.4, 34.0, 31.0, 29.1, 24.3, 23.4, 23.3, 21.8, 19.3, 12.0, 11.8; HR ESIMS  $m/z$  405.3011 [M-H]<sup>-</sup>, C<sub>25</sub>H<sub>41</sub>O<sub>4</sub> requires 405.3005.

*6 $\alpha$ -ethyl-3 $\alpha$ , 7 $\alpha$ -dihydroxy-24-nor-5 $\beta$ -cholan-23-ol* (NorECDCOH, **77**).

Compound **95** (200 mg, 0.5 mmol) was dissolved in 50 mL of dry methanol and treated with *p*-toluenesulfonic acid in catalytic amount. The solution was left to stand at room temperature for 2 h. The mixture was quenched by addition until the neutrality of NaHCO<sub>3</sub> saturated solution. Most of the solvent was evaporated, and the residue was extracted with EtOAc. To a solution of crude solid (220 mg, quantitative yield) in dry THF (10 mL), at 0 °C dry methanol (158  $\mu$ L, 3.90 mmol) and LiBH<sub>4</sub> (1.90 mL, 2M in THF, 3.90 mmol) was added. The resulting mixture was stirred for 1 h at 0 °C. The mixture was quenched by addition of 1.0 M NaOH (1.1 mL) and then ethyl acetate. The organic phase was washed with water, dried (Na<sub>2</sub>SO<sub>4</sub>) and concentrated. Silica gel chromatography eluting with hexane/EtOAc 6:4 afforded compound **77** (191 mg, 98% over two steps). An analytical sample was obtained by on a Nucleodur 100-5 C18 (5  $\mu$ m; 4.6 mm i.d. x 250 mm) with MeOH/H<sub>2</sub>O (88:12) as eluent (flow rate 1 mL/min,  $t_R$ =10.8 min);  $[\alpha]_D^{25} = +4.4$  ( $c = 1.42$ , CH<sub>3</sub>OH); <sup>1</sup>H and <sup>13</sup>C NMR spectroscopic data in CD<sub>3</sub>OD given in Tables 1 and 2; HR ESIMS  $m/z$  393.3374 [M+H]<sup>+</sup>, C<sub>25</sub>H<sub>45</sub>O<sub>3</sub> requires 393.3369.

*6 $\alpha$ -ethyl-3 $\alpha$ , 7 $\alpha$ -dihydroxy-24-nor-5 $\beta$ -cholan-23-nitrile* (NorECDCN, **78**). To a solution of **94** (200 mg, 0.5 mmol) in dry THF (10 mL), at 0 °C dry methanol (142  $\mu$ L, 3.50 mmol) and LiBH<sub>4</sub> (1.80 mL, 2M in THF, 3.50 mmol) was added. The resulting mixture was stirred for 2 h at 0 °C. The mixture was quenched by addition of 1 M NaOH (1 mL) and then ethyl acetate. The organic phase was washed with water, dried (Na<sub>2</sub>SO<sub>4</sub>) and concentrated. HPLC purification on a Nucleodur 100-5 C18 (5  $\mu$ m; 10 mm i.d. x 250 mm) with MeOH/H<sub>2</sub>O (88:12) as eluent (flow rate 3 mL/min), gave 805 mg of **78** (79%,  $t_R$ =15.2 min).  $[\alpha]_D^{25} = -13.4$  ( $c = 0.47$ , CH<sub>3</sub>OH); selected <sup>1</sup>H NMR (700 MHz, CD<sub>3</sub>OD):  $\delta$  3.66 (1H, br s), 3.31 (1H, ovl), 2.46 (1H, dd,  $J = 3.8, 16.9$  Hz), 2.34 (1H, dd,  $J = 7.4, 16.9$  Hz) 1.16 (3H, d,  $J = 6.5$  Hz), 0.91 (3H, t,  $J = 7.5$  Hz), 0.92 (3H, s), 0.73 (3H, s); <sup>13</sup>C NMR (175

MHz, CD<sub>3</sub>OD):  $\delta$  120.3, 72.9, 70.9, 56.1, 51.5, 46.7, 43.4, 42.9, 41.4, 40.2, 36.5, 36.2, 34.3 (2C), 34.2, 30.7, 29.2, 24.9, 24.4, 23.4, 23.3, 21.9, 18.5, 12.1, 11.6; HR ESIMS  $m/z$  388.3221 [M+H]<sup>+</sup>, C<sub>25</sub>H<sub>42</sub>NO<sub>2</sub> requires 388.3216.

**Synthesis of 3 $\alpha$ -hydroxy-, 3-deoxy-, 3 $\beta$ -hydroxy-6-ethylnorcholane and bis-homo-6-ethylcholane derivatives.**

*Methyl 3 $\alpha$ -hydroxy-7-keto-24-nor-5 $\beta$ -cholan-23-oate (98).* 7-KLCA (2.0 g, 5.1 mmol) was subjected to Beckmann degradation at C24 and methylation at C-23 furnishing **98** in 66% yield. The Beckmann degradation was previously described for the synthesis of 3 $\alpha$ ,7 $\alpha$ -dihydroxy-6-ethylnorcholane derivatives.

*Methyl (E)-3 $\alpha$ -acetoxy-6-ethylidene-7-keto-24-nor-5 $\beta$ -cholan-23-oate (99).* At the solution of the methyl ester **98** (1.32 g, 3.38 mmol) in dry pyridine (10 mL), an excess of acetic anhydride (3.2 mL, 34 mmol) was added. After 2 h, the pyridine was concentrated under vacuum. The residue was poured into cold water (100 mL) and extracted with ethyl acetate (3  $\times$  50 mL). The combined organic phases were dried (Na<sub>2</sub>SO<sub>4</sub>) and concentrated to give a residue that was further purified by flash chromatography on silica gel using hexane/ethyl acetate 95:5 and 0.5% of triethylamine as eluent. To a solution of diisopropylamine (7.2 mL, 51 mmol) in dry THF (50 mL) was added dropwise a solution of *n*-butyllithium (19.0 mL, 2.5 M in hexane, 47.6 mmol) at -78 °C. After 30 min, trimethylchlorosilane (8.20 mL, 64.6 mmol) was added. After additional 30 min, a solution of residue (1.46 g, 3.40 mmol) in dry THF (10 mL) was added. The reaction was stirred at -78 °C for 45 min and then triethylamine (16.6 mL, 119 mmol) was added. After 1 h, the reaction mixture was allowed to warm to -20 °C, treated with aqueous saturated solution of NaHCO<sub>3</sub> (100 mL) and brought up to room temperature in 2 h. The aqueous phase was extracted with ethyl acetate (3 x 50 mL). The combined organic phases were washed then with saturated solution of NaHCO<sub>3</sub>, water and brine. After drying, the residue was evaporated under *vacuum* to give 2 g of residue, that was diluted in dry CH<sub>2</sub>Cl<sub>2</sub> (20 mL) and cooled at -78 °C. At this stirred solution acetaldehyde (960  $\mu$ L, 17.0 mmol) and BF<sub>3</sub>·OEt<sub>2</sub> (4.2 mL, 34 mmol) were added dropwise. The reaction mixture was stirred for 1 h at -60 °C and allowed to warm to room temperature. The mixture was quenched with saturated aqueous solution of NaHCO<sub>3</sub> and extracted with CH<sub>2</sub>Cl<sub>2</sub>. The combined organic phases were washed with brine, dried over anhydrous Na<sub>2</sub>SO<sub>4</sub> and

concentrated under *vacuum*. Purification by silica gel (hexane-ethyl acetate 99:1 and 0.5% TEA) gave compound **99** (940 mg, 60% over three steps). NMR analysis demonstrated a diastomeric ratio *E/Z* >95%. The *E* configuration at the exocyclic double bond was established by dipolar coupling H<sub>3</sub>-25 ( $\delta$  1.67)/H-5 ( $\delta$  2.61) in NOESY spectrum (400 MHz, mixing time 400 ms).  $[\alpha]_D^{25} = -3.31$  ( $c = 3.25$ , CH<sub>3</sub>OH); selected <sup>1</sup>H NMR (400 MHz, CDCl<sub>3</sub>):  $\delta$  6.17 (1H, q,  $J = 7.2$  Hz, H-24), 4.75 (1H, m, H-3), 3.64 (3H, s, COOCH<sub>3</sub>), 2.61 (1H, dd,  $J = 13.1, 4.0$  Hz, H-5), 1.98 (3H, s, COCH<sub>3</sub>), 1.67 (3H, d,  $J = 7.2$  Hz, H<sub>3</sub>-25), 1.00 (3H, s, H<sub>3</sub>-19), 0.97 (3H, d,  $J = 6.8$  Hz, H<sub>3</sub>-21), 0.67 (3H, s, H<sub>3</sub>-18); <sup>13</sup>C NMR (100 MHz, CDCl<sub>3</sub>):  $\delta$  204.5, 174.2, 170.5, 143.0, 130.6, 72.5, 54.7, 51.4, 50.7, 48.6, 45.3, 43.7, 41.5, 39.1, 38.8, 34.6, 34.2, 33.6, 33.4, 28.5, 25.9 (2C), 22.8, 21.3 (2C), 19.7, 12.7, 12.1; HR ESIMS  $m/z$  459.3107 [M+H]<sup>+</sup>, C<sub>28</sub>H<sub>43</sub>O<sub>5</sub> requires 459.3110.

*Methyl 3 $\alpha$ -acetoxy-6 $\beta$ -ethyl-7-keto-24-nor-5 $\beta$ -cholan-23-oate (100)*. A solution of **99** (600 x 10<sup>-3</sup> g, 1.30 mmol) in THF dry/MeOH dry (100 mL, 1:1 v/v) was hydrogenated in presence of Pd(OH)<sub>2</sub> 20% wt on activated carbon (100 mg) Degussa type. The mixture was transferred to a standard Parr apparatus and flushed with nitrogen and hydrogen several times. The apparatus was shacked under 50 psi of H<sub>2</sub>. The reaction was stirred at room temperature for 12 h. The catalyst was filtered through Celite, and the recovered filtrate was concentrated under vacuum to give **100** (600 mg, quantitative yield). The  $\beta$ -configuration of ethyl group at C-6 was determined by dipolar couplings H<sub>3</sub>-25 ( $\delta$  0.83)/ H<sub>3</sub>-19 ( $\delta$  1.22) in NOESY spectrum (400 MHz, mixing time 400 ms).  $[\alpha]_D^{25} = +10.4$  ( $c = 0.39$ , CH<sub>3</sub>OH); selected <sup>1</sup>H NMR (400 MHz, CDCl<sub>3</sub>):  $\delta$  4.65 (1H, m, H-3), 3.67 (3H, s, COOCH<sub>3</sub>), 2.60 (1H, t,  $J = 11.2$  Hz, H-8), 2.43 (1H, dd,  $J = 14.2, 2.6$  Hz, H-22a), 1.98 (3H, s, COCH<sub>3</sub>), 1.88 (1H, m ovl, H-6), 1.22 (3H, s, H<sub>3</sub>-19), 0.98 (3H, d,  $J = 6.4$  Hz, H<sub>3</sub>-21), 0.83 (3H, t,  $J = 7.0$  Hz, H<sub>3</sub>-25), 0.70 (3H, s, H<sub>3</sub>-18); <sup>13</sup>C NMR (100 MHz, CDCl<sub>3</sub>):  $\delta$  215.3, 174.0, 170.5, 72.8, 61.9, 55.0, 51.4, 49.2, 48.7, 45.5, 42.9, 42.6, 41.4, 38.7 (2C), 35.6, 35.3, 34.9, 28.3 (2C), 26.5, 25.9, 24.8, 21.4, 21.3, 19.6, 13.0, 12.1; HR ESIMS  $m/z$  461.3265 [M+H]<sup>+</sup>, C<sub>28</sub>H<sub>45</sub>O<sub>5</sub> requires 461.3267.

*6 $\beta$ -ethyl-3 $\alpha$ ,7 $\beta$ -hydroxy-24-nor-5 $\beta$ -cholan-23-ol (79)* and *6 $\beta$ -ethyl-3 $\alpha$ ,7 $\alpha$ -hydroxy-24-nor-5 $\beta$ -cholan-23-ol (81)*. A methanol solution of compound **100**

(100 mg, 0.2 mmol), a large excess of NaBH<sub>4</sub> was added at 0 °C. The mixture was left at room temperature for 10 h and then water and MeOH was added dropwise during a period of 15 min at 0 °C with effervescence being observed. Then after evaporation of the solvents, the residue was diluted with water and extracted with ethyl acetate (3 x 50 mL). The combined extract was washed with brine, dried with Na<sub>2</sub>SO<sub>4</sub>, and evaporated to give 90 mg of a crude residue that was subjected to the next step without further purification. To a solution of crude residue (90.0 mg, 0.214 mmol) in dry THF (15 mL), at 0 °C dry methanol (60.0 μL, 1.49 mmol) and LiBH<sub>4</sub> (749 μL, 2 M in THF, 1.49 mmol) were added. The resulting mixture was stirred for 2 h at 0 °C. The mixture was quenched by addition of 1.0 M NaOH (0.43 mL) and then ethyl acetate. The organic phase was washed with water, dried (Na<sub>2</sub>SO<sub>4</sub>) and concentrated. HPLC purification on a Nucleodur 100-5 C18 (5 μm; 10 mm i.d. x 250 mm) with MeOH/H<sub>2</sub>O (86:14) as eluent (flow rate 3 mL/min), gave 47 mg of **79** (54%, *t<sub>R</sub>*= 11 min) and 20 mg of **81** (23%, *t<sub>R</sub>*= 15 min).

*6β-ethyl-3α,7β-hydroxy-24-nor-5β-cholan-23-ol (79)*.  $[\alpha]_D^{25} = +11.57$  (*c* = 0.14, CH<sub>3</sub>OH); selected <sup>1</sup>H NMR (400 MHz, CD<sub>3</sub>OD): δ 3.73 (1H, dd, *J* = 10.5, 5.5 Hz, H-7), 3.61 (1H, m, H-23a), 3.51 (1H, m, ovl, H-23b), 3.51 (1H, m, ovl, H-3), 0.98 (3H, d, ovl, H<sub>3</sub>-21), 0.97 (3H, s, H<sub>3</sub>-19), 0.96 (3H, t, ovl, H<sub>3</sub>-25), 0.70 (3H, s, H<sub>3</sub>-18); <sup>13</sup>C NMR (100 MHz, CD<sub>3</sub>OD): δ 75.2, 71.8, 60.8, 57.5, 56.6, 51.5, 45.5, 44.8, 42.0, 41.4, 40.7, 40.3, 39.9, 36.9, 36.0, 34.2, 30.5, 29.6, 28.3, 26.2, 23.4, 22.0, 19.4, 14.7, 12.9; HR ESIMS *m/z* 393.3365 [M+H]<sup>+</sup>, C<sub>25</sub>H<sub>45</sub>O<sub>3</sub> requires 393.3369.

*6β-ethyl-3α,7α-hydroxy-24-nor-5β-cholan-23-ol (81)*.  $[\alpha]_D^{25} = +9.16$  (*c* = 0.62, CH<sub>3</sub>OH); selected <sup>1</sup>H NMR (400 MHz, CD<sub>3</sub>OD): δ 3.63 (1H, m, H-23a), 3.60 (1H, m, H-7), 3.55 (1H, m, H-23b), 3.37 (1H, m, H-3), 2.30 (1H, q, *J* = 12.5 Hz, H-4a), 0.97 (3H, d, *J* = 6.6 Hz, H<sub>3</sub>-21), 0.95 (3H, s, H<sub>3</sub>-19), 0.95 (3H, t, *J* = 7.0 Hz, H<sub>3</sub>-25), 0.72 (3H, s, H<sub>3</sub>-18); <sup>13</sup>C NMR (100 MHz, CD<sub>3</sub>OD): δ 72.8, 72.7, 60.8, 57.9, 52.7, 51.4, 47.5, 43.7, 42.3, 41.0, 39.9, 37.5, 37.3, 36.7, 34.2, 33.3, 31.0, 29.6, 29.4, 26.2, 24.8, 21.6, 19.3, 14.5, 12.1; HR ESIMS *m/z* 393.3367 [M+H]<sup>+</sup>, C<sub>25</sub>H<sub>45</sub>O<sub>3</sub> requires 393.3369.

*6β-ethyl-3α,7β-hydroxy-24-nor-5β-cholan-23-oic acid (80)*. To a methanol solution of compound **100** (200 x 10<sup>-3</sup> g, 0.440 mmol), a large excess of NaBH<sub>4</sub>

was added at 0 °C. The mixture was left at room temperature for 2 h and then water and MeOH were added dropwise during a period of 15 min at 0 °C with effervescence being observed. After evaporation of the solvents, the residue was diluted with water and extracted with ethyl acetate (3 x 50 mL). The combined extract was washed with brine, dried with Na<sub>2</sub>SO<sub>4</sub> and evaporated to give 216 mg of **101** that was subjected to the next step without further purification. Compound **101** (216 mg, 0.520 mmol) was hydrolyzed with NaOH (207 mg, 5.17 mmol) in a solution of MeOH:H<sub>2</sub>O 1:1 v/v (20 mL). The resulting solution was then concentrated under vacuum, diluted with water, acidified with HCl 6 M and extracted with ethyl acetate (3 x 50 mL). The collected organic phases were washed with brine, dried over Na<sub>2</sub>SO<sub>4</sub> anhydrous and evaporated under reduced pressure. HPLC purification on a Nucleodur 100-5 C18 (5 μm; 10 mm i.d. x 250 mm) with MeOH/H<sub>2</sub>O (86:14) as eluent (flow rate 3 mL/min), gave compound **80** (147 mg, 0.360 mmol) as a white solid (82%, *t*<sub>R</sub> = 9 min). [ $\alpha$ ]<sub>D</sub><sup>25</sup> = +23.7 (*c* = 0.14, CH<sub>3</sub>OH); selected <sup>1</sup>H NMR (400 MHz, CD<sub>3</sub>OD):  $\delta$  3.74 (1H, dd, *J* = 10.1, 5.7 Hz, H-7), 3.50 (1H, m, ovl, H-3), 2.42 (1H, d, *J* = 11.0 Hz, H-22a), 1.02 (3H, d, ovl, H<sub>3</sub>-21), 1.00 (3H, s, H<sub>3</sub>-19), 0.96 (3H, t, *J* = 7.0 Hz, H<sub>3</sub>-25), 0.76 (3H, s, H<sub>3</sub>-18); HR ESIMS *m/z* 405.3001 [M-H]<sup>-</sup>, C<sub>25</sub>H<sub>41</sub>O<sub>4</sub> requires 405.3005.

*6-ethylidene-3 $\alpha$ ,7 $\beta$ -dihydroxy-24-nor-5 $\beta$ -cholan-23-ol* (**82**). Compound **99** (100 mg, 0.2 mmol) was subjected to the same operative condition previously described for compounds **79** and **81**. HPLC purification on a Nucleodur 100-5 C18 (5 μm; 10 mm i.d. x 250 mm) with MeOH/H<sub>2</sub>O (86:14) as eluent (flow rate 3 mL/min), gave 73 mg of compound **82** (*t*<sub>R</sub> = 8 min, 85% over two steps). [ $\alpha$ ]<sub>D</sub><sup>25</sup> = +20.6 (*c* = 2.43, CH<sub>3</sub>OH); selected <sup>1</sup>H NMR (400 MHz, CD<sub>3</sub>OD):  $\delta$  5.66 (1H, q, *J* = 6.8 Hz, H-24), 3.92 (1H, d, *J* = 9.8 Hz, H-7), 3.60 (1H, m, H-23a), 3.56 (1H, m, H-3), 3.55 (1H, m, H-23b), 2.52 (1H, dd, *J* = 3.7, 13.2 Hz, H-5), 1.63 (3H, d, *J* = 6.8 Hz, H<sub>3</sub>-25), 0.98 (3H, d, *J* = 6.5 Hz, H<sub>3</sub>-21), 0.95 (3H, s, H<sub>3</sub>-19), 0.71 (3H, s, H<sub>3</sub>-18); <sup>13</sup>C NMR (100 MHz, CD<sub>3</sub>OD):  $\delta$  143.7, 115.4, 74.1, 71.8, 60.8, 58.0, 57.1, 46.1, 45.9, 45.1, 41.6, 41.1, 39.9, 37.0, 36.4, 35.8, 34.1, 30.9, 29.8, 28.1, 23.5, 22.5, 19.5, 12.7, 12.6; HR ESIMS *m/z* 391.3208 [M+H]<sup>+</sup>, C<sub>25</sub>H<sub>43</sub>O<sub>3</sub> requires 391.3212.

*6 $\alpha$ -ethyl-3 $\alpha$ ,7 $\beta$ -dihydroxy-24-nor-5 $\beta$ -cholan-23-ol (83)*. A solution of **82** (30.0 mg, 0.0760 mmol) in THF dry/MeOH dry (5 mL, 1:1 v/v) was hydrogenated in presence of Pd(OH)<sub>2</sub> 20% wt on activated carbon (10 mg) Degussa type. The reaction was stirred at room temperature for 12 h. The catalyst was filtered through Celite, and the recovered filtrate was concentrated under vacuum to give **83** (30 mg, quantitative yield).  $[\alpha]_D^{25} = -3.3$  ( $c = 0.10$ , CH<sub>3</sub>OH); selected <sup>1</sup>H NMR (400 MHz, CD<sub>3</sub>OD):  $\delta$  3.62 (1H, m, H-23a), 3.54 (1H, m, H-23b), 3.45 (1H, m, H-3), 3.08 (1H, t,  $J = 9.8$  Hz, H-7), 0.97 (3H, d,  $J = 6.5$  Hz, H<sub>3</sub>-21), 0.95 (3H, s, H<sub>3</sub>-19), 0.86 (3H, t,  $J = 7.4$  Hz, H<sub>3</sub>-25), 0.73 (3H, s, H<sub>3</sub>-18); <sup>13</sup>C NMR (100 MHz, CD<sub>3</sub>OD):  $\delta$  76.4, 72.5, 60.8, 57.9, 57.2, 46.2, 45.1, 44.7, 41.8, 41.2, 40.0, 39.8, 36.5, 35.6, 34.2, 31.2, 30.9, 29.9, 27.9, 24.1, 22.7, 22.0, 19.5, 12.7, 11.7; HR ESIMS  $m/z$  393.3365 [M+H]<sup>+</sup>, C<sub>25</sub>H<sub>45</sub>O<sub>3</sub> requires 393.3369.

*Methyl 3 $\alpha$ -toxyloxy-6 $\alpha$ -ethyl-7-keto-24-nor-5 $\beta$ -cholan-23-oate (102)*. Compound **100** (300 x 10<sup>-3</sup> g, 0.650 mmol) was treated with 0.5 M MeONa (13 mL) in dry methanol and stirred at room temperature over night, in order to obtain the de-acetylation at C-3 and inversion at C-6. Then after addition of water and evaporation of the solvents, the residue was diluted with water and extracted with ethyl acetate (3 x 50 mL). The combined extract was washed with brine, dried with Na<sub>2</sub>SO<sub>4</sub> and evaporated to give 240 mg of a crude residue that was subjected to the next step without further purification. To a solution of a crude residue (240 mg, 0.520 mmol) in dry pyridine (10 mL), tosyl chloride (1.11 g, 12.2 mmol) was added, and the mixture was stirred at room temperature for 6 h. It was poured into cold water (30 mL) and extracted with CH<sub>2</sub>Cl<sub>2</sub> (3 x 30 mL), to give 270 mg of **102** (73% over two steps) that was subjected to the next step without further purification.

*6 $\alpha$ -ethyl-7 $\alpha$ -hydroxy-24-nor-5 $\beta$ -cholan-23-ol (84)*. Lithium bromide (50.0 mg, 0.580 mmol) and lithium carbonate (42.2 mg, 0.580 mmol) were added to a solution of compound **102** (150 mg, 0.26 mmol) in dry DMF (10 mL), and the mixture was refluxed for 2 h. After cooling to room temperature, the mixture was slowly poured into 10% HCl solution (10 mL) and extracted with CH<sub>2</sub>Cl<sub>2</sub> (3 x 30 mL). The combined organic layer was washed successively with water, saturated NaHCO<sub>3</sub> solution and water, and then dried over anhydrous MgSO<sub>4</sub> and evaporated to dryness to give 145 mg of oily residue (quantitative yield),



that was subjected to next step without any purification. An oven-dried 10 mL flask was charged with 10% palladium on carbon (5 mg) and the product obtained (145 mg, 0.250 mmol) and the flask was evacuated and flushed with argon. Absolute methanol (5 mL) and dry THF (5 mL) were added, and the flask was flushed with hydrogen. The reaction was stirred at room temperature under H<sub>2</sub> (1 atm) over night. The mixture was filtered through celite and the recovered filtrate was concentrated to give 110 mg of **103** (0.026 mmol, quantitative yield over two steps). Dry methanol (35.0  $\mu$ L, 0.870 mmol) and LiBH<sub>4</sub> (435  $\mu$ L, 2 M in THF, 0.870 mmol) were added to a solution of **103** (50.0 mg, 0.124 mmol) in dry THF (5 mL) at 0 °C under argon and the resulting mixture was stirred for 3 h at 0 °C. The mixture was quenched by addition of NaOH (1.0 M, 0.25 mL) and then allowed to warm to room temperature. Ethyl acetate was added and the separated aqueous phase was extracted with ethyl acetate (3  $\times$  15 mL). The combined organic phases were washed with water, dried (Na<sub>2</sub>SO<sub>4</sub>) and concentrated. HPLC purification on a Nucleodur 100-5 C18 (5 $\mu$ m; 5 mm i.d.  $\times$  250 mm) with MeOH/H<sub>2</sub>O (9:1) as eluent (flow rate 1 mL/min), gave 32.5 mg of **84** (*t<sub>R</sub>* = 17.2 min, 70%). [ $\alpha$ ]<sub>D</sub><sup>25</sup> = +1.0 (*c* = 2.15, CH<sub>3</sub>OH); selected <sup>1</sup>H NMR (400 MHz, CD<sub>3</sub>OD):  $\delta$  3.66 (1H, br s, H-7), 3.61 (1H, m, H-23a), 3.54 (1H, m, H-23b), 0.96 (3H, d, *J* = 6.7 Hz, H<sub>3</sub>-21), 0.91 (3H, s, H<sub>3</sub>-19), 0.89 (3H, t, *J* = 7.3 Hz, H<sub>3</sub>-25), 0.70 (3H, s, H<sub>3</sub>-18); <sup>13</sup>C NMR (100 MHz, CD<sub>3</sub>OD):  $\delta$  71.5, 60.8, 57.8, 51.7, 48.6, 43.8, 43.3, 41.5, 41.1, 39.9, 39.2, 37.4, 34.5, 34.2, 29.4, 28.8, 25.0, 24.6 (2C), 23.5, 22.5, 22.0, 19.4, 12.2, 12.1; HR ESIMS *m/z* 377.3423 [M+H]<sup>+</sup>, C<sub>25</sub>H<sub>45</sub>O<sub>2</sub> requires 377.3420.

*6 $\alpha$ -ethyl-7 $\alpha$ -hydroxy-24-nor-5 $\beta$ -cholan-23-oic acid (85)*. Compound **103** (60.0 mg, 0.150 mmol) was hydrolyzed with NaOH (57.6 mg, 1.44 mmol) in a solution of MeOH:H<sub>2</sub>O 1:1 v/v (6 mL) on reflux for 4 h. Crude carboxylic acid intermediate (65 mg, 0.17 mmol) was treated with LiBH<sub>4</sub> by analogous procedures to those detailed above for compound **84**. Purification by silica gel (CH<sub>2</sub>Cl<sub>2</sub>-MeOH 99:1) furnished 53.5 mg of compound **85** (0.140 mmol, 92%). [ $\alpha$ ]<sub>D</sub><sup>25</sup> = +1.5 (*c* = 0.27, CH<sub>3</sub>OH); selected <sup>1</sup>H NMR (400 MHz, CD<sub>3</sub>OD):  $\delta$  3.64 (1H, br s, H-7), 2.41 (1H, dd, *J* = 11.0, 2.6 Hz, H-22a), 1.00 (3H, d, *J* = 6.0 Hz, H<sub>3</sub>-21), 0.90 (3H, s, H<sub>3</sub>-19), 0.87 (3H, t, *J* = 7.4 Hz, H<sub>3</sub>-25), 0.71 (3H, s, H<sub>3</sub>-18);

$^{13}\text{C}$  NMR (100 MHz,  $\text{CD}_3\text{OD}$ ):  $\delta$  178.9, 71.6, 57.5, 51.7, 48.6, 43.8, 43.4, 43.3, 41.5, 40.9, 39.1, 37.4, 35.2, 34.6, 29.4, 28.8, 25.0, 24.6 (2C), 23.5, 22.4, 22.0, 20.1, 12.2, 12.1; HR ESIMS  $m/z$  389.3052  $[\text{M}-\text{H}]^-$ ,  $\text{C}_{25}\text{H}_{41}\text{O}_3$  requires 389.3056.

*Methyl 3 $\beta$ -hydroxy-6 $\alpha$ -ethyl-7-keto-24-nor-5 $\beta$ -cholan-23-oate (104)*. A solution of intermediate **102** ( $100 \times 10^{-3}$  g, 0.170 mmol) and  $\text{CH}_3\text{COOK}$  (18 mg, 0.18 mmol) dissolved in water (1 mL) and *N,N*-dimethylformamide (DMF, 4 mL), was refluxed for 3 h. The solution was cooled at room temperature and then ethyl acetate and water were added. The separated aqueous phase was extracted with ethyl acetate ( $3 \times 30$  mL). The combined organic phases were washed with water, dried ( $\text{Na}_2\text{SO}_4$ ) and evaporated to dryness to give intermediate **104** (100 mg) that was used as starting material in the synthesis of compounds **86** and **87** without further purification.

*6 $\alpha$ -ethyl-3 $\beta$ ,7 $\alpha$ -dihydroxy-24-nor-5 $\beta$ -cholan-23-ol (86)*. Compound **104** (60.0 mg, 0.140 mmol) was subjected at  $\text{LiBH}_4$  reduction with the same procedures previous described for compound **84**, to give 55 mg of a crude residue. HPLC purification on a Nucleodur 100-5 C18 (5  $\mu\text{m}$ ; 5 mm i.d. x 250 mm) with  $\text{MeOH}/\text{H}_2\text{O}$  (8:2) as eluent (flow rate 1 mL/min), gave 31 mg of **86** ( $t_{\text{R}} = 14$  min, 57%).  $[\alpha]_{\text{D}}^{25} = +7.1$  ( $c = 1.23$ ,  $\text{CH}_3\text{OH}$ ); selected  $^1\text{H}$  NMR (400 MHz,  $\text{CD}_3\text{OD}$ ):  $\delta$  3.97 (1H, br s, H-3), 3.67 (1H, br s, H-7), 3.61 (1H, m, H-23a), 3.55 (1H, m, H-23b), 0.97 (3H, d,  $J = 6.6$  Hz,  $\text{H}_3$ -21), 0.95 (3H, s,  $\text{H}_3$ -19), 0.91 (3H, t,  $J = 7.4$  Hz,  $\text{H}_3$ -25), 0.71 (3H, s,  $\text{H}_3$ -18);  $^{13}\text{C}$  NMR (100 MHz,  $\text{CD}_3\text{OD}$ ):  $\delta$  71.4, 67.4, 60.8, 57.9, 51.8, 43.8, 42.8, 41.5, 41.2, 41.1, 39.9, 37.0, 34.2, 33.8, 31.3, 31.2, 29.4, 28.3, 24.6, 24.2, 23.3, 22.3, 19.4, 12.2, 12.1; HR ESIMS  $m/z$  393.3365  $[\text{M}+\text{H}]^+$ ,  $\text{C}_{25}\text{H}_{45}\text{O}_3$  requires 393.3369.

*6 $\alpha$ -ethyl-3 $\beta$ ,7 $\alpha$ -dihydroxy-24-nor-5 $\beta$ -cholan-23-oic acid (87)*. Compound **104** (40.0 mg, 0.0950 mmol) was hydrolyzed with sodium hydroxide in a solution of  $\text{MeOH}:\text{H}_2\text{O}$  1:1 (5 mL) overnight under reflux. The resulting solution was then concentrated under vacuum, diluted with water, acidified with  $\text{HCl}$  6 M and extracted with ethyl acetate ( $3 \times 50$  mL). The collected organic phases were washed with brine, dried over  $\text{Na}_2\text{SO}_4$  anhydrous and evaporated under reduced pressure, to give a crude residue (35 mg, 0.086 mmol) that was subjected at  $\text{LiBH}_4$  reduction, with the same procedures previous described for compound **85**. HPLC

purification on a Nucleodur 100-5 C18 (5  $\mu$ m; 5 mm i.d. x 250 mm) with MeOH/H<sub>2</sub>O (88:12) as eluent (flow rate 3 mL/min), gave 22.5 mg of **87** as a white solid (58% over two steps,  $t_R$  = 9 min).  $[\alpha]_D^{25} = +2.0$  ( $c = 0.47$ , CH<sub>3</sub>OH); selected <sup>1</sup>H NMR (400 MHz, CD<sub>3</sub>OD):  $\delta$  3.97 (1H, br s, H-3), 3.66 (1H, br s, H-7), 2.42 (1H, dd,  $J = 11.3, 3.3$  Hz, H-22a), 1.02 (3H, d,  $J = 6.0$  Hz, H<sub>3</sub>-21), 0.94 (3H, s, H<sub>3</sub>-19), 0.91 (3H, t,  $J = 7.3$  Hz, H<sub>3</sub>-25), 0.73 (3H, s, H<sub>3</sub>-18); <sup>13</sup>C NMR (100 MHz, CD<sub>3</sub>OD):  $\delta$  177.7, 71.3, 67.4, 57.4, 51.8, 43.8 (2C), 42.8, 41.5, 41.2, 41.0, 37.0, 35.1, 33.8, 31.3, 31.2, 29.4, 28.3, 24.6, 24.2, 23.3, 22.2, 20.0, 12.2, 12.1; HR ESIMS  $m/z$  405.3003 [M-H]<sup>-</sup>, C<sub>25</sub>H<sub>41</sub>O<sub>4</sub> requires 405.3005.

*6 $\alpha$ -ethyl-3 $\alpha$ ,7 $\alpha$ -di(tert-butyltrimethylsilyloxy)-5 $\beta$ -cholan-24-ol (106)*. 2,6-lutidine (5.35 mL, 46.0 mmol) and *tert*-butyltrimethylsilyl trifluoromethanesulfonate (3.15 mL, 13.7 mmol) were added at 0 °C to a solution of compound **105**, prepared as previously reported, (1.0 g, 2.3 mmol) in 30 mL of CH<sub>2</sub>Cl<sub>2</sub>. After 2 h stirring at 0 °C, the reaction was quenched by addition of aqueous NaHSO<sub>4</sub> (1 M, 100 mL). The layers were separated and the aqueous phase was extracted with CH<sub>2</sub>Cl<sub>2</sub> (3  $\times$  50 mL). The combined organic layers were washed with NaHSO<sub>4</sub>, water, saturated aqueous NaHCO<sub>3</sub>, and brine and evaporated *in vacuo* to give 2.2 g of methyl *6 $\alpha$ -ethyl-3 $\alpha$ ,7 $\alpha$ -di(tert-butyltrimethylsilyloxy)-5 $\beta$ -cholan-24-oate* in the form of colorless needles, that was subjected to next step without any purification. To a solution of methyl ester (2.2 g, 3.4 mmol) in dry THF (30 mL), at 0 °C dry methanol (413  $\mu$ L, 10.2 mmol) and LiBH<sub>4</sub> (5.10 mL, 2M in THF, 10.2 mmol) was added. The resulting mixture was stirred for 2 h at 0 °C. The mixture was quenched by addition of 1.0 M NaOH (6.8 mL) and then ethyl acetate. The organic phase was washed with water, dried (Na<sub>2</sub>SO<sub>4</sub>) and concentrated. Purification by silica gel (hexane/ethyl acetate 99:1 and 0.5% TEA) gave **106** as a white solid (1 g, 68% over two steps).

*Methyl 6 $\alpha$ -ethyl-3 $\alpha$ ,7 $\alpha$ -di(tert-butyltrimethylsilyloxy)-25,26-bis-homo-5 $\beta$ -chol-24-en-26-oate (107)*. DMSO (1.56 mL, 22.0 mmol) was added dropwise for 15 min to a solution of oxalyl chloride (5.49 mL, 11.0 mmol) in dry dichloromethane (30 mL) at -78 °C under argon atmosphere. After 30 min a solution of alcohol **106** (1.0 g, 1.6 mmol) in dry CH<sub>2</sub>Cl<sub>2</sub> was added via cannula and the mixture was stirred at -78 °C for 30 min. Et<sub>3</sub>N (2.18 mL, 15.7 mmol) was added dropwise. After 1 h methyl (triphenylphosphoranylidene)acetate (1.64 g, 4.70 mmol) was

added and the mixture was allowed to warm to room temperature. A saturated solution of NaCl was added and the aqueous phase was extracted with diethyl ether (3 × 50 mL). The combined organic phases were washed with water, dried (Na<sub>2</sub>SO<sub>4</sub>) and concentrated. Purification by silica gel (hexane-ethyl acetate 995:5 and 0.5% TEA) gave compound **107** as colorless oil (850 mg, 79%).

*Methyl 6 $\alpha$ -ethyl-3 $\alpha$ ,7 $\alpha$ -dihydroxy-25, 26-bis-homo-5 $\beta$ -cholan-26-oate (88)*. A solution of compound **107** (850 mg, 1.2 mmol) in THF dry/MeOH dry (5 mL/5 mL, v/v) was hydrogenated in presence of Pd(OH)<sub>2</sub> 5% wt on activated carbon Degussa type (5 mg). The flask was evacuated and flushed first with argon and then with hydrogen. After 12 h, the reaction was complete. The catalyst was filtered through celite, and the recovered filtrate was concentrated under vacuum to give the methyl ester, which was dissolved in methanol (40 mL). At the solution was added 1 mL of HCl 37% v/v. After 1h, silver carbonate was added at the solution to precipitate chloride. Then the reaction mixture was centrifuged and the supernatant was concentrated *in vacuo* to give compound **88** as colourless amorphous solids (500 mg, 88%). An analytical sample was purified by HPLC on a Nucleodur 100-5 C18 (5 $\mu$ m; 4.6 mm i.d. x 250 mm) with MeOH/H<sub>2</sub>O (98:2) as eluent (flow rate 1 mL/min), to give compound **88** ( $t_R$  = 7min).  $[\alpha]_D^{25} = +6.85$  ( $c = 0.14$ , CH<sub>3</sub>OH); selected <sup>1</sup>H NMR (400 MHz, CD<sub>3</sub>OD):  $\delta$  3.66 (3H, s, COOCH<sub>3</sub>), 3.65 (1H, ovl, H-7), 3.31 (1H, ovl, H-3), 2.32 (2H, t,  $J = 7.71$  Hz, H<sub>2</sub>-25), 0.94 (3H, d,  $J = 6.4$  Hz, H<sub>3</sub>-21), 0.92 (3H, s, H<sub>3</sub>-19), 0.91 (3H, t,  $J = 6.8$  Hz, H<sub>3</sub>-28), 0.69 (3H, s, H<sub>3</sub>-18); <sup>13</sup>C NMR (175 MHz, CD<sub>3</sub>OD):  $\delta$  176.0, 73.2, 71.2, 57.7, 51.9, 51.7, 47.0, 43.7, 43.1, 41.6, 41.1, 37.1, 36.9, 36.8, 36.6, 34.5, 34.4 (2C), 31.3, 29.4, 26.7, 26.4, 24.6, 23.8, 23.5, 22.0, 19.2, 12.3, 12.1; HR ESIMS  $m/z$  463.3783 [M+H]<sup>+</sup>, C<sub>29</sub>H<sub>51</sub>O<sub>4</sub> requires 463.3787

*6 $\alpha$ -ethyl-3 $\alpha$ ,7 $\alpha$ -dihydroxy-25,26-bis-homo5 $\beta$ -cholan-26-oic acid (89)*. Compound **88** (200 × 10<sup>-3</sup> g, 0.430 mmol) was hydrolyzed with sodium hydroxide in a solution of MeOH:H<sub>2</sub>O 1:1 (10 mL) overnight under reflux. The resulting solution was then concentrated under vacuum, diluted with water, acidified with HCl 6 M and extracted with ethyl acetate (3 x 50 mL). The collected organic phases were washed with brine, dried over Na<sub>2</sub>SO<sub>4</sub> anhydrous and evaporated under reduced pressure. HPLC purification on a Nucleodur 100-5 C18 (5 $\mu$ m; 4.6 mm i.d. x 250

mm) with MeOH/H<sub>2</sub>O (92:8) as eluent (flow rate 1 mL/min), gave 172 mg of **89** as a white solid (89%,  $t_R$  = 7 min).  $[\alpha]_D^{25} = -0.72$  ( $c = 0.08$ , CH<sub>3</sub>OH); selected <sup>1</sup>H NMR (400 MHz, CD<sub>3</sub>OD):  $\delta$  3.66 (1H, br s, H-7), 3.31 (1H, m ovl, H-3), 2.24 (2H, t,  $J = 7.3$  Hz, H<sub>2</sub>-25), 0.95 (3H, d,  $J = 6.4$  Hz, H<sub>3</sub>-21), 0.92 (3H, s, H<sub>3</sub>-19), 0.91 (3H, t,  $J = 6.9$  Hz, H<sub>3</sub>-28), 0.70 (3H, s, H<sub>3</sub>-18); <sup>13</sup>C NMR (175 MHz, CD<sub>3</sub>OD):  $\delta$  186.7, 73.3, 71.3, 57.7, 51.7, 47.0, 43.7, 43.1, 41.6, 41.1, 37.1, 36.9, 36.8, 36.6, 34.5, 34.4 (2C), 31.3, 29.4, 27.0 (2C), 24.6, 23.8, 23.5, 22.0, 19.2, 12.2, 12.0; HR ESIMS  $m/z$  447.3469 [M-H]<sup>-</sup>, C<sub>28</sub>H<sub>47</sub>O<sub>4</sub> requires 447.3474.

*6 $\alpha$ -ethyl-3 $\alpha$ ,7 $\alpha$ -dihydroxy-25,26-bis-homo-5 $\beta$ -cholan-26-ol* (**90**). Compound **88** (300 x 10<sup>-3</sup> g, 0.650 mmol) was subjected to a LiBH<sub>4</sub> reduction with the same procedure previous described for compound **106**, to give 280 mg of crude residue. HPLC purification on a Nucleodur 100-5 C18 (5 $\mu$ m; 4.6 mm i.d. x 250 mm) with MeOH/H<sub>2</sub>O (9:1) as eluent (flow rate 1 mL/min), gave 220 mg of **90** (78%,  $t_R$  = 14 min).  $[\alpha]_D^{25} = +10.6$  ( $c = 0.25$ , CH<sub>3</sub>OH); selected <sup>1</sup>H NMR (400 MHz, CD<sub>3</sub>OD):  $\delta$  3.64 (1H, br s, H-7), 3.53 (2H, t,  $J = 6.6$  Hz, H<sub>2</sub>-26), 3.30 (1H, m ovl, H-3), 0.94 (3H, d,  $J = 6.7$  Hz, H<sub>3</sub>-21), 0.91 (3H, s, H<sub>3</sub>-19), 0.90 (3H, t,  $J = 7.0$  Hz, H<sub>3</sub>-28), 0.68 (3H, s, H<sub>3</sub>-18); <sup>13</sup>C NMR (175 MHz, CD<sub>3</sub>OD):  $\delta$  73.3, 71.3, 63.1, 57.7, 51.7, 47.0, 43.7, 43.1, 41.6, 41.1, 37.1, 36.8 (2C), 36.6, 34.5, 34.4, 33.7, 31.3, 29.5, 27.4, 27.0, 24.6, 23.8, 23.5, 22.0, 19.3, 12.3, 12.0; HR ESIMS  $m/z$  435.3835 [M+H]<sup>+</sup>, C<sub>28</sub>H<sub>51</sub>O<sub>3</sub> requires 435.3838.

*6 $\alpha$ -ethyl-3 $\alpha$ ,7 $\alpha$ -dihydroxy-25,26-bis-homo-5 $\beta$ -cholan-26-yl-26-sodium sulfate* (**91**). The triethylamine-sulfur trioxide complex (65.3 mg, 0.360 mmol) was added to a solution of compound **90** (50.0 mg, 0.120 mmol) in DMF dry (3 mL) under an argon atmosphere, and the mixture was stirred at 70°C for 24 h. The solvent was concentrated *in vacuo*. The residue was poured over a RP18 column. Fraction eluted with MeOH 100% gave a mixture that was further purified by HPLC on a Nucleodur 100-5 C18 (5  $\mu$ m; 4.6 mm i.d. x 250 mm) with MeOH/H<sub>2</sub>O (78:22) as eluent (flow rate 1 mL/min), to give 16 mg (0.030 mmol, 25%) of compound **91** ( $t_R$  = 16 min).  $[\alpha]_D^{25} = -6.14$  ( $c = 0.07$ , CH<sub>3</sub>OH); selected <sup>1</sup>H NMR (400 MHz, CD<sub>3</sub>OD):  $\delta$  3.99 (2H, t,  $J = 6.6$  Hz, H<sub>2</sub>-26), 3.65 (1H, br s, H-7), 3.31 (1H, m ovl, H-3), 0.94 (3H, d,  $J = 6.2$  Hz, H<sub>3</sub>-21), 0.91 (3H, s, H<sub>3</sub>-19), 0.90 (3H, t,  $J = 7.0$  Hz,

H<sub>3</sub>-28), 0.69 (3H, s, H<sub>3</sub>-18); HR ESIMS *m/z* 513.3247 [M-Na]<sup>+</sup>, C<sub>28</sub>H<sub>49</sub>O<sub>6</sub>S requires 513.3250.

**Specific biological assay used for compound 77**

**Chemicals.** Design and synthesis of **77** (6 $\alpha$ -ethyl-3 $\alpha$ , 7 $\alpha$ -dihydroxy-24-nor-5 $\beta$ -cholan-23-ol or BAR502) has been described previously. The agent was dissolved daily in drinking water containing 1% methyl cellulose before its administration by gavage (100  $\mu$ L).

**Animal Studies of ANIT.** GP-BAR1 null mice (GP-BAR1-B6= GP-BAR12/2 mice, generated directly into C57BL/6NCrl background), and congenic littermates on C57BL/6NCrl mice were kindly gifted by Dr. Galya Vassileva (Schering-Plough Research Institute, Kenilworth). Mice were housed under controlled temperatures (22uC) and photoperiods (12:12-hour light/dark cycle), allowed unrestricted access to standard mouse chow and tap water and allowed to acclimate to these conditions for at least 5 days before inclusion in an experiment. Protocol for ANIT administration was approved by Ministry of Health (decree N°245/2013-B). Mice (6 male for group) were treated 9 days with ANIT (Sigma-Aldrich) dissolved in corn oil (10 mg/kg, os) or corn oil alone (control mice). At the end of the treatment mice were subjected to intradermal injection of 25  $\mu$ g DCA, 6-ECDCa, UDCA, compound **77** and the scratching response was recorded for 60 min. Serum levels of total bilirubin, aspartate aminotransferase (AST) and alkaline phosphatase were measured by routine clinical chemistry testing performed on a Hitachi 717 automatic analyzer.

**Animal model of NASH.** C57BL6 mice 24 weeks old were fed a high fat diet containing 60% kj fat (ssniff® EF acc. D12492 (I) mod.) and fructose in drinking water (42 g/l) or normal diet (6 mice) for 18 weeks<sup>11–13</sup>. After 10 weeks of HFD, mice were randomized to receive HFD alone (9 mice) or HFD plus BAR502 (15 mg/kg/day) body weight by gavage (9 mice) for 8 weeks. HFD mice were administered 100  $\mu$ L of 1% methyl cellulose in drinking water. Mice were housed under controlled temperatures (22 °C) and photoperiods (12:12-hour light/dark cycle), allowed unrestricted access to standard mouse chow and tap water and allowed to acclimate to these conditions for at least 5 days before inclusion in an experiment. The care and use of the animals were approved by the Institutional Animal Care and Use Committee of the University of Perugia and

were in accordance to European guidelines for care of experimental animals. Protocols were approved by the Italian Minister of Health and Istituto Superiore di Sanità (Italy) and were in agreement with the European guideline for use of experimental animals (permission n. 41/2014-B released to AD). The general health of the animals was monitored daily by the Veterinarian in the animal facility. The study protocol caused minor suffering, however, animals that lost more than 25% of the initial body weight were euthanized. At the day of sacrifice mice were deeply anesthetized with a mixture of tiletamine hydrochloride and zolazepam hydrochloride/xylazine at a dose of 50/5 mg/kg. Food intake was estimated as the difference of weight between the offered and the remnant amount of food at 7-days intervals. The food was provided as pressed pellets and the residual spillage was not considered.

**Liver fibrosis.** Liver fibrosis was induced by carbon tetrachloride (CCl<sub>4</sub>) administration according to a previously published method.<sup>139</sup> For this purpose, C57BL6 mice were administered i.p. 500  $\mu$ L/kg body weight of CCl<sub>4</sub> in an equal volume of paraffin oil twice a week for 8 weeks. CCl<sub>4</sub> mice were randomized to receive BAR502 (15 mg/kg daily by gavage) or vehicle (distilled water).

**Tissue histology.** For histological examination, portions of the right and left liver lobes and epididymal white adipose tissue (epWAT) were fixed in 10% formalin, embedded in paraffin, sectioned and stained with Sirius red and hematoxylin/eosin (H&E), for morphometric analysis. NASH severity was scored in H&E-stained cross sections using an adapted grading system of human NASH. The level of macrovesicular and microvesicular steatosis was determined at 40  $\times$  magnification relative to the total liver area analyzed and expressed as a percentage. Inflammation was scored by counting the number of aggregates of inflammatory cells per field using a 100  $\times$  magnification. The average of five random fields was taken. Relative values against the average of the HFC control group were calculated. Hepatic fibrosis was identified using Sirius Red stained slides and evaluated using an adapted grading system of human NASH. The presence of pathological collagen deposition was scored as either absent (0), observed within perisinusoidal/perivenular or periportal area (1), within both perisinusoidal and periportal areas (2), bridging fibrosis (3) or cirrhosis (4). The sum of the scores (degree of steatosis, hepatocyte ballooning, lobular

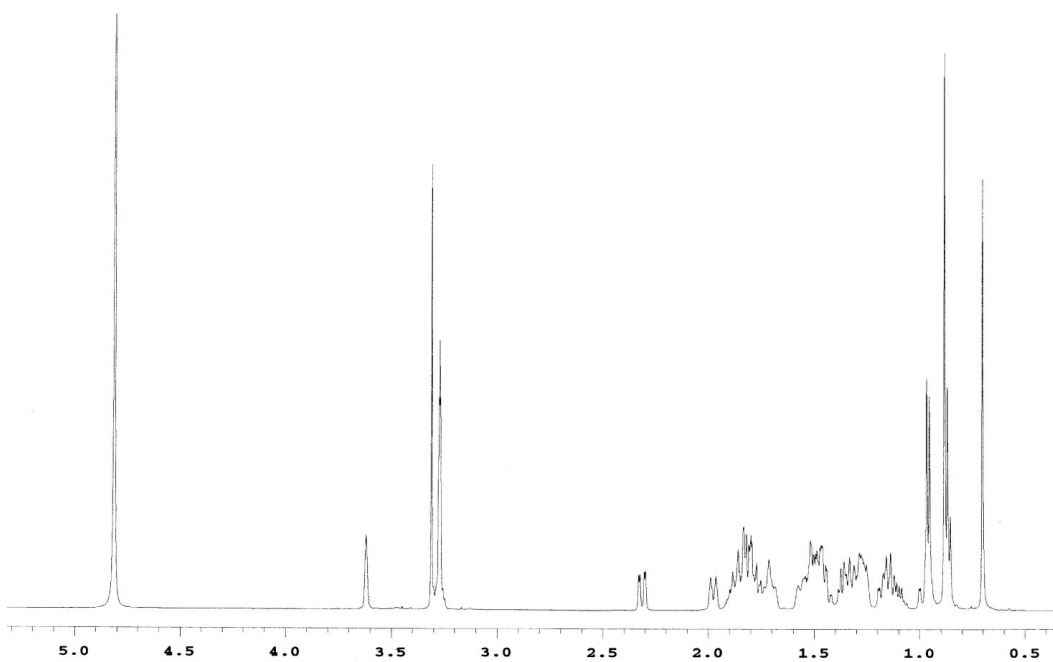
inflammation, and portal inflammation) was considered as the total pathology score.

**Biochemical analyses.** AST, triglyceride, total- and HDL- cholesterol, albumin and fasting glucose concentrations were quantified using an automated clinical chemistry analyzer (Cobas, Roche) with enzymatic methods. Plasma insulin levels were measured by ELISA assays according to the manufacturer's instructions. The homeostatic model assessment (HOMA) of IR and insulin sensitivity index was calculated by the concentrations of plasma glucose and insulin.

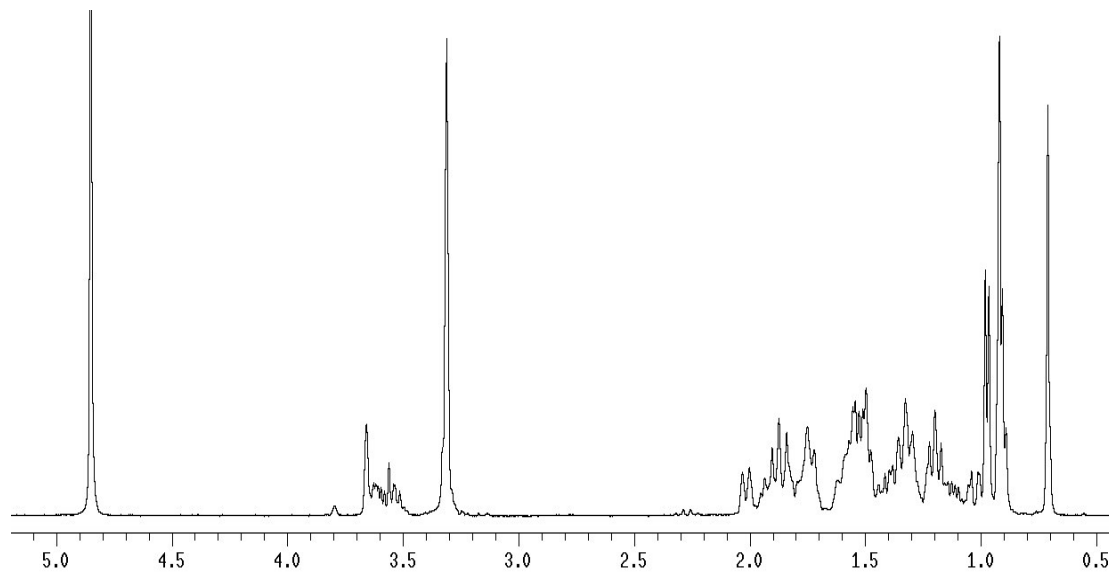


**Spectroscopic data**

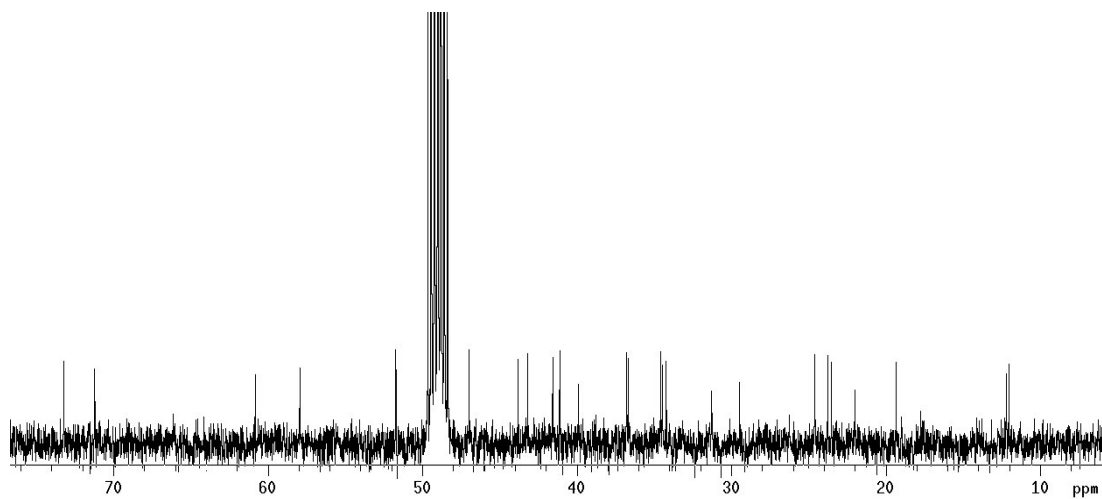
$^1\text{H}$  NMR (500 MHz,  $\text{CD}_3\text{OD}$ ) of compound **76**



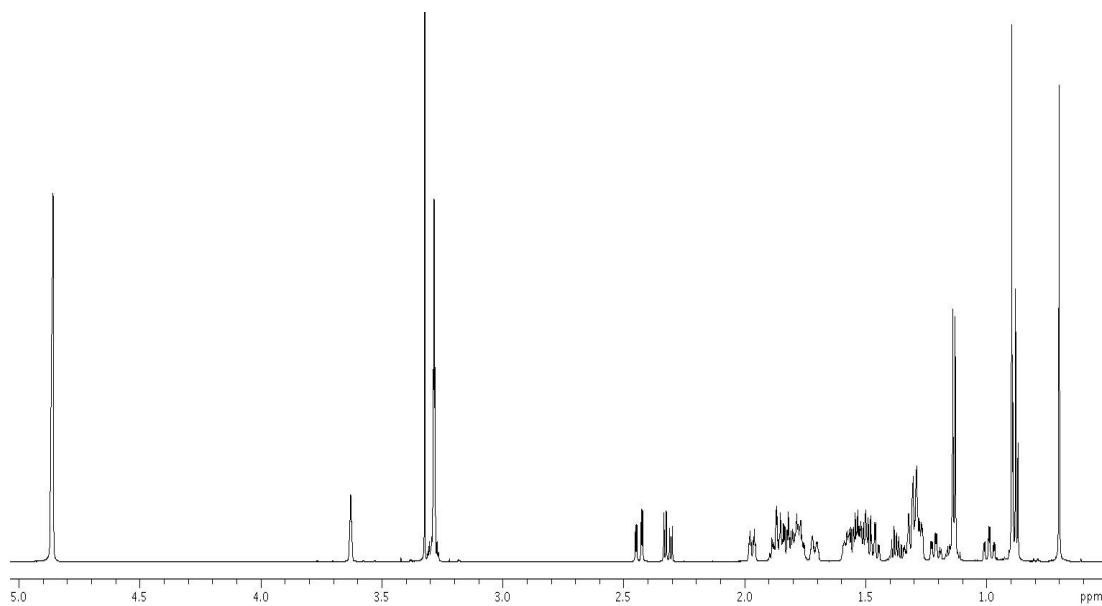
$^1\text{H}$  NMR (400 MHz,  $\text{CD}_3\text{OD}$ ) of compound **77**



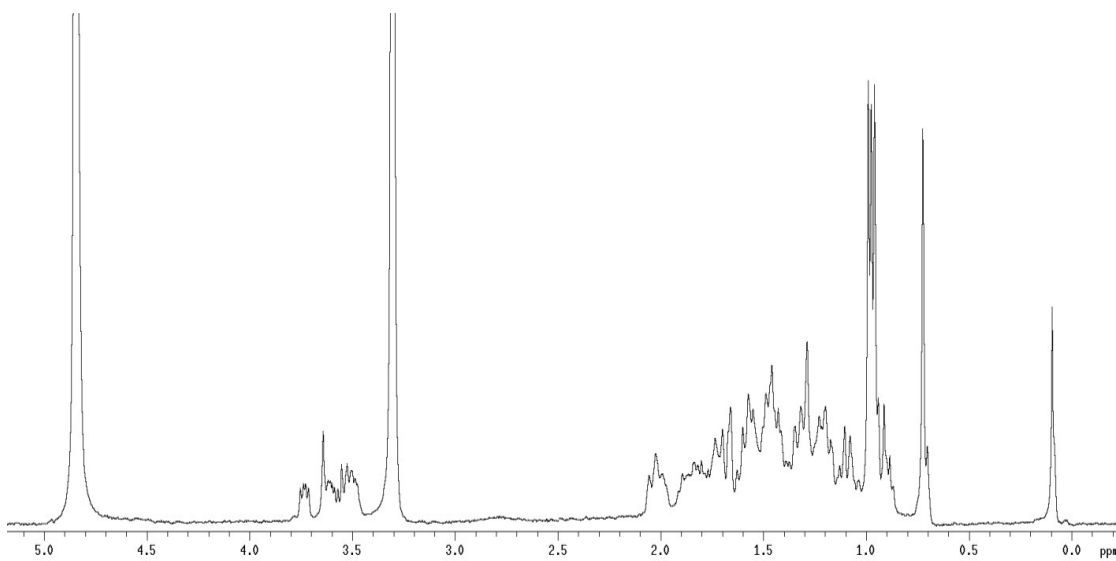
$^{13}\text{C}$  NMR (100 MHz,  $\text{CD}_3\text{OD}$ ) of compound **77**



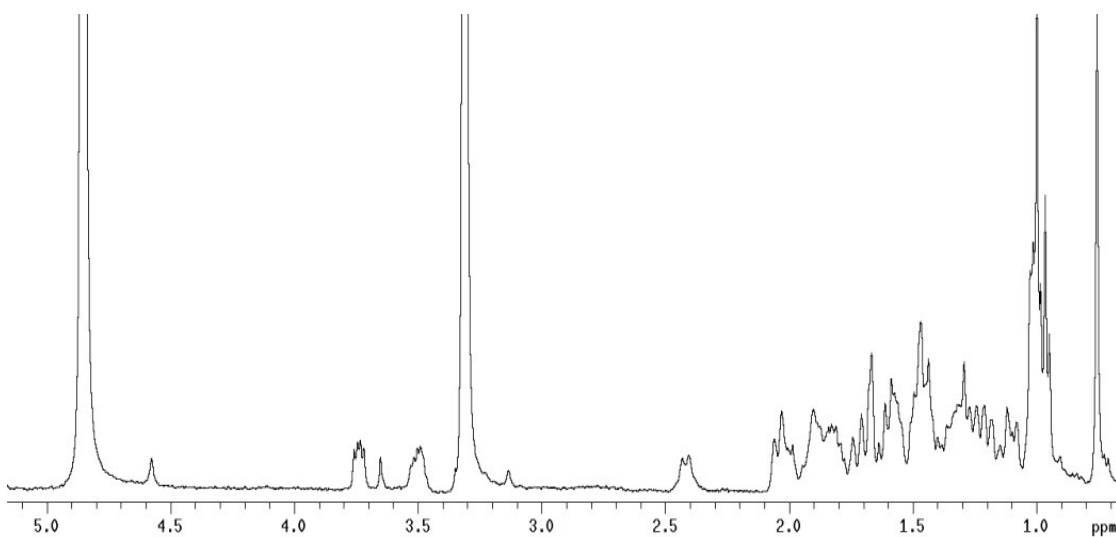
$^1\text{H}$  NMR (700 MHz,  $\text{CD}_3\text{OD}$ ) of compound **78**



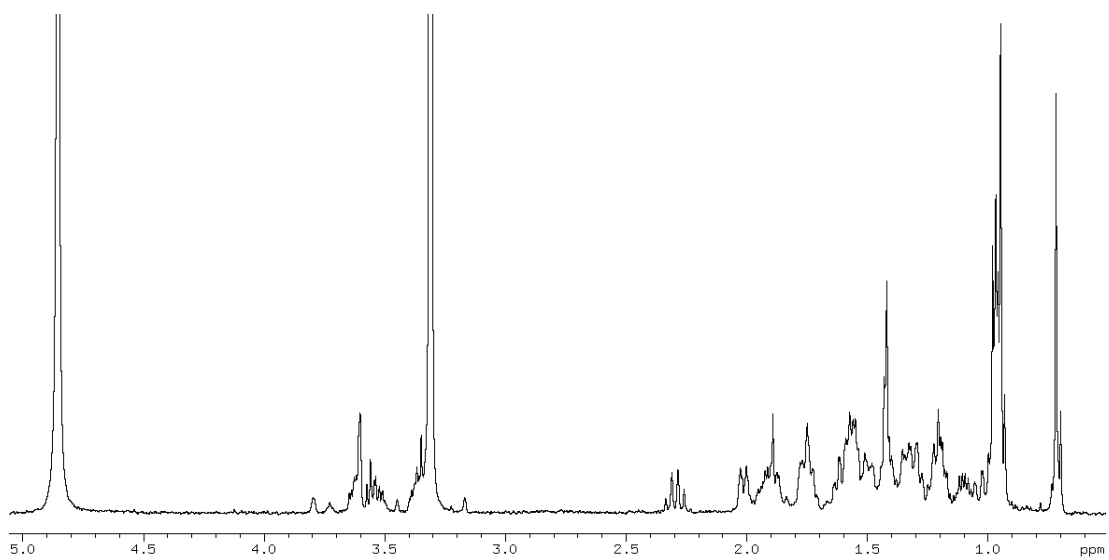
$^1\text{H}$  NMR (400 MHz,  $\text{CD}_3\text{OD}$ ) of compound **79**



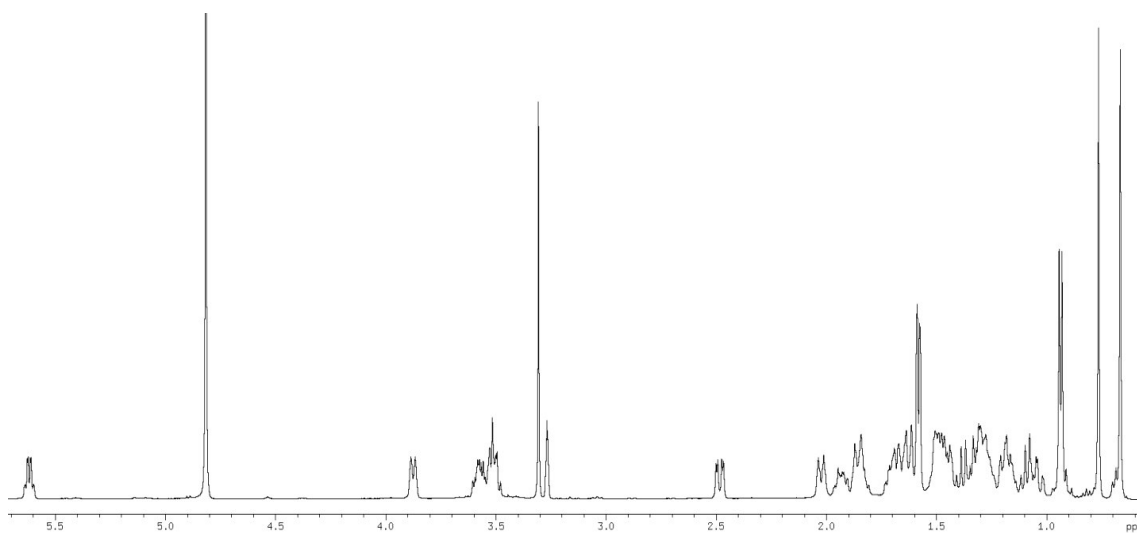
$^1\text{H}$  NMR (400 MHz,  $\text{CD}_3\text{OD}$ ) of compound **80**



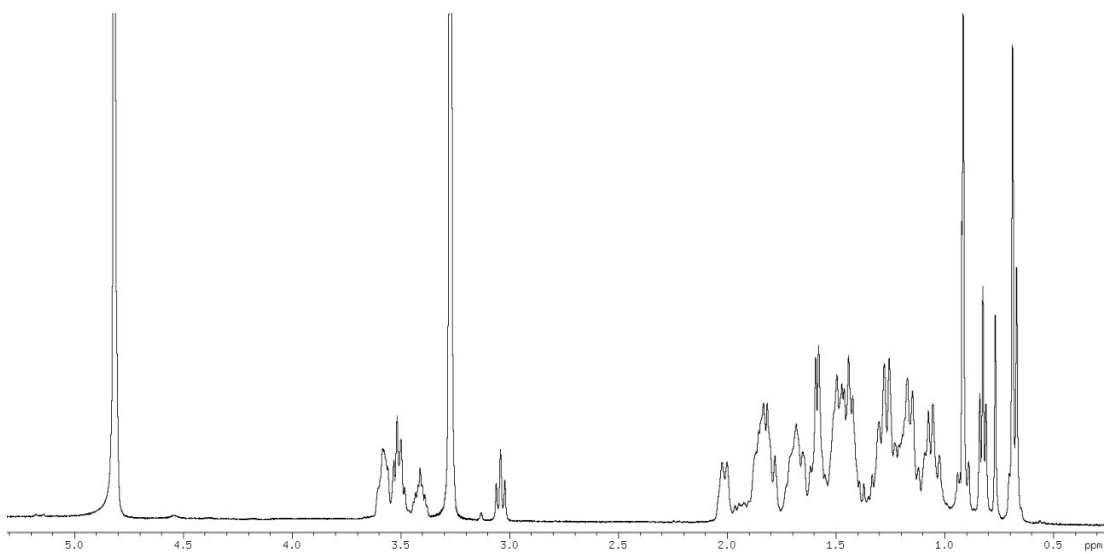
$^1\text{H}$  NMR (400 MHz,  $\text{CD}_3\text{OD}$ ) of compound **81**



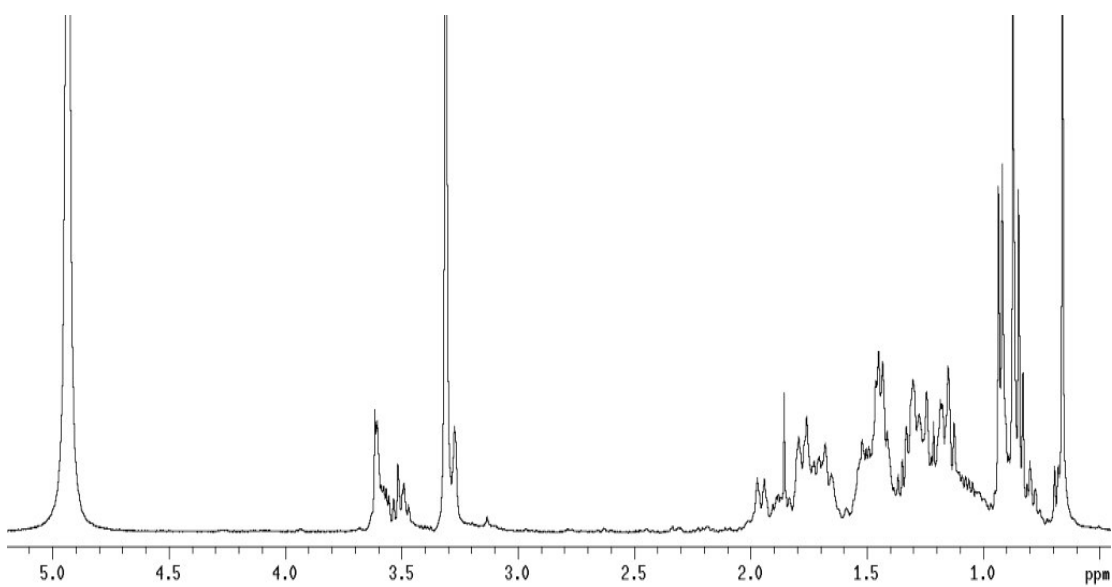
$^1\text{H}$  NMR (400 MHz,  $\text{CD}_3\text{OD}$ ) of compound **82**



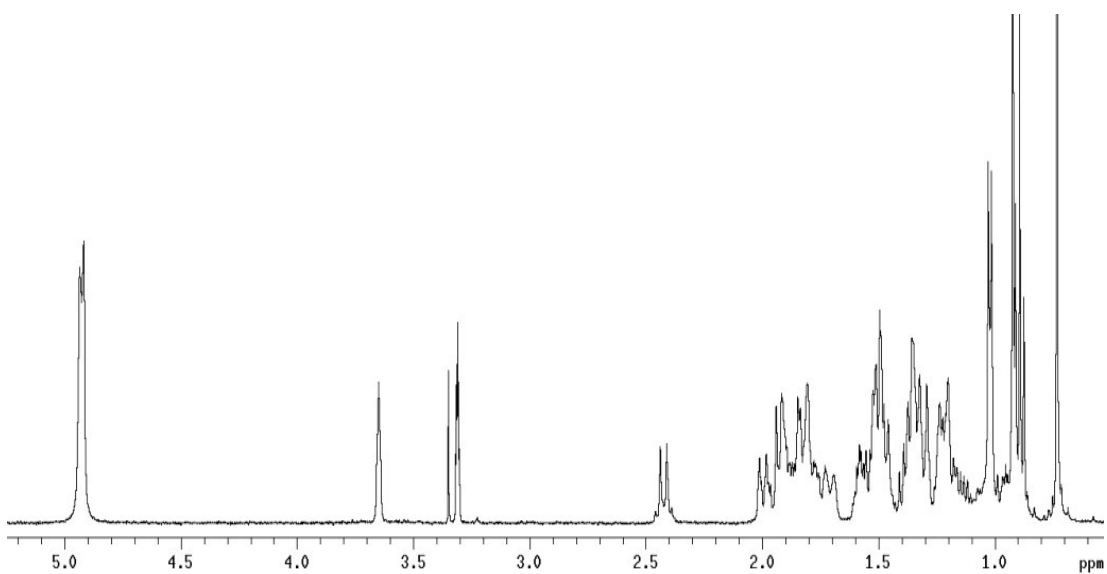
$^1\text{H}$  NMR (400 MHz,  $\text{CD}_3\text{OD}$ ) of compound **83**



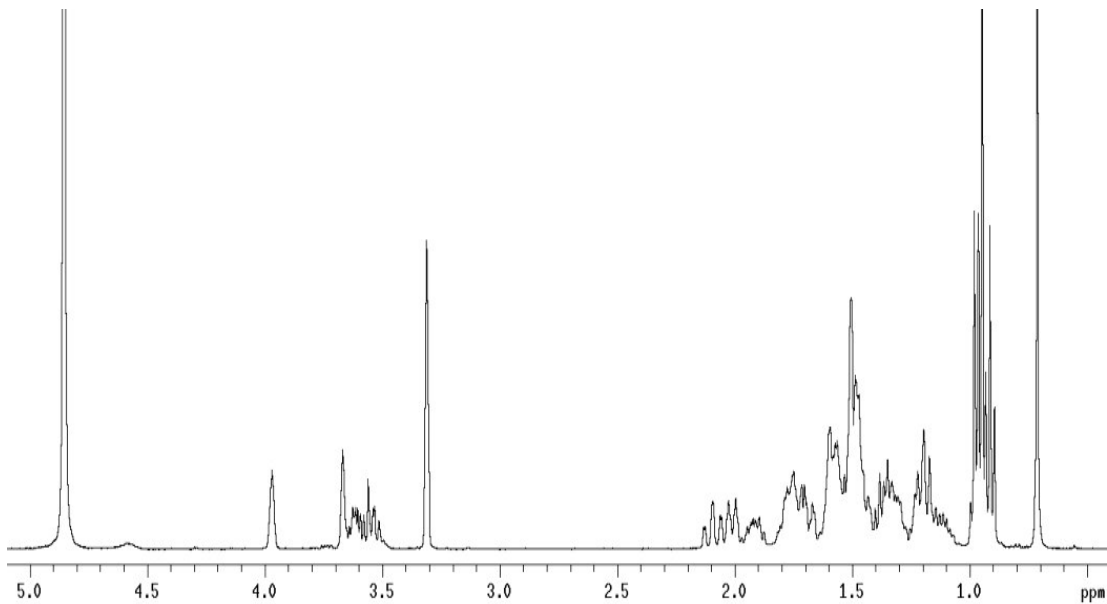
$^1\text{H}$  NMR (400 MHz,  $\text{CD}_3\text{OD}$ ) of compound **84**



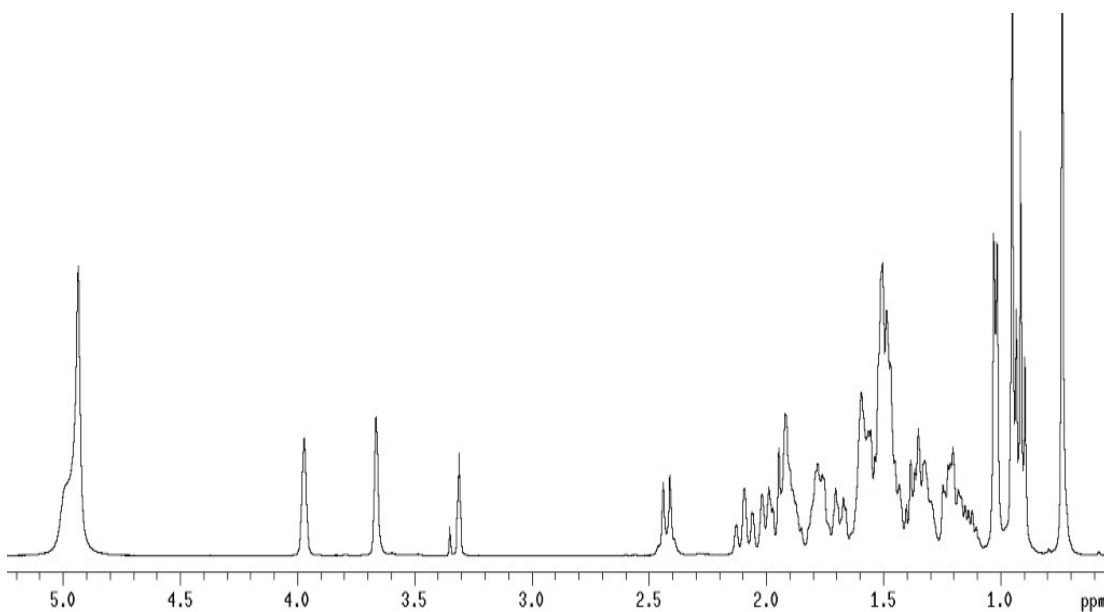
$^1\text{H}$  NMR (400 MHz,  $\text{CD}_3\text{OD}$ ) of compound **85**



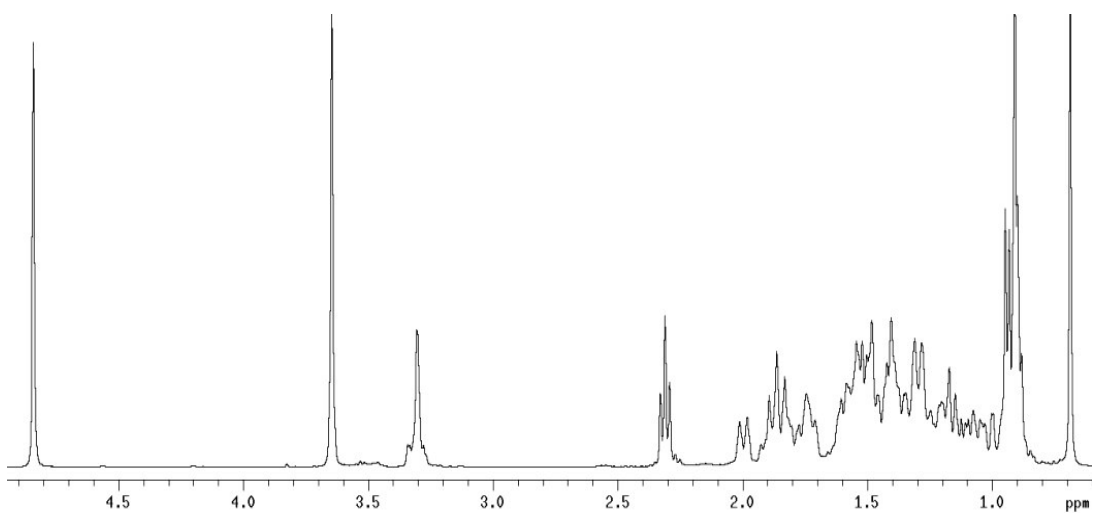
$^1\text{H}$  NMR (400 MHz,  $\text{CD}_3\text{OD}$ ) of compound **86**



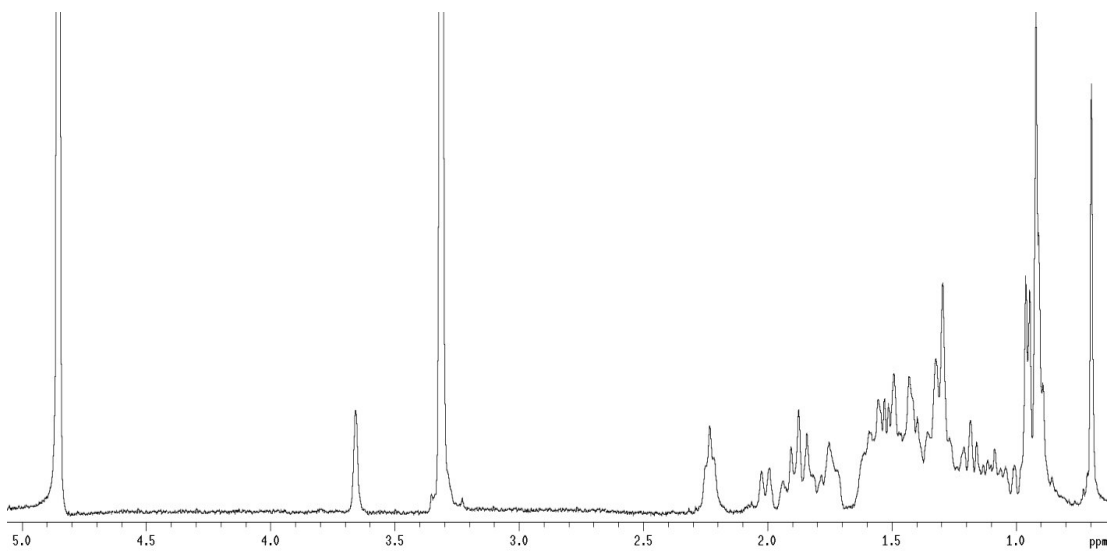
$^1\text{H}$  NMR (400 MHz,  $\text{CD}_3\text{OD}$ ) of compound **87**



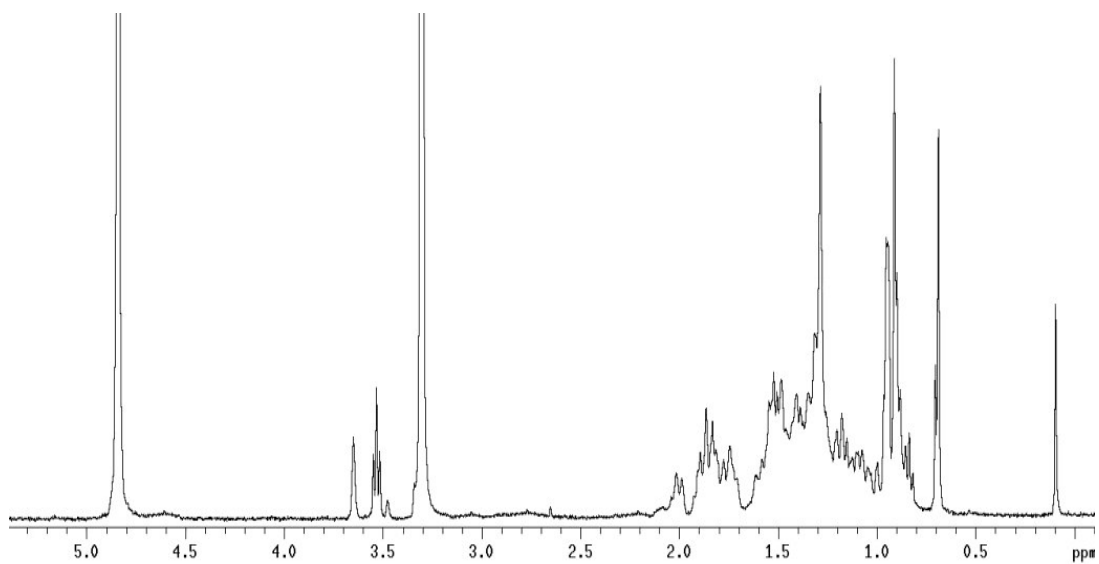
$^1\text{H}$  NMR (400 MHz,  $\text{CD}_3\text{OD}$ ) of compound **88**



$^1\text{H}$  NMR (400 MHz,  $\text{CD}_3\text{OD}$ ) of compound **89**



$^1\text{H}$  NMR (400 MHz,  $\text{CD}_3\text{OD}$ ) of compound **90**





## V. Experimental procedures for benzo-fused cyclic amines

### General procedure for the intramolecular Heck reaction

A solution of the corresponding substituted 2-iodobenzyl sulfinyl amide **1** (1.0 equiv), Pd(OAc)<sub>2</sub> (0.1 equiv), PPh<sub>3</sub> (0.2 equiv), Et<sub>3</sub>N (2.0 equiv) and Ag<sub>2</sub>CO<sub>3</sub> (2.0 equiv) in toluene (0.1 M) was heated to 70 LC for 12 h. The solvent was removed under reduced pressure, and the crude product was purified by flash chromatography to give compounds **5**. Compounds **5a–d** have previously been described, and their spectroscopic data are in fully agreement with the literature.<sup>142</sup>

### General procedure for the ring-closing enyne metathesis

A solution of **21** (1.0 equiv), 1,7-octadiene (8.0 equiv) and Grubbs II catalyst (0.05 equiv) in CH<sub>2</sub>Cl<sub>2</sub> (0.1 M) was heated to 90 LC for 24 h. The solvent was removed under reduced pressure, and the crude product was purified by flash chromatography to give compounds **22**.

*(R<sub>S</sub>)-2-Methyl-N-[(S)-4-(1-phenylvinyl)-1,2-dihydronaphthalen-1-yl]propane-2-sulfinamide (22a)*. The title compound was obtained following the general procedure described above. Flash chromatography [*n*-hexane/EtOAc (1:1)] afforded compound **22a** as a brown solid (99 %). [α]<sub>D</sub><sup>25</sup> = +24.3 (*c* = 1.0; CHCl<sub>3</sub>); selected <sup>1</sup>H NMR (300 MHz, CDCl<sub>3</sub>): δ 1.23 (s, 9H), 2.68 (ddd, *J* = 17.2, 7.1, 4.9 Hz, 1H), 2.89 (ddd, *J* = 17.2, 5.7, 4.3 Hz, 1H), 3.51 (d, *J* = 8.1 Hz, 1H), 4.59 (dd, *J* = 13.7, 7.2 Hz, 1H), 5.35 (d, *J* = 1.6 Hz, 1H), 5.67 (d, *J* = 1.6 Hz, 1H), 6.10 (t, *J* = 4.5 Hz, 1H), 7.00 (dd, *J* = 7.6, 1.2 Hz, 1H), 7.10 (td, *J* = 7.5, 1.5 Hz, 1H), 7.17 (td, *J* = 7.4, 1.5 Hz, 1H), 7.23 (d, *J* = 1.9 Hz, 1H), 7.25 (d, *J* = 2.0 Hz, 1H), 7.26 (s, 1H), 7.36–7.43 (m, 3H); <sup>13</sup>C NMR (75 MHz, CDCl<sub>3</sub>): δ 22.7 (3xCH<sub>3</sub>), 32.6 (CH<sub>2</sub>), 54.3 (CH), 56.1 (C), 115.4 (CH<sub>2</sub>), 125.1 (CH), 126.3 (CH), 126.6 (2xCH), 126.8 (CH), 127.3 (CH), 127.7 (CH), 128.0 (CH), 128.3 (2xCH), 133.5 (C), 135.6 (C), 139.6 (C), 139.7 (C), 147.9 (C); HRMS (EI) calculated for C<sub>22</sub>H<sub>25</sub>NOS [M+H]<sup>+</sup>: 352.1730, found: 352.1737.

*(R<sub>S</sub>)-N-[(S)-7-Methoxy-4-(1-phenylvinyl)-1,2-dihydronaphthalen-1-yl]-2-methylpropane-2-sulfinamide (22b)*. The title compound was obtained following the general procedure described above. Flash chromatography [*n*-hexane/EtOAc

(1:1)] afforded compound **22b** as a brown solid (82 %).  $[\alpha]_{\text{D}}^{25} = +21.0$  ( $c = 1.0$ ;  $\text{CHCl}_3$ ); selected  $^1\text{H}$  NMR (300 MHz,  $\text{CDCl}_3$ ):  $\delta$  1.25 (s, 9H), 2.62 (ddd,  $J = 16.9, 8.0, 4.6$  Hz, 1H), 2.87 (ddd,  $J = 16.9, 5.7, 4.5$  Hz, 1H), 3.49 (d,  $J = 7.5$  Hz, 1H), 3.76 (s, 3H), 4.49–4.60 (m, 1H), 5.34 (d,  $J = 1.7$  Hz, 1H), 5.64 (d,  $J = 1.7$  Hz, 1H), 5.97 (t,  $J = 4.5$  Hz, 1H), 6.61 (dd,  $J = 8.5, 2.7$  Hz, 1H), 6.91 (d,  $J = 8.5$  Hz, 1H), 6.97 (d,  $J = 2.7$  Hz, 1H), 7.21–7.26 (m, 3H), 7.37–7.42 (m, 2H);  $^{13}\text{C}$  NMR (75 MHz,  $\text{CDCl}_3$ ):  $\delta$  22.7, 32.7, 54.9, 55.2, 56.2, 112.3, 112.8, 115.2, 122.7, 126.6, 127.7, 128.3, 137.7, 139.3, 139.8, 148.1, 158.8; HRMS (EI) calculated for  $\text{C}_{23}\text{H}_{27}\text{NO}_2\text{S}$   $[\text{M}+\text{H}]^+$ : 382.1762, found: 382.1760.

*(R\_S)*-*N*-[*(S)*-4-(1-(3-Methoxyphenyl)vinyl)-1,2-dihydronaphthalen-1-yl]-2-methylpropane-2-sulfonamide (**22c**). The title compound was obtained following the general procedure described above. Flash chromatography [*n*-hexane/EtOAc (1:1)] afforded compound **22c** as a brown solid (95 %).  $[\alpha]_{\text{D}}^{25} = +5.0$  ( $c = 1.0$ ;  $\text{CHCl}_3$ ); selected  $^1\text{H}$  NMR (300 MHz,  $\text{CDCl}_3$ ):  $\delta$  1.23 (s, 9H), 2.67 (ddd,  $J = 17.2, 7.3, 4.8$  Hz, 1H), 2.88 (ddd,  $J = 17.2, 5.8, 4.3$  Hz, 1H), 3.51 (d,  $J = 8.5$  Hz, 1H), 3.76 (s, 3H), 4.57 (dd,  $J = 13.9, 7.6$  Hz, 1H), 5.34 (d,  $J = 1.6$  Hz, 1H), 5.66 (d,  $J = 1.6$  Hz, 1H), 6.08 (t,  $J = 4.5$  Hz, 1H), 6.78 (ddd,  $J = 8.2, 2.5, 0.9$  Hz, 1H), 6.95–6.99 (m, 2H), 7.01 (dd,  $J = 7.5, 1.4$  Hz, 1H), 7.08–7.20 (m, 3H), 7.35–7.41 (m, 1H);  $^{13}\text{C}$  NMR (75 MHz,  $\text{CDCl}_3$ ):  $\delta$  22.7 (3x $\text{CH}_3$ ), 32.7 ( $\text{CH}_2$ ), 54.5 ( $\text{CH}$ ), 55.2 ( $\text{CH}_3$ ), 56.1 ( $\text{C}$ ), 112.7 ( $\text{CH}$ ), 112.7 ( $\text{CH}$ ), 115.7 ( $\text{CH}_2$ ), 119.3 ( $\text{CH}$ ), 125.2 ( $\text{CH}$ ), 126.3 ( $\text{CH}$ ), 126.6 (2x $\text{CH}$ ), 127.4 ( $\text{CH}$ ), 127.9 (2x $\text{CH}$ ), 129.3 ( $\text{CH}$ ), 133.5 ( $\text{C}$ ), 135.7 ( $\text{C}$ ), 139.6 ( $\text{C}$ ), 141.3 ( $\text{C}$ ), 147.8 ( $\text{C}$ ), 159.6 ( $\text{C}$ ); HRMS (EI) calculated for  $\text{C}_{23}\text{H}_{27}\text{NO}_2\text{S}$   $[\text{M}+\text{H}]^+$ : 382.1835, found: 382.1819.

*(R\_S)*-*N*-[*(S)*-4-(1-(3,5-Bis(trifluoromethyl)phenyl)vinyl)-1,2-dihydronaphthalen-1-yl]-2-methylpropane-2-sulfonamide (**22d**). The title compound was obtained following the general procedure described above. Flash chromatography [*n*-hexane/EtOAc (1:1)] afforded compound **22d** as a brown solid (73%).  $[\alpha]_{\text{D}}^{25} = +15.0$  ( $c = 1.0$ ;  $\text{CHCl}_3$ ); selected  $^1\text{H}$  NMR (300 MHz,  $\text{CDCl}_3$ ):  $\delta$  1.22 (s, 9H), 2.74 (ddd,  $J = 17.4, 7.1, 4.8$  Hz, 1H), 2.92 (ddd,  $J = 17.3, 6.0, 4.3$  Hz, 1H), 3.48 (d,  $J = 8.8$  Hz, 1H), 4.58 (dd,  $J = 15.2, 6.7$  Hz, 1H), 5.56 (d,  $J = 0.7$  Hz, 1H), 5.78 (d,  $J = 0.9$  Hz, 1H), 6.15 (t,  $J = 4.5$  Hz, 1H), 6.90 (dd,  $J = 7.6, 1.1$  Hz, 1H), 7.13 (td,  $J = 7.5, 1.4$  Hz, 1H), 7.22 (td,  $J = 7.5, 1.4$  Hz, 1H), 7.41 (d,  $J = 7.4$  Hz, 1H), 7.75 (s,

1H), 7.80 (s, 2H);  $^{19}\text{F}$  NMR (282 MHz,  $\text{CDCl}_3$ ):  $\delta$  -62.84 ( $2\times\text{CF}_3$ );  $^{13}\text{C}$  NMR (75 MHz,  $\text{CDCl}_3$ ):  $\delta$  22.6 ( $3\times\text{CH}_3$ ), 32.7 ( $\text{CH}_2$ ), 54.4 (CH), 56.2 (C), 119.1 ( $\text{CH}_2$ ), 121.5 (d,  $^3J_{\text{CF}} = 5.5$  Hz,  $2\times\text{CH}$ ), 125.9 (CH), 126.6(CH), 126.8 (q,  $^1J_{\text{CF}} = 272.9$  Hz,  $2\times\text{CF}_3$ ), 126.9 (CH), 127.1 (CH), 127.9 (CH), 128.1 (CH), 131.8 (d,  $^2J_{\text{CF}} = 33.2$  Hz,  $2\times\text{C}$ ), 132.4 (C), 135.9 (C), 138.2 (C), 142.2 (C), 145.7 (C); HRMS (EI) calculated for  $\text{C}_{24}\text{H}_{23}\text{NOF}_6\text{S}$   $[\text{M}+\text{H}]^+$ : 488.1477, found: 488.1464.

*(R\_S)*-*N*-[*(S)*-4-(1-(4-Methoxyphenyl)vinyl)-1,2-dihydronaphthalen-1-yl]-2-methylpropane-2-sulfonamide (**22e**). The title compound was obtained following the general procedure described above. Flash chromatography [*n*-hexane/EtOAc (1:1)] afforded compound **22e** as a brown solid (98 %).  $[\alpha]_{\text{D}}^{25} = +6.0$  ( $c = 1.0$ ;  $\text{CHCl}_3$ ); selected  $^1\text{H}$  NMR (300 MHz,  $\text{CDCl}_3$ ):  $\delta$  1.23 (s, 9H), 2.66 (ddd,  $J = 17.2, 7.2, 4.8$  Hz, 1H), 2.88 (ddd,  $J = 17.1, 5.7, 4.3$  Hz, 1H), 3.52 (d,  $J = 8.1$  Hz, 1H), 3.76 (s, 3H), 4.58 (dd,  $J = 13.7, 7.4$  Hz, 1H), 5.24 (d,  $J = 1.6$  Hz, 1H), 5.57 (d,  $J = 1.7$  Hz, 1H), 6.08 (t,  $J = 4.5$  Hz, 1H), 6.74–6.80 (m, 2H), 7.00 (dd,  $J = 7.5, 1.3$  Hz, 1H), 7.10 (td,  $J = 7.5, 1.5$  Hz, 1H), 7.17 (td,  $J = 7.4, 1.5$  Hz, 1H), 7.30–7.36 (m, 2H), 7.39 (d,  $J = 6.9$  Hz, 1H);  $^{13}\text{C}$  NMR (75 MHz,  $\text{CDCl}_3$ ):  $\delta$  22.7 ( $3\times\text{CH}_3$ ), 32.6 ( $\text{CH}_2$ ), 54.4 (CH), 55.2 ( $\text{CH}_3$ ), 56.1 (C), 113.6 ( $\text{CH}_2$ ), 113.7 (CH), 124.9 (CH), 126.4 ( $2\times\text{CH}$ ), 126.7 (CH), 127.3 (CH), 127.8 ( $2\times\text{CH}$ ), 128.0 (CH), 132.3(C), 133.6 (C), 135.6 (C), 139.8 (C), 147.3 (C), 159.3 (C); HRMS (EI) calculated for  $\text{C}_{23}\text{H}_{27}\text{NO}_2\text{S}$   $[\text{M}+\text{H}]^+$ : 382.1835, found: 382.1833.

*(R\_S)*-*N*-[*(S)*-4-(Hex-1-en-2-yl)-1,2-dihydronaphthalen-1-yl]-2-methylpropane-2-sulfonamide (**22f**). The title compound was obtained following the general procedure described above. Flash chromatography [*n*-hexane/EtOAc (1:1)] afforded compound **22f** as a brown solid (50 %).  $[\alpha]_{\text{D}}^{25} = +7.9$  ( $c = 1.0$ ;  $\text{CHCl}_3$ ); selected  $^1\text{H}$  NMR (300 MHz,  $\text{CDCl}_3$ ):  $\delta$  0.86 (t,  $J = 7.1$  Hz, 3H), 1.18 (s, 9H), 1.28–1.35 (m, 2H), 1.47 (d,  $J = 4.8$  Hz, 2H), 2.24 (t,  $J = 7.0$  Hz, 2H), 2.58 (ddd,  $J = 17.0, 6.9, 5.0$  Hz, 1H), 2.73 (ddd,  $J = 17.0, 5.6, 4.3$  Hz, 1H), 3.47 (d,  $J = 8.7$  Hz, 1H), 4.45 (dd,  $J = 14.8, 6.5$  Hz, 1H), 5.00 (d,  $J = 2.3$  Hz, 1H), 5.08 (ddd,  $J = 2.3, 1.2$  Hz, 1.2 Hz, 1H), 5.86 (t,  $J = 4.5$  Hz, 1H), 7.19–7.28 (m, 3H), 7.35–7.40 (m, 1H);  $^{13}\text{C}$  NMR (75 MHz,  $\text{CDCl}_3$ ):  $\delta$  13.9 ( $\text{CH}_3$ ), 22.2 ( $\text{CH}_2$ ), 22.6 ( $3\times\text{CH}_3$ ), 30.5 ( $\text{CH}_2$ ), 32.4 ( $\text{CH}_2$ ), 35.5 ( $\text{CH}_2$ ), 54.7 (CH), 56.1 (C), 114.2 ( $\text{CH}_2$ ), 122.0 (CH),

125.7 (CH), 126.7 (CH), 127.3 (CH), 127.9 (CH), 133.3 (C), 136.3 (C), 140.8 (C),  
148.7 (C); HRMS (EI) calculated for C<sub>20</sub>H<sub>29</sub>NOS [M+H]<sup>+</sup>: 332.2043, found:  
332.2040.

**REFERENCES**

---

1. Makishima, M.; Okamoto, A.Y.; Repa, J.J.; et al. Identification of a nuclear receptor for bile acids. *Science* 284, 1362-1365 (1999).
2. Parks, D.J.; Blanchard, S.G.; Bledsoe, R.K.; et al. Bile acids: natural ligands for an orphan nuclear receptor. *Science* 284, 1365-1368 (1999).
3. Wang, H.; Chen, J.; Hollister, K.; et al. Endogenous bile acids are ligands for the nuclear receptor FXR/BAR. *Mol. Cell* 3, 543-553 (1999).
4. Makishima, M.; Lu, T.T.; Xie, W.; et al. Vitamin D receptor as an intestinal bile acid sensor. *Science* 296, 1313-1316 (2002).
5. Maruyama, T.; Miyamoto, Y.; Nakamura, T.; et al. Identification of membrane type receptor for bile acids (M-BAR). *Biochem. Biophys. Res. Commun.* 298, 714-719 (2002).
6. Sheikh Abdul Kadir, S.H.; Miragoli, M.; Abu-Hayyeh, S.; et al. Bile acid-induced arrhythmia is mediated by muscarinic M2 receptors in neonatal rat cardiomyocytes. *PLoS One* 5, e9689 (2010).
7. Fiorucci, S.; Rizzo, G.; Donini, A.; et al. Targeting farnesoid X receptor for liver and metabolic disorders. *Trends Mol. Med.* 13, 298-309 (2007).
8. Swanson, H.I.; Wada, T.; Xie, W.; et al. Role of nuclear receptors in lipid dysfunction and obesity-related diseases. *Drug Metab. Dispos.* 41, 1-11 (2013).
9. Fiorucci, S.; Mencarelli, A.; Distrutti, E.; et al. Farnesoid X receptor: from medicinal chemistry to clinical applications. *Future Med. Chem.* 4, 877-891 (2012).
10. Fiorucci, S.; Zampella, A.; Distrutti, E. Development of FXR, PXR and CAR agonists and antagonists for treatment of liver disorders. *Curr. Top. Med. Chem.* 12, 605-624 (2012).
11. Cipriani, S.; Baldelli, F.; et al. Bile acid-activated receptors in the treatment of dyslipidemia and related disorders. *Prog. Lipid Res.* 49, 171-185 (2010).
12. Fiorucci, S.; Mencarelli, A.; Palladino, G.; et al. Bile-acid-activated receptors: targeting TGR5 and farnesoid-X-receptor in lipid and glucose disorders. *Trends Pharmacol. Sci.* 30, 570-580 (2009).

13. Inagaki, T.; Choi, M.; Moschetta, A.; et al. Fibroblast growth factor 15 functions as an enterohepatic signal to regulate bile acid homeostasis. *Cell Metab.* 2, 217-225 (2005).
14. Goodwin, B.; et al. A regulatory cascade of the nuclear receptors FXR, SHP-1, and LRH-1 represses bile acid biosynthesis. *Mol Cell.* 6, 517-526 (2000).
15. Boyer, J.L.; et al. Up-regulation of a basolateral FXR-dependent bile acid efflux transporter OSTalpha-OSTbeta in cholestasis in humans and rodents. *Am. J. Physiol. Gastrointest. Liver Physiol.* 290, G1124-G1130 (2006).
16. Owen, B.M.; Mangelsdorf, D.J.; Kliewer, S.A. Tissue-specific actions of the metabolic hormones FGF15/19 and FGF21. *Trends Endocrinol. Metab.* 26, 22-29 (2015).
17. Fiorucci, S.; Distrutti, E.; Ricci, P.; et al. Targeting FXR in cholestasis: hype or hope. *Expert Opin. Ther. Targets* 12, 1449-1459 (2014).
18. Momah, N.; Lindor, K.D. Primary biliary cirrhosis in adults. *Expert Rev. Gastroenterol. Hepatol.* 4, 427-433 (2014).
19. Mayo, M.J. Cholestatic liver disease overlap syndromes. *Clin. Liver Dis.* 2, 243-253 (2013).
20. Hirschfield, G.M.; Karlsen, T.H.; Lindor, K.D.; et al. Primary sclerosing cholangitis. *Lancet* 382, 1587-1599 (2013).
21. Ahmed, K.T.; Almashhrawi, A.A.; Rahman, R.N.; et al. Liver diseases in pregnancy: diseases unique to pregnancy. *World J. Gastroenterol.* 43, 7639-7646 (2013).
22. Rizzo, G.; et al. The farnesoid X receptor promotes adipocyte differentiation and regulates adipose cell function in vivo. *Mol. Pharmacol.* 70, 1164-1173 (2006).
23. Mencarelli, A.; et al. Dissociation of intestinal and hepatic activities of FXR and LXRA supports metabolic effects of terminal ileum interposition in rodents. *Diabetes* 62, 3384-3393 (2013).
24. Singh, R.B.; Niaz, M.A.; Ghosh, S. Hypolipidemic and antioxidant effects of *Commiphora mukul* as an adjunct to dietary therapy in patients with hypercholesterolemia. *Cardiovasc. Drugs Ther.* 4, 659-664 (1994).
25. Sinal, C.J.; Gonzalez, F.J. Guggulsterone: an old approach to a new problem. *Trends Endocrin. Met.* 13, 275-276 (2002).

26. Urizar, N.L.; Liverman, A.B.; Dodds, D.T.; et al. A natural product that lowers cholesterol as an antagonist ligand for FXR. *Science* 296, 1703-1706 (2002).
27. Wu, J.; Xia, C.; Meier, J.; et al. The hypolipidemic natural product guggulsterone acts as an antagonist of the bile acid receptor. *Mol. Endocrinol.* 16, 1590-1597 (2002).
28. Cui, J.; Huang, L.; Zhao, A.; et al. Guggulsterone is a farnesoid X receptor antagonist in coactivator association assays but acts to enhance transcription of bile salt export pump. *J. Biol. Chem.* 278, 10214-10220 (2003).
29. Szapary, P.O.; Wolfe, M.L.; Bloedon, L.T.; et al. Guggulipid for the treatment of hypercholesterolemia: a randomized controlled trial. *J. Am. Med. Assoc.* 290, 765-772 (2003).
30. Burris, T.P.; Montrose, C.; Houck, K.A.; et al. The hypolipidemic natural product guggulsterone is a promiscuous steroid receptor ligand. *Mol. Pharmacol.* 67, 948-954 (2005).
31. Meng, Q.; Chen, X.; Wang, C.; et al. Alisol B 23-acetate promotes liver regeneration in mice after partial hepatectomy via activating farnesoid X receptor. *Biochem. Pharmacol.* 92, 289-298 (2014).
32. Zou, J.; Jiang, J.; Diao, Y.-Y. ; et al. Cycloartane triterpenoids from the stems of *Schisandra glaucescens* and their bioactivity. *Fitoterapia* 83, 926-931 (2012).
33. Carter, B.A.; Taylor, O.A.; Prendergast D.R.; et al. Stigmasterol, a Soy lipid-derived phytosterol, is an antagonist of the bile acid nuclear receptor FXR. *Pediatric Research* 62, 301-306 (2007).
34. Fiorucci, S.; Distrutti, E.; Bifulco, G.; et al. Marine sponge steroids as nuclear receptor ligands. *Trends Pharmacol. Sci.* 33, 591-601 (2012).
35. De Marino, S.; Ummarino, R.; D'Auria, M.V.; et al. Theonellasterols and conicasterols from *Theonella swinhoei*. Novel marine natural ligands for human nuclear receptors. *J. Med. Chem.* 54, 3065-3075 (2011).
36. De Marino, S.; Ummarino, R.; D'Auria, M.V.; et al. 4-Methylenesterols from *Theonella swinhoei* sponge are natural pregnane-X-receptor agonists and farnesoid-X-receptor antagonists that modulate innate immunity. *Steroids* 77, 484-495 (2012).
37. Sepe, V.; Ummarino, R.; D'Auria, M.V.; et al. Conicasterol E, a small heterodimer partner sparing farnesoid X receptor modulator endowed with a

- pregnane X receptor agonistic activity, from the marine sponge *Theonella swinhoei*. *J. Med. Chem.* 55, 84-93 (2012).
38. Chini, M.G.; Jones, C.R.; Zampella, A.; et al. Quantitative NMR-derived interproton distances combined with quantum mechanical calculations of <sup>13</sup>C chemical shifts in the stereochemical determination of conicasterol F, a nuclear receptor ligand from *Theonella swinhoei*. *J. Org. Chem.* 77, 1489-1496 (2012).
39. Renga, B.; Mencarelli, A.; D'Amore, C.; et al. Discovery that theonellasterol a marine sponge sterol is a highly selective FXR antagonist that protects against liver injury in cholestasis. *PLoS One* 7, e30443 (2012).
40. Pellicciari, R.; Fiorucci, S.; Camaioni, E.; et al. 6R-ethyl-chenodeoxycholic acid (6-ECDCA), a potent and selective FXR agonist endowed with anticholestatic activity. *J. Med. Chem.* 45, 3569-3572 (2002).
41. Fiorucci, S.; Cipriani, S.; Mencarelli, A.; et al. Farnesoid X receptor agonist for the treatment of liver and metabolic disorders: focus on 6-ethyl-CDCA. *Mini-Rev. Med. Chem.* 11, 753-62 (2011).
42. Mencarelli, A.; Palladino, G.; et al. FXR activation reverses insulin resistance and lipid abnormalities and protects against liver steatosis in Zucker (*fa/fa*) obese rats. *J. Lipid Res.* 51, 771-84 (2010).
43. Fickert, P.; Fuchsichler, A.; Moustafa, T.; et al. Farnesoid X receptor critically determines the fibrotic response in mice but is expressed to a low extent in human hepatic stellate cells and periductal myofibroblasts. *Am. J. Pathol.* 175, 2392-405 (2009).
44. Verbeke, L.; Farre, R.; Trebicka, J.; et al. Obeticholic acid, a farnesoid X receptor agonist, improves portal hypertension by two distinct pathways in cirrhotic rats. *Hepatology* 59, 2286-98 (2014).
45. Mudaliar, S.; Henry, R.R.; Sanyal, A.J.; et al. Efficacy and safety of the farnesoid X receptor agonist obeticholic acid in patients with type 2 diabetes and nonalcoholic fatty liver disease. *Gastroenterology* 145, 574-82 (2013).
46. Neuschwander-Tetri, B.A.; Loomba, R.; Sanyal, A.J.; et al. Farnesoid X nuclear receptor ligand obeticholic acid for non-cirrhotic, non-alcoholic steatohepatitis (FLINT): a multicentre, randomised, placebo-controlled trial. *Lancet* S0140-6736, 61933-4 (2014).



47. Mason, A.; Luketic, V.; Lindor, K.; et al. Farnesoid-X receptor agonists: a new class of drugs for the treatment of PBC? An international study evaluating the addition of INT-747 to ursodeoxycholic acid. *J. Hepatol.* 52, S1-S2 (2010).
48. D'Amore, C.; Di Leva, F.S.; Sepe, V.; et al. Design, synthesis, and biological evaluation of potent dual agonists of nuclear and membrane bile acid receptors. *J. Med. Chem.* 57, 937-54 (2014).
49. Alemi, F.; Kwon, E.; Poole, D.P.; et al. The TGR5 receptor mediates bile acid-induced itch and analgesia. *J. Clin. Invest.* 123, 1513-30 (2013).
50. Rizzo, G.; et al. Functional characterization of the semisynthetic bile acid derivative INT-767, a dual farnesoid X receptor and TGR5 agonist. *Mol. Pharmacol.* 78, 617-630 (2010).
51. Pellicciari, R.; et al. Nongenomic actions of bile acids. Synthesis and preliminary characterization of 23- and 6,23-alkyl-substituted bile acid derivatives as selective modulators for the G-protein coupled receptor TGR5. *J. Med. Chem.* 50, 4265-4268 (2007).
52. Gege, C.; Kinzel, O.; Steeneck, C.; et al. Knocking on FXR's Door: the "hammerhead"-structure series of FXR agonists-amphiphilic isoxazoles with potent *in vitro* and *in vivo* activities. *Curr. Top. Med. Chem.* 14, 2143-58 (2014).
53. Phenex Pharmaceuticals AG. Novel FXR (NR1H4) binding and activity modulating compounds. WO 2011020615 A1 (2011).
54. Katsuma, S.; Hirasawa, A.; Tsujimoto, G. Bile acids promote glucagon-like peptide-1 secretion through TGR5 in a murine enteroendocrine cell line STC-1. *Biochem. Biophys. Res. Commun.* 1, 386-390 (2005).
55. Lieu, T.; Jayaweera, G.; Bunnett, N.W. GPBA: a GPCR for bile acids and an emerging therapeutic target for disorders of digestion and sensation. *Br. J. Pharmacol.* 171, 1156-1166 (2014).
56. Poole, D.P.; Godfrey, C.; Cattaruzza, F.; et al. Expression and function of the bile acid receptor GP-BAR1 (TGR5) in the murine enteric nervous system. *Neurogastroenterol. Motil.* 22, 814-825 (2010).
57. Bunnett, N.W. Neuro-humoral signalling by bile acids and the TGR5 receptor in the gastrointestinal tract. *J. Physiol.* 592, 2943-2950 (2014).

58. Camilleri, M.; Vazquez-Roque, M.I.; Carlson, P.; et al. Association of bile acid receptor TGR5 variation and transit in health and lower functional gastrointestinal disorders. *Neurogastroenterol. Motil.* 11, 95-99 (2011).
59. Fiorucci, S.; Cipriani, S.; Mencarelli, A.; et al. Counter-regulatory role of bile acid activated receptors in immunity and inflammation. *Curr. Mol. Med.* 6, 79-95 (2010).
60. Baghdasaryan, A.; et al. Protective role of membrane bile acid receptor TGR5 (GPBAR1) in DDC-induced sclerosing cholangitis in mice. *J. Hepatol.* 60, S197-S198 (2014).
61. Pols, T.W.H.; Noriega, L.G.; Nomura, M.; Auwerx, J.; Schoonjans, K. The bile acid membrane receptor TGR5 as an emerging target in metabolism and inflammation. *J. Hepatol.* 54, 1263–1272 (2011).
62. Watanabe, M.; Houten, S. M.; Matakai, C.; Christoffolete, M.A.; Kim, B.W.; Sato, H.; Messaddeq, N.; Harney, J.W.; Ezaki, O.; Kodama, T.; Schoonjans, K.; Bianco, A.C.; Auwerx, J. Bile acids induce energy expenditure by promoting intracellular thyroid hormone activation. *Nature* 439, 484–489 (2006).
63. Rainer, E.M.; Bissantz, C.; Gavelle, O.; Kuratli, C.; Dehmlow, H.; Richter, H.G.F.; Obst Sander, U.; Erickson, S.D.; Kim, K.; Pietranico-Cole, S.L.; Alvarez-Sánchez, R.; Ullmer, C. 2-Phenoxy-nicotinamides are Potent Agonists at the Bile Acid Receptor GPBAR1 (TGR5). *ChemMedChem* 8, 569-576, (2013).
64. Tiwari, A.; Maiti, P. TGR5: an emerging bile acid G-protein-coupled receptor target for the potential treatment of metabolic disorders. *Drug Discov. Today* 14, 523-530 (2009).
65. Fiorucci, S.; Baldelli, F. Farnesoid X receptor agonists in biliary tract disease. *Curr. Opin. Gastroenterol.* 25, 252-259 (2009).
66. Sepe, V.; Ummarino, R.; D'Auria, M.V.; Lauro, G.; Bifulco, G.; D'Amore, C.; Renga, B.; Fiorucci, S.; Zampella, A. Modification in the side chain of solomonsterol A: discovery of cholestandisulfate as a potent pregnane-X-receptor agonist. *Org. Biomol. Chem.* 10, 6350-6362 (2012).
67. Parker, H.E.; Wallis, K.; le Roux, C.W.; Wong, K.Y.; Reimann, F.; Gribble, F.M. Molecular mechanisms underlying bile acid-stimulated glucagon-like peptide-1 secretion. *Br. J. Pharmacol.* 165, 414-423 (2012).

68. Hirschfield, G.M.; et al. Efficacy of obeticholic acid in patients with primary biliary cirrhosis and inadequate response to ursodeoxycholic acid. *Gastroenterology* 148, 751-761 (2015).
69. Intercert Pharmaceuticals Inc. Preparation, uses and solid forms of obeticholic acid. WO 2013192097 A1 (2013).
70. Sato, H.; Macchiarulo, A.; Thomas, C.; Gioiello, A.; Une, M.; Hofmann, A.F.; Saladin, R.; Schoonjans, K.; Pellicciari, R.; Auwerx, J. Novel potent and selective bile acid derivatives as TGR5 agonists: biological screening, structure-activity relationships, and molecular modeling studies. *J. Med. Chem.* 51, 1831-1841 (2008).
71. Festa, C.; Renga, B.; D'Amore, C.; Sepe, V.; Finamore, C.; De Marino, S.; Carino, A.; Cipriani, S.; Monti, M.C.; Zampella, A.; Fiorucci, S. Exploitation of cholane scaffold for the discovery of potent and selective farnesoid X receptor (FXR) and G-protein coupled bile acid receptor 1 (GP-BAR1) ligands. *J. Med. Chem.* 57, 8477-8495 (2014).
72. Gioiello, A.; Macchiarulo, A.; Carotti, A.; Filipponi, P.; Costantino, G.; Rizzo, G.; Adorini, L.; Pellicciari, R. Extending SAR of bile acids as FXR ligands: discovery of 23-N-(carbocinnamyloxy)-3 $\alpha$ ,7 $\alpha$ -dihydroxy-6 $\alpha$ -ethyl-24-nor-5 $\beta$ -cholan-23-amine. *Bioorg. Med. Chem.* 19, 2650-2658 (2011).
73. Renga, B.; Cipriani, S.; Carino, A.; Simonetti, M.; Zampella, A.; Fiorucci, S. Reversal of Endothelial Dysfunction by GPBAR1 Agonism in Portal Hypertension Involves a AKT/FOXO1 Dependent Regulation of H2S Generation and Endothelin-1. *PLoS One* 10(11), e0141082 (2015).
74. Rockey, D.C. Vasoactive agents in intrahepatic portal hypertension and fibrogenesis: implications for therapy. *Gastroenterology* 118, 1261-1265 (2000).
75. Gupta, T.K.; Toruner, M.; Chung, M.K.; Groszmann, R.J. Endothelial dysfunction and decreased production of nitric oxide in the intrahepatic microcirculation of cirrhotic rats. *Hepatology* 28, 926-931 (1998).
76. Shah, V.; Haddad, F.G.; Garcia-Gardena, G.; Frangos, J.A.; Mennone, A.; Groszmann, R.J.; et al. Liver sinusoidal endothelial cells are responsible for nitric oxide modulation of resistance in hepatic sinusoids. *J. Clin. Invest.* 100, 2923-2930 (1997).

77. Distrutti, E.; Mencarelli, A.; Santucci, L.; Renga, B.; Orlandi, S.; et al. The methionine connection: homocysteine and hydrogen sulfide exert opposite effects on hepatic microcirculation in rats. *Hepatology* 47, 659–667 (2008).
78. Shah, V.; Cao, S.; Hendrickson, H.; Yao, J.; Katusic, Z.S. Regulation of hepatic eNOS by caveolin and cal-modulin after bile duct ligation in rats. *Am. J. Physiol.* 280, G1209–G1216 (2001).
79. Renga, B.; Bucci, M.; Cipriani, S.; Carino, A.; Monti, M.C.; Zampella, A.; et al. Cystationine  $\gamma$ -liase, a H<sub>2</sub>S generating enzyme, is a GPBAR1 regulated gene and contribute to vasodilation caused by secondary bile acids. *Am. J. Physiol.: Heart Circ. Physiol.* 309(1), H114-26. (2015).
80. Horowitz, J.H.; Rypins, E.B.; Henderson, J.M.; Heymsfield, S.B.; Moffitt, S.D.; Bain, R.P.; et al. Evidence for impairment of transsulfuration pathway in cirrhosis. *Gastroenterology* 81, 668–75 (1981).
81. Martin-Duce, A.; Ortiz, P.; Cabero, C.; Mato, J.M. S-Adenosyl-l-methionine synthase and phospholipid methyltransferase are inhibited in human cirrhosis. *Hepatology* 8, 65–8 (1988).
82. Stipanuk, M.H. Sulfur amino acid metabolism: pathways for production and removal of homocysteine and cysteine. *Annu. Rev. Nutr.* 24, 539–577 (2004).
83. Bosity-Westphal, A.; Petersen, S.; Hinrichsen, H.; Czech, N.; J Muller, M. Increased plasma homocysteine in liver cirrhosis. *Hepatol. Res.* 20, 28–38 (2001).
84. Renga, B.; Mencarelli, A.; Migliorati, M.; Distrutti, E.; Fiorucci, S. Bile-acid-activated farnesoid X receptor regulates hydrogen sulfide production and hepatic microcirculation. *World J. Gastroenterol.* 15, 2097–2108 (2009).
85. Renga, B.; Mencarelli, A.; D'Amore, C.; Cipriani, S.; Baldelli, F.; Zampella, A.; et al. Glucocorticoid receptor mediates the gluconeogenic activity of the farnesoid X receptor in the fasting condition. *FASEB J.* 26, 3021–3031 (2012).
86. Vassileva, G.; Golovko, A.; Markowitz, L.; Abbondanzo, S.J.; Zeng, M.; Yang, S.; et al. Targeted deletion of GP-BAR1 protects mice from cholesterol gallstone formation. *Biochem. J.* 398, 423–430 (2006).
87. Grossman, H.J.; Grossman, V.L.; Bhathal, P.S. Hemodynamic characteristics of the intrahepatic portal vascular bed over an extended flow range: a study in the isolated perfused rat liver. *Hepatology* 21, 162–168 (1995).

88. Reiter, C.E.; Kim, J.A.; Quon, M.J. Green tea polyphenol epigallocatechin gallate reduces endothelin-1 expression and secretion in vascular endothelial cells: roles for AMP-activated protein kinase, Akt, and FOXO1. *Endocrinology* 151, 103–14. (2010).
89. León, J.; Casado, J.; Jiménez Ruiz, S.M.; Zurita, M.S.; González-Puga, C.; et al. Melatonin reduces endothelin-1 expression and secretion in colon cancer cells through the inactivation of FoxO-1 and NF- $\kappa$ B. *J. Pineal Res.* 56, 415–26 (2014).
90. Wang, Y.; Zhou, Y.; Graves, D.T. FOXO transcription factors: their clinical significance and regulation. *BioMed. Res. Int.* 2014, 925350 (2014).
91. Carbajo-Pescador, S.; Mauriz, J.L.; García-Palomo, A.; González-Gallego, J. FoxO proteins: regulation and molecular targets in liver cancer. *Curr. Med. Chem.* 21, 1231–46 (2014).
92. Woods, M.; Wood, E.G.; Bardswell, S.C.; Bishop-Bailey, D.; Barker, S.; Wort, S.J.; et al. Role for nuclear factor-kappaB and signal transducer and activator of transcription 1/interferon regulatory factor-1 in cytokine-induced endothelin-1 release in human vascular smooth muscle cells. *Mol. Pharmacol.* 64, 923–31 (2003).
93. Kida, T.; Tsubosaka, Y.; Hori, M.; Ozaki, H.; Murata, T. Bile acid receptor TGR5 agonism induces NO production and reduces monocyte adhesion in vascular endothelial cells. *Arterioscler. Thromb. Vasc. Biol.* 33, 1663–169 (2013).
94. Hendrickson, H.; Chatterjee, S.; Cao, S.; Morales Ruiz, M.; Sessa, W.C.; Shah, V. Influence of caveolin on constitutively activated recombinant eNOS: insights into eNOS dysfunction in BDL rat liver. *Am. J. Physiol.: Gastrointest. Liver Physiol.* 285, G652–60 (2003).
95. Wiest, R.; Groszmann, R.J. The paradox of nitric oxide in cirrhosis and portal hypertension: too much, not enough. *Hepatology* 35, 478–91 (2002).
96. Keitel, V.; Reinehr, R.; Gatsios, P.; Rupprecht, C.; Görg, B.; Selbach, O.; et al. The G-protein coupled bile salt receptor TGR5 is expressed in liver sinusoidal endothelial cells. *Hepatology* 45, 695–704 (2007).
97. Sepe, V., Distrutti, E., Limongelli, V., Fiorucci, S. & Zampella, A. Steroidal scaffolds as FXR and GPBAR1 ligands: from chemistry to therapeutic application. *Future Med. Chem.* 7, 1109-1135 (2015).

98. Di Leva, F.S.; *et al.* Structure-based drug design targeting the cell membrane receptor GPBAR1: exploiting the bile acid scaffold towards selective agonism. *Sci Rep.* 5, 16605 (2015).
99. Sepe, V.; *et al.* Insights on FXR selective modulation. Speculation on bile acid chemical space in the discovery of potent and selective agonists. *Sci. Rep.* 6, 19008 (2016).
100. Mi, L.Z.; Devarakonda, S.; Harp, J.M.; Han, Q.; Pellicciari, R.; Willson, T.M.; Khorasanizadeh, S.; Rastinejad, F. Structural basis for bile acid binding and activation of the nuclear receptor FXR. *Mol. Cell.* 11, 1093-1100 (2003).
101. Butler, A.E.; Campbell-Thompson, M.; Gurlo, T.; Dawson, D.W.; Atkinson, M.; Butler, P.C. Marked expansion of exocrine and endocrine pancreas with incretin therapy in humans with increased exocrine pancreas dysplasia and the potential for glucagon-producing neuroendocrine tumors. *Diabetes* 62, 2595-2604 (2013).
102. Sepe, V.; Ummarino, R.; D'Auria, M.V.; Renga, B.; Fiorucci, S.; Zampella, A. The first total synthesis of solomonsterol B, a marine pregnane X receptor agonist. *Eur. J. Org. Chem.* 5187–5194 (2012).
103. Tserng, K.Y.; Klein, P.D. Formylated bile acids: improved synthesis, properties, and partial deformylation. *Steroids* 29, 635–648 (1977).
104. Schteingart, C.D.; Hofmann, A.F. Synthesis of 24-nor-5-beta-cholan-23-oic acid derivatives: a convenient and efficient one-carbon degradation of the side chain of natural bile acids. *J. Lipid Res.* 10, 1387–1395 (1988).
105. Cipriani, S.; Renga, B.; D'Amore, C.; Simonetti, M.; De Tursi, A.A.; Carino, A.; Monti, M.C.; Sepe, V.; Zampella, A.; Fiorucci, S. Impaired itching perception in murine models of cholestasis is supported by dysregulation of GPBAR1 signaling. *PLoS One* 10(7), e0129866 (2015).
106. Sherif, Z.A.; *et al.* Global Epidemiology of Nonalcoholic Fatty Liver Disease and Perspectives on US Minority Populations. *Dig. Dis. Sci.* 6, 1214–25 (2016).
107. Rosselli, M.; *et al.* The metabolic syndrome and chronic liver disease. *Curr. Pharm. Des.* 20, 5010–24 (2014).
108. Baffy, G.; Brunt, E.M.; & Caldwell S.H. Hepatocellular carcinoma in non-alcoholic fatty liver disease: an emerging menace. *J. Hepatol.* 56, 1384–1391 (2012).

109. Angulo, P.; et al. Liver fibrosis, but no other histologic features, is associated with long-term outcomes of patients with nonalcoholic fatty liver disease. *Gastroenterology* 149, 389–397 (2015).
110. Silverstein, R.L.; & Febbraio, M. CD36, a scavenger receptor involved in immunity, metabolism, angiogenesis, and behavior. *Sci. Signaling* 2, re3. doi: 10.1126/scisignal.272re3 (2009).
111. Jakulj, L.; et al. ABCG5/G8 polymorphisms and markers of cholesterol metabolism: systematic review and meta-analysis. *J. Lipid Res.* 51, 3016–23 (2010).
112. Fiorucci, S.; & Distrutti, E. Targeting the transsulfuration-H<sub>2</sub>S pathway by FXR and GPBAR1 ligands in the treatment of portal hypertension. *Pharmacol. Res.* 111, 749–756 (2016).
113. Goto, J., Sano, Y., Chikai, T., Nambara, T. Synthesis of disulfates of unconjugated and conjugated bile acids. *Chem. Pharm. Bull.* 35, 4562-4567 (1987).
114. Song, X.; et al. Mechanistic insights into isoform-dependent and species-specific regulation of bile salt export pump by farnesoid X receptor. *J. Lipid Res.* 54, 3030-3044 (2013).
115. Finamore, C.; Festa, C.; Renga, B.; Sepe, V.; Carino, A.; Masullo, D.; Biagioli, M.; Marchianò, S.; Capolupo, A.; Monti, M.C.; Fiorucci, S.; Zampella, A. Navigation in bile acid chemicals space: discovery of novel FXR and GPBAR1 ligands. *Sci. Rep.* 6, 29320 (2016).
116. Collins, S.; Barlett, S.; Nie, F.; Sore, H.F; Spring, D.R. Diversity-Oriented Synthesis of Macrocyclic Libraries for Drug Discovery and Chemical Biology. *Synthesis* 48, 1457 (2016).
117. Serba C.; Winssinger, N. Following the Lead from Nature: Divergent Pathways in Natural Product Synthesis and Diversity-Oriented Synthesis. *Eur. J. Org. Chem.* 20, 4195 (2013).
118. MacLellan, P.; Nelson, A. A conceptual framework for analysing and planning synthetic approaches to diverse lead-like scaffolds. *Chem. Commun.* 49, 2383 (2013).

119. Beckmann, H.S.G.; O'Connor, C.J.; Spring, D.R. Diversity-oriented synthesis: producing chemical tools to dissect biology. *Chem. Soc. Rev.* 41, 4444 (2012).
120. Burke, M.D.; Schreiber, S.L. A planning strategy for diversity-oriented synthesis. *Angew. Chem. Int. Ed.* 43, 46 (2004).
121. Schreiber, S.L. Target-Oriented and Diversity-Oriented Organic Synthesis in Drug Discovery. *Science* 287, 1964 (2000).
122. Lazaro, R.; Román, R.; Sedgwick, D.M.; Haufe, G.; Barrio, P.; Fustero, S. Asymmetric Synthesis of Monofluorinated 1-Amino-1,2-dihydronaphthalene and 1,3-Amino Alcohol Derivatives. *Org. Lett.* 18, 948 (2016).
123. Fustero, S.; Lazaro, R.; Aiguabella, N.; Riera, A.; Simon-Fuentes, A.; Barrio, P. Asymmetric Allylation/Pauson–Khand Reaction: A Simple Entry to Polycyclic Amines. Application to the Synthesis of Aminosteroid Analogues. *Org. Lett.* 16, 1224 (2014).
124. Fustero, S.; Lazaro, R.; Herrera, L.; Rodriguez, E.; Mateu, N.; Barrio, P. Asymmetric Allylation/Ring Closing Metathesis: One-Pot Synthesis of Benzo-fused Cyclic Homoallylic Amines. Application to the Formal Synthesis of Sertraline Derivatives. *Org. Lett.* 15, 3770 (2013).
125. Fustero, S.; Rodriguez, E.; Lazaro, R.; Herrera, L.; Catalan, S.; Barrio, P. Relay Catalysis: Enantioselective Synthesis of Cyclic Benzo-Fused Homoallylic Alcohols by Chiral Brønsted Acid-Catalyzed Allylboration/Ring Closing Metathesis. *Adv. Synth. Catal.* 355, 1058 (2013).
126. Fustero, S.; Rodriguez, E.; Herrera, L.; Asensio, A.; Maestro, M.A.; Barrio, P. Intramolecular Michael Reaction of *tert*-ButylsulfinylKetimines: Asymmetric Synthesis of 3-Substituted Indanones. *Org. Lett.* 13, 6564 (2011).
127. Barrio, P.; Ibañez, I.; Herrera, L.; Román, R.; Catalan, S.; Fustero, S. Asymmetric Synthesis of Fluorinated Isoindolinones through Palladium-Catalyzed Carbonylative Amination of Enantioenriched Benzylic Carbamate. *Chem. Eur. J.* 21, 11579 (2015).
128. Fustero, S.; Ibañez, I.; Barrio, P.; Maestro, M.A.; Catalan, S. Gold-Catalyzed Intramolecular Hydroamination of *o*-AlkynylbenzylCarbamates: A Route to Chiral Fluorinated Isoindoline and Isoquinoline Derivatives. *Org. Lett.* 15, 832 (2013).



129. Fustero, S.; Herrera, L.; Lazaro, R.; Rodriguez, E.; Maestro, M.A.; Mateu, N.; Barrio, P. Base-Dependent Stereodivergent Intramolecular Aza-Michael Reaction: Asymmetric Synthesis of 1,3-Disubstituted Isoindolines. *Chem. Eur. J.* 19, 11776 (2013).
130. Fustero, S.; Moscardó, J.; Sanchez-Roselló, M.; Rodriguez, E.; Barrio, P. Tandem Nucleophilic Addition–Intramolecular Aza-Michael Reaction: Facile Synthesis of Chiral Fluorinated Isoindolines. *Org. Lett.* 12, 5494 (2010).
131. Barrio, P.; Rodriguez, E.; Fustero, S. Recent Developments in the Chiral Brønsted Acid-catalyzed Allylboration Reaction with Polyfunctionalized Substrates. *Chem. Rec.* 16(4), 2046 (2016).
132. Villar, H.; Frings, M.; Bolm, C. Ring closing enyne metathesis: A powerful tool for the synthesis of heterocycles. *Chem. Soc. Rev.* 36, 55 (2007).
133. Rodriguez, E.; Grayson, M.N.; Asensio, A.; Barrio, P.; Houk, K.N.; Fustero, S. Chiral Brønsted Acid-Catalyzed Asymmetric Allyl(propargyl)boration Reaction of *ortho*-Alkynyl Benzaldehydes: Synthetic Applications and Factors Governing the Enantioselectivity. *ACS Catal.* 6, 2506 (2016).
134. Fustero, S.; Bello, P.; Miró, J.; Simon, A.; del Pozo, C. 1,7-Octadiene-Assisted Tandem Multicomponent Cross-Enyne Metathesis (CEYM)-Diels–Alder Reactions: A Useful Alternative to Mori’s Conditions. *Chem. Eur. J.* 18, 10991 (2012).
135. Lázaro, R.; Barrio, P.; Finamore, C.; Román, R.; Fustero, S. Homoallylic o-halobenzylamines: asymmetric diversity-oriented synthesis of benzo-fused cyclic amines. *Struct. Chem.* 28, 445-452 (2017).
136. Forman, B.M.; Goode, E.; Chen, J.; Oro, A.E.; Bradley, D.J.; Perlmann, T.; Noonan, D.J.; Burka, L.T.; McMorris, T.; Lamph, W.W.; Evans, R.M.; Weinberger, C. Identification of a nuclear receptor that is activated by farnesol metabolites. *Cell.* 81, 687-693 (1995).
137. Ogundare, M.; *et al.* Cerebrospinal fluid steroidomics: are bioactive bile acids present in brain? *J. Biol. Chem.* 285, 4666-4679 (2010).
138. Sepe, V.; *et al.* Modification on ursodeoxycholic acid (UDCA) scaffold. discovery of bile acid derivatives as selective agonists of cell-surface G-protein coupled bile acid receptor 1 (GP-BAR1). *J. Med. Chem.* 57, 7687–7701 (2014).

139. Fiorucci, S.; et al. The nuclear receptor SHP mediates inhibition of hepatic stellate cells by FXR and protects against liver fibrosis. *Gastroenterology* 127, 1497–512 (2004).
140. Fiorucci, S.; Antonelli, E.; Mencarelli, A.; Orlandi, S.; Renga, B.; Rizzo, G.; et al. The third gas: H<sub>2</sub>S regulates perfusion pressure in both the isolated and perfused normal rat liver and in cirrhosis. *Hepatology* 42, 539–548 (2005).
141. Fiorucci, S.; Distrutti, E.; Cirino, G.; Wallace, J.L. The emerging roles of hydrogen sulfide in the gastrointestinal tract and liver. *Gastroenterology* 131, 259–271 (2006).
142. Sirvent, J.A.; Foubelo, F.; Yus, M. Chiral Aminated  $\alpha$ -Methylenebenzocycloalkenes from *o*-Bromoaryl Aldehydes and Ketones. *Eur. J. Org. Chem.* 2013(12), 2461-2471 (2013).

## **ACKNOWLEDGEMENTS**

---

### **My Mentors:**



A special acknowledgement is dedicated to my mentors, Prof. Angela Zampella and Dr. Valentina Sepe, my tutor, to give me the possibility to spend these three years of doctorate in their laboratory of organic chemistry, driving me and allowing me to grow professionally. They've transmitted me their passion for the chemistry and it was a pleasure for me to work with them.



### **Santos Fustero's group:**

Another special thank is for the Prof. Santos Fustero with his research group, for welcoming me with all the availability and for making me feel so at home during that six months. In particular I want to thank my supervisor Rachel Román for her constant support and my colleagues of the Centro de Investigación Príncipe Felipe, Daniel Mark Sedgwick and Lidia Herrera Muñoz, to have helped to integrate me and for sharing with me this beautiful experience.



### **Our research group**



Moreover, I would to thank my research group, especially the Drs. Dario Masullo and Carmen Festa, which have become other than two colleagues, also good friends for me. I also thank the Prof. Maria Valeria D'Auria, Prof. Franco Zollo and the Dr. Simona De Marino, for their precious advices and for letting me to learn many things in these years. At the end, of course, I want to thank all students that I've met during my doctorate, starting from the first to the last. Everyone taught me that you never stop learning and is a piece of my heart.

**My family**

I want to thank also my beautiful family, in particular my parents, which have supported me from the beginning to the end as they have supported all the choices of my life. I can only say you an enormous “thanks”!

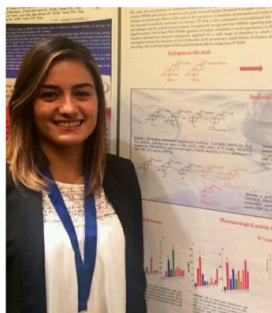
I would also thank my best friend Mara, which represents an important reference point in my life and also she’s as a sister for me.

**My boyfriend**

At last but not for importance, I would to thank my boyfriend Antonio, which is present in my life for six years and that better of any other he knows my sacrifices and has shared with me this important run.

## **CURRICULUM VITAE**

---



**Claudia Finamore**

University of Naples "Federico II"

claudia.finamore@unina.it

claudia.finamore@unina.it

Claudia Finamore obtained a Master's Degree in Pharmacy in December 2013 at the University of Naples "Federico II", Department of Pharmacy and she discussed an experimental thesis entitled: «Synthesis and pharmacological evaluation of a dual agonist of bile acid receptors GP-BAR1/FXR.»

In 2014 she entered the XXIX cycle of the PhD program in Pharmaceutical Sciences, Dept. of Pharmacy in Naples. Her research is focused on Organic Chemistry, in particular her field of interest concerns the synthesis of bile acid derivatives.

### **UNIVERSITY CAREER:**

**2014-present:** PhD student in Pharmaceutical Sciences, University "Federico II", Naples.

**April 2016-September 2016:** Training for doctorate of six months in fluorine and non fluorine chemistry at C.I.P.F (Centro de Investigación Principe Felipe, Valencia, Spain).

**2013:** Master Degree in Pharmacy (100/100 with honors).

## PUBLICATIONS

---

1. Festa, C., Renga, B., D'Amore, C., Sepe, V., Finamore, C., et al. "Exploitation of cholane scaffold for the discovery of potent and selective farnesoid X receptor (FXR) and G-protein coupled bile acid receptor 1 (GP-BAR1) ligands." *J. Med. Chem.* 57, 8477-8495 (2014).
2. Sepe, V., Renga, B., Festa, C., Finamore, C., et al. "Investigation on bile acid receptor regulators. Discovery of cholanoic acid derivatives with dual G-protein coupled bile acid receptor 1 (GPBAR1) antagonistic and farnesoid X receptor (FXR) modulatory activity." *Steroids* 105, 59-67 (2015).
3. Sepe, V., Festa, C., Renga, B., Carino, A., Cipriani, S., Finamore, C., et al. "Insights on FXR selective modulation. Speculation on bile acid chemical space in the discovery of potent and selective agonists." *Sci. Rep.* 6, 19008 (2016).
4. Finamore, C., Renga, B., Sepe, V., Carino, A., Masullo, D., Del Gaudio, F., Monti, M. C., Fiorucci, S., and Zampella, A. "Navigation in bile acid chemical space. Discovery of novel FXR and GPBAR1 ligands." *Sci. Rep.* 6, 29320 (2016).
5. Lázaro, R., Barrio, P., Finamore, C., Román, R., Fustero, S. "Homoallylic *o*-halobenzylamines: asymmetric diversity-oriented synthesis of benzo-fused cyclic amines." *Struct. Chem.* 28, 445-452 (2017).
6. De Marino, S., Carino, A., Masullo, D., Finamore, C., et al. "Hyodeoxycholic acid derivatives as liver X receptor a and G-protein-coupled bile acid receptor agonists." *Sci. Rep.* 7, 43290 (2017).

## POSTER AND ORAL COMMUNICATIONS

### Posters:

1. "Discovery of UDCA derivatives as new modulators of bile acid receptors." (XXV National Conference S.C.I., Arcavacata di Rende, 7- 12 September 2014 and International Summer School on Natural Products (ISSNP), Naples, 6-10 July 2015).
2. "Synthesis of Cholanoic acid derivatives with a dual activity on GPBAR1 and FXR receptors." (XV Edition of Sigma-Aldrich Young Chemists Symposium (S.A.Y.C.S.), Rimini, 27-29 October 2015).

### Short Oral communications:

1. "Towards FXR selectivity: manipulation of 6-ethylcholane scaffold." (XLI Edition of the "Attilio Corbella" International Summer School on Organic Synthesis, Gargnano, 12-17 June 2016).
2. "Navigation in bile acid chemical space: discovery of novel FXR and GPBAR1 modulators." (1st WG meeting MuTaLig COST Action, 19-20 November 2016, Hotel Novotel Budapest Danube, Hungary).

## Exploitation of Cholane Scaffold for the Discovery of Potent and Selective Farnesoid X Receptor (FXR) and G-Protein Coupled Bile Acid Receptor 1 (GP-BAR1) Ligands

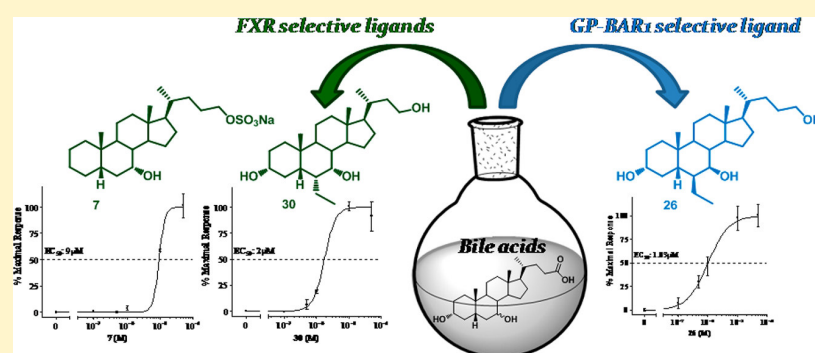
Carmen Festa,<sup>†</sup> Barbara Renga,<sup>‡</sup> Claudio D'Amore,<sup>‡</sup> Valentina Sepe,<sup>†</sup> Claudia Finamore,<sup>†</sup> Simona De Marino,<sup>†</sup> Adriana Carino,<sup>‡</sup> Sabrina Cipriani,<sup>‡</sup> Maria Chiara Monti,<sup>§</sup> Angela Zampella,<sup>\*,†</sup> and Stefano Fiorucci<sup>‡</sup>

<sup>†</sup>Department of Pharmacy, University of Naples "Federico II", Via D. Montesano 49, I-80131 Naples, Italy

<sup>‡</sup>Department of Surgery and Biomedical Sciences, Nuova Facoltà di Medicina, P.zza L. Severi, I-06132 Perugia, Italy

<sup>§</sup>Department of Pharmacy, University of Salerno, Via Giovanni Paolo II 132, I-84084, Fisciano, Salerno, Italy

**S** Supporting Information



**ABSTRACT:** Nuclear and G-protein coupled receptors are considered major targets for drug discovery. FXR and GP-BAR1, two bile acid-activated receptors, have gained increasing consideration as druggable receptors. Because endogenous bile acids often target both receptor families, the development of selective ligands has been proven difficult, exposing patients to side effects linked to an unwanted activation of one of the two receptors. In the present study, we describe a novel library of semisynthetic bile acid derivatives obtained by modifications on the cholane scaffold. The pharmacological characterization of this library led to the discovery of 7 $\alpha$ -hydroxy-5 $\beta$ -cholan-24-sulfate (7), 6 $\beta$ -ethyl-3 $\alpha$ ,7 $\beta$ -dihydroxy-5 $\beta$ -cholan-24-ol (EUDCOH, 26), and 6 $\alpha$ -ethyl-3 $\alpha$ ,7 $\alpha$ -dihydroxy-24-nor-5 $\beta$ -cholan-23-ol (NorECDCOH, 30) as novel ligands for FXR and GP-BAR1 that might hold utility in the treatment of FXR and GP-BAR1 mediated disorders.

### INTRODUCTION

Bile acids (BAs), the end-products of cholesterol catabolism, are signaling molecules activating several cellular networks<sup>1,2</sup> through the recognition of nuclear and membrane receptors. At least four members of the nuclear receptors (NRs) superfamily, the farnesoid-X-receptor (FXR), the constitutive androstane receptor (CAR), the pregnane-X- receptor (PXR), the vitamin D receptor (VDR),<sup>3–7</sup> and G-protein-coupled receptor, GP-BAR1 (also known as M-BAR, TGR5, or BG37), are activated at physiological concentrations by primary and secondary bile acids.<sup>8,9</sup>

BAs are generated in the liver as primary bile acids, cholic acid (CA) and chenodeoxycholic acid (CDCA) conjugated with glycine and taurine and then secreted in the small intestine and transformed by the intestinal microbiota into secondary bile acids, deoxycholic acid (DCA) and lithocholic acid (LCA). CDCA (1 in Figure 1) and its conjugated forms are endogenous ligands for FXR, while LCA and its corresponding

tauro- and glyco-conjugates (TLCA 2 in Figure 1) are the most potent natural agonists for GP-BAR1. The main physiological role for FXR is to function as a bile acids sensor. FXR regulates bile acids absorption, synthesis, and secretion in the intestine, liver, and kidney and is considered a promising target in cholestasis, a liver disorder that occurs primarily in the context of genetic mutation of basolateral or apical membrane transporters in hepatocytes.<sup>10</sup> Cholestasis represents the main biochemical feature of primary biliary cirrhosis<sup>11,12</sup> (PBC) and sclerosing cholangitis (PSC), two immune-mediated disorders characterized by progressive bile duct destruction for which medical therapy is still poorly effective.<sup>11,12</sup> In this context, the use of endogenous bile acids, with the exception of ursodeoxycholic acid (UDCA), is poorly effective due to their toxicity and for their promiscuity in activating G-protein-

**Received:** June 27, 2014

**Published:** September 23, 2014

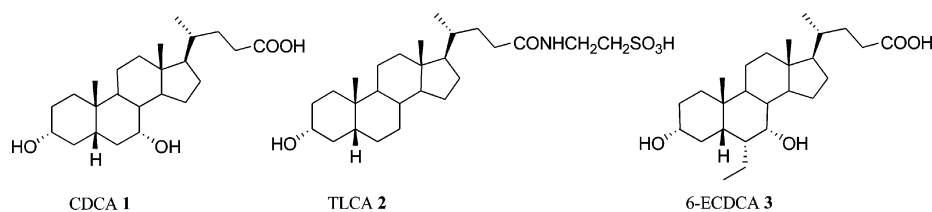


**Figure 1.** CDCA and TLCA, the most potent endogenous activators of FXR and GP-BAR1, respectively. 6-ECDCA, a potent semisynthetic dual agonist.

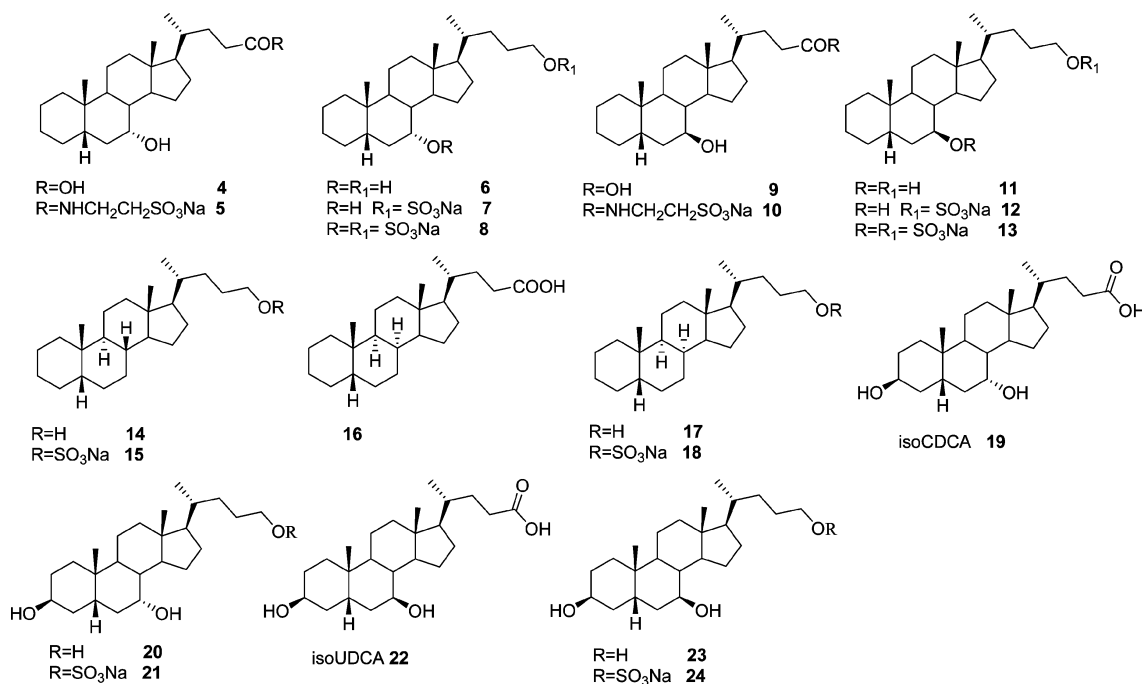


**Figure 2.** Natural bile acid derivatives generated in this study.

coupled receptors, including GP-BAR1. Although GP-BAR1 agonists represent a novel opportunity in the treatment of enterohepatic and metabolic disorders such as nonalcoholic steatohepatitis (NASH) and type 2 diabetes,<sup>2,13,14</sup> a recent study has provided evidence that this receptor is the physiological mediator of pruritus,<sup>15</sup> a common symptom observed in cholestasis and a highly frequent side effect occurring in clinical trials<sup>16</sup> in PBC patients administered with 6 $\alpha$ -ethyl-chenodeoxycholic acid (6-ECDCA, obeticholic acid, **3** in Figure 1), a dual FXR and GP-BAR1 ligand.<sup>17,18</sup> Thus, it can be predicted that highly selective FXR agonists, devoid of GP-BAR1 agonism, will avoid this side effect and might have utility in the treatment of PBC.

On the other hand, selective GP-BAR1 ligands hold utility in the treatment of metabolic disorders through their ability to trigger the release of glucagon-like peptide (GLP)-1, an insulinotropic and antidiabetic hormone.

In this frame, bile acid scaffold has been subjected to intense medicinal chemistry modifications, producing several derivatives with different pharmacological profile, ranging from dual modulators to selective agonists toward FXR and GP-BAR1. In detail, the introduction of an ethyl at C-6 on the CDCA ring B has produced potent dual agonists. Structure–activity analysis has demonstrated that this change retains its potent effect and is not modulated by changes in the side chain. Indeed,

harnessing the carboxyl group of 6-ECDCA by the introducing a sulfate group at position 23 or at position 24 on a shortened side chain increases the potency toward both FXR and GP-BAR1.<sup>18,19</sup> In contrast, a marked selectivity toward GP-BAR1 over FXR has been achieved with the methylation at C-23 position.<sup>20</sup> Interestingly, the removal of the hydroxyl group at C-3 on CDCA scaffold impacts on bile acid receptor selectivity generating a derivative, 3-deoxy-CDCA, that still transactivates FXR but is devoid of any activity toward GP-BAR1.<sup>21</sup> The same pattern was observed by modifying the hydroxyl group at C-3 on LCA or its tauro-conjugated **2**. Indeed, removal or isomerization (iso-LCA) of the 3R-hydroxyl group as well as its substitution with a sulfate moiety robustly attenuates the agonistic activity on GP-BAR1.<sup>21</sup>

In the present report, we describe the generation of a novel family of selective FXR and GP-BAR1 ligands based on the UDCA and CDCA scaffolds. Specifically, we have harnessed around the functionality of tetracyclic core, including a speculation on the stereochemistry of ring junctions, and on the functional groups on the side chain, to obtain a novel library of steroidal derivatives (Figure 2).

Our investigation was also expanded on the 6-ethylcholane scaffold, providing evidence that the stereochemical arrangement of ring B substituents as well as the length and the nature of the end group on the side chain (Figure 3) allow modulation



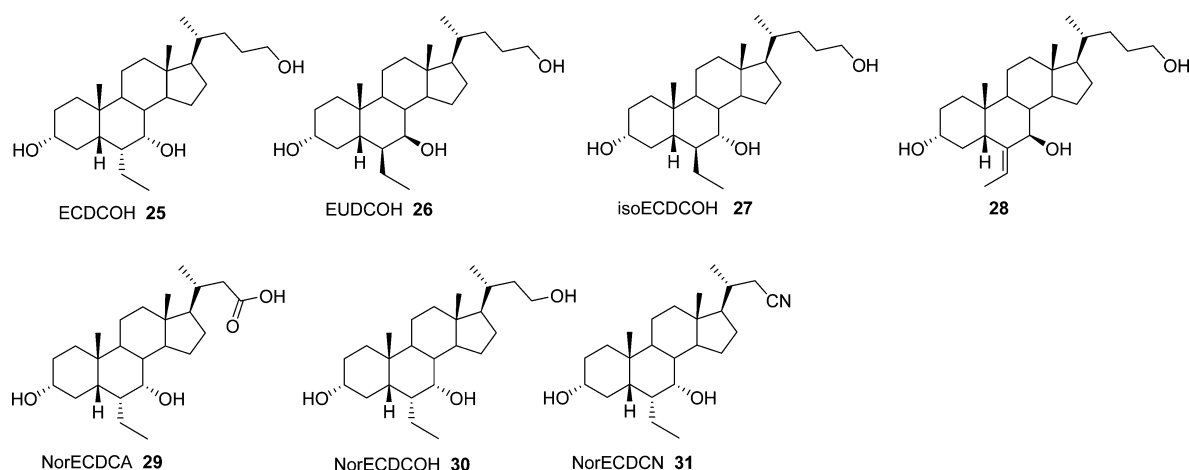
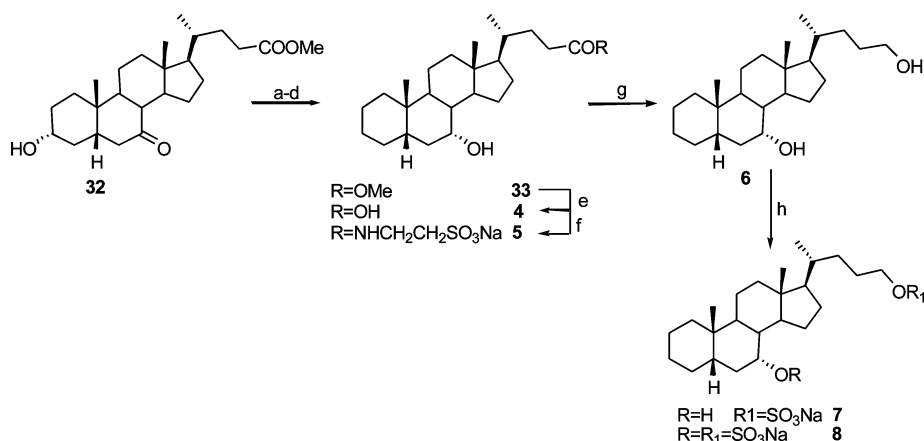


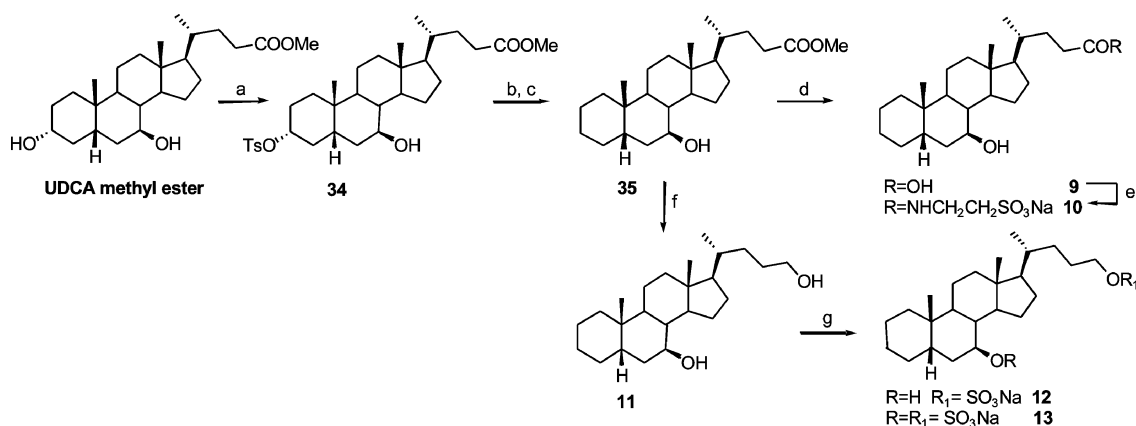
Figure 3. 6-Ethylcholane scaffold derivatives generated in this study.

### Scheme 1. 3-Deoxy-chenocholane Derivatives<sup>a</sup>

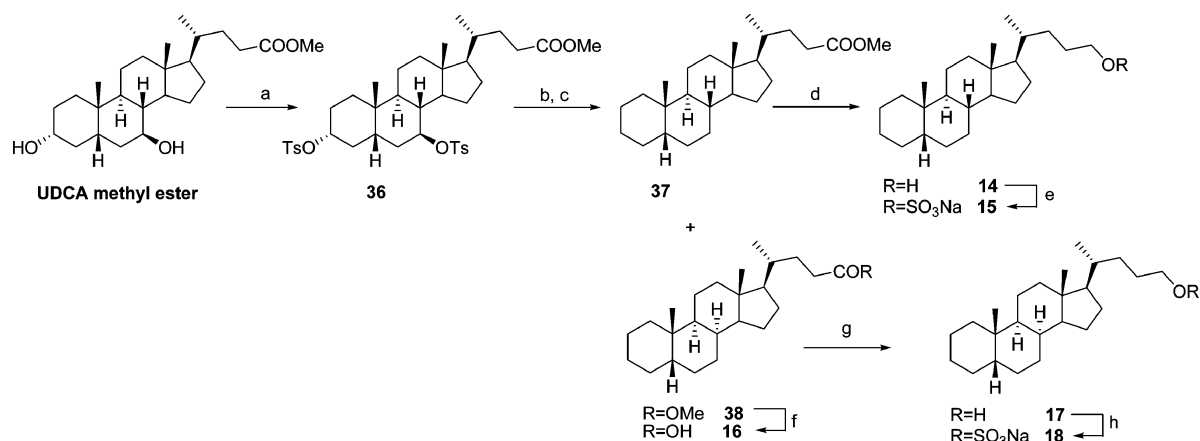


<sup>a</sup>Reagents and conditions: (a) *p*-TsCl, pyridine; (b) LiBr, Li<sub>2</sub>CO<sub>3</sub>, DMF, reflux; (c) H<sub>2</sub> (1 atm), Pd/C, THF/MeOH 1:1; (d) NaBH<sub>4</sub>, THF/H<sub>2</sub>O 4:1 v/v, quantitative yield over four steps; (e) NaOH 5% in MeOH/H<sub>2</sub>O 1:1 v/v, quantitative yield; (f) DMT-MM, Et<sub>3</sub>N, taurine, DMF dry, 35%; (g) LiBH<sub>4</sub>, MeOH dry, THF, 0 °C, 79%; (h) Et<sub>3</sub>N-SO<sub>3</sub>, DMF, 80 °C.

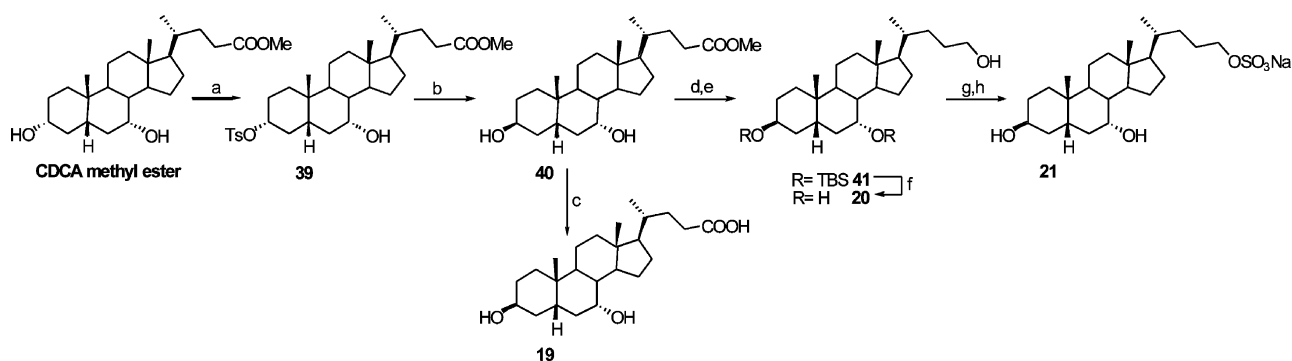
### Scheme 2. 3-Deoxy-ursocholane Derivatives<sup>a</sup>



<sup>a</sup>Reagents and conditions: (a) *p*-TsCl, pyridine, 58%; (b) LiBr, Li<sub>2</sub>CO<sub>3</sub>, DMF, reflux, quantitative yield; (c) H<sub>2</sub> (1 atm), Pd/C, THF/MeOH 1:1, 78%; (d) NaOH 5% in MeOH/H<sub>2</sub>O 1:1 v/v, quantitative yield; (e) DMT-MM, Et<sub>3</sub>N, taurine, DMF dry, 27%; (f) LiBH<sub>4</sub>, MeOH dry, THF, 0 °C, 91%; (g) Et<sub>3</sub>N-SO<sub>3</sub>, DMF, 80 °C.

Scheme 3.  $5\beta$ -Cholane Derivatives<sup>a</sup>

<sup>a</sup>Reagents and conditions: (a) *p*-TsCl, pyridine, quantitative yield; (b) LiBr, Li<sub>2</sub>CO<sub>3</sub>, DMF, reflux, quantitative yield; (c) H<sub>2</sub> (1 atm), Pd/C, THF/MeOH 1:1; (d) NaOH 5% in MeOH/H<sub>2</sub>O 1:1 v/v, 84%; (e) DMT-MM, Et<sub>3</sub>N, taurine, DMF dry, 23%; (f) NaOH 5% in MeOH/H<sub>2</sub>O 1:1 v/v, 78%; (g) LiBH<sub>4</sub>, MeOH dry, THF, 0 °C, 78%; (g) Et<sub>3</sub>N·SO<sub>3</sub>, DMF, 80 °C, 43%.

Scheme 4.  $3\beta$ -Chenodeoxycholate Derivatives<sup>a</sup>

<sup>a</sup>Reagents and conditions: (a) *p*-TsCl, pyridine, quantitative yield; (b) CH<sub>3</sub>COOK, DMF; H<sub>2</sub>O 5:1, reflux, 75%; (c) NaOH 5% in MeOH/H<sub>2</sub>O 1:1 v/v, 89%; (d) 2,6-lutidine, *t*-butyldimethylsilyltrifluoromethanesulfonate, CH<sub>2</sub>Cl<sub>2</sub>, 0 °C; (e) LiBH<sub>4</sub>, MeOH dry, THF, 0 °C, 84% over two steps; (f) HCl 37%, MeOH, 96%; (g) Et<sub>3</sub>N·SO<sub>3</sub>, DMF, 80 °C; (h) HCl 37%, MeOH, 76% over two steps.

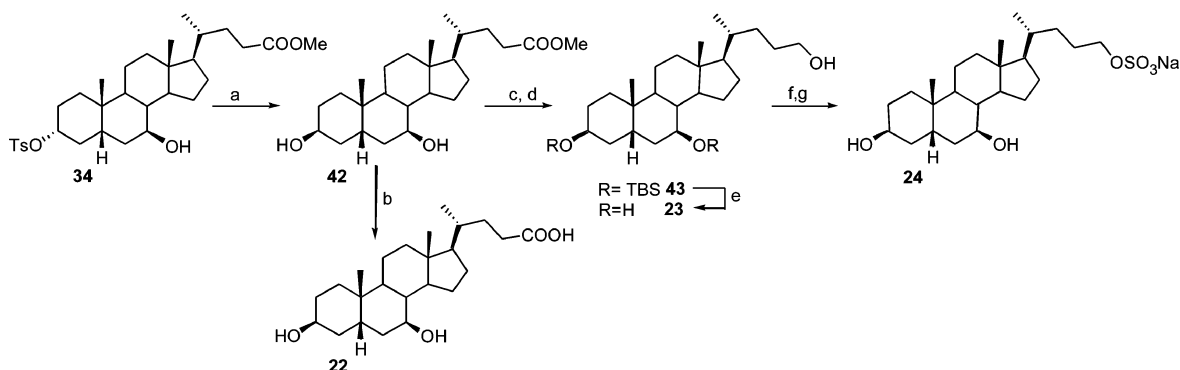
of the specificity toward FXR and GP-BAR1. Deep pharmacological investigations resulted in the identification of several compounds as potent and selective bile acid receptor agonists.

## RESULTS

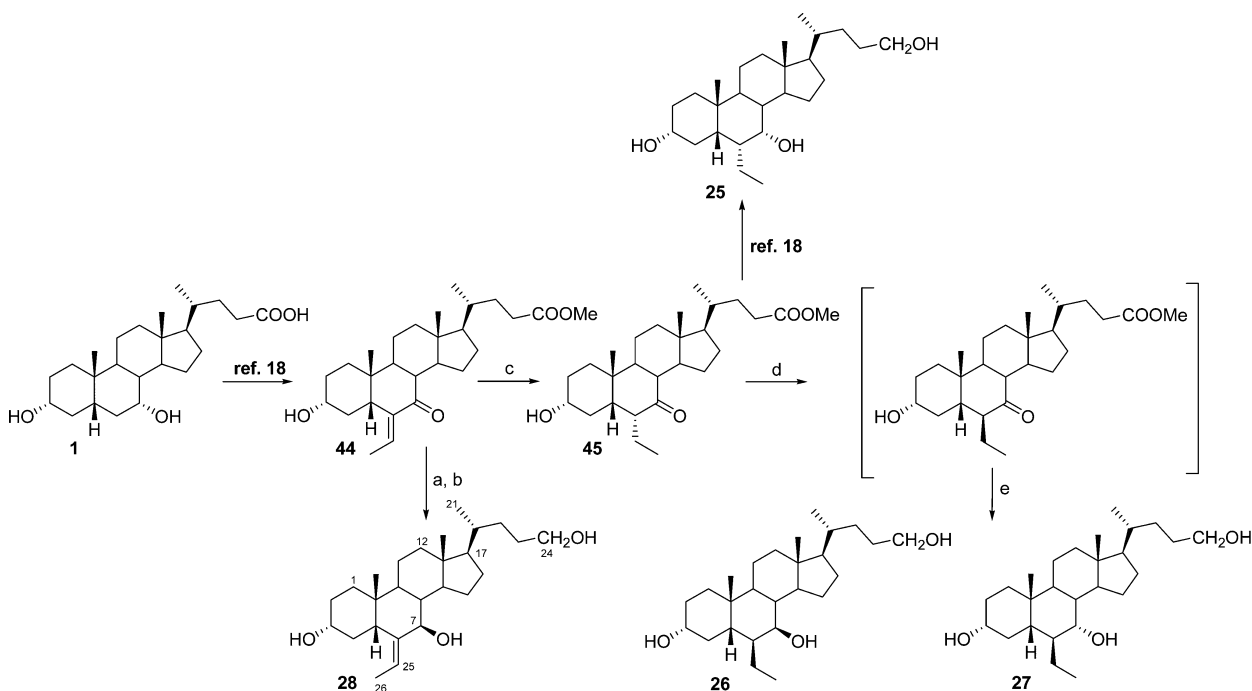
**Modification on CDCA: Preparation of 3-Deoxy-chenocholane Derivatives.** As previously described, regioselective CDCA oxidation followed by methylation furnished methyl ester 32 in quantitative yield.<sup>18</sup> Tosylation and elimination at C-3 hydroxyl group followed by double bond reduction and subsequent sodium borohydride treatment gave methyl 3-deoxy-cholanoate 33 in quantitative chemical yield over four steps (Scheme 1). Alkaline hydrolysis furnished 3-deoxy-cholanoic acid (4) in quantitative chemical yield, that in a small aliquot was subjected to the reaction of amidation with taurine.<sup>22</sup> Purification on RP-18 column followed by HPLC furnished 5 in pure form and as sodium salt. An aliquot of methyl ester 33 was transformed in the corresponding C-24 alcohol 6 (LiBH<sub>4</sub>, MeOH/THF) that in turn was subjected to sulfation (Et<sub>3</sub>N·SO<sub>3</sub> 1.5 equiv), affording a mixture of disulfate derivative 8 and side chain monosulfate derivative 7 that was efficiently separated by HPLC.

**Modification on UDCA: Preparation of 3-Deoxy-ursocholane Derivatives.** UDCA methyl ester treatment with 1.5 equiv of tosyl chloride resulted in a mixture of 3- and 7-monotosyl derivatives that was efficiently separated by silica gel column, affording pure 34 in 58% yield. Following the same synthetic protocol described before for the corresponding cheno-derivative, derivatives 9–13 (Scheme 2) were obtained in high chemical yield.

**$5\beta$ -Cholane Derivatives.** UDCA methyl ester was ditosylated at C-3 and C-7 hydroxyl groups, furnishing intermediate 36 that was subjected to LiBr/Li<sub>2</sub>CO<sub>3</sub> treatment to achieve the double elimination on ring A and ring B (Scheme 3). Hydrogenation (H<sub>2</sub>, Pd/C, THF/MeOH) on the crude reaction product furnished a mixture of the saturated methyl esters 37 and 38, epimers at C-8 and generated through the attack of hydrogen on the up and down face of  $\Delta^7$  double bond, respectively. Treatment of  $5\beta$ -cholane methyl ester 37 with LiBH<sub>4</sub> and then with Et<sub>3</sub>N·SO<sub>3</sub> furnished alcohol 14 and its sulfate derivative 15. C-8 epimer 38 was subjected to the same synthetic protocol, including also basic hydrolysis of methyl ester function, obtaining acid carboxylic derivative 16, alcohol 17, and the corresponding sulfate derivative 18.

Scheme 5.  $3\beta$ -Ursodeoxycholate Derivatives<sup>a</sup>

<sup>a</sup>Reagents and conditions: (a)  $\text{CH}_3\text{COOK}$ , DMF;  $\text{H}_2\text{O}$  5:1, reflux, 82%; (b)  $\text{NaOH}$  5% in  $\text{MeOH}/\text{H}_2\text{O}$  1:1 v/v, 87%; (c) 2,6-lutidine, *t*-butyldimethylsilyltrifluoromethanesulfonate,  $\text{CH}_2\text{Cl}_2$ , 0 °C, 96%; (d)  $\text{LiBH}_4$ ,  $\text{MeOH}$  dry, THF, 0 °C, 94% over two steps; (e)  $\text{HCl}$  37%,  $\text{MeOH}$ , 96%; (f)  $\text{Et}_3\text{N}\cdot\text{SO}_3$ , DMF, 80 °C; (g)  $\text{HCl}$  37%,  $\text{MeOH}$ , 67% over two steps.

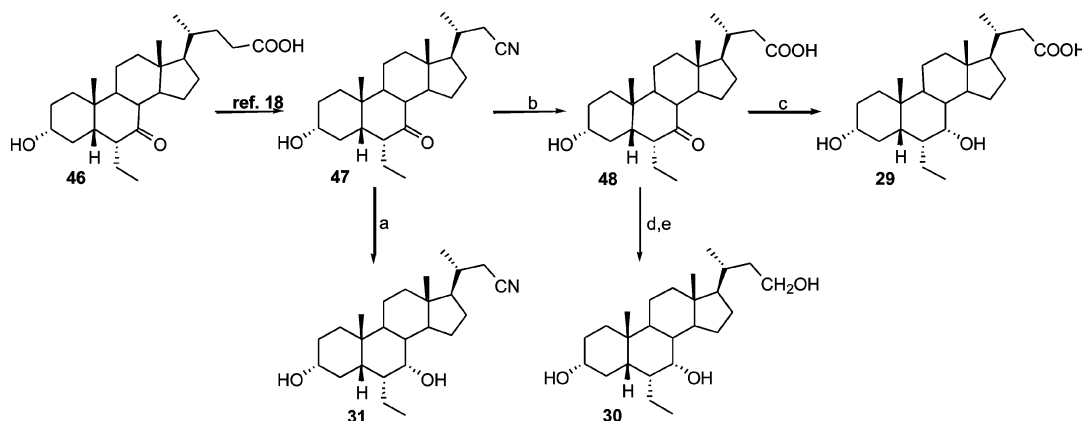
Scheme 6. Modification on Ring B of 6-Ethylcholate Scaffold<sup>a</sup>

<sup>a</sup>Reagents and conditions: (a)  $\text{NaBH}_4$ ,  $\text{MeOH}$ ; (b)  $\text{LiBH}_4$ ,  $\text{MeOH}$  dry, THF, 0 °C, 85% over two steps; (c)  $\text{H}_2$  (1 atm),  $\text{Pd}/\text{C}$ , THF/ $\text{MeOH}$  1:1; (d)  $\text{NaBH}_4$ ,  $\text{MeOH}$ ; (e)  $\text{LiBH}_4$ ,  $\text{MeOH}$  dry, THF, 0 °C.

**Preparation of  $3\beta$ -Chenodeoxycholate and  $3\beta$ -Ursodeoxycholate Derivatives.** Regioselective tosylation at C-3 hydroxyl group on CDCA methyl ester followed by inversion of configuration with potassium acetate in DMF/ $\text{H}_2\text{O}$  (Scheme 4) afforded the  $3\beta$ -hydroxy derivative 40 in 74% over two steps. Hydrolysis at C-24 methyl ester gave isoCDCA (19), whereas protection at C-3 and C-7 carbinols and then reduction at C-24 methyl ester furnished the protected intermediate 41. Sulfation and then deprotection afforded monosulfate derivative 21 whereas direct deprotection gave isoCDCOH (20).

As depicted in Scheme 5, the corresponding  $3\beta$ -ursodeoxycholate derivatives 22–24 were prepared starting from methyl ester 34 and following the same synthetic protocol reported in Scheme 4.

**Modification on 6-Ethylcholate Scaffold.** As previously demonstrated, the introduction of an  $\alpha$ -ethyl group at C-6 on CDCA ring B profoundly improves the activity of the endogenous bile acid, producing 6-ECDCA (3, in Figure 1), a potent dual FXR/GP-BAR1 agonist. Even if also the corresponding  $7\beta$ -isomer,  $6\alpha$ -ethylUDCA, was proved to be effective in fibrosis, to data analysis on the effect produced in term of biological activity and selectivity by the modification in the configuration of ring B substituents has not been faced. Moreover starting from the well demonstrated ability of bile alcohols to activate FXR, also the modification on carboxyl group of 6-ECDCA could be instrumental in generating selective modulators. Thus, an intense medicinal chemistry protocol was also performed on 6-ethylcholate scaffold.

Scheme 7. Modification on the Side Chain of 6 $\alpha$ -Ethylcholan Scaffold<sup>a</sup>

<sup>a</sup>Reagents and conditions: (a) LiBH<sub>4</sub>, MeOH dry, THF, 0 °C, 79%; (b) KOH 30% in MeOH/H<sub>2</sub>O 1:1 v/v, 2 h; (c) LiBH<sub>4</sub>, MeOH dry, THF, 0 °C, 89%; (d) *p*-TsOH, MeOH dry; (e) LiBH<sub>4</sub>, MeOH dry, THF, 0 °C, 98% over two steps.

An aliquot of **44**, prepared in a 77% yield starting from CDCA,<sup>18</sup> was subjected to NaBH<sub>4</sub> reduction at C-7 ketone followed by treatment with LiBH<sub>4</sub> to afford triol **28** in good chemical yield (Scheme 6). Interestingly, sodium borohydride treatment on **44** proceeded in a stereoselective manner, affording the exclusive formation of 7 $\beta$ -hydroxyl derivative as judged by the shape of H-7 as a doublet ( $J = 9.8$  Hz) which is consistent with an axial disposition for this proton, and therefore with the  $\beta$ -orientation of the hydroxyl group on ring B. Dipolar couplings H-7/H-25 and Me-26/H-5 in the NOESY spectrum allowed definition the *E* configuration for the exocyclic double bond as depicted in **28**.

Exocyclic double bond hydrogenation (H<sub>2</sub> on Pd/C) on **44** afforded **45** in quantitative yield that was transformed in the compound **25** following the synthetic procedure previously described.<sup>18</sup> In agreement with the steric influence played by the ethyl group at C-6 and by the ring A, both oriented on the  $\alpha$ -face of ring B, and as demonstrated by the shape of H-7 signal as a singlet, NaBH<sub>4</sub> treatment on free carboxyl acid proceeded in a stereoselective manner, affording the exclusive formation of 6 $\alpha$ -ethyl-3 $\alpha$ ,7 $\alpha$ -dihydroxy-5 $\beta$ -cholan-24-ol (ECD-COH, **25**) through the approach of the hydride from the upper-face of the steroid nucleus. The stereochemical assignment reported for **25** was substantiated by the almost complete superimposition of proton resonances of all nuclei belonging to the tetracyclic nucleus with those reported for **3**.<sup>18,23</sup>

To access C-6 and/or C-7 epimers of compound **25**, we devised an alternative synthetic procedure encompassing NaBH<sub>4</sub> treatment on methyl ester **45** and then LiBH<sub>4</sub>. As depicted in Scheme 6, prolonged NaBH<sub>4</sub> treatment in methanol produced extensive C-6 epimerization and partial reduction at C-7 carbonyl group. LiBH<sub>4</sub> reduction on the crude reaction product afforded a mixture whose HPLC purification (88% MeOH:H<sub>2</sub>O) gave pure 6 $\beta$ -ethyl derivatives **26** and **27**, epimeric at C-7 in a 69/31 ratio. Structural and stereochemical characterization on 6 $\beta$ -ethyl-3 $\alpha$ ,7 $\alpha$ -dihydroxy-5 $\beta$ -cholan-24-ol (isoECDCOH, **27**) was based on careful comparison of NMR data with those of **25** (Supporting Information, Tables S1 and S2).

As in **25**, H-7 proton in **27** resonated as a singlet ( $\delta_{\text{H}}$  3.60), thus establishing the equatorial disposition for this proton and therefore the  $\alpha$ -configuration of the hydroxyl group at C-7. The remaining resonances in the <sup>1</sup>H NMR spectra of **25** and **27**

were almost similar in the shape and in the chemical shift values, with the exception of the down-field shifted signals for H<sub>2</sub>-4 ( $\delta_{\text{H}}$  2.30, 1.55 in **27** vs  $\delta_{\text{H}}$  1.88, 1.73 in **25**) and for Me-26 ( $\delta_{\text{H}}$  0.95 in **27** vs 0.90 in **25**), which suggested the inverted configuration at C-6 in **27**.

The <sup>13</sup>C NMR spectrum of **27** (Supporting Information, Table S2), interpreted with the help of HSQC and HMBC experiments, confirmed this hypothesis, revealing a profound modification in the chemical shift of several carbon centers around C-6 (i.e., C-4  $\delta_{\text{C}}$  41.4 in **27** vs 34.3 in **25**; C-6  $\delta_{\text{C}}$  51.7 in **27** vs 42.9 in **25**; C-8  $\delta_{\text{C}}$  36.4 in **27** vs 41.3 in **25**).

In the <sup>1</sup>H NMR spectrum of 6 $\beta$ -ethyl-3 $\alpha$ ,7 $\beta$ -dihydroxy-5 $\beta$ -cholan-24-ol (EUDCOH, **26**), H-7 was observed as a doublet ( $\delta_{\text{H}}$  3.74, dd,  $J = 10.3, 6.0$  Hz) with a large coupling constant with H-8, thus pointing toward their *trans* diaxial relationship and therefore to the  $\beta$ -orientation of the hydroxyl group at C-7. ROESY cross-peaks H-7/H-9, H-7/H-14, and H-7/H-6 confirmed the inversion of configuration at C-7 and also suggested the *cis* stereochemical arrangement of the substituents at C-6 and C-7. Definitive confirmation of the  $\beta$ -orientation of the ethyl group at C-6 derived from the observed good match in the carbon resonances of all ring A nuclei with those of compound **27** (Supporting Information, Table S2).

Next, we turned our attention to 6-ECDC side chain, investigating also the effect of the length and the functional group on bile acid receptor selectivity (Scheme 7).

3 $\alpha$ -Hydroxy-6 $\alpha$ -ethyl-7-keto-5 $\beta$ -cholan-24-oic acid (**46**) was subjected to Beckmann degradation at C-24 as previously described,<sup>18</sup> and the resulting nor-nitrile **47** was subjected to LiBH<sub>4</sub> reduction at C-7 carbonyl group, affording 6 $\alpha$ -ethyl-3 $\alpha$ ,7 $\alpha$ -dihydroxy-24-*nor*-5 $\beta$ -cholan-23-nitrile (NorECD-CN, **31**) in high yield and as a single diastereoisomer (HPLC purity >95%).

Nor-nitrile **47** was used also as starting material in the preparation of NorECDCA (**29**) and the corresponding alcohol, NorECDCOH (**30**). Prolonged alkaline hydrolysis afforded carboxylic acid **48** that was in turn subjected to LiBH<sub>4</sub> reduction at C-7. Purification by silica gel (CH<sub>2</sub>Cl<sub>2</sub>:MeOH 9:1) gave NorECDCA (**29**) as a white solid in 89% chemical yield. Methyl ester formation on intermediate **48**, followed by simultaneous reduction at C-23 methyl ester function and at C-7 carbonyl group, furnished **30** in 98% yield. In this case, no epimerization at C-6 was observed and all attempts to obtain

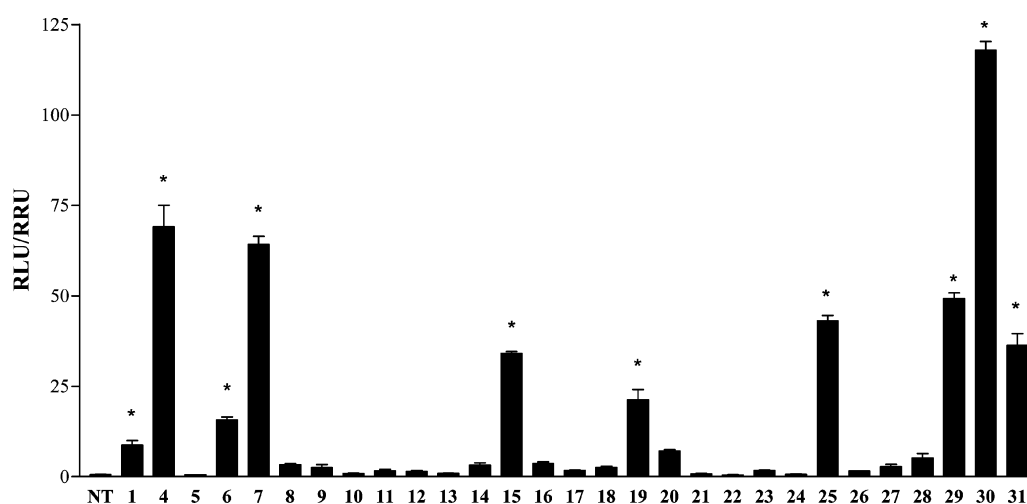


**Figure 4.** Transactivation assays on FXR. HepG2 cells were transfected with pSG5-FXR, pSG5-RXR, pCMV- $\beta$ gal, and p(hsp27)TKLUC vectors. Cells were stimulated with compounds 4–31 (10  $\mu$ M). CDCA (1, 10  $\mu$ M) was used as a positive control. Results are expressed as mean  $\pm$  standard error; \* $p$  < 0.05 versus not treated cells (NT).

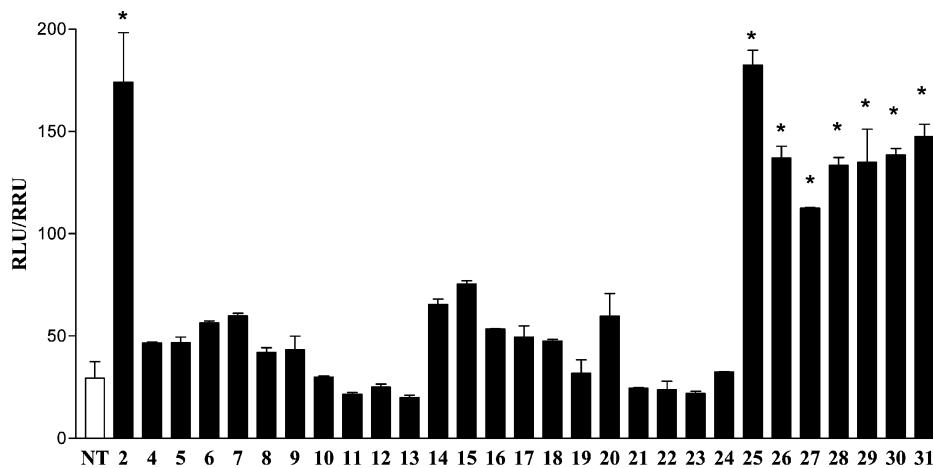


**Figure 5.** Transactivation assays on GP-BAR1. HEK-293T cells were cotransfected with GP-BAR1 and a reporter gene containing a cAMP responsive element in front of the luciferase gene. Twenty-four h post transfection, cells were stimulated with 4–31 (10  $\mu$ M). Luciferase activity served as a measure of the rise in intracellular cAMP following activation of GP-BAR1. TLCA (2, 10  $\mu$ M) was used as a positive control. Results are expressed as mean  $\pm$  standard error. \* $p$  < 0.05 versus not treated cells (NT).

alternative stereochemical arrangements of the substituents at C-6 and C-7 on *nor* 6-ethylcholane scaffold failed, producing invariably the 6 $\alpha$ -ethyl-7 $\alpha$ -hydroxy relationship.

**Pharmacological Evaluation.** Derivatives 4–31 were tested for their activity on FXR and GP-BAR1. For this purpose, we used a luciferase reporter assay with HepG2 and HEK-293T cells transfected with FXR and GP-BAR1, respectively (Figures 4 and 5).

Results shown in Figures 4 and 5 demonstrated that several compounds generated in this study were potent agonists for FXR or GP-BAR1. As reported in Figure 4, we found that the deletion of the hydroxyl group at C-3 in the CDCA scaffold produces potent and selective FXR agonists.

In detail, with the exception of the 7,24-disulfate derivative 8, all the 3-deoxy-chenocholane derivatives maintain the ability to transactivate FXR independently from the functional group at C-24 on the side chain (COOH in 4, CH<sub>2</sub>OH in 6, and CH<sub>2</sub>OSO<sub>3</sub><sup>-</sup> in 7). Tauro conjugation of the carboxyl group on the side chain completely abolishes the agonism on FXR

(compare 5 versus 4 in Figure 4) and thus eradicates the therapeutic potential of derivative 4 in FXR mediated diseases. Interestingly, the substitution of carboxyl end group with a nonconjugable functional group such as the sulfate group produces the equipotent derivative 7, devoid of any GP-BAR1 activity (Figure 5), as a promising selective FXR agonist.

As expected, the corresponding urso-derivatives 9–13, all sharing the  $\beta$ -configuration at the C-7 hydroxyl group, were inactive toward FXR, thus demonstrating, once again, that the configuration at C-7 is a key structural feature in FXR recognition. Even if the sulfate derivative 15 showed a potency comparable to that of CDCA, the endogenous ligand of FXR, the general trend observed for 5 $\beta$ -cholane derivatives 14–18 demonstrates that the elimination of the hydroxyl group at C-7 is detrimental for FXR (compare 14 versus 6, and 15 versus 7) activity.

The modification in B/C ring junction produces derivatives 16–18, devoid of any activity toward FXR, thus confirming the

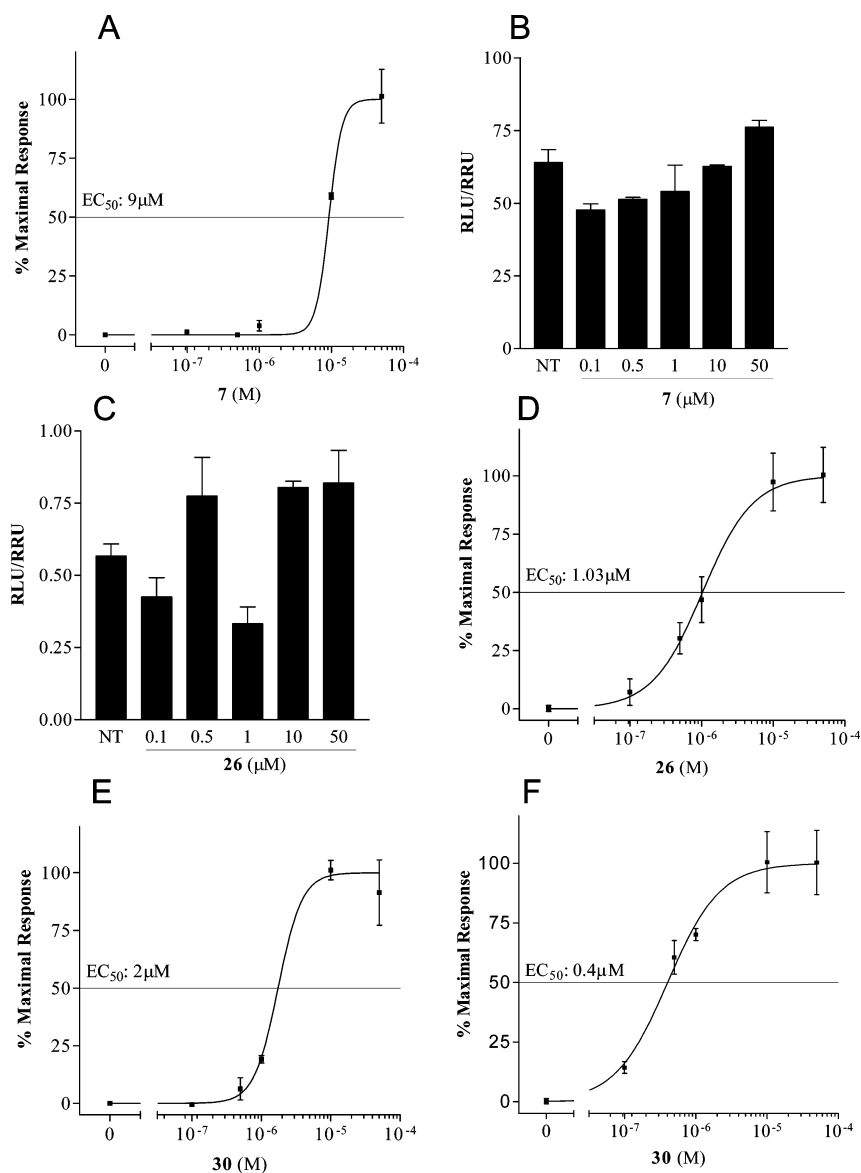


**Figure 6.** Concentration–response curve of **7**, **26**, and **30** on FXR (A,C,E) and GP-BAR1 (B,D,F). FXR transactivation was measured in a luciferase reporter assay using HepG2 cells transfected with FXR. GP-BAR1 activity was measured in HEK-293T cells cotransfected with GP-BAR1 and a reporter gene containing a cAMP responsive element in front of the luciferase gene (CRE). Twenty-four h post transfection, cells were stimulated with increasing concentrations of each agent: range from 100 nM to 50 μM. Results are expressed as mean ± standard error. \**p* < 0.05 versus not treated cells (NT).

profound impact engaged by bile acid molecular shape in fitting in FXR-LBD.

Of interest are also the results of epimerization at position C-3. As shown in Figure 4, isochenodeoxycholic acid (isoCDCA, **19**) is more potent than the cognate CDCA in transactivating FXR. This result, along with the well-known bile acids epimerization at C-3 occurring in the intestine by bacterial enzymes, open the way to further pharmacological speculation on isoCDCA as FXR modulator.

Results of transactivations of CREB-responsive elements in HEK-293T transiently transfected with the membrane bile acid receptor GP-BAR1 (Figure 5) revealed that, independently by the functional group on the side chain, the elimination/epimerization of the hydroxyl groups on the tetracyclic core of

5β-cholane scaffold is detrimental in terms of activation of GP-BAR1 (compounds **4–24** in Figure 5).

Profoundly different were the results on 6-ethylcholane derivatives **25–31**. As shown in Figures 4 and 5, the analysis of the biological results for the compounds in this subset indicates that the C-6 and C-7 configuration represents a key structural feature for FXR activity, whereas it is in-influent in terms of GP-BAR1 activity. Indeed, C-24 side chain alcohols **26–28** resulted potent and selective membrane bile acid receptor agonists, whereas derivative **25**, with both ethyl and the hydroxyl groups on ring B α-oriented, is a dual agonist. Of interest, NorECDCOH (**30**), the corresponding *nor*-derivative of **25**, shows a residual GP-BAR1 activity but represents the most potent FXR agonist generated in this study. The specificity of **30** is completely reverted by the replacement of the C-23

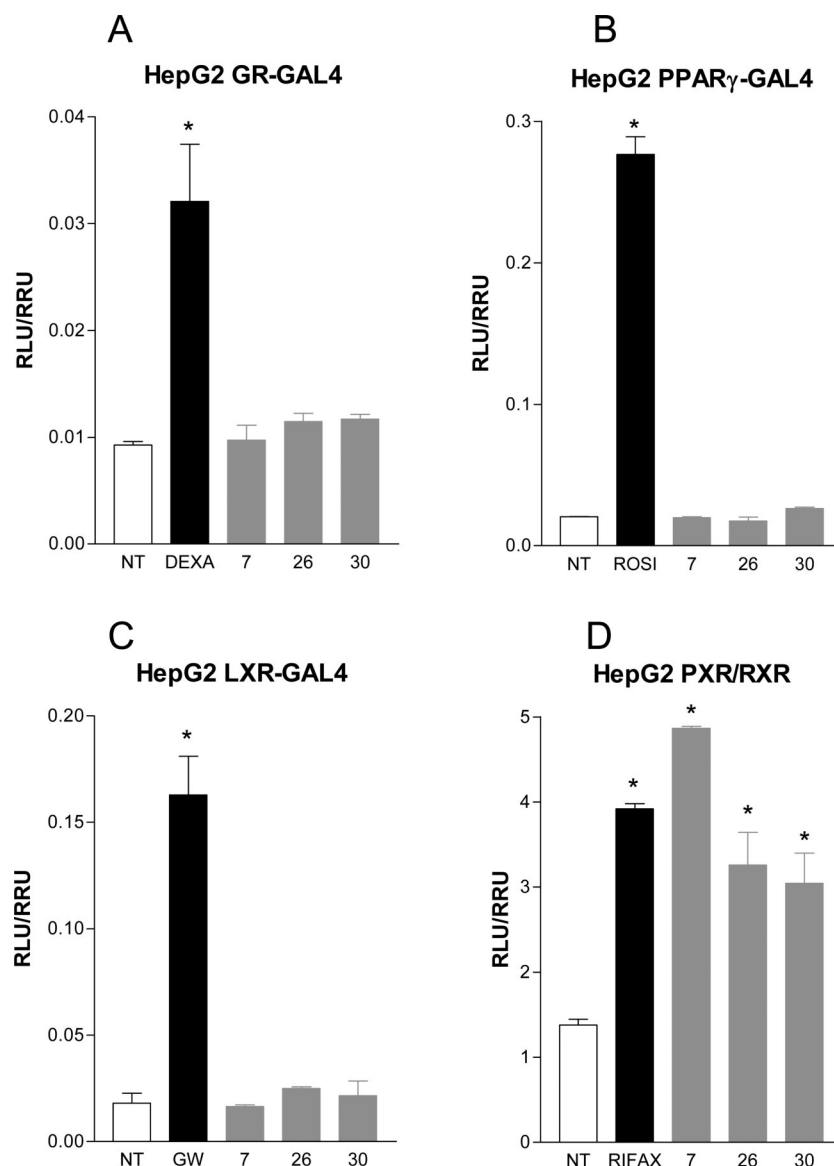


**Figure 7.** Specificity of **7**, **26**, and **30** on other nuclear receptors. (A–C) HepG2 cells were cotransfected with the Gal4 luciferase reporter vector and with a series of chimeras in which the Gal4 DNA binding domain is fused to the LBD of the indicated nuclear receptors. Cells were treated 18 h with the specific agonists (10  $\mu$ M) or with **7**, **26**, and **30** (10  $\mu$ M). (D) HepG2 cells were cotransfected with pSG5-PXR, pSG5-RXR, and with the reporter pCYP3A4 promoter-TKLuc and then stimulated with rifaximin (10  $\mu$ M), a PXR agonist, or with **7**, **26**, and **30** (10  $\mu$ M). Data are the mean  $\pm$  SE of three experiments. \* $p$  < 0.05 versus not treated cells (NT). DEXA, dexamethasone; ROSI, rosiglitazone; GW, GW3965; RIFAX, rifaximin.

alcoholic moiety with a carboxyl or a nitrile group as in **29** and **31**, respectively, showing a clear shift of their selectivity toward GP-BAR1.

**Pharmacological Evaluation on 7 $\alpha$ -Hydroxy-5 $\beta$ -cholan-24-sulfate (**7**), EUDCOH (**26**), and NorEUDCOH (**30**).** Among all tested compounds, 7 $\alpha$ -hydroxy-5 $\beta$ -cholan-24-sulfate (**7**), NorEUDCOH (**30**), and EUDCOH (**26**) represent promising templates for generating selective bile acid receptor modulators.

The relative potency of selected members of this novel family of semisynthetic cholane derivatives was first investigated by a detailed measurement of concentration–response curve of compounds **7**, **26**, and **30** on FXR and GP-BAR1 transactivation. As illustrated in Figure 6A,C,E, **7** and **30** transactivate FXR with an EC<sub>50</sub> of 9 and 2  $\mu$ M, respectively,

while **26** failed to transactivate FXR at any concentration tested. In addition, **26** and **30** transactivate GP-BAR1 with EC<sub>50</sub>s of 1.03 and 0.4  $\mu$ M (Figure 6D,F), respectively, while **7** failed to transactivate GP-BAR1 at any concentration tested (Figure 7B).

To further investigate the specificity of the above selected compounds, we have tested whether **7**, **26**, and **30** interact with other nuclear receptors including GR, PPAR $\gamma$ , LXR, and PXR. As shown in Figure 7A–C, these compounds at the concentration of 10  $\mu$ M failed to transactivate GR, PPAR $\gamma$ , and LXR, respectively. It is noteworthy that **7**, **26**, and **30** transactivate the nuclear receptor PXR (Figure 7D).

We have subsequently analyzed whether **7**, **26**, and **30** regulate canonical functions exerted by FXR and GP-BAR1. As shown in Figure 8A,B, both **26** and **30** were able to induce the

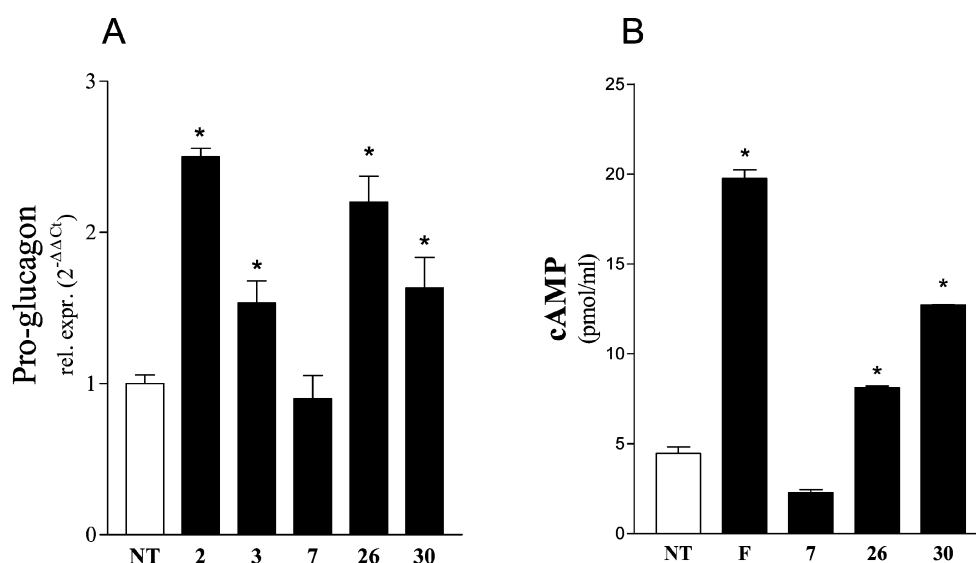


**Figure 8.** In vitro pharmacological evaluation of GP-BAR1 functions on 7, 26, and 30. (A) Real-time PCR analysis of mRNA expression of GP-BAR1 target gene Pro-glucagon in GLUTAg cells primed with 7, 26, and 30 ( $10 \mu\text{M}$ ). TLCA (2) and 6-ECDCA (3) were tested as positive controls ( $10 \mu\text{M}$ ). Values are normalized relative to GAPDH mRNA and are expressed relative to those of not treated cells (NT), which are arbitrarily set to 1:  $*p < 0.05$  versus not treated cells (NT). (B) Effect of 7, 26, and 30 ( $10 \mu\text{M}$ ) on intracellular generation of cAMP in THP-1 cells. The data are the mean  $\pm$  SE of three experiments:  $*p < 0.05$  versus not treated cells (NT). F: forskolin  $10 \mu\text{M}$ .

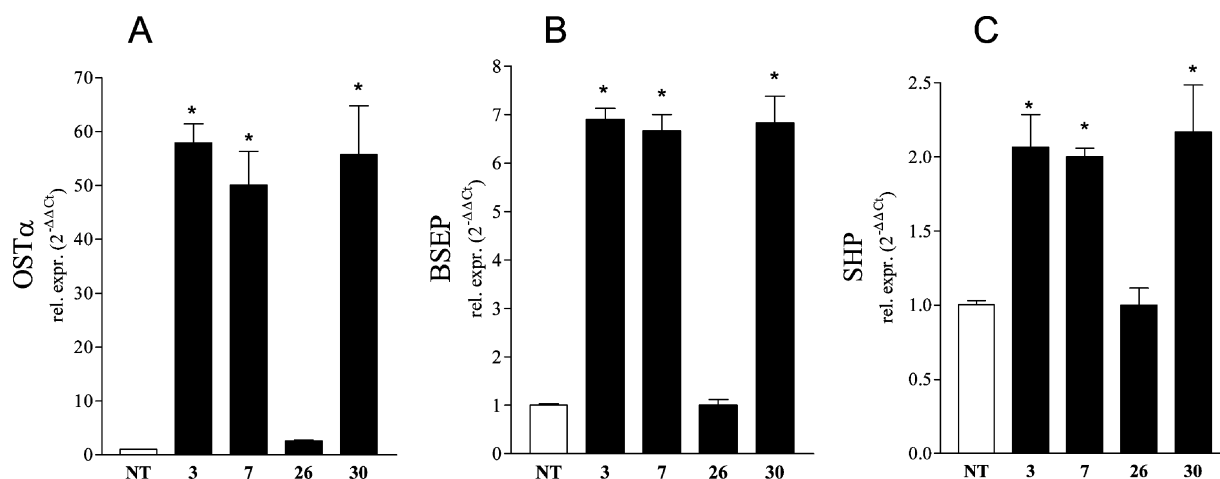


**Figure 9.** In vitro pharmacological evaluation of FXR target genes on 7, 26, and 30. Real-time PCR analysis of mRNA expression of FXR target genes OST $\alpha$  (A), BSEP (B), and SHP (C) in HepG2 cells primed with 7, 26, and 30, respectively ( $10 \mu\text{M}$ ). 6-ECDCA (3) was tested as positive control ( $10 \mu\text{M}$ ). Values are normalized relative to GAPDH mRNA and are expressed relative to those of not treated cells (NT), which are arbitrarily set to 1:  $*p < 0.05$  vs NT.

expression of pro-glucagon mRNA in GLUTAg cells, an intestinal endocrine cell line, as well as to increase cAMP concentrations in THP-1 cells, while 7 failed to regulate these canonical GP-BAR1 functions.

In vitro characterization of FXR target genes (i.e., OST $\alpha$ , BSEP, and SHP) was carried out by assessing the response of HepG2 cells primed with 7, 26, and 30. As illustrated in Figure 9, both 7 and 30 induce the expression of OST $\alpha$ , BSEP, and SHP, while 26 failed to regulate these canonical FXR target genes.

To measure the ability of the more active compounds to straightly recruit SRC-1, a coactivator recruitment assay using Alphascreen technology was applied. In this assay, the ligand induces the recruitment of a coactivator to the LBD of hFXR. Data shown in Figure 10 clearly confirm the transactivation

results and also substantiate the delineated structure–activity relationship.

CDCA (1) and 6-ECDCA (3) were tested as positive controls and reference molecules (the effect of CDCA was arbitrarily settled as 100%), 7, 15, and 25–31 were tested at fixed concentration of  $4 \mu\text{M}$ , and the results were compared to the assay carried out in absence of ligand (response at 10%). Compound 30 showed a very potent activity in the recruitment of SRC-1 coactivator and high affinity to FXR, almost comparable to that measured for 3. Compounds 7, 15, 25, 29, and 31 showed a moderate recruitment of SRC-1, and 26–28 resulted completely unable to recruit the coactivator.

**In Vivo Effects.** Since it has previously demonstrated that bile acids cause itch through the activation of GP-BAR1,<sup>15</sup> we have next investigated whether compound 30, a potent FXR



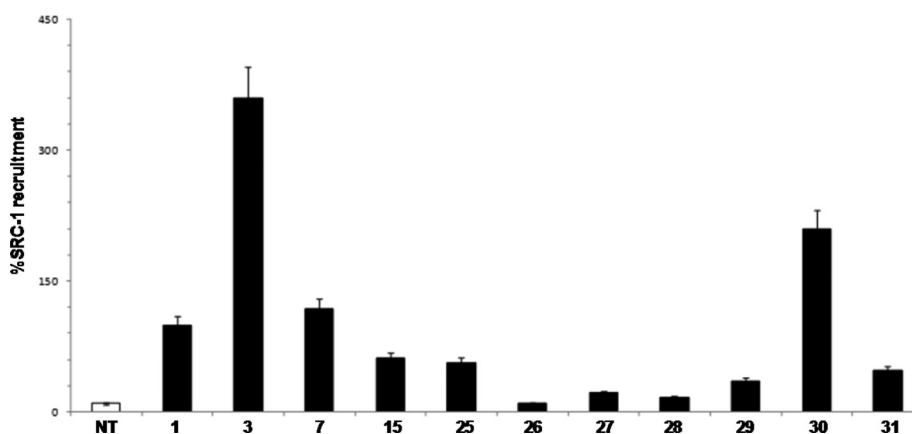


**Figure 10.** Coactivator recruitment assay measuring a direct interaction of FXR with Src-1. Anti-GST-coated acceptor beads captured GST-fusion FXR-LBD and the biotinylated-SRC-1 peptide was captured by the streptavidin donor beads. FXR-LBD recruited SRC-1 in the presence of ligand at 4  $\mu$ M and, upon illumination at 680 nm, chemical energy is transferred from donor to acceptor beads across the complex streptavidin-donor/Src-1-biotin/ligand/GSTFXR-LBD/anti-GST-acceptor and a signal is produced. Results are expressed as percentage of the effect of CDCA (1) arbitrarily settled as 100%. NT is referred to the experiment carried out in absence of ligand. Results are expressed as mean  $\pm$  standard error.

agonist endowed with a residual GP-BAR1 activity, triggers itching behavior in a mouse model of pruritus linked to the activation of GP-BAR1.

For this purpose, GP-BAR1<sup>+/+</sup> and GP-BAR1<sup>-/-</sup> mice were treated with ANIT for 9 days and then subjected to intradermal injection of bile acids (i.e., 3, DCA, UDCA) and compound 30.

As shown in Figure 11, ANIT treatment significantly increased AST levels in GP-BAR1<sup>-/-</sup> animals in comparison with GP-BAR1<sup>+/+</sup> mice (Figure 11D, \* $p < 0.05$ ), while no significant changes in total bilirubin and alkaline phosphatase were observed among these groups (Figure 11B,C). It is noteworthy that mice were rendered cholestatic by treatment with ANIT developed a GP-BAR1 dependent itching when challenged with bile acids DCA or 6-ECDCA (3) (Figure 11, panel E, \* $p < 0.05$ ), while UDCA and compound 30 failed to induce itching, thus demonstrating that 30 is an FXR agonist despite its residual activity on GP-BAR1.

## DISCUSSION AND CONCLUSION

Bile acid activated receptors are a family of nuclear and G protein activated receptors that are currently investigated for their potential in the treatment of a variety of gastrointestinal and metabolic disorders.<sup>2</sup> Receptors activated by bile acids are largely concentrated in the liver and gastrointestinal tract and are promiscuous in term of ligand specificity. FXR is the main bile acid sensor in the gastrointestinal tract and liver, and its activation reduces bile acid synthesis while increasing detoxification. For these reason, FXR has been deemed a target for treating cholestasis.<sup>1,2</sup> However, preclinical studies have shown that FXR activation worsens liver damage in rodent model of cholestasis, while FXR ablation attenuates liver injury in bile duct ligated mice. In mild nonobstructive cholestasis, FXR activation ameliorates bile flow impairment. These observations have led to the concept that FXR activation could be beneficial in treating cholestasis in PBC patients. Clinical trials carried out with 6-ECDCA (3, INT747, or obeticholic acid), a compound we first developed in 2002,<sup>17</sup> has led however to exacerbation of itching, a side effect that greatly limits the benefit of this approach.<sup>12,16</sup> It has to be noted, however, that 6-ECDCA is a dual FXR and GP-BAR1 ligand, and GP-BAR1 has recently been demonstrated to be the main

receptor involved in mediating itching caused by bile acids.<sup>15</sup> Thus, it appears that dual FXR/GP-BAR1 ligands hold the potential for detrimental side effects in cholestasis.

In the present study, we have harnessed on the CDCA and UDCA scaffolds to generate semisynthetic derivatives that are selective for FXR or GP-BAR1. The results of this investigation has led to the discovery of compound 7, a selective FXR ligand, compound 26, a selective GP-BAR1 ligand, and compound 30, a highly preferential FXR ligand endowed with a minimal GP-BAR1 agonistic activity.

7 $\alpha$ -Hydroxy-5 $\beta$ -cholan-24-sulfate (7) transactivates FXR in transactivation assay with an EC<sub>50</sub> of  $\sim 9 \mu$ M that is approximately 10–15 fold less potent than 6-ECDCA (3) in this assay (Supporting Information, Figure S1). However, its potency in inducing the expression of OST $\alpha$ , a FXR target gene in the liver, is comparable to that of 6-ECDCA (Figure 9). In comparison to 6-ECDCA, compound 7 has no effect on GP-BAR1, nor does it induces a GP-BAR1 target gene such as proglucagon in GLUTAg cells. GLUTAg cells are a line of murine L cells, an enteroendocrine cell population highly concentrated in the terminal ileum that releases GLP-1, a hormone involved in insulin secretion and a well validated target in the treatment of diabetes.<sup>24</sup> The fact that 7 has no effect on GP-BAR1 should make this agent an ideal candidate in the treatment of cholestasis. This compound should avoid the risk of itching, a common side effect of 6-ECDCA,<sup>12</sup> likely due to GP-BAR1 activation.

EUDCOH (26) is an alcohol generated on the ursodeoxycholine scaffold and represents the first example of UDCA derivative substituted at C-6 with a  $\beta$ -oriented ethyl group. Results from detailed analysis of its activity demonstrate that this derivative is devoid of FXR agonistic activity as is the parent compound UDCA. However, in comparison to UDCA, EUDCOH (26) is a rather potent ligand for GP-BAR1 and stimulates pro-glucagon mRNA accumulation in GLUTAg cells. Because GLP-1, a peptide that represents the product of proglucagon, is a major pharmacological target in the treatment of type 2 diabetes,<sup>25</sup> one might speculate that compound 26 could be an important tool for targeting the GLP-1/insulin axis in diabetes. Its pharmacological characterization is ongoing.

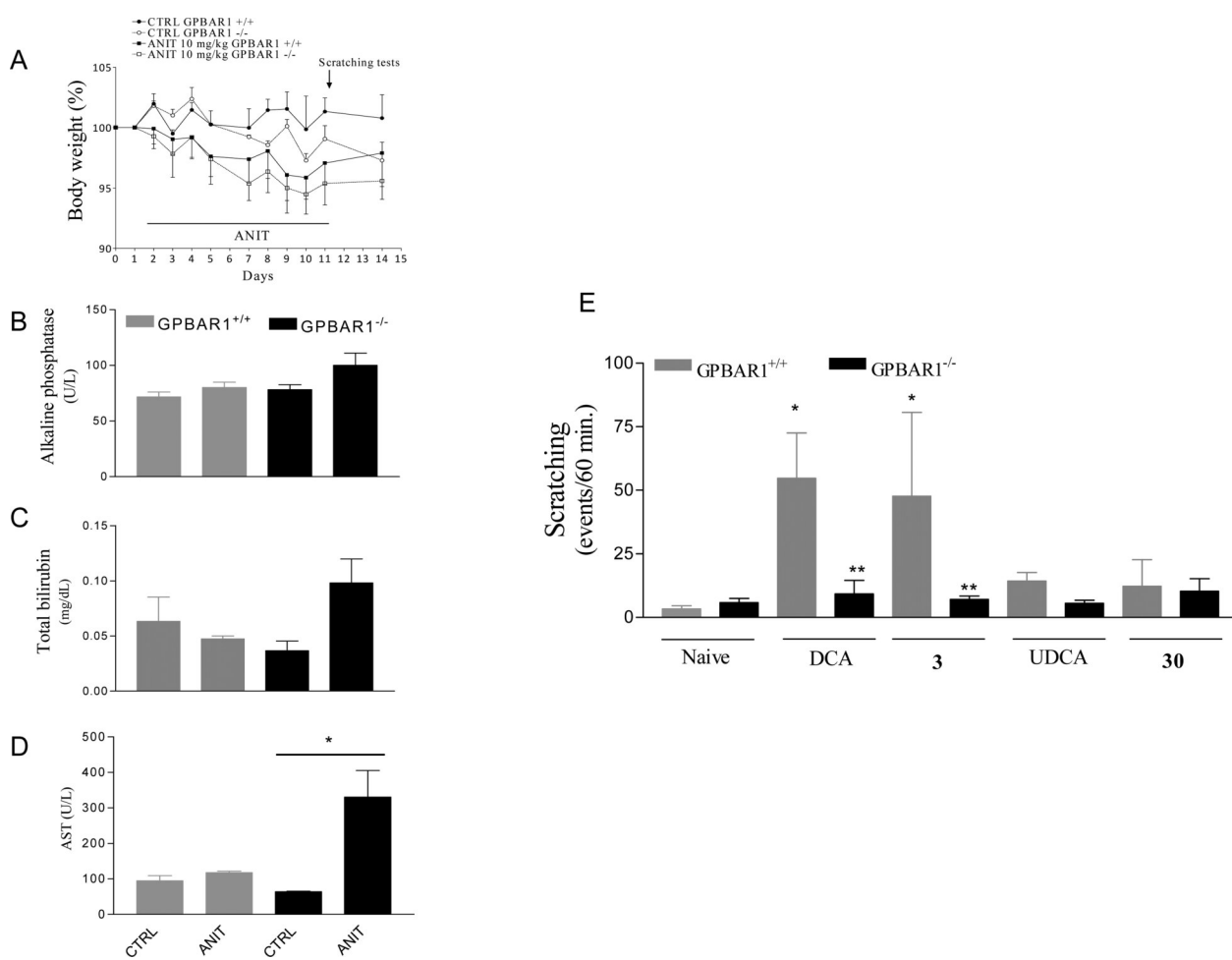


**Figure 11.** Effects of **30** on scratching in GP-BAR1<sup>+/+</sup> and GP-BAR1<sup>-/-</sup> mice. GP-BAR1<sup>+/+</sup> and GP-BAR1<sup>-/-</sup> mice were administered with ANIT for 9 days. At the end of the treatments, mice were subjected to intradermal injection of deoxycholic acid (DCA), 6-ECDCA (**3**), UDCA, and **30**. Scratching tests were performed at day 11 as summarized in (A). Serum levels of (B) alkaline phosphatase, (C) total bilirubin, and (D) AST in GP-BAR1<sup>+/+</sup> and GP-BAR1<sup>-/-</sup> animals not treated or administered with ANIT. (E) DCA and **3** robustly stimulated scratching in GP-BAR1-WT mice but not in GP-BAR1<sup>-/-</sup> mice, while spontaneous scratching was the same in GP-BAR1<sup>+/+</sup> and GP-BAR1<sup>-/-</sup> mice subjected to intradermal injection of UDCA and **30**. Results are the mean  $\pm$  standard error of six animals for group and were expressed as the number of scratching events during 60 min of observation.

NorECDCOH (**30**), a truncated side chain alcohol with both substituents on ring B in  $\alpha$ -configuration, is a potent FXR ligand with an EC<sub>50</sub> of 2  $\mu$ M, very close to that of 6-ECDCA (**3**). The two agents induce the expression of OST $\alpha$  with the same potency. In addition to the ability to transactivate FXR, NorECDCOH (**30**) retains a certain capacity of inducing GP-BAR1 and, indeed, it increases pro-glucagon gene expression in GLUTAg cells. Because its potency in inducing FXR target genes largely overwhelms that on GP-BAR1, NorECDCOH (**30**) should be considered a highly preferential FXR ligand. Supporting this view it does not induce itching when administered in vivo.

Pruritus is a common finding in cholestasis and remains an unmet clinical need.<sup>26</sup> Despite autotaxin having been shown to be a candidate mediator for itching in cholestasis,<sup>27,28</sup> administration of PBC patients with 6-ECDCA/obeticholic acid causes/worsens pruritus that is severe enough to cause drug discontinuation in 40% of patients. The high incidence of pruritus was unexpected and not predicted on the basis of FXR agonism. Nevertheless, the fact that 6-ECDCA/obeticholic acid

activates GP-BAR1 provides a rational molecular explanation for this side effect. This view is further strengthened by the consideration that UDCA, which is a weak ligand for GP-BAR1, does not cause itching. Whether or not itching caused by 6-ECDCA/obeticholic acid in PBC patients is mediated by GP-BAR1 needs additional investigations and other molecular mechanisms could be involved. In the present study, we have developed a model to investigate whether pruritus in cholestasis is linked to GP-BAR1 activation. The results presented in Figure 11 demonstrate that itching in animals administered with ANIT, a common model for drug induced liver injury and cholestasis, is GP-BAR1 dependent. Indeed, while 6-ECDCA induced itching and this effect was lost in GP-BAR1<sup>-/-</sup> mice, compound **30** failed to trigger an itching behavior. These data establish that compound **30** might have utility in cholestatic conditions.

By using a chenodeoxycholine scaffold, we have demonstrated that modification at C-3 hydroxyl group could be instrumental in generating selective FXR agonists (e.g., compounds **4**, **6**, **7**, **19**). Indeed, **7** represents the most potent

agonist so far generated with a simplified cholane scaffold whose total synthesis is therefore amenable of scale up. Moreover, from a metabolic point of view, the presence of the stable and nonconjugable sulfate group on its side chain highlights the therapeutic potential of derivative **7** in human FXR mediated diseases.

Of interest are also the results on 6-ethylcholane derivatives **25–31**. Data shown in the Figures 4 and 5 indicate that the C-6 and C-7  $\alpha$ -configuration represents a key structural feature for FXR activity with epimerized alcohols **26–28** resulting in potent and selective GP-BAR1 agonists, whereas derivative **25**, with both ethyl and the hydroxyl groups on ring B  $\alpha$ -oriented, is a dual agonist. Looking to *nor* derivatives **29–31**, pharmacological results emphasize the side chain as the pointer in determining FXR/GP-BAR1 selectivity on semisynthetic  $6\alpha,7\alpha$ -substituted cholane derivatives. In fact, the introduction of an hydroxyl group on a C-24 side chain improves GP-BAR1 selectivity (**25**) with respect to the corresponding C-24 carboxyl acid (6-ECDC) and also C-24 sulfate derivative, both potent dual agonists.<sup>18</sup> On the contrary, the shortening of the side chain generates a potent FXR agonist when an hydroxyl group is present as side chain end terminus as in NorECDCOH (**30**), whereas the introduction of a negative charge, NorECDC (a **29**), or a neutral end group, NorECDCN (**31**), improve GP-BAR1 selectivity (compare **30** vs **29** and **31** in Figures 4 and 5).

In summary, in the present report, we describe a novel series of FXR and GP-BAR1 selective agonists using known bile acid scaffold. The pharmacological characterization of several members of this series has led to the discovery of novel potential leads that might hold utility in the treatment of FXR and GP-BAR1 mediated disorders.

## EXPERIMENTAL SECTION

**Chemistry.** Specific rotations were measured on a Jasco P-2000 polarimeter. High-resolution ESI-MS spectra were performed with a Micromass Q-TOF mass spectrometer. NMR spectra were obtained on Varian Inova 400, 500, and 700 NMR spectrometers (<sup>1</sup>H at 400, 500, and 700 MHz, <sup>13</sup>C at 100, 125, and 175 MHz, respectively) equipped with a SUN microsystem ultra5 hardware and recorded in CD<sub>3</sub>OD ( $\delta_{\text{H}} = 3.31$  and  $\delta_{\text{C}} = 49.0$  ppm) and CDCl<sub>3</sub> ( $\delta_{\text{H}} = 7.26$  and  $\delta_{\text{C}} = 77.0$  ppm). All of the detected signals were in accordance with the proposed structures. Coupling constants (*J* values) are given in hertz (Hz), and chemical shifts ( $\delta$ ) are reported in ppm and referred to CHD<sub>2</sub>OD and CHCl<sub>3</sub> as internal standards. Spin multiplicities are given as s (singlet), br s (broad singlet), d (doublet), t (triplet), or m (multiplet). Through-space <sup>1</sup>H connectivities were evidenced using a ROESY experiment with mixing times of 200 and 250 ms, respectively.

HPLC was performed with a Waters model 510 pump equipped with Waters Rheodine injector and a differential refractometer, model 401. Reaction progress was monitored via thin-layer chromatography (TLC) on Alugram silica gel G/UV254 plates. Silica gel MN Kieselgel 60 (70–230 mesh) from Macherey-Nagel Company was used for column chromatography. All chemicals were obtained from Sigma-Aldrich, Inc.

Silica gel (200–400 mesh) from Macherey-Nagel Company was used for flash chromatography. All chemicals were obtained from Sigma-Aldrich, Inc. Solvents and reagents were used as supplied from commercial sources with the following exceptions. Hexane, ethyl acetate, chloroform, dichloromethane, tetrahydrofuran, and triethylamine were distilled from calcium hydride immediately prior to use. Methanol was dried from magnesium methoxide as follows. Magnesium turnings (5 g) and iodine (0.5 g) were refluxed in a small (50–100 mL) quantity of methanol until all of the magnesium has reacted. The mixture was diluted (up to 1 L) with reagent grade methanol, refluxed for 2–3 h, and then distilled under nitrogen. All

reactions were carried out under argon atmosphere using flame-dried glassware.

The purities of compounds were determined to be greater than 95% by HPLC. Compounds **25**, **32**, **44**, **45**, **47**, and **48** were prepared as previously reported.<sup>18,23</sup>

**Synthetic Procedures.** *Methyl 7 $\alpha$ -Hydroxy-5 $\beta$ -cholane-24-oate (33).* To a solution of **32** (130 mg, 0.32 mmol) in dry pyridine (10 mL), tosyl chloride (613 mg, 3.22 mmol) was added, and the mixture was stirred at room temperature for 4 h. It was poured into cold water (10 mL) and extracted with CH<sub>2</sub>Cl<sub>2</sub> (3  $\times$  10 mL). The combined organic layer was washed with saturated NaHCO<sub>3</sub> solution (10 mL) and water (10 mL) and then dried over anhydrous MgSO<sub>4</sub> and evaporated in vacuo to give 180 mg of methyl 3 $\alpha$ -tosyloxy-7-keto-5 $\beta$ -cholane-24-oate (quantitative yield) in the form of colorless needles, which was subjected to the next step without any purification.

Lithium bromide (55 mg, 0.64 mmol) and lithium carbonate (47 mg, 0.64 mmol) were added to a solution of methyl 3 $\alpha$ -tosyloxy-7-keto-5 $\beta$ -cholane-24-oate (180 mg, 0.32 mmol) in dry DMF (10 mL), and the mixture was refluxed for 3 h. After cooling to room temperature, the mixture was slowly poured into 10% HCl solution (50 mL) and extracted with CH<sub>2</sub>Cl<sub>2</sub> (3  $\times$  30 mL). The combined organic layer was washed successively with water, saturated NaHCO<sub>3</sub> solution, and water and then dried over anhydrous MgSO<sub>4</sub> and evaporated to dryness to give 124 mg of oily residue (quantitative yield) that was subjected to next step without any purification.

An oven-dried 25 mL flask was charged with 10% palladium on carbon (30 mg) and the previously obtained crude intermediate (124 mg, 0.32 mmol), and the flask was evacuated and flushed with argon. Absolute methanol (5 mL) and dry THF (5 mL) were added, and the flask was flushed with hydrogen. The reaction was stirred at room temperature under H<sub>2</sub> (1 atm) overnight. The mixture was filtered through Celite, and the recovered filtrate was concentrated to give 125 mg of methyl 7-keto-5 $\beta$ -cholane-24-oate (quantitative yield), which was subjected to the next step without any purification.

Methyl 7-keto-5 $\beta$ -cholane-24-oate (125 mg, 0.32 mmol) was dissolved in a solution of tetrahydrofuran/water (10 mL, 4/1 v/v) and treated at 0 °C with NaBH<sub>4</sub> (722 mg, 1.9 mmol). After 2 h, water and MeOH were added dropwise during a period of 15 min at 0 °C, with effervescence being observed. Then after evaporation of the solvents, the residue was diluted with water, acidified with HCl 1 N, and extracted with AcOEt (3  $\times$  10 mL). The combined organic phases were washed with brine, dried over Na<sub>2</sub>SO<sub>4</sub> anhydrous, and evaporated under reduced pressure to obtain 125 mg of **33** (quantitative yield); [ $\alpha$ ]<sub>D</sub><sup>25</sup> = +3.5 (*c* 2.82, CH<sub>3</sub>OH). Selected <sup>1</sup>H NMR (500 MHz CDCl<sub>3</sub>):  $\delta$  3.84 (1H, s), 3.66 (3H, s), 2.34 (1H, m), 2.22 (1H, m), 0.92 (3H, d, *J* = 6.5 Hz), 0.90 (3H, s), 0.66 (3H, s). HRMS-ESI *m/z* 391.3216 [M + H]<sup>+</sup>, C<sub>25</sub>H<sub>43</sub>O<sub>3</sub> requires 391.3212.

*7 $\alpha$ -Hydroxy-5 $\beta$ -cholane-24-oic Acid (4).* Compound **33** (56 mg, 0.14 mmol) was hydrolyzed with a methanol solution of sodium hydroxide (5%, 10 mL) in H<sub>2</sub>O (2 mL) overnight under reflux. The resulting solution was then concentrated under vacuum, diluted with water, acidified with HCl 6 N, and extracted with ethyl acetate (3  $\times$  50 mL). The collected organic phases were washed with brine, dried over Na<sub>2</sub>SO<sub>4</sub> anhydrous, and evaporated under reduced pressure to give compound **4** in quantitative yield (54 mg). An analytic sample was obtained by HPLC on a Nucleodur 100–5 C18 (5  $\mu$ m; 4.6 mm i.d.  $\times$  250 mm) with MeOH/H<sub>2</sub>O (95:5) as eluent (flow rate 1 mL/min, *t*<sub>R</sub> = 8.2 min); [ $\alpha$ ]<sub>D</sub><sup>25</sup> = –5.3 (*c* 0.03, CH<sub>3</sub>OH). Selected <sup>1</sup>H NMR (400 MHz CD<sub>3</sub>OD):  $\delta$  3.79 (1H, s), 2.33 (1H, m), 2.23 (1H, m), 0.96 (3H, d, *J* = 6.4 Hz), 0.93 (3H, s), 0.70 (3H, s). <sup>13</sup>C NMR (100 MHz CD<sub>3</sub>OD):  $\delta$  178.3, 69.4, 57.3, 51.5, 44.9, 43.7, 41.1, 40.8, 38.8, 37.0, 36.2, 34.1, 32.4, 31.6, 30.8, 29.2, 29.0, 24.6, 24.2, 23.4, 22.6, 21.8, 18.8, 12.2. HRMS-ESI *m/z* 375.2903 [M – H]<sup>–</sup>, C<sub>24</sub>H<sub>39</sub>O<sub>3</sub> requires 375.2899.

*7 $\alpha$ -Hydroxy-5 $\beta$ -cholane-24-oyl Taurine Sodium Salt (5).* Compound **4** (15 mg, 0.04 mmol) in DMF dry (3 mL) was treated with DMT-MM (33 mg, 0.12 mmol) and triethylamine (140  $\mu$ L, 1 mmol), and the mixture was stirred at room temperature for 10 min. Then to the mixture was added taurine (30 mg, 0.24 mmol). After 24 h, the reaction mixture was concentrated under vacuo and dissolved in water

(5 mL). The solution was poured over a C18 silica gel column. Fraction eluted with H<sub>2</sub>O/MeOH 99:1 gave a mixture that was further purified by HPLC on a Nucleodur 100–5 C18 (5  $\mu$ m; 4.6 mm i.d.  $\times$  250 mm) with MeOH/H<sub>2</sub>O (83:17) as eluent (flow rate 1 mL/min) to give 7 mg (35%) of compound 5 ( $t_R$  = 7.6 min);  $[\alpha]_D^{25}$  = –58.2 (c 0.02, CH<sub>3</sub>OH). Selected <sup>1</sup>H NMR (500 MHz CD<sub>3</sub>OD):  $\delta$  3.79 (1H, s), 3.59 (2H, t,  $J$  = 7.3 Hz), 2.96 (2H, t,  $J$  = 7.3 Hz), 0.97 (3H, d,  $J$  = 7.1 Hz), 0.93 (3H, s), 0.69 (3H, s). HRESIMS  $m/z$  482.2951 [M – Na]<sup>–</sup>, C<sub>26</sub>H<sub>44</sub>NO<sub>5</sub>S requires 482.2940.

**7 $\alpha$ -Hydroxy-5 $\beta$ -cholan-24-ol (6).** Dry methanol (50  $\mu$ L, 1.26 mmol) and LiBH<sub>4</sub> (630  $\mu$ L, 2 M in THF, 1.26 mmol) were added to a solution of the compound 33 (70 mg, 0.18 mmol) in dry THF (10 mL) at 0 °C under argon, and the resulting mixture was stirred for 3 h at 0 °C. The mixture was quenched by addition of NaOH (1 M, 0.4 mL) and then allowed to warm to room temperature. Ethyl acetate was added, and the separated aqueous phase was extracted with ethyl acetate (3  $\times$  15 mL). The combined organic phases were washed with water, dried (Na<sub>2</sub>SO<sub>4</sub>), and concentrated. Purification by silica gel eluting with ethyl acetate–hexane (85:15) gave the alcohol 6 as a white solid (52 mg, 79%). An analytic sample was obtained by HPLC on a Nucleodur 100–5 C18 (5  $\mu$ m; 4.6 mm i.d.  $\times$  250 mm) with MeOH/H<sub>2</sub>O (95:5) as eluent (flow rate 1 mL/min,  $t_R$  = 8 min);  $[\alpha]_D^{25}$  = +5.2 (c 0.53, CH<sub>3</sub>OH). Selected <sup>1</sup>H NMR (400 MHz CD<sub>3</sub>OD):  $\delta$  3.79 (1H, br s), 3.51 (2H, t,  $J$  = 6.6 Hz), 0.97 (3H, d,  $J$  = 6.6 Hz), 0.93 (3H, s), 0.70 (3H, s). <sup>13</sup>C NMR (100 MHz CD<sub>3</sub>OD):  $\delta$  69.4, 63.6, 57.6, 51.6, 45.6, 43.6, 42.8, 41.1, 40.9, 38.9, 37.0, 36.2, 34.1, 33.3, 31.6, 30.3, 29.3, 29.0, 24.7, 24.5, 22.6, 21.8, 19.2, 12.2. HRMS-ESI  $m/z$  363.3271 [M + H]<sup>+</sup>, C<sub>24</sub>H<sub>42</sub>O<sub>2</sub> requires 363.3263.

**7 $\alpha$ -Hydroxy-5 $\beta$ -cholan-24-yl-24-sodium Sulfate (7) and 5 $\beta$ -Cholan-7 $\alpha$ ,24-diy-7,24-disodium Disulfate (8).** At a solution of diol 6 (40 mg, 0.11 mmol) in DMF dry (3 mL) was added triethylamine–sulfur trioxide complex (88 mg, 0.55 mmol) under an argon atmosphere, and the mixture was stirred at 80 °C for 24 h. Most of the solvent was evaporated, and the residue was poured over a RP18 column to remove excess SO<sub>3</sub>–NEt<sub>3</sub>. Fraction eluted with MeOH/H<sub>2</sub>O 45:55 gave a mixture that was further purified by HPLC on a Nucleodur 100–5 C18 (5  $\mu$ m; 4.6 mm i.d.  $\times$  250 mm) with MeOH/H<sub>2</sub>O (50:50) as eluent (flow rate 1 mL/min), to give 24 mg (39%) of compound 8 ( $t_R$  = 20.4 min);  $[\alpha]_D^{25}$  = –9.3 (c 0.14, CH<sub>3</sub>OH). Selected <sup>1</sup>H NMR (400 MHz CD<sub>3</sub>OD):  $\delta$  4.42 (1H, s), 3.95 (2H, br t,  $J$  = 6.5 Hz), 0.96 (3H, d,  $J$  = 6.5 Hz), 0.94 (3H, s), 0.69 (3H, s). HRESIMS  $m/z$  543.2070 [M – Na]<sup>–</sup>, C<sub>24</sub>H<sub>40</sub>O<sub>8</sub>S<sub>2</sub>Na requires 543.2062.

Fraction eluted with MeOH gave a mixture that was further purified by HPLC on a Nucleodur 100–5 C18 (5  $\mu$ m; 4.6 mm i.d.  $\times$  250 mm) with MeOH/H<sub>2</sub>O (90:10) as eluent (flow rate 1 mL/min), to give 28 mg (55%) of compound 7 ( $t_R$  = 6.6 min);  $[\alpha]_D^{25}$  = –7.0 (c 0.28, CH<sub>3</sub>OH). Selected <sup>1</sup>H NMR (400 MHz CD<sub>3</sub>OD):  $\delta$  3.96 (2H, t,  $J$  = 6.6 Hz), 3.78 (1H, br s), 3.30 (1H, ovl), 0.96 (3H, d,  $J$  = 6.5 Hz), 0.92 (3H, s), 0.69 (3H, s). <sup>13</sup>C NMR (100 MHz CD<sub>3</sub>OD):  $\delta$  69.7, 69.4, 57.7, 51.6, 45.0, 43.8, 41.2, 41.0, 39.0, 37.1, 36.3, 34.2, 33.3, 34.2, 33.3, 31.7, 29.5, 29.0, 27.3, 24.3, 22.7, 21.9, 19.2, 12.3. HRESIMS  $m/z$  441.2679 [M – Na]<sup>–</sup>, C<sub>24</sub>H<sub>41</sub>O<sub>5</sub>S requires 441.2675.

**Methyl 3 $\alpha$ -Tosyloxy-7 $\beta$ -hydroxy-5 $\beta$ -cholan-24-oate (34).** To a solution of UDCA methyl ester (400 mg, 0.99 mmol) in dry pyridine (10 mL), tosyl chloride (280 mg, 1.5 mmol) was added, and the mixture was stirred at room temperature for 2 h. It was poured into cold water (10 mL) and extracted with CH<sub>2</sub>Cl<sub>2</sub> (3  $\times$  10 mL). Purification by silica gel eluting with ethyl acetate–hexane (8:2) gave compound 34 (320 mg, 58%) as a white solid;  $[\alpha]_D^{25}$  = +37.6 (c 0.70, CH<sub>3</sub>OH). Selected <sup>1</sup>H NMR (400 MHz CDCl<sub>3</sub>):  $\delta$  7.79 (2H, d,  $J$  = 8.5 Hz), 7.33 (2H, d,  $J$  = 8.5 Hz), 4.40 (1H, m), 3.52 (1H, m), 2.46 (3H, s), 2.35 (1H, m), 2.23 (1H, m), 0.92 (3H, d, ovl), 0.91 (3H, s), 0.66 (3H, s). HRESIMS  $m/z$  561.3259 [M + H]<sup>+</sup>, C<sub>32</sub>H<sub>49</sub>O<sub>6</sub>S requires 561.3250.

**7 $\beta$ -Hydroxy-5 $\beta$ -cholan-24-oic Acid (9).** Lithium bromide (73 mg, 0.84 mmol) and lithium carbonate (62 mg, 0.84 mmol) were added to a solution of methyl ester 34 (220 mg, 0.42 mmol) in dry DMF (10 mL), and the mixture was refluxed for 2 h. After cooling to room temperature, the mixture was slowly poured into 10% HCl solution

(10 mL) and extracted with CH<sub>2</sub>Cl<sub>2</sub> (3  $\times$  30 mL). The combined organic layer was washed successively with water, saturated NaHCO<sub>3</sub> solution, and water and then dried over anhydrous MgSO<sub>4</sub> and evaporated to dryness to give 162 mg of oily residue (quantitative yield), which was subjected to next step without any purification.

An oven-dried 25 mL flask was charged with 10% palladium on carbon (5 mg) and the product obtained (162 mg, 0.42 mmol), and the flask was evacuated and flushed with argon. Absolute methanol (5 mL) and dry THF (5 mL) were added, and the flask was flushed with hydrogen. The reaction was stirred at room temperature under H<sub>2</sub> (1 atm) overnight. The mixture was filtered through Celite, and the recovered filtrate was concentrated to give 128 mg of compound 35 (78%). An amount of compound 35 (40 mg, 10.2  $\times$  10<sup>–2</sup> mmol) was hydrolyzed with a methanol solution of sodium hydroxide (5%, 5 mL) in H<sub>2</sub>O (1 mL) overnight under reflux. The resulting solution was then concentrated under vacuum, diluted with water, acidified with HCl 6 N, and extracted with ethyl acetate (3  $\times$  20 mL). The collected organic phases were washed with brine, dried over Na<sub>2</sub>SO<sub>4</sub> anhydrous, and evaporated under reduced pressure to give 9 in a quantitative yield (39.5 mg). An analytic sample was obtained by HPLC on a Nucleodur 100–5 C18 (5  $\mu$ m; 4.6 mm i.d.  $\times$  250 mm) with MeOH/H<sub>2</sub>O (78:22) as eluent (flow rate 1 mL/min,  $t_R$  = 13.2 min);  $[\alpha]_D^{25}$  = –95.0 (c 0.08, CH<sub>3</sub>OH). Selected <sup>1</sup>H NMR (400 MHz CD<sub>3</sub>OD):  $\delta$  3.45 (1H, m), 2.32 (1H, m), 2.21 (1H, m), 0.96 (3H, s), 0.95 (3H, d, ovl), 0.71 (3H, s). HRESIMS  $m/z$  375.2901 [M – H]<sup>–</sup>, C<sub>24</sub>H<sub>39</sub>O<sub>3</sub> requires 375.2899.

**7 $\beta$ -Hydroxy-5 $\beta$ -cholan-24-oyl Taurine Sodium Salt (10).** Compound 9 (9 mg, 23.9  $\times$  10<sup>–3</sup> mmol) in DMF dry (3 mL) was treated with DMT-MM (20 mg, 71.7  $\times$  10<sup>–3</sup> mmol) and triethylamine (85  $\mu$ L, 0.6 mmol), and the mixture was stirred at room temperature for 10 min. Then to the mixture was added taurine (18 mg, 0.14 mmol). After 24 h, the reaction mixture was concentrated under vacuo and dissolved in water (5 mL). The solution was poured over a C18 silica gel column. Fraction eluted with H<sub>2</sub>O/MeOH 99:1 gave a mixture that was further purified by HPLC on a Nucleodur 100–5 C18 (5  $\mu$ m; 4.6 mm i.d.  $\times$  250 mm) with MeOH/H<sub>2</sub>O (73:27) as eluent (flow rate 1 mL/min), to give 3.3 mg of 10 (27%,  $t_R$  = 18 min);  $[\alpha]_D^{25}$  = +4.8 (c 0.08, CH<sub>3</sub>OH). Selected <sup>1</sup>H NMR (400 MHz CD<sub>3</sub>OD):  $\delta$  3.57 (2H, t,  $J$  = 7.2 Hz), 3.46 (1H, m), 2.95 (2H, t,  $J$  = 7.2 Hz), 0.96 (6H, ovl), 0.70 (3H, s). HRESIMS  $m/z$  482.2945 [M – Na]<sup>–</sup>, C<sub>24</sub>H<sub>39</sub>O<sub>3</sub> requires 482.2940.

**7 $\beta$ -Hydroxy-5 $\beta$ -cholan-24-ol (11).** Dry methanol (22  $\mu$ L, 0.55 mmol) and LiBH<sub>4</sub> (276  $\mu$ L, 2 M in THF, 0.55 mmol) were added to a solution of the compound 35 (71.9 mg, 18.4  $\times$  10<sup>–2</sup> mmol) in dry THF (10 mL) at 0 °C under argon, and the resulting mixture was stirred for 3 h at 0 °C. The mixture was quenched by addition of NaOH (1 M, 364  $\mu$ L) and then allowed to warm to room temperature. Ethyl acetate was added, and the separated aqueous phase was extracted with ethyl acetate (3  $\times$  15 mL). The combined organic phases were washed with water, dried (Na<sub>2</sub>SO<sub>4</sub>), and concentrated to give 61 mg of 11 as a white solid (91%). An analytic sample was obtained by HPLC on a Nucleodur 100–5 C18 (5  $\mu$ m; 4.6 mm i.d.  $\times$  250 mm) with MeOH/H<sub>2</sub>O (95:5) as eluent (flow rate 1 mL/min,  $t_R$  = 16 min);  $[\alpha]_D^{25}$  = +114.6 (c 0.04 CH<sub>3</sub>OH). Selected <sup>1</sup>H NMR (400 MHz CD<sub>3</sub>OD):  $\delta$  3.51 (2H, t,  $J$  = 6.5 Hz), 3.46 (1H, m), 0.96 (3H, s), 0.95 (3H, d, ovl), 0.71 (3H, s). HRMS-ESI  $m/z$  363.3268 [M + H]<sup>+</sup>, C<sub>24</sub>H<sub>42</sub>O<sub>2</sub> requires 363.3263.

**5 $\beta$ -Cholan-7 $\beta$ ,24-diy-7,24-disodium Disulfate (13) and 7 $\beta$ -Hydroxy-5 $\beta$ -cholan-24-yl-24-sodium Sulfate (12).** At a solution of diol 11 (50 mg, 0.138 mmol) in DMF dry (5 mL) was added triethylamine–sulfur trioxide complex (125 mg, 0.69 mmol) under an argon atmosphere, and the mixture was stirred at 80 °C for 24 h. Most of the solvent was evaporated, and the residue was poured over a RP18 column to remove excess SO<sub>3</sub>–NEt<sub>3</sub>. Fraction eluted over a RP18 column with H<sub>2</sub>O:MeOH 1:1 gave a mixture that was further purified by HPLC on a Nucleodur 100–5 C18 (5  $\mu$ m; 4.6 mm i.d.  $\times$  250 mm) with MeOH/H<sub>2</sub>O (65:35) as eluent (flow rate 1 mL/min), to give 32 mg of 13 (41%,  $t_R$  = 12.4 min);  $[\alpha]_D^{25}$  = –15.4 (c 0.03, CH<sub>3</sub>OH). Selected <sup>1</sup>H NMR (400 MHz CD<sub>3</sub>OD):  $\delta$  3.96 (2H, m), 3.49 (1H, m), 0.97 (6H, ovl), 0.71 (3H, s). HRESIMS  $m/z$  543.2069 [M – Na]<sup>–</sup>, C<sub>24</sub>H<sub>40</sub>O<sub>8</sub>S<sub>2</sub>Na requires 543.2062.

Fraction eluted over a RP18 column with MeOH gave a mixture that was further purified by HPLC on a Nucleodur 100–5 C18 (5  $\mu$ m; 4.6 mm i.d.  $\times$  250 mm) with MeOH/H<sub>2</sub>O (83:17) as eluent (flow rate 1 mL/min), to give 26 mg of compound **12** (41%,  $t_R$  = 5.4 min);  $[\alpha]_D^{25}$  = +21.4 (c 1.46, CH<sub>3</sub>OH). Selected <sup>1</sup>H NMR (400 MHz CD<sub>3</sub>OD):  $\delta$  4.28 (1H, m), 3.96 (2H, m), 0.99 (3H, s), 0.98 (3H, d, ovl), 0.72 (3H, s). <sup>13</sup>C NMR (100 MHz CD<sub>3</sub>OD):  $\delta$  81.0, 70.9, 56.6 (2C), 45.4, 44.8, 42.6, 41.3, 40.5, 38.3, 36.8, 35.6, 35.2, 33.1, 29.5, 28.8, 28.2, 27.0, 26.9, 24.6, 22.1, 21.8, 19.1, 12.5. HRESIMS  $m/z$  441.2681 [M – Na]<sup>+</sup>, C<sub>24</sub>H<sub>41</sub>O<sub>5</sub>S requires 441.2675.

**Methyl 3 $\alpha$ ,7 $\beta$ -Ditosyloxy-5 $\beta$ -cholan-24-oate (36).** To a solution of UDCA methyl ester (300 mg, 0.73 mmol) in dry pyridine (20 mL), tosyl chloride (1.39 g, 7.3 mmol) was added and the mixture was stirred at room temperature for 6 h. It was poured into cold water (30 mL) and extracted with CH<sub>2</sub>Cl<sub>2</sub> (3  $\times$  30 mL). Purification by silica gel eluting with ethyl acetate–hexane (8:2) gave **36** (521 mg, quantitative yield) as a white solid;  $[\alpha]_D^{25}$  = –11 (c 0.48, CH<sub>3</sub>OH). Selected <sup>1</sup>H NMR (400 MHz CDCl<sub>3</sub>):  $\delta$  7.79 (2H, d,  $J$  = 8.3 Hz), 7.75 (2H, d,  $J$  = 8.3 Hz), 7.36 (2H, d,  $J$  = 8.3 Hz), 7.32 (2H, d,  $J$  = 8.3 Hz), 4.58 (1H, m), 4.38 (1H, m), 3.67 (3H, s), 2.47 (3H, s), 2.45 (3H, s), 2.33 (1H, m), 2.22 (1H, m), 0.91 (3H, d,  $J$  = 6.5 Hz), 0.88 (3H, s), 0.61 (3H, s). HRESIMS  $m/z$  715.3333 [M + H]<sup>+</sup>, C<sub>39</sub>H<sub>53</sub>O<sub>8</sub>S<sub>2</sub> requires 715.3338.

**Methyl 5 $\beta$ -Cholan-24-oate (37) and 8 $\alpha$  Epimer 38.** Lithium bromide (45 mg, 0.52 mmol) and lithium carbonate (38 mg, 0.52 mmol) were added to a solution of **36** (190 mg, 0.26 mmol) in dry DMF (20 mL), and the mixture was refluxed for 3 h. After cooling to room temperature, the mixture was slowly poured into 10% HCl solution (50 mL) and extracted with CH<sub>2</sub>Cl<sub>2</sub> (3  $\times$  30 mL). The combined organic layer was washed successively with water, saturated NaHCO<sub>3</sub> solution, and water and then dried over anhydrous MgSO<sub>4</sub> and evaporated to dryness to give 124 mg of oily residue (quantitative yield), which was subjected to next step without any purification.

An oven-dried 25 mL flask was charged with 10% palladium on carbon (10 mg) and the crude product (124 mg, 0.23 mmol), and the flask was evacuated and flushed with argon. Absolute methanol (5 mL) and dry THF (5 mL) were added, and the flask was flushed with hydrogen. The reaction was stirred at room temperature under H<sub>2</sub> (1 atm) overnight. The mixture was filtered through Celite, and the recovered filtrate was concentrated to give 95 mg of crude product, which was further purified by HPLC on a Nucleodur 100–5 C18 (5  $\mu$ m; 10 mm i.d.  $\times$  250 mm) with MeOH/H<sub>2</sub>O (99.5:0.5) as eluent (flow rate 3 mL/min), to give 25 mg of compound **38** (26%,  $t_R$  = 25.5 min) and 32 mg of compound **37** (33%;  $t_R$  = 33 min).

**Methyl 5 $\beta$ -Cholan-24-oate (37).**  $[\alpha]_D^{25}$  = –3.0 (c 0.03, CH<sub>3</sub>OH). Selected <sup>1</sup>H NMR (400 MHz CDCl<sub>3</sub>):  $\delta$  3.66 (3H, s), 2.33 (1H, m), 2.20 (1H, m), 0.91 (6H, ovl), 0.65 (3H, s). <sup>13</sup>C NMR (100 MHz CDCl<sub>3</sub>):  $\delta$  171.9, 56.6, 56.0, 51.5, 43.8, 40.5 (2C), 40.3, 37.7, 35.9, 35.4 (2C), 31.0 (2C), 28.2, 27.5, 27.3, 27.1, 26.5, 24.2 (2C), 21.3, 20.8, 18.2, 12.0. HRESIMS  $m/z$  375.3267 [M + H]<sup>+</sup>, C<sub>25</sub>H<sub>43</sub>O<sub>2</sub> requires 375.3263.

**Compound 38.**  $[\alpha]_D^{25}$  = +19.7 (c 0.02, CH<sub>3</sub>OH). Selected <sup>1</sup>H NMR (400 MHz CDCl<sub>3</sub>):  $\delta$  3.68 (3H, s), 2.46 (1H, m), 2.35 (1H, dd,  $J$  = 10.1, 5.3 Hz), 0.95 (3H, d,  $J$  = 6.5 Hz), 0.84 (3H, s), 0.81 (3H, s). <sup>13</sup>C NMR (100 MHz CDCl<sub>3</sub>):  $\delta$  172.2, 56.6, 51.5, 43.9 (2C), 37.3, 37.1, 36.7, 35.9, 35.3 (2C), 34.1, 31.0, 30.8, 27.7, 27.1 (2C), 26.6, 25.7, 24.9, 24.6, 21.7, 19.4, 18.7, 18.3. HRESIMS  $m/z$  375.3265 [M + H]<sup>+</sup>, C<sub>25</sub>H<sub>43</sub>O<sub>2</sub> requires 375.3263.

**5 $\beta$ -Cholan-24-ol (14).** Dry methanol (8  $\mu$ L, 0.19 mmol) and LiBH<sub>4</sub> (95  $\mu$ L, 2 M in THF, 0.19 mmol) were added to a solution of **37** (10 mg, 26.7  $\times$  10<sup>–3</sup> mmol) in dry THF (5 mL) at 0 °C under argon, and the resulting mixture was stirred for 3 h at 0 °C. The mixture was quenched by addition of NaOH (1 M, 55  $\mu$ L) and then allowed to warm to room temperature. Ethyl acetate was added, and the separated aqueous phase was extracted with ethyl acetate (3  $\times$  15 mL). The combined organic phases were washed with water, dried (Na<sub>2</sub>SO<sub>4</sub>), and concentrated to give 7.8 mg of **14** (84%). An analytic sample was obtained by HPLC on a Nucleodur 100–5 C18 (5  $\mu$ m; 4.6 mm i.d.  $\times$  250 mm) with MeOH/H<sub>2</sub>O (99.5:0.5) as eluent (flow rate 1 mL/min,  $t_R$  = 18 min);  $[\alpha]_D^{25}$  = +20.5 (c 0.20, CH<sub>3</sub>OH). Selected <sup>1</sup>H NMR (400 MHz CDCl<sub>3</sub>):  $\delta$  3.62 (2H, m), 0.94 (3H, d, ovl), 0.92 (3H,

s), 0.65 (3H, s). <sup>13</sup>C NMR (100 MHz CDCl<sub>3</sub>):  $\delta$  63.7, 56.7, 56.3, 43.9, 42.8, 40.6 (2C), 40.3, 37.8, 36.0, 35.6, 31.9, 29.5, 28.3, 27.6, 27.3 (2C), 27.0, 26.8, 24.4, 21.4, 20.9, 18.7, 12.2. HRESIMS  $m/z$  347.3321 [M + H]<sup>+</sup>, C<sub>24</sub>H<sub>43</sub>O requires 347.3314.

**5 $\beta$ -Cholan-24-yl-24-sodium sulfate (15).** At a solution of **14** (5 mg, 14.5  $\times$  10<sup>–3</sup> mmol) in DMF dry (3 mL) was added triethylamine–sulfur trioxide complex (12 mg, 72.5  $\times$  10<sup>–3</sup> mmol) under an argon atmosphere, and the mixture was stirred at 80 °C for 24 h. Most of the solvent was evaporated, and the residue was poured over a RP18 column to remove excess SO<sub>3</sub>–NEt<sub>3</sub>. Fraction eluted with MeOH gave 1.5 mg of compound **15** (23%). An analytic sample was obtained by HPLC on a Nucleodur 100–5 C18 (5  $\mu$ m; 4.6 mm i.d.  $\times$  250 mm) with MeOH/H<sub>2</sub>O (98:2) as eluent (flow rate 1 mL/min,  $t_R$  = 9.9 min);  $[\alpha]_D^{25}$  = +9.0 (c 0.88, CH<sub>3</sub>OH). Selected <sup>1</sup>H NMR (400 MHz CD<sub>3</sub>OD):  $\delta$  3.64 (2H, m), 0.96 (3H, d, ovl), 0.95 (3H, s), 0.69 (3H, s). <sup>13</sup>C NMR (100 MHz CD<sub>3</sub>OD):  $\delta$  69.7, 57.6, 47.9, 45.2, 43.8, 41.9, 41.6, 38.7, 37.3, 36.8, 36.5, 33.2, 29.3, 28.6, 28.4, 28.2, 27.7, 27.1, 25.3, 24.8, 22.4, 22.0, 19.2, 12.5. HRESIMS  $m/z$  425.2732 [M – H]<sup>–</sup>, C<sub>24</sub>H<sub>41</sub>O<sub>4</sub>S requires 425.2726.

**Compound 16.** Compound **38** (12 mg, 32.0  $\times$  10<sup>–3</sup> mmol) was hydrolyzed with a methanol solution of sodium hydroxide (5%, 5 mL) in H<sub>2</sub>O (1 mL) overnight under reflux. The resulting solution was then concentrated under vacuum, diluted with water, acidified with HCl 6 N, and extracted with ethyl acetate (3  $\times$  50 mL). The collected organic phases were washed with brine, dried over Na<sub>2</sub>SO<sub>4</sub> anhydrous, and evaporated under reduced pressure to give 9 mg of carboxyl acid **16** (78%). An analytic sample was obtained by HPLC on a Nucleodur 100–5 C18 (5  $\mu$ m; 4.6 mm i.d.  $\times$  250 mm) with MeOH/H<sub>2</sub>O (99:1) as eluent (flow rate 1 mL/min,  $t_R$  = 21 min);  $[\alpha]_D^{25}$  = +12.7 (c 0.28, CHCl<sub>3</sub>). Selected <sup>1</sup>H NMR (400 MHz CDCl<sub>3</sub>):  $\delta$  2.42 (1H, m), 2.28 (1H, m), 0.97 (3H, d,  $J$  = 6.8 Hz), 0.85 (3H, s), 0.81 (3H, s). HRESIMS  $m/z$  359.2958 [M – H]<sup>–</sup>, C<sub>24</sub>H<sub>39</sub>O<sub>2</sub> requires 359.2950.

**Compound 17.** Compound **17** (18 mg, 97%) was synthesized, starting from compound **38** (20 mg, 53.5  $\times$  10<sup>–3</sup> mmol), by analogous procedures to those detailed above for compound **14**. An analytic sample was obtained by HPLC on a Nucleodur 100–5 C18 (5  $\mu$ m; 4.6 mm i.d.  $\times$  250 mm) with MeOH/H<sub>2</sub>O (99.5:0.5) as eluent (flow rate 1 mL/min,  $t_R$  = 15.8 min);  $[\alpha]_D^{25}$  = +2.9 (c 0.18, CHCl<sub>3</sub>). Selected <sup>1</sup>H NMR (400 MHz CDCl<sub>3</sub>):  $\delta$  3.64 (2H, m), 0.97 (3H, d,  $J$  = 6.3 Hz), 0.85 (3H, s), 0.81 (3H, s). <sup>13</sup>C NMR (100 MHz CDCl<sub>3</sub>):  $\delta$  63.6, 56.9, 44.1 (2C), 42.6, 37.4 (2C), 36.7, 36.1, 35.3, 34.2, 31.7, 29.3, 27.7, 27.2, 27.1, 26.6, 25.8, 24.9, 24.6, 21.7, 19.5, 19.1, 18.1. HR ESIMS  $m/z$  347.3318 [M + H]<sup>+</sup>, C<sub>24</sub>H<sub>43</sub>O requires 347.3314.

**Compound 18.** Compound **18** (8.8 mg, 43%) was synthesized, starting from compound **17** (16 mg, 46.2  $\times$  10<sup>–3</sup> mmol), by an analogous procedure to that detailed above for compound **15**. An analytic sample was obtained by HPLC on a Nucleodur 100–5 C18 (5  $\mu$ m; 4.6 mm i.d.  $\times$  250 mm) with MeOH/H<sub>2</sub>O (98:2) as eluent (flow rate 1 mL/min,  $t_R$  = 9 min);  $[\alpha]_D^{25}$  = +9.7 (c 0.15, CH<sub>3</sub>OH). Selected <sup>1</sup>H NMR (400 MHz CD<sub>3</sub>OD):  $\delta$  3.96 (2H, m), 0.98 (3H, d,  $J$  = 6.3 Hz), 0.87 (3H, s), 0.81 (3H, s). HRESIMS  $m/z$  425.2733 [M – Na]<sup>–</sup>, C<sub>24</sub>H<sub>41</sub>O<sub>4</sub>S requires 425.2726.

**Methyl 3 $\alpha$ -Tosyloxy-7 $\alpha$ -hydroxy-5 $\beta$ -cholan-24-oate (39).** To a solution of CDCA methyl ester (400 mg, 1.0 mmol) in dry pyridine (10 mL), tosyl chloride (382 mg, 2.0 mmol) was added and the mixture was stirred at room temperature for 4 h. It was poured into cold water (20 mL) and extracted with CH<sub>2</sub>Cl<sub>2</sub> (3  $\times$  50 mL). The combined organic layer was washed with saturated NaHCO<sub>3</sub> solution (30 mL) and water (30 mL) and then dried over anhydrous MgSO<sub>4</sub> and evaporated in vacuo to give 555 mg of **39** (quantitative yield) in the form of colorless oil;  $[\alpha]_D^{25}$  = +22.6 (c 0.93, CH<sub>3</sub>OH). Selected <sup>1</sup>H NMR (500 MHz CDCl<sub>3</sub>):  $\delta$  7.80 (2H, d,  $J$  = 8.5 Hz), 7.34 (2H, d,  $J$  = 8.5 Hz), 4.38 (1H, m), 3.83 (1H, s), 3.62 (3H, s), 2.40 (3H, s) 2.35 (1H, m), 2.23 (1H, m), 0.93 (3H, d,  $J$  = 6.4 Hz), 0.89 (3H, s), 0.65 (3H, s). HRESIMS  $m/z$  561.3288 [M + H]<sup>+</sup>, C<sub>32</sub>H<sub>49</sub>O<sub>6</sub>S requires 561.3283.

**Methyl 3 $\beta$ ,7 $\alpha$ -Dihydroxy-5 $\beta$ -cholan-24-oate (40).** A solution of **39** (555 mg, 0.99 mmol) and CH<sub>3</sub>COOK (97 mg, 0.99 mmol) dissolved in water (2 mL) and *N,N'*-dimethylformamide (DMF, 10 mL) was refluxed for 2 h. The solution was cooled at room temperature, and

then ethyl acetate and water were added. The separated aqueous phase was extracted with ethyl acetate (3 × 30 mL). The combined organic phases were washed with water, dried (Na<sub>2</sub>SO<sub>4</sub>), and evaporated to dryness to give 600 mg of mixture. Purification by silica gel (hexane–ethyl acetate 7:3 and 0.5% TEA) gave **40** as oily oil (300 mg, 75%); [ $\alpha$ ]<sub>D</sub><sup>25</sup> = +2.6 (c 1.5, CH<sub>3</sub>OH). Selected <sup>1</sup>H NMR (400 MHz CD<sub>3</sub>OD):  $\delta$  3.96 (1H, s), 3.79 (1H, s), 3.63 (3H, s), 2.47 (dt, *J* = 2.3, 13.7 Hz), 2.36 (1H, m), 2.26 (1H, m), 0.95 (3H, s), 0.94 (3H, d, ovl), 0.68 (3H, s). <sup>13</sup>C NMR (100 MHz CD<sub>3</sub>OD):  $\delta$  171.7, 69.3, 67.7, 57.3, 52.0, 51.6, 43.7, 41.1, 40.7, 37.5 (2C), 36.7 (2C), 35.5, 33.4, 32.3, 31.9, 31.0, 29.3, 28.6, 24.6, 23.8, 22.1, 18.8, 12.2. HRESIMS *m/z* 407.3173 [M + H]<sup>+</sup>, C<sub>25</sub>H<sub>43</sub>O<sub>4</sub> requires 407.3161.

**3 $\beta$ ,7 $\alpha$ -Dihydroxy-5 $\beta$ -cholan-24-*oic* Acid (19).** Compound **40** (70 mg, 17.2 × 10<sup>-2</sup> mmol) was hydrolyzed with a methanol solution of sodium hydroxide (5%, 5 mL) in H<sub>2</sub>O (1 mL) overnight under reflux. The resulting solution was then concentrated under vacuum, diluted with water, acidified with HCl 6 N, and extracted with ethyl acetate (3 × 50 mL). The collected organic phases were washed with brine, dried over Na<sub>2</sub>SO<sub>4</sub> anhydrous, and evaporated under reduced pressure. HPLC purification on a Nucleodur 100–5 C18 (5  $\mu$ m; 5 mm i.d. × 250 mm) with MeOH/H<sub>2</sub>O (75:25) as eluent (flow rate 1 mL/min) gave 60 mg of **19** as a white solid (89%, *t*<sub>R</sub> = 22 min); [ $\alpha$ ]<sub>D</sub><sup>25</sup> = +11 (c 0.07, CH<sub>3</sub>OH). Selected <sup>1</sup>H NMR (400 MHz CD<sub>3</sub>OD):  $\delta$  3.97 (1H, s), 3.79 (1H, s), 2.47 (1H, dt, *J* = 2.34, 13.8 Hz), 2.28 (1H, m), 2.13 (1H, m), 0.96 (3H, d, ovl), 0.95 (3H, s), 0.69 (3H, s). HR ESIMS *m/z* 391.2856 [M – H]<sup>-</sup>, C<sub>24</sub>H<sub>39</sub>O<sub>4</sub> requires 391.2848.

**3 $\beta$ ,7 $\alpha$ -Dihydroxy-5 $\beta$ -cholan-24-*ol* (20).** 2,6-lutidine (570  $\mu$ L, 4.9 mmol) and *tert*-butyldimethylsilyltrifluoromethanesulfonate (336  $\mu$ L, 1.5 mmol) were added at 0 °C to a solution of **40** (200 mg, 0.49 mmol) in 10 mL of CH<sub>2</sub>Cl<sub>2</sub>. After 2 h stirring at 0 °C, the reaction was quenched by addition of aqueous NaHSO<sub>4</sub> (1 M, 30 mL). The layers were separated, and the aqueous phase was extracted with CH<sub>2</sub>Cl<sub>2</sub> (3 × 100 mL). The combined organic layers were washed with NaHSO<sub>4</sub>, water, saturated aqueous NaHCO<sub>3</sub>, and brine and evaporated in vacuo to give 310 mg of methyl 3 $\beta$ ,7 $\alpha$ -di(*tert*-butyldimethylsilyloxy)-5 $\beta$ -cholan-24-*oate* (quantitative yield) in the form of colorless needles, which was subjected to the next step without any purification. To a solution of methyl ester (310 mg, 0.49 mmol) in dry THF (10 mL) at 0 °C, dry methanol (140  $\mu$ L, 3.4 mmol) and LiBH<sub>4</sub> (1.7 mL, 2 M in THF, 3.4 mmol) were added. The resulting mixture was stirred for 1 h at 0 °C. The mixture was quenched by addition NaOH 1 M (1 mL) and then ethyl acetate. The organic phase was washed with water, dried (Na<sub>2</sub>SO<sub>4</sub>), and concentrated to give 250 mg of **41** as a white solid (84%). Methyl ester **41** (200 mg, 0.33 mmol) was dissolved in methanol (5 mL), and 500  $\mu$ L of HCl 37% v/v were added. After 2 h, silver carbonate was added at the solution to precipitate chloride. Then the reaction mixture was centrifuged and the supernatant was concentrated in vacuo. HPLC purification on a Nucleodur 100–5 C18 (5  $\mu$ m; 5 mm i.d. × 250 mm) with MeOH/H<sub>2</sub>O (9:1) as eluent (flow rate 1 mL/min) gave 120 mg of compound **20** as a white solid (96%, *t*<sub>R</sub> = 7 min); [ $\alpha$ ]<sub>D</sub><sup>25</sup> = +22.8 (c 0.06, CH<sub>3</sub>OH). Selected <sup>1</sup>H NMR (500 MHz CD<sub>3</sub>OD):  $\delta$  3.98 (1H, s), 3.80 (1H, s), 3.50 (2H, m), 0.97 (3H, d, *J* = 6.7 Hz), 0.96 (3H, s), 0.70 (3H, s). <sup>13</sup>C NMR (125 MHz CD<sub>3</sub>OD):  $\delta$  69.3, 67.7, 63.6, 57.6, 51.6, 43.7, 41.1, 40.7, 37.5, 37.4, 37.1, 36.7, 35.5, 33.4, 33.2, 31.0, 30.3, 29.3, 28.5, 24.6, 23.8, 22.1, 19.2, 12.2. HRESIMS *m/z* 379.3219 [M + H]<sup>+</sup>, C<sub>24</sub>H<sub>43</sub>O<sub>3</sub> requires 379.3212.

**3 $\beta$ ,7 $\alpha$ -Dihydroxy-5 $\beta$ -cholan-24-*yl*-24-*sodium* Sulfate (21).** The triethylamine–sulfur trioxide complex (65.6 mg, 0.41 mmol) was added to a solution of **41** (50 mg, 82.5 × 10<sup>-3</sup> mmol) in DMF dry (5 mL) under an argon atmosphere, and the mixture was stirred at 80 °C overnight. The solution was then concentrated under vacuum to give 100 mg of crude mixture. The solid was dissolved in methanol (5 mL) and at the solution was added 300  $\mu$ L of HCl 37% v/v. After 1 h, silver carbonate was added at the solution to precipitate chloride. Then the reaction mixture was centrifuged, and the supernatant was concentrated in vacuo. HPLC purification on a Nucleodur 100–5 C18 (5  $\mu$ m; 5 mm i.d. × 250 mm) with MeOH/H<sub>2</sub>O (55:45) as eluent (flow rate 1 mL/min) gave 30 mg of **21** as colorless amorphous solid (76% over two steps, *t*<sub>R</sub> = 11.4 min); [ $\alpha$ ]<sub>D</sub><sup>25</sup> = +18.4 (c 0.04,

CH<sub>3</sub>OH). Selected <sup>1</sup>H NMR (500 MHz CD<sub>3</sub>OD):  $\delta$  3.97 (3H, m), 3.80 (1H, s), 2.49 (1H, t, *J* = 14.3 Hz), 0.97 (3H, d, ovl), 0.96 (3H, s), 0.70 (3H, s). HRESIMS *m/z* 457.2632 [M – Na]<sup>-</sup>, C<sub>24</sub>H<sub>41</sub>O<sub>6</sub>S requires 457.2624.

**Methyl 3 $\beta$ ,7 $\beta$ -Dihydroxy-5 $\beta$ -cholan-24-*oate* (42).** A solution of compound **34** (100 mg, 0.18 mmol) and CH<sub>3</sub>COOK (18 mg, 0.18 mmol) dissolved in water (1 mL) and *N,N*-dimethylformamide (DMF, 4 mL) was refluxed for 3 h. The solution was cooled at room temperature, and then ethyl acetate and water were added. The separated aqueous phase was extracted with ethyl acetate (3 × 30 mL). The combined organic phases were washed with water, dried (Na<sub>2</sub>SO<sub>4</sub>), and evaporated to dryness. Purification by silica gel (hexane–ethyl acetate 7:3 and 0.5% TEA) gave **42** as an oil (60 mg, 82%); [ $\alpha$ ]<sub>D</sub><sup>25</sup> = +27.4 (c 0.10, CH<sub>3</sub>OH). Selected <sup>1</sup>H NMR (500 MHz CDCl<sub>3</sub>):  $\delta$  4.06 (1H, s), 3.65 (3H, s), 3.54 (1H, m), 2.34 (1H, m), 2.21 (1H, m), 0.98 (3H, s), 0.92 (3H, d, *J* = 6.8 Hz), 0.67 (3H, s). HRESIMS *m/z* 407.3169 [M + H]<sup>+</sup>, C<sub>25</sub>H<sub>43</sub>O<sub>4</sub> requires 407.3161.

**3 $\beta$ ,7 $\beta$ -Dihydroxy-5 $\beta$ -cholan-24-*oic* Acid (22).** Compound **42** (30 mg, 73.9 × 10<sup>-3</sup> mmol) was hydrolyzed with a methanol solution of sodium hydroxide (5%, 5 mL) in H<sub>2</sub>O (1 mL) overnight under reflux. The resulting solution was then concentrated under vacuum, diluted with water, acidified with HCl 6 N, and extracted with ethyl acetate (3 × 50 mL). The collected organic phases were washed with brine, dried over Na<sub>2</sub>SO<sub>4</sub> anhydrous, and evaporated under reduced pressure. HPLC purification on a Nucleodur 100–5 C18 (5  $\mu$ m; 5 mm i.d. × 250 mm) with MeOH/H<sub>2</sub>O (75:25) as eluent (flow rate 1 mL/min) gave 25 mg of **22** as white solid (87%, *t*<sub>R</sub> = 10.5 min); [ $\alpha$ ]<sub>D</sub><sup>25</sup> = +38.1 (c 0.14, CH<sub>3</sub>OH). Selected <sup>1</sup>H NMR (400 MHz CD<sub>3</sub>OD):  $\delta$  4.00 (1H, s), 3.44 (1H, m), 0.99 (3H, s), 0.96 (3H, d, *J* = 6.3 Hz), 0.69 (3H, s). HRESIMS *m/z* 391.2853 [M – H]<sup>-</sup>, C<sub>25</sub>H<sub>39</sub>O<sub>4</sub> requires 391.2848.

**3 $\beta$ ,7 $\beta$ -Dihydroxy-5 $\beta$ -cholan-24-*ol* (23).** 2,6-Lutidine (86  $\mu$ L, 0.74 mmol) and *tert*-butyldimethylsilyltrifluoromethanesulfonate (51  $\mu$ L, 9 mmol) were added at 0 °C to a solution of **42** (30 mg, 73.9 × 10<sup>-3</sup> mmol) in 5 mL of CH<sub>2</sub>Cl<sub>2</sub>. After 2 h stirring at 0 °C, the reaction was quenched by addition of aqueous NaHSO<sub>4</sub> (1 M, 10 mL). The layers were separated, and the aqueous phase was extracted with CH<sub>2</sub>Cl<sub>2</sub> (3 × 20 mL). The combined organic layers were washed with NaHSO<sub>4</sub>, water, saturated aqueous NaHCO<sub>3</sub>, and brine and evaporated in vacuo to give 45 mg of methyl 3 $\beta$ ,7 $\beta$ -di(*tert*-butyldimethylsilyloxy)-5 $\beta$ -cholan-24-*oate* (96%) in the form of colorless needles, which was subjected to next step without any purification. To a solution of methyl ester (45 mg, 71 × 10<sup>-3</sup> mmol) in dry THF (5 mL), at 0 °C dry methanol (20  $\mu$ L, 0.50 mmol) and LiBH<sub>4</sub> (250  $\mu$ L, 2 M in THF, 0.50 mmol) was added. The resulting mixture was stirred for 1 h at 0 °C. The mixture was quenched by addition NaOH 1 M (35  $\mu$ L) and then ethyl acetate. The organic phase was washed with water, dried (Na<sub>2</sub>SO<sub>4</sub>), and concentrated to give 40 mg of **43** as a white solid (94%), which was dissolved in methanol (3 mL) and treated with 100  $\mu$ L of HCl 37% v/v. After 2 h, silver carbonate was added at the solution to precipitate chloride. Then the reaction mixture was centrifuged and the supernatant was concentrated in vacuo. HPLC purification on a Nucleodur 100–5 C18 (5  $\mu$ m; 10 mm i.d. × 250 mm) with MeOH/H<sub>2</sub>O (9:1) as eluent (flow rate 1 mL/min) gave 18 mg of compound **23** as a white solid (96%, *t*<sub>R</sub> = 6.5 min); [ $\alpha$ ]<sub>D</sub><sup>25</sup> = +32.5 (c 0.31, CH<sub>3</sub>OH). Selected <sup>1</sup>H NMR (400 MHz CD<sub>3</sub>OD):  $\delta$  4.00 (1H, s), 3.52 (2H, m), 3.43 (1H, m), 1.00 (3H, s), 0.96 (3H, d, *J* = 6.5 Hz), 0.72 (3H, s). <sup>13</sup>C NMR (100 MHz CD<sub>3</sub>OD):  $\delta$  72.0, 67.4, 63.6, 57.6, 56.7, 44.8, 44.4, 41.6, 40.1, 38.6, 38.3, 37.0, 35.6, 35.2, 33.3, 30.8, 30.3, 29.7, 28.4, 27.9, 24.5, 22.7, 19.4, 12.7. HRESIMS *m/z* 379.3219 [M + H]<sup>+</sup>, C<sub>24</sub>H<sub>43</sub>O<sub>3</sub> requires 379.3212.

**3 $\beta$ ,7 $\beta$ -Dihydroxy-5 $\beta$ -cholan-24-*yl*-24-*sodium* Sulfate (24).** The triethylamine–sulfur trioxide complex (20 mg, 0.12 mmol) was added to a solution of **43** (15 mg, 24.7 × 10<sup>-3</sup> mmol) in DMF dry (5 mL) under an argon atmosphere, and the mixture was stirred at 80 °C for 24 h. The solution was then concentrated under vacuum. The solid was dissolved in methanol (3 mL) and at the solution was added 50  $\mu$ L of HCl 37% v/v. After 1 h, silver carbonate was added at the solution to precipitate chloride. Then the reaction mixture was centrifuged and the supernatant was concentrated in vacuo. HPLC purification on a Nucleodur 100–5 C18 (5  $\mu$ m; 5 mm i.d. × 250 mm)

with MeOH/H<sub>2</sub>O (55:45) as eluent (flow rate 1 mL/min) gave 8 mg of **24** as colorless amorphous solid (67% over two steps,  $t_R = 13.5$  min);  $[\alpha]_D^{25} = +30$  ( $c$  0.26, CH<sub>3</sub>OH). Selected <sup>1</sup>H NMR (500 MHz CD<sub>3</sub>OD):  $\delta$  4.00 (1H, s), 3.96 (2H, m), 3.44 (1H, m), 0.99 (3H, s), 0.97 (3H, d,  $J = 6.6$  Hz), 0.72 (3H, s). HRESIMS  $m/z$  457.2631 [M - Na]<sup>-</sup>, C<sub>24</sub>H<sub>41</sub>O<sub>6</sub>S requires 457.2624.

**Compound 28.** To a methanol solution of compound **44** (400 mg, 0.93 mmol), a large excess of NaBH<sub>4</sub> was added at 0 °C. The mixture was left at room temperature for 10 h, and then water and MeOH was added dropwise during a period of 15 min at 0 °C with effervescence being observed. Then after evaporation of the solvents, the residue was diluted with water and extracted with AcOEt (3 × 50 mL). The combined extract was washed with brine, dried with Na<sub>2</sub>SO<sub>4</sub>, and evaporated to give 400 mg of a crude residue that was subjected to the next step without further purification. To a solution of crude residue (400 mg, 0.93 mmol) in dry THF (30 mL), at 0 °C dry methanol (260  $\mu$ L, 6.51 mmol) and LiBH<sub>4</sub> (3.2 mL, 2 M in THF, 6.51 mmol) were added. The resulting mixture was stirred for 2 h at 0 °C. The mixture was quenched by addition of 1 M NaOH (2 mL) and then ethyl acetate. The organic phase was washed with water, dried (Na<sub>2</sub>SO<sub>4</sub>), and concentrated. HPLC purification on a Nucleodur 100–5 C18 (5  $\mu$ m; 10 mm i.d. × 250 mm) with MeOH/H<sub>2</sub>O (88:12) as eluent (flow rate 3 mL/min) gave 320 mg of **28** (85% over two steps,  $t_R = 9.2$  min);  $[\alpha]_D^{25} = +18.1$  ( $c$  0.36, CH<sub>3</sub>OH). <sup>1</sup>H and <sup>13</sup>C NMR spectroscopic data in CD<sub>3</sub>OD are given in Supporting Information, Tables S1 and S2. HRESIMS  $m/z$  405.3373 [M + H]<sup>+</sup>, C<sub>26</sub>H<sub>43</sub>O<sub>3</sub> requires 405.3369.

**6 $\beta$ -Ethyl-3 $\alpha$ ,7 $\beta$ -dihydroxy-5 $\beta$ -cholan-24-ol (26) and 6 $\beta$ -Ethyl-3 $\alpha$ ,7 $\alpha$ -dihydroxy-5 $\beta$ -cholan-24-ol (27).** To a methanol solution of **45** (1.1 g, 2.5 mmol), a large excess of NaBH<sub>4</sub> was added at 0 °C. The mixture was left at room temperature for 10 h, and then water and MeOH was added dropwise during a period of 15 min at 0 °C with effervescence being observed. Then after evaporation of the solvents, the residue was diluted with water and extracted with AcOEt (3 × 50 mL). The combined extract was washed with brine, dried with Na<sub>2</sub>SO<sub>4</sub>, and evaporated to give 1.3 g of a crude residue that was subjected to the next step without further purification. To a solution of crude residue (1.1 g, 2.5 mmol) in dry THF (30 mL), at 0 °C dry methanol (708  $\mu$ L, 17.5 mmol) and LiBH<sub>4</sub> (8.7 mL, 2 M in THF, 17.5 mmol) were added. The resulting mixture was stirred for 2 h at 0 °C. The mixture was quenched by addition of 1 M NaOH (6 mL) and then ethyl acetate. The organic phase was washed with water, dried (Na<sub>2</sub>SO<sub>4</sub>), and concentrated. HPLC purification on a Nucleodur 100–5 C18 (5  $\mu$ m; 10 mm i.d. × 250 mm) with MeOH/H<sub>2</sub>O (88:12) as eluent (flow rate 3 mL/min) gave 805 mg of **26** (79%,  $t_R = 11$  min) and 361 mg of **27** (35%,  $t_R = 20.4$  min).

**6 $\beta$ -Ethyl-3 $\alpha$ ,7 $\beta$ -dihydroxy-5 $\beta$ -cholan-24-ol (26).**  $[\alpha]_D^{25} = +15.2$  ( $c$  1.21, CH<sub>3</sub>OH). <sup>1</sup>H and <sup>13</sup>C NMR spectroscopic data in CD<sub>3</sub>OD given in Supporting Information, Tables S1 and S2. HRESIMS  $m/z$  407.3529 [M + H]<sup>+</sup>, C<sub>26</sub>H<sub>47</sub>O<sub>3</sub> requires 407.3525.

**6 $\beta$ -Ethyl-3 $\alpha$ ,7 $\alpha$ -dihydroxy-5 $\beta$ -cholan-24-ol (27).**  $[\alpha]_D^{25} = +5.1$  ( $c$  5.74, CH<sub>3</sub>OH). <sup>1</sup>H and <sup>13</sup>C NMR spectroscopic data in CD<sub>3</sub>OD given in Supporting Information, Tables S1 and S2. HRESIMS  $m/z$  407.3532 [M + H]<sup>+</sup>, C<sub>26</sub>H<sub>47</sub>O<sub>3</sub> requires 407.3525.

**6 $\alpha$ -Ethyl-3 $\alpha$ ,7 $\alpha$ -dihydroxy-24-nor-5 $\beta$ -cholan-23-nitrile (31).** To a solution of **47** (200 mg, 0.52 mmol) in dry THF (10 mL), at 0 °C dry methanol (150  $\mu$ L, 3.6 mmol) and LiBH<sub>4</sub> (1.8 mL, 2 M in THF, 3.6 mmol) was added. The resulting mixture was stirred for 2 h at 0 °C. The mixture was quenched by addition of 1 M NaOH (1 mL) and then ethyl acetate. The organic phase was washed with water, dried (Na<sub>2</sub>SO<sub>4</sub>), and concentrated. HPLC purification on a Nucleodur 100–5 C18 (5  $\mu$ m; 10 mm i.d. × 250 mm) with MeOH/H<sub>2</sub>O (88:12) as eluent (flow rate 3 mL/min) gave 805 mg of **31** (79%,  $t_R = 15.2$  min);  $[\alpha]_D^{25} = -13.4$  ( $c$  0.47, CH<sub>3</sub>OH). <sup>1</sup>H NMR (700 MHz CD<sub>3</sub>OD):  $\delta$  3.66 (1H, br s), 3.31 (1H, ovl), 2.46 (1H, dd,  $J = 3.8, 16.9$  Hz), 2.34 (1H, dd,  $J = 7.4, 16.9$  Hz), 1.16 (3H, d,  $J = 6.5$  Hz), 0.91 (3H, t,  $J = 7.5$  Hz), 0.92 (3H, s), 0.73 (3H, s). <sup>13</sup>C NMR (175 MHz CD<sub>3</sub>OD):  $\delta$  120.3, 72.9, 70.9, 56.1, 51.5, 46.7, 43.4, 42.9, 41.4, 40.2, 36.5, 36.2, 34.3 (2C), 34.2, 30.7, 29.2, 24.9, 24.4, 23.4, 23.3, 21.9, 18.5, 12.1, 11.6. HRESIMS  $m/z$  388.3221 [M + H]<sup>+</sup>, C<sub>25</sub>H<sub>42</sub>NO<sub>2</sub> requires 388.3216.

**6 $\alpha$ -Ethyl-3 $\alpha$ ,7 $\alpha$ -dihydroxy-24-nor-5 $\beta$ -cholan-23-oic Acid (29).** To a solution of **48** (500 mg, 1.2 mmol) in dry THF (30 mL), at 0 °C dry methanol (360  $\mu$ L, 8.4 mmol) and LiBH<sub>4</sub> (4.2 mL, 2 M in THF, 8.4 mmol) was added. The resulting mixture was stirred for 1 h at 0 °C. The mixture was quenched by addition of 1 M NaOH (2.4 mL) and then ethyl acetate. The organic phase was washed with water, dried (Na<sub>2</sub>SO<sub>4</sub>), and concentrated. Purification by silica gel (CH<sub>2</sub>Cl<sub>2</sub>/MeOH 9:1) gave **29** as a white solid (400 mg, 82%). An analytic sample was obtained by HPLC on a Nucleodur 100–5 C18 (5  $\mu$ m; 4.6 mm i.d. × 250 mm) with MeOH/H<sub>2</sub>O (88:12) as eluent (flow rate 1 mL/min,  $t_R = 9.6$  min);  $[\alpha]_D^{25} = +3.3$  ( $c$  1.04, CH<sub>3</sub>OH). <sup>1</sup>H NMR (500 MHz CD<sub>3</sub>OD):  $\delta$  3.66 (1H, s), 3.32 (1H, ovl), 2.35 (1H, dd,  $J = 13.4, 3.3$  Hz), 1.00 (3H, d,  $J = 6.4$  Hz), 0.92 (3H, s), 0.90 (3H, t,  $J = 7.1$  Hz), 0.74 (3H, s). <sup>13</sup>C NMR (125 MHz CD<sub>3</sub>OD):  $\delta$  178.0, 72.9, 70.9, 57.6, 51.4, 46.7, 43.7, 43.6, 42.8, 41.2, 40.8, 36.8, 36.0, 34.8, 34.4, 34.0, 31.0, 29.1, 24.3, 23.4, 23.3, 21.8, 19.3, 12.0, 11.8; HR ESIMS  $m/z$  405.3011 [M - H]<sup>-</sup>, C<sub>25</sub>H<sub>41</sub>O<sub>4</sub> requires 405.3005.

**6 $\alpha$ -Ethyl-3 $\alpha$ ,7 $\alpha$ -dihydroxy-24-nor-5 $\beta$ -cholan-23-ol (30).** Compound **48** (420 mg, 1.0 mmol) was dissolved in 90 mL of dry methanol and treated with *p*-toluenesulfonic acid in catalytic amount. The solution was left to stand at room temperature for 2 h. The mixture was quenched by addition until the neutrality of NaHCO<sub>3</sub> saturated solution. Most of the solvent was evaporated, and the residue was extracted with EtOAc. To a solution of crude solid (420 mg, quantitative yield) in dry THF (10 mL), at 0 °C dry methanol (300  $\mu$ L, 7.0 mmol) and LiBH<sub>4</sub> (3.5 mL, 2 M in THF, 7.0 mmol) was added. The resulting mixture was stirred for 1 h at 0 °C. The mixture was quenched by addition of 1 M NaOH (2.0 mL) and then ethyl acetate. The organic phase was washed with water, dried (Na<sub>2</sub>SO<sub>4</sub>), and concentrated. Silica gel chromatography eluting with hexane/EtOAc 6:4 afforded compound **30** (383 mg, 98% over two steps). An analytic sample was obtained by HPLC on a Nucleodur 100–5 C18 (5  $\mu$ m; 4.6 mm i.d. × 250 mm) with MeOH/H<sub>2</sub>O (88:12) as eluent (flow rate 1 mL/min,  $t_R = 10.8$  min);  $[\alpha]_D^{25} = +4.4$  ( $c$  1.42, CH<sub>3</sub>OH). <sup>1</sup>H and <sup>13</sup>C NMR spectroscopic data in CD<sub>3</sub>OD given in Supporting Information, Tables S1 and S2. HR ESIMS  $m/z$  393.3374 [M + H]<sup>+</sup>, C<sub>25</sub>H<sub>45</sub>O<sub>3</sub> requires 393.3369.

**Cell Cultures.** HepG2 cells were cultured in E-MEM supplemented with 10% FBS, 1% glutamine, 1% penicillin/streptomycin.

GLUTAg cells were originally donated by Dr. D. J. Drucker, Banting and Best Diabetes Centre, University of Toronto, Toronto General Hospital, 200 Elizabeth Street MBRW-4R402, Toronto, Canada M5G 2C4. GLUTAg cells were cultured in D-MEM, supplemented with 10% FBS, 1% glutamine, and 1% penicillin/streptomycin.

THP-1 cells were cultured in RPM-1 supplemented with 10% FBS, 1% glutamine, and 1% penicillin/streptomycin.

**Transactivation Assay.** For FXR mediated transactivation, HepG2 cells were plated at 5 × 10<sup>4</sup> cells/well in a 24 well plate. Cells were transfected with 200 ng of the reporter vector p(hsp27)-TK-LUC containing the FXR response element IR1 cloned from the promoter of heat shock protein 27 (hsp27), 100 ng of pSG5-FXR, 100 ng of pSG5-RXR, and 100 of pGL4.70 (Promega), a vector encoding the human Renilla gene. The reporter plasmid p(hsp27)-TKLUC has been developed and validated for FXR reporter activity as previously reported.<sup>29</sup>

At 24 h post-transfection, cells were stimulated 18 h with 10  $\mu$ M CDCA (**1**) and compounds **4–31**. For GP-BAR1 mediated transactivation, HEK-293T cells were plated at 1 × 10<sup>4</sup> cells/well in a 24 well-plate and transfected with 200 ng of pGL4.29 (Promega), a reporter vector containing a cAMP response element (CRE) that drives the transcription of the luciferase reporter gene luc2P, with 100 ng of pCMVSPORT6-human GP-BAR1, and with 100 ng of pGL4.70. At 24 h post-transfection, cells were stimulated 18 h with 10  $\mu$ M TLCA (**2**) and compounds **4–31**. After treatments, 10  $\mu$ L of cellular lysates were read using Dual Luciferase Reporter Assay System (Promega Italia srl, Milan, Italy) according manufacturer specifications using the Glomax20/20 luminometer (Promega Italia srl, Milan, Italy). For dose-response curves, cells were transfected as described above and then treated with increasing concentrations of **7**, **26**, and **30** (0.1,

0.5, 1, and 10 and 50  $\mu\text{M}$ ); luciferase activities were assayed and normalized with Renilla activities.

To investigate the specificity of compounds **7**, **26**, and **30**, HepG2 cells were transiently transfected with 200 ng of reporter vector p(UAS)<sub>SX</sub>TKLuc, 100 ng of pGL4.70, and with a series of vectors containing the ligand binding domain of various nuclear receptors (PPAR $\gamma$ , LXR, and GR) cloned upstream of the GAL4-DNA binding domain (i.e., pSG5-PPAR $\gamma$ LBD-GAL4DBD, pSG5-LXRLBD-GAL4DBD, and pSG5-GRLBD-GAL4DBD). At 48 h post-transfection, cells were stimulated 18 h with the appropriate nuclear receptor agonist or with **7**, **26**, and **30**. To investigate the PXR mediated transactivation, HepG2 cells were transfected with 100 ng of pSG5-PXR, 100 ng of pSG5-RXR, 100 ng of pGL4.70, and with 200 ng of the reporter vector containing the PXR target gene promoter (CYP3A4 gene promoter) cloned upstream of the luciferase gene (pCYP3A4promoter-TKLuc). At 48 h post-transfection, cells were stimulated 18 h with 10  $\mu\text{M}$  rifaximin or with **7**, **26**, and **30**.

**Real-Time PCR.** Total RNA was isolated using the TRIzol reagent according to the manufacturer's specifications (Invitrogen). One microgram of purified RNA was treated with DNaseI for 15 min at room temperature, followed by incubation at 95 °C for 3 min in the presence of 2.5 mmol/L EDTA. The RNA was reverse transcribed with Superscript III (Invitrogen) in 20  $\mu\text{L}$  reaction volume using random primers. For Real Time PCR, a 10 ng template was dissolved in 25  $\mu\text{L}$  containing 200 nmol/L of each primer and 12.5  $\mu\text{L}$  of 2 $\times$  SYBR FAST Universal ready mix (Invitrogen). All reactions were performed in triplicate, and the thermal cycling conditions were as follows: 2 min at 95 °C, followed by 40 cycles of 95 °C for 20 s and 60 °C for 30 s in iCycler iQ instrument (Biorad). The relative mRNA expression was calculated and expressed as  $2^{-(\Delta\Delta\text{Ct})}$ . Forward and reverse primer sequences were the following: human GAPDH, gaaggtgaaggtcggagt and catgggtggaatcatattggaa; human OST $\alpha$ , tgttggcccttccaatac and ggctcccatgtctgctcac; human BSEP, gggccattgacgagatcctaa and tgcaccgtctttcactttctg; human SHP, gctgtctggagtcctctgg and ccaatgataggcgcaagaagag; mouse GAPDH, ctgagtgtctgtggagtctac and gttgtgtgtcaggatgctcattg; mouse Pro-glucagon, tgaagacaacgccaactac and caatgtgttccggttcctc.

**cAMP Measurement.** cAMP generation in THP-1 cells was assayed using the Direct Cyclic AMP enzyme immuno-assay kit (Arbor Assay cat. no. K019-H1). THP-1 cells were serum starved overnight and then stimulated for 30 min with 10  $\mu\text{M}$  forskolin or **7**, **26**, and **30**.

**Animal Studies.** GP-BAR1 null mice (GP-BAR1-B6 = GP-BAR12/2 mice, generated directly into C57BL/6NcrJ background) and congenic littermates on C57BL/6NcrJ mice were kindly gifted by Dr. Galya Vassileva (Schering-Plough Research Institute, Kenilworth). Mice were housed under controlled temperatures (22 °C) and photoperiods (12:12 h light/dark cycle), allowed unrestricted access to standard mouse chow and tap water, and allowed to acclimate to these conditions for at least 5 days before inclusion in an experiment. Protocol for ANIT administration was approved by Ministry of Health (decree no. 245/2013-B). Mice (six males per group) were treated for nine days with ANIT (Sigma-Aldrich) dissolved in corn oil (10 mg/kg, os) or corn oil alone (control mice). At the end of the treatment, mice were subjected to intradermal injection of 25  $\mu\text{g}$  of DCA, 6-ECDC, UDCA, and compound **30** and the scratching response was recorded for 60 min. Serum levels of total bilirubin, aspartate aminotransferase (AST), and alkaline phosphatase were measured by routine clinical chemistry testing performed on a Hitachi 717 automatic analyzer.

**Direct Interaction on FXR by Alphascreen Technology in a Coactivator Recruitment Assay.** Anti-GST-coated acceptor beads were used to capture the GST-fusion FXR-LBD, whereas the biotinylated-SRC-1 peptide was captured by the streptavidin donor beads. Upon illumination at 680 nm, chemical energy is transferred from donor to acceptor beads across the complex streptavidin-donor/Src-1-biotin/GSTFXR-LBD/anti-GST-acceptor and a signal is produced. The assay was performed in white, low-volume, 384-well Opti plates (PerkinElmer) using a final volume of 25  $\mu\text{L}$  containing final concentrations of 10 nM of purified GST-tagged FXR-LBD protein, 30 nM biotinylated Src-1 peptide, 20  $\mu\text{g}/\text{mL}$  anti-GST acceptor beads acceptor beads, and 10  $\mu\text{g}/\text{mL}$  of streptavidin donor bead

(PerkinElmer). The assay buffer contained 50 mM Tris (pH 7.4), 50 mM KCl, 0.1% BSA, and 1 mM DTT. The stimulation times with 1  $\mu\text{L}$  of tested compound (dissolved in 50% DMSO/H<sub>2</sub>O) were fixed to 30 min at room temperature. The concentration of DMSO in each well was maintained at a final concentration of 4%. After the addition of the detection mix (acceptor and donor beads), the plates were incubated in the dark for 4 h at room temperature and then were read in an Envision microplate analyzer (PerkinElmer).

## ■ ASSOCIATED CONTENT

### 📄 Supporting Information

Concentration–response curve of 6-ECDC (3) on FXR and GP-BAR1. Tabulated NMR data for compounds **25–28** and **30**, tabulated analytical data for all tested compounds (HPLC ks, MS data), and NMR spectra for all tested compounds. This material is available free of charge via the Internet at <http://pubs.acs.org>.

## ■ AUTHOR INFORMATION

### Corresponding Author

\*Phone: (0039) 081-678525. Fax: (0039) 081-678552. E-mail: [angela.zampella@unina.it](mailto:angela.zampella@unina.it).

### Notes

The authors declare no competing financial interest.

## ■ ACKNOWLEDGMENTS

This work was supported by grants from PSC Partners (5237 South Kenton Way, Englewood, Colorado 80111 USA) and grants from BAR Pharmaceuticals, Srl, Italy.

## ■ ABBREVIATIONS USED

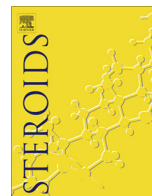
CAR, androstane receptor; CDCA, chenodeoxycholic acid; FXR, farnesoid-X-receptor; GLP-1, glucagon-like peptide 1; GP-BAR1, G-protein coupled bile acid receptor 1; HepG2, human hepatoma cell line; HEK-293T, human embryonic kidney 293 cells; LBD, ligand binding domain; LCA, lithocholic acid; NASH, nonalcoholic steato-hepatitis; OST $\alpha$ , organic solute transporter  $\alpha$ ; PBC, primary biliary cirrhosis; PSC, primary sclerosing cholangitis; SRC-1, steroid receptor coactivator 1; TLCA, tauro-lithocholic acid; UDCA, ursodeoxycholic acid

## ■ REFERENCES

- (1) Fiorucci, S.; Rizzo, G.; Donini, A.; Distrutti, E.; Santucci, L. Targeting farnesoid X receptor for liver and metabolic disorders. *Trends Mol. Med.* **2007**, *13*, 298–309.
- (2) Fiorucci, S.; Mencarelli, A.; Palladino, G.; Cipriani, S. Bile-acid-activated receptors: targeting TGR5 and farnesoid-X-receptor in lipid and glucose disorders. *Trends Pharmacol. Sci.* **2009**, *30*, 570–580.
- (3) Makishima, M.; Okamoto, A. Y.; Repa, J. J.; Tu, H.; Learned, R. M.; Luk, A.; Hull, M. V.; Lustig, K. D.; Mangelsdorf, D. J.; Shan, B. Identification of a nuclear receptor for bile acids. *Science* **1999**, *284*, 1362–1365.
- (4) Parks, D. J.; Blanchard, S. G.; Bledsoe, R. K.; Chandra, G.; Consler, T. G.; Kliewer, S. A.; Stimmel, J. B.; Willson, T. M.; Zavacki, A. M.; Moore, D. D.; Lehmann, J. M. Bile acids: natural ligands for an orphan nuclear receptor. *Science* **1999**, *284*, 1365–1368.
- (5) Wang, H.; Chen, J.; Hollister, K.; Sowers, L. C.; Forman, B. M. Endogenous bile acids are ligands for the nuclear receptor FXR/BAR. *Mol. Cell* **1999**, *3*, 543–553.
- (6) Xie, W.; Radomska-Pandya, A.; Shi, Y.; Simon, C. M.; Nelson, M. C.; Ong, E. S.; Waxman, D. J.; Evans, R. M. An essential role for nuclear receptors SXR/PXR in detoxification of cholestatic bile acids. *Proc. Natl. Acad. Sci. U. S. A.* **2001**, *98*, 3375–3380.



- (7) Makishima, M.; Lu, T. T.; Xie, W.; Whitfield, G. K.; Domoto, H.; Evans, R. M.; Haussler, M. R.; Mangelsdorf, D. J. Vitamin D receptor as an intestinal bile acid sensor. *Science* **2002**, *296*, 1313–1316.
- (8) Maruyama, T.; Miyamoto, Y.; Nakamura, T.; Tamai, Y.; Okada, H.; Sugiyama, E.; Nakamura, T.; Itadani, H.; Tanaka, K. Identification of membrane type receptor for bile acids (M-BAR). *Biochem. Biophys. Res. Commun.* **2002**, *298*, 714–719.
- (9) Sheikh Abdul Kadir, S. H.; Miragoli, M.; Abu-Hayyeh, S.; Moshkov, A. V.; Xie, Q.; Keitel, V.; Nikolaev, V. O.; Williamson, C.; Gorelik, J. Bile acid-induced arrhythmia is mediated by muscarinic M2 receptors in neonatal rat cardiomyocytes. *PLoS One* **2010**, *5*, e9689.
- (10) Mencarelli, A.; Renga, B.; Distrutti, E.; Fiorucci, S. Antiatherosclerotic effect of farnesoid X receptor. *Am. J. Physiol.: Heart Circ. Physiol.* **2009**, *296*, 272–281.
- (11) Fiorucci, S.; Baldelli, F. Farnesoid X receptor agonists in biliary tract disease. *Curr. Opin. Gastroenterol.* **2009**, *25*, 252–259.
- (12) Fiorucci, S.; Cipriani, S.; Mencarelli, A.; Baldelli, F.; Bifulco, G.; Zampella, A. Farnesoid X receptor agonist for the treatment of liver and metabolic disorders: focus on 6-ethyl-CDCA. *Mini-Rev. Med. Chem.* **2011**, *11*, 753–762.
- (13) Fiorucci, S.; Cipriani, S.; Baldelli, F.; Mencarelli, A. Bile acid-activated receptors in the treatment of dyslipidemia and related disorders. *Prog. Lipid Res.* **2010**, *49*, 171–185.
- (14) Tiwari, A.; Maiti, P. TGR5: an emerging bile acid G-protein-coupled receptor target for the potential treatment of metabolic disorders. *Drug Discovery Today* **2009**, *14*, 523–530.
- (15) Alemi, F.; Kwon, E.; Poole, D. P.; Lieu, T.; Lyo, V.; Cattaruzza, F.; Cevikbas, F.; Steinhoff, M.; Nassini, R.; Materazzi, S.; Guerrero-Alba, R.; Valdez-Morales, E.; Cottrell, G. S.; Schoonjans, K.; Geppetti, P.; Vanner, S. J.; Bunnett, N. W.; Corvera, C. U. The TGR5 receptor mediates bile acid-induced itch and analgesia. *J. Clin. Invest.* **2013**, *123*, 1513–1530.
- (16) Fiorucci, S.; Mencarelli, A.; Distrutti, E.; Zampella, A. Farnesoid X receptor: from medicinal chemistry to clinical applications. *Future Med. Chem.* **2012**, *4*, 877–891.
- (17) Pellicciari, R.; Fiorucci, S.; Camaioni, E.; Clerici, C.; Costantino, G.; Maloney, P. R.; Morelli, A.; Parks, D. J.; Willson, T. M. 6- $\alpha$ -Ethylchenodeoxycholic acid (6-ECDCA), a potent and selective FXR agonist endowed with anticholestatic activity. *J. Med. Chem.* **2002**, *45*, 3569–3572.
- (18) D'Amore, C.; Di Leva, F. S.; Sepe, V.; Renga, B.; Del Gaudio, C.; D'Auria, M. V.; Zampella, A.; Fiorucci, S.; Limongelli, V. Design, synthesis, and biological evaluation of potent dual agonists of nuclear and membrane bile acid receptors. *J. Med. Chem.* **2014**, *57*, 937–954.
- (19) Pellicciari, R.; Fiorucci, S.; Pruzanski, M. Preparation of bile acid derivatives as FXR ligands for the prevention or treatment of FXR-mediated diseases or conditions. PCT Int. WO 2008002573 A2 20080103, 2008.
- (20) Pellicciari, R.; Sato, H.; Gioiello, A.; Costantino, G.; Macchiarulo, A.; Sadeghpour, B. M.; Giorgi, G.; Schoonjans, K.; Auwerx, J. Nongenomic actions of bile acids. Synthesis and preliminary characterization of 23- and 6,23-alkyl-substituted bile acid derivatives as selective modulators for the G-protein coupled receptor TGR5. *J. Med. Chem.* **2007**, *50*, 4265–4268.
- (21) Sato, H.; Macchiarulo, A.; Thomas, C.; Gioiello, A.; Une, M.; Hofmann, A. F.; Saladin, R.; Schoonjans, K.; Pellicciari, R.; Auwerx, J. Novel potent and selective bile acid derivatives as TGR5 agonists: biological screening, structure–activity relationships, and molecular modeling studies. *J. Med. Chem.* **2008**, *51*, 1831–1841.
- (22) Sepe, V.; Ummarino, R.; D'Auria, M. V.; Lauro, G.; Bifulco, G.; D'Amore, C.; Renga, B.; Fiorucci, S.; Zampella, A. Modification in the side chain of solomonsterol A: discovery of cholestansulfate as a potent pregnane-X-receptor agonist. *Org. Biomol. Chem.* **2012**, *10*, 6350–6362.
- (23) Sepe, V.; Ummarino, R.; D'Auria, M. V.; Chini, M. G.; Bifulco, G.; Renga, B.; D'Amore, C.; Debitus, C.; Fiorucci, S.; Zampella, A. Conicasterol E, a small heterodimer partner sparing farnesoid X receptor modulator endowed with a pregnane X receptor agonistic activity, from the marine sponge *Theonella swinhoei*. *J. Med. Chem.* **2012**, *55*, 84–93.
- (24) Parker, H. E.; Wallis, K.; le Roux, C. W.; Wong, K. Y.; Reimann, F.; Gribble, F. M. Molecular mechanisms underlying bile acid-stimulated glucagon-like peptide-1 secretion. *Br. J. Pharmacol.* **2012**, *165*, 414–423.
- (25) Butler, A. E.; Campbell-Thompson, M.; Gurlo, T.; Dawson, D. W.; Atkinson, M.; Butler, P. C. Marked expansion of exocrine and endocrine pancreas with incretin therapy in humans with increased exocrine pancreas dysplasia and the potential for glucagon-producing neuroendocrine tumors. *Diabetes* **2013**, *62*, 2595–2604.
- (26) Fiorucci, S.; Distrutti, E.; Ricci, P.; Giuliano, V.; Donini, A.; Baldelli, F. Targeting FXR in cholestasis: hype or hope. *Expert Opin. Ther. Targets* **2014**, DOI: 10.1517/14728222.2014.956087.
- (27) Hashimoto, T.; Ohata, H.; Momose, K. Itch–scratch responses induced by lysophosphatidic acid in mice. *Pharmacology* **2004**, *72*, 51–56.
- (28) Kremer, A. E.; Martens, J. J.; Kulik, W.; Ruëff, F.; Kuiper, E. M.; van Buuren, H. R.; van Erpecum, K. J.; Kondrackiene, J.; Prieto, J.; Rust, C.; Geenes, V. L.; Williamson, C.; Moolenaar, W. H.; Beuers, U.; Oude Elferink, R. P. Lysophosphatidic acid is a potential mediator of cholestatic pruritus. *Gastroenterology* **2010**, *139*, 1008–1018.
- (29) Forman, B. M.; Goode, E.; Chen, J.; Oro, A. E.; Bradley, D. J.; Perlmann, T.; Noonan, D. J.; Burka, L. T.; McMorris, T.; Lamph, W. W.; Evans, R. M.; Weinberger, C. Identification of a nuclear receptor that is activated by farnesol metabolites. *Cell* **1995**, *81*, 687–693.



# Investigation on bile acid receptor regulators. Discovery of cholanoic acid derivatives with dual G-protein coupled bile acid receptor 1 (GPBAR1) antagonistic and farnesoid X receptor (FXR) modulatory activity



Valentina Sepe<sup>a</sup>, Barbara Renga<sup>b</sup>, Carmen Festa<sup>a</sup>, Claudia Finamore<sup>a</sup>, Dario Masullo<sup>a</sup>, Adriana Carino<sup>b</sup>, Sabrina Cipriani<sup>b</sup>, Eleonora Distrutti<sup>c</sup>, Stefano Fiorucci<sup>b</sup>, Angela Zampella<sup>a,\*</sup>

<sup>a</sup> Department of Pharmacy, University of Naples "Federico II", Via D. Montesano, 49, I-80131 Naples, Italy

<sup>b</sup> Department of Surgery and Biomedical Sciences, Nuova Facoltà di Medicina, P.zza L. Severi, I-06132 Perugia, Italy

<sup>c</sup> Hospital S. Maria della Misericordia, S. Andrea delle Fratte, 06126 Perugia, Italy

## ARTICLE INFO

### Article history:

Received 1 July 2015

Received in revised form 12 November 2015

Accepted 17 November 2015

Available online 1 December 2015

### Keywords:

Bile acids

Farnesoid X receptor

G protein-coupled bile acid receptor

GPBAR1 antagonists

FXR modulators

## ABSTRACT

Bile acids, the end products of cholesterol metabolism, activate multiple mechanisms through the interaction with membrane G-protein coupled receptors including the bile acid receptor GPBAR1 and nuclear receptors such as the bile acid sensor, farnesoid X receptor (FXR). Even if dual FXR/GPBAR1 agonists are largely considered a novel opportunity in the treatment of several liver and metabolic diseases, selective targeting of one of these receptors represents an attractive therapeutic approach for a wide range of disorders in which dual modulation is associated to severe side effects. In the present study we have investigated around the structure of LCA generating a small library of cholane derivatives, endowed with dual FXR agonism/GPBAR1 antagonism. To the best of our knowledge, this is the first report of bile acid derivatives able to antagonize GPBAR1.

© 2015 Elsevier Inc. All rights reserved.

**Abbreviations:** BSEP, bile salt export pump; CDCA, chenodeoxycholic acid; CRE, cAMP response element; CREB, cAMP-response element binding protein; DMT-MM, 4-(4,6-dimethoxy-1,3,5-triazin-2-yl)-4-methylmorpholinium chloride; 6-ECDCA/OCA, 6-ethylchenodeoxycholic acid/obeticholic acid; ESI-MS, electrospray ionization mass spectrometry; FXR, farnesoid X receptor; GPBAR1, G protein-coupled bile acid receptor 1; HEK293T, human embryonic kidney 293 cells; HepG2, hepatocellular carcinoma human cell line; LCA, lithocholic acid; NAFLD, nonalcoholic fatty liver disease; NASH, nonalcoholic steatohepatitis; OST $\alpha$ , organic solute transporter alpha; PBC, primary biliary cirrhosis; PSC, primary sclerosing cholangitis; PXR, pregnane X receptor; RT-PCR, real-time polymerase chain reaction; SHP, small heterodimer partner; TLCA, tauroolithocholic acid; VDR, vitamin D receptor.

**Reagent lists:** CH<sub>3</sub>COOK; potassium acetate; DMF, *N,N*-dimethylformamide; DMT-MM, 4-(4,6-dimethoxy-1,3,5-triazin-2-yl)-4-methylmorpholinium chloride; Et<sub>3</sub>N, triethylamine; Et<sub>3</sub>N-SO<sub>3</sub>, sulfur trioxide triethylamine complex; HCOOH, formic acid; HClO<sub>4</sub>, perchloric acid; KOH, potassium hydroxide; LiBH<sub>4</sub>, lithium borohydride; LiBr, lithium bromide; Li<sub>2</sub>CO<sub>3</sub>, lithium carbonate; MeOH, methanol; NaNO<sub>2</sub>, sodium nitrite; NaOH, sodium hydroxide; Pd/C, palladium on carbon; Pd(OH)<sub>2</sub>/C, palladium hydroxide on carbon; TFA, trifluoroacetic acid; THF, tetrahydrofuran; *p*-TsOH, *p*-toluenesulfonic acid monohydrate; *p*-TsCl, *p*-toluenesulfonyl chloride.

\* Corresponding author.

E-mail address: [angela.zampella@unina.it](mailto:angela.zampella@unina.it) (A. Zampella).

## 1. Introduction

Bile acids, the end product of cholesterol metabolism, are amphipathic molecules essential for lipid and fat-soluble vitamins solubilization, absorption and metabolism. Bile acids produced in hepatocytes, as primary bile acids, cholic acid (CA) and chenodeoxycholic acid (CDCA), are secreted in the bile ducts, stored in the gallbladder, and then released into the duodenum upon ingestion of a meal to facilitate absorption of triglycerides, cholesterol, and lipid-soluble vitamins [1–5]. In the intestine, primary bile acids undergo a complex metabolism by the intestinal microbiota resulting in generation of secondary bile acids, deoxycholic acid (DCA) and lithocholic acid (LCA). Bile acids are efficiently reabsorbed (>95%) from the intestine, mainly by active transport mediated by the ileal bile acid transporters but also through passive diffusion in the upper small intestine and colon. Synthesis and transport of bile salts are undergo extensive feedback and feed-forward regulation by transcriptional and post-transcriptional mechanisms.

Basic research in the past 2 decades showed that bile acids are signaling molecules activating several cellular networks through the recognition of nuclear and membrane receptors, such as the

farnesoid X receptor (FXR), pregnane X receptor (PXR), vitamin D receptor (VDR), and the cell surface G protein-coupled receptor (GPCR), GPBAR1 [1–6].

A key regulator of hepatocellular bile salt homeostasis is the bile acid receptor farnesoid X receptor (FXR) [1–3]. FXR, is the main sensor of bile acid levels in hepatocytes and in enterocytes and regulates the expression/activity of a number of downstream targets by binding to specific DNA response elements as an heterodimeric complex with the retinoid X receptor (RXR). One FXR target gene is SHP, which encodes an atypical nuclear receptor that lacks a ligand-binding domain and dimerizes with and inactivates both LRH1 and LXR $\alpha$ , resulting in a decrease in CYP7A1 expression and inhibition of bile acid synthesis through the neutral pathway [1–3]. In addition, FXR ligands negatively regulate basolateral bile acid uptake by hepatocytes via repression of NTCP and OATP-1 and -4, while stimulate the overall gene expression of both canalicular MRP3 (multidrug resistance-associated protein 3) and BSEP and alternative basolateral efflux transporters, MRP4 and OST $\alpha$  and  $\beta$  (SLC51 solute carrier family 51,  $\alpha$  and  $\beta$  subunit). In hepatocytes, FXR activation increases the expression of genes encoding for proteins involved in bile acid detoxification: CYP3A4 (cytochrome P450, family 3, subfamily A, polypeptide 4), UGT1A3, (UDP-glucuronosyltransferase 1A3) and Sult2A1 (sulfotransferase family, cytosolic, 2A member 1) [1–3]. Together, these changes lead to a reduced uptake, reduced *de novo* synthesis and increased excretion of bile acids by hepatocytes. In the intestine, FXR activation modulates the expression of specific transporters by repressing the human apical sodium bile acids transporter (ASBT) and inducing the basolateral organic solute transporters (OST $\alpha$  and OST $\beta$ ). Importantly, activation of intestinal FXR increases the expression and causes the release of FGF-15, (FGF-19 in humans) [1–5] which, after binding to the type-4 of FGF receptor (FGF-R4) in hepatocytes, represses Cyp7A1 [1–3].

FXR is validated target in the treatment of liver and metabolic disorders. Currently, FXR ligands have shown beneficial effects in treating cholestasis, in patients affected by primary biliary cirrhosis (PBC) and primary sclerosing cholangitis (PSC), two immune-mediated disorders characterized by progressive bile duct destruction [7,8]. FXR also has an important role in regulating glucose metabolism through regulation of gluconeogenesis and glycogenolysis in the liver, as well as regulation of peripheral insulin sensitivity in striated muscle and adipose tissue, suggesting potential beneficial effects of FXR agonists in patients with type II diabetes, nonalcoholic fatty liver disease (NAFLD) and nonalcoholic steatohepatitis (NASH) [9–11].

In addition to their role of signal molecules activating the nuclear receptor FXR, bile acids also activates the G-protein coupled receptor GPBAR1 (or TGR5) [6]. GPBAR1 is highly expressed along the intestinal tract, with the highest expression found in the ileum and colon [12]. Despite the liver being a major bile acid target organ, GPBAR1 expression in the liver is very low. GPBAR1 is expressed in liver sinusoidal endothelial cells, gallbladder epithelial cells, and Kupffer cells. GPBAR1 is also expressed in nontraditional bile acid target organs including white and brown adipose, spleen, kidney, pancreas, lung, macrophages, and the central nervous system [12,13]. It is generally recognized that GPBAR1 signaling plays important roles in energy and glucose metabolism as well as anti-inflammation in the digestive system.

Both conjugated bile acids and free bile acids are known to bind and activate FXR and GPBAR1. Indeed the activity toward the two bile acid receptors is structure dependent, with CDCA (EC<sub>50</sub> approximately 10  $\mu$ M) and its conjugated forms the most potent endogenous FXR activators and LCA and tauroolithocholic acid (TLCA, EC<sub>50</sub> value of 0.53  $\mu$ M), the strongest natural agonists of GPBAR1.

In the last years bile acid scaffold has been subjected to intense medicinal chemistry strategies, affording to the identification of potent steroidal derivatives with different pharmacological profiles, from dual to selective agonists toward FXR and GPBAR1 [14]. Sure dual agonists represent a novel opportunity in the treatment of dyslipidemia and related disorders [9–11]. On the other hands, cholestasis is the main therapeutic area for potent FXR agonists. 6-ECDC/OCA (obeticholic acid) (a dual FXR/GPBAR1 agonist) [15,16] and Px-102 (non steroidal agonist) have been investigated in clinical trials and the results of the phase II trial with OCA support the notion that FXR activation could be beneficial in this setting [17,18]. However, the use of OCA associates with several side effects the most disturbing of which was itching that was not observed in Phase II pilot study in patients with NAFLD with Px102, a non-steroidal ligand [19]. The explanation for this side effect remains unclear but the recent demonstration that GPBAR1 is the physiological mediator of pruritus [20], suggests that the development of highly selective FXR agonists, devoid of GPBAR1 agonism, could be a rational strategy to circumvent the side effect and might have utility in the treatment of PBC.

Intrinsically steroidal ligands are promiscuous covering the same chemical space of the endogenous activators of FXR and GPBAR1. Indeed the recent observation that the elimination of the hydroxyl groups on the tetracyclic core of 5 $\beta$ -cholane scaffold is detrimental in term of GPBAR1 activation [21,22], could be instrumental in generating selective FXR ligands devoid of any activity toward GPBAR1. In this context and in the frame of our interest in the discovery of nuclear receptor modulators, we have decided to manipulate LCA chemical scaffold modifying the functionalities of tetracyclic core, the stereochemistry of A/B rings junction, the length and the functionalization of the side chain. Pharmacological investigations on the so generated small library of cholane derivatives (Fig. 1) resulted in the identification for the first time of potent FXR agonists/GP-BAR1 antagonists.

## 2. Material and methods

### 2.1. General experimental procedures

Specific rotations were measured on a Jasco P-2000 polarimeter. High-resolution ESI-MS spectra were performed with a Micromass Q-TOF mass spectrometer. NMR spectra were obtained on Varian Inova 400, 500 and 700 NMR spectrometers (<sup>1</sup>H at 400, 500 and 700 MHz, <sup>13</sup>C at 100, 125 and 175 MHz, respectively) equipped with a SUN microsystem ultra5 hardware and recorded in CD<sub>3</sub>OD ( $\delta_H$  = 3.30 and  $\delta_C$  = 49.0 ppm) and CDCl<sub>3</sub> ( $\delta_H$  = 7.26 and  $\delta_C$  = 77.0 ppm). All of the detected signals were in accordance with the proposed structures. Coupling constants (*J* values) are given in Hertz (Hz), and chemical shifts ( $\delta$ ) are reported in ppm and referred to CHD<sub>2</sub>OD and CHCl<sub>3</sub> as internal standards. Spin multiplicities are given as s (singlet), br s (broad singlet), d (doublet), or m (multiplet). Through-space <sup>1</sup>H connectivities were evidenced using a ROESY experiment with mixing times of 200 and 250 ms, respectively.

HPLC was performed with a Waters Model 510 pump equipped with Waters Rheodine injector and a differential refractometer, model 401. Reaction progress was monitored via thin-layer chromatography (TLC) on Alugram silica gel G/UV254 plates. Silica gel MN Kieselgel 60 (70–230 mesh) from Macherey–Nagel Company was used for column chromatography. All chemicals were obtained from Sigma–Aldrich, Inc.

All chemicals were obtained from Sigma–Aldrich, Inc. Solvents and reagents were used as supplied from commercial sources with the following exceptions. Tetrahydrofuran and triethylamine were distilled from calcium hydride immediately prior to use. Methanol

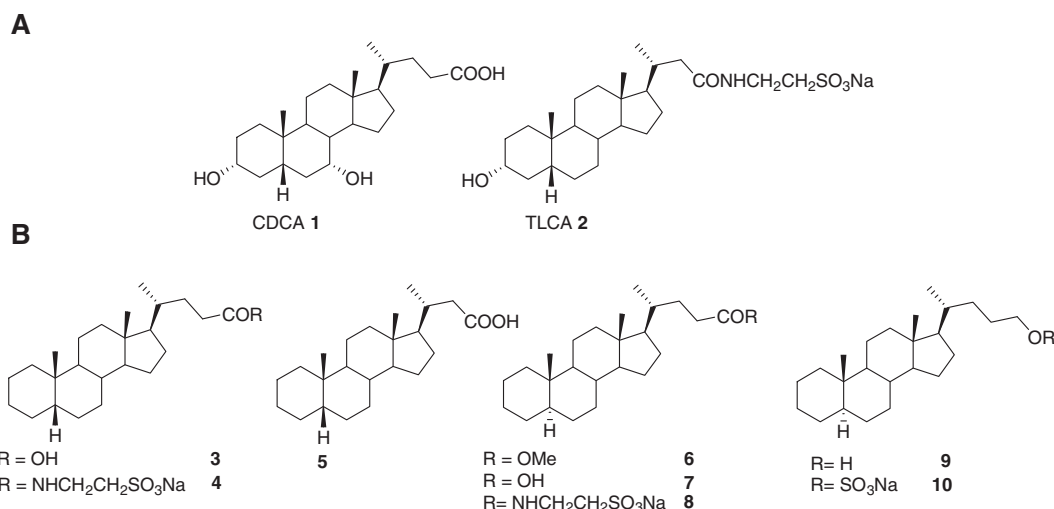


**Fig. 1.** A: CDCA and TLCA, the endogenous activators of FXR and GPBAR1, respectively. B: 5 $\beta$ - and 5 $\alpha$ -cholane derivatives generated in this study.

was dried from magnesium methoxide as follow. Magnesium turnings (5 g) and iodine (0.5 g) are refluxed in a small (50–100 mL) quantity of methanol until all of the magnesium has reacted. The mixture is diluted (up to 1 L) with reagent grade methanol, refluxed for 2–3 h then distilled under nitrogen. All reactions were carried out under argon atmosphere using flame-dried glassware.

The purities of compounds were determined to be greater than 95% by HPLC. Compound **20** was prepared as previously reported [23,24].

## 2.2. Synthetic methods

### 2.2.1. Methyl 3 $\alpha$ -tosiloxy-5 $\beta$ -cholan-24-oate (**12**)

To a solution of lithocholic acid (2 g, 5.31 mmol), dissolved in 50 mL of dry methanol was added *p*-toluenesulfonic acid (4.5 g, 26.5 mmol). The solution was left to stand at room temperature for 1 h. The mixture was quenched by addition until the neutrality of NaHCO<sub>3</sub> saturated solution. After the evaporation of the methanol, the residue was extracted with ethyl acetate. The combined extract was washed with brine, dried with Na<sub>2</sub>SO<sub>4</sub>, and evaporated to give the methyl ester as amorphous solid (2.1 g, quantitative yield).

At the solution of the methyl ester (2 g, 5.13 mmol) in dry pyridine (30 mL), tosyl chloride (4.9 g, 25.6 mmol) was added, and the mixture was stirred at room temperature for 8 h. It was poured into cold water (50 mL) and extracted with CH<sub>2</sub>Cl<sub>2</sub> (3  $\times$  50 mL). The combined organic phases were washed with saturated NaHCO<sub>3</sub> solution (50 mL) and water (50 mL), dried (Na<sub>2</sub>SO<sub>4</sub>) and concentrated to give 2.57 g of **12** as a white solid (92%). [ $\alpha$ ]<sub>D</sub><sup>25</sup> = +59.5 (c 0.02, CH<sub>3</sub>OH); selected <sup>1</sup>H NMR (500 MHz, CDCl<sub>3</sub>):  $\delta$ <sub>H</sub> 7.77 (2H, d, *J* = 8.2 Hz), 7.31 (2H, d, *J* = 8.2 Hz), 4.43 (1H, m), 3.64 (3H, s), 2.32 (1H, m), 2.19 (1H, m), 0.88 (3H, d, *J* = 6.6 Hz), 0.86 (3H, s), 0.60 (3H, s); HR ESIMS *m/z* 545.3309 [M+H]<sup>+</sup>, C<sub>32</sub>H<sub>49</sub>O<sub>5</sub>S requires 545.3301.

### 2.2.2. Methyl 5 $\beta$ -cholan-24-oate (**13**)

Lithium bromide (800 mg, 9.2 mmol) and lithium carbonate (680 mg, 9.2 mmol) were added to a solution of compound **12** (2.5 g, 4.6 mmol) in dry DMF (30 mL), and the mixture was refluxed for 2 h. After cooling to room temperature, the mixture was slowly poured into saturated NaHCO<sub>3</sub> solution (50 mL) and extracted with ethyl acetate (3  $\times$  50 mL). The combined organic layer was washed successively with water, and then dried over anhydrous MgSO<sub>4</sub> and evaporated to dryness to give 1.7 g of oily

residue (quantitative yield), that was subjected to next step without any purification.

A solution of compound previously obtained (1.7 g, 4.6 mmol) in THF dry/MeOH dry (10 mL/10 mL, v/v) was hydrogenated in presence of Pd(OH)<sub>2</sub> 20% wt on activated carbon Degussa type (30 mg) in PARR apparatus. The flask was evacuated and flushed first with argon and then with hydrogen (about 5 atm). After 12 h, the reaction was complete. The mixture was filtered through celite, and the recovered filtrate was concentrated to give 1.7 g of crude product. Purification by silica gel (hexane/ethyl acetate 95:5) gave compound **13** as a colorless oil (1.27 g, 74%). [ $\alpha$ ]<sub>D</sub><sup>25</sup> = -3.0 (c 0.03, CH<sub>3</sub>OH); selected <sup>1</sup>H NMR (400 MHz, CDCl<sub>3</sub>):  $\delta$  3.68 (3H, s), 2.37 (1H, m), 2.24 (1H, m), 0.94 (3H, d, ovl), 0.93 (3H, s), 0.66 (3H, s). <sup>13</sup>C NMR (100 MHz, CDCl<sub>3</sub>):  $\delta$  175.2, 56.9, 56.3, 51.8, 44.0 (2C), 40.8, 40.6, 37.9, 36.2, 35.7, 31.4 (2C), 28.5, 27.8, 27.6, 27.4, 26.9 (2C), 24.6, 21.6, 21.2, 18.6, 12.4. HR ESIMS *m/z* 375.3267 [M+H]<sup>+</sup>, C<sub>25</sub>H<sub>43</sub>O<sub>2</sub> requires 375.3263.

### 2.2.3. 5 $\beta$ -cholan-24-oic acid (**3**)

Compound **13** (500 mg, 1.33 mmol) was hydrolyzed with a methanol solution of sodium hydroxide (5%, 5 mL) in H<sub>2</sub>O (5 mL) overnight under reflux. The resulting solution was then concentrated under vacuum, diluted with water, acidified with HCl 6 N and extracted with ethyl acetate (3  $\times$  50 mL). The collected organic phases were washed with brine, dried over Na<sub>2</sub>SO<sub>4</sub> anhydrous and evaporated under reduced pressure to give 480 mg of compound **3** (quantitative yield). An analytic sample was obtained by HPLC on a Nucleodur 100–5 C18 (5  $\mu$ m; 10 mm i.d.  $\times$  250 mm) with MeOH/H<sub>2</sub>O (999.5:0.5) as eluent (flow rate 3 mL/min, *t*<sub>R</sub> = 21 min); [ $\alpha$ ]<sub>D</sub><sup>25</sup> = +13.3 (c 0.32, CHCl<sub>3</sub>); selected <sup>1</sup>H NMR (400 MHz CDCl<sub>3</sub>):  $\delta$  2.39 (1H, m), 2.26 (1H, m), 0.93 (3H, d, *J* = 6.6 Hz), 0.91 (3H, s), 0.66 (3H, s). <sup>13</sup>C NMR (100 MHz CDCl<sub>3</sub>):  $\delta$  179.1, 56.8, 56.2, 50.6, 43.9, 43.0, 40.7, 40.5, 37.8, 36.1 (2C), 35.6 (2C), 31.1, 28.4, 27.7, 27.5, 27.3, 26.8, 24.5, 21.6, 21.0, 18.5, 12.3. HR ESIMS *m/z* 359.2956 [M-H]<sup>-</sup>, C<sub>24</sub>H<sub>39</sub>O<sub>2</sub> requires 359.2950.

### 2.2.4. 5 $\beta$ -cholan-24-oil taurine sodium salt (**4**)

Compound **3** (50 mg, 0.14 mmol) in DMF dry (3 mL) was treated with DMT-MM (77.5 mg, 0.28 mmol) and triethylamine (70  $\mu$ L, 0.49 mmol) and the mixture was stirred at room temperature for 10 min. Then to the mixture was added taurine (15 mg, 0.16 mmol). After 24 h, the reaction mixture was concentrated under vacuo and dissolved in water (5 mL). The mixture was purified by HPLC on a Nucleodur 100–5 C18 (5  $\mu$ m; 4.6 mm i.d.  $\times$  250 mm) with

MeOH/H<sub>2</sub>O (83:17) as eluent (flow rate 1 mL/min), to give 3.5 mg of compound **4** ( $t_R = 11$  min);  $[\alpha]_{25}^D = +22.5$  (c 0.05, CH<sub>3</sub>OH); selected <sup>1</sup>H NMR (400 MHz, CD<sub>3</sub>OD):  $\delta$  3.58 (2H, t,  $J = 7.0$  Hz), 2.95 (2H, t,  $J = 7.0$  Hz), 2.24 (1H, m), 2.08 (1H, m), 0.95 (3H, d, ovl), 0.94 (3H, s), 0.68 (3H, s). HR ESIMS  $m/z$  480.3150 [M–Na]<sup>–</sup>, C<sub>27</sub>H<sub>46</sub>NO<sub>4</sub>S requires 480.3153.

#### 2.2.5. 3 $\alpha$ -formyloxy-5 $\beta$ -cholan-24-oic acid (14)

A solution of lithocholic acid **11** (500 mg, 1.3 mmol) in 10 mL of 90% formic acid containing 25  $\mu$ L of 70% perchloric acid was stirred at 47–50 °C for 12 h. The temperature of the heating bath was lowered to 40 °C, then 5 mL of acetic anhydride was added and the mixture was stirred for 15 min. The solution was cooled to room temperature, poured into 50 mL of water and extracted with diethyl ether. The organic layers were washed with saturated NaHCO<sub>3</sub> solution (50 mL) and water to neutrality, dried over Na<sub>2</sub>SO<sub>4</sub>, and evaporated to give 540 mg of **14** (quantitative yield). An analytic sample was obtained by silica gel chromatography eluting with CH<sub>2</sub>Cl<sub>2</sub>:MeOH 9:1. Selected <sup>1</sup>H NMR (400 MHz CD<sub>3</sub>OD):  $\delta$  8.04 (1H, s), 4.85 (1H, m), 2.39 (1H, m), 2.25 (1H, m), 0.93 (3H, s), 0.92 (3H, d,  $J = 6.7$  Hz), 0.65 (3H, s); <sup>13</sup>C NMR (100 MHz CD<sub>3</sub>OD):  $\delta$  178.1, 160.8, 74.4, 56.5, 55.9, 41.9, 40.5, 40.2, 40.1, 35.8 (3C), 35.4 (2C), 32.3, 30.8, 30.7, 28.2, 27.0, 26.3, 24.2, 23.4, 20.8, 18.2, 12.1; HRMS-ESI  $m/z$  405.2997 [M+H]<sup>+</sup>, C<sub>25</sub>H<sub>41</sub>O<sub>4</sub> requires 405.2999.

#### 2.2.6. 3 $\alpha$ -formyloxy-24-nor-5 $\beta$ -cholan-23-nitrile (15)

Crude **14** (500 mg, 1.2 mmol), 3.8 mL of cold trifluoroacetic acid, and 1 mL (7.2 mmol) of trifluoroacetic anhydride were stirred at 0 °C until dissolution. Sodium nitrite (248 mg, 3.6 mmol) was added to the solution. The reaction mixture was stirred first at 0–5 °C for 1 h, then at 45–50 °C for 3 h. When the reaction was completed, it was neutralized with NaOH 2 N, then the product was extracted with 50 mL of diethyl ether (3  $\times$  50 mL), followed by washing with brine and dried over anhydrous Na<sub>2</sub>SO<sub>4</sub>. The ether was removed under reduced pressure to afford 380 mg of **15** (85%), that was subjected to next step without any purification.

#### 2.2.7. 24-nor-lithodeoxycholic acid (16)

Compound **15** (350 mg, 0.94 mmol) was refluxed in ca. 50 mL of methanol–water 1:1 with 30% KOH. After 2 h, the basic aqueous solution was neutralized with HCl 6 N. Then methanol was evaporated and the residue was extracted with ethyl acetate (3  $\times$  50 mL) and then with CH<sub>2</sub>Cl<sub>2</sub> (3  $\times$  50 mL). The organic layers were washed with brine, dried and evaporated to dryness to give white solid residue, that was purified by silica gel chromatography, eluting with CH<sub>2</sub>Cl<sub>2</sub>:MeOH 9:1 (340 mg, quantitative yield). An analytic sample was purified by HPLC on a Nucleodur 100–5 C18 (5  $\mu$ m; 4.6 mm i.d.  $\times$  250 mm) with MeOH/H<sub>2</sub>O (95:5) as eluent (flow rate 1 mL/min), to give compound **16** ( $t_R = 10.5$  min).  $[\alpha]_{25}^D = +21.9$  (c 0.58, CH<sub>3</sub>OH); selected <sup>1</sup>H NMR (400 MHz CD<sub>3</sub>OD):  $\delta$  3.54 (1H, m), 2.41 (2H, m), 1.00 (3H, d,  $J = 7.0$  Hz), 0.94 (3H, s), 0.71 (3H, s). <sup>13</sup>C NMR (100 MHz CD<sub>3</sub>OD):  $\delta$  178.0, 72.5, 57.9, 57.5, 43.6, 42.5, 41.9, 41.4, 37.2, 37.1, 36.5, 35.7, 34.9, 31.1, 29.3, 28.3, 27.6, 25.2, 23.9, 21.9, 19.9, 12.5; HRMS-ESI  $m/z$  363.2895 [M+H]<sup>+</sup>, C<sub>23</sub>H<sub>39</sub>O<sub>3</sub> requires 363.2899.

#### 2.2.8. 24-nor-5 $\beta$ -cholanoic acid (5)

Compound **5** (210 mg, 75% over five steps) was synthesized, starting from compound **16** (300 mg, 0.82 mmol) as described in Scheme 2, by an analogous procedure to that detailed above for compound **3**. An analytic sample was obtained by HPLC on a Nucleodur 100–5 C18 (5  $\mu$ m; 10 mm i.d.  $\times$  250 mm) with MeOH/H<sub>2</sub>O (99.5:0.5) as eluent (flow rate 3 mL/min,  $t_R = 20$  min);  $[\alpha]_{25}^D = +24.6$  (c 0.03, CH<sub>3</sub>OH); selected <sup>1</sup>H NMR (400 MHz CD<sub>3</sub>OD):  $\delta$  2.41 (1H, m), 1.00 (3H, d,  $J = 6.0$  Hz), 0.95 (3H, s), 0.72 (3H, s); <sup>13</sup>C NMR (100 MHz CD<sub>3</sub>OD):  $\delta$  178.0, 58.0, 57.6, 45.2, 44.0, 42.8, 41.9, 41.5,

38.7, 37.3, 36.5, 35.0, 29.3, 28.6, 28.4, 28.2, 27.7, 25.3, 24.8, 22.4, 21.9, 20.0, 12.5; HR ESIMS  $m/z$  347.2947 [M+H]<sup>+</sup>, C<sub>23</sub>H<sub>39</sub>O<sub>2</sub> requires 347.2950.

#### 2.2.9. Methyl cholan-3,5-dien-24-oate (21)

At a solution of the ditosylate **20** (500 mg, 0.7 mmol) in water (3 mL) and *N,N*-dimethylformamide (DMF; 27 mL) was added CH<sub>3</sub>COOK (206 mg, 2.1 mmol) and the mixture was refluxed for 36 h. The solution was cooled at room temperature, then water and ethyl acetate were added and the separated aqueous phase was extracted with ethyl acetate (3  $\times$  20 mL). The combined organic phases were washed with water, dried (Na<sub>2</sub>SO<sub>4</sub>) and concentrated to give a mixture. Purification by silica gel eluting with hexane–ethyl acetate (99:1) gave the diene **21** (200 mg, 78%). selected <sup>1</sup>H NMR (400 MHz CD<sub>3</sub>OD):  $\delta$  5.92 (1H, d,  $J = 9.7$  Hz), 5.58 (1H, d,  $J = 11.3$  Hz), 5.38 (1H, m), 3.66 (3H, s), 2.34 (1H, m), 2.22 (1H, m), 0.94 (3H, d,  $J = 5.8$  Hz), 0.92 (3H, s), 0.70 (3H, s); <sup>13</sup>C NMR (100 MHz CD<sub>3</sub>OD):  $\delta$  174.8, 141.5, 129.1, 125.2, 123.2, 57.0, 55.8, 51.5, 48.4, 43.4, 39.8, 35.4, 33.8, 31.9, 31.8, 31.7, 31.0, 30.9, 28.1, 24.2, 23.9, 23.0, 20.9, 18.8, 12.0. HR ESIMS  $m/z$  371.2947 [M+H]<sup>+</sup>, C<sub>25</sub>H<sub>39</sub>O<sub>2</sub> requires 371.2950.

#### 2.2.10. Methyl 5 $\alpha$ -cholan-24-oate (6)

A solution of methyl chol-3,5-dien-24-oate **21** (150 mg, 0.40 mmol) in absolute methanol (5 mL) and dry THF (5 mL) was added in an oven-dried 50 mL flask, that was charged with 10% palladium on carbon (10 mg). The flask was evacuated and flushed first with argon and then with hydrogen. The reaction was stirred at room temperature under H<sub>2</sub> (1 atm) for 1 h. The mixture was filtered through celite, and the recovered filtrate was concentrated to give 147 mg of compound **6** (quantitative yield).  $[\alpha]_{25}^D = -2.9$  (c 2.54, CH<sub>3</sub>OH); selected <sup>1</sup>H NMR (400 MHz CDCl<sub>3</sub>):  $\delta$  3.66 (3H, s), 2.34 (1H, m), 2.21 (1H, m), 0.91 (3H, d,  $J = 6.4$  Hz), 0.77 (3H, s), 0.64 (3H, s); <sup>13</sup>C NMR (100 MHz CDCl<sub>3</sub>):  $\delta$  176.0, 56.9, 56.2, 55.0, 51.6, 47.3, 40.4, 39.0 (2C), 35.7 (3C), 32.5, 31.4, 31.3, 29.4, 29.3, 28.4, 27.2, 24.5, 22.6, 21.2, 18.6, 12.5, 12.4; HR ESIMS  $m/z$  375.3269 [M+H]<sup>+</sup>, C<sub>25</sub>H<sub>43</sub>O<sub>2</sub> requires 375.3263.

#### 2.2.11. 5 $\alpha$ -cholan-24-oic acid (7)

Compound **6** (50 mg, 0.13 mmol) was hydrolyzed with a methanol solution of sodium hydroxide (5%, 5 mL) in H<sub>2</sub>O (1 mL) overnight under reflux. The resulting solution was then concentrated under vacuum, diluted with water, acidified with HCl 6 N and extracted with ethyl acetate (3  $\times$  30 mL). The collected organic phases were washed with brine, dried over Na<sub>2</sub>SO<sub>4</sub> anhydrous and evaporated under reduced pressure to give compound **7** (40 mg, 87%). An analytic sample was obtained by HPLC on a Nucleodur 100–5 C18 (5  $\mu$ m; 4.6 mm i.d.  $\times$  250 mm) with MeOH/H<sub>2</sub>O (92:8) as eluent (flow rate 1 mL/min,  $t_R = 12$  min);  $[\alpha]_{25}^D = +17.7$  (c 0.14, CH<sub>3</sub>OH); selected <sup>1</sup>H NMR (400 MHz, CD<sub>3</sub>OD):  $\delta$  2.31 (1H, m), 2.20 (1H, m), 0.94 (3H, d,  $J = 6.2$  Hz), 0.81 (3H, s), 0.69 (3H, s). HR ESIMS  $m/z$  359.2953 [M–H]<sup>–</sup>, C<sub>24</sub>H<sub>39</sub>O<sub>2</sub> requires 359.2950.

#### 2.2.12. 5 $\alpha$ -cholan-24-oyl-taurine sodium salt (8)

Compound **7** (10 mg, 27.8  $\times$  10<sup>–3</sup> mmol) in DMF dry (3 mL) was treated with DMT-MM (16 mg, 58.2  $\times$  10<sup>–3</sup> mmol) and triethylamine (70  $\mu$ L, 0.49 mmol) and the mixture was stirred at room temperature for 10 min. Then to the mixture was added taurine (15 mg, 0.16 mmol). After 24 h, the reaction mixture was concentrated under vacuo and dissolved in water (5 mL). The mixture was purified by HPLC on a Nucleodur 100–5 C18 (5  $\mu$ m; 4.6 mm i.d.  $\times$  250 mm) with MeOH/H<sub>2</sub>O (83:17) as eluent (flow rate 1 mL/min), to give 3.5 mg (27%) of compound **8** ( $t_R = 10.4$  min);  $[\alpha]_{25}^D = +37$ . (c 0.03, CH<sub>3</sub>OH); selected <sup>1</sup>H NMR (400 MHz, CD<sub>3</sub>OD):  $\delta$  3.58 (2H, t,  $J = 7.0$  Hz), 2.96 (2H, t,  $J = 7.0$  Hz), 2.24 (1H, m), 2.09

(1H,m), 0.95 (3H,d, $J$  = 6.2 Hz), 0.82 (3H,s), 0.69 (3H,s). HR ESIMS  $m/z$  452.2840  $[M-Na]^-$ ,  $C_{25}H_{42}NO_4S$  requires 452.2835.

### 2.2.13. 5 $\alpha$ -cholan-24-ol (9)

Dry methanol (40  $\mu$ L, 0.94 mmol) and  $LiBH_4$  (470  $\mu$ L, 2 M in THF, 0.94 mmol) were added to a solution of the compound **8** (50 mg, 0.13 mmol) in dry THF (10 mL) at 0 °C under argon and the resulting mixture was stirred for 2 h at 0 °C. The mixture was quenched by addition of NaOH (1 M, 260  $\mu$ L) and then allowed to warm to room temperature. Ethyl acetate was added and the separated aqueous phase was extracted with ethyl acetate (3  $\times$  15 mL). The combined organic phases were washed with water, dried ( $Na_2SO_4$ ) and concentrated. Purification by silica gel eluting with  $CH_2Cl_2$ -MeOH (85:15) gave the alcohol **9** as a white solid (45 mg, quantitative yield). An analytic sample was obtained by HPLC on a Nucleodur 100–5 C18 (5  $\mu$ m; 4.6 mm i.d.  $\times$  250 mm) with MeOH/ $H_2O$  (92:8) as eluent (flow rate 1 mL/min,  $t_R$  = 17.6 min);  $[\alpha]_{25}^D = +5.5$  (c 1.14,  $CH_3OH$ ); selected  $^1H$  NMR (400 MHz  $CDCl_3$ ):  $\delta$  3.51 (2H, m), 0.87 (3H, d,  $J$  = 6.3 Hz), 0.72 (3H,s), 0.60 (3H,s).  $^{13}C$  NMR (100 MHz  $CDCl_3$ ):  $\delta$  63.6, 56.6, 56.1, 54.7, 47.0, 42.6, 40.1, 38.6, 35.6, 35.5 (2C), 32.2, 31.8, 29.3, 29.0 (2C), 28.2, 26.8, 24.2, 22.2, 20.8, 18.6, 12.2, 12.1; HR ESIMS  $m/z$  347.3318  $[M+H]^+$ ,  $C_{24}H_{43}O$  requires 347.3314.

### 2.2.14. 5 $\alpha$ -cholan-24-yl-24-triethylammonium sulfate (10)

At a solution of compound **9** (10 mg, 0.028 mmol) in DMF dry (3 mL) was added triethylamine-sulfur trioxide complex (26 mg, 0.144 mmol) under an argon atmosphere, and the mixture was stirred at 95 °C for 12 h. Most of the solvent was evaporated and the residue was poured over a RP18 column to remove excess  $SO_3-NEt_3$ . Fraction eluted with MeOH: $H_2O$  1:1 contained **10** as ammonium salt. HPLC on a Nucleodur 100–5 C18 (5  $\mu$ m; 4.6 mm i.d.  $\times$  250 mm) with MeOH/ $H_2O$  (90:10) as eluent (flow rate 1 mL/min), gave 1.4 mg of compound **10** (18%,  $t_R$  = 5 min) as sodium salt.  $[\alpha]_{25}^D = -26.7$  (c 0.02,  $CH_3OH$ ); selected  $^1H$  NMR (400 MHz,  $CD_3OD$ ):  $\delta$  3.95 (2H,t, $J$  = 6.7 Hz), 0.94 (3H,d, $J$  = 6.5 Hz), 0.81 (3H,s), 0.69 (3H,s). HR ESIMS  $m/z$  425.2730  $[M-Na]^-$ ,  $C_{24}H_{41}O_4S$  requires 425.2726.

## 2.3. Pharmacological assays

### 2.3.1. Cell culture

HepG2, an immortalized epatocarcinoma cell line, was cultured and maintained at 37 °C and 5%  $CO_2$  in E-MEM additioned with 10% FBS, 1% glutamine and 1% penicillin/streptomycin.

HEK-293T and GlutaG cells were cultured and maintained at 37 °C and 5%  $CO_2$  in D-MEM additioned with 10% FBS, 1% glutamine and 1% penicillin/streptomycin.

### 2.3.2. Luciferase reporter gene assay

To evaluate FXR mediated transactivation, HepG2 cells were transfected with 100 ng of human pSG5-FXR, 100 ng of human pSG5-RXR, 200 ng of the reporter vector p(hsp27)-TK-LUC containing the FXR response element IR1 cloned from the promoter of heat shock protein 27 (hsp27) and with 100 ng of pGL4.70 (Promega), a vector encoding the human Renilla gene. To evaluate GPBAR1 mediated transactivation, HEK-293T cells were transfected with 200 ng of human pGL4.29 (Promega), a reporter vector containing a cAMP response element (CRE) that drives the transcription of the luciferase reporter gene luc2P, with 100 ng of pCMVSPORT6-human GPBAR1, and with 100 ng of pGL4.70. At 24 h post-transfection, cells were stimulated 18 h with 10  $\mu$ M CDCA (**1**), TLCA (**2**) and compounds **3–10**. In another experimental setting,

at 24 h post-transfection, cells were stimulated with 50  $\mu$ M of compounds **3–10** in combination with 10  $\mu$ M CDCA (**1**) or TLCA (**2**). Luciferase activities were assayed and normalized with Renilla activities.

To calculate the  $IC_{50}$  of **3** and **7** versus GPBAR1, a dose response curve was performed in HEK-293T transfected as described above and stimulated 18 h with 1, 5, 25 and 50  $\mu$ M of compounds **3** and **7**. After treatments, 10  $\mu$ L of cellular lysates were read using Dual Luciferase Reporter Assay System (Promega Italia srl, Milan, Italy) according manufacturer specifications using the Glomax20/20 luminometer (Promega Italia srl, Milan, Italy). Luciferase activities were assayed and normalized with Renilla activities.

### 2.3.3. Real-Time PCR

Total RNA was isolated from HepG2 or GlutaG cells using the TRIzol reagent according to the manufacturer's specifications (Invitrogen). One microgram of purified RNA was treated with DNase-I and reverse transcribed with Superscript II (Invitrogen). For Real Time PCR, 10 ng template was dissolved in 25  $\mu$ L containing 200 nmol/L of each primer and 12.5  $\mu$ L of 2 $\times$  SYBR FAST Universal ready mix (Invitrogen). All reactions were performed in triplicate, and the thermal cycling conditions were as follows: 2 min at 95 °C, followed by 40 cycles of 95 °C for 20 s and 60 °C for 30 s in iCycler iQ instrument (Biorad). The relative mRNA expression was calculated and expressed as 2 $-(\Delta\Delta Ct)$ . Forward and reverse primer sequences were the following: human GAPDH, gaaggtgaaggctggagt and catgggtggaatcatattggaa; human OST $\alpha$ , tgtgggccccttccaatac and ggctcccatgttctgctcac; human BSEP, gggccattgtacgagatcctaa and tgcaccgtctttcactttctg; human SHP, gctgtctggagtccttctgg and ccaatgatagggcgaaagaagag; mouse GAPDH, ctgagtatgctgtggagtctac and gttgtgtgtgcaggatgcatg; mouse Pro-glucagon, tgaagacaaaacgccaactcac and caatgttgttccggcttctc.

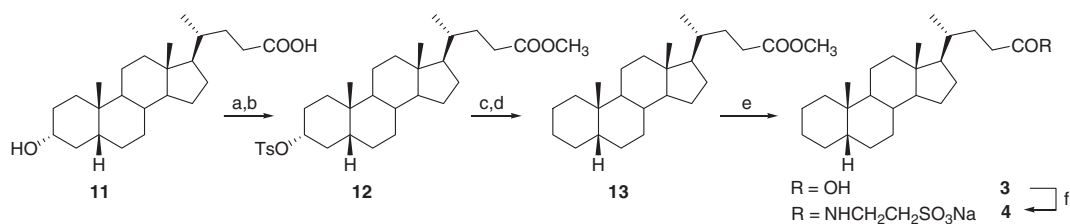
## 3. Results

### 3.1. Chemistry

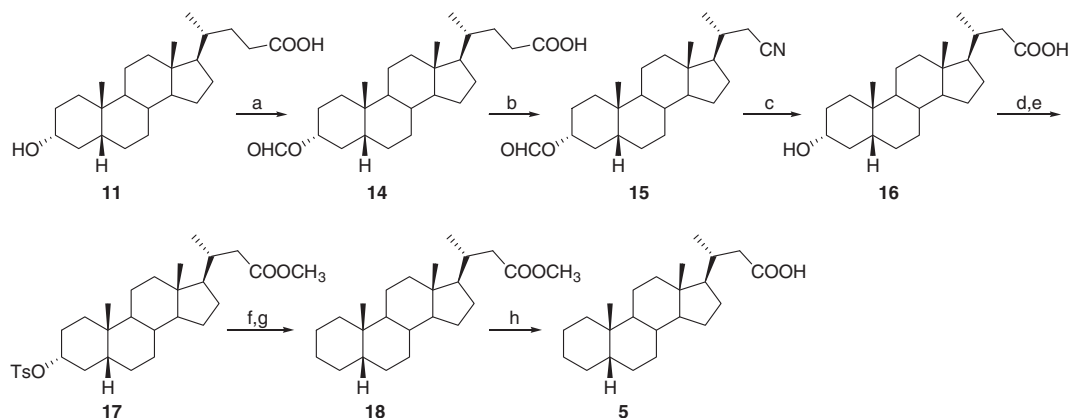
#### 3.1.1. 5 $\beta$ -cholane derivatives (Schemes 1 and 2)

5 $\beta$ -cholanic acid **3** was prepared from LCA in a five steps reaction protocol (Scheme 1). LCA methyl ester intermediate was tosylated at C-3 hydroxyl group furnishing **12** in a 92% yield over two steps. Elimination ( $LiBr/Li_2CO_3$ ) and subsequent hydrogenation ( $H_2$ , Pd(OH) $_2$ , THF/MeOH) on the crude reaction product furnished methyl 5 $\beta$ -cholanoate **13** that in turn was transformed in the corresponding C24 acid **3** by alkaline hydrolysis (NaOH, MeOH/ $H_2O$ ) in quantitative chemical yield. A small aliquot of the so obtained 5 $\beta$ -cholanic acid **3** was then subjected to the reaction of amidation with taurine in the presence of the versatile coupling agent DMTMM, 4-(4,6-dimethoxy-1,3,5-triazin-2-yl)-4-methylmorpholinium chloride [25], giving the amide derivative as ammonium sulfate salt. Purification on RP-18 column followed by HPLC furnished **4** in pure form and as sodium salt.

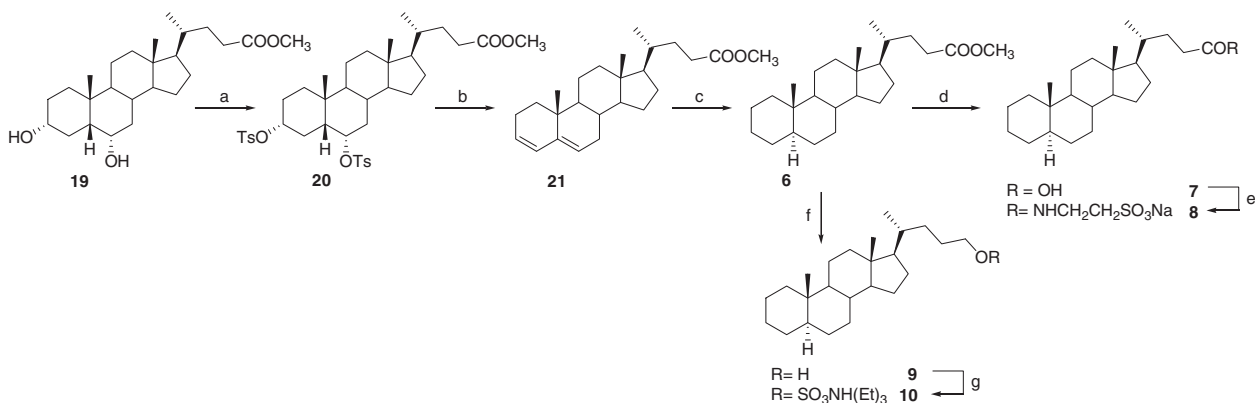
The synthetic protocol towards *nor*-cholanic acid **5** (Scheme 2) encompassed Beckmann one carbon degradation [26,27]. LCA was protected as performate derivative **14** by treatment of LCA with formic acid in presence of catalytic amounts of perchloric acid. Treatment with sodium nitrite in a mixture of trifluoroacetic anhydride and trifluoroacetic acid afforded 23-nitrile intermediate **15** in 85% yield over two steps (Scheme 2) that was in turn transformed in the corresponding *nor*LCA **16** through prolonged alkaline hydrolysis. Methanol/*p*-toluenesulfonic acid treatment gave C23 methyl ester that was subjected to the same synthetic protocol depicted in the Scheme 1. Briefly, tosylation/elimination at C3 and then hydrogenation of the double bond on ring A afforded



**Scheme 1.** 5 $\beta$ -Cholane derivatives: *Reagents and Conditions.* (a) *p*-TsOH, MeOH dry; (b) *p*-TsCl, pyridine, 92% over two steps; (c) LiBr, Li<sub>2</sub>CO<sub>3</sub>, DMF, reflux; (d) H<sub>2</sub> 3 atm, Pd(OH)<sub>2</sub>/C degussa type, THF/MeOH 1:1, 74% over two steps; (e) NaOH, MeOH:H<sub>2</sub>O 1:1 v/v, quantitative; (f) DMT-MM, Et<sub>3</sub>N, taurine, DMF dry.



**Scheme 2.** Preparation of *nor*-cholanic acid **5** *Reagents and Conditions.* (a) HCOOH, HClO<sub>4</sub>, quantitative; (b) TFA, trifluoroacetic anhydride, NaNO<sub>2</sub>, 85%; (c) KOH 30% in MeOH/H<sub>2</sub>O 1:1 v/v, quantitative; (d) *p*-TsOH, MeOH dry, 97%; (e) *p*-TsCl, pyridine, quantitative; (f) LiBr, Li<sub>2</sub>CO<sub>3</sub>, DMF, reflux; (g) H<sub>2</sub> 3 atm, Pd(OH)<sub>2</sub>/C degussa type, THF/MeOH 1:1, 78% over two steps; (h) NaOH, MeOH:H<sub>2</sub>O 1:1 v/v, quantitative.



**Scheme 3.** 5 $\alpha$ -Cholane derivatives *Reagents and Conditions.* (a) *p*-TsCl, pyridine; (b) CH<sub>3</sub>COOK, DMF/H<sub>2</sub>O 9:1, reflux, 78% over two steps; (c) H<sub>2</sub>, Pd/C, THF/MeOH 1:1, room temperature, quantitative; (d) NaOH 5% in MeOH/H<sub>2</sub>O 5:1 v/v, 87%; (e) DMT-MM, Et<sub>3</sub>N, taurine, DMF dry; (f) LiBH<sub>4</sub>, MeOH dry, THF, 0 °C, quantitative yield; (g) Et<sub>3</sub>N·SO<sub>3</sub>, DMF, 95 °C.

methyl ester **18**. Finally basic hydrolysis of methyl ester function gave the desiderated *nor* 5 $\beta$ -cholanic acid **5** in 64% overall chemical yield.

### 3.1.2. 5 $\alpha$ -Cholane derivatives (Scheme 3)

Treatment of methyl hydoxycholanoate **19** with tosyl chloride in pyridine afforded the 3 $\alpha$ ,6 $\alpha$ -ditosyloxy-5 $\beta$ -cholanoate (**20**) in satisfactory yield (quantitative yield) (see Scheme 3).

Refluxing in DMF and CH<sub>3</sub>COOK for 1 h produced elimination at C-3 and C-6 to give the dyene **21**, which in turn was hydrogenated to afford the required A/B *trans* ring junction in methyl ester **6**.

Hydrolysis at C-23 methyl ester gave *nor* 5 $\alpha$ -cholanic acid **7**, that in a small aliquot was subjected to the reaction of amidation with taurine and purification (RP-18/HPLC) giving the tauro-conjugate **8** sodium salt. An aliquot of methyl ester **6** was

transformed in the corresponding C-23 alcohol **9** that in turn was subjected to sulfation affording the side chain sulfate derivative **10**.

### 3.2. Pharmacological evaluation

Derivatives **3–10** were tested for their activity on FXR and GPBAR1 in a luciferase reporter assay on HepG2 and HEK-293T cells transfected with human FXR and GPBAR1, respectively (Figs. 2 and 3).

As previously demonstrated [21], 5 $\beta$ -cholanic acid **3** transactivated FXR with a potency comparable with the endogenous activator CDCA (**1**) and, interestingly this activity was also shared by the corresponding 5 $\alpha$ -cholanoic acid **7**, thus demonstrating that, in absence of the hydroxyl groups at C-3 and at C-7, also a flat cholane scaffold could activate FXR. *Nor*-carboxyl acid derivative **5** was

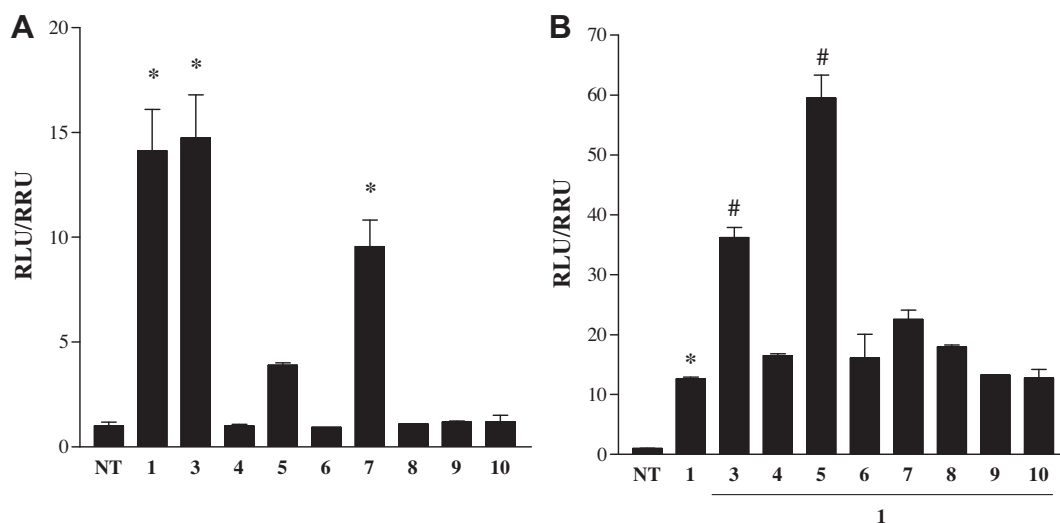


**Fig. 2.** Transactivation assays on FXR. A, Luciferase reporter assay performed in HepG2 transiently transfected with human pSG5-FXR, pSG5-RXR, pCMV- $\beta$ gal, and p(hsp27) TKLUC vectors and measured as RLU/RRU (Relative Luciferase Unit/Relative Renilla Unit). Twenty-four hours post transfection, cells were stimulated with compounds **3–10** (10  $\mu$ M). CDCA (**1**, 10  $\mu$ M) was used as a positive control. Results are expressed as mean  $\pm$  standard error; \* $p$  < 0.05 versus not treated cells (NT). B, HepG2 cells were transfected as described in A. Twenty-four hours post transfection cells were stimulated with 10  $\mu$ M CDCA (**1**) alone or in combination with compounds **3–10** (50  $\mu$ M). \* $p$  < 0.05 versus not treated cells (NT). # $p$  < 0.05 versus CDCA (**1**) stimulated cells.

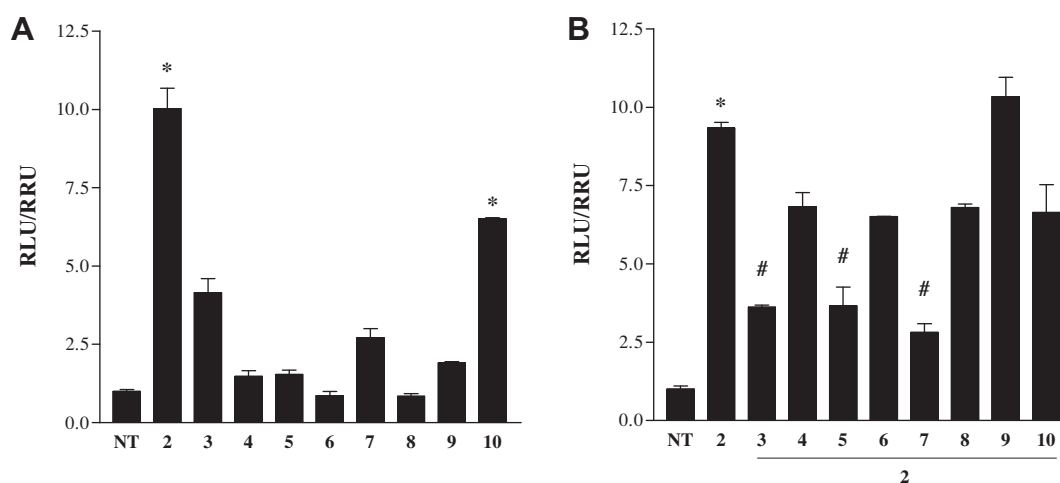


**Fig. 3.** Transactivation assays on GPBAR1. A, Luciferase reporter assay performed in HEK-293T cells transiently transfected with human GPBAR1 and a reporter gene containing a cAMP responsive element in front of the luciferase gene and measured as RLU/RRU (Relative Luciferase Unit/Relative Renilla Unit). Twenty-four hours post transfection, cells were stimulated with compounds **3–10** (10  $\mu$ M). TLCA (**2**, 10  $\mu$ M) was used as a positive control. Results are expressed as mean  $\pm$  standard error. \* $p$  < 0.05 versus not treated cells (NT). B, HEK-293T cells were transfected as described in A. Twenty-four hours post transfection cells were stimulated with 10  $\mu$ M TLCA (**2**) alone or in combination with compounds **3–10** (50  $\mu$ M). \* $p$  < 0.05 versus not treated cells (NT). # $p$  < 0.05 versus TLCA stimulated cells.

almost inactive when tested at 10  $\mu$ M (Fig. 2A). Moreover, when **5** was tested at 50  $\mu$ M in the presence of CDCA (Fig. 2B), the ratio RLU/RRU was higher than that of CDCA, indicating that **5** might be a weak FXR agonist.

Data shown in Fig. 3 revealed that the elimination of the hydroxyl group at C-3 on the tetracyclic core of LCA is detrimental in term of activation of the membrane bile acid receptor (compounds **3–9** in Fig. 3, Panel A). Indeed data in Panel B are quite interesting. Cell stimulation in presence of TLCA **2** reveals that, among this series, derivatives **3**, **5**, **7** were relatively effective in inhibiting GPBAR1 activation caused by TLCA, thus behaving as antagonists and this result represents the first report of cholanic acid derivatives as dual modulators of FXR/GPBAR1 with an agonistic profile toward the nuclear bile acid sensor and an antagonistic behavior toward the membrane receptor.

Antagonistic activity of compounds **3** and **7** was further investigated by a detailed measurement of concentration–response curve

on GPBAR1. As illustrated in Fig. 4, compounds **3** and **7** inhibited the transactivation of GPBAR1 with an IC<sub>50</sub> of 28 and 22  $\mu$ M, respectively.

Compound **3** was further investigated in vitro and its effects on FXR and GPBAR1 target genes assessed by RT-PCR. As shown in Fig. 5, panels A–D, 5 $\beta$ -cholanic acid **3** was able to induce the expression of BSEP, SHP and OST $\alpha$  genes in HepG2 cells whereas antagonized the expression of pro-glucagon mRNA in GLUTAg cells, thus demonstrating that this molecule is an effective FXR agonist endowed with antagonistic activity toward GPBAR1.

#### 4. Discussion and conclusion

FXR senses the intracellular presence of bile acids by activating multiple mechanisms, such as promotion of bile acid export from liver, down-regulation of bile acid import and also attenuation of



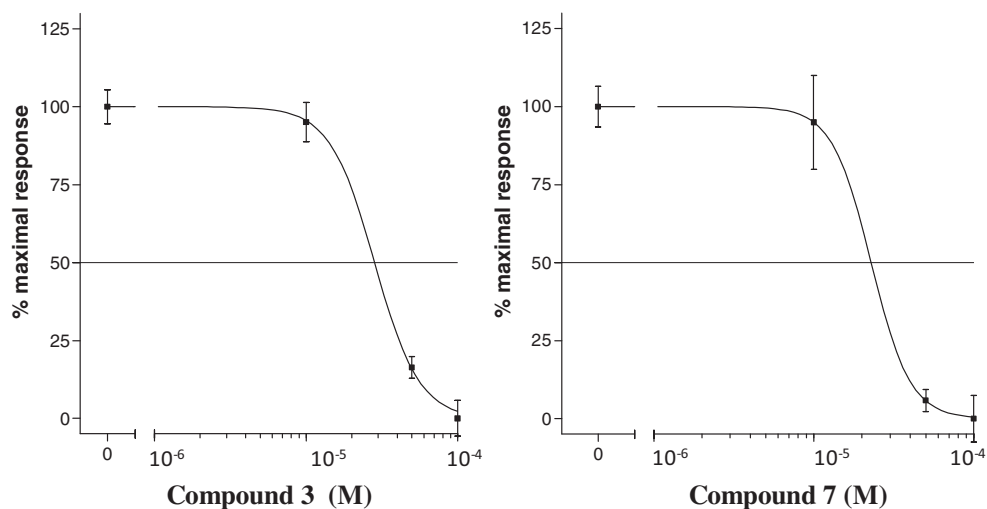


**Fig. 4.** Concentration–response curve of compounds 3 and 7 on GPBAR1. GPBAR1 activity was measured in HEK-293T cells cotransfected with human GPBAR1 and a reporter gene containing a cAMP responsive element in front of the luciferase gene (CRE). Twenty-four hours post transfection, cells were co-stimulated with 10  $\mu$ M TLCA (2) and increasing concentrations of each compound: range from 1 to 50  $\mu$ M. Results are expressed as mean  $\pm$  standard error.

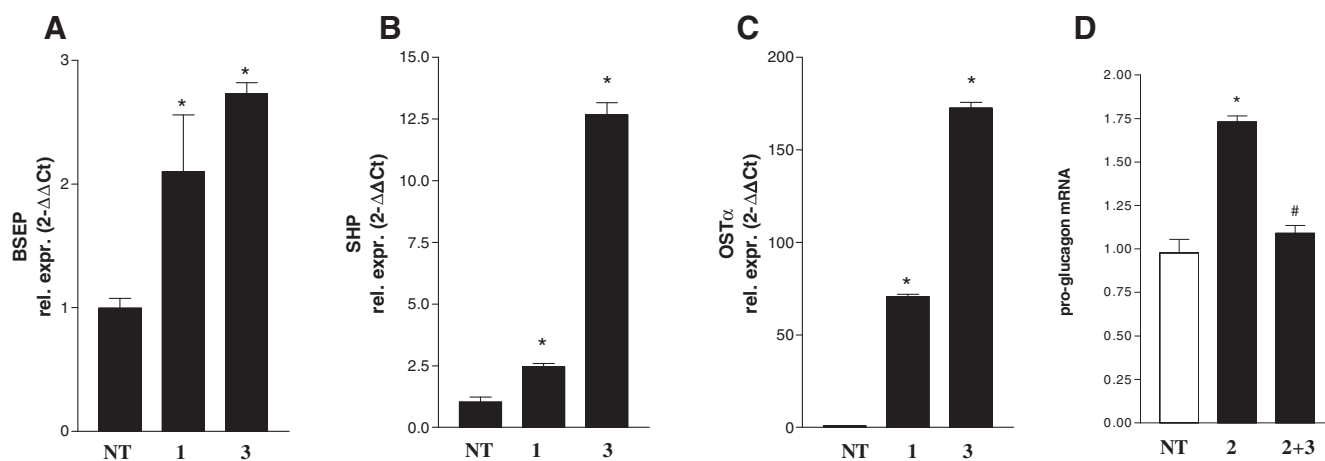


**Fig. 5.** Effect of compound 3 on FXR and GPBAR1 target genes. (A–C) Real-time PCR analysis of mRNA expression of FXR target genes BSEP (A), SHP (B), and OST $\alpha$  (C) in HepG2 cells primed with 10  $\mu$ M of compound 3. CDCA (1) was used as positive control (10  $\mu$ M). (D) Real-time PCR analysis of mRNA expression of GPBAR1 target gene pro-glucagon in Glutag cells stimulated with 10  $\mu$ M TLCA (2) alone or in combination with 50  $\mu$ M of compound 3 (2 + 3). Values are normalized relative to GAPDH mRNA and are expressed relative to those of not treated cells (NT), which are arbitrarily set to 1. The relative mRNA expression is expressed as 2 $^{-\Delta\Delta C_t}$ . \* $p$  < 0.05 versus NT (non treated cells). # $p$  < 0.05 versus TLCA (2) stimulated cells.

*de novo* bile acid synthesis. As a consequence, FXR has been identified as an appealing target in the treatment of cholestasis and liver steatosis, where bile acid levels are impaired. In addition, FXR plays a crucial beneficial role in hepatic triglyceride homeostasis, and in glucose metabolism. Therefore, FXR agonists are promising for the treatment of NAFLD, dyslipidemia and type 2 diabetes [7–10]. After FXR de-orphanization by endogenous bile acids [1–3], bile acid scaffold has been subjected to intense medicinal chemistry modifications, producing several steroidal derivatives with different pharmacological profiles, and, of interest, endowed with good physicochemical properties and higher drug-like profiles when compared to non-steroidal ligands.

Since steroidal ligands cover the same chemical space of the endogenous activators, they are intrinsically promiscuous toward FXR and GPBAR1 and, with few exception, this kind of speculation mainly afforded dual modulators [14,22,28].

Besides this promiscuity supports the use of dual FXR/GPBAR1 agonists in the treatment of nonalcoholic steatohepatitis (NASH) and type 2 diabetes [9], the recent identification of GPBAR1 as

the physiological mediator of pruritus [20], a common symptom observed in cholestasis, highly limits the pharmacological utility of dual agonists in the treatment of primary biliary cirrhosis (PBC) and related cholestatic disorders. In this context, the discovery of highly selective FXR agonists, devoid of GPBAR1 agonism, represents a good promise in the identification of new pharmacological protocols for PBC, an orphan disease for which therapeutic options are limited and poorly effective. In the present study, we have harnessed on the LCA scaffold modifying the functionalities of tetracyclic core, the stereochemistry of A/B ring junction, the length and the functionalization of the side chain. The results of this investigation has led to the discovery of compounds 3, 5 and 7, 5 $\beta$ -cholanoic acid, 5 $\beta$ -norcholanoic acid, and 5 $\alpha$ -cholanoic acid, respectively, as the first examples of bile acid derivatives endowed with FXR agonism and GPBAR1 antagonism. Analysis of transactivation data clearly affirms the carboxylic group on the side chain as a key structural feature in GPBAR1 antagonism. Independently by the length of the side chain (C24 in 3 and C23 in 5) and by the shape of the tetracyclic core, all carboxylic acids generated in

this study were relatively effective in inhibiting GPBAR1 activation caused by TLCA. In fact, both 5 $\beta$ -cholanoic acid **3** and 5 $\alpha$ -cholanoic acid **7**, with a bent and a flat shape (A/B *cis* junction in **3** and the A/B *trans* junction in **5**), inhibited TLCA-induced transactivation of GPBAR1 with comparable IC<sub>50</sub> values (28  $\mu$ M and 22  $\mu$ M, respectively, Fig. 4). Of interest is the observation that the presence of a larger negative charged end group such as the sulfate group in **10** and the sulfonate group in the tauro-conjugated derivatives **4** and **8**, is detrimental in term of GPBAR1 antagonism for both 5 $\alpha$ - and 5 $\beta$ -cholane derivatives.

In conclusion, on the best of our knowledge, this result represents the first report of cholanoic acid derivatives able to antagonize GPBAR1. These compounds represent novel chemical probes, useful component of today's research arsenal of bile acid derivatives, in dissecting and in shedding light on the complex biological pathways under GPBAR1 control.

The analysis of their *in vivo* effects could result in the identification of new therapeutic approach to FXR mediated liver disorders in which the concomitant activation of GPBAR1 is associated to severe side-effects.


### Appendix A. Supplementary data

Supplementary data associated with this article can be found, in the online version, at <http://dx.doi.org/10.1016/j.steroids.2015.11.003>.

### References

- [1] M. Makishima, A.Y. Okamoto, J.J. Repa, H. Tu, R.M. Learned, A. Luk, et al., Identification of a nuclear receptor for bile acids, *Science* 284 (1999) 1362–1365.
- [2] D.J. Parks, S.G. Blanchard, R.K. Bledsoe, G. Chandra, T.G. Consler, S.A. Kliewer, et al., Bile acids: natural ligands for an orphan nuclear receptor, *Science* 284 (1999) 1365–1368.
- [3] H. Wang, J. Chen, K. Hollister, L.C. Sowers, B.M. Forman, Endogenous bile acids are ligands for the nuclear receptor FXR/BAR, *Mol. Cell* 3 (1999) 543–553.
- [4] W. Xie, A. Radominska-Pandya, Y. Shi, C.M. Simon, M.C. Nelson, E.S. Ong, et al., An essential role for nuclear receptors SXR/PXR in detoxification of cholestatic bile acids, *Proc. Natl. Acad. Sci. USA* 98 (2001) 3375–3380.
- [5] M. Makishima, T.T. Lu, W. Xie, G.K. Whitfield, H. Domoto, R.M. Evans, et al., Vitamin D receptor as an intestinal bile acid sensor, *Science* 296 (2002) 1313–1316.
- [6] T. Maruyama, Y. Miyamoto, T. Nakamura, Y. Tamai, H. Okada, E. Sugiyama, et al., Identification of membrane type receptor for bile acids (M-BAR), *Biochem. Biophys. Res. Commun.* 298 (2002) 714–719.
- [7] S. Fiorucci, F. Baldelli, Farnesoid X receptor agonists in biliary tract disease, *Curr. Opin. Gastroenterol.* 25 (2009) 252–259.
- [8] S. Fiorucci, S. Cipriani, A. Mencarelli, F. Baldelli, G. Bifulco, A. Zampella, Farnesoid X receptor agonist for the treatment of liver and metabolic disorders: focus on 6-ethyl-CDCA, *Mini Rev. Med. Chem.* 11 (2011) 753–762.
- [9] S. Fiorucci, A. Mencarelli, G. Palladino, S. Cipriani, Bile-acid-activated receptors: targeting TGR5 and farnesoid-X-receptor in lipid and glucose disorders, *Trends. Pharmacol. Sci.* 30 (2009) 570–580.
- [10] S. Fiorucci, S. Cipriani, F. Baldelli, A. Mencarelli, Bile acid-activated receptors in the treatment of dyslipidemia and related disorders, *Prog. Lipid Res.* 49 (2010) 171–185.
- [11] A. Tiwari, P. Maiti, TGR5: an emerging bile acid G-protein-coupled receptor target for the potential treatment of metabolic disorders, *Drug Discovery Today* 14 (2009) 523–530.
- [12] Y. Kawamata, R. Fujii, M. Hosoya, M. Harada, H. Yoshida, M. Miwa, et al., A G protein-coupled receptor responsive to bile acids, *J. Biol. Chem.* 278 (2003) 9435–9440.
- [13] V. Keitel, B. Görg, H.J. Bidmon, I. Zemtsova, L. Spomer, K. Zilles, et al., The bile acid receptor TGR5 (Gpbar-1) acts as a neurosteroid receptor in brain, *Glia* 58 (2010) 1794–1805.
- [14] V. Sepe, E. Distrutti, V. Limongelli, S. Fiorucci, A. Zampella, Steroidal scaffolds as FXR and GPBAR1 ligands. From chemistry to therapeutic application, *Future Med. Chem.* 7 (2015) 1109–1135.
- [15] G. Rizzo, D. Passeri, F. De Franco, G. Ciaccioli, L. Donadio, G. Rizzo, et al., Functional characterization of the semisynthetic bile acid derivative INT-767, a dual farnesoid X receptor and TGR5 agonist, *Mol. Pharmacol.* 78 (2010) 617–630.
- [16] R. Pellicciari, H. Sato, A. Gioiello, G. Costantino, A. Macchiarulo, B.M. Sadeghpour, et al., Non genomic actions of bile acids. Synthesis and preliminary characterization of 23- and 6,23-alkyl-substituted bile acid derivatives as selective modulators for the G-protein coupled receptor TGR5, *J. Med. Chem.* 50 (2007) 4265–4268.
- [17] G.M. Hirschfeld, A. Mason, V. Luketic, K. Lindor, S.C. Gordon, M. Mayo, K.V. Kowdley, et al., Efficacy of obeticholic acid in patients with primary biliary cirrhosis and inadequate response to ursodeoxycholic acid, *Gastroenterology* 148 (2015) 751–761.
- [18] B.A. Neuschwander-Tetri, R. Looma, A.J. Sanyal, J.E. Lavine, M.L. Van Natta, M. F. Abdelmalek, et al., Farnesoid X nuclear receptor ligand obeticholic acid for non-cirrhotic, non-alcoholic steatohepatitis (FLINT): a multicentre, randomised, placebo-controlled trial, *Lancet* 385 (2015) 956–965.
- [19] <<https://clinicaltrials.gov/ct2/show/NCT01999101>>.
- [20] F. Alemi, E. Kwon, D.P. Poole, T. Lieu, V. Lyo, F. Cattaruzza, et al., The TGR5 receptor mediates bile acid-induced itch and analgesia, *J. Clin. Invest.* 123 (2013) 1513–1530.
- [21] H. Sato, A. Macchiarulo, C. Thomas, A. Gioiello, M. Une, A.F. Hofmann, et al., Novel potent and selective bile acid derivatives as TGR5 agonists: biological screening, structure-activity relationships, and molecular modeling studies, *J. Med. Chem.* 51 (2008) 1831–1841.
- [22] C. Festa, B. Renga, C. D'Amore, V. Sepe, C. Finamore, S. De Marino, et al., Exploitation of cholane scaffold for the discovery of potent and selective farnesoid X receptor (FXR) and G-protein coupled bile acid receptor 1 (GP-BAR1) ligands, *J. Med. Chem.* 57 (2014) 8477–8495.
- [23] V. Sepe, R. Ummarino, M.V. D'Auria, A. Mencarelli, C. D'Amore, B. Renga, et al., Total synthesis and pharmacological characterization of solomonsterol A, a potent marine pregnane-X-receptor agonist endowed with anti-inflammatory activity, *J. Med. Chem.* 54 (2011) 4590–4599.
- [24] T. Iida, G. Kakiyama, Y. Hibiya, S. Miyata, T. Inoue, K. Ohno, et al., Chemical synthesis of the 3-sulfoxy-7-N-acetylglucosaminyl-24-amidated conjugates of 3 $\beta$ ,7 $\beta$ -dihydroxy-5-cholen-24-oic acid, and related compounds: unusual, major metabolites of bile acid in a patient with Niemann–Pick disease type C1, *Steroids* 71 (2006) 18–29.
- [25] V. Sepe, R. Ummarino, M.V. D'Auria, G. Lauro, G. Bifulco, C. D'Amore, et al., Modification in the side chain of solomonsterol A: discovery of cholestan disulfate as a potent pregnane-X-receptor agonist, *Org. Biomol. Chem.* 10 (2012) 6350–6362.
- [26] C.D. Scheingart, A.F. Hofmann, Synthesis of 24-nor-5 $\beta$ -cholane-23-oic acid derivatives: a convenient and efficient one-carbon degradation of the side chain of natural bile acids, *J. Lipid Res.* 29 (1988) 1387–1395.
- [27] V. Sepe, R. Ummarino, M.V. D'Auria, B. Renga, S. Fiorucci, A. Zampella, The first total synthesis of solomonsterol B, a marine pregnane X receptor agonist, *Eur. J. Org. Chem.* (2012) 5187–5194.
- [28] C. D'Amore, F.S. Di Leva, V. Sepe, B. Renga, C. Del Gaudio, M.V. D'Auria, et al., Design, synthesis, and biological evaluation of potent dual agonists of nuclear and membrane bile acid receptors, *J. Med. Chem.* 57 (2014) 937–954.

# SCIENTIFIC REPORTS



OPEN

## Insights on FXR selective modulation. Speculation on bile acid chemical space in the discovery of potent and selective agonists

Received: 24 September 2015

Accepted: 02 December 2015

Published: 07 January 2016

Valentina Sepe<sup>1</sup>, Carmen Festa<sup>1</sup>, Barbara Renga<sup>2</sup>, Adriana Carino<sup>2</sup>, Sabrina Cipriani<sup>2</sup>, Claudia Finamore<sup>1</sup>, Dario Masullo<sup>1</sup>, Federica del Gaudio<sup>3,4</sup>, Maria Chiara Monti<sup>3</sup>, Stefano Fiorucci<sup>2</sup> & Angela Zampella<sup>1</sup>

Bile acids are the endogenous modulators of the nuclear receptor FXR and the membrane receptor GPBAR1. FXR represents a promising pharmacological target for the treatment of cholestatic liver disorders. Currently available semisynthetic bile acid derivatives cover the same chemical space of bile acids and therefore they are poorly selective toward BA receptors, increasing patient risk for adverse side effects. In this report, we have investigated around the structure of CDCA describing the synthesis and the *in vitro* and *in vivo* pharmacological characterization of a novel family of compounds modified on the steroidal tetracyclic core and on the side chain. Pharmacological characterization resulted in the identification of several potent and selective FXR agonists. These novel agents might add utility in the treatment of cholestatic disorders by potentially mitigating side effects linked to unwanted activation of GPBAR1.

Farnesoid X receptor (FXR) is one of the 48 ligand-activated nuclear transcription factor proteins. Mostly expressed in hepatocytes, biliary epithelium, small bowel enterocytes, renal tubular cells and adrenal glands, FXR senses the intracellular presence of bile acids (BAs) by inducing changes in gene expression<sup>1,2</sup>. The results of the consequent activated multiple mechanisms include promotion of bile acid export from liver, down-regulation of bile acid import and also attenuation of *de-novo* bile acid synthesis<sup>3</sup>. Thus, FXR has been identified as an appealing target in the treatment of cholestasis and liver steatosis<sup>4-6</sup>. In addition to its canonical role in regulating bile acid homeostasis, FXR plays a crucial beneficial role in hepatic triglyceride (TG) homeostasis, as well as in glucose metabolism. FXR lowers hepatic TG content and serum TG levels and improves insulin resistance and hyperglycemia. Therefore, FXR agonists are promising for the treatment of non-alcoholic fatty liver disease (NAFLD), dyslipidemia and type 2 diabetes<sup>7-10</sup>.

Among endogenous occurring BAs, chenodeoxycholic acid (CDCA, **1** in Fig. 1) is the most potent natural FXR ligand ( $EC_{50} \sim 10 \mu\text{M}$ ), whereas deoxycholic acid and lithocholic acid are weaker natural ligands<sup>11</sup>.

In addition, secondary BAs activate the membrane G-protein-coupled receptor GPBAR1 (also known as M-BAR, TGR5 or BG37)<sup>12</sup>, and the exogenous dual control over the two receptors represents an attractive strategy for the treatment of non-alcoholic steatohepatitis (NASH) and type 2 diabetes<sup>13-15</sup>.

On the other hands, GPBAR1 has been recently identified as the physiological mediator of pruritus<sup>16</sup>, a common symptom observed in cholestasis and the severity of this side effect limits the pharmacological utility of dual agonists in the treatment of primary biliary cirrhosis (PBC) and related cholestatic disorders. In this context, the discovery of highly selective FXR agonists, devoid of GPBAR1 agonism, represents a promising approach in the identification of new pharmacological protocols for PBC, an orphan disease for which therapeutic options are limited and poorly effective.

<sup>1</sup>Department of Pharmacy, University of Naples "Federico II", Via D. Montesano, 49, 80131 Naples, Italy.

<sup>2</sup>Department of Surgery and Biomedical Sciences, Nuova Facoltà di Medicina, P.zza L. Severi 1, 06132 Perugia, Italy.

<sup>3</sup>PhD Program in Drug Discovery and Development, University of Salerno, Via Giovanni Paolo II 132, 84084 Fisciano (Salerno), Italy. <sup>4</sup>Department of Pharmacy, University of Salerno, Via Giovanni Paolo II, 132, 84084 Fisciano (Salerno), Italy. Correspondence and requests for materials should be addressed to A.Z. (email: angela.zampella@unina.it)

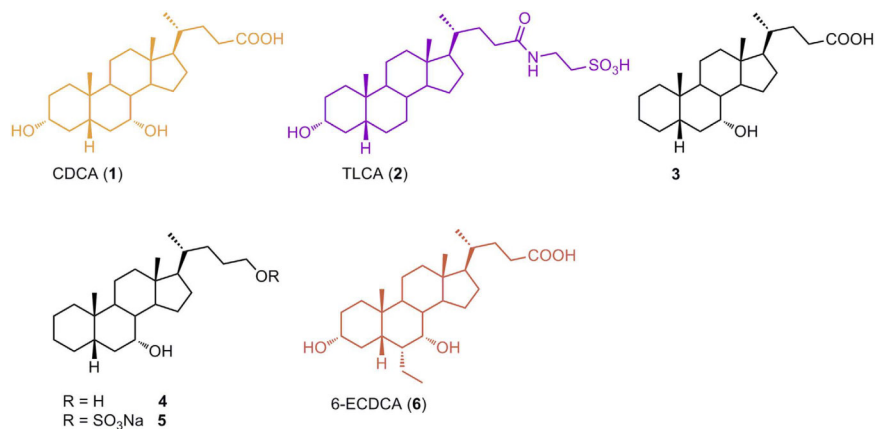


**Figure 1.** CDCA and TLCA, the most potent endogenous activators of FXR and GPBAR1, respectively. 3-Deoxy-5 $\beta$ -cholane derivatives 3–5 as selective FXR ligands and 6-ECDCA, a potent semi-synthetic dual agonist.

Indeed, in the last ten years bile acid scaffold has been subjected to intense medicinal chemistry modifications, producing several steroidal derivatives modified on the side chain in the length and in the nature of the end-group and on the tetracyclic core. Since steroidal ligands cover the same chemical space of BAs, they are intrinsically promiscuous toward FXR and GPBAR1 and, with few exception, this kind of speculation mainly afforded dual modulators<sup>17,18</sup>. Indeed, the removal or isomerization of the hydroxyl group at C-3 on LCA or its tauro-conjugated form (TLCA, **2** in Fig. 1), the most potent GPBAR1 agonist among endogenous BAs<sup>19</sup>, is detrimental in term of GPBAR1 agonism, and this observation was recently translated on CDCA scaffold demonstrating that 3-deoxy-5 $\beta$ -cholane derivatives are selective FXR ligands<sup>17</sup>. Independently from the functional group at C-24 on the side chain, derivatives 3–5 (Fig. 1) were demonstrated selective FXR agonists with 7 $\alpha$ -hydroxy-5 $\beta$ -cholan-24-sulfate (**5**) transactivating FXR with an EC<sub>50</sub> of ~9  $\mu$ M. Even if less potent in trans-activation assay than 6-ethylchenodeoxycholic acid, 6-ECDCA/OCA (**6**), the most potent steroidal FXR agonist generated so far, the potency of compound **5** in inducing the expression of OST $\alpha$ , a FXR target gene in the liver, is comparable to that of 6-ECDCA. However 6-ECDCA is also a GPBAR1 activator<sup>20,21</sup>, and administration of PBC patients has led to exacerbation of itching causing drug discontinuation in 40% of patients<sup>22</sup>.

With this background in mind, we decided to proceed in the modification of the hydroxyl group at C-3 on 6-ethylcholane scaffold generating a library of 6-ethylcholane derivatives that are divided in two subsets (Fig. 2): subset A includes the 3-deoxy-6-ethyl derivatives, and subset B includes the 3 $\beta$ -hydroxyl derivatives.

As shown in the Fig. 2, in each subset, our investigation was also expanded on the side chain-end group and on the stereochemical arrangement of 6-ethyl and 7-hydroxyl substituents on ring B affording to the discovery of several derivatives as potent and selective FXR agonists.

## Results

### Modification on 6-ethylchenodeoxycholine scaffold in the preparation of subset A derivatives (Fig. 3).

Methyl ester formation and acetylation at C-3 hydroxyl group on 7-KLCA furnished intermediate **22** in 84% yield over two steps. Aldolic addition to a silyl enol ether intermediate generated **23**. Hydrogenation at the exocyclic double bond (H<sub>2</sub> on Pd(OH)<sub>2</sub>) afforded exclusively the 6 $\beta$ -ethyl group in **24** (80% yield over three steps) as demonstrated by dipolar couplings Me-26 ( $\delta$  0.83)/Me-19 ( $\delta$  1.22) and H-8 ( $\delta$  2.56)/H-25 ( $\delta$  1.83) in Noesy spectrum. First, compound **24** was treated with MeONa in methanol to effect de-acetylation at C-3 and inversion at C-6 and then with tosyl chloride to afford **25** in quantitative yield over two steps. Elimination by LiBr/Li<sub>2</sub>CO<sub>3</sub> treatment and hydrogenation of the unsaturated-ring A transient intermediate furnished the key derivative **26**. LiBH<sub>4</sub> treatment produced the concomitant reduction at C-24 methyl ester and at C-7 carbonyl group furnishing **7** in high chemical yield and a small aliquot of the corresponding epimer at C-7 (**8**), efficiently separated by HPLC.

Chemoselective sulfation at C-24 hydroxyl group on a small aliquot of **7** gave the corresponding sulfate derivative **9**. Intermediate **26** was also used as starting material for the preparation of compounds **10** and **11**. Alkaline hydrolysis of the methyl ester followed by LiBH<sub>4</sub> treatment furnished **10** in high chemical yield with about 10% of 6 $\alpha$ -ethyl-7 $\beta$ -hydroxy-5 $\beta$ -cholan-24-oic acid (**11**) that was isolated by HPLC. Amidation with taurine on the major 6 $\alpha$ -ethyl-7 $\alpha$ -hydroxy-5 $\beta$ -cholan-24-oic acid (**10**) and C18 silica gel column/HPLC purification provided the corresponding tauro-conjugated **12**.

As previously demonstrated, stereochemical arrangement of the substituents at C-6 and C-7 on ring B profoundly affects bile acid receptor selectivity<sup>17</sup>. Invariably the presence of the 6 $\alpha$ -ethyl and the 7 $\alpha$ -hydroxyl groups produces potent agonists with dual FXR/GPBAR1 activity whereas the 6-epimers (6 $\beta$ -ethyl derivatives) are selective GPBAR1 agonists. To access to 3-deoxy-6 $\beta$ -ethylchenodeoxycholine derivatives, compound **24** was treated with MeONa in MeOH for 2 h reaction time affording de-acetylation at C-3 without epimerization at C-6. Tosylation on the crude reaction product furnished **27** that was subjected to the same operative condition described for compound **26**, to obtain **28** in 94% yield over two steps. Treatment of **28** with NaBH<sub>4</sub> in methanol followed by LiBH<sub>4</sub> reduction on the crude reaction product to secure the complete reduction of the methyl ester

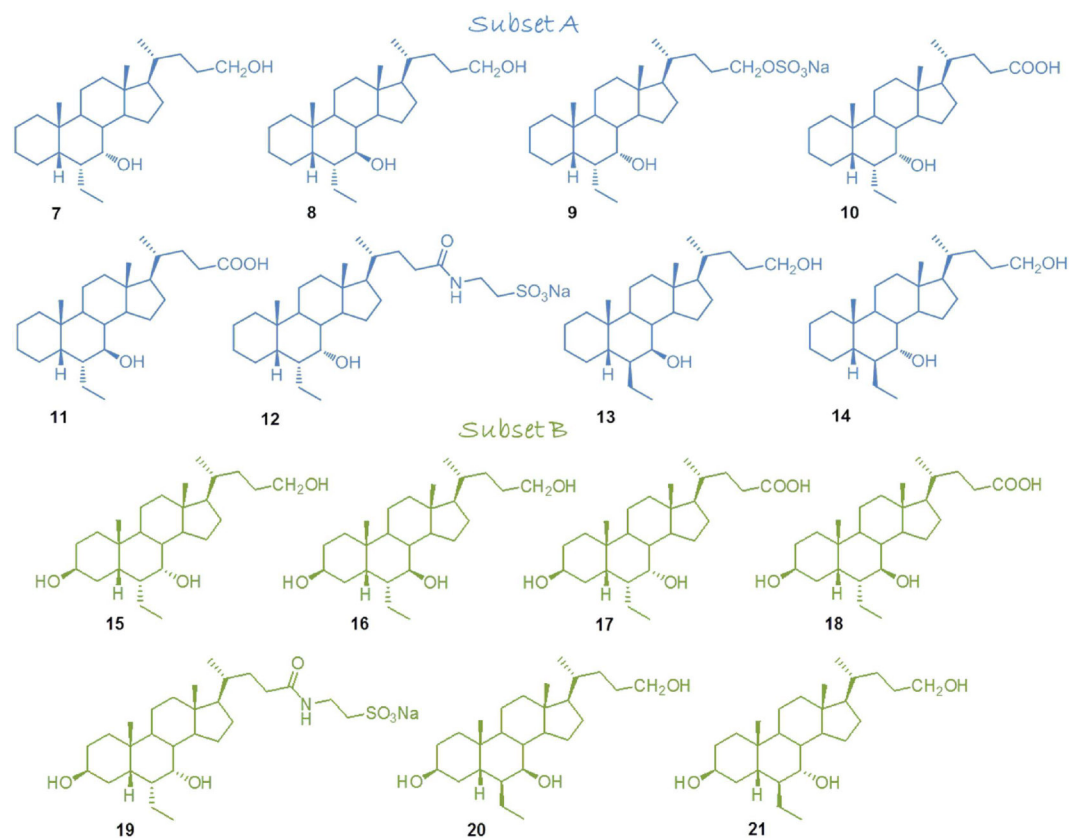


**Figure 2.** 6-Ethylcholate scaffold derivatives generated in this study. Subset A: 3-deoxy-6-ethylchenodeoxycholate derivatives; subset B: 3 $\beta$ -hydroxy-6-ethylchenodeoxycholate derivatives.

on the side chain afforded a mixture whose HPLC purification gave pure **13** in a 54% yield respect to the corresponding C7 epimer, compound **14**.

**Modification on 6-ethylchenodeoxycholate scaffold in the preparation of subset B derivatives (Fig. 4).** As previously demonstrated, modification at C-3 impacts on BAs selectivity and activity towards FXR and GPBAR1. Isomerization of the 3R-hydroxyl group on LCA robustly attenuates the agonistic activity on GPBAR1 with iso-LCA less potent respect to the cognate LCA. On the other hand, isochenodeoxycholic acid (iso-CDCA) is more potent than CDCA in transactivating FXR and notably has only very weak activity towards GPBAR1<sup>17</sup>.

With this background in mind, our speculation on 6-ethylchenodeoxycholate scaffold was expanded to the preparation of 3 $\beta$ -hydroxyl derivatives.

As depicted in Fig. 4, in a convergent protocol, inversion at C-3 on **27** with potassium acetate in DMF/H<sub>2</sub>O followed by treatment with MeONa/MeOH gave **29** (74% over two steps) that was used as starting material in the synthesis of derivatives **15–19**. In detail NaOH hydrolysis followed by LiBH<sub>4</sub> treatment gave **17** and small amounts (about 10%) of the corresponding 7 $\beta$ -hydroxyl derivative **18**, efficiently separated by HPLC. Tauro-conjugation on a small aliquot of **17** proceeded smoothly to the formation of **19** in good chemical yield. In a parallel protocol, intermediated **29** was subjected to LiBH<sub>4</sub> treatment affording alcohol **15** in presence of a small amount of 6 $\alpha$ -ethyl-3 $\beta$ ,7 $\beta$ -dihydroxy-5 $\beta$ -cholan-24-ol (**16**).

Compound **27** was also used as starting material for the preparation of compounds **20–21** (Fig. 4). Inversion at C-3 followed by reduction at C-7 and C-24 with NaBH<sub>4</sub>/LiBH<sub>4</sub> treatment as described for the corresponding 3-deoxy derivatives (Fig. 3) furnished **20** and **21** as a mixture, then separated by HPLC.

**Preparation of the reference compound, 6-ECDCA (6) (Fig. 5).** Methyl ester **24** was also converted in 6-ECDCA (**6**), used as reference compound in the pharmacological evaluation of our library of 6-ethylcholate derivatives. Basic treatment (NaOH, MeOH/H<sub>2</sub>O) on **24** proceeded in a straightforward manner affording the concomitant hydrolysis on side chain methyl ester, de-acetylation at C-3 and inversion at C-6 ethyl group. LiBH<sub>4</sub> reduction of the C7-carbonyl group on intermediate **30** furnished 6-ECDCA (**6**) in 69% over two steps.

**In vitro pharmacological evaluation.** Derivatives **7–21** were tested for FXR and GPBAR1 activity, in a luciferase reporter assay with HepG2 and HEK-293T cells transfected with FXR and GPBAR1, respectively (Figs 6, 8 and 9). As reported in Fig. 6A, all 6 $\alpha$ /7 $\alpha$  derivatives (compounds **7**, **9**, **10** in subset A and **15**, **17** in subset B) are potent agonists of FXR. Within 6 $\alpha$ /7 $\alpha$  stereochemical arrangement, the presence of a negative charge

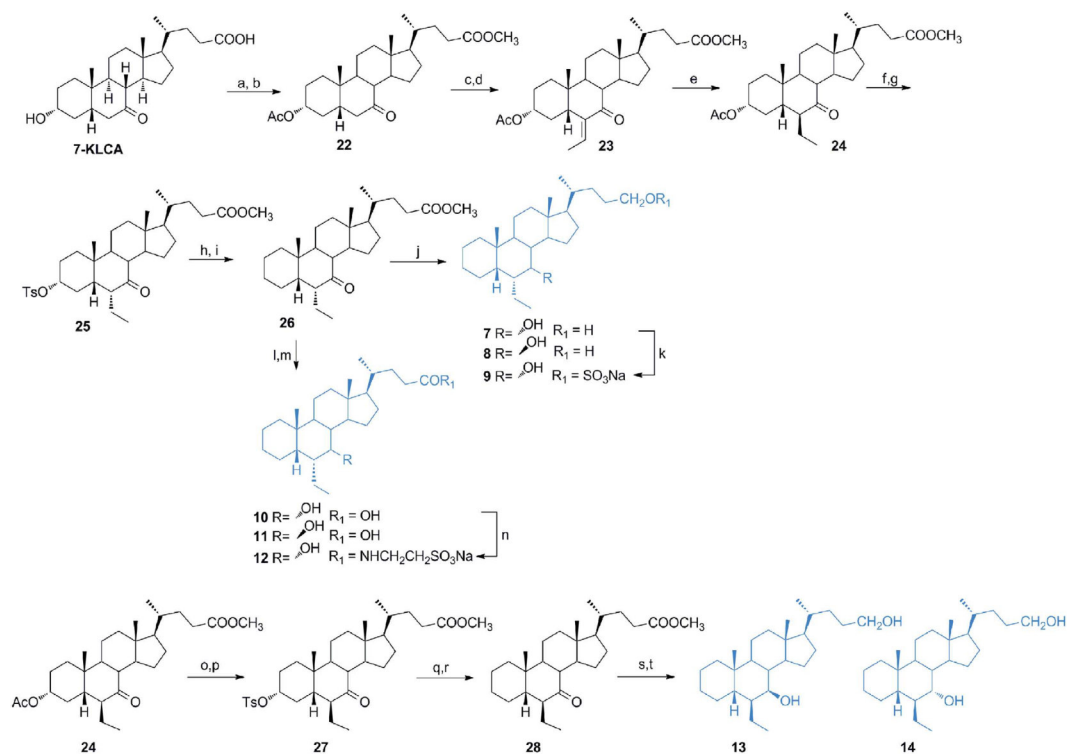


**Figure 3. Preparation of 3-deoxy-6-ethylchenocholeane derivatives (subset A).** Reagents and conditions: (a) *p*-TsOH, MeOH dry; (b) acetic anhydride, pyridine, 84% yield over two steps; (c) DIPA, *n*-BuLi, TMSCl, TEA dry, THF dry  $-78^\circ\text{C}$ ; (d) acetaldehyde,  $\text{BF}_3(\text{OEt})_2$ ,  $\text{CH}_2\text{Cl}_2$ ,  $-60^\circ\text{C}$ , 80% over two steps; (e)  $\text{H}_2$ ,  $\text{Pd}(\text{OH})_2$ , THF/MeOH 1:1, quantitative yield; (f) MeONa, MeOH; (g) *p*-TsCl, pyridine, quantitative yield over two steps; (h) LiBr,  $\text{Li}_2\text{CO}_3$ , DMF, reflux, (i)  $\text{H}_2$ ,  $\text{Pd}(\text{OH})_2$ , THF/MeOH 1:1, room temperature, 88% over two steps; (j)  $\text{LiBH}_4$ , MeOH dry, THF,  $0^\circ\text{C}$ , 77%; (k)  $\text{Et}_3\text{N}\cdot\text{SO}_3$ , DMF,  $95^\circ\text{C}$ ; (l) NaOH, MeOH:H<sub>2</sub>O 1:1 v/v, 98%; (m)  $\text{LiBH}_4$ , MeOH dry, THF,  $0^\circ\text{C}$ , 83%; (n) DMT-MM,  $\text{Et}_3\text{N}$ , taurine, DMF dry; (o) MeONa, MeOH; (p) *p*-TsCl, pyridine, quantitative yield over two steps; (q) LiBr,  $\text{Li}_2\text{CO}_3$ , DMF, reflux; (r)  $\text{H}_2$ ,  $\text{Pd}(\text{OH})_2$ , THF/MeOH 1:1, room temperature, 94% over two steps; (s)  $\text{NaBH}_4$ , MeOH; (t)  $\text{LiBH}_4$ , MeOH dry, THF,  $0^\circ\text{C}$ , 78% over two steps.

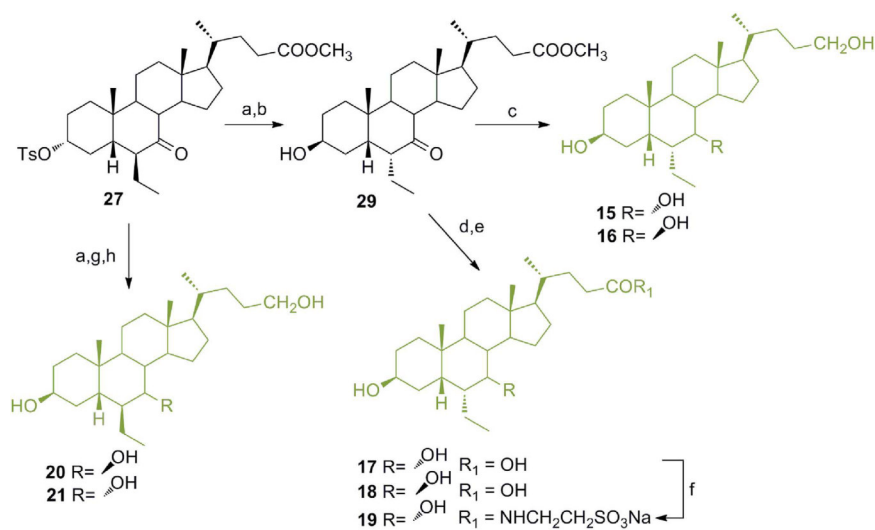


**Figure 4. Preparation of 3β-hydroxy-6-ethylchenocholeane derivatives (subset B).** Reagents and conditions: (a)  $\text{CH}_3\text{COOK}$ , DMF:H<sub>2</sub>O 5:1 v/v; (b) NaOMe, MeOH, 74% over two steps; (c)  $\text{LiBH}_4$ , MeOH dry, THF,  $0^\circ\text{C}$ , 58%; (d) NaOH, MeOH:H<sub>2</sub>O 1:1 v/v; (e)  $\text{LiBH}_4$ , MeOH dry, THF,  $0^\circ\text{C}$ , 74% over two steps; (f) DMT-MM,  $\text{Et}_3\text{N}$ , taurine, DMF dry; (g)  $\text{NaBH}_4$ , MeOH; (h)  $\text{LiBH}_4$ , MeOH dry, THF,  $0^\circ\text{C}$ , 74% over three steps.

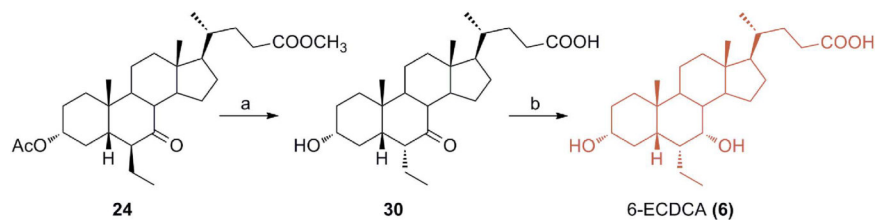


**Figure 5.** Preparation of the reference compound, 6-ECDCA (6). Reagents and conditions: (a) NaOH, MeOH:H<sub>2</sub>O 1:1 v/v; (b) LiBH<sub>4</sub>, MeOH dry, THF, 0 °C, 69% over two steps.

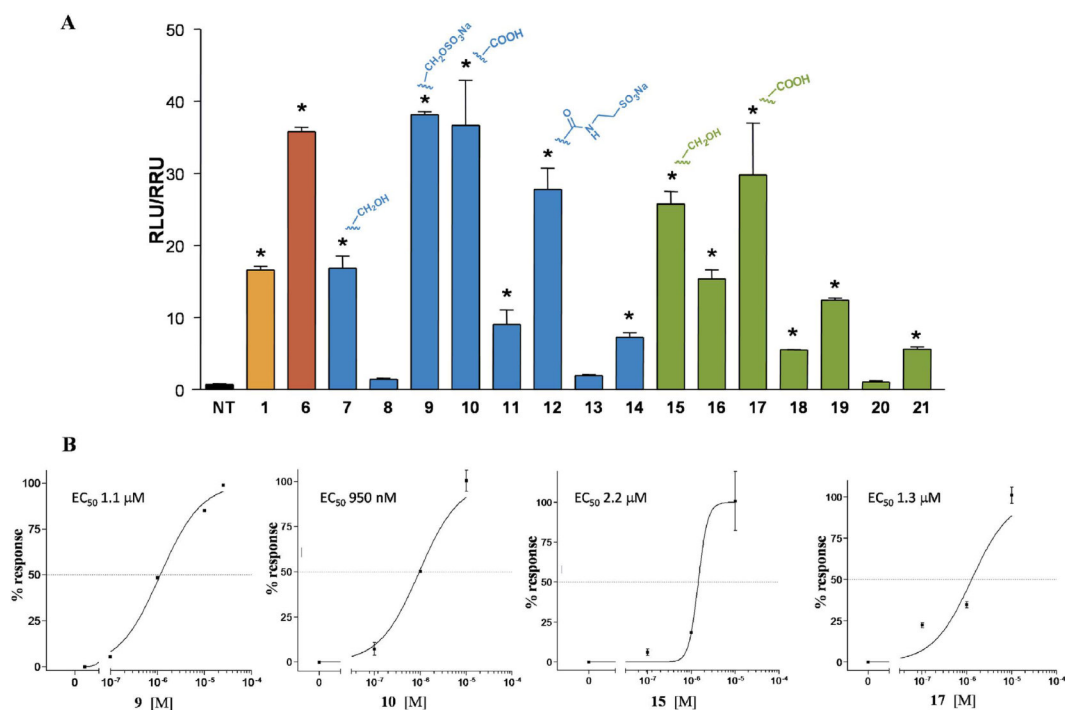


**Figure 6.** Transactivation assays on FXR. (A) HepG2 cells were transfected with pSG5-FXR, pSG5-RXR, pCMV-βgal, and p(hsp27)TKLUC vectors. Cells were stimulated with compounds 7–21 (10 μM). CDCA (1, 10 μM) and 6-ECDCA (6, 1 μM) were used as a positive control. Results are expressed as mean ± standard error; \*p < 0.05 versus not treated cells (NT); (B) Concentration-response curve of 9, 10, 15 and 17 on FXR in a luciferase reporter assay using HepG2 cells transfected with FXR. Twenty-four hour post transfection cells were stimulated with increasing concentrations of each agent: range from 100 nM to 10 μM.

on the side chain favors the 3-deoxy derivatives with the carboxylic acid **10** and the sulfate derivative **9** potent FXR activators whereas the alcoholic function at C-24 improves FXR activity of the corresponding 3β-hydroxyl derivatives (compare **10** vs **17** and **15** vs **7**). Of interest are also the cellular assay results on compounds with one of the two substituents on ring B in a β-configuration (C6α/C7β or C6β/C7α) revealing a remarkable decrease in FXR activity when compared to the corresponding 6α/7α substituted derivatives. In detail, one again, the activity is related to the functional group on the side chain and to the presence/absence of the hydroxyl group at C-3. First derivative **8**, a C3-deoxy/C24-alcohol with the C6α/C7β stereochemical arrangement is completely inactive towards FXR whereas the corresponding carboxylic acid **11**, even if less potent than CDCA (**1**), retains a certain activity. Opposite is the behavior of the corresponding 3β-hydroxyl derivatives where the presence of the alcoholic function at C-24 on the side chain improves FXR activity (compare **16** vs **18**).

Finally, the complete loss of activity for compounds **13** and **20** points the attention on the pharmacophoric role of the C6/C7 stereochemical arrangement with the 6β/7β relationship detrimental in FXR binding.

The relative potency of selected members of this novel family was then investigated by a detailed measurement of concentration-response curve of the 3-deoxy sulfate derivative **9**, the corresponding carboxylic acid **10**, and the 3β-hydroxyl alcohol **15** and carboxylic acid derivative **17**, all sharing the 6α/7α configuration, on FXR transactivation. As illustrated in Fig. 6B, compounds **9**, **10**, **15** and **17** transactivate FXR with an EC<sub>50</sub> of 1.1 μM, 950 nM, 2.2 μM and 1.3 μM, respectively, with compound **10** showing a comparable potency with the reference compound, 6-ECDCA, EC<sub>50</sub> = 500 nM in the same assay (Supporting Information, Figure S1). Of interest, the ability in transactivating FXR is also maintained by the corresponding tauro-conjugated **12** (Fig. 6A, compare **10** vs **12**),

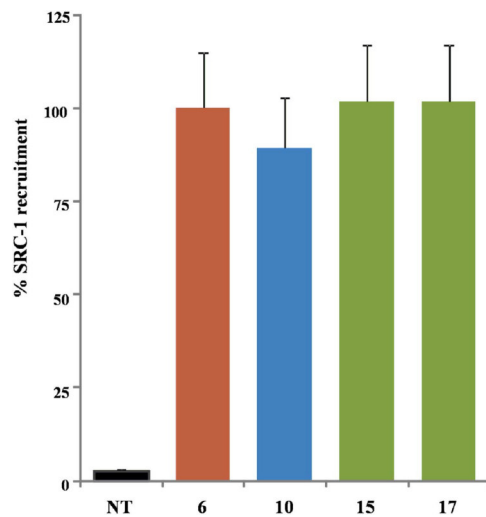


**Figure 7. Coactivator recruitment assay measuring a direct interaction of FXR with SRC-1.** Anti-GST-coated acceptor beads captured GST-fusion FXR-LBD and the biotinylated-SRC-1 peptide was captured by the streptavidin donor beads. FXR-LBD recruited SRC-1 in the presence of ligand at  $2\ \mu\text{M}$  and, upon illumination at 680 nm, chemical energy is transferred from donor to acceptor beads across the complex streptavidin-donor/Src-1-biotin/ligand/GSTFXR-LBD/anti-GST-acceptor and a signal is produced. Results are expressed as percentage of the effect of **6** arbitrarily settled as 100%. NT is referred to the experiment carried out in absence of ligand. Results are expressed as mean  $\pm$  standard error.

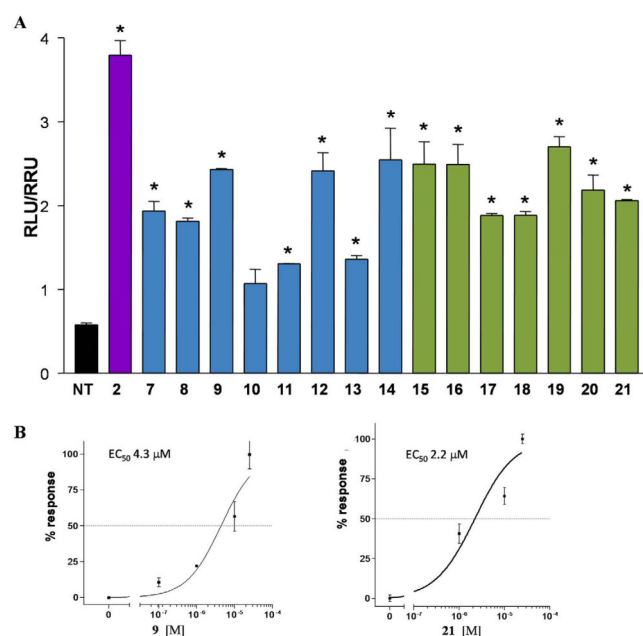


**Figure 8. Agonism on GPBAR1 by transactivation assay.** (A) HEK-293T cells were co-transfected with GPBAR1 and a reporter gene containing a cAMP responsive element in front of the luciferase gene. Twenty-four hour post transfection cells were stimulated with **7–21** ( $10\ \mu\text{M}$ ). Luciferase activity served as a measure of the rise in intracellular cAMP following activation of GPBAR1. TLCA (**2**,  $10\ \mu\text{M}$ ) was used as a positive control. Results are expressed as mean  $\pm$  standard error. \* $p < 0.05$  versus not treated cells (NT); (B) Concentration-response curve of **9** and **21** on GPBAR1 in HEK-293T cells co-transfected with GPBAR1 and a reporter gene containing a cAMP responsive element in front of the luciferase gene (CRE). Twenty-four hour post transfection cells were stimulated with increasing concentrations of each agent: range from 100 nM to  $50\ \mu\text{M}$ . Results are expressed as mean  $\pm$  standard error.

thus highlighting the therapeutical potential of  $6\alpha$ -ethyl- $7\alpha$ -hydroxy- $5\beta$ -cholan-24-oic acid (**10**) in human FXR mediated diseases. On the contrary, tauro-conjugation on carboxylic acid **17** produces a considerable decrease in FXR transactivation activity (compare **19** vs **17** in Fig. 6A), thus first demonstrating that a longer negative



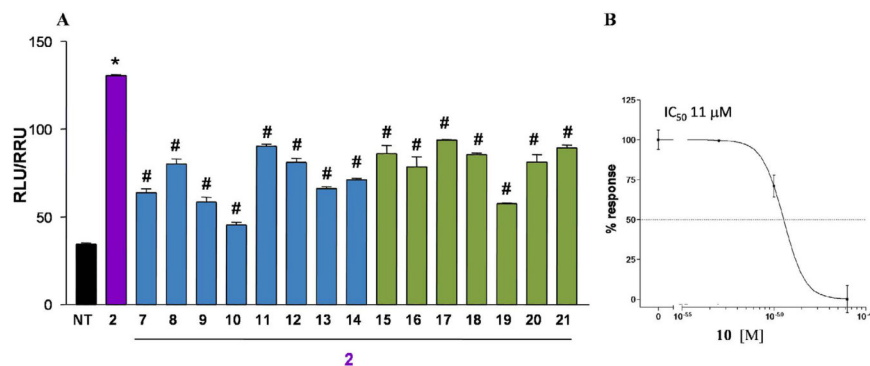


**Figure 9. Antagonism on GPBAR1 by transactivation assay.** (A) HEK-293T cells were transfected as described in Fig. 8. Twenty-four hour post transfection cells were stimulated with 10  $\mu$ M TLCA (2) alone or in combination with 25  $\mu$ M compounds 7–21. \* $p < 0.05$  versus TLCA stimulated cells; (B) Concentration-response curve of 10 on GPBAR1 in combination with TLCA (2, 10  $\mu$ M) and with increasing concentrations of 10: range from 5 to 25  $\mu$ M. Results are expressed as mean  $\pm$  standard error.

charged side chain is detrimental in FXR binding when a 3 $\beta$ -hydroxyl group is present on the steroidal scaffold and second, reducing the pharmacological impact of compound 17. Finally the ability of the more active compounds in transactivating FXR was measured as recruitment of the coactivator SRC-1, using Alphascreen technology. In this assay, the ligand induces the recruitment of the coactivator to the LBD of hFXR. 6-ECDCA (6) was used as positive control and reference molecule setting its effect as 100% (Fig. 7). All tested derivatives, 6 $\alpha$ -ethyl-7 $\alpha$ -hydroxy-5 $\beta$ -cholan-24-oic acid (10), 6 $\alpha$ -ethyl-3 $\beta$ ,7 $\alpha$ -dihydroxy-5 $\beta$ -cholan-24-ol (15) and the corresponding carboxylic acid, 6 $\alpha$ -ethyl-3 $\beta$ ,7 $\alpha$ -dihydroxy-5 $\beta$ -cholan-24-oic acid (17) showed a very potent activity in the recruitment of SRC-1 co-activator and high affinity to FXR, almost comparable to that measured for 6, thus confirming the transactivation results.

Results of transactivations of CREB-responsive elements in HEK-293T, transiently transfected with the membrane bile acid receptor GPBAR1 (Fig. 8A), revealed that the strategy of elimination or inversion at C-3 hydroxyl group could be instrumental in shifting the selectivity of 6-ethylcholine derivatives toward FXR.

Indeed, independently by the functional group on the side chain, the stereochemical arrangement of C6/C7 substituents and the presence/absence of the hydroxyl group at C-3, all derivatives generated in this study are weak agonists, substantially less potent than TLCA (2) in modulating GPBAR1. By way of example, the concentration-response curve on compounds 9 and 21 (Fig. 8B) resulted in EC<sub>50</sub> values of 4.3 and 2.2  $\mu$ M, substantially lesser than the corresponding value for TLCA (EC<sub>50</sub> = 0.29  $\mu$ M)<sup>19</sup>. As a consequent, compound 9 should be considered a preferential FXR modulator with a residual activity on GPBAR1 whereas compound 21, less potent than CDCA in transactivating FXR (Fig. 6A), is a weak but preferential GPBAR1 activator.

Moreover, 6 $\alpha$ -ethyl-7 $\alpha$ -hydroxy-5 $\beta$ -cholan-24-oic acid (10), one of the most potent derivative in transactivating FXR is inactive towards GPBAR1 in agonistic mode (Fig. 8A). Of interest, when administered in presence of 10  $\mu$ M TLCA (2), compound 10 showed inhibitory activity against GPBAR1 transactivation induced by TLCA (Fig. 9A). The above result was also confirmed by a concentration-response curve in HEK-293T transiently transfected with GPBAR1, revealing for 10 an IC<sub>50</sub> value of 11  $\mu$ M in antagonizing the effect of TLCA (Fig. 9B). To the best of our knowledge, this result represents the first report of a 6-ethylcholanoic derivative endowed by potent FXR agonism and able to antagonize GPBAR1. This discovery opens the way to a new and promising field of research. First, the speculation of the *in vivo* effects of this compound could result in the identification of new therapeutical approach to FXR mediated liver disorders in which the concomitant activation of GPBAR1 is associated to severe side effects. Second, compound 10 represents a novel tool compound, useful component of today's research arsenal of BA derivatives, in dissecting and in shedding light on the complex biological pathways under GPBAR1 control.

***In vivo* pharmacological characterization (Figs. 10,11).** C57BL6 mice were administered with compound 10 (15 mg/kg, ip). At 6 h post-treatment, livers and blood were collected. As shown in Fig. 10, compound 10 significantly up-regulated the relative mRNA expression of canonical FXR molecular targets such as OST $\alpha$ , SHP and BSEP in the liver exposed 6 h to 10 (\* $p < 0.05$  versus control mice).

Analysis of plasmatic concentrations of unconjugated and tauro-conjugated bile acids demonstrated that *in vivo* administration of 10 significantly reduced total unconjugated bile acids while the quote of tauro-conjugated tMu, tCA, tHCA, tCDCA, tDCA and tLCA was unaffected (Fig. 11, \* $p < 0.05$  versus control mice). Compound 10 was only found in the conjugated form with taurine (data not shown).

## Discussion and Conclusion

In addition to their role in lipid absorption, and similarly to other cholesterol metabolites, bile acids are signaling molecules.

Each bile acid interacts with more than one receptor, however, FXR and GPBAR1 are differentially activated by CDCA > DCA > LCA > CA and LCA > DCA > CDCA > CA, respectively. In addition to endogenous ligands,

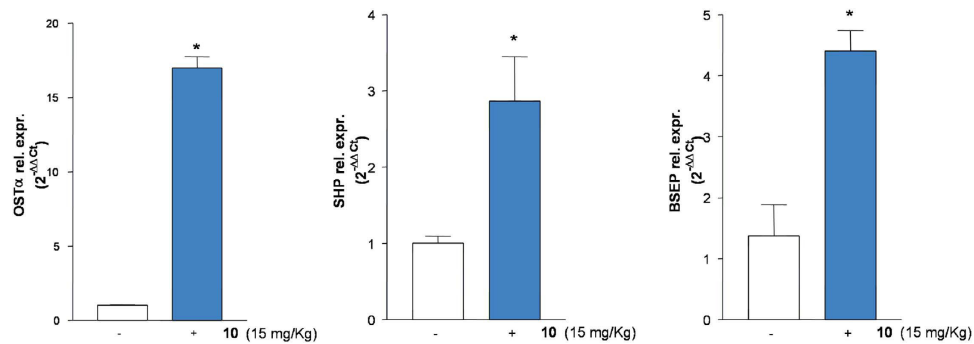


**Figure 10.** *In vivo* effect of **10** on FXR target genes. C57BL/6 mice were administered with **10** (15 mg/Kg) for 6 h. After treatment liver were removed and the relative mRNA expression of OST $\alpha$ , SHP and BSEP was assayed by quantitative Real-Time PCR. \* $p < 0.05$  versus control mice.

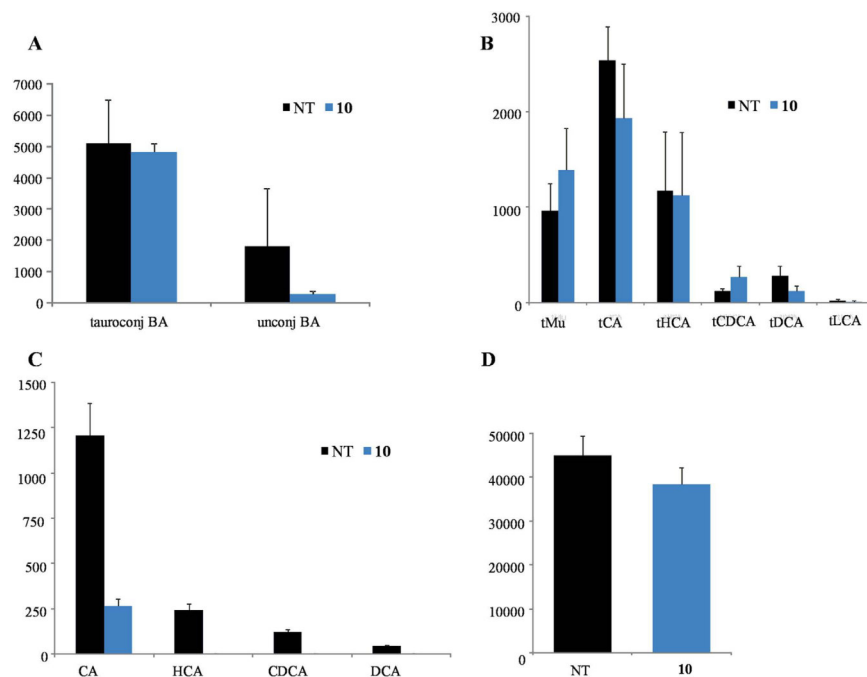


**Figure 11.** Blood concentrations of (A) total tauro-conjugated and total unconjugated bile acids; (B) individual conjugated and (C) unconjugated bile acids; (D) 7 $\alpha$ -hydroxy-4-cholesten-3-one before and after *in vivo* administration of **10** at 15 mg/Kg.

several semisynthetic bile acids and non-steroidal FXR ligands are currently under evaluation in the treatment of metabolic (NASH) and cholestatic liver diseases (PBC).

Obeticholic acid (OCA, or 6-ECDCA (**6**), or INT-747), a semi-synthetic dual FXR and GPBAR1 ligand and a derivative of CDCA, has been recently evaluated in the multicenter, double-blind, randomized NASH (FLINT) trial<sup>23</sup>. Although 6-ECDCA/OCA significantly improved the primary histological outcome (NAFLD activity score) and fibrosis score compared with placebo, NASH resolution occurred in only 22% of patients after 72 weeks ( $p = 0.08$  vs. placebo). In addition, a 5% decrease in HDL-C levels coupled with a 16% increase in LDL-C was observed with OCA as compared to placebo and the impact of these changes on long-term cardiovascular risk in NASH is unknown. One major limitation of the use of OCA is the high incidence of pruritus, occurring in up to 80% patients with primary biliary cirrhosis receiving OCA and primarily responsible for high rate of drug discontinuation in 40% of patients<sup>23,24</sup>. Indeed, OCA is a dual FXR/GPBAR1 agonist<sup>20,21</sup>, and GPBAR1 has recently been demonstrated a physiological mediator of itching<sup>15</sup>, indicating that highly selective FXR agonists might have utility in the treatment of PBC. In this context, we have modified BA scaffold generating a library of 6-ethylcholane derivatives having variable and peculiar activity toward FXR and GPBAR1.

From a chemical perspective of structure-activity relationship, our investigation has been focused primarily on three areas: (1) the modification at C-3 hydroxyl group (elimination/inversion) on the 6-ethylcholane scaffold; (2) changes to the end group on side chain; and (3) the stereochemical orientation of C6/C7 substituents on ring B. The first consideration to be drawn is that all 6-ethylcholane derivatives prepared in this study

are at least weak GPBAR1 agonists (Fig. 8), thus affirming the key pharmacophoric role of the 3 $\alpha$ -hydroxyl group for GPBAR1 activation by BA scaffold. Second, as expected, the presence of both substituents on ring B in  $\alpha$ -configuration favors FXR binding generating potent agonists<sup>25</sup>. Among the two subsets of semisynthetic bile acid derivatives, 3-deoxy-chenodeoxycholate derivatives (subset A) **9** and **10**, differing in the nature of the negative charged side chain end group (sulfate in **9** and carboxylic acid in **10**) transactivate FXR with EC<sub>50</sub> values of 1.1  $\mu$ M and 950 nM, respectively. Both values are comparable to that of 6-ECDCA (**6**) (Figure S1) and the above potency was also shared by the corresponding 3 $\beta$ -hydroxyl carboxylic acid **17** (EC<sub>50</sub> values of 1.3  $\mu$ M). Of interest are also the results of tauro-conjugation on the potent FXR agonists, carboxylic acids **10** and **17**. As shown in Fig. 6A, tauro-conjugation on the 3-deoxy derivative **10** produces **12**, still a potent FXR agonist whereas tauro-conjugation on the 3 $\beta$ -hydroxyl carboxylic acid **17** is detrimental in term of FXR activation (compound **19** in Fig. 6A). Because endogenous bile acids and semisynthetic bile acid derivatives undergo to extensive liver conjugation at the carboxyl acid end group (tauro-conjugation in mice and glyco-conjugation in human), this result highlights the therapeutical potential of compound **10** in human FXR mediated diseases. Indeed compound **10** is devoid of any activity toward GPBAR1 in agonistic mode (Fig. 8A) but when administered in combination with TLCA, it inhibited TLCA mediated GPBAR1 activation with an IC<sub>50</sub> value of 11  $\mu$ M (Fig. 9B). Thus, to the best of our knowledge, compound **10** represents the first example of a 6-ethyl bile acid derivative endowed with FXR agonism/GPBAR1 antagonism.

Further investigating its pharmacological properties, compound **10** at the dose of 15 mg/kg was administered to intact mice. As illustrated in Fig. 10, this agent significantly increased the expression of three canonical FXR target genes in the liver. Indeed, compound **10** increased the expression of OST $\alpha$ , SHP and BSEP in the liver as early as 6 h after administration. Because these three genes are endowed with canonical FXR-responsive elements in their promoter, their induction is fully consistent with the nature of compound **10** as potent FXR ligand. This view was further confirmed by analysis of bile acids in the blood of mice administered with compound **10**. Indeed, as shown in Fig. 11, exposure to this agent results in a marked reduction of total and single unconjugated bile acids, a feature that is consistent with its FXR agonistic profile. Indeed, activation of FXR in the liver inhibits the activity of CYP7A1, thus causing a reduction of the synthesis of primary bile acids. Further supporting this view, **10** reduced the blood concentrations of 7 $\alpha$ -hydroxy-4-cholesten-3-one (Fig. 11D), an intermediate in the synthesis of primary bile acids, that is widely used to indirectly measure CYP7A1 activity *in vivo*. The fact that 7 $\alpha$ -hydroxy-4-cholesten-3-one levels were reduced in mice administered with compound **10** further supports this compound as a potent FXR agonist.

In summary, in the present study we describe the synthesis and the *in vitro* and *in vivo* pharmacological characterization of a novel family of compounds including several potent and selective FXR agonists. These novel agents might add utility in the treatment of cholestatic disorders avoiding side effects linked to unwanted activation of GPBAR1.

## Methods

**Chemistry.** High-resolution ESI-MS spectra were performed with a Micromass Q-TOF mass spectrometer. NMR spectra were obtained on Varian Inova 400, 500 and 700 NMR spectrometers (<sup>1</sup>H at 400, 500 and 700 MHz, <sup>13</sup>C at 100, 125 and 175 MHz, respectively) equipped with a SUN microsystem ultra 5 hardware and recorded in CD<sub>3</sub>OD ( $\delta_{\text{H}} = 3.31$  and  $\delta_{\text{C}} = 49.0$  ppm) and CDCl<sub>3</sub> ( $\delta_{\text{H}} = 7.26$  and  $\delta_{\text{C}} = 77.0$  ppm). All of the detected signals were in accordance with the proposed structures. Coupling constants (*J* values) are given in Hertz (Hz), and chemical shifts ( $\delta$ ) are reported in ppm and referred to CHD<sub>2</sub>OD and CHCl<sub>3</sub> as internal standards. Spin multiplicities are given as s (singlet), br s (broad singlet), d (doublet), or m (multiplet). Through-space <sup>1</sup>H connectivities were evidenced using a NOESY experiment with mixing times of 400 ms, respectively.

HPLC was performed with a Waters Model 510 pump equipped with Waters Rheodine injector and a differential refractometer, model 401. Reaction progress was monitored via thin-layer chromatography (TLC) on Alugram silica gel G/UV254 plates. Silica gel MN Kieselgel 60 (70–230 mesh) from Macherey-Nagel Company was used for column chromatography.

All chemicals were obtained from Sigma-Aldrich, Inc. Solvents and reagents were used as supplied from commercial sources with the following exceptions. Dichloromethane, tetrahydrofuran and triethylamine were distilled from calcium hydride immediately prior to use. Methanol was dried from magnesium methoxide as follow. Magnesium turnings (5 g) and iodine (0.5 g) were refluxed in a small (50–100 mL) quantity of methanol until all of the magnesium has reacted. The mixture was diluted (up to 1 L) with reagent grade methanol, refluxed for 2–3 h then distilled under nitrogen. All reactions were carried out under argon atmosphere using flame-dried glassware.

The purities of compounds were determined to be greater than 95% by HPLC.

**Synthetic procedures.** See the Supporting Information.

**Transactivation assay.** To evaluate the transcriptional activity of FXR, HepG2 cells were transiently transfected with Fugene HD reagent (Promega) using the followings plasmids: pCMVSPORT-humanFXR, pSG5RXR, p(hsp27)TKLUC and pGL4.70, a plasmid containing the Renilla gene used for luciferase normalization. At 24 h post transfection, cells were stimulated with compounds **7–21** (10  $\mu$ M). CDCA (**1**, 10  $\mu$ M) and 6-ECDCA (**6**, 1  $\mu$ M) were used as a positive controls. Dose-response curves were performed in HepG2 cells transfected as described above and treated with increasing concentrations of **9**, **10**, **15** and **17** (from 100 nM to 10  $\mu$ M).

To investigate GPBAR1 activation, HEK-293T cells were transiently transfected with Fugene HD reagent (Promega) using the following vectors: pCMVSPORT6-human GPBAR1, pGL4.29 (Promega), a reporter vector containing a cAMP response element (CRE) cloned upstream to the luciferase reporter gene luc2P and pGL4.70. At 24 h post transfection, cells were stimulated with compounds **7–21** (10  $\mu$ M) and TLCA (**2**, 10  $\mu$ M) were used as

a positive controls. Dose-response curves were performed in HEK-293T cells transfected as described above and treated with increasing concentrations of **9** and **21** (from 100 nM to 50  $\mu$ M). To evaluate the  $IC_{50}$  of compound **10**, a dose response curve was performed in HEK-293T cells stimulated with 10  $\mu$ M TLCA and with increasing concentrations of **10**: range from 5 to 25  $\mu$ M. At 18 h post stimulations, cellular lysate was assayed for luciferase and renilla activities using the Dual-Luciferase Reporter assay system (E1980, Promega). Luminescence was measured using Glomax 20/20 luminometer (Promega). Luciferase activities were normalized with Renilla activities.

**Direct Interaction on FXR by Alphascreen Technology in a Coactivator Recruitment Assay.** Anti-GST-coated acceptor beads were used to capture the GST-fusion FXR-LBD, whereas the biotinylated-SRC-1 peptide was captured by the streptavidin donor beads. Upon illumination at 680 nm, chemical energy is transferred from donor to acceptor beads across the complex streptavidin-donor/Src-1-biotin/GSTFXR-LBD/anti-GST-acceptor and a signal is produced. The assay was performed in white, low-volume, 384-well Optiplates (PerkinElmer) using a final volume of 25  $\mu$ L containing final concentrations of 10 nM of purified GST-tagged FXR-LBD protein, 30 nM biotinylated Src-1 peptide, 20  $\mu$ g/mL anti-GST acceptor beads, and 10  $\mu$ g/mL of streptavidin donor bead (PerkinElmer). The assay buffer contained 50 mM Tris (pH 7.4), 50 mM KCl, 0.1% BSA, and 1 mM DTT. The stimulation times with 1  $\mu$ L of tested compound (dissolved in 50% DMSO/H<sub>2</sub>O) were fixed to 30 min at room temperature. The concentration of DMSO in each well was maintained at a final concentration of 4%. After the addition of the detection mix (acceptor and donor beads), the plates were incubated in the dark for 4 h at room temperature and then were read in an Envision microplate analyzer (PerkinElmer).

**Animal Studies.** All animal experimental procedures were approved by the Ethics Committee of the University of Perugia and by the Italian Health Ministry, according to the Italian guideline for care and use of laboratory animals. C57BL6 mice were treated 6 h with compound **10** (15 mg/kg, ip). At the end of the treatment, mice were sacrificed and liver and blood samples were collected respectively to perform real-time PCR and bile acids quantization.

**RT-PCR.** Total RNA was extracted using the TRIzol reagent (Life Technologies). First, 1  $\mu$ g of RNA was purified of the genomic DNA by DNase I treatment (Life Technologies) and random reverse-transcribed with Superscript II (Life Technologies) in a 20  $\mu$ L reaction volume. Then 10 ng of cDNA was amplified in a final volume of 20  $\mu$ L in a mix containing 200 nM of each sense/antisense primers and 10  $\mu$ L of 2 $\times$  SYBR Select Master mix (Life Technologies). RT-PCR reactions were performed in duplicate and the thermal cycling conditions were: 2 min at 95  $^{\circ}$ C, followed by 40 cycles of 95  $^{\circ}$ C for 20 s, 60  $^{\circ}$ C for 30 s on Step One Plus Instrument (ABI). The relative mRNA expression was calculated and expressed as  $2^{-\Delta\Delta Ct}$ . Sense and antisense primer sequences were the following: mouse GAPDH, ctgagtatgctgtggagctac and gttgtgtgtgcaggatgcatg; mOST $\alpha$ , cagtggacatagccctacc and gaccaaagcagcagaacaca; mBSEP, aaatcggatggttgcactgc and tgacagcagaatcaccaag; mSHP, tctcttctccgctcatca and aagggctgctggacagtta.

**Bile acid and 7 $\alpha$ -hydroxy-4-cholesten-3-one determinations.** See the Supporting Information.

## References

- Makishima, M. *et al.* Identification of a nuclear receptor for bile acids. *Science* **284**, 1362–1365 (1999).
- Parks, D. J. *et al.* Bile acids: natural ligands for an orphan nuclear receptor. *Science* **284**, 1365–1368 (1999).
- Goodwin, B. *et al.* A regulatory cascade of the nuclear receptors FXR, SHP-1, and LXR-1 represses bile acid biosynthesis. *Mol. Cell* **6**, 517–526 (2000).
- Fiorucci, S., & Baldelli, F. Farnesoid X receptor agonists in biliary tract disease. *Curr. Opin. Gastroenterol.* **25**, 252–259 (2009).
- Fiorucci, S. *et al.* Targeting FXR in cholestasis: hype or hope. *Expert Opin. Ther. Targets* **12**, 1449–1459 (2014).
- Fiorucci, S., Mencarelli, A., Distrutti, E., & Zampella, A. Farnesoid X receptor: from medicinal chemistry to clinical applications. *Future Med. Chem.* **4**, 877–891 (2012).
- Cipriani, S., Mencarelli, A., Palladino, G., & Fiorucci, S. FXR activation reverses insulin resistance and lipid abnormalities and protects against liver steatosis in Zucker (fa/fa) obese rats. *J. Lipid Res.* **51**, 771–784 (2010).
- Rizzo, G. *et al.* The farnesoid X receptor promotes adipocyte differentiation and regulates adipose cell function *in vivo*. *Mol. Pharmacol.* **70**, 1164–1173 (2006).
- Fiorucci, S., Rizzo, G., Donini, A., Distrutti, E., & Santucci, L. Targeting farnesoid X receptor for liver and metabolic disorders. *Trends Mol. Med.* **13**, 298–309 (2007).
- Mencarelli, A. *et al.* Dissociation of intestinal and hepatic activities of FXR and LXR $\alpha$  supports metabolic effects of terminal ileum interposition in rodents. *Diabetes* **62**, 3384–3393 (2013).
- Wang, H., Chen, J., Hollister, K., Sowers, L. C. & Forman, B. M. Endogenous bile acids are ligands for the nuclear receptor FXR/BAR. *Mol. Cell* **3**, 543–553 (1999).
- Maruyama, T., *et al.* Identification of membrane type receptor for bile acids (M-BAR). *Biochem. Biophys. Res. Commun.* **298**, 714–719 (2002).
- Fiorucci, S., Mencarelli, A., Palladino, G., & Cipriani, S. Bile-acid activated receptors: targeting TGR5 and farnesoid-X-receptor in lipid and glucose disorders. *Trends Pharmacol. Sci.* **30**, 570–580 (2009).
- Fiorucci, S., Cipriani, S., Baldelli, F., & Mencarelli, A. Bile acid activated receptors in the treatment of dyslipidemia and related disorders. *Prog. Lipid Res.* **49**, 171–185 (2010).
- Tiwari, A. & Maiti, P. TGR5: an emerging bile acid G-protein coupled receptor target for the potential treatment of metabolic disorders. *Drug Discovery Today* **14**, 523–530 (2009).
- Alemi, F. *et al.* The TGR5 receptor mediates bile acid-induced itch and analgesia. *J. Clin. Invest.* **123**, 1513–1530 (2013).
- Festa, C. *et al.* Exploitation of cholane scaffold for the discovery of potent and selective farnesoid X receptor (FXR) and G-protein coupled bile acid receptor 1 (GP-BAR1) ligands. *J. Med. Chem.* **57**, 8477–8495 (2014).
- Sepe, V., Distrutti, E., Limongelli, V., Fiorucci, S., & Zampella, A. Steroidal scaffolds as FXR and GPBAR1 ligands: from chemistry to therapeutical application. *Future Med. Chem.* **7**, 1109–1135 (2015).

19. Sato, H. *et al.* Novel potent and selective bile acid derivatives as TGR5 agonists: biological screening, structure-activity relationships, and molecular modeling studies. *J. Med. Chem.* **51**, 1831–1841 (2008).
20. Rizzo, G. *et al.* Functional characterization of the semisynthetic bile acid derivative INT-767, a dual farnesoid X receptor and TGR5 agonist. *Mol. Pharmacol.* **78**, 617–630 (2010).
21. Pellicciari, R. *et al.* Nongenomic actions of bile acids. Synthesis and preliminary characterization of 23- and 6,23-alkyl-substituted bile acid derivatives as selective modulators for the G-protein coupled receptor TGR5. *J. Med. Chem.* **50**, 4265–4268 (2007).
22. Hirschfield, G. M. *et al.* Efficacy of obeticholic acid in patients with primary biliary cirrhosis and inadequate response to ursodeoxycholic acid. *Gastroenterology* **148**, 751–761 (2015).
23. Neuschwander-Tetri, B. A. *et al.* Farnesoid X nuclear receptor ligand obeticholic acid for non-cirrhotic, non-alcoholic steatohepatitis (FLINT): a multicentre, randomised, placebo-controlled trial. *Lancet* **385**, 956–965 (2015).
24. Fiorucci, S. *et al.* Farnesoid X receptor agonist for the treatment of liver and metabolic disorders: focus on 6-ethyl-CDCA. *Mini-Rev. Med. Chem.* **11**, 753–762 (2011).
25. Mi, L. Z. *et al.* Structural basis for bile acid binding and activation of the nuclear receptor FXR. *Mol. Cell.* **11**, 1093–1100 (2003).

## Acknowledgements

This work was supported by grants from PSC Partners, 5237 South Kenton Way, Englewood, Colorado 80111 USA and from POR Campania FESR 2007–2013 - O.O. 2.1 (FarmaBioNet).

## Author Contributions

V.S., C.F., C.F., D.M. and A.Z. designed and performed synthesis; B.R., A.C., S.C. and S.F. designed and performed pharmacological experiments; F.d.G. and M.C.M. designed and performed MS experiments; S.F. and A.Z. analyzed and interpreted the data. All authors contributed to manuscript writing and approved the final version.

## Additional Information

**Supplementary information** accompanies this paper at <http://www.nature.com/srep>

**Competing financial interests:** The authors declare no competing financial interests.

**How to cite this article:** Sepe, V. *et al.* Insights on FXR selective modulation. Speculation on bile acid chemical space in the discovery of potent and selective agonists. *Sci. Rep.* **6**, 19008; doi: 10.1038/srep19008 (2016).



This work is licensed under a Creative Commons Attribution 4.0 International License. The images or other third party material in this article are included in the article's Creative Commons license, unless indicated otherwise in the credit line; if the material is not included under the Creative Commons license, users will need to obtain permission from the license holder to reproduce the material. To view a copy of this license, visit <http://creativecommons.org/licenses/by/4.0/>

# SCIENTIFIC REPORTS



OPEN

## Navigation in bile acid chemical space: discovery of novel FXR and GPBAR1 ligands

Received: 01 April 2016

Accepted: 16 June 2016

Published: 06 July 2016

Claudia Finamore<sup>1</sup>, Carmen Festa<sup>1</sup>, Barbara Renga<sup>2</sup>, Valentina Sepe<sup>1</sup>, Adriana Carino<sup>2</sup>, Dario Masullo<sup>1</sup>, Michele Biagioli<sup>2</sup>, Silvia Marchianò<sup>2</sup>, Angela Capolupo<sup>3</sup>, Maria Chiara Monti<sup>3</sup>, Stefano Fiorucci<sup>2</sup> & Angela Zampella<sup>1</sup>

Bile acids are signaling molecules interacting with nuclear receptors and membrane G-protein-coupled receptors. Among these receptors, the farnesoid X receptor (FXR) and the membrane G-coupled receptor (GPBAR1) have gained increasing consideration as druggable receptors and their exogenous dual regulation represents an attractive strategy in the treatment of enterohepatic and metabolic disorders. However, the therapeutic use of dual modulators could be associated to severe side effects and therefore the discovery of selective GPBAR1 and FXR agonists is an essential step in the medicinal chemistry optimization of bile acid scaffold. In this study, a new series of 6-ethylcholane derivatives modified on the tetracyclic core and on the side chain has been designed and synthesized and their *in vitro* activities on FXR and GPBAR1 were assayed. This speculation resulted in the identification of compound 7 as a potent and selective GPBAR1 agonist and of several derivatives showing potent dual agonistic activity.

Next to their ancestral roles in lipid digestion and solubilization, bile acids (BAs), the principal constituent of bile, are today recognized signaling molecules involved in many physiological functions and these signaling pathways involve the activation of several metabolic nuclear receptors, mainly the BAs sensor FXR<sup>1,2</sup>, and the dedicated membrane G-protein-coupled receptor, GPBAR1 (TGR5)<sup>3</sup>.

Principally, FXR functions as a sensor of bile acid level playing an important role in the regulation of their intracellular levels in hepatocytes<sup>4</sup>. FXR is activated by CDCA (1)<sup>1,2,5</sup> and upon CDCA binding, FXR forms a heterodimer with the retinoid X receptor (RXR) that binds specific DNA sequences within the promoter regions of target genes. The canonical gene expression program activated by FXR leads to the reduction in the intracellular bile acid levels by increasing the export of bile acids out of cells, decreasing bile acid uptake and decreasing bile acid synthesis<sup>6–8</sup>. As a consequence, FXR has been identified as an appealing target in the treatment of cholestasis disorders such as primary biliary cirrhosis (PBC) and liver steatosis<sup>9–11</sup>, two severe human conditions in which bile acids homeostasis is impaired.

PBC is an immunologically mediated progressive liver disease characterized by the destruction of small intrahepatic bile ducts, with accumulation of bile acids in the liver and consequently inflammation, fibrosis, and potential cirrhosis. Fatigue and pruritus are the most common symptoms of primary biliary cirrhosis, and both can be debilitating in some patients. Cholestasis causes intense, sometimes intolerable, itch leading to scratching, excoriation, sleep deprivation, and depression<sup>12</sup>.

In addition, FXR plays a crucial beneficial role in hepatic triglyceride homeostasis, as well as in glucose metabolism and therefore, FXR agonists are also promising for the treatment of non-alcoholic fatty liver disease (NAFLD), dyslipidemia and type 2 diabetes (T2DM)<sup>13–16</sup>.

In addition to FXR and other nuclear hormone receptors, BAs can also signal through a membrane-receptor (GPBAR1/TGR5/M-BAR)<sup>3</sup>. The most potent endogenous GPBAR1 activator is TLCA (2) followed by DCA, while other BAs are less potent. GPBAR1<sup>-/-</sup> mice display prolonged cholestasis, exacerbated inflammatory response and more severe liver injury after partial hepatectomy<sup>17</sup>. In addition, in a mouse model of xenobiotic (DDC)-induced sclerosing cholangitis, mice overexpressing GPBAR1 showed less liver injury while mice lacking

<sup>1</sup>Department of Pharmacy, University of Naples "Federico II", Via D. Montesano, 49, 80131 Naples, Italy. <sup>2</sup>Department of Surgery and Biomedical Sciences, Nuova Facoltà di Medicina, P.zza L. Severi 1, 06132 Perugia, Italy. <sup>3</sup>Department of Pharmacy, University of Salerno, Via Giovanni Paolo II, 132, 84084 Fisciano (Salerno), Italy. Correspondence and requests for materials should be addressed to A.Z. (email: angela.zampella@unina.it)

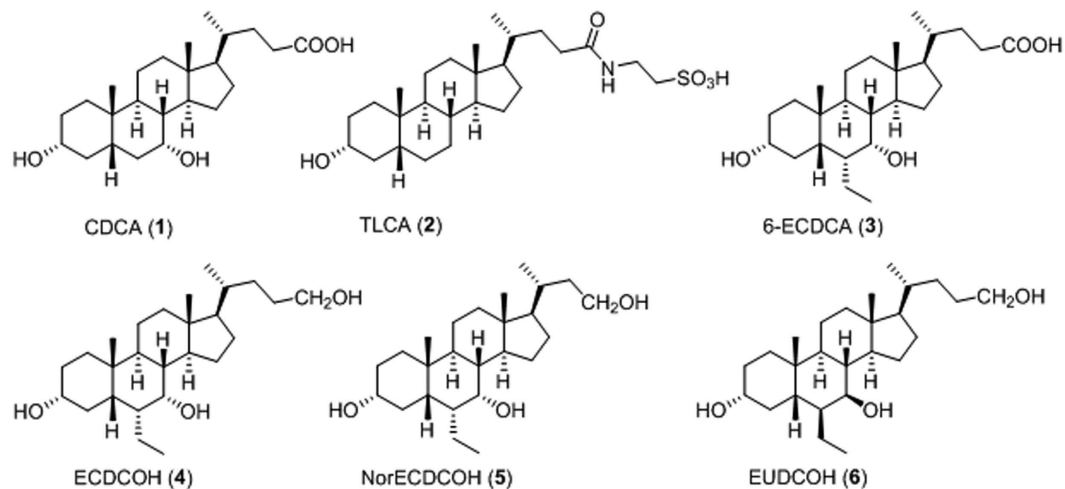


**Figure 1.** CDCA and TLCA, the most potent endogenous activators of FXR and GPBAR1, respectively. 6-ECDCA and 6 $\alpha$ -ethylchenodeoxycholanol derivatives 4 and 5 as dual ligands and EUDCOH (6), a selective GPBAR1 agonist.

GPBAR1 showed aggravation of inflammation and fibrosis<sup>18</sup>. Collectively, these findings suggest a critical role of GPBAR1 for liver protection against BA overload but activation of GPBAR1 should be also associated with severe side effects, especially in the context of impaired bile acid level in the liver.

In fact, GPBAR1 has been recently identified as the physiological mediator of pruritus<sup>19</sup>, a common symptom observed in cholestasis and the severity of this side effect limits the pharmacological utility of dual agonists in the treatment of primary biliary cirrhosis (PBC) and related cholestatic disorders.

On the other hand, responses to GPBAR1 activation include increased energy expenditure, improved intestinal motility, glucose metabolism and insulin sensitivity<sup>20,21</sup>. The latter two occur through the release of the glucagon-like peptide 1 (GLP-1) by intestinal L cells upon GPBAR1 activation<sup>22</sup>. Therefore, the exogenous regulation of this receptor represents an attractive strategy to treat metabolic disorders such as NASH, hypercholesterolemia, hypertriglyceridemia, and T2DM<sup>23,24</sup>. Thus, in the window of metabolic disorders, the development of ligands endowed with dual activity toward GPBAR1 and FXR appears to be a promising strategy<sup>23–26</sup>. In contrast, the discovery of highly selective FXR agonists could represent a new frontier in the treatment of primary biliary cirrhosis (PBC) and related cholestatic disorders where the concomitant activation of GPBAR1 could increase patient risk for adverse side effects. Indeed, results from PBC phase II clinical trial with 6-ECDCA/OCA (3), a potent semi-synthetic steroidal FXR agonist<sup>27</sup>, have shown that while the compound exerts benefit, its use has associated with pruritus. In fact, up to 40% of PBC patients halted the treatment due to the severity of itching in one trial and approx. 80% of patients experienced the symptoms. The reason why OCA causes itching is unclear. However, this agent is almost equally potent on FXR and GPBAR1<sup>28,29</sup> and it is predictable that the severity of this side effect could prevent its use in stage III and IV PBC patients<sup>30</sup>.

Medicinal chemistry on 6-ECDCA scaffold and on bile acid scaffold has produced several derivatives modified on the side chain in the length and in the nature of the end-group and on the tetracyclic core<sup>11,31–33</sup>. Indeed these derivatives cover the same chemical space of BAs that are intrinsically promiscuous toward FXR and GPBAR1 and therefore, with few exceptions, this kind of speculation mainly afforded dual modulators<sup>33</sup>. The most interesting results have been obtained with compounds 4–6 (Fig. 1).

The replacement of the negative charged end group with a neutral polar group produced derivative 4, again a potent dual agonist and the above activity was also maintained by the corresponding *nor*-derivative 5, with one carbon less on the side chain. Of interest compound 5 attenuates liver damage in animal models of non-obstructive cholestasis without inducing itching<sup>34</sup>. Finally, speculation on stereochemical modification on ring B produced 6, a C-24 alcohol that represents the first example of ursodeoxycholanol derivative substituted at C-6 with a  $\beta$ -oriented ethyl group. Pharmacological assays demonstrated that this derivative is a rather potent ligand for GPBAR1 (EC<sub>50</sub> 1.03  $\mu$ M) failing in transactivating FXR at any concentration tested<sup>26</sup>.

Recently we have also demonstrated that compound 6 exerts portal pressure-lowering effects in rodent models of portal hypertension by directly regulating the expression/activity of cystathionine  $\gamma$ -lyase (CSE) and endothelial nitric oxide synthases (eNOS) in liver sinusoidal endothelial cells (LSEC), thus affirming this compound as a novel approach to attenuate the hemodynamic changes in patients with liver cirrhosis<sup>35</sup>.

In addition, in our recent contribution, we have extended the structure-activity relationship on C24 6-ethylcholane scaffold modifying the hydroxyl group at C-3 and demonstrating that the elimination or the inversion of the above functionality on ring A could shift the activity toward FXR<sup>36</sup>.

Prompted by these promising results, we decided to expand our investigation proceeding in the modification of the side chain length on the 6-ethylcholane scaffold. As shown in the Fig. 2, a small library of C23 6-substituted cholane derivatives, compounds 7–15, have been prepared.

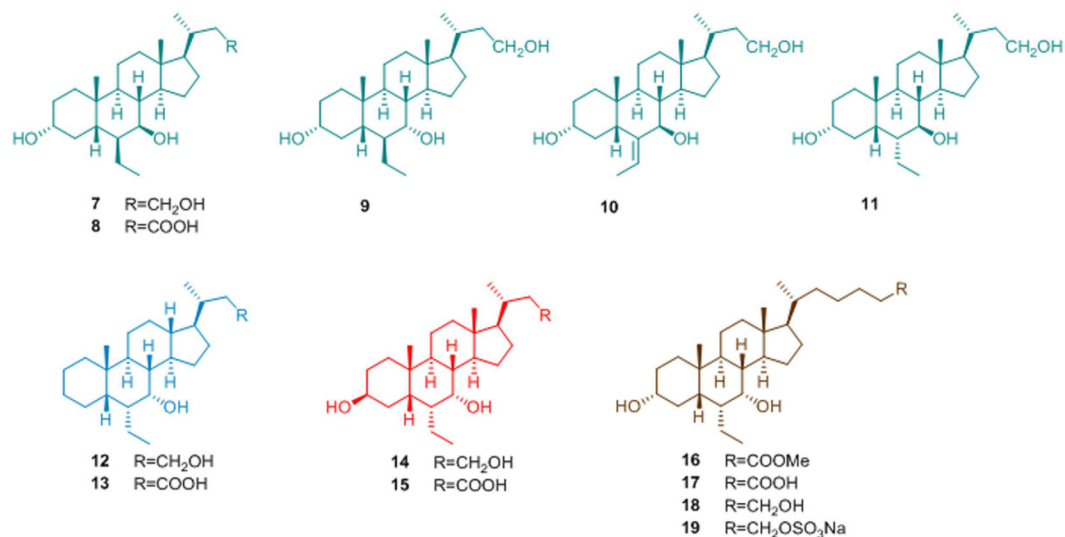


**Figure 2.** 6-Ethylcholane derivatives generated in this study.

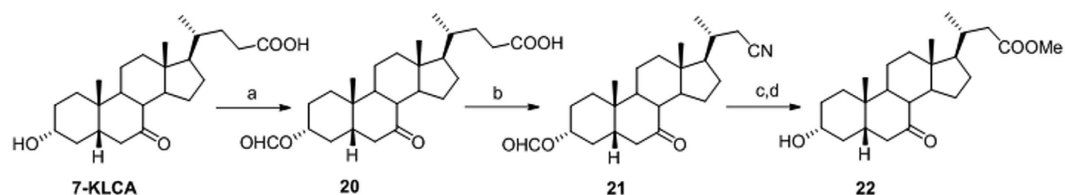


**Figure 3.** Preparation of 7-keto-norLCA methyl ester (**22**). Reagents and conditions: (a) HCOOH, HClO<sub>4</sub>; (b) TFA, trifluoroacetic anhydride, NaNO<sub>2</sub>; (c) KOH 30% in MeOH/H<sub>2</sub>O 1:1 v/v, 66% over three steps; (d) p-TsOH, MeOH dry, quantitative yield.

In this framework, the effects of the stereochemical arrangement of the cholane C-6/C-7 positions and the substituents adorning the C-3 position and the C-23 side chain end group (OH or COOH) have been explored in term of potency/selectivity toward FXR and GPBAR1.

In addition, the chemical diversity of available bile acid receptor modulators have been increased preparing bis-*homo* 6-ethylcholane derivatives **16–19**. Pharmacological investigations resulted in the identification of compounds **7** and **19** as a potent and selective GPBAR1 agonist and a potent dual agonist respectively.

## Results

In the synthesis of 6-ethyl *nor*cholane derivatives **7–15**, the first step was the preparation of the key intermediate 7-keto-*nor*LCA methyl ester **22** from 7-KLCA (Fig. 3). A reaction sequence comprising Fisher's esterification with formic acid and perchloric acid generated the formiate derivative **20** that was subjected to a Beckmann rearrangement with treatment with sodium nitrite in a trifluoroacetic anhydride/trifluoroacetic acid mixture obtaining the 23-nitrile derivative **21**<sup>37</sup>. Prolonged alkaline hydrolysis afforded the corresponding carboxylic acid that was in turn transformed in the methyl ester derivative **22** by methanol/*p*-toluensulfonic acid treatment (66% yield from 7-KLCA).

**Preparation of 3 $\alpha$ -hydroxy-6-ethyl*nor*cholane derivatives.** Acetylation at C-3 on **22** and aldolic addition to a silyl enol ether intermediate generated the intermediate **23** (60% over three steps) that was hydrogenated at the exocyclic double bond (H<sub>2</sub> on Pd(OH)<sub>2</sub>) affording exclusively the 6 $\beta$ -ethyl group in the compound **24** (quantitative yield). Treatment of **24** with an excess of NaBH<sub>4</sub> in methanol followed by LiBH<sub>4</sub> reduction on the crude reaction product to secure the reduction at the methyl ester on the side chain, gave the concomitant deacetylation at C-3 and reduction at C-7 keto and at C-23 methyl ester groups (Fig. 4).

HPLC purification gave the main product **7** and small amount of its epimer at C-7, compound **9**. When intermediate **24** was treated with a stoichiometric amount of NaBH<sub>4</sub>, the reduction occurred exclusively at C-7 keto group giving the methyl ester **25**, that was subjected to basic hydrolysis furnishing the carboxylic acid **8** in 82% over two steps.

Intermediate **23** was also used as starting material in the preparation of **10** and **11**. Sodium borohydride/LiBH<sub>4</sub> treatment on **23** proceeded in a stereoselective manner, affording the exclusive formation of 7 $\beta$ -hydroxyl derivative as judged by the shape of H-7 as a doublet ( $J = 9.8$  Hz) which is consistent with an axial disposition for this proton, and therefore with the  $\beta$ -orientation of the hydroxyl group on ring B. Dipolar couplings H-7/H-24



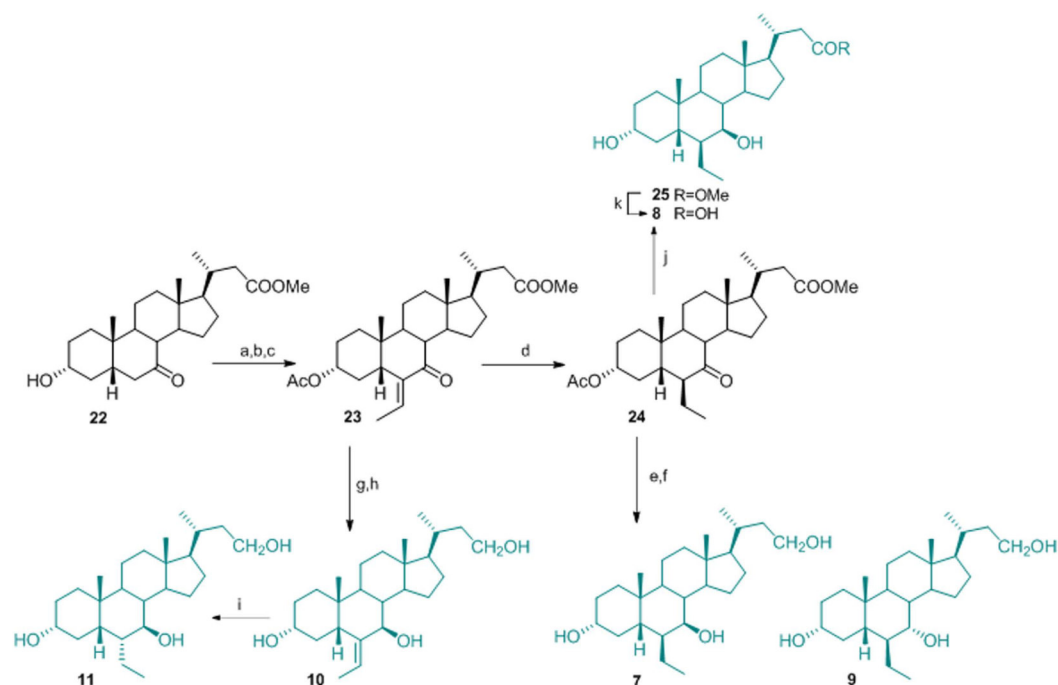


**Figure 4. Synthesis of 3 $\alpha$ -hydroxy-6-ethylnorcholane derivatives.** Reagents and conditions: (a) acetic anhydride, pyridine; (b) DIPA, *n*-BuLi, TMSCl, TEA dry, THF dry  $-78^{\circ}\text{C}$ ; (c) acetaldehyde,  $\text{BF}_3(\text{OEt})_2$ ,  $\text{CH}_2\text{Cl}_2$ ,  $-60^{\circ}\text{C}$ , 60% over three steps; (d)  $\text{H}_2$ ,  $\text{Pd}(\text{OH})_2$ , THF/MeOH 1:1, quantitative yield; (e)  $\text{NaBH}_4$ , MeOH dry,  $0^{\circ}\text{C}$ ; (f)  $\text{LiBH}_4$ , MeOH, THF dry,  $0^{\circ}\text{C}$ , 77% over two steps; (g)  $\text{NaBH}_4$ , MeOH; (h)  $\text{LiBH}_4$ , MeOH dry, THF,  $0^{\circ}\text{C}$ , 85% over two steps; (i)  $\text{H}_2$ ,  $\text{Pd}(\text{OH})_2$ , THF:MeOH 1:1 v/v, quantitative yield; (j)  $\text{NaBH}_4$ , MeOH dry,  $0^{\circ}\text{C}$ ; (k) NaOH, MeOH:H<sub>2</sub>O 1:1 v/v, 82% over two steps.

and Me-25/H-5 in the NOESY spectrum allowed definition the E configuration for the exocyclic double bond as depicted in **10**. Hydrogenation on  $\text{Pd}(\text{OH})_2$  catalyst afforded derivative **11** with the ethyl group at C-6  $\alpha$ -oriented.

**Preparation of 3-deoxy- and 3 $\beta$ -hydroxy-6 $\alpha$ -ethylnorcholane derivatives.** In the preparation of 3-deoxy- and 3 $\beta$ -hydroxy-6-ethylnorcholane derivatives **12–15**, a convergent protocol was applied starting from the methyl ester **24**, that was first treated with MeONa in methanol to effect de-acetylation at C-3 and inversion at C-6 and then with tosyl chloride to afford **26** in 73% yield over two steps (Fig. 5).

Elimination by  $\text{LiBr}/\text{Li}_2\text{CO}_3$  treatment and hydrogenation of the unsaturated-ring A transient intermediate furnished **27** that was used as starting material for the preparation of compounds **12** and **13**.

$\text{LiBH}_4$  treatment produced the concomitant reduction at C-24 methyl ester and at C-7 carbonyl group furnishing **12** whereas alkaline hydrolysis of the methyl ester followed by  $\text{LiBH}_4$  treatment gave **10** in high chemical yield.

Finally, treatment of the tosyl derivative **26** with potassium acetate in DMF/H<sub>2</sub>O afforded inversion at C-3 on **28**. Reduction at C-7 and C-24 with  $\text{LiBH}_4$  and hydrolysis at methyl ester group on the side chain gave **14** and **15**, respectively.

**Preparation of bis-homo 6-ethylcholane derivatives.** In the preparation of bis-homo-6-ethylcholane derivatives **16**, a four-steps reaction sequence on **29**, previously prepared in our laboratory<sup>25,26</sup>, including protection of the alcoholic functions at C3 and C7, reduction of the side chain methyl ester, and subsequent one pot Swern oxidation/Wittig C2 homologation, gave the protected methyl ester of  $\Delta^{24,25}$  bis-homoECDCA **31** (Fig. 6).

Side chain double bond hydrogenation and alcoholic function deprotection gave the methyl ester **16** that was used as starting material in the preparation of the carboxylic acid **17** and the corresponding alcohol **18** through treatment with LiOH and  $\text{LiBH}_4$ , respectively. Chemoselective sulfation at C-26 hydroxyl group on a small aliquot of **18** gave the corresponding sulfate derivative **19**<sup>38</sup>.

## Discussion and Conclusion

Derivatives **7–19** were tested in the luciferase reporter assays on HepG2 and HEK-293T cells transfected with FXR and GPBAR1, respectively. Data shown in Fig. 7, panel A, reporting the results of the transactivation assay on FXR, reaffirm the 6 $\alpha$ /7 $\alpha$  stereochemical arrangement around ring B as the most important feature in FXR activity with derivatives **7–11**, with one or two substituents on ring B in  $\beta$  configuration, devoid of any activity at 10  $\mu\text{M}$  dose. Of interest is the behavior of derivatives **12–15**, with both substituents on ring B in  $\alpha$ -configuration and a shortened (C23) side chain. In a cross comparison between the above compounds, it is quite evident that the presence of a negative charge on the side chain favors the 3-deoxy derivatives (compare **13** with COOH vs **12** with  $\text{CH}_2\text{OH}$ ), whereas the alcoholic function at C-24 improves FXR activity of the corresponding 3 $\beta$ -hydroxyl

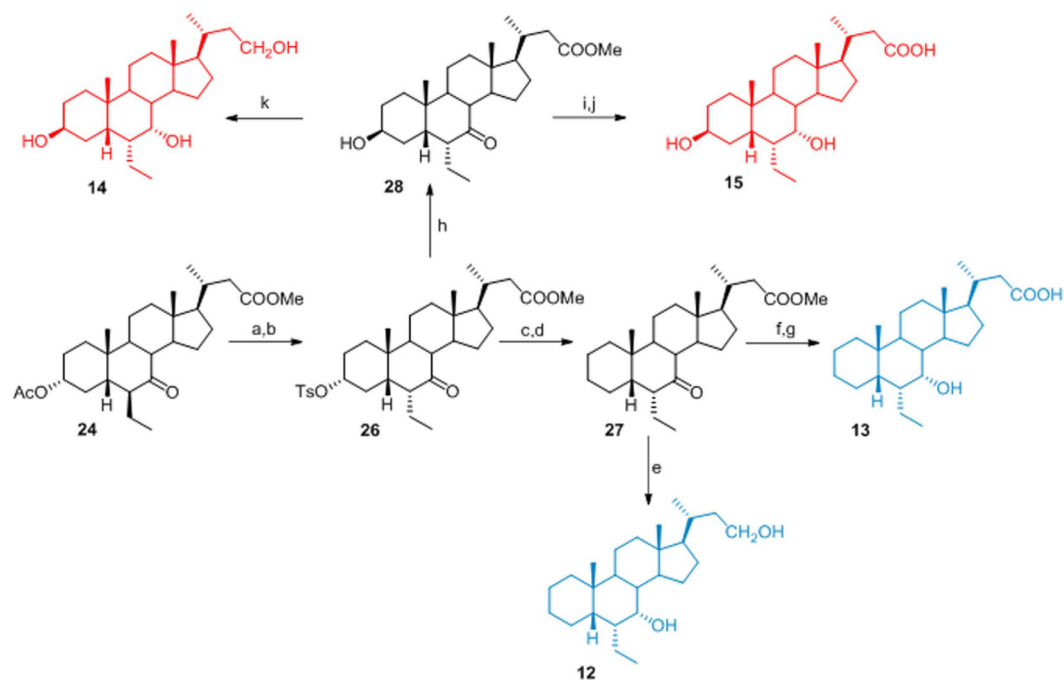


**Figure 5. Synthesis of 3-deoxy- and 3 $\beta$ -hydroxy-6 $\alpha$ -ethylnorcholeane derivatives.** *Reagents and conditions:* (a) MeONa, MeOH; (b) p-TsCl, pyridine, 73% over two steps; (c) LiBr, Li<sub>2</sub>CO<sub>3</sub>, DMF, reflux, (d) H<sub>2</sub>, Pd(OH)<sub>2</sub>, THF/MeOH 1:1, room temperature, quantitative yield over two steps; (e) LiBH<sub>4</sub>, MeOH dry, THF, 0 °C, 70%; (f) NaOH, MeOH:H<sub>2</sub>O 1:1 v/v; (g) LiBH<sub>4</sub>, MeOH dry, THF, 0 °C, 92% over two steps; (h) CH<sub>3</sub>COOK, DMF:H<sub>2</sub>O 5:1 v/v; (i) NaOH, MeOH:H<sub>2</sub>O 1:1 v/v; (j) LiBH<sub>4</sub>, MeOH dry, THF, 0 °C, 58% over two steps; (k) LiBH<sub>4</sub>, MeOH dry, THF, 0 °C, 57%.

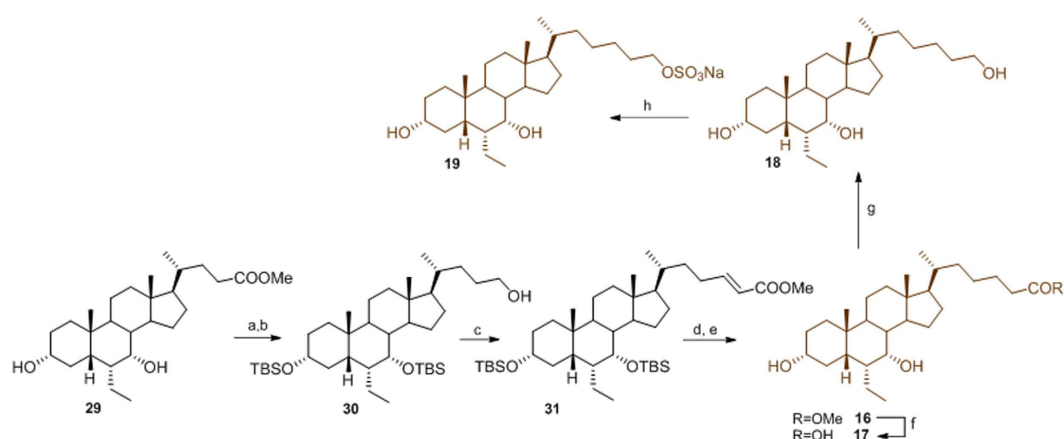


**Figure 6. Preparation of bis-homo 6-ethylcholeane derivatives.** *Reagents and conditions:* (a) 2,6-lutidine, t-butyltrimethylsilyl trifluoromethanesulfonate, CH<sub>2</sub>Cl<sub>2</sub>, 0 °C; (b) LiBH<sub>4</sub>, MeOH dry, THF, 0 °C, 68% over two steps; (c) DMSO, oxalyl chloride, TEA dry, CH<sub>2</sub>Cl<sub>2</sub>, -78 °C then methyl(triphenylphosphoranylidene)acetate, 79%; (d) H<sub>2</sub>, Pd(OH)<sub>2</sub>/C Degussa type, THF/MeOH 1:1, quantitative yield; (e) HCl 37%, MeOH, 88%; (f) NaOH 5% in MeOH/H<sub>2</sub>O 1:1 v/v, 89%; (g) LiBH<sub>4</sub>, MeOH dry, THF, 0 °C, 78%; (h) Et<sub>3</sub>N·SO<sub>3</sub>, DMF, 95 °C, 25%.

derivative (compare **14** with CH<sub>2</sub>OH vs **15** with COOH). In addition, results on derivatives **16–19** demonstrate that side chain elongation on the 6-ethyl scaffold could be instrumental in generation potent FXR agonists. In this subset, the nature of the side chain end group produces a remarkable effect in FXR transactivation with the sulfate derivative **19**, the most potent FXR agonist generated in this study.

Results of transactivations of CREB-responsive elements in HEK-293T transiently transfected with the membrane bile acid receptor GPBAR1 are showed in Fig. 7, panel B. Compounds **7** and **8**, with both the ethyl and the hydroxyl groups on ring B  $\beta$ -oriented, were demonstrated inducers of cAMP-luciferase reporter gene, with **7** showing a potency similar to that of TLCA (**2**), the most potent endogenous GPBAR1 agonist. As expected, all derivatives with both substituents on ring B in  $\alpha$ -configuration are endowed with GPBAR1 agonistic activity, and

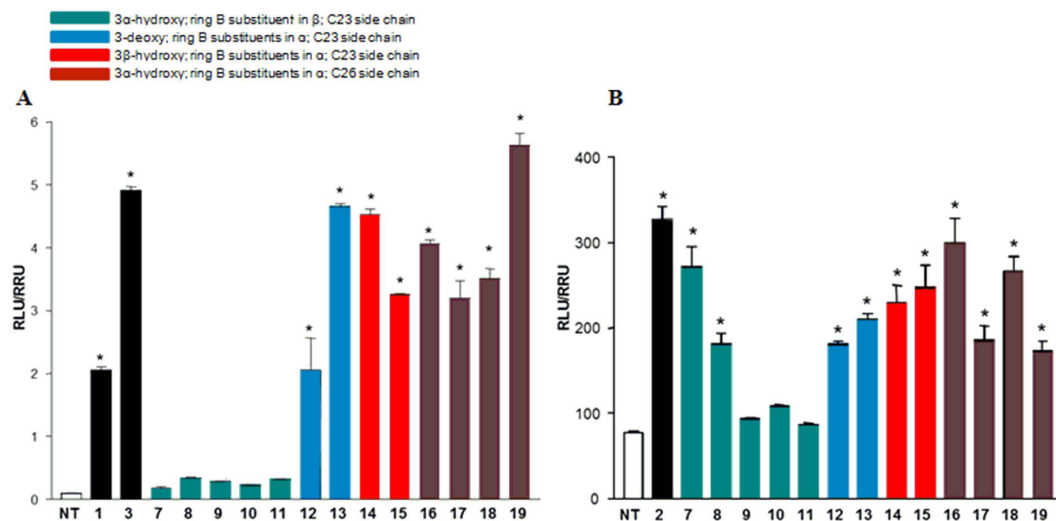


**Figure 7. Agonism on bile acid receptors by transactivation assay.** (A) HepG2 cells were transfected with pSG5-FXR, pSG5-RXR, pCMV- $\beta$ gal, and p(hsp27)TKLUC vectors. Cells were stimulated with compounds 7–19 (10  $\mu$ M). CDCA (1, 10  $\mu$ M) and 6-ECDCA (3, 1  $\mu$ M) were used as a positive control. (B) HEK-293T cells were co-transfected with GPBAR1 and a reporter gene containing a cAMP responsive element in front of the luciferase gene. Cells were stimulated with 7–19 (10  $\mu$ M). TLCA (2, 10  $\mu$ M) was used as a positive control. Luciferase activity served as a measure of the rise in intracellular cAMP following activation of GPBAR1. In both panels, results are expressed as mean  $\pm$  standard error. \* $p < 0.05$  versus not treated cells (NT).

the above activity is quite independent of the length and the functionalization of the side chain and by the substitution at C-3 with 3 $\alpha$ -, 3 $\beta$ -hydroxy and 3-deoxy derivatives sharing a similar behavior. Even if, by comparing FXR and GPBAR1 transactivation results, derivatives 12–19 are to be considered dual agonists, there is a considerable difference in GPBAR1 activity of C26 derivatives 16–19. It is quite evident that the presence of a neutral (COOMe in 16) or a non-charged polar group (CH<sub>2</sub>OH in 18) on the elongated side chain is preferable respect to a negative charged end group such as the COOH in 17 and the sulfate in 19.

The relative potency of selected members of this novel family was then investigated by a detailed measurement of the concentration-response curve of the 3-deoxy C-23 carboxylic acid derivative 13, the 3 $\beta$ -hydroxyl C-23 alcohol 14 and the C-26 sulfate derivative 19, all sharing the 6 $\alpha$ /7 $\alpha$  configuration, on FXR and GPBAR1 transactivation.

As illustrated in Figs 8 and 9, compounds 13, 14, and 19 transactivate FXR with an EC<sub>50</sub> of 2.3  $\mu$ M, 5.3  $\mu$ M and 1.7  $\mu$ M, respectively. In addition, 13, 14, and 19 transactivate GPBAR1 with EC<sub>50</sub> of 4.3  $\mu$ M, 1.0  $\mu$ M and 0.95  $\mu$ M, respectively. Combining these data, compound 19 represents the most potent FXR/GPBAR1 dual agonist identified in this study. Finally, compound 7 exerted a concentration-dependent effect on activation of cAMP responsive element in HEK-293T cells transfected with GPBAR1 with an EC<sub>50</sub> of 0.91  $\mu$ M.

The ability of compound 19, the most potent FXR agonist in these series, in the recruitment of the coactivator SRC-1 was also measured through Alpha screen technology. CDCA (1) and 6-ECDCA (3) were used as positive controls at 2  $\mu$ M concentration and the effect of 6-ECDCA (3) was settled as 100%. As shown in Fig. 10, panel A, compound 19 showed an activity in the recruitment of SRC-1 co-activator at least comparable, if not better, to that measured for 3, thus confirming the transactivation results. Interestingly, the presence of the non-conjugable functional group such as the sulfate group on the side chain instead of the carboxyl end group as in 6-ECDCA (3) points the attention on the positive pharmacokinetic properties of compound 19 and therefore on its therapeutic potential in liver FXR mediated diseases. On the other hand, panel A in Fig. 10 shows compounds 7, 9 and 10 completely unable to recruit SRC-1 in cell free Alpha screen assay, thus excluding any pharmacokinetic elements in their FXR inactivity on cellular luciferase assays (Fig. 7, panel A) and indirectly reaffirming compound 7 as a selective GPBAR1 agonist (Fig. 7, panel B).

RT-PCR further confirmed 19 as a dual FXR/GPBAR1 agonist and the GPBAR1 mediated pharmacological effect of compound 7. As shown in Fig. 10 panels B–D, 19 was able to induce the expression of BSEP and OST $\alpha$ , two canonical FXR targeted genes, whereas both compounds increased pro-glucagon gene expression in GLUTag cells. The observed 2 fold of BSEP upregulation as well as the robust induction of OST $\alpha$  mRNA is consistent with the activation of the FXR-mediated effect by compound 19<sup>39</sup>.

In summary, a series of 6-ethylcholane derivatives were designed and synthesized and all the newly synthesized compounds were evaluated *in vitro* for their activity towards FXR and GPBAR1. Concerning the structural features,  $\alpha$ -substituents introduced at C-6 and C-7 positions play a significant role in FXR and GPBAR1 activity, with all derivatives showing this configurational disposition able to transactivate both receptors. Even if the sulfate derivative 19 is the most potent FXR agonist discovered in this study, the dual modulation is a general trend within compounds 12–19, independently by the length and the functional group of the side chain as well as by the substitution at C-3. On the contrary, modification at the configurational disposition of one or both substituents

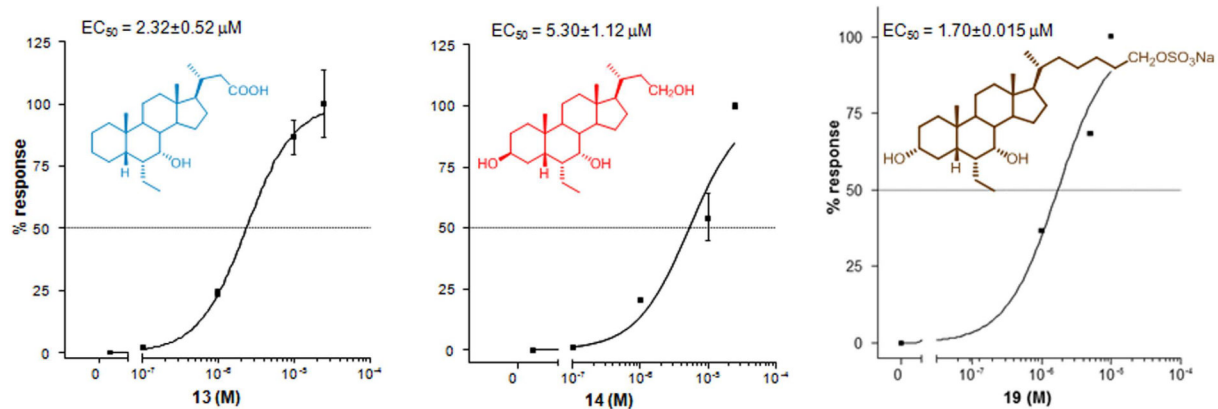


**Figure 8. Concentration-response curve of 13, 14, and 19 on FXR.** HepG2 cells were transfected with FXR as described above and used in a luciferase reporter assay. Twenty-four hour post transfection cells were stimulated with increasing concentrations of each agent: range from 100 nM to 25  $\mu$ M. Results are expressed as mean  $\pm$  standard error.

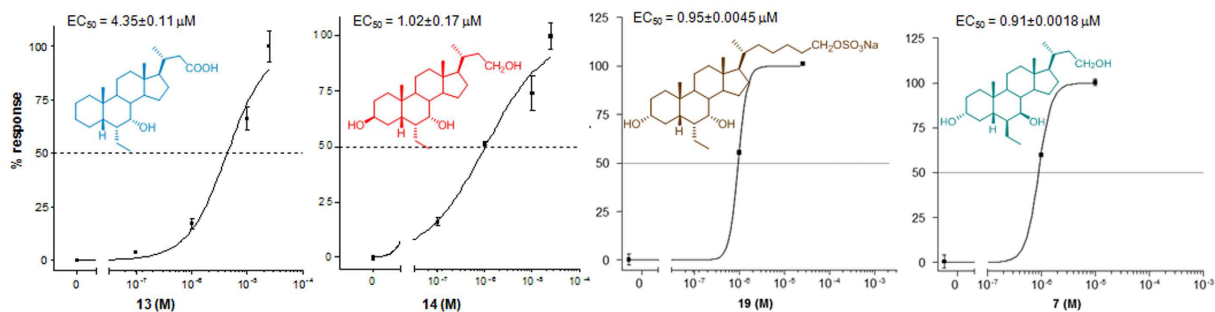


**Figure 9. Concentration-response curve of compounds 13, 14 and 19 on FXR.** HepG2 cells were transfected with FXR as described above and used in a luciferase reporter assay. Twenty-four hour post transfection cells were stimulated with increasing concentrations of each agent: range from 100 nM to 25  $\mu$ M. Results are expressed as mean  $\pm$  standard error.

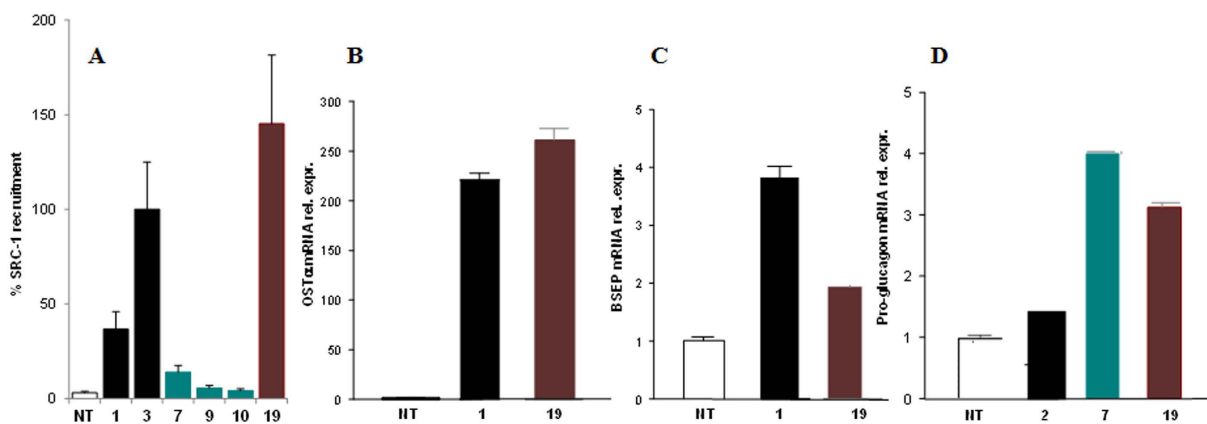


**Figure 10. (A)** Coactivator recruitment assay measuring a direct interaction of FXR with SRC-1; ligands at 2  $\mu$ M. Results are expressed as percentage of the effect of 3 arbitrarily settled as 100%. NT is referred to the experiment in absence of ligand. Results are expressed as mean  $\pm$  standard error. **(B,C)** Real-time PCR analysis of mRNA expression on FXR target genes BSEP **(B)**, and OST $\alpha$  **(C)** in HepG2 cells primed with 10  $\mu$ M of compound 19. CDCA (1) was used as a positive control at 10  $\mu$ M. **(D)** Real-time PCR analysis of mRNA expression of GPBAR1 target gene Pro-glucagon in GLUTAg cells stimulated with 10  $\mu$ M of compounds 7 and 19, and TLCA (2) used as a positive control at 10  $\mu$ M. Values are normalized to GAPDH and are expressed relative to those of not treated cells (NT) which are arbitrarily settled to 1. The relative mRNA expression is expressed as  $2(-\Delta\Delta Ct)$ .

on ring B is clearly deleterious in term of FXR activation but represents a promising strategy in the identification and development of selective GPBAR1 agonists with compound 7, the most potent GPBAR1 activator identified in this study.

## Methods

**Chemistry.** Specific rotations were measured on a Jasco P-2000 polarimeter. High-resolution ESI-MS spectra were performed with a Micromass Q-TOF mass spectrometer. NMR spectra were obtained on Varian Inova 400, 500 and 700 NMR spectrometers ( $^1\text{H}$  at 400 and 700 MHz,  $^{13}\text{C}$  at 100 and 175 MHz, respectively) equipped with a SUN microsystem ultra5 hardware and recorded in  $\text{CD}_3\text{OD}$  ( $\delta_{\text{H}} = 3.30$  and  $\delta_{\text{C}} = 49.0$  ppm) and  $\text{CDCl}_3$  ( $\delta_{\text{H}} = 7.26$  and  $\delta_{\text{C}} = 77.0$  ppm). All of the detected signals were in accordance with the proposed structures. Coupling constants ( $J$  values) are given in Hertz (Hz), and chemical shifts ( $\delta$ ) are reported in ppm and referred to  $\text{CHD}_2\text{OD}$  and  $\text{CHCl}_3$  as internal standards. Spin multiplicities are given as s (singlet), br s (broad singlet), d (doublet), or m (multiplet). Through-space  $^1\text{H}$  connectivities were evidenced using NOESY experiment with mixing time of 400 ms. HPLC was performed with a Waters Model 510 pump equipped with Waters Rheodine injector and a differential refractometer, model 401. Reaction progress was monitored via thin-layer chromatography (TLC) on Alugram silica gel G/UV254 plates. Silica gel MN Kieselgel 60 (70–230 mesh) from Macherey-Nagel Company was used for column chromatography. All chemicals were obtained from Sigma-Aldrich, Inc. Solvents and reagents were used as supplied from commercial sources with the following exceptions. Tetrahydrofuran and triethylamine were distilled from calcium hydride immediately prior to use. Methanol was dried from magnesium methoxide as follow. Magnesium turnings (5 g) and iodine (0.5 g) are refluxed in a small (50–100 mL) quantity of methanol until all of the magnesium has reacted. The mixture is diluted (up to 1 L) with reagent grade methanol, refluxed for 2–3 h then distilled under nitrogen. All reactions were carried out under argon atmosphere using flame-dried glassware. The purities of compounds were determined to be greater than 95% by HPLC.

**Synthetic procedures.** See the Supporting Information.

**Transactivation assay.** For FXR and GPBAR1 mediated transactivations, HepG2 cells and HEK293T cells were transfected as described previously<sup>25</sup>. At 24 h post-transfection, cells were stimulated 18 h with  $10\ \mu\text{M}$  CDCA (1), TLCA (2), 6-ECDCA (3) and compounds 7–19. After treatments,  $20\ \mu\text{L}$  of cellular lysates were read using Dual Luciferase Reporter Assay System (Promega Italia s.r.l., Milan, Italy) according manufacturer specifications using the Glomax 20/20 luminometer (Promega Italia s.r.l., Milan, Italy). To evaluate GPBAR1 mediated transactivation, HEK-293T cells were transfected with 200 ng of human pGL4.29 (Promega), a reporter vector containing a cAMP response element (CRE) that drives the transcription of the luciferase reporter gene luc2P, with 100 ng of pCMVSPORT6-human GPBAR1, and with 100 ng of pGL4.70. Dose-response curves were performed in HepG2 and HEK-293T cells transfected as described above and then treated with increasing concentrations of compounds 7 (1– $10\ \mu\text{M}$ ), 13, 14 and 19 (100 nM– $25\ \mu\text{M}$ ). At 18 h post stimulations, cellular lysates were assayed for luciferase and Renilla activities using the Dual-Luciferase Reporter assay system (E1980, Promega). Luminescence was measured using Glomax 20/20 luminometer (Promega). Luciferase activities were normalized with Renilla activities.

**RNA isolation and RT-PCR.** Total RNA was isolated from HepG2 or GLUTAg cells using the TRIzol reagent according to the manufacturer's specifications (Invitrogen). One microgram of purified RNA was treated with DNase-I and reverse transcribed with Superscript II (Invitrogen). For Real Time PCR, 10 ng template was dissolved in  $25\ \mu\text{L}$  containing 200 nmol/L of each primer and  $12.5\ \mu\text{L}$  of  $2 \times$  SYBR FAST Universal ready mix (Invitrogen). All reactions were performed in triplicate, and the thermal cycling conditions were as follows: 2 min at  $95\ ^\circ\text{C}$ , followed by 40 cycles of  $95\ ^\circ\text{C}$  for 20 s and  $60\ ^\circ\text{C}$  for 30 s in iCycler iQ instrument (Biorad). The relative mRNA expression was calculated and expressed as  $2^{-\Delta\Delta\text{Ct}}$ . Forward and reverse primer sequences were the following: human GAPDH, gaagtggaaggtcggagt and catgggtggaatcatattgga; human OST $\alpha$ , tgttggccctttccaatac and ggctcccatgttctgctcac; human BSEP, gggccattgtacgagatcctaa and tgcaccgtctttcacttctg; mouse GAPDH, ctgag-tatgtcgtggagtctac and gttggtggtgcaggatgcattg; mouse Pro-glucagon, tgaagacaacgcccactac and caatgtttccggtctctc.

### Direct interaction on FXR by Alpha screen technology in a coactivator recruitment assay.

Anti-GST-coated acceptor beads were used to capture the GST-fusion FXR-LBD whereas the biotinylated-SRC-1 peptide was captured by the streptavidin donor beads. Upon illumination at 680 nm, chemical energy is transferred from donor to acceptor beads across the complex streptavidin-Donor/Src-1-Biotin/GSTFXR-LBD/Anti-GST-Acceptor and a signal is produced. The assay was performed in white, low-volume, 384-well Optiplates (PerkinElmer) using a final volume of  $25\ \mu\text{L}$  containing final concentrations of 10 nM of purified GST-tagged FXR-LBD protein, 30 nM biotinylated Src-1 peptide,  $20\ \mu\text{g}/\text{mL}$  anti-GST acceptor beads acceptor beads and  $10\ \mu\text{g}/\text{mL}$  of streptavidin donor bead (PerkinElmer). The assay buffer contained 50 mM Tris (pH 7.4), 50 mM KCl, 0.1% BSA, and 1 mM DTT. The stimulation times with  $1\ \mu\text{L}$  of tested compound (dissolved in 50% DMSO/ $\text{H}_2\text{O}$ ) were fixed to 30 min at room temperature. The concentration of DMSO in each well was maintained at a final concentration of 4%. After the addition of the detection mix (acceptor and donor beads) the plates were incubated in the dark for 4 h at room temperature and then were read in Envision microplate analyzer (PerkinElmer).

## References

- Makishima, M. *et al.* Identification of a nuclear receptor for bile acids. *Science* **284**, 1362–1365 (1999).
- Parks, D. J. *et al.* Bile acids: natural ligands for an orphan nuclear receptor. *Science* **284**, 1365–1368 (1999).
- Maruyama, T. *et al.* Identification of membrane type receptor for bile acids (M-BAR). *Biochem. Biophys. Res. Commun.* **298**, 714–719 (2002).

4. Modica, S., Gadaleta, R. M. & Moschetta, A. Deciphering the nuclear bile acid receptor FXR paradigm. *Nucl. Recept. Signal.* **8**, e005 (2010).
5. Wang, H., Chen, J., Hollister, K., Sowers, L. C. & Forman, B. M. Endogenous bile acids are ligands for the nuclear receptor FXR/BAR. *Mol. Cell.* **3**, 543–553 (1999).
6. Goodwin, B. *et al.* A regulatory cascade of the nuclear receptors FXR, SHP-1, and LXR-1 represses bile acid biosynthesis. *Mol. Cell.* **6**, 517–526 (2000).
7. Ananthanarayanan, M., Balasubramanian, N., Makishima, M., Mangelsdorf, D. J. & Suchy, F. J. Human bile salt export pump promoter is transactivated by the farnesoid X receptor/bile acid receptor. *J. Biol. Chem.* **276**, 28857–28865 (2001).
8. Boyer, J. L. *et al.* Upregulation of a basolateral FXR-dependent bile acid efflux transporter OSTalpha-OSTbeta in cholestasis in humans and rodents. *Am. J. Physiol. Gastrointest. Liver Physiol.* **290**, G1124–G1130 (2006).
9. Fiorucci, S. & Baldelli, F. Farnesoid X receptor agonists in biliary tract disease. *Curr. Opin. Gastroenterol.* **25**, 252–259 (2009).
10. Fiorucci, S. *et al.* Targeting FXR in cholestasis: hype or hope. *Expert Opin. Ther. Targets* **12**, 1449–1459 (2014).
11. Fiorucci, S., Mencarelli, A., Distrutti, E. & Zampella, A. Farnesoid X receptor: from medicinal chemistry to clinical applications. *Future Med. Chem.* **4**, 877–891 (2012).
12. Beuers, U., Kremer, A. E., Bolier, R. & Elferink, R. P. Pruritus in cholestasis: facts and fiction. *Hepatology* **60**, 399–407 (2014).
13. Cipriani, S., Mencarelli, A., Palladino, G. & Fiorucci, S. FXR activation reverses insulin resistance and lipid abnormalities and protects against liver steatosis in Zucker (fa/fa) obese rats. *J. Lipid Res.* **51**, 771–784 (2010).
14. Rizzo, G. *et al.* The farnesoid X receptor promotes adipocyte differentiation and regulates adipose cell function *in vivo*. *Mol. Pharmacol.* **70**, 1164–1173 (2006).
15. Fiorucci, S., Rizzo, G., Donini, A., Distrutti, E. & Santucci, L. Targeting farnesoid X receptor for liver and metabolic disorders. *Trends Mol. Med.* **13**, 298–309 (2007).
16. Mencarelli, A. *et al.* Dissociation of intestinal and hepatic activities of FXR and LXR $\alpha$  supports metabolic effects of terminal ileum interposition in rodents. *Diabetes* **62**, 3384–3393 (2013).
17. Pean, N. *et al.* The receptor TGR5 protects the liver from bile acid overload during liver regeneration in mice. *Hepatology* **58**, 1451–1460 (2013).
18. Baghdasaryan, A. *et al.* Protective role of membrane bile acid receptor TGR5 (GPBAR1) in DDC-induced sclerosing cholangitis in mice. *J. Hepatol.* **60**, S197–S198 (2014).
19. Alemi, F. *et al.* The TGR5 receptor mediates bile acid-induced itch and analgesia. *J. Clin. Invest.* **123**, 1513–1530 (2013).
20. Watanabe, M. *et al.* Bile acids induce energy expenditure by promoting intracellular thyroid hormone activation. *Nature* **439**, 484–489 (2006).
21. Thomas, C. *et al.* TGR5-mediated bile acid sensing controls glucose homeostasis. *Cell Metab.* **10**, 167–177 (2009).
22. Parker, H.E. *et al.* Molecular mechanisms underlying bile acid-stimulated glucagon-like peptide-1 secretion. *Br. J. Pharmacol.* **165**, 414–423 (2012).
23. Fiorucci, S., Mencarelli, A., Palladino, G. & Cipriani, S. Bile-acid-activated receptors: targeting TGR5 and farnesoid-X-receptor in lipid and glucose disorders. *Trends Pharmacol. Sci.* **30**, 570–580 (2009).
24. Fiorucci, S., Cipriani, S., Baldelli, F. & Mencarelli, A. Bile acid-activated receptors in the treatment of dyslipidemia and related disorders. *Prog. Lipid Res.* **49**, 171–185 (2010).
25. D'Amore, C. *et al.* Design, synthesis, and biological evaluation of potent dual agonists of nuclear and membrane bile acid receptors. *J. Med. Chem.* **57**, 937–954 (2014).
26. Festa, C. *et al.* Exploitation of cholane scaffold for the discovery of potent and selective farnesoid X receptor (FXR) and G-protein coupled bile acid receptor 1 (GP-BAR1) ligands. *J. Med. Chem.* **57**, 8477–8495 (2014).
27. Pellicciari, R. *et al.* 6- $\alpha$ -Ethylchenodeoxycholic acid (6-ECDCA), a potent and selective FXR agonist endowed with anticholestatic activity. *J. Med. Chem.* **45**, 3569–3572 (2002).
28. Rizzo, G. *et al.* Functional characterization of the semisynthetic bile acid derivative INT-767, a dual farnesoid X receptor and TGR5 agonist. *Mol. Pharmacol.* **78**, 617–630 (2010).
29. Pellicciari, R. *et al.* Non genomic actions of bile acids. Synthesis and preliminary characterization of 23- and 6,23-alkyl-substituted bile acid derivatives as selective modulators for the G-protein coupled receptor TGR5. *J. Med. Chem.* **50**, 4265–4268 (2007).
30. Hirschfield, G. M. *et al.* Efficacy of obeticholic acid in patients with primary biliary cirrhosis and inadequate response to ursodeoxycholic acid. *Gastroenterology* **148**, 751–761 (2015).
31. Fiorucci, S., Zampella, A. & Distrutti, E. Development of FXR, PXR and CAR agonists and antagonists for treatment of liver disorders. *Curr. Top. Med. Chem.* **12**, 605–624 (2012).
32. Sepe, V., Distrutti, E., Limongelli, V., Fiorucci, S. & Zampella, A. Steroidal scaffolds as FXR and GPBAR1 ligands: from chemistry to therapeutic application. *Future Med. Chem.* **7**, 1109–1135 (2015).
33. Di Leva, F. S. *et al.* Structure-based drug design targeting the cell membrane receptor GPBAR1: exploiting the bile acid scaffold towards selective agonism. *Sci Rep.* **5**, 16605 (2015).
34. Cipriani, S. *et al.* Impaired itching perception in murine models of cholestasis is supported by dysregulation of GPBAR1 signaling. *PLoS One* **10**, e0129866 (2015).
35. Renga, B. *et al.* Reversal of endothelial dysfunction by GPBAR1 agonism in portal hypertension involves a AKT/FOXO1 dependent regulation of H<sub>2</sub>S generation and endothelin-1. *PLoS One* **10**, e0141082 (2015).
36. Sepe, V. *et al.* Insights on FXR selective modulation. Speculation on bile acid chemical space in the discovery of potent and selective agonists. *Sci. Rep.* **6**, 19008 (2016).
37. Scheingart, C. D. & Hofmann, A. F. Synthesis of 24-nor-5 beta-cholan-23-oic acid derivatives: a convenient and efficient one-carbon degradation of the side chain of natural bile acids. *J. Lipid Res.* **10**, 1387–1395 (1988).
38. Goto, J., Sano, Y., Chikai, T. & Nambara, T. Synthesis of disulfates of unconjugated and conjugated bile acids. *Chem. Pharm. Bull.* **35**, 4562–4567 (1987).
39. Song, X. *et al.* Mechanistic insights into isoform-dependent and species-specific regulation of bile salt export pump by farnesoid X receptor. *J. Lipid Res.* **54**, 3030–3044 (2013).

## Acknowledgements

This work was supported by grants from PSC Partners (5237 South Kenton Way, Englewood, Colorado 80111 USA) and grants from POR Campania FESR 2007-2013-O.O.2.1 (FarmaBioNet).

## Author Contributions

C.F., Ca.F., V.S., D.M. and A.Z. designed and performed synthesis; B.R., A.C., S.M., M.B. and S.F. designed and performed pharmacological experiments; M.C.M. and A.C. designed and performed Alpha screen experiments; S.F. and A.Z. analyzed and interpreted the data. All authors contributed to manuscript writing and approved the final version.

### Additional Information

**Supplementary information** accompanies this paper at <http://www.nature.com/srep>

**Competing financial interests:** The authors declare no competing financial interests.

**How to cite this article:** Finamore, C. *et al.* Navigation in bile acid chemical space: discovery of novel FXR and GPBAR1 ligands. *Sci. Rep.* **6**, 29320; doi: 10.1038/srep29320 (2016).



This work is licensed under a Creative Commons Attribution 4.0 International License. The images or other third party material in this article are included in the article's Creative Commons license, unless indicated otherwise in the credit line; if the material is not included under the Creative Commons license, users will need to obtain permission from the license holder to reproduce the material. To view a copy of this license, visit <http://creativecommons.org/licenses/by/4.0/>

# Homoallylic *o*-halobenzylamines: asymmetric diversity-oriented synthesis of benzo-fused cyclic amines

Rubén Lázaro<sup>1</sup> · Pablo Barrio<sup>1</sup> · Claudia Finamore<sup>2</sup> · Raquel Román<sup>2</sup> · Santos Fustero<sup>1,2</sup> 

Received: 2 September 2016 / Accepted: 7 September 2016  
© Springer Science+Business Media New York 2016

**Abstract** The presence of a halogen atom in the proximity of a homoallylic amine, obtained by asymmetric addition of allylzinc bromide to the corresponding *tert*-butyl sulfinimine, makes them versatile building blocks suitable to participate in several palladium-catalyzed processes, such as the intramolecular Heck reaction or the Sonogashira cross-coupling. The thus obtained *ortho*-alkynyl derivatives display two unsaturated functional groups which may be further modified by means of the intramolecular Pauson–Khand reaction or the ring-closing enyne metathesis. In this way, a variety of benzo-fused amines can be obtained in 2–3 steps from readily available starting materials.

**Keywords** Homoallylic amine · Pauson–Khand reaction · Sonogashira cross-coupling · Intramolecular Heck reaction · Diversity-oriented synthesis · Asymmetric synthesis

## Introduction

Diversity-oriented synthesis (DOS) aims to provide maximum coverage of the chemical space, from a common precursor, by using the minimum number of steps (usually 4–5) [1–6]. Usually, the key for the success of such a strategy is the identification of a suitable substrate carrying specific functional groups at appropriate positions. In this way, the product of a given transformation becomes the substrate of the subsequent. These functional groups must be able to participate in as many different reactions as possible, thus increasing the achievable molecular complexity. In this context, during the last few years, our group has studied the use of 2-halobenzaldehyde derivatives as common building blocks for the asymmetric synthesis of benzo-fused carbo—[7–11] and heterocycles [12–15] (Scheme 1) [16].

The use of this strategy has allowed us to synthesize interesting building blocks such as fluorinated [13, 14] and non-fluorinated isoindolines [14], indanones [11] and, more recently, fluorinated isoindolinones [12] and amino steroid derivatives [8]. In the course of the latter study, we found that significant amounts of an undesired intramolecular Heck reaction by-product **4a** was obtained upon Sonogashira cross-coupling of homoallylic *o*-bromobenzylsulfinamide **3a** (Scheme 2). The formation of **4a** was unambiguously determined by the presence of two characteristic methylene protons at 5.1 and 5.5 ppm in the <sup>1</sup>H-NMR spectrum, as well as the corresponding signal at 104.4 ppm at the <sup>13</sup>C-NMR spectrum.

In our previous communication [7], the formation of this undesired by-product could be suppressed by increasing the amount of alkyne (from 3 to 5 equivalents) and the reaction concentration (from 0.1 to 0.5 M), thus favoring the intermolecular Sonogashira cross-coupling over the

---

Dedicated to Professor George A. Olah on the occasion of his 90th birthday.

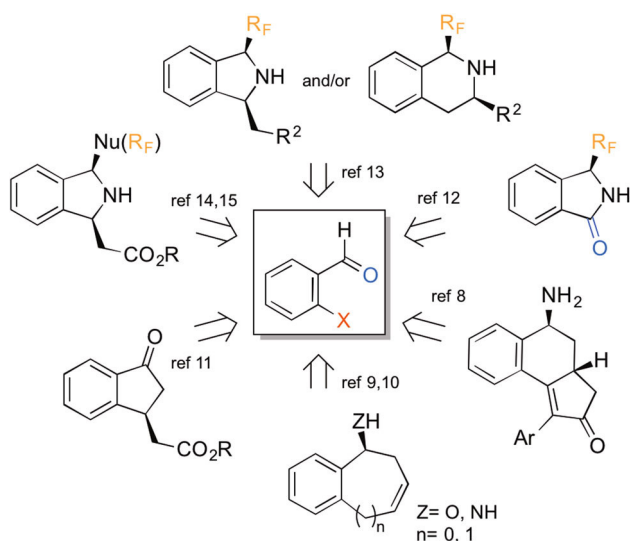
✉ Pablo Barrio  
pablo.barrio@uv.es

✉ Santos Fustero  
santos.fustero@uv.es

<sup>1</sup> Departamento de Química Orgánica, Universidad de Valencia, 46100 Burjassot, Spain

<sup>2</sup> Laboratorio de Moléculas Orgánicas, Centro de Investigación Príncipe Felipe, 46012 Valencia, Spain





**Scheme 1** 2-Halobenzaldehyde in DOS

intramolecular Heck reaction. In this report, we describe the optimization of the intramolecular Heck reaction along with the implementation of a one-pot condensation/asymmetric allylation/intramolecular PKR protocol for the synthesis of tricyclic amines. In addition, the RCEYM reaction of intermediates **3** will also be discussed.

## Results and discussion

### Intramolecular Heck reaction

Obtaining the undesired intramolecular Heck reaction product as a by-product of the Sonogashira reaction of substrate **1a** was the starting point for trying to optimize this process, as mentioned in the introduction (Scheme 2). Of course, we started by removing the no-longer necessary alkyne and the CuI from the reaction medium (Table 1, Entry 1). By doing so, we obtained an overall moderate yield; however, a significant amount of it in the form of the isomerized product **6**. Replacing Et<sub>3</sub>N with an inorganic base (Ag<sub>2</sub>CO<sub>3</sub>) suppressed the formation of the undesired isomerized product, giving exclusively the desired product in moderate yield (Table 1, Entry 2). The use of microwave irradiation both in toluene and THF did not bring any beneficial effect, nor did the addition of external ligands (Table 1, Entries 3–6). Finally, the use of an equimolar ratio of Et<sub>3</sub>N and Ag<sub>2</sub>CO<sub>3</sub> as base gave rise to an optimized 70 % yield (Table 1, Entry 7). It should be noted that recently, Yus et al. [17] have described similar reaction conditions for this transformation.

Once an optimized set of reaction conditions had been established, a small library of 3-methylene-1-aminoindane derivatives were synthesized in moderate to good yields

(Scheme 3). For substrate **1b**, the isomerized product **4b'** was obtained in 68 % yield.<sup>1</sup>

Aiming toward a more sustainable and practical methodology, and in view of our own experience in the use of one-pot reactions in the context of DOS, we then studied the one-pot condensation/asymmetric allylation/Heck reaction sequence on 2-iodobenzaldehyde **8a** achieving the desired product in 70 % yield over the three steps and as a single diastereoisomer (Scheme 4).

In order to increase the range of molecular structures available through our methodology, two simple transformations were carried out on the exocyclic double bond of the unsubstituted substrate **4a**, namely the hydrogenation and the oxidative cleavage (Scheme 5). As expected, the Pd/C-catalyzed heterogeneous hydrogenation of the double bond proceeded with high *anti* selectivity affording the *cis* product **9** in excellent yield (Scheme 5). On the other hand, the oxidative cleavage of the *exo*-methylene afforded the 3-aminoindanone derivative **10** in good yield (Scheme 5). Note that the –SO<sub>t</sub>Bu group was concomitantly oxidized to the –SO<sub>2</sub>tBu group under the reaction conditions. Compound **10** was further transformed into *cis* 1,3-aminoalcohol **11** by BH<sub>3</sub>·THF-mediated diastereoselective reduction of the ketone (Scheme 5).

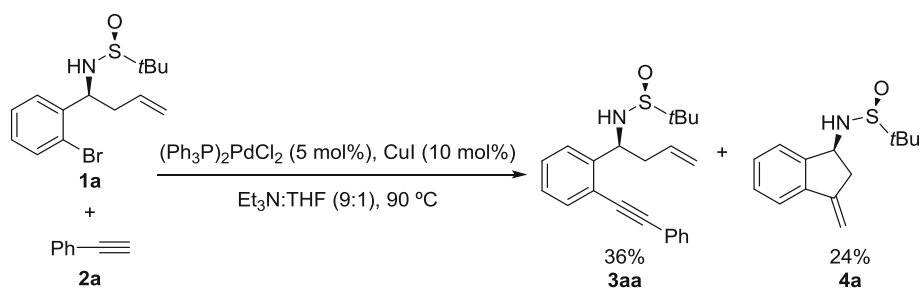
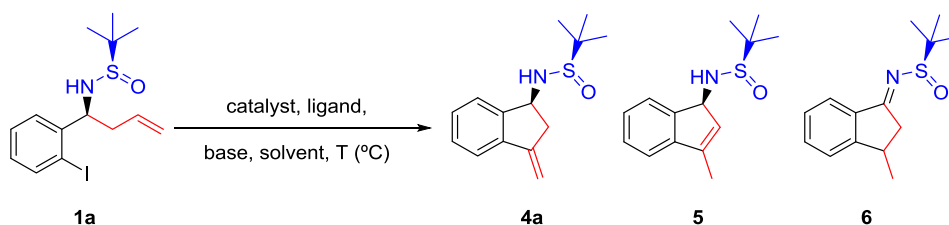
The relative configuration of the chiral centers in products **9** and **11** was determined by means of 2D-NMR NOESY experiments, which showed cross peaks between the NH and the CH<sub>3</sub> protons, and also between the two benzylic methyne protons H<sub>a</sub> and H<sub>b</sub> (Fig. 1). In both cases, these observations are in agreement with a *cis* arrangement. For compound **9**, this result could be foreseen since catalytic heterogeneous hydrogenations usually proceed on the less hindered face of the olefin, in this case *anti* to the bulky NHSOtBu group, resulting in the observed *cis* product.

### Ring-closing enyne metathesis (RCEYM)

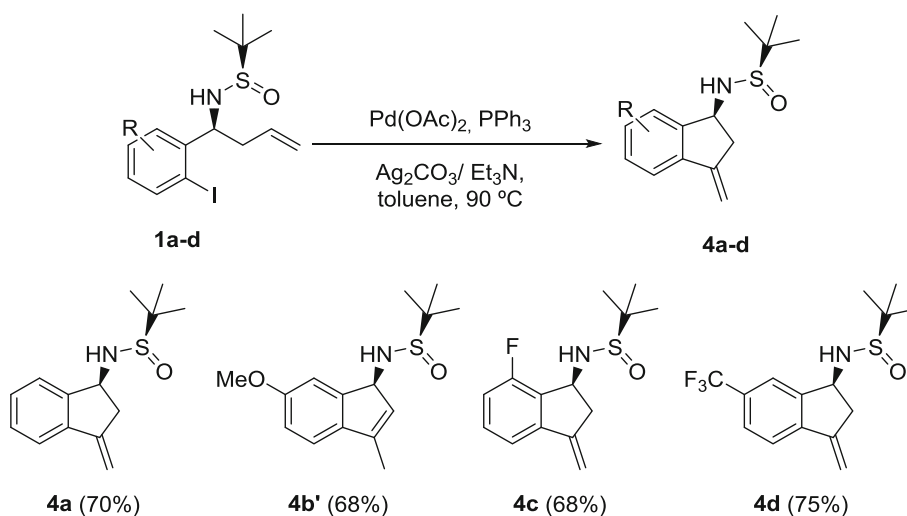
Taking advantage of the densely functionalized intermediates **3** synthesized in our recent report [8], we envisioned to expand their reactivity to other well-established transformations of enynes. Among these, RCEYM has become a powerful tool for the creation of carbo- and heterocycles of several ring sizes with the added value of presenting an exocyclic conjugated vinyl moiety amenable for subsequent transformations [18].

Using **3a** as a model substrate, an optimization of the reaction conditions was carried out using our recently reported parent transformation on the corresponding

<sup>1</sup> Under the reaction conditions described by Yus the isomerized product is also obtained, see Sirvent et al. [17].

**Scheme 2** Preliminary results**Table 1** Optimization of the intramolecular Heck reaction conditions

Entry	Catalyst	Ligand	Base	Solvent	<i>T</i> (°C)	1 (%)	4 (%)	5 (%)	6 (%)
1	Pd(OAc) <sub>2</sub>	PPh <sub>3</sub>	Et <sub>3</sub> N	Tol.	120	–	25	–	31
2	Pd(OAc) <sub>2</sub>	PPh <sub>3</sub>	Ag <sub>2</sub> CO <sub>3</sub>	Tol.	120	–	66	–	–
3	Pd(dba) <sub>2</sub>	PPh <sub>3</sub>	Ag <sub>2</sub> CO <sub>3</sub>	Tol.	120 MW	–	50	–	–
4	Pd(dba) <sub>2</sub>	PPh <sub>3</sub>	Ag <sub>2</sub> CO <sub>3</sub>	THF	100 MW	–	25	25	–
5	Pd(dba) <sub>2</sub>	XANP	Ag <sub>2</sub> CO <sub>3</sub>	THF	100 MW	–	37.5	12.5	–
6	Pd(dba) <sub>2</sub>	JOHNP	Ag <sub>2</sub> CO <sub>3</sub>	THF	100 MW	80	–	–	–
7	Pd(OAc) <sub>2</sub>	PPh <sub>3</sub>	Et <sub>3</sub> N/Ag <sub>2</sub> CO <sub>3</sub>	Tol.	90	–	70	–	–

**Scheme 3** Scope and limitations

alcohols as starting point (second generation Grubbs' catalyst [Ru-II], DCM, 45 °C, 1,7-octadiene) (Table 2) [19, 20].

Under the original reaction conditions, a moderate 55 % yield was obtained (Table 2, entry 1). We envisioned that this modest result might be the result of an inefficient in situ ethylene formation along with some catalyst

deactivation. In an attempt to tackle these issues, we carried out the reaction in a sealed tube and added two portions of both the catalyst and 1,7-octadiene, obtaining an excellent yield (Table 2, entry 2). The reaction time could be shortened by rising the temperature, however, at expense of chemical yield (Table 2, entry 3). Finally, while the addition of a Lewis acid improved the catalytic activity

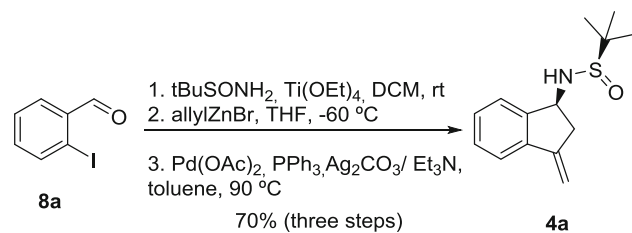
(Table 2, entry 4), the results were not as satisfactory as the ones obtained in entry 2. Hence, the reaction conditions shown in entry 2 were used for the study of the reaction scope.

With a small library of enynes **12** from our previous study in hand [8], the scope of this transformation was studied using the optimized conditions shown in Table 2, entry 2 (Scheme 6).

Substitution at both aromatic rings is well tolerated without significantly modifying the high chemical yield (Scheme 6, **12a-e**). On the other hand, replacing the aryl substituent at the triple bond by an alkyl one results in a significant drop, although still obtaining a synthetically useful 50 % yield (Scheme 6, **12f**). The better performance of aryl- over alkyl-substituted triple bonds might be rationalized by the higher stabilization of the resulting diene by conjugation with the aromatic ring, since RCEYM is an enthalpy driven transformation.

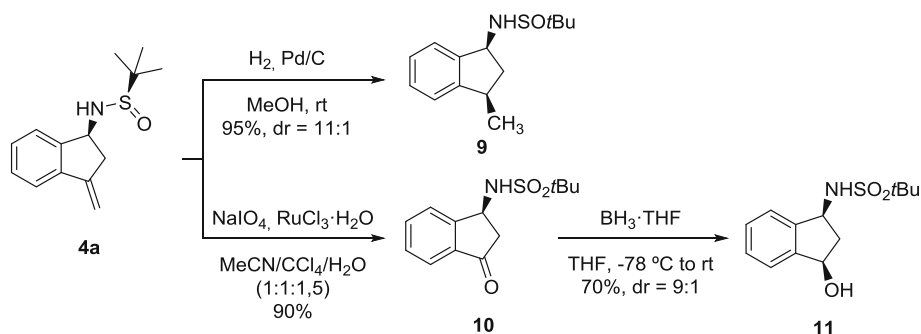
With the aim of further increasing the structural complexity and diversity affordable with our strategy, a Diels–Alder reaction of diene **12a** with dimethyl acetylene dicarboxylate (DMAD) was envisioned. However, no reaction was observed even after prolonged heating in DCE (Scheme 7).

We believe the reason behind this unexpectedly low reactivity of diene **12a** in Diels–Alder reactions could be its preference for the *s-trans* over the required *s-cis* conformation, due to the steric hinderance between the *ortho* protons at the aromatic substituents of the dienic moiety, which would clash by adopting such conformation (Fig. 2).



**Scheme 4** One-pot condensation/asymmetric allylation/Heck reaction sequence

**Scheme 5** Transformations on the 1-amino-3-methyleneindane skeleton



### Study of the one-pot condensation/asymmetric allylation/intramolecular Pauson–Khand reaction (PKR) sequence

Finally, building on our own experience in the area of one-pot transformations with Ellman's sulfonimides [9], we envisioned setting up a one-pot protocol for our recently reported asymmetric synthesis of tricyclic enones by means of intramolecular PKR [8]. We started our study using the simplest starting material and tackling the most ambitious four-step one-pot transformation (condensation/allylation/

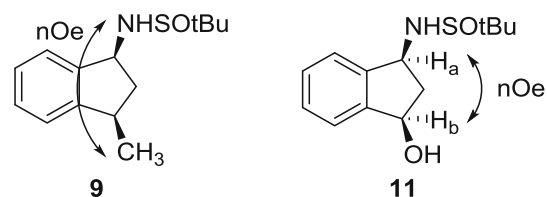
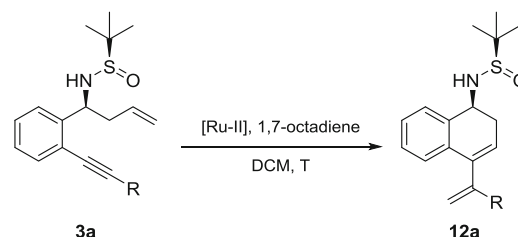


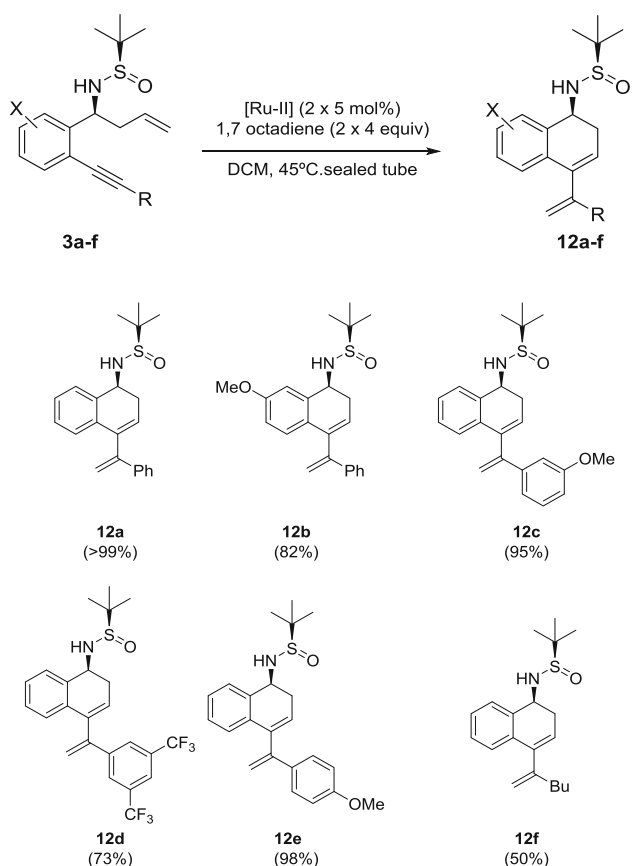
**Fig. 1** Assignment of the relative stereochemistry of products **9** and **11**

**Table 2** Optimization of the RCEYM reaction conditions

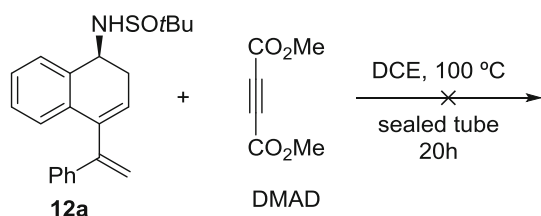


Entry	<i>T</i> (°C)	<b>12a</b> (%)
1	45	55
2 <sup>a,b,c</sup>	45	>99
3 <sup>a,b,c</sup>	90	73
4 <sup>a,d</sup>	45	84

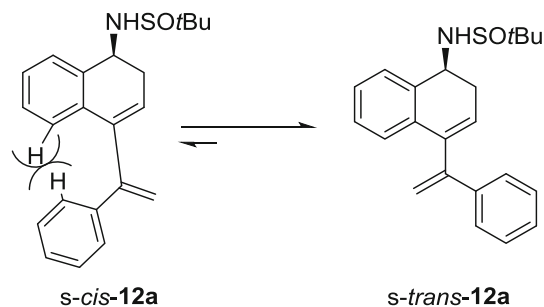
<sup>a</sup> Sealed tube, <sup>b</sup> 2 × 5 mol % catalyst loading, <sup>c</sup> 2 × 4 equiv 1,7-octadiene, <sup>d</sup> 1 equiv Ti(OEt)<sub>4</sub>



Scheme 6 Scope and limitations



Scheme 7 Failed Diels–Alder reaction between 12a and DMAD

Fig. 2 *S-cis/S-trans* conformational equilibrium of 12a

Sonogashira/PKR). However, although the desired product **13a** was detected in the crude reaction mixture, most of the recovered material was identified as **1a**, suggesting that the

Sonogashira reaction was not fully compatible with the reaction medium from the previous condensation/allylation steps (Scheme 8).

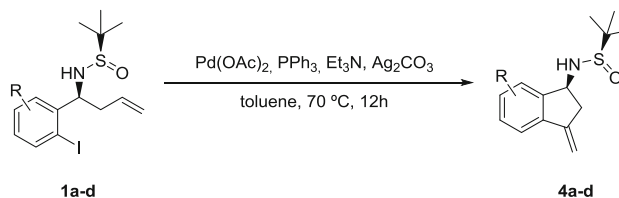
Since the Sonogashira coupling seemed to be the bottleneck for this one-pot procedure, we decided to carry out this step independently and then run the one-pot procedure on the corresponding *o*-alkynylbenzaldehyde derivatives **14a, b** (Scheme 9). In both examples, the chemical yield of the one-pot procedure is significantly lower than the corresponding stepwise protocol (Scheme 9). The one-pot methodology, though, benefits from operational simplicity. Regarding the diastereoselectivity, for **14a**, a diminished *dr* was obtained, as expected (Scheme 9). This is due to the dependence of the diastereoselectivity with the substitution at the triple bond that we described in our previous report [8]. The isolation of a single diastereoisomer for **14b** might be due to the loss of small quantities of minor diastereoisomers during purification, which would also account for the low chemical yield (Scheme 9).

## Conclusions

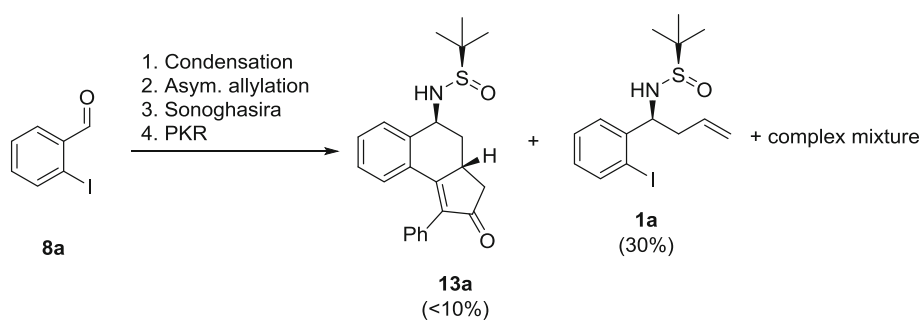
In recent years, 2-iodobenzaldehyde has shown its superior performance as a substrate for diversity-oriented synthesis. In this report, we have further increased the molecular variability accessible from this readily available starting material. More specifically, the asymmetric allylation of the corresponding Ellman's imines followed by intramolecular Heck reaction affords 3-methylene-1-aminointhane derivatives. On the other hand, the introduction of an alkynyl group at the *ortho*-position affords substrates suitable for a RCEYM reaction achieving conjugated dienes. One-pot procedures have been developed for both the asymmetric allylation/intramolecular Heck reaction and the condensation/asymmetric allylation/Pauson–Kahnd reaction sequence.

## Experimental section

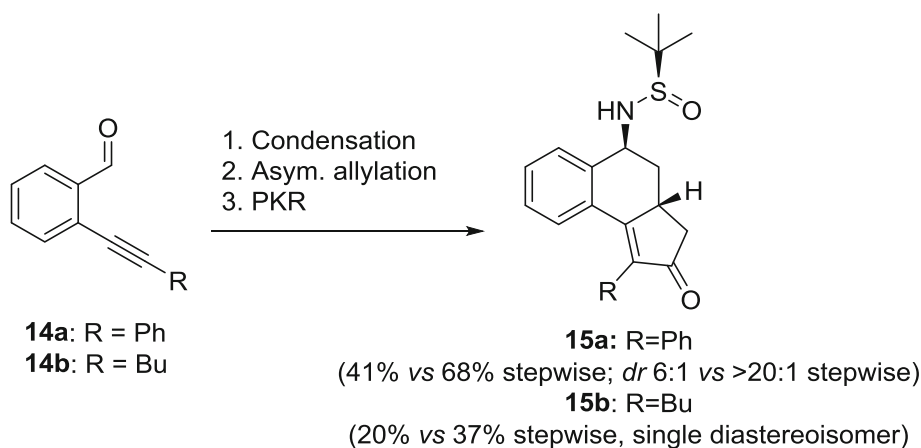
### General procedure for the intramolecular Heck reaction



**Scheme 8** One-pot condensation/asymmetric allylation/Sonogashira coupling//PKR



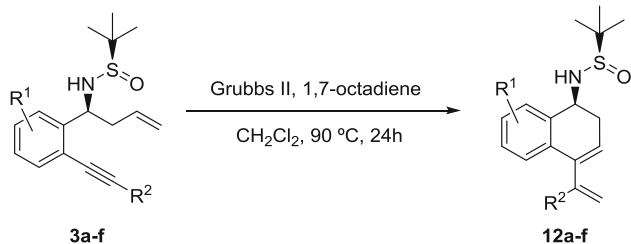
**Scheme 9** One-pot condensation/asymmetric allylation/PKR sequence



A solution of the corresponding substituted 2-iodobenzyl sulfinyl amide **1** (1.0 equiv), Pd(OAc)<sub>2</sub> (0.1 equiv), PPh<sub>3</sub> (0.2 equiv), Et<sub>3</sub>N (2.0 equiv) and Ag<sub>2</sub>CO<sub>3</sub> (2.0 equiv) in toluene (0.1 M) was heated to 70 °C for 12 h. The solvent was removed under reduced pressure, and the crude product was purified by flash chromatography to give compounds **4**.

Compounds **4a–d** have previously been described, and their spectroscopic data are in fully agreement with the literature [17].

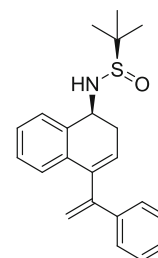
### General procedure for the ring-closing enyne metathesis



A solution of **3** (1.0 equiv), 1,7-octadiene (8.0 equiv) and Grubbs II catalyst (0.05 equiv) in CH<sub>2</sub>Cl<sub>2</sub> (0.1 M) was

heated to 90 °C for 24 h. The solvent was removed under reduced pressure, and the crude product was purified by flash chromatography to give compounds **12**.

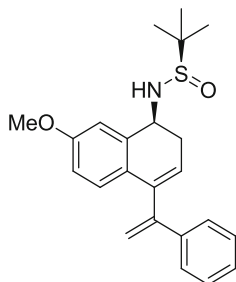
(*R*<sub>S</sub>)-2-Methyl-*N*-[(*S*)-4-(1-phenylvinyl)-1,2-dihydronaphthalen-1-yl]propane-2-sulfinamide (**12a**)



The title compound was obtained following the general procedure described above. Flash chromatography [*n*-hexane/EtOAc (1:1)] afforded compound **12a** as a brown solid (>99 %). [ $\alpha$ ]<sub>D</sub><sup>25</sup> = +24.3 (c 1.0; CHCl<sub>3</sub>). <sup>1</sup>H RMN (300 MHz, CDCl<sub>3</sub>)  $\delta$  1.23 (s, 9H), 2.68 (ddd, *J* = 17.2, 7.1, 4.9 Hz, 1H), 2.89 (ddd, *J* = 17.2, 5.7, 4.3 Hz, 1H), 3.51 (d, *J* = 8.1 Hz, 1H), 4.59 (dd, *J* = 13.7, 7.2 Hz, 1H), 5.35 (d, *J* = 1.6 Hz, 1H), 5.67 (d, *J* = 1.6 Hz, 1H), 6.10 (t, *J* = 4.5 Hz, 1H), 7.00 (dd, *J* = 7.6, 1.2 Hz, 1H), 7.10 (td, *J* = 7.5, 1.5 Hz, 1H), 7.17 (td, *J* = 7.4, 1.5 Hz, 1H), 7.23 (d, *J* = 1.9 Hz, 1H), 7.25 (d, *J* = 2.0 Hz, 1H), 7.26 (s, 1H), 7.36–7.43 (m, 3H). <sup>13</sup>C RMN (75 MHz, CDCl<sub>3</sub>)

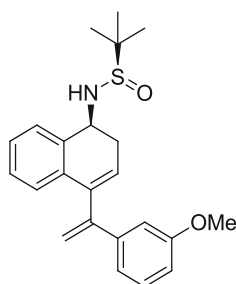
$\delta$  22.7 (3xCH<sub>3</sub>), 32.6 (CH<sub>2</sub>), 54.3 (CH), 56.1 (C), 115.4 (CH<sub>2</sub>), 125.1 (CH), 126.3 (CH), 126.6 (2xCH), 126.8 (CH), 127.3 (CH), 127.7 (CH), 128.0 (CH), 128.3 (2xCH), 133.5 (C), 135.6 (C), 139.6 (C), 139.7 (C), 147.9 (C). HRMS (EI) calcd for C<sub>22</sub>H<sub>25</sub>NOS [M + H]<sup>+</sup>: 352.1730, found: 352.1737.

(*R<sub>S</sub>*)-*N*-[(*S*)-7-Methoxy-4-(1-phenylvinyl)-1,2-dihydronaphthalen-1-yl]-2-methylpropane-2-sulfinamide (12b)



The title compound was obtained following the general procedure described above. Flash chromatography [*n*-hexane/EtOAc (1:1)] afforded compound **12b** as a brown solid (82 %).  $[\alpha]_D^{25} = + 21.0$  (c 1.0; CHCl<sub>3</sub>). <sup>1</sup>H RMN (300 MHz, CDCl<sub>3</sub>)  $\delta$  1.25 (s, 9H), 2.62 (ddd, *J* = 16.9, 8.0, 4.6 Hz, 1H), 2.87 (ddd, *J* = 16.9, 5.7, 4.5 Hz, 1H), 3.49 (d, *J* = 7.5 Hz, 1H), 3.76 (s, 3H), 4.49–4.60 (m, 1H), 5.34 (d, *J* = 1.7 Hz, 1H), 5.64 (d, *J* = 1.7 Hz, 1H), 5.97 (t, *J* = 4.5 Hz, 1H), 6.61 (dd, *J* = 8.5, 2.7 Hz, 1H), 6.91 (d, *J* = 8.5 Hz, 1H), 6.97 (d, *J* = 2.7 Hz, 1H), 7.21–7.26 (m, 3H), 7.37–7.42 (m, 2H). <sup>13</sup>C RMN (75 MHz, CDCl<sub>3</sub>)  $\delta$  22.7, 32.7, 54.9, 55.2, 56.2, 112.3, 112.8, 115.2, 122.7, 126.6, 127.7, 128.3, 137.7, 139.3, 139.8, 148.1, 158.8. HRMS (EI) calcd for C<sub>23</sub>H<sub>27</sub>NO<sub>2</sub>S [M + H]<sup>+</sup>: 382.1762, found: 382.1760.

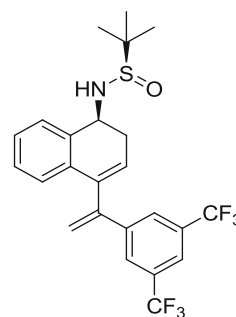
(*R<sub>S</sub>*)-*N*-[(*S*)-4-(1-(3-Methoxyphenyl)vinyl)-1,2-dihydronaphthalen-1-yl]-2-methylpropane-2-sulfinamide (12c)



The title compound was obtained following the general procedure described above. Flash chromatography [*n*-hexane/EtOAc (1:1)] afforded compound **12c** as a brown solid (95 %).  $[\alpha]_D^{25} = + 5.0$  (c 1.0; CHCl<sub>3</sub>). <sup>1</sup>H RMN

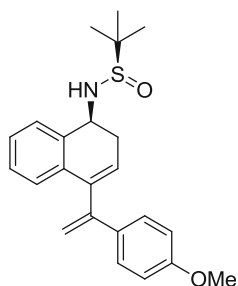
(300 MHz, CDCl<sub>3</sub>)  $\delta$  1.23 (s, 9H), 2.67 (ddd, *J* = 17.2, 7.3, 4.8 Hz, 1H), 2.88 (ddd, *J* = 17.2, 5.8, 4.3 Hz, 1H), 3.51 (d, *J* = 8.5 Hz, 1H), 3.76 (s, 3H), 4.57 (dd, *J* = 13.9, 7.6 Hz, 1H), 5.34 (d, *J* = 1.6 Hz, 1H), 5.66 (d, *J* = 1.6 Hz, 1H), 6.08 (t, *J* = 4.5 Hz, 1H), 6.78 (ddd, *J* = 8.2, 2.5, 0.9 Hz, 1H), 6.95–6.99 (m, 2H), 7.01 (dd, *J* = 7.5, 1.4 Hz, 1H), 7.08–7.20 (m, 3H), 7.35–7.41 (m, 1H). <sup>13</sup>C RMN (75 MHz, CDCl<sub>3</sub>)  $\delta$  22.7 (3xCH<sub>3</sub>), 32.7 (CH<sub>2</sub>), 54.5 (CH), 55.2 (CH<sub>3</sub>), 56.1 (C), 112.7 (CH), 112.7 (CH), 115.7 (CH<sub>2</sub>), 119.3 (CH), 125.2 (CH), 126.3 (CH), 126.6 (2xCH), 127.4 (CH), 127.9 (2xCH), 129.3 (CH), 133.5 (C), 135.7 (C), 139.6 (C), 141.3 (C), 147.8 (C), 159.6 (C). HRMS (EI) calcd for C<sub>23</sub>H<sub>27</sub>NO<sub>2</sub>S [M + H]<sup>+</sup>: 382.1835, found: 382.1819.

(*R<sub>S</sub>*)-*N*-[(*S*)-4-(1-(3,5-Bis(trifluoromethyl)phenyl)vinyl)-1,2-dihydronaphthalen-1-yl]-2-methylpropane-2-sulfinamide (12d)



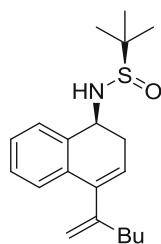
The title compound was obtained following the general procedure described above. Flash chromatography [*n*-hexane/EtOAc (1:1)] afforded compound **12d** as a brown solid (73 %).  $[\alpha]_D^{25} = + 15.0$  (c 1.0; CHCl<sub>3</sub>). <sup>1</sup>H RMN (300 MHz, CDCl<sub>3</sub>)  $\delta$  1.22 (s, 9H), 2.74 (ddd, *J* = 17.4, 7.1, 4.8 Hz, 1H), 2.92 (ddd, *J* = 17.3, 6.0, 4.3 Hz, 1H), 3.48 (d, *J* = 8.8 Hz, 1H), 4.58 (dd, *J* = 15.2, 6.7 Hz, 1H), 5.56 (d, *J* = 0.7 Hz, 1H), 5.78 (d, *J* = 0.9 Hz, 1H), 6.15 (t, *J* = 4.5 Hz, 1H), 6.90 (dd, *J* = 7.6, 1.1 Hz, 1H), 7.13 (td, *J* = 7.5, 1.4 Hz, 1H), 7.22 (td, *J* = 7.5, 1.4 Hz, 1H), 7.41 (d, *J* = 7.4 Hz, 1H), 7.75 (s, 1H), 7.80 (s, 2H). <sup>19</sup>F RMN (282 MHz, CDCl<sub>3</sub>)  $\delta$  -62.84 (2xCF<sub>3</sub>). <sup>13</sup>C RMN (75 MHz, CDCl<sub>3</sub>)  $\delta$  22.6 (3xCH<sub>3</sub>), 32.7 (CH<sub>2</sub>), 54.4 (CH), 56.2 (C), 119.1 (CH<sub>2</sub>), 121.5 (d, <sup>3</sup>*J*<sub>CF</sub> = 5.5 Hz, 2xCH), 125.9 (CH), 126.6 (CH), 126.8 (q, <sup>1</sup>*J*<sub>CF</sub> = 272.9 Hz, 2xCF<sub>3</sub>), 126.9 (CH), 127.1 (CH), 127.9 (CH), 128.1 (CH), 131.8 (d, <sup>2</sup>*J*<sub>CF</sub> = 33.2 Hz, 2xC), 132.4 (C), 135.9 (C), 138.2 (C), 142.2 (C), 145.7 (C). HRMS (EI) calcd for C<sub>24</sub>H<sub>23</sub>NOF<sub>6</sub>S [M + H]<sup>+</sup>: 488.1477, found: 488.1464.

(*R<sub>S</sub>*)-*N*-[(*S*)-4-(1-(4-Methoxyphenyl)vinyl)-1,2-dihydronaphthalen-1-yl]-2-methylpropane-2-sulfinamide (12e)



The title compound was obtained following the general procedure described above. Flash chromatography [*n*-hexane/EtOAc (1:1)] afforded compound **12e** as a brown solid (98 %).  $[\alpha]_D^{25} = +6.0$  (c 1.0; CHCl<sub>3</sub>). <sup>1</sup>H RMN (300 MHz, CDCl<sub>3</sub>) δ 1.23 (s, 9H), 2.66 (ddd, *J* = 17.2, 7.2, 4.8 Hz, 1H), 2.88 (ddd, *J* = 17.1, 5.7, 4.3 Hz, 1H), 3.52 (d, *J* = 8.1 Hz, 1H), 3.76 (s, 3H), 4.58 (dd, *J* = 13.7, 7.4 Hz, 1H), 5.24 (d, *J* = 1.6 Hz, 1H), 5.57 (d, *J* = 1.7 Hz, 1H), 6.08 (t, *J* = 4.5 Hz, 1H), 6.74–6.80 (m, 2H), 7.00 (dd, *J* = 7.5, 1.3 Hz, 1H), 7.10 (td, *J* = 7.5, 1.5 Hz, 1H), 7.17 (td, *J* = 7.4, 1.5 Hz, 1H), 7.30–7.36 (m, 2H), 7.39 (d, *J* = 6.9 Hz, 1H). <sup>13</sup>C RMN (75 MHz, CDCl<sub>3</sub>) δ 22.7 (3xCH<sub>3</sub>), 32.6 (CH<sub>2</sub>), 54.4 (CH), 55.2 (CH<sub>3</sub>), 56.1 (C), 113.6 (CH<sub>2</sub>), 113.7 (CH), 124.9 (CH), 126.4 (2xCH), 126.7 (CH), 127.3 (CH), 127.8 (2xCH), 128.0 (CH), 132.3 (C), 133.6 (C), 135.6 (C), 139.8 (C), 147.3 (C), 159.3 (C). HRMS (EI) calcd for C<sub>23</sub>H<sub>27</sub>NO<sub>2</sub>S [M + H]<sup>+</sup>: 382.1835, found: 382.1833.

(*R*<sub>S</sub>)-*N*-[(*S*)-4-(Hex-1-en-2-yl)-1,2-dihydronaphthalen-1-yl]-2-methylpropane-2-sulfonamide (**12f**)



The title compound was obtained following the general procedure described above. Flash chromatography [*n*-hexane/EtOAc (1:1)] afforded compound **12f** as a brown solid (50 %).  $[\alpha]_D^{25} = +7.9$  (c 1.0; CHCl<sub>3</sub>). <sup>1</sup>H RMN (300 MHz, CDCl<sub>3</sub>) δ 0.86 (t, *J* = 7.1 Hz, 3H), 1.18 (s, 9H), 1.28–1.35 (m, 2H), 1.47 (d, *J* = 4.8 Hz, 2H), 2.24 (t, *J* = 7.0 Hz, 2H), 2.58 (ddd, *J* = 17.0, 6.9, 5.0 Hz, 1H),

2.73 (ddd, *J* = 17.0, 5.6, 4.3 Hz, 1H), 3.47 (d, *J* = 8.7 Hz, 1H), 4.45 (dd, *J* = 14.8, 6.5 Hz, 1H), 5.00 (d, *J* = 2.3 Hz, 1H), 5.08 (ddd, *J* = 2.3, 1.2 Hz, 1.2 Hz, 1H), 5.86 (t, *J* = 4.5 Hz, 1H), 7.19–7.28 (m, 3H), 7.35–7.40 (m, 1H). <sup>13</sup>C RMN (75 MHz, CDCl<sub>3</sub>) δ 13.9 (CH<sub>3</sub>), 22.2 (CH<sub>2</sub>), 22.6 (3xCH<sub>3</sub>), 30.5 (CH<sub>2</sub>), 32.4 (CH<sub>2</sub>), 35.5 (CH<sub>2</sub>), 54.7 (CH), 56.1 (C), 114.2 (CH<sub>2</sub>), 122.0 (CH), 125.7 (CH), 126.7 (CH), 127.3 (CH), 127.9 (CH), 133.3 (C), 136.3 (C), 140.8 (C), 148.7 (C). HRMS (EI) calcd for C<sub>20</sub>H<sub>29</sub>NOS [M + H]<sup>+</sup>: 332.2043, found: 332.2040.

**Acknowledgments** We thank the Spanish MINECO (CTQ2013-43310) and Generalitat Valenciana (PROMETEOII/2014/073) for their financial support. R. L. thanks the Spanish MINECO for a predoctoral fellowship.

## References

- Collins S, Barlett S, Nie F, Sore HF, Spring DR (2016) *Synthesis* 48:1457
- Serba C, Winssinger N (2013) *Eur J Org Chem* 2013:4195
- MacLellan P, Nelson A (2013) *Chem Commun* 49:2383
- O'Connor CJ, Beckmann HSG, Spring DR (2012) *Chem Soc Rev* 41:4444
- For some representative early reports, see: Burke MD, Schreiber SL (2004) *Angew Chem Int Ed* 43:46
- Schreiber SL (2000) *Science* 287:1964
- Lázaro R, Román R, Sedgwick DM, Haufe G, Barrio P, Fustero S (2016) *Org Lett* 18:948
- Fustero S, Lázaro R, Aiguabella N, Riera A, Simón-Fuentes A, Barrio P (2014) *Org Lett* 16:1224
- Fustero S, Lázaro R, Herrera L, Rodríguez E, Mateu N, Barrio P (2013) *Org Lett* 15:3770
- Fustero S, Rodríguez E, Lázaro R, Herrera L, Catalán S, Barrio P (2013) *Adv Synth Catal* 355:1058
- Fustero S, Rodríguez E, Herrera L, Asensio A, Maestro MA, Barrio P (2011) *Org Lett* 13:6564
- Barrio P, Ibañez I, Herrera L, Román R, Catalán S, Fustero S (2015) *Chem Eur J* 21:11579
- Fustero S, Ibañez I, Barrio P, Maestro MA, Catalán S (2013) *Org Lett* 15:832
- Fustero S, Herrera L, Lázaro R, Rodríguez E, Maestro MA, Mateu N, Barrio P (2013) *Chem Eur J* 19:11776
- Fustero S, Moscardó J, Sánchez-Roselló M, Rodríguez E, Barrio P (2010) *Org Lett* 12:5494
- Barrio P, Rodríguez E, Fustero S (2016) *Chem Rec* 18(4):2046
- Sirvent JA, Foubelo F, Yus M (2013) *Eur J Org Chem* 2013:2461
- Villar H, Frings M, Bolm C (2007) *Chem Soc Rev* 36:55
- Rodríguez E, Grayson MN, Asensio A, Barrio P, Houk KN, Fustero S (2016) *ACS Cat* 6:2506
- Fustero S, Bello P, Miró J, Simón A, del Pozo C (2012) *Chem Eur J* 18:10991

# SCIENTIFIC REPORTS



OPEN

## Hyodeoxycholic acid derivatives as liver X receptor $\alpha$ and G-protein-coupled bile acid receptor agonists

Simona De Marino<sup>1</sup>, Adriana Carino<sup>2</sup>, Dario Masullo<sup>1</sup>, Claudia Finamore<sup>1</sup>, Silvia Marchianò<sup>2</sup>, Sabrina Cipriani<sup>2</sup>, Francesco Saverio Di Leva<sup>1</sup>, Bruno Catalanotti<sup>1</sup>, Ettore Novellino<sup>1</sup>, Vittorio Limongelli<sup>1,3</sup>, Stefano Fiorucci<sup>2,\*</sup> & Angela Zampella<sup>1,\*</sup>

Received: 05 October 2016

Accepted: 23 January 2017

Published: 24 February 2017

Bile acids are extensively investigated for their potential in the treatment of human disorders. The liver X receptors (LXRs), activated by oxysterols and by a secondary bile acid named hyodeoxycholic acid (HDCA), have been found essential in the regulation of lipid homeostasis in mammals. Unfortunately, LXR $\alpha$  activates lipogenic enzymes causing accumulation of lipid in the liver. In addition to LXRs, HDCA has been also shown to function as ligand for GPBAR1, a G protein coupled receptor for secondary bile acids whose activation represents a promising approach to liver steatosis. In the present study, we report a library of HDCA derivatives endowed with modulatory activity on the two receptors. The lead optimization of HDCA moiety was rationally driven by the structural information on the binding site of the two targets and results from pharmacological characterization allowed the identification of hyodeoxycholane derivatives with selective agonistic activity toward LXR $\alpha$  and GPBAR1 and notably to the identification of the first example of potent dual LXR $\alpha$ /GPBAR1 agonists. The new chemical entities might hold utility in the treatment of dyslipidemic disorders.

Liver X receptor  $\alpha$  and  $\beta$  (LXRs) are ligand activated transcription factors. LXRs function as heterodimers with the retinoid X receptor (RXR) and are activated by naturally occurring cholesterol metabolites known as oxysterols<sup>1,2</sup>. LXR $\alpha$  and LXR $\beta$  share a high structural homology<sup>3</sup>, but are differentially expressed in mammalian tissues. Thus, while LXR $\alpha$  is primarily expressed in liver, intestine, adipose tissue, and macrophages, LXR $\beta$  is ubiquitously expressed.

Upon ligand-induced activation, both LXR isoforms regulate gene expression through binding to LXR response elements (LXREs) in the promoter regions of the target genes. In the liver, LXR $\alpha$  directly induces cytochrome 7A1 (CYP7A1), promoting the conversion of cholesterol into bile acids. In macrophages and adipocytes, LXRs induce the expression of ATP-binding cassettes ABCA1, ABCG1 and apolipoprotein (apoE), increasing the efflux of cholesterol from cells<sup>4,5</sup>, and exerts anti-inflammatory activities<sup>6,7</sup> with beneficial effects in rodent models of diabetes and insulin resistance<sup>8,9</sup>.

These genetic and pharmacological approaches have shown that LXRs are potentially druggable receptors that might hold utility in the treatment of highly prevalent human diseases including obesity, diabetes, neurodegenerative diseases and chronic inflammatory states<sup>10,11</sup>. Unfortunately, the available synthetic agonists for LXR $\alpha$  cause the activation of hepatic lipogenic enzymes, thereby increasing triglyceride synthesis and accumulation, hampering their clinical utility in cardiovascular disease<sup>12</sup>. In mammals, hyodeoxycholic acid (HDCA, **1** in Fig. 1), a naturally occurring secondary bile acid generated in human small intestine by bacterial C-6 hydroxylation of lithocholic acid (LCA, **2**)<sup>13</sup>, is a weak LXR $\alpha$  agonist<sup>14</sup>. Indeed, HDCA has been shown effective in the treatment of rodent models of metabolic disorders<sup>15,16</sup> and a diet enriched with HDCA was found to protect against atherosclerotic plaques formation in LDL receptor-knockout mice by reducing intestinal cholesterol absorption and increasing HDL-mediated cholesterol efflux from foam cells and macrophages<sup>17</sup>. In addition, HDCA exerts hypolipidemic effect in mice, reducing in liver the gene expression of sterol regulatory element binding protein

<sup>1</sup>Department of Pharmacy, University of Naples "Federico II", Via D. Montesano, 49, I-80131 Naples, Italy.

<sup>2</sup>Department of Surgery and Biomedical Sciences, Nuova Facoltà di Medicina, P.zza L. Severi 1-06132, Perugia, Italy. <sup>3</sup>Università della Svizzera Italiana (USI), Faculty of Informatics, Institute of Computational Science - Center for Computational Medicine in Cardiology, Via G. Buffi 13, CH-6900 Lugano, Switzerland. \*These authors contributed equally to this work. Correspondence and requests for materials should be addressed to A.Z. (email: angela.zampella@unina.it)



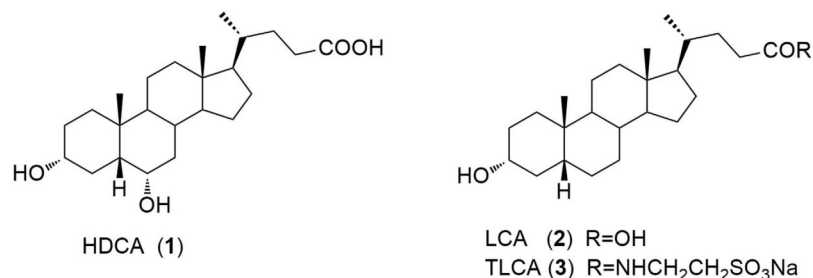


**Figure 1. Naturally occurring bile acids.** HDCA, a weak LXR $\alpha$ /GPBAR1 dual agonist and LCA and its tauro-conjugated derivative, TLCA, the most potent endogenous activators of GPBAR1.

1c (SREPB1c), acetyl-CoA carboxylase (ACoA synthase), fatty acid synthase (FAS), and stearyl-CoA desaturase (S-CoA Des)<sup>18</sup>.

*In vitro* studies have also demonstrated that HDCA is a weak agonist for the G-protein-coupled bile acid receptor GPBAR1 (also known as TGR5), with an EC<sub>50</sub> of 31.6  $\mu$ M<sup>19</sup>. GPBAR1 is a membrane bile acid receptor<sup>20</sup>, highly expressed in non-parenchymal liver cells, gallbladder, intestine, heart, spleen, kidney, placenta, leukocytes, skeletal muscle and brown adipose tissue (BAT)<sup>21</sup>. GPBAR1 is preferentially activated by LCA (2) and taurolithocholic acid (TLCA, 3 in Fig. 1), with EC<sub>50</sub> of 0.53  $\mu$ M and 0.29  $\mu$ M, respectively<sup>22</sup>.

GPBAR1 activation leads to genomic and non-genomic effects. While non-genomic effects are mediated by the modulation of intracellular concentrations of cAMP, the genomic effects are mediated by the PKA-dependent phosphorylation of CREB (cAMP response element-binding protein), a cellular transcription factor that binds to specific DNA sequences called cAMP response elements (CRE), in the promoter of target genes. In muscles and brown adipose tissue, GPBAR1 increases energy expenditure and oxygen consumption<sup>23</sup>, while in the entero-endocrine L cells, stimulates the secretion of glucagon-like peptide (GLP)-1, an incretin that increases insulin release, thus regulating glucose blood levels, gastrointestinal motility and appetite<sup>24</sup>.

Similarly to LXRs, GPBAR1 is a potentially druggable receptor and might have application in the treatment of metabolic disorders including obesity, diabetes, dyslipidemias, atherosclerosis, liver steatohepatitis, and neurologic disorders<sup>25,26</sup>.

In this framework, we have set to explore the chemical space of HDCA with the aim to develop ligands endowed with dual agonist activity towards LXR $\alpha$  and GPBAR1. The newly identified compounds by simultaneously activating LXR $\alpha$  and GPBAR1 could allow targeting metabolic/inflammatory disorders with a novel mechanism of action.

With this background in mind, a large family of hyodeoxycholane derivatives was prepared through various chemical modifications. As shown in Fig. 2, we first introduced on the HDCA scaffold numerous apolar side chains, differing in length, ramification and presence/absence of unsaturation (Subset A). The rationale of this choice relies on the structural features of the ligand-binding site of both LXR $\alpha$  and GPBAR1. In particular, the binding pocket of LXR $\alpha$  is rather amphipathic and thus able to host ligands endowed with both polar and hydrophobic branches<sup>27</sup>. On the other hand, the GPBAR1 ligand-binding pocket presents a small lipophilic cleft that might be targeted by relatively short hydrophobic chains (Fig. 3). Therefore, the introduction on the HDCA steroidal scaffold of hydrophobic side chains with different length can help in deciphering the structural requisites to achieve a dual activity on the two receptors. The obtained set of derivatives was then subjected to a second round of chemical modifications focused on the steroidal scaffold. This step allowed investigating the effect of the A/B ring junction, the stereochemistry at C-3 and the hydroxyl group at C-6 on the ligand affinity towards the receptors (Subset B, Fig. 4). Pharmacological experiments resulted in the identification of several compounds endowed with selective agonistic activity toward LXR $\alpha$  and GPBAR1 and notably to the identification of compound **14**, the first example of potent dual LXR $\alpha$ /GPBAR1 modulator. *In vivo* administration of this modulator, allowed us to investigate the effects of dual LXR $\alpha$ /GPBAR1 activation on mice metabolism.

## Results

**Preparation of Subset A derivatives.** Aldehyde **34** was used as a cornerstone intermediate in the preparation of compounds **4–12**. A four-step reaction sequence on HDCA, including preparation of methyl ester **31**, protection of alcoholic functions at C-3 and C-6, reduction of the side chain methyl ester and subsequent Swern oxidation furnished aldehyde **34** in quantitative yield (Fig. 5).

As depicted in Fig. 6, Wittig olefination with isopropyl triphenylphosphonium iodide followed by the removal of 3 $\alpha$ , 6 $\alpha$ -dihydroxy protective groups gave **4** that was also used as starting material in double bond hydrogenation affording the saturated derivative **5** in quantitative yield.

Compounds **6–12**<sup>28</sup> (Figs 6 and 7) were prepared following the same synthetic protocol and using isobutyl triphenylphosphonium iodide, methyl triphenylphosphonium iodide and benzyl triphenylphosphonium iodide, respectively in Wittig olefination.

Figures 8 and 9 illustrate the synthetic protocols for the preparation of HDCA derivatives with *nor* and *bisnor* alkenyl and alkyl side chains. As previously reported<sup>29</sup>, HDCA was subjected to one-carbon degradation at C-24 through the so-called second order “Beckmann rearrangement” affording the 24-*normethyl* ester **37** (Fig. 8). Protection at C-3 and C-6 hydroxyl groups, followed by reduction of side chain methyl ester and subsequent Swern oxidation furnished key intermediate aldehyde **38** in 94% yield.

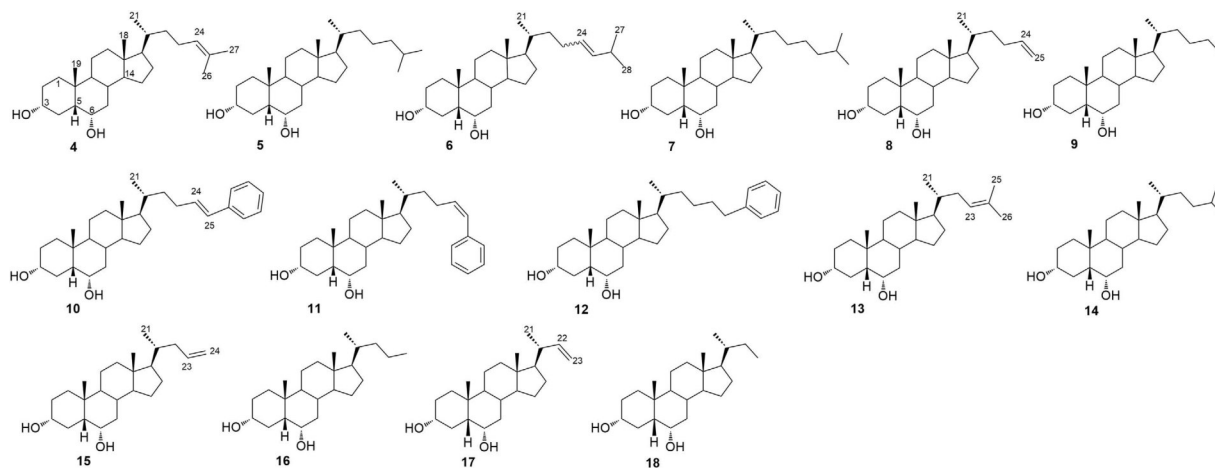


**Figure 2. Subset A: installation of a hydrophobic side chain on hydoexocholane scaffold.**

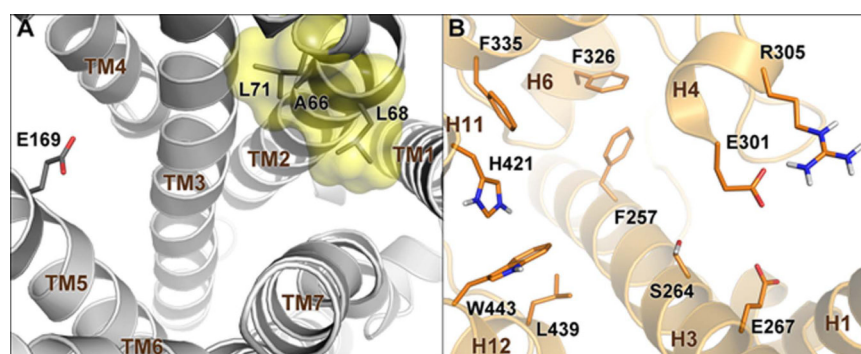


**Figure 3. Ligand binding sites of GPBAR1 and LXR $\alpha$ .** In (A) the amino acids defining the small lipophilic cleft in GPBAR1 are highlighted as yellow transparent surface. (B) Shows the amphipathic nature of LXR $\alpha$ -LBD characterized by the presence of both polar and hydrophobic residues. GPBAR1 and LXR $\alpha$  are shown as gray and orange cartoons, respectively. In both receptors, representative residues are depicted as sticks. Non-polar hydrogens are omitted for clarity.

Wittig olefination and double bond hydrogenation, in the same operative conditions described for the preparation of derivatives **4/5** and **8/9**, gave the corresponding *nor* derivatives **13/14** and **15/16**.

The preparation of C23-analogues **17** and **18** began with the acetylation of HDCA (Fig. 9). Radical oxidative decarboxylation of protected carboxylic acid **39** by treatment with Cu(OAc)<sub>2</sub> and Pb(OAc)<sub>4</sub> furnished the  $\Delta^{22}$  derivative **40**. Sodium methoxide treatment gave the alkene **17** in 90% yield that in turn was also used as starting material to obtain the corresponding saturated derivative **18**.

**Preparation of subset B derivatives.** At this point, our chemical speculation was extended to the tetracyclic nucleus exploring the influence of the hydroxyl group at C-6 as well as the configuration of the hydroxyl group at C-3 and the A/B ring junction. Thus, to obtain the corresponding 6-deoxy derivatives **19–24**, LCA was subjected to the four-step sequence depicted in Fig. 10 including TBS-protection at C-3, methyl ester formation at C-24, reduction to the corresponding primary alcohol and finally Swern oxidation to obtain aldehyde **41**. Wittig olefination with methyl triphenylphosphonium iodide and with isopropyl triphenylphosphonium iodide furnished the installation of a terminal alkene and a dimethyl branched alkene as side chain end group in **19** and **21**, respectively. Hydrogenation with Pd(OH)<sub>2</sub> as catalyst on a small portion of each compound end group gave the corresponding saturated derivatives **20** and **22**. Finally, oxidative decarboxylation on 3-O-acetyl LCA **42** followed by removal of the protecting group at C-3 position gave the alkene **23** that in turn was hydrogenated to the corresponding C23-alkyl derivative **24** (Fig. 10).

In the preparation of 3 $\beta$ -hydroxy-5 $\alpha$ -cholane derivatives **25–30**, HDCA was transformed in the methyl 3 $\beta$ -hydroxy-5 $\alpha$ -cholan-24-oate **43** following our previously published procedure (Fig. 11)<sup>30</sup>.

Then, conversion to aldehyde **44** and Wittig olefination/reduction gave compounds **25–28**, following the same synthetic protocol described in Fig. 6.

Intermediate **43** was also used as starting material in the oxidative decarboxylation affording alkene **29** in 62% yield. Hydrogenation at the side chain double bond furnished compound **30**.

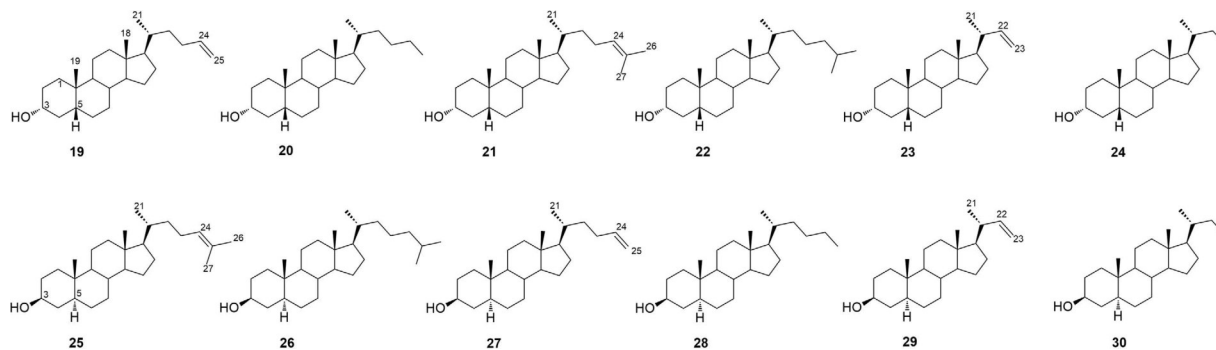


**Figure 4. Subset B: installation of a hydrophobic side chain on modified A-B ring hydoexycholane scaffold.**

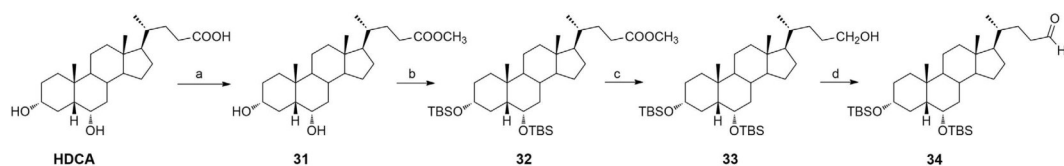


**Figure 5. Synthesis of key aldehyde 34. Reagents and conditions:** (a) p-TsOH, MeOH dry, quantitative yield; (b) 2,6-lutidine, t-butyldimethylsilyltrifluoromethanesulfonate,  $\text{CH}_2\text{Cl}_2$ , 0 °C, quantitative yield; (c)  $\text{LiBH}_4$ , MeOH dry, THF, 0 °C, 56%; (d) DMSO, oxalyl chloride, TEA dry,  $\text{CH}_2\text{Cl}_2$ , -78 °C, quantitative yield.

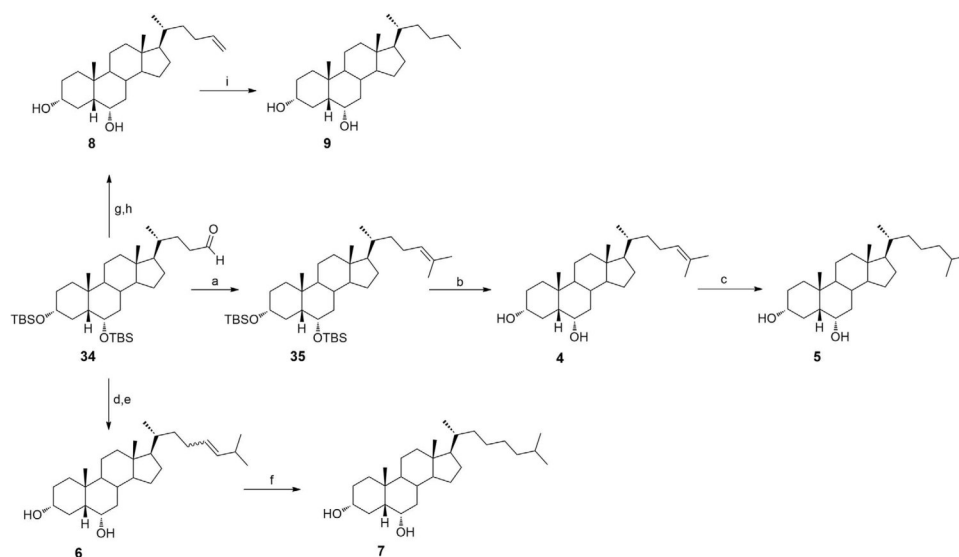


**Figure 6. Preparation of Subset A derivatives: introduction of C25 linear and C26/C27 branched aliphatic side chains on hydoexycholane scaffold. Reagents and conditions:** (a) *n*-BuLi, isopropyl triphenylphosphonium iodide, THF dry, r.t., 84%; (b) HCl 37%, MeOH, quantitative yield; (c)  $\text{H}_2$ , Pd(OH)<sub>2</sub> degussa type, THF:MeOH dry 1:1, quantitative yield; (d) *n*-BuLi, isobutyl triphenylphosphonium iodide, THF dry, r.t.; (e) HCl 37%, MeOH; (f)  $\text{H}_2$ , Pd(OH)<sub>2</sub> degussa type, THF:MeOH dry 1:1; (g) *n*-BuLi, methyl triphenylphosphonium iodide, THF dry, r.t., 60%; (h) HCl 37%, MeOH, quantitative yield; (i)  $\text{H}_2$ , Pd(OH)<sub>2</sub> degussa type, THF:MeOH dry 1:1, 70%.

**In vitro pharmacological evaluation.** Derivatives 4–30 were tested for their activity in a luciferase reporter assay with HepG2 and HEK-293T cells transfected with LXR $\alpha,\beta$  and GPBAR1, respectively. Table 1 reports the efficacy of tested compounds compared to those of reference compounds, GW3965 for LXR $\alpha/\beta$  and TLCA for GPBAR1.

Each compound was tested at the concentration of 10  $\mu\text{M}$  and transactivation activity of GW3965 on LXRs and TLCA on CRE (i.e. TGR5/GPBAR1) was considered equal to 100%.

As shown in Table 1, the introduction of a hydrophobic side chain on the hydoexycholane scaffold (Subset A, compounds 4–18) produced beneficial effects on LXR $\alpha$ . Inspection of biological activity clearly indicates that

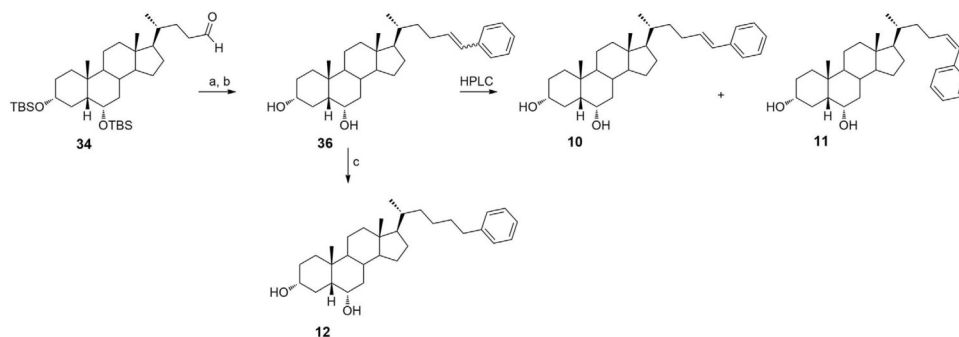


**Figure 7. Preparation of Subset A derivatives: introduction of an aromatic end-group side chain on hedeoerycholine scaffold.** Reagents and conditions: (a) *n*-BuLi, benzyl triphenylphosphoniumiodide, THF dry; (b) HCl 37%, MeOH, 67% over two steps; (c) H<sub>2</sub>, Pd(OH)<sub>2</sub> degussa type, THF:MeOH dry 1:1, quantitative yield.

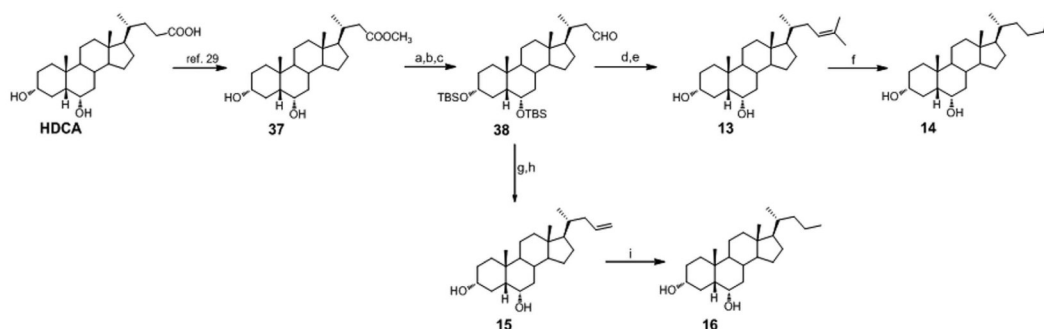


**Figure 8. Preparation of Subset A derivatives: introduction of C24 linear and C25 branched aliphatic side chains on hedeoerycholine scaffold.** Reagents and conditions: (a) 2,6-lutidine, *t*-butyldimethylsilyltrifluoromethanesulfonate, CH<sub>2</sub>Cl<sub>2</sub>, 0 °C; (b) LiBH<sub>4</sub>, MeOH dry in THF dry; (c) DMSO, oxalyl chloride, TEA dry, CH<sub>2</sub>Cl<sub>2</sub>, -78 °C, 94% over three steps; (d) *n*-BuLi, isopropyl triphenylphosphonium iodide, THF dry, r.t.; (e) HCl 37%, MeOH, 80% over two steps; (f) H<sub>2</sub>, Pd(OH)<sub>2</sub> degussa type, THF/MeOH 1:1, 90%; (g) *n*-BuLi, methyl triphenylphosphonium iodide, THF dry; (h) HCl 37%, MeOH, 95% over two steps; (i) H<sub>2</sub>, Pd(OH)<sub>2</sub> degussa type, THF/MeOH dry 1:1, 88%.

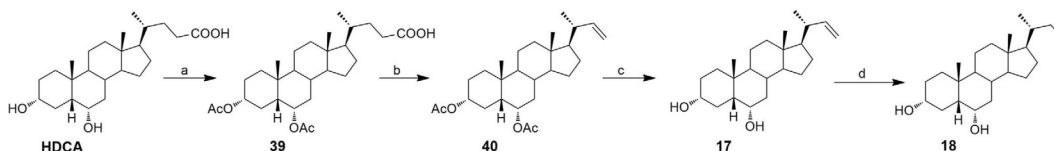


**Figure 9. Preparation of Subset A derivatives: introduction of a C23 linear aliphatic side chain on hedeoerycholine scaffold.** Reagents and conditions: (a) Ac<sub>2</sub>O, pyridine, quantitative yield; (b) Cu(OAc)<sub>2</sub> · H<sub>2</sub>O, Pb(OAc)<sub>4</sub> in toluene dry/pyridine dry, 17%; (c) CH<sub>3</sub>ONa, CHCl<sub>3</sub> dry/MeOH dry 5:3 v/v, 90%; (d) H<sub>2</sub>, Pd(OH)<sub>2</sub> degussa type, THF dry/MeOH dry 1:1 v/v, quantitative yield.

in the above subset, the efficacy in transactivating LXR $\alpha$  is in correlation with the size of the installed side chain and with the presence of a double bond. The correlation activity/side chain length is not linear with a reduction in LXR $\alpha$  activity for derivatives with too long (compounds 6 and 7) or too short side chain (compounds 15–18) whereas, as general trend, the presence of a double bond leads to a reduction of the efficacy. Therefore, the best match has been found for compounds 5, 12 and 14 with an efficacy of 73%, 63% and 109%, respectively.

On the other hand, the length of side chain produces opposite effects on GPBAR1 with improved efficacy of hedeoerycholine derivatives with shortened side chains (derivatives 13–17).

Analysis of biological data for subset B compounds reveals that the elimination of the hydroxyl group at C-6 is detrimental in term of LXR $\alpha$  transactivation whereas produce positive effects on GPBAR1. Derivatives 19–30 shows GPBAR1 efficacy in a 51–96% range.

While the above activity is slightly affected by the configuration of the hydroxyl group at C-3 and of the A/B ring junction, the GPBAR1 efficacy is favored with the shortening of the side chain with compounds 24 and 29, the most efficacious GPBAR1 selective agonists identified in this study. Of interest the presence of a double bond

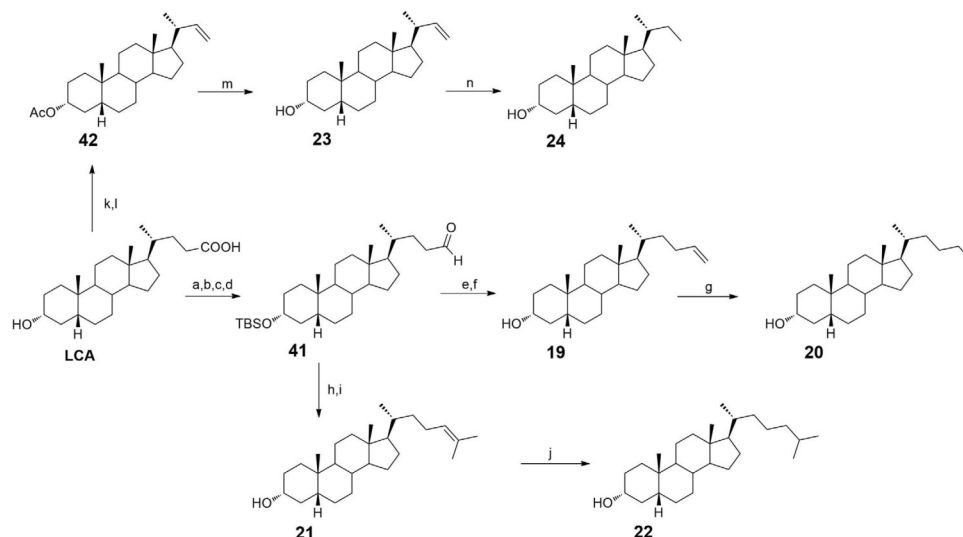


**Figure 10. Preparation of Subset B derivatives. Linear C23/C25 and branched C26 aliphatic side chains on 6-deoxyhydrodeoxycholate scaffold.** Reagents and conditions: (a) *p*-TsOH, MeOH dry; (b) 2,6-lutidine, *t*-butyldimethylsilyltrifluoromethanesulfonate, CH<sub>2</sub>Cl<sub>2</sub>, 0 °C; (c) LiBH<sub>4</sub>, MeOH dry, THF, 0 °C; (d) DMSO, oxalyl chloride, TEA dry, CH<sub>2</sub>Cl<sub>2</sub>, -78 °C, 72% over four steps; (e) *n*-BuLi, methyl triphenylphosphonium iodide, THF dry, r.t.; (f) HCl 37%, MeOH, quantitative yield over two steps; (g) H<sub>2</sub>, Pd(OH)<sub>2</sub> degussa type, THF:MeOH dry 1:1, 86%; (h) *n*-BuLi, isopropyl triphenylphosphonium iodide, THF dry, r.t.; (i) HCl 37%, MeOH, 40% over two steps; (j) H<sub>2</sub>, Pd(OH)<sub>2</sub> degussa type, THF:MeOH dry 1:1, quantitative yield; (k) Ac<sub>2</sub>O, Pyr; (l) Cu(OAc)<sub>2</sub> H<sub>2</sub>O, Pb(OAc)<sub>4</sub> in toluene dry/pyridine dry, quantitative yield over two steps; (m) CH<sub>3</sub>ONa, CHCl<sub>3</sub> dry/MeOH dry 5:3 v/v, 27%; (n) H<sub>2</sub>, Pd(OH)<sub>2</sub> degussa type, THF dry/MeOH dry 1:1 v/v, 22%.

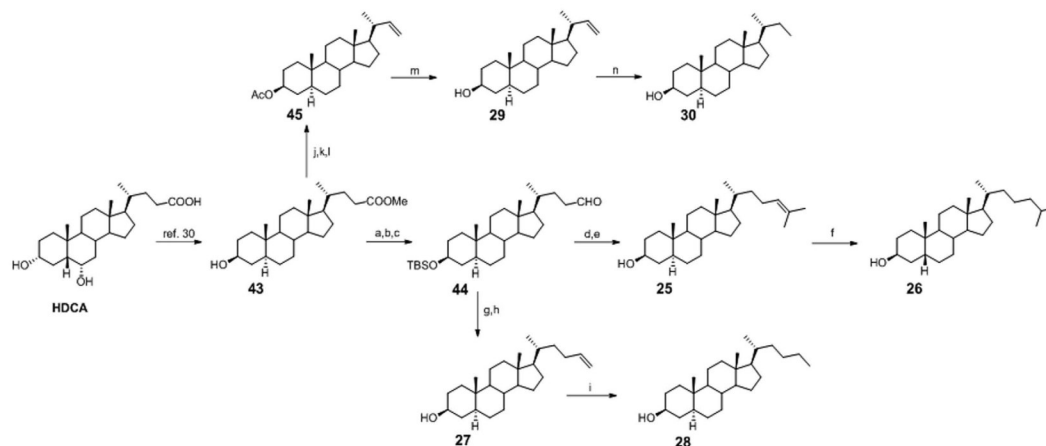


**Figure 11. Preparation of Subset B derivatives. Linear C23/C25 and branched C26 aliphatic side chains on 3β-hydroxy-6-deoxy-5α-hydrodeoxycholate scaffold.** Reagents and conditions: (a) 2,6-lutidine, *t*-butyldimethylsilyltrifluoromethanesulfonate, CH<sub>2</sub>Cl<sub>2</sub>, 0 °C; (b) LiBH<sub>4</sub>, MeOH dry, THF, 0 °C; (c) DMSO, oxalyl chloride, TEA dry, CH<sub>2</sub>Cl<sub>2</sub>, -78 °C, 34% over three steps; (d) *n*-BuLi, isopropyl triphenylphosphonium iodide, THF dry, r.t.; (e) HCl 37%, MeOH, 34% over two steps; (f) H<sub>2</sub>, Pd(OH)<sub>2</sub> degussa type, THF:MeOH dry 1:1, quantitative yield; (g) *n*-BuLi, methyl triphenylphosphonium iodide, THF dry, r.t.; (h) HCl 37%, MeOH, 38% over two steps; (i) H<sub>2</sub>, Pd(OH)<sub>2</sub> degussa type, THF:MeOH dry 1:1, quantitative yield; (j) NaOH, MeOH/H<sub>2</sub>O 1:1 v/v, reflux; (k) Ac<sub>2</sub>O, pyridine; (l) Cu(OAc)<sub>2</sub> H<sub>2</sub>O, Pb(OAc)<sub>4</sub> in toluene dry/pyridine dry, 78%; (m) CH<sub>3</sub>ONa, CHCl<sub>3</sub> dry/MeOH dry 5:3 v/v, 62%; (n) H<sub>2</sub>, Pd(OH)<sub>2</sub> degussa type, THF dry/MeOH dry 1:1 v/v, quantitative yield.

on the side chain increases the efficacy of the derivatives with *trans* A/B ring junction (compare efficacy of **25** vs **26**, **27** vs **28** and **29** vs **30**).

The behavior of compounds with 5β-configuration is quite the contrary, thus indicating that the introduction of a saturated side chain produces beneficial effects on bent shaped nuclei (compare efficacy of **24** vs **23**). None of tested compounds was able to transactivate LXRβ (Table 1) and FXR (Figure S1).

Compound	GPBAR1*		LXR $\alpha$ **		LXR $\beta$
	Efficacy		Efficacy		Efficacy
	(% vs TLCA)	(% vs HDCA)	(% vs GW3965)	(% vs HDCA)	(% vs GW3965)
HDCA	26		15, 5		NA***
4	26, 3	101, 0	49, 3	317, 1	NA
5	14, 9	57, 5	72, 8	468, 1	NA
6	65, 0	249, 8	32, 6	209, 7	NA
7	26, 3	101, 2	28, 0	180, 1	NA
8	25, 5	98, 0	42, 9	276, 3	NA
9	27, 0	103, 9	54, 1	348, 3	NA
10	26, 0	100, 0	12, 2	78, 5	NA
11	33, 2	127, 7	26, 2	168, 3	NA
12	18, 6	71, 7	63, 1	406, 1	NA
13	52, 6	202, 4	36, 1	232, 0	NA
14	55, 1	211, 9	109, 3	703, 3	NA
15	68, 7	264, 0	NA	—	NA
16	53, 7	206, 6	23, 8	153, 0	NA
17	53, 1	204, 3	17, 3	111, 7	NA
18	22, 8	87, 6	NA	—	NA
19	75, 1	288, 7	NA	—	NA
20	74, 0	284, 6	20, 0	128, 6	NA
21	73, 0	280, 7	NA	—	NA
22	77, 1	296, 5	NA	—	NA
23	59, 6	229, 1	NA	—	NA
24	92, 9	357, 1	NA	—	NA
25	58, 1	223, 2	NA	—	NA
26	50, 9	195, 8	NA	—	NA
27	64, 4	247, 7	NA	—	NA
28	54, 9	211, 1	NA	—	NA
29	96, 0	368, 8	15, 0	96, 7	NA
30	58, 1	223, 5	NA	—	NA

**Table 1. GPBAR1 and LXRs efficacy of compounds 4–30.** \*Activity toward GPBAR1 in a reporter assay was assessed in HEK-293T cells transfected with a cAMP responsive element (CRE) cloned upstream to the luciferase gene. For calculation of efficacy data, maximal transactivation of CRE caused by each compound (10  $\mu$ M) was compared to maximal transactivation caused by TLCA (10  $\mu$ M) and by HDCA (10  $\mu$ M). \*\*Activity toward LXR $\alpha$  in a reporter assay was assessed in HepG2 cells transfected with an LXR $\alpha$  responsive element (LRE) cloned upstream to the luciferase gene. For calculation of efficacy data, maximal transactivation of LRE caused by each compound (10  $\mu$ M) was compared to maximal transactivation caused by GW3965 (10  $\mu$ M) and by HDCA (10  $\mu$ M). \*\*\*NA: no activity at 10  $\mu$ M.

Table 2 shows EC<sub>50</sub> values of the most efficacious compounds identified in this study.

Compounds **14** was further investigated *in vitro* to evaluate its effects on LXR $\alpha$  and GPBAR1 target genes by RT-PCR. The HepG2 and Glutag cells ( $1 \times 10^6$ ) were plated and, after 24 hours of starvation, were stimulated with receptor agonists GW3965, TLCA and HDCA (10  $\mu$ M) and with increasing concentration of compound **14** (1, 5, 10, 25, 50  $\mu$ M). As shown in Fig. 12, compound **14** was able to induce the expression of ABCA1 and SREBP1c genes in HepG2 cells in dose-dependent manner with an EC<sub>50</sub> of 8.3  $\mu$ M and 5.8  $\mu$ M respectively.

The compound was also able to activate the expression of pro-glucagon mRNA in Glutag cells; however, the induction is dose-dependent only until the 10  $\mu$ M concentration with an EC<sub>50</sub> of 6.5  $\mu$ M. These results demonstrate that this compound is a potent, effective and selective LXR $\alpha$  and GPBAR1 dual agonist.

Compound **14** was also investigated *in vivo* to verify whether the LXR $\alpha$  activation causes lipid accumulation in the liver. C57BL6 mice were administered with **14** (30 mg/Kg daily by oral gavage) for two weeks. As showed in Fig. 13, no effects were observed in mice treated with compound **14** on the plasmatic levels of AST, cholesterol and triglycerides (Fig. 13A). Liver histology (H&E staining), in which no differences were observed between control group and mice treated with **14** (Fig. 13B), confirmed this result. Real-Time PCR assayed on liver tissue demonstrated that the compound does not induce the expression of steatosis markers genes, FAS, SREBP1c, CD36 and PPARs (Fig. 13C). Of interest, compound **14** increases the expression of GPBAR1 target genes GLP1 and Fgf21 in terminal ileum (Fig. 13D). These results demonstrate that, despite its activity on LXR $\alpha$ , compound **14** does not induce lipid accumulation and liver steatosis and this positive effect is closely related to the simultaneous activation of GPBAR1, as evidenced by the *in vivo* induction of GPBAR1 target genes in the gut.

	GPBAR1	LXR $\alpha$
Compound	Affinity ( $\mu$ M)*	Affinity ( $\mu$ M)
Selective LXR $\alpha$ agonists		
4		6.99 $\pm$ 0.31
5		8.2 $\pm$ 0.16
8		2.7 $\pm$ 0.65
9		5.1 $\pm$ 0.43
12		12.4 $\pm$ 0.41
GPBAR1/LXR $\alpha$ dual agonists		
13	4.2 $\pm$ 0.79	22.3 $\pm$ 3.05
14	4.9 $\pm$ 0.2	3.2 $\pm$ 0.03
Selective GPBAR1 agonists		
15	3.7 $\pm$ 0.38	
17	2.54 $\pm$ 0.015	
20	6.8 $\pm$ 0.08	
21	5.9 $\pm$ 0.055	
24	0.91 $\pm$ 0.092	
25	7.6 $\pm$ 0.71	
27	1 $\pm$ 0.062	
29	4.9 $\pm$ 0.06	
30	1.98 $\pm$ 0.145	

**Table 2.** EC<sub>50</sub> values for selected compounds. \*Data are mean  $\pm$  SE of 3 experiments in duplicate.

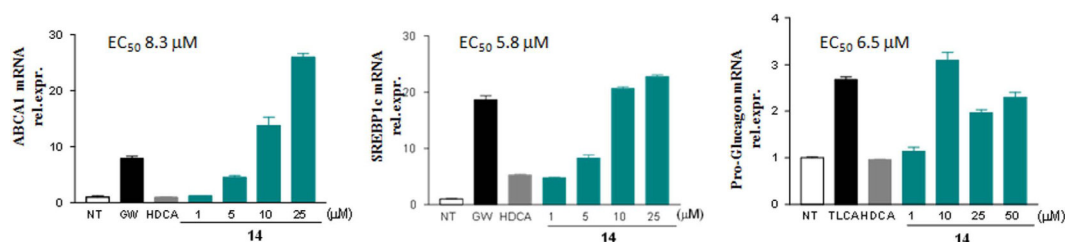


**Figure 12.** Quantitative Real-Time PCR analysis of mRNA expression on LXR $\alpha$  and GPBAR1 target genes. ABCA1 (A) and SREBP1c (B) expression in HepG2 cells primed with increasing concentration of compound **14** (1, 5, 10 and 25  $\mu$ M). GW3965 and HDCA were used as positive controls. Pro-glucagon (C) expression in Glutag cells stimulated with increasing dose of compound **14** (1, 10, 25 and 50  $\mu$ M). TLCA and HDCA were used as a positive control. Values are normalized to GAPDH and are expressed relative to those of not treated cells (NT) which are arbitrarily settled to 1. The relative mRNA expression is expressed as  $2^{(-\Delta\Delta C_t)}$ .

**Molecular Modeling.** In order to investigate the molecular bases of the dual LXR $\alpha$ /GPBAR1 activity of **14**, a thorough computational study has been carried out. First, we performed docking calculations of **14** in the homology model of GPBAR1 that we have previously developed and successfully used for drug design<sup>31</sup>. The best scored docking pose (Fig. 14A) shows that **14** binds to GPBAR1 similarly to other bile acids recently reported by us as agonists of this receptor<sup>31–33</sup>. Nevertheless, some differences can be found. In detail, while the ligand 3 $\alpha$ -hydroxyl group engages the typical H-bond interaction with the Glu169 side chain, the hydrophobic side chain of **14** occupies the small lipophilic pocket formed by Ala66, Leu68 and Leu71 on TM2. This orientation of the side chain in the binding site is different respect to that of the derivatives with polar functional groups on the side chain, which occupy the site interacting with the serine residues of transmembrane helices TM7 and TM1. The ligand binding mode is further stabilized by a set of hydrophobic interactions established by the steroidal scaffold with the side chains of Leu71, Phe96, Leu174 and Trp237.

In order to elucidate the binding mode of **14** to LXR $\alpha$ , docking simulations were performed using the crystal structure of the ligand binding domain (LBD) of the receptor (PDB code: 3IPU)<sup>34</sup>. In this case, docking calculations suggest two possible binding modes, A and B, where the ligand assumes two opposite orientations in the LBD (Figure S2). Specifically, in A the hydrophobic chain of **14** is oriented towards the helices 11 and 12 of LXR $\alpha$ , while the 3 $\alpha$ - and 6 $\alpha$ -hydroxyl groups interact with the residues of the  $\beta$ -sheet close to H1. In B, the steroidal scaffold is oriented in the opposite direction relative to A in the LBD. In particular, the 3 $\alpha$ - and 6 $\alpha$ -hydroxyl groups are close to His421 of helix 11, while the hydrophobic side chain extends towards the  $\beta$ -sheet in the ligand binding pocket. We decided to further investigate the two binding modes assessing their stability through over 100 ns molecular dynamics (MD) calculations. In particular, we evaluated, during the simulation, the conservation of the interactions engaged by the ligand with the protein and the geometrical stability of the ligand by computing the root mean square displacement (rmsd) of its heavy atoms relative to their starting position (see

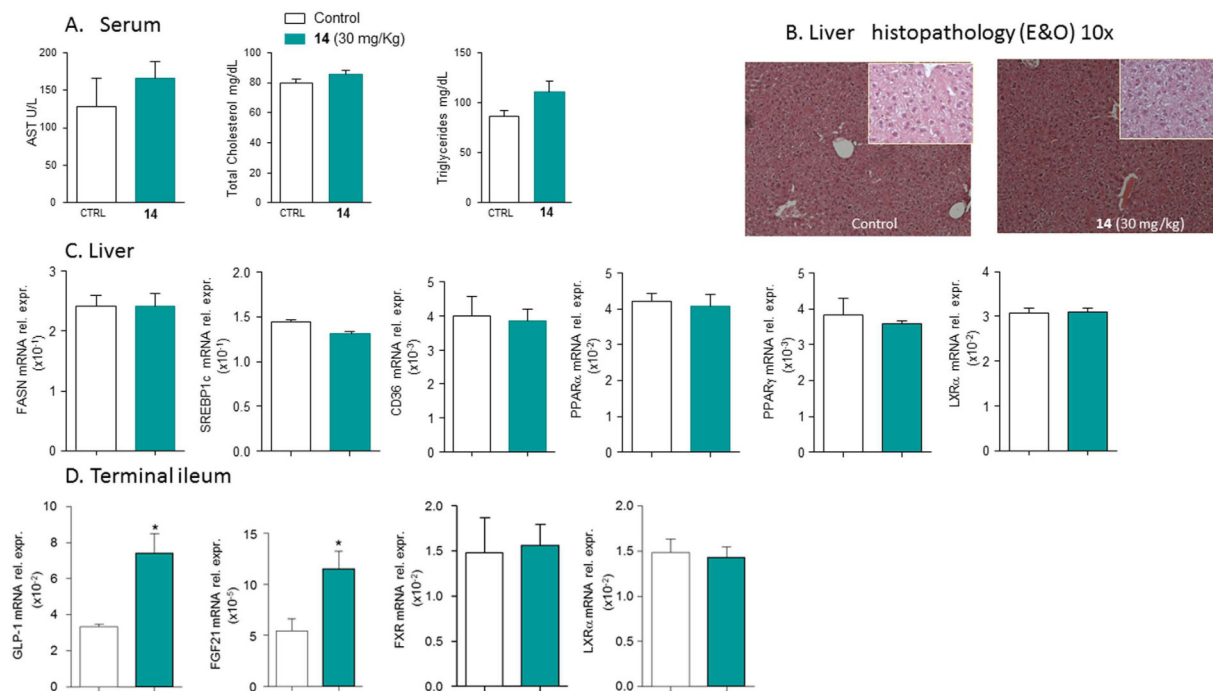


**Figure 13. Effects of compound 14 on hepatic lipid metabolism and on terminal ileum after administration on intact mice.** C57BL6 mice were treated with 14 (30 mg/Kg daily per os) for two weeks. Results are the mean  $\pm$  SE of 3–5 mice per group; \* $p < 0.05$  versus control mice. (A) Serum levels of AST, total cholesterol and triglycerides; (B) Histopathology analysis (Hematoxylin and Eosin) of liver sections. Magnification 4x. Insets magnification 40x. The images show that no fat deposition occurs in the liver of mice treated up to 2 weeks with 14 at the dose of 30 mg/Kg; (C) Relative hepatic mRNA expression of genes involved in fatty acids metabolism (FASN, SREBP1C, CD36) and genes for nuclear receptors (PPAR $\alpha$ , PPAR $\gamma$ , LXR $\alpha$ ); (D) Relative hepatic mRNA expression of GLP-1, FGF21, FXR and LXR $\alpha$  genes in terminal ileum.

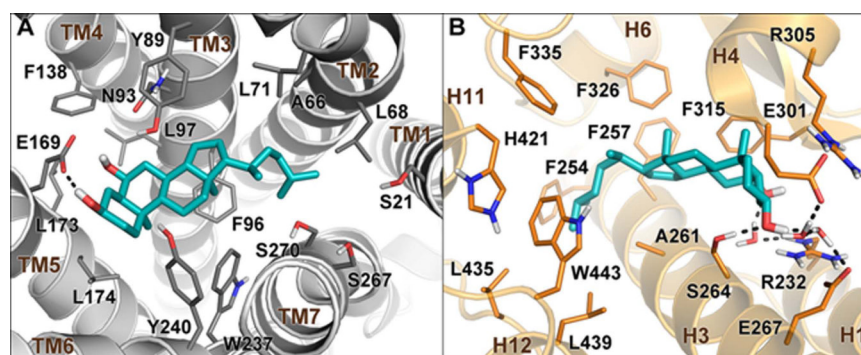


**Figure 14. Binding mode of 14 in GPBAR1 and in LXR $\alpha$ .** (A) Docking pose in the homology model of GPBAR1. (B) Conformation obtained from MD simulations within the LXR $\alpha$  LBD (PDB code: 3IPU). Compound 14 is represented as cyan sticks. GPBAR1 and LXR $\alpha$  are shown as gray and orange cartoons, respectively. Amino acids important for ligand binding are depicted as sticks. Non-polar hydrogens are omitted for clarity.

Figure S3 for details). In B, the original ligand/protein interactions, such as the H-bond between 14 and His421, are lost and the ligand rmsd value increases during the simulation showing instability of this binding mode. At variance with B, in A the ligand rmsd values are low (Figure S3) and all the starting ligand/protein interactions are conserved throughout the simulation. The MD results prompted us to consider only binding mode A for further analysis. In this pose (Fig. 14B and S4), the steroidal scaffold of 14 establishes favorable contacts with lipophilic residues such as Phe257, Phe315 and Phe326, while the 3 $\alpha$ -group of 14 H-bonds with the Ser264 side chain. Additional water-mediated interactions are engaged by both the ligand hydroxyl groups with the side chains of Arg232, Glu267 and Glu301. On the other hand, the ligand hydrophobic side chain inserts into a deep lipophilic pocket shaped by helices (H) 3, 4, 6, 11, and 12, where it can establish favorable contacts with several residues such as Phe254, Phe335, Leu435, Leu439 and Trp443. This hydrophobic network stabilizes the position of Trp443



in the binding site favoring its interaction through a cation- $\pi$  interaction with His421. Such interaction is considered fundamental for the activation of nuclear receptors like LXR $\alpha$ , since it allows the C-terminal H12 to adopt a conformation competent for the binding of co-activator peptides. This event triggers in turn the LXR $\alpha$ /RXR dimerization and the transcription of target genes<sup>27</sup>. Although **14** is devoid of a polar side chain, its binding mode to LXR $\alpha$  is overall similar to that reported for some oxysterols<sup>27</sup> and to the crystallographic binding pose of 24(S), 25-epoxycholesterol in LXR $\beta$  (Figure S4)<sup>35</sup>. Furthermore, the binding mode of **14** is in line with the mutagenesis data that suggest a functional role of Glu267 in the binding of oxysterols to LXRs<sup>27</sup>.

## Discussion and Conclusion

Understanding the structural requisites for selective affinity of a ligand towards its molecular target is of paramount relevance in drug design. This task can be particularly difficult when proteins involved in different cellular pathways discriminate among ligands with small chemical changes as in the case of bile acid receptors. On the other hand, one might exploit the possibility to simultaneously activate more than one molecular target developing multi-target compounds that could be beneficial from the therapeutic point of view. In the present work, we have explored the chemical space of hydoxycholeic acid (HDCA) introducing a hydrophobic side chain on hydoxycholane scaffold and on A/B ring modified hydoxycholane scaffold. Several selective LXR $\alpha$  and GPBAR1 agonists as well the first example of LXR $\alpha$ /GPBAR1 dual modulators have been identified. The lead optimization of HDCA was rationally driven by the structural informations on the binding site of the two targets. Moreover, the information coming from binding calculations of **14** in GPBAR1 and LXR $\alpha$  and the pharmacological activity of structurally related compounds, allowed us to delineate the structural requirements for ligand binding to either receptor. In particular, the binding mode of **14** to LXR $\alpha$  suggests that the 3 $\alpha$ - and 6 $\alpha$ -hydroxyl groups as well as C25/C26 hydrophobic chains are crucial for ligand activity. In fact, compounds without the 6 $\alpha$ -OH group (**19–30**) or endowed with too short side chains (linear C24/C23, compounds **15–18**) and too long (branched C27, compounds **6** and **7**) are inactive towards LXR $\alpha$ . At variance with LXR $\alpha$ , the 6 $\alpha$ -hydroxyl group is not a prerequisite for ligand binding to GPBAR1, with compounds **19–30** invariably able in transactivating GPBAR1 (Table 1), while in this receptor, compounds with a hydrophobic side chain longer than C25 are inactive since their lipophilic branch can difficultly insert into the small hydrophobic cleft of the receptor binding site. Overall, our results lead to conclude that subset A derivatives (Fig. 2) with linear C25 (compounds **8** and **9**), phenyl-substituted C25 (compound **12**) and methyl-branched C26 (compounds **4** and **5**) side chains are LXR $\alpha$  selective. On the other hand, subset A derivatives with linear C24/C23 side chains (compounds **15–17**) and compounds without the 6 $\alpha$ -hydroxyl group (Subset B in Fig. 4) turn out to be active only on GPBAR1. Finally, the concurrent presence of the 6 $\alpha$ -OH group and of a C-25 methyl-branched side chain as in compounds **13** and **14** allow achieving dual LXR $\alpha$ /GPBAR1 activity.

Compound **14** was effective in modulating the expression of canonical LXR $\alpha$  and GPBAR1 target genes. We have shown that **14** increases the expression of SREBP1c, ABCG1 and GLP1 *in vitro*. Noteworthy, *in vivo* administration of compound **14** on intact mice demonstrated beneficial effects. Compound **14** does not induced the typical effects of LXR $\alpha$  agonists, which usually activate lipogenic enzymes causing accumulation of lipid in the liver. Conversely, the expression of steatosis marker genes FAS, SREBP1c and CD36 was not modulated compared to the control group. This positive effect is closely related to the simultaneous activation of GPBAR1, as demonstrated by the *in vivo* induction of GLP1 expression in the gut. Collectively, these data strongly support a further pharmacological characterization of the newly discovered agent in rodent models of metabolic disorders. In summary, we have generated a novel series of HDCA derivatives that allowed targeting metabolic disorders including diabetes, chronic inflammatory states and neurodegenerative diseases, by exploiting a completely novel mechanism of action, i.e. the simultaneous activation of LXR $\alpha$  and GPBAR1.

## Methods

**Chemistry.** High-resolution ESI-MS spectra were performed with a Micromass Q-TOF mass spectrometer. NMR spectra were obtained on Varian Inova 400 NMR spectrometer (<sup>1</sup>H at 400, MHz, <sup>13</sup>C at 100 MHz, respectively) equipped with a SUN microsystem ultra 5 hardware and recorded in CD<sub>3</sub>OD ( $\delta_{\text{H}} = 3.31$  and  $\delta_{\text{C}} = 49.0$  ppm) and CDCl<sub>3</sub> ( $\delta_{\text{H}} = 7.26$  and  $\delta_{\text{C}} = 77.0$  ppm). All of the detected signals were in accordance with the proposed structures. Coupling constants (*J* values) are given in Hertz (Hz), and chemical shifts ( $\delta$ ) are reported in ppm and referred to CHD<sub>2</sub>OD and CHCl<sub>3</sub> as internal standards. Spin multiplicities are given as s (singlet), br s (broad singlet), d (doublet), or m (multiplet).

HPLC was performed with a Waters Model 510 pump equipped with Waters Rheodine injector and a differential refractometer, model 401. Reaction progress was monitored via thin-layer chromatography (TLC) on Alugram silica gel G/UV254 plates. Silica gel MN Kieselgel 60 (70–230 mesh) from Macherey-Nagel Company was used for column chromatography. All chemicals were obtained from Sigma-Aldrich, Inc. Solvents and reagents were used as supplied from commercial sources with the following exceptions. Dichloromethane, tetrahydrofuran and trimethylamine were distilled from calcium hydride immediately prior to use. Methanol was dried from magnesium methoxide as follow. Magnesium turnings (5 g) and iodine (0.5 g) were refluxed in a small (50–100 mL) quantity of methanol until all of the magnesium has reacted. The mixture was diluted (up to 1 L) with reagent grade methanol, refluxed for 2–3 h then distilled under nitrogen. All reactions were carried out under argon atmosphere using flame-dried glassware.

The purities of compounds were determined to be greater than 95% by HPLC.

**Synthetic procedures.** See the Supporting Information.

**Cell culture.** HepG2, an immortalized human hepatocarcinoma cell line, was cultured and maintained at 37 °C and 5% CO<sub>2</sub> in E-MEM added with 10% FBS, 1% glutamine and 1% penicillin/streptomycin. HEK-293T and Glutag cells were cultured and maintained at 37 °C and 5% CO<sub>2</sub> in D-MEM added with 10% FBS, 1% glutamine and 1% penicillin/streptomycin.

**Luciferase reporter gene assay and dose-response curves.** To evaluate LXR $\alpha$  mediated transactivation, HepG2 cells were transfected with 20 ng of the reporter vector p(UAS)5XTKLuc, 100 ng of a vector containing the ligand binding domain of LXR $\alpha$  cloned upstream of the GAL4-DNA binding domain (i.e. pSG5-LXR $\alpha$ LBD-GAL4DBD) and 100 of pGL4.70 (Promega), a vector encoding the human Renilla gene. To evaluate GPBAR1 mediated transactivation, HEK-293T cells were transfected with 200 ng of human pGL4.29 (Promega), a reporter vector containing a cAMP response element (CRE) that drives the transcription of the luciferase reporter gene luc2P, with 100 ng of pCMVSPORT6-human GPBAR1, and with 100 ng of pGL4.70 Renilla. To evaluate FXR mediated transactivation, HepG2 cells were transfected with 100 ng of human pSG5-FXR, 100 ng of human pSG5-RXR, 200 ng of the reporter vector p(hsp27)-TK-LUC containing the FXR response element IR1 cloned from the promoter of heat shock protein 27 (hsp27) and with 100 ng of pGL4.70 Renilla. At 24 h post-transfection, cells were stimulated 18 h with 10  $\mu$ M GW3965, TLCA, or CDCA and compounds **4–30** (10  $\mu$ M). Luciferase activities were assayed and normalized with Renilla activities. Dose-response curves were performed in HepG2 and HEK-293T cells transfected as described above and then treated with increasing concentrations of compounds **4, 5, 8, 9, 12–15, 17, 20, 21, 24, 25, 27, 29, 30** (1, 5, 10, 25 and 50  $\mu$ M). At 18 h post stimulations, cellular lysates were assayed for luciferase and Renilla activities using the Dual-Luciferase Reporter assay system (E1980, Promega). Luminescence was measured using Glomax 20/20 luminometer (Promega). Luciferase activities (RLU) were normalized with Renilla activities (RRU).

**Animal model.** C57BL6 mice were originally donated by Dr. Galya Vassileva (Schering-Plough Research Institute, Kenilworth). The colonies were maintained in the animal facility of University of Perugia. Mice were treated with compound **14** (30 mg/Kg daily by oral gavage) or vehicle (distilled water) for two weeks. Mice were housed under controlled temperatures (22 °C) and photoperiods (12:12-h light/dark cycle), allowed unrestricted access to standard mouse chow and tap water and allowed to acclimate to these conditions for at least 5 days before inclusion in an experiment. The study was conducted in agreement with the Italian law and the protocol was approved by ethical committee of University of Perugia and by National committee of Ministry of Health (permission n. 42/2014-B). The Veterinarian monitored the health and body conditions of the animals daily in the animal facility. The study protocol caused minor suffering; however, animals that lost more than 25% of the initial body weight were euthanized. At the day of sacrifice mice were deeply anesthetized with a mixture of tiletamine hydrochloride and zolazepam hydrochloride/xylazine at a dose of 50/5 mg/Kg. Blood, liver and terminal ileum were collected for further analysis. Aspartate aminotransferase (AST), total cholesterol and triglycerides were measured by routine biochemical clinical chemistry. For histological examination, portions of liver lobes were fixed in 10% formalin, embedded in paraffin, sectioned (5  $\mu$ m thin) and stained with Hematoxylin/Eosin (H&E) for morphometric analysis.

**RNA isolation and RT-PCR.** HepG2 and Glutag cells were plated at  $1 \times 10^6$  cells/well in a 6 well plate. After an overnight incubation, cells were starved and then stimulated for 18 h with GW3965 or TLCA (10  $\mu$ M), HDCA (10  $\mu$ M), and with increasing concentrations of compound **14** (1, 5, 10, 25, 50  $\mu$ M).

Total RNA was isolated from HepG2 or Glutag cells and from animal tissues (liver and terminal ileum) using the TRIzol reagent according to the manufacturer's specifications (Invitrogen). One microgram of purified RNA was treated with DNase-I and reverse transcribed with Superscript II (Invitrogen). For Real Time PCR, 25 ng template was dissolved in 25  $\mu$ L containing 200 nmol/L of each primer and 12.5  $\mu$ L of  $2 \times$  SYBR FAST Universal ready mix (Invitrogen). All reactions were performed in triplicate, and the thermal cycling conditions were as follows: 2 min at 95 °C, followed by 40 cycles of 95 °C for 20 s and 60 °C for 30 s in StepOnePlus (Applied Biosystems). The relative mRNA expression was calculated and expressed as  $2^{(-\Delta\Delta Ct)}$ . Forward and reverse primer sequences were the following: human GAPDH, gaaggtgaaggtcggag and catgggtggaatcatattggaa; human ABCA1, gcttggaagattatgacagg and aggggatgattgaagcagtaa; human SREBP1c, gcaaggccatcgactacatt and ggctcagtgtgctcctcacct; mouse GAPDH, ctgagtatgctgtggagtctac and gttggtggtcaggatgcttg; mouse Pro-glucagon, tgaagacaacgccactcac and caatgtgttccggttcctc; mouse FAS, tcaagatgaaggtggcagagtgct and ttgagcagtgcgggattcgg; mouse SREBP1c, gatcaaa-gaggagcagtcg and tagatggtggctgctgagtg; mouse CD36, cggagacatgcttattgagaa and actctgtatgtgaaggacct; mouse PPAR $\alpha$ , cagaggtccgattctccac and gatcagcatcccgtgtttgt; mouse PPAR $\gamma$ , gccagtttcgatccgtagaa and aatccttggcctct-gagat; mouse LXR $\alpha$ , ggctcaccagcttcattagc and gcaggaccagctccaagtag; mouse FXR, tgtgagggctgcaaaggttt and acatcccattctctgac; mouse Fgf21, acacagatgacgaccaagacac and aagtgaggcgtatcatagagag.

**Molecular docking.** The Glide (version 7.1) software package<sup>36</sup> was used to perform molecular docking calculations in the three-dimensional model of hGPBAR1<sup>31</sup> and in the crystal structure of LXR $\alpha$ -LBD bound to a synthetic benzisoxazole urea agonist (PDB code: 3IPU)<sup>34</sup>.

This structure was selected among the several available using the following criteria: i) the higher resolution of the electron density map; ii) the presence of all amino acids in helix 1, which is not fully resolved in all the LXR $\alpha$  crystal structures; iii) the presence of an agonist with bulkiness comparable to bile acid derivatives. Missing residues in the loop connecting H1 with H3 were added and refined using Prime<sup>37</sup>. Ligand and receptors structures were prepared as described in a previous paper<sup>32</sup>.

For both GPBAR1 and LXR $\alpha$ , a box of  $30 \times 30 \times 30$  Å centered on the ligand binding cavities was created. The standard precision (SP) mode of the GlideScore function<sup>38,39</sup> was used to score the predicted binding poses.

**Molecular dynamics.** All the simulations were performed with NAMD 2.10<sup>40</sup> using the *ff14SB*<sup>41</sup> and *gaff*<sup>42</sup> Amber force field parameters for the protein and the ligand, respectively. Each complex was solvated in a 12.0 Å layer cubic water box using the TIP3P water model parameters<sup>43</sup>. The addition of 2 Na<sup>+</sup> ions ensured neutrality. Amber charges were applied to the proteins and water molecules, whereas the ligand charges were computed using the restrained electrostatic potential (RESP) fitting procedure<sup>44</sup>. The ESP was first calculated by means of the Gaussian09 package<sup>45</sup> using a 6–31 G\* basis set at Hartree-Fock level of theory, and then the RESP charges were obtained by a two-stages fitting procedure using Antechamber<sup>46</sup>. A 10 Å cutoff (switched at 8.0 Å) was used for atom-pair interactions<sup>47,48</sup>. The long-range electrostatic interactions were computed by means of the particle mesh Ewald (PME) method<sup>49</sup>, using a 1.0 Å grid spacing in periodic boundary conditions. The SHAKE algorithm was applied to constraint bonds involving hydrogen atoms, and thus an integration time step of 2 fs could be used. Each complex was heated up to 300 K while putting harmonic constraints on the protein and the ligand, which were gradually released along the thermalization process. Production runs were then performed under NPT conditions at 1 atm and 300 K.

All figures were rendered using PyMOL (<http://www.pymol.org>).

## References

- Janowski, B. A., Willy, P. J., Devi, T. R., Falck, J. R. & Mangelsdorf, D. J. An oxysterol signalling pathway mediated by the nuclear receptor LXR alpha. *Nature* **383**, 728–731 (1996).
- Lehmann, J. M. *et al.* Activation of the nuclear receptor LXR by oxysterols defines a new hormone response pathway. *J. Biol. Chem.* **272**, 3137–3140 (1997).
- Svensson, S. *et al.* Crystal structure of the heterodimeric complex of LXR $\alpha$  and RXR $\beta$  ligand-binding domains in a fully agonistic conformation. *EMBO J.* **22**, 4625–4633 (2003).
- Venkateswaran, A. *et al.* Control of cellular cholesterol efflux by the nuclear oxysterol receptor LXR alpha. *Proc. Natl. Acad. Sci USA* **97**, 12097–12102 (2000).
- Repa, J. J. *et al.* Regulation of absorption and ABC1-mediated efflux of cholesterol by RXR heterodimers. *Science* **289**, 1524–1529 (2000).
- Joseph, S. B. *et al.* LXR-dependent gene expression is important for macrophage survival and the innate immune response. *Cell* **119**, 299–309 (2004).
- A-Gonzalez, N. *et al.* Apoptotic cells promote their own clearance and immune tolerance through activation of the nuclear receptor LXR. *Immunity* **31**, 245–258 (2009).
- Laffitte, B. A. *et al.* Activation of liver X receptor improves glucose tolerance through coordinate regulation of glucose metabolism in liver and adipose tissue. *Proc. Natl. Acad. Sci USA* **100**, 5419–5424 (2003).
- Commerford, S. R. *et al.* Dissection of the insulin-sensitizing effect of liver X receptor ligands. *Mol. Endocrinol.* **21**, 3002–3012 (2007).
- Hong, C. & Tontonoz, P. Liver X receptors in lipid metabolism: opportunities for drug discovery. *Nat. Rev. Drug Discov.* **6**, 433–444 (2014).
- Tice, C. M. *et al.* The medicinal chemistry of liver X receptor (LXR) modulators. *J. Med. Chem.* **57**, 7182–7205 (2014).
- Grefhorst, A. *et al.* Stimulation of lipogenesis by pharmacological activation of the liver X receptor leads to production of large, triglyceride-rich very low density lipoprotein particles. *J. Biol. Chem.* **277**, 34182–34190 (2002).
- Eyssen, H. J., De Pauw, G. & Van Eldere, J. Formation of hyodeoxycholic acid from muricholic acid and hyocholic acid by an unidentified gram-positive rod termed HDCA-1 isolated from rat intestinal microflora. *Appl. Environ. Microbiol.* **65**, 3158–3163 (1999).
- Song, C., Hiipakka, R. A. & Liao, S. Selective activation of liver X receptor alpha by 6-alpha-hydroxy bile acids and analogs. *Steroids* **65**, 423–427 (2000).
- Singhal, A. K., Cohen, B. I., Finver-Sadowsky, J., McSherry, C. K. & Mosbach, E. H. Role of hydrophilic bile acids and of sterols on cholelithiasis in the hamster. *J. Lipid Res.* **25**, 564–570 (1984).
- Singhal, A. K. *et al.* Prevention of cholesterol-induced gallstones by hyodeoxycholic acid in the prairie dog. *J. Lipid Res.* **25**, 539–549 (1984).
- Shih, D. M. *et al.* Hyodeoxycholic acid improves HDL function and inhibits atherosclerotic lesion formation in LDLR-knockout mice. *FASEB J.* **9**, 3805–3817 (2013).
- Watanabe, S. & Fujita, K. Dietary hyodeoxycholic acid exerts hypolipidemic effects by reducing farnesoid X receptor antagonist bile acids in mouse enterohepatic tissues. *Lipids* **49**, 963–973 (2014).
- Sato, H. *et al.* Novel potent and selective bile acid derivatives as TGR5 agonists: biological screening, structure-activity relationships, and molecular modeling studies. *J. Med. Chem.* **51**, 1831–1841 (2008).
- Maruyama, T. *et al.* Identification of membrane type receptor for bile acids (M-BAR). *Biochem. Biophys. Res. Commun.* **298**, 714–719 (2002).
- Keitel, V. & Haussinger, D. Perspective: TGR5 (Gpbar-1) in liver physiology and disease. *Clin. Res. Hepatol. Gastroenterol.* **36**, 412–419 (2012).
- Kawamata, Y. *et al.* A G protein-coupled receptor responsive to bile acids. *J. Biol. Chem.* **278**, 9435–9440 (2003).
- Watanabe, M. *et al.* Bile acids induce energy expenditure by promoting intracellular thyroid hormone activation. *Nature* **439**, 484–489 (2006).
- Thomas, C. *et al.* TGR5-mediated bile acid sensing controls glucose homeostasis. *Cell Metab.* **10**, 167–177 (2009).
- Pols, T. W. *et al.* TGR5 activation inhibits atherosclerosis by reducing macrophage inflammation and lipid loading. *Cell Metab.* **14**, 747–757 (2011).
- Stepanov, V., Stankov, K. & Mikov, M. The bile acid membrane receptor TGR5: a novel pharmacological target in metabolic, inflammatory and neoplastic disorders. *J. Recept. Signal Transduct. Res.* **33**, 213–223 (2013).
- Svensson, S. *et al.* Crystal structure of the heterodimeric complex of LXR $\alpha$  and RXR $\beta$  ligand-binding domains in a fully agonistic conformation. *EMBO J.* **22**, 4625–4633 (2003).
- Compound **6** was obtained as inseparable mixture of the two diastereoisomers at the side chain double bond.
- Sepe, V. *et al.* The first total synthesis of solomonsterol B, a marine pregnane X receptor agonist. *Eur. J. Org. Chem.* 5187–5194 (2012).
- Sepe, V. *et al.* Total synthesis and pharmacological characterization of solomonsterol A, a potent marine pregnane-X-receptor agonist endowed with anti-inflammatory activity. *J. Med. Chem.* **54**, 4590–4599 (2011).
- D'Amore C. *et al.* Design, synthesis, and biological evaluation of potent dual agonists of nuclear and membrane bile acid receptors. *J. Med. Chem.* **57**, 937–954 (2014).
- Sepe, V. *et al.* Modification on ursodeoxycholic acid (UDCA) scaffold. Discovery of bile acid derivatives as selective agonists of cell-surface G-protein coupled bile acid receptor 1 (GP-BAR1). *J. Med. Chem.* **57**, 7687–701 (2014).
- Di Leva, F. S. *et al.* Structure-based drug design targeting the cell membrane receptor GPBAR1: exploiting the bile acid scaffold towards selective agonism. *Sci. Rep.* **5**, 16605 (2015).

34. Fradera, X. *et al.* X-ray structures of the LXR $\alpha$  LBD in its homodimeric form and implications for heterodimer signaling. *J. Mol. Biol.* **399**, 120–132 (2010).
35. Williams, S. *et al.* X-ray crystal structure of the liver X receptor beta ligand binding domain: regulation by a histidine-tryptophan switch. *J. Biol. Chem.* **278**, 27138–27143 (2003).
36. Glide, version 7.1, Schrödinger, LLC, New York, NY (2016).
37. Prime, version 4.4, Schrödinger, LLC, New York, NY (2016).
38. Halgren, T. A. *et al.* Glide: A new approach for rapid, accurate docking and scoring. 2. Enrichment factors in database screening. *J. Med. Chem.* **47**, 1750–1759 (2004).
39. Friesner, R. A. *et al.* Glide: A new approach for rapid, accurate docking and scoring. 1. Method and assessment of docking accuracy. *J. Med. Chem.* **47**, 1739–1749 (2004).
40. Phillips, J. C. *et al.* Scalable molecular dynamics with NAMD. *J. Comput. Chem.* **26**, 1781–1802 (2005).
41. Maier, J. A. *et al.* ff14SB: Improving the accuracy of protein side chain and backbone parameters from ff99SB. *J. Chem. Theory Comput.* **11**, 3696–3713 (2015).
42. Wang, J., Wolf, R. M., Caldwell, J. W., Kollman, P. A. & Case, D. A. Development and testing of a general amber force field. *J. Comput. Chem.* **25**, 1157–1174 (2004).
43. Jorgensen, W. L., Chandrasekhar, J., Madura, J. D., Impey, R. W. & Klein, M. L. Comparison of simple potential functions for simulating liquid water. *J. Chem. Phys.* **79**, 926–935 (1983).
44. Bayly, C. L., Cieplak, P., Cornell, W. D. & Kollman, P. A. A well-behaved electrostatic potential based method using charge restraints for determining atom-centered charges: The RESP Model. *J. Phys. Chem.* **97**, 10269–10280 (1993).
45. Frisch, M. J. *et al.* Gaussian 09 Revision D.01, Gaussian, Inc: Wallingford, CT (2010).
46. Wang, J., Wang, W., Kollman, P. A. & Case, D. A. Automatic atom type and bond type perception in molecular mechanics. *J. Mol. Graphics Model.* **25**, 247–260 (2006).
47. Anzini, M. *et al.* Ethyl 8-Fluoro-6-(3-nitrophenyl)-4H-imidazo[1,5-a][1,4]benzodiazepine-3-carboxylate as novel, highly potent, and safe anti-anxiety agent. *J. Med. Chem.* **51**, 4730–4743 (2008).
48. Anzini, M. *et al.* New insight into the central benzodiazepine receptor ligand interactions: design, synthesis, biological evaluation, and molecular modeling of 3-substituted 6-phenyl-4H-imidazo[1,5-a]-[1,4]benzodiazepines and related compounds. *J. Med. Chem.* **54**, 5694–5711 (2011).
49. Darden, T., York, D. & Pedersen, L. Particle mesh Ewald: an N-log(N) method for Ewald sums in large systems. *J. Chem. Phys.* **98**, 10089–10092 (1993).

## Acknowledgements

This work was supported by grants from PSC Partners, 5237 South Kenton Way, Englewood, Colorado 80111 USA, MIUR-ITALY PRIN2015 “Top-down and Bottom-up approach in the development of new bioactive chemical entities inspired on natural products scaffolds” (Project N. 2015MSCCKCE\_003) and the Swiss National Science Foundation (Project N. 200021\_163281). Computational resources were provided by the Swiss National Supercomputing Center (CSCS) [project ID s557]. The authors also thank the COST action CA15135 (Multi-target paradigm for innovative ligand identification in the drug discovery process MuTaLig) for the support.

## Author Contributions

S.D.M., D.M., C.F., B.C. and A.Z. designed and performed synthesis; A.C., S.C., S.M. and S.F. designed and performed pharmacological experiments; F.S.D.L., E.N. and V.L. designed and performed computational studies. All authors contributed to manuscript writing and approved the final version.

## Additional Information

**Supplementary information** accompanies this paper at <http://www.nature.com/srep>

**Competing financial interests:** The authors declare no competing financial interests.

**How to cite this article:** De Marino, S. *et al.* Hyodeoxycholic acid derivatives as liver X receptor  $\alpha$  and G-protein-coupled bile acid receptor agonists. *Sci. Rep.* **7**, 43290; doi: 10.1038/srep43290 (2017).

**Publisher's note:** Springer Nature remains neutral with regard to jurisdictional claims in published maps and institutional affiliations.



This work is licensed under a Creative Commons Attribution 4.0 International License. The images or other third party material in this article are included in the article's Creative Commons license, unless indicated otherwise in the credit line; if the material is not included under the Creative Commons license, users will need to obtain permission from the license holder to reproduce the material. To view a copy of this license, visit <http://creativecommons.org/licenses/by/4.0/>

© The Author(s) 2017